TRAC-WSMR-TR-99-001(R)

Effects of Vegetation on Line-of-Sight (LOS) for Dismounted Infantry Operations

Study Proponent

US Army Models and Simulation Office
ODCSOPS, ATTN: DAMO-ZS
400 Army Pentagon
Washington, DC 20310-0400

Study Organization

TRADOC Analysis Center-White Sands Missile Range (TRAC-WSMR)
White Sands Missile Range, NM 88002-5502

DEPARTMENT OF THE ARMY

June 1999

Distribution authorized to US Government agencies and their contractors; administrative or operational use; June 1999. Other requests for this document must be referred to Director, TRADOC Analysis Center-White Sands Missile Range, ATTN: ATRC-WE, WSMR, NM 88002-5502

Notice

This report has been prepared by the TRADOC Analysis Center-White Sands Missile Range under the sponsorship of US Army Models and Simulation Office, ODCSOPS, ATTN: DAMO-ZS 400 Army Pentagon Washington, DC 20310-0400. This report documents analysis based on best available data, scenarios, and model versions at the time of the analysis. The findings in this report have not been reviewed by the US Army Models and Simulation Office and may not be construed as an official US Army position unless so designated by other official documents.

Destruction Notice

Destroy in accordance with the procedures in DOD 5200.22-M, Industrial Security Manual, Section 11-19 or DOD 5200.1-R, Information Security Program Regulation, Chapter IX.

TRAC-WSMR-TR-99-001(R)

Effects of Vegetation on Line-of-Sight (LOS) for Dismounted Infantry Operations

Study Proponent

US Army Models and Simulation Office
ODCSOPS, ATTN: DAMO-ZS
400 Army Pentagon
Washington, DC 20310-0400

Study Organization

TRADOC Analysis Center-White Sands Missile Range (TRAC-WSMR)
White Sands Missile Range, NM 88002-5502

Authors

Danny C. Champion, TRAC-WSMR
Louis A. Fatale, TEC
Paul F. Krause, Ph.D., TEC

Released by:

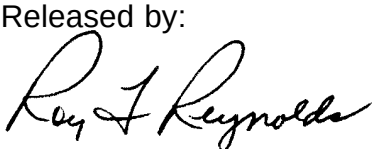

ROY F. REYNOLDS
SES, US Army
Director, TRAC-WSMR

June 1999

Distribution authorized to US Government agencies and their contractors; administrative or operational use; June 1999. Other requests for this document must be referred to Director, TRADOC Analysis Center-White Sands Missile Range, ATTN: ATRC-WE, WSMR, NM 88002-5502

REPORT DOCUMENTATION PAGE

Form Approved
OMB No. 0704-0188

Public reporting burden for this collection of information is estimated to average 1 hour per response, including the time for reviewing instructions, searching existing data sources, gathering and maintaining the data needed, and completing and reviewing the collection of information. Send comments regarding this burden estimate or any other aspect of this collection of information, including suggestions for reducing this burden, to Washington Headquarters Services, Directorate for Information Operations and Reports, 1215 Jefferson Davis Highway, Suite 1204, Arlington, VA 22202-4302, and to the Office of Management and Budget, Paperwork Reduction Project (0704–0188) Washington, DC 20503

1. AGENCY USE ONLY *(Leave blank)*	2. REPORT DATE	3. REPORT TYPE AND DATES COVERED
	June 1999	Final, September 1997 - May 1999

4. TITLE AND SUBTITLE
Effects of Vegetation on Line-of-Sight (LOS) for Dismounted Infantry Operations

5. FUNDING NUMBERS

6. AUTHOR(S)
Danny C. Champion, Louis A. Fatale, Paul F. Krause, Ph.D.

7. PERFORMING ORGANIZATION NAME(S) AND ADDRESS(ES)
Director, TRAC-WSMR
ATTN: ATRC-WE
White Sands Missile Range, NM 88002-5502

8. PERFORMING ORGANIZATION REPORT NUMBER
TRAC-WSMR-TR-99-001(

9. SPONSORING/MONITORING AGENCY NAME(S) AND ADDRESS(ES)
US Army Models and Simulation Office
ODCSOPS, ATTN: DAMO-ZS
400 Army Pentagon
Washington, DC 20310-0400

10. SPONSORING/MONITORING AGENCY REPORT NUMBER

11. SUPPLEMENTARY NOTES

12a. DISTRIBUTION/AVAILABILITY STATEMENT
Distribution authorized to US Government agencies and their contractors; administrative or operational use; June 1999. Other requests for this document must be referred to Director, US Army TRADOC Analysis Center-White Sands Missile Range, ATTN: ATRC-WE, WSMR, NM 88002-5502

12b. DISTRIBUTION CODE

13. ABSTRACT (*Maximum 200 words)*

Prediction of realistic line-of-sight (LOS) conditions has always been an essential aspect of combat simulations. The representation of LOS in areas with surface features (vegetation) has never been extensively examined. However, recent advances in weapons systems, combat simulators, and the evolving mission requirements of the modern Army have demonstrated the need for a more precise understanding of how vegetation impacts LOS prediction. This study will: (1) identify geotypical feature density zones; (2) document typical LOS within each with a field collection effort and; (3) predict future LOS performance. The output of this study will: (1) facilitate the selection of a standard algorithm for LOS which performs effectively in varied feature densities and (2) provide recommendations on how to improve the play of surface features in combat models.

14. SUBJECT TERMS
LOS, detection, acquisition, vegetation, infantry, intervisibility

15. NUMBER OF PAGES

16. PRICE CODE

17. SECURITY CLASSIFICATION OF REPORT	18. SECURITY CLASSIFICATION OF THIS PAGE	19. SECURITY CLASSIFICATION OF ABSTRACT	20. LIMITATION OF ABSTRACT
UNCLASSIFIED	UNCLASSIFIED	UNCLASSIFIED	

Effects of Vegetation on Line-of-Sight (LOS) for Dismounted Infantry Operations

Study Gist

Purpose. This research provides a better understanding of line-of-sight (LOS) in vegetated areas. It also provides equations and parameters for those equations allowing analysts involved in combat simulation to depict dismounted infantry engagements more accurately.

Critical Issues Addressed. Prediction of realistic LOS has always been an essential aspect of combat simulations. The representation of LOS in areas with surface features (vegetation) has never been extensively examined. With recent advances in weapons systems, the increased use of combat simulators, and the evolving mission requirements of the modern Army have demonstrated the requirement for a more precise understanding of how vegetation impacts LOS prediction.

Objectives. Provide analysts with a standard algorithm providing accurate LOS in varied vegetation densities and provide recommendations on how to improve the simulation of LOS in vegetation for combat models.

Principal Findings. Vegetation varies throughout the world and, thus, impacts LOS differently. This research examined vegetation as a function of vegetative biome (a combination of climate and vegetation) and provides algorithms accurately portraying LOS in different densities and types of vegetation.

Impact/Utility to the Army. Even before the analysis was complete, a major combat simulation, the Combined Arms Support Task Force Evaluation Model (CASTFOREM), was modified to incorporate data and algorithms from this study in order to portray LOS in vegetation more realistically. Ultimately, this work will improve the simulation of dismounted infantry combat in other combat simulations.

Main Assumptions. The field-collected data is representative of the vegetation for each study area. The field-collected data can be extrapolated to areas with similar vegetation, climate, soil, latitude, and elevation.

Principal Limitations. Several world vegetation types had to be omitted from this study. These include areas void or nearly void of vegetation (i.e., desert and tundra), areas inaccessible to the data collection team (i.e., Australia and Siberia) or areas where deployment of troops is unlikely (i.e., the Great Lakes region).

Scope. The scope of this research was limited to collecting visibility data between dismounted infantry units. Since it is unlikely that two units will encounter each other randomly, this work focused on a unit in defense and a unit in attack.

Approach. The approach used in this study included the following steps: identify data collection locations (general geographic areas), select a tactically sound defensive position and a tactical field of view, collect data consisting of how much of a kneeling infantryman is visible as a function of range, and provide a fit to three different types of curves (exponential, field exponential, and pole-zero) representing LOS in vegetation as a function of range.

Study Sponsor. United States (US) Army Models and Simulation Organization

Performing Organization and Principal Authors. Mr. Danny C. Champion of the Training and Doctrine Command (TRADOC) Analysis Agency-White Sands Missile Range (TRAC-WSMR), and Mr. Louis A. Fatale and Dr. Paul Krause of the US Army Topographic Engineering Agency (TEC)

Literature Search. A literature search examined documents which: focused on forestry research, included a keyword search of Defense Technical Information Center (DTIC), and included internet searches. Also, modeling and simulation agencies (both US and allied forces) were contacted to determine if any similar work had been conducted.

DTIC Accession Number. DA358645

Start and Completion Dates. September 1997 through May 1999

Table of Contents

Study Gist iii
List of Figures vii
List of Tables xi
Preface xii

Introduction 1
Background 1
Purpose 3
Scope 3
Limitations 3
Assumptions 3
Difference Between LOS and Detection 3
Methodology 5
  Introduction 5
  Geographic Selection for Data Collection 5
  Site Selection 10
  Tactical Considerations for Data Collection 10
  Data Collection Methodology 10
Analysis 15
  Introduction 15
Raw Data 16
  Curve Fits 16
  Representative Data Sites 18
  Parameter Selection 19
  Relationship of the Undergrowth to the LOS Parameters 27
  Panama Discussion 28
  Data Collection Observations 28
Conclusions 29
Recommendations 30

Appendix A. Probability of Detection (PDET) 31
Appendix B. Description of Data Collection Locations and Sites 37
Appendix C. Climates 65
Appendix D. Vegetative Sub-Biome Descriptions 69
Appendix E. Analysis 79

Bibliography 357
Acronyms 359
Distribution 361

List of Figures

Figure 1. Moths on Tree Bark - Fully Visible, Difficult to Detect 4
Figure 2. Moths on Tree Bark - Fully Visible, Easy to Detect 5
Figure 3a. Vegetation Biomes for the World 6
Figure 3b. Vegetation Biomes for the World 7
Figure 4. Kneeling Target Silhouette 11
Figure 5. Sample Azimuth 12
Figure 6. Sample Data Collection Sheet 14
Figure 7. A Sample of the Plots Developed From the Field Collection 17
Figure 8. The Raw Data for Five Selected Sites Where a Prone Defender is Looking at a Kneeling Attacker 26
Figure 9. The Exponential Fits for Five Selected Sites Where a Prone Defender is Looking at a Kneeling Attacker 26
Figure 10. The Field Exponential Fits for Five Selected Sites Where a Prone Defender is Looking at a Kneeling Attacker 26
Figure 11. The Pole-Zero Fits for Five Selected Sites Where a Prone Defender is Looking at a Kneeling Attacker 27
Figure A-1. Probability of Detection for Different Light Conditions - Fully Exposed Kneeling Target on the Move 35
Figure A-2. Probability of Detection for Different Light Conditions - Fully Exposed Prone Target on the Move 36
Figure B-1a. Vegetation Biomes for the World 38
Figure B-1b. Vegetation Biomes for the World 39
Figure B-2. CONUS Vegetation Analogs to Korea Vegetation 43
Figure B-3. CONUS Vegetation Analogs to the Former Yugoslavia 44
Figure D-1a. Vegetation Biomes for the World 73
Figure D-1b. Vegetation Biomes for the World 74
Figure E-1. Panama, From Defender Point of View, Site gam1 108
Figure E-2. Panama, From Attacker Point of View, Site gam1 110
Figure E-3. Panama, From Defender Point of View, Site gam2 112
Figure E-4. Panama, From Attacker Point of View, Site gam2 114
Figure E-5. Panama, From Defender Point of View, Site gam3 116
Figure E-6. Panama, From Attacker Point of View, Site gam3 118
Figure E-7. Panama, From Defender Point of View, Site skh1 120
Figure E-8. Panama, From Attacker Point of View, Site skh1 122
Figure E-9. Panama, From Defender Point of View, Site mck1 124
Figure E-10. Panama, From Attacker Point of View, Site mck1 126
Figure E-11. Panama, From Defender Point of View, Site elv1 128
Figure E-12. Panama, From Attacker Point of View, Site elv1 130
Figure E-13. Panama - Wet, From Defender Point of View, Site gam1w 132
Figure E-14. Panama - Wet, From Attacker Point of View, Site gam1w 134
Figure E-15. Panama - Wet, From Defender Point of View, Site gam2w 136
Figure E-16. Panama - Wet, From Attacker Point of View, Site gam2w 138
Figure E-17. Panama - Wet, From Defender Point of View, Site gam3w 140
Figure E-18. Panama - Wet, From Attacker Point of View, Site gam3w 142
Figure E-19. Panama - Wet, From Defender Point of View, Site shk1w 144
Figure E-20. Panama - Wet, From Attacker Point of View, Site shk1w 146
Figure E-21. Panama - Wet, From Defender Point of View, Site mck1w 148
Figure E-22. Panama - Wet, From Attacker Point of View, Site mck1w 150
Figure E-23. Panama - Wet, From Defender Point of View, Site elv1w 152
Figure E-24. Panama - Wet, From Attacker Point of View, Site elv1w 154
Figure E-25. Eglin AFB, From Defender Point of View, Site egl_B2 156
Figure E-26. Eglin AFB, From Attacker Point of View, Site egl_B2 158
Figure E-27. Eglin AFB, From Defender Point of View, Site egl_B12 160
Figure E-28. Eglin AFB, From Attacker Point of View, Site egl_B12 162

Figure E-29. Eglin AFB, From Defender Point of View, Site egl_X8 164
Figure E-30. Eglin AFB, From Attacker Point of View, Site egl_X8 166
Figure E-31. Eglin AFB, From Defender Point of View, Site egl_X11 168
Figure E-32. Eglin AFB, From Attacker Point of View, Site egl_X11 170
Figure E-33. Fort Hood, From Defender Point of View, Site hood1 172
Figure E-34. Fort Hood, From Attacker Point of View, Site hood1 174
Figure E-35. Fort Hood, From Defender Point of View, Site hood2 176
Figure E-36. Fort Hood, From Attacker Point of View, Site hood2 178
Figure E-37. Fort Hood, From Defender Point of View, Site hood3 180
Figure E-38. Fort Hood, From Attacker Point of View, Site hood3 182
Figure E-39. Fort Hood, From Defender Point of View, Site hood4 184
Figure E-40. Fort Hood, From Attacker Point of View, Site hood4 186
Figure E-41. Fort Carson, From Defender Point of View, Site car28 188
Figure E-42. Fort Carson, From Attacker Point of View, Site car28 190
Figure E-43. Fort Carson, From Defender Point of View, Site car41 192
Figure E-44. Fort Carson, From Attacker Point of View, Site car41 194
Figure E-45. Fort Carson, From Defender Point of View, Site car43 196
Figure E-46. Fort Carson, From Attacker Point of View, Site car43 198
Figure E-47. Fort Carson, From Defender Point of View, Site afa1 200
Figure E-48. Fort Carson, From Attacker Point of View, Site afa1 202
Figure E-49. Fort Hunter-Liggett, From Defender Point of View, Site hl2 204
Figure E-50. Fort Hunter-Liggett, From Attacker Point of View, Site hl2 206
Figure E-51. Fort Hunter-Liggett, From Defender Point of View, Site hl5 208
Figure E-52. Fort Hunter-Liggett, From Attacker Point of View, Site hl5 210
Figure E-53. Fort Hunter-Liggett, From Defender Point of View, Site hl9 212
Figure E-54. Fort Hunter-Liggett, From Attacker Point of View, Site hl9 214
Figure E-55. Fort Hunter-Liggett, From Defender Point of View, Site hl10 216
Figure E-56. Fort Hunter-Liggett, From Attacker Point of View, Site hl10 218
Figure E-57. Fort Lewis, From Defender Point of View, Site lew3 220
Figure E-58. Fort Lewis, From Attacker Point of View, Site lew3 222
Figure E-59. Fort Lewis, From Defender Point of View, Site lew8 224
Figure E-60. Fort Lewis, From Attacker Point of View, Site lew8 226
Figure E-61. Fort Lewis, From Defender Point of View, Site lew10 228
Figure E-62. Fort Lewis, From Attacker Point of View, Site lew10 230
Figure E-63. Fort Lewis, From Defender Point of View, Site lew19 232
Figure E-64. Fort Lewis, From Attacker Point of View, Site lew19 234
Figure E-65. Fort Benning, From Defender Point of View, Site ben_D12 236
Figure E-66. Fort Benning, From Attacker Point of View, Site ben_D12 238
Figure E-67. Fort Benning, From Defender Point of View, Site ben_L3 240
Figure E-68. Fort Benning, From Attacker Point of View, Site ben_L3 242
Figure E-69. Fort Benning, From Defender Point of View, Site ben_T3 244
Figure E-70. Fort Benning, From Attacker Point of View, Site ben_T3 246
Figure E-71. Fort Benning, From Defender Point of View, Site ben_T4 248
Figure E-72. Fort Benning, From Attacker Point of View, Site ben_T4 250
Figure E-73. Smoky Mountains, From Defender Point of View, Site NC1 252
Figure E-74. Smoky Mountains, From Attacker Point of View, Site NC1 254
Figure E-75. Smoky Mountains, From Defender Point of View, Site TN1 256
Figure E-76. Smoky Mountains, From Attacker Point of View, Site TN1 258
Figure E-77. Smoky Mountains, From Defender Point of View, Site TN2 260
Figure E-78. Smoky Mountains, From Attacker Point of View, Site TN2 262
Figure E-79. Smoky Mountains, From Defender Point of View, Site TN3 264
Figure E-80. Smoky Mountains, From Attacker Point of View, Site TN3 266
Figure E-81. Willow Grove NAS, From Defender Point of View, Site WG2 268
Figure E-82. Willow Grove NAS, From Attacker Point of View, Site WG2 270
Figure E-83. Willow Grove NAS, From Defender Point of View, Site WG4 272
Figure E-84. Willow Grove NAS, From Attacker Point of View, Site WG4 274
Figure E-85. Willow Grove NAS, From Defender Point of View, Site WG5 276
Figure E-86. Willow Grove NAS, From Attacker Point of View, Site WG5 278

Figure E-87. Willow Grove NAS, From Defender Point of View, Site WG6 280
Figure E-88. Willow Grove NAS, From Attacker Point of View, Site WG6 282
Figure E-89. Natchaug SF, From Defender Point of View, Site Nat1 284
Figure E-90. Natchaug SF, From Attacker Point of View, Site Nat1 286
Figure E-91. Natchaug SF, From Defender Point of View, Site Nat2 288
Figure E-92. Natchaug SF, From Attacker Point of View, Site Nat2 290
Figure E-93. Natchaug SF, From Defender Point of View, Site Nat4 292
Figure E-94. Natchaug SF, From Attacker Point of View, Site Nat4 294
Figure E-95. Natchaug SF, From Defender Point of View, Site Nat5 296
Figure E-96. Natchaug SF, From Attacker Point of View, Site Nat5 298
Figure E-97. Fort Drum, From Defender Point of View, Site 7B 300
Figure E-98. Fort Drum, From Attacker Point of View, Site 7B 302
Figure E-99. Fort Drum, From Defender Point of View, Site 7E 304
Figure E-100. Fort Drum, From Attacker Point of View, Site 7E 306
Figure E-101. Fort Drum, From Defender Point of View, Site 7G 308
Figure E-102. Fort Drum, From Attacker Point of View, Site 7G 310
Figure E-103. Fort Drum, From Defender Point of View, Site 8C 312
Figure E-104. Fort Drum, From Attacker Point of View, Site 8C 314
Figure E-105. Gagetown, NB, From Defender Point of View, Site Gage07 316
Figure E-106. Gagetown, NB, From Attacker Point of View, Site Gage07 318
Figure E-107. Gagetown, NB, From Defender Point of View, Site Gage08 320
Figure E-108. Gagetown, NB, From Attacker Point of View, Site Gage08 322
Figure E-109. Gagetown, NB, From Defender Point of View, Site Gage27 324
Figure E-110. Gagetown, NB, From Attacker Point of View, Site Gage27 326
Figure E-111. Gagetown, NB, From Defender Point of View, Site Gage31 328
Figure E-112. Gagetown, NB, From Attacker Point of View, Site Gage31 330
Figure E-113. Fort Greely, From Defender Point of View, Site G00 332
Figure E-114. Fort Greely, From Attacker Point of View, Site G00 334
Figure E-115. Fort Greely, From Defender Point of View, Site G02 336
Figure E-116. Fort Greely, From Attacker Point of View, Site G02 338
Figure E-117. Fort Greely, From Defender Point of View, Site G05 340
Figure E-118. Fort Greely, From Attacker Point of View, Site G05 342
Figure E-119. Fort Greely, From Defender Point of View, Site G22 344
Figure E-120. Fort Greely, From Attacker Point of View, Site G22 346
Figure E-121. Fort Greely, From Defender Point of View, Site G24 348
Figure E-122. Fort Greely, From Attacker Point of View, Site G24 350
Figure E-123. Fort Greely, From Defender Point of View, Site G25 352
Figure E-124. Fort Greely, From Attacker Point of View, Site G25 354

List of Tables

Table 1. Vegetative Sub-Biome/Climate and Vegetation Definitions of Data Collection Localities 9
Table 2. Best Representative Sites for Each Location 18
Table 3. Data Fits for the Exponential Decay From a Prone Defender to a Prone Attacker 20
Table 4. Data Fits for the Exponential Decay From a Prone Defender to a Kneeling Attacker 20
Table 5. Data Fits for the Exponential Decay From a Prone Attacker to a Prone Defender 21
Table 6. Data Fits for the Exponential Decay From a Crouching Attacker to a Prone Defender 21
Table 7. Data Fits for the Field Exponential Decay From a Prone Defender to a Prone Attacker 22
Table 8. Data Fits for the Field Exponential Decay From a Prone Defender to a Kneeling Attacker 22
Table 9. Data Fits for the Field Exponential Decay From a Prone Attacker to a Prone Defender 23
Table 10. Data Fits for the Field Exponential Decay From a Crouching Attacker to a Prone Defender 23
Table 11. Data Fits for the Pole-Zero Decay From a Prone Defender to a Prone Attacker 24
Table 12. Data Fits for the Pole-Zero Decay From a Prone Defender to a Kneeling Attacker 24
Table 13. Data Fits for the Pole-Zero Decay From a Prone Attacker to a Prone Defender 25
Table 14. Data Fits for the Pole-Zero Decay From a Crouching Attacker to a Prone Defender 25
Table 15. Correlation of Collected Data and Exponential Parameters for the Prone Defender Looking at the Kneeling Attacker 27
Table A-1. Values of Apparent Contrast as a Function of Range in a European Scenario 33
Table A-2. Minimum Resolvable Frequency for Different Light Levels and Different Values of AC 34
Table A-3. MRF Values for Five Light Conditions 34
Table A-4. Value of N for Different Light Conditions - Fully Exposed Kneeling Target on the Move 35
Table A-5. Value of N for Different Light Conditions - Fully Exposed Prone Target on the Move 35
Table B-1. Vegetative Sub-Biome/Climate and Vegetation Definitions of Data Collection Locations 41
Table B-2. Location of Field Collection Locations 44
Table B-3. Climate Information About Data Collection Locations 45
Table B-4. Exact Locations of Field Collection Sites Including Easting, Northing, and Elevation 46
Table B-5. Canopy Closure, Tree Types, and Undergrowth Information for all Data Collection Sites 47
Table D-1. World Vegetation Sub-Biomes by Continent and Country 75
Table E-1. Exact Locations of Field Collection Sites Including Easting, Northing, and Elevation 79
Table E-2. Data Fits for the Exponential Decay From a Prone Defender to a Prone Attacker 82
Table E-3. Data Fits for the Exponential Decay From a Prone Defender to a Kneeling Attacker 83

Table E-4. Data Fits for the Exponential Decay From a Crouching Defender to a Prone Attacker 84
Table E-5. Data Fits for the Exponential Decay From a Crouching Defender to a Kneeling Attacker 85
Table E-6. Data Fits for the Exponential Decay From a Prone Attacker to a Prone Defender 86
Table E-7. Data Fits for the Exponential Decay From a Prone Attacker to a Kneeling Defender 87
Table E-8. Data Fits for the Exponential Decay From a Crouching Attacker to a Prone Defender 88
Table E-9. Data Fits for the Exponential Decay From a Crouching Attacker to a Kneeling Defender 89
Table E-10. Data Fits for the Field Exponential Decay From a Prone Defender to a Prone Attacker 90
Table E-11. Data Fits for the Field Exponential Decay From a Prone Defender to a Kneeling Attacker 91
Table E-12. Data Fits for the Field Exponential Decay From a Crouching Defender to a Prone Attacker 92
Table E-13. Data Fits for the Field Exponential Decay From a Crouching Defender to a Kneeling Attacker 93
Table E-14. Data Fits for the Field Exponential Decay From a Prone Attacker to a Prone Defender 94
Table E-15. Data Fits for the Field Exponential Decay From a Prone Attacker to a Kneeling Defender 95
Table E-16. Data Fits for the Field Exponential Decay From a Crouching Attacker to a Prone Defender 96
Table E-17. Data Fits for the Field Exponential Decay From a Crouching Attacker to a Kneeling Defender 97
Table E-18. Data Fits for the Pole-Zero Decay From a Prone Defender to a Prone Attacker 98
Table E-19. Data Fits for the Pole-Zero Decay From a Prone Defender to a Kneeling Attacker 99
Table E-20. Data Fits for the Pole-Zero Decay From a Crouching Defender to a Prone Attacker 100
Table E-21. Data Fits for the Pole-Zero Decay From a Crouching Defender to a Prone Attacker 101
Table E-22. Data Fits for the Pole-Zero Decay From a Prone Attacker to a Prone Defender 102
Table E-23. Data Fits for the Pole-Zero Decay From a Prone Attacker to a Kneeling Defender 103
Table E-24. Data Fits for the Pole-Zero Decay From a Crouching Attacker to a Prone Defender 104
Table E-25. Data Fits for the Pole-Zero Decay From a Crouching Attacker to a Kneeling Defender 105
Table E-26. Best Representative Sites for Each Location 106

Preface

This study was conducted between the period September 1997 until March 1999. During this period, several organizations generously provided funding to this work. They are:

United States (US) Army Modeling and Simulation Organization (AMSO)

US Army Training and Doctrine Command (TRADOC) Analysis Center-White Sands Missile Range (TRAC-WSMR), NM

US Army Topographic Engineering Center (TEC), Alexandria, VA

US Test and Evaluation Command (TECOM), Yuma Proving Ground, Yuma, AZ

Rapid Force Projection Initiative, Huntsville, AL

Directorate Land Operations Research, Ottawa, Canada

Special thanks go out to the following people from TRAC-WSMR: Ms. Donna Vargas, Mr. Walt Butler, Ms. Lounell Southard, and Mr. Joseph Bebbs of the Brigade Models and Simulation Directorate for allowing time to conduct this study; Mr. Robert Williams of the Technical Reports Office for helping develop the field collection methodology, produce all of the briefing slides, and providing most of the figures for the report; Sergeant First Class (SFC) James Nicholson for assisting in the field collection and providing software support during the analysis; Staff Sergeant (SSG) Raymond Heiskell for helping to develop the data collection methodology, assisting in the data collection, and providing an infantryman's perspective to the work; Sergeant (SGT) David Bliss for spending many thankless hours putting together many of the graphics seen in this report and double checking all of the data; Dr. Kathy Nau for providing constant sanity checks on the analysis; SFC Gus Williams and SSG Patrick Quenga for assisting in the data collection effort; Ms. Donna Johnson for assisting in the data collection effort, developing the software to fit the raw data with exponential and pole-zero curves, and providing significant enhancements to the written report; Ms. Rita Baird, Ms. Gretchen Lindsay, Ms. Soyla Ward, Ms. Jackie Reyes, and Ms. Annaliza Arvizu of the Technical Reports Office, whose patience and tireless effort brought all of this work together into the final report. Finally, the authors would like to thank Mr. Peter Shugart for reviewing the report and making changes that make the report better and not just different.

Special thanks go out to the following people from TEC: Mr. Jeffery Messmore for his work on the original proposal and his continued motivation and support during the long field collection process; Mr. William Clark and Ms. Kathy Flood for their support to the Korea/Yugoslavia analog work; all members of the Information Services and Support Branch, especially Mr. Cedric Key and Ms. Angela Straub for graphics support; and Mr. Paul Cerevich, Mr. Tom Cox, and Mr. Dan Oimoen for their advice and invaluable support in supplying the survey equipment used in this study.

Special thanks also goes out to Dr. James P. Reilly of New Mexico State University for allowing us to borrow surveying equipment during development of the data collection methodology.

The authors' gratitude is also extended to Dr. Arthur N. Strahler and John Wiley and Sons Publishing Company for their generous permission to reproduce graphics and text which played an important role in the development of the study.

Special thanks also goes out to SSG Todd Antal from the Northern Warfare Training Center at Fort Greely, AK, for providing input about arctic infantry operations and for his assistance in selecting sites that were representative of a boreal climate and in the subsequent data collection. Additionally, we wish to thank the following people at the Tropical Test Center, Corozal, Panama: Larry Havrilo (Ch.), Rolando Ayala, Tamara Paredes, Alcibiades Grajales (Sr. and Jr.), Alonso Iglesias, Ricardo Martinez, Dinorah Tijerino, Lloyd Hay, Juventino Serrano, and James Bryan without whose support the tropical analyses of this study could not have been completed.

Special appreciation is also extended to Messrs. Lance Vanderzyl, Acting Director of the Tropic Test Center and Mr. Ruben Hernandez, Optical Development and Integration Branch, Yuma Proving Ground whose unwavering support of the study and foresight regarding tropical environments facilitated the development of a substantially improved final report.

John D'Errico, a retired infantryman from the Dismounted Battlespace Battle Lab, provided an infantry perspective to the field collection at Fort Benning, assisted with the field collection, and provided many of the field supplies used during the course of the study.

Finally, the authors would like to thank Mr. Pierre Ladouceur and Ms. Mary Ellen Campbell, Canadian National Defence Headquarters, Ottawa, Ontario, Canada, for their coordination of the New Brunswick, Canada data collection effort which provided the opportunity for the incorporation of a valuable international site into the study.

Mr. Roy Reynolds was the Director and Colonel (COL) Gary G. Swenson was the Senior Military Analyst of TRAC-WSMR at the time of the publication of this report. Dr. William E. Roper was Director of the Topographic Engineering Center (TEC) at the time of the publication of this report.

Effects of Vegetation on Line-of-Sight (LOS) for Dismounted Infantry Operations

Introduction

The realistic representation of line-of-sight (LOS) is an essential aspect of combat simulations. Until the end of the cold war, combat modeling had focused on large armored forces where the representation of surface features (e.g., vegetation and urban structures) was not of primary importance in the calculation of LOS.

Since 1989, the United States (US) Army has deployed over a dozen times. With the exception of Desert Storm, all of the deployments have focused on smaller operations using dismounted infantry units. Therefore, there is today a new emphasis on the operations of relatively small and rapidly deployable forces and a consequent increased effort to simulate the dynamic combat of dismounted infantry. Additionally, this emphasis is also driven largely by the emergence of Dismounted Interactive Simulation systems where virtual, live, and constructive simulations are combined.

In combat, dismounted soldiers maneuver and fight using surface features for concealment. There is a modeling shortfall in the realistic simulation of LOS in areas containing a high density of surface features.

Background

LOS is, by definition, a point-to-point measure. A sensor and a target are represented by a pair of (x, y, z) coordinates. LOS is defined to exist if there are no obstructions in the straight line between the two points. For this study, assume the target is represented as a two dimensional area with a boundary. The questions to be addressed here are:

- Taking into account the surface features of the terrain, does LOS exist between the sensor and any point on the target?
- When such LOS exists, what percent of the target area is visible?

Over the last 30 years, there has been very little research examining LOS in areas with surface features. Since 1994, the US Army Training and Doctrine (TRADOC) Analysis Center-White Sands Missile Range (TRAC-WSMR) and the Topographic Engineering Center (TEC) have worked together to improve LOS representation for high resolution combat simulations. Unfortunately, this research was limited to areas void of significant surface features (Fort Irwin and Twentynine Palms, CA; Yakima Training Center, WA; and Yuma Proving Grounds, AZ).

Currently, LOS in vegetated areas is generally played using one of the following methods:

- The surface feature completely blocks LOS. With this methodology, surface features are simulated as a solid object. Units can move within the features, but there is no visibility into the feature, out of the feature, or within the feature.
- The surface feature completely blocks LOS with one exception. The user inputs the distance sensors can see into and out of the surface feature. This methodology allows units to deploy just inside a tree line while maintaining LOS to the battlefield. Although based on operational experience and common sense (no one would deliberately take up a position in which the LOS to the region under surveillance does not exist), there is no quantitative basis for this "see-through" distance, which gives units perfect visibility until the "see-through" value is exceeded. From then on, the visibility is governed by the characteristics of the terrain and surface features at the end of the "see-through" distance. If obstructing surface features are present, the visibility goes to zero.
- A probability of LOS is defined for a unit of distance (usually 25 meters) into an area with surface features. For example, if the user input is 0.9 and a sensor is trying to see 75 meters into trees, the probability of LOS is 0.729 (0.9 • 0.9 • 0.9). However, the input probability has no quantitative basis.
- A virtual simulator draws all the features between the sensor and the target one at a time in order to play their effects. This can be a time consuming process. Typically, the individual trees are stylized fonts (i.e., they are either all the same tree or there are a small number of different trees) and the number of trees that can be represented in a small area is constrained by the polygon limits of the simulator. The shortfall of this method was emphasized in a 1997 National Imagery and Mapping Agency (NIMA) study examining the requirements for high resolution modeling in which the soldiers who evaluated the database felt the representation of vegetation was not realistic in the NIMA database.

The above examples illustrate the lack of quantitative data to support LOS calculations in models of high resolution dismounted combat in a vegetative environment. A set of quantitative LOS data in areas of high feature density would help modelers portray combat in a more realistic manner. Recent advances in weapon systems, combat simulators, and the evolving mission requirements of the modern Army (i.e., stability and support operations, hostage rescue operations, peacekeeping operations, and low intensity conflict) require a more precise understanding of the impact of vegetation on LOS prediction. TRAC-WSMR and TEC recognized this problem and developed this study to:

- Identify a wide variety of vegetation types with associated climate zones.
- Collect data within each area to determine the percent of target visible when the LOS existed at a given range.
- Provide functions, based on the analysis of the collected data, which will enable the calculation of the percent of target visible using the range of the LOS and the terrain classification.

This report documents these efforts, draws conclusions, and makes recommendations to the modeling and simulation (M&S) community as to the selection of a standard algorithm to depict LOS in varied vegetation densities and how to improve play of surface features in combat models.

Purpose

This research provides a better understanding of LOS in vegetated areas through a set of graphs showing the portion of a target visible in different vegetation types as a function of range. Also provided are tables containing parameters used in equations generating the graphs. All of the graphs and equation parameters are based on empirical data.

Scope

The scope of this research was limited to collecting visibility data between dismounted infantry units. It is unlikely two units in a vegetated area will encounter each other at random. A more common scenario is an attacking unit encountering a defensive position. Therefore, this research focused on the LOS between a unit in a tactically sound defensive position and a unit in attack.

Limitations

Several vegetation types were excluded from this study. These included desert, arctic tundra, and areas inaccessible to the data collectors.

Assumptions

The field collection sites were representative of the vegetation in each study area.

The field-collected data can be extrapolated to areas with similar vegetation types, climate, soil types, latitude, and elevation (in order of importance).

Within a given vegetative zone, it was assumed types and densities of vegetation growing in flat areas are equivalent to vegetation growing on rolling terrain. Therefore, the field collection effort took place in areas where the change in ground elevation was negligible.

Difference Between LOS and Detection

Briefly, LOS is a geometry problem and detection is a physics and physiology problem using LOS and target presented area (the measures collected here) as factors. The current detection model is discussed at length in appendix A. However, in order to gain insight into the details involved in calculating probability of detection, some of the inputs provided by the combat simulation are listed below:

- Target contrast (the ratio of target brightness and background brightness)
- Visible light
- Sky over ground (SOG) ratio (contrast between the sky and the ground)
- Type of sensor (naked eyes, binoculars, night vision devices)
- Atmospheric attenuation effects
- Minimum resolvable contrast
- Whether or not the target is stationary or moving

Figures 1 and 2 illustrate the difference between LOS and detection. Figure 1 depicts three moths on a tree that are fully visible but very difficult to detect. By changing the contrast of the tree (see figure 2), the moths become much easier to detect.

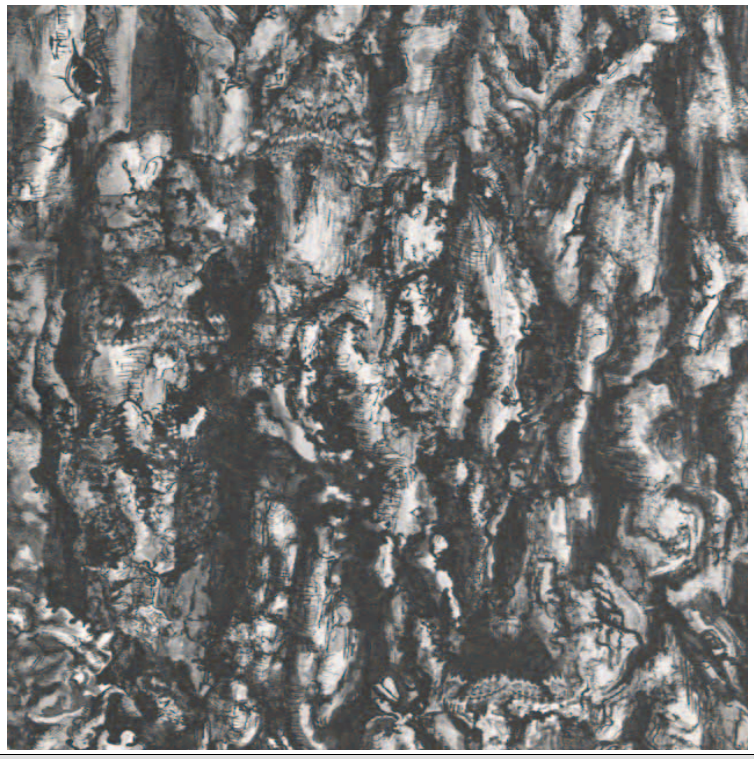

Figure 1. Moths on Tree Bark – Fully Visible, Difficult to Detect

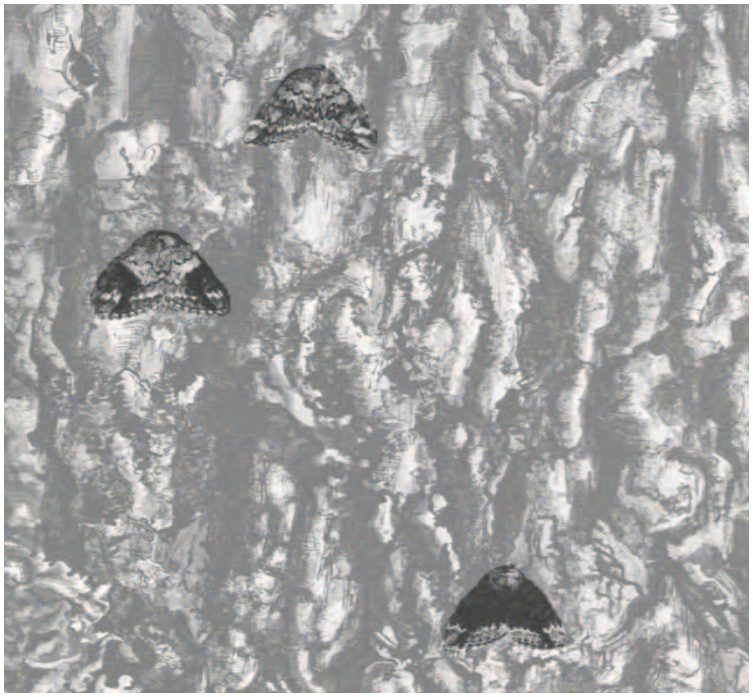

Figure 2. Moths on Tree Bark – Fully Visible, Easy to Detect

Methodology

Introduction

There are four steps to the methodology for this study: (1) the selection of data collection locations (the general geographical area), (2) the selection of site (the defensive positions where data were collected), (3) determination of the tactical considerations of data collection, and (4) determination of how the data would actually be collected.

Geographic Selection for Data Collection

Initially, the locations for data collection were to cover all of the climates in the continental US (CONUS). An analysis of vegetation types located within each climate zone indicated that vegetation varied greatly within each zone. Vegetative biomes, which are related to climate, provided a better method to delineate vegetation types. To provide even better detail about vegetation types, biomes have been divided into sub-biomes. Figure 3 shows a vegetative sub-biome map for the entire world.

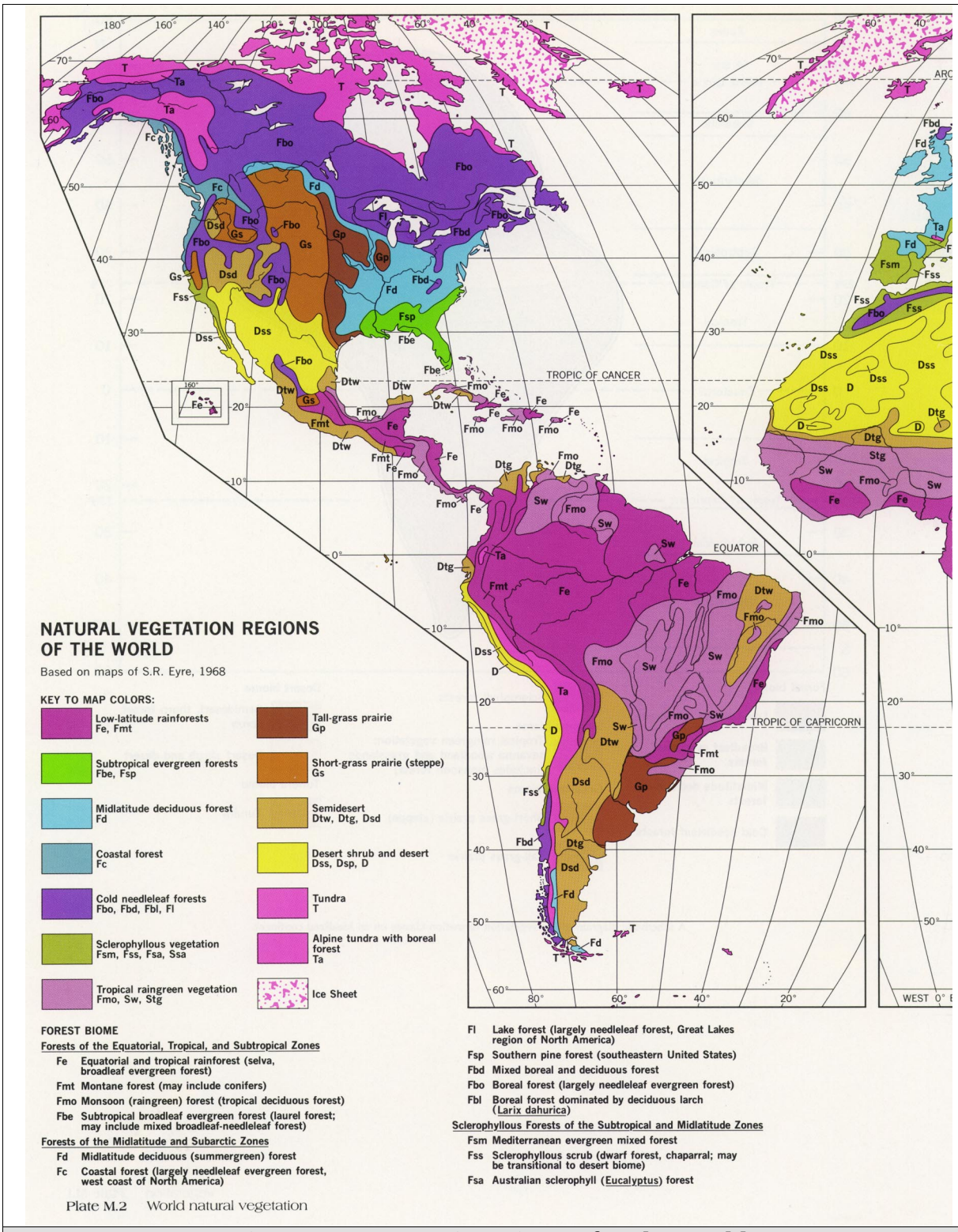

Figure 3a. Vegetation Biomes for the World

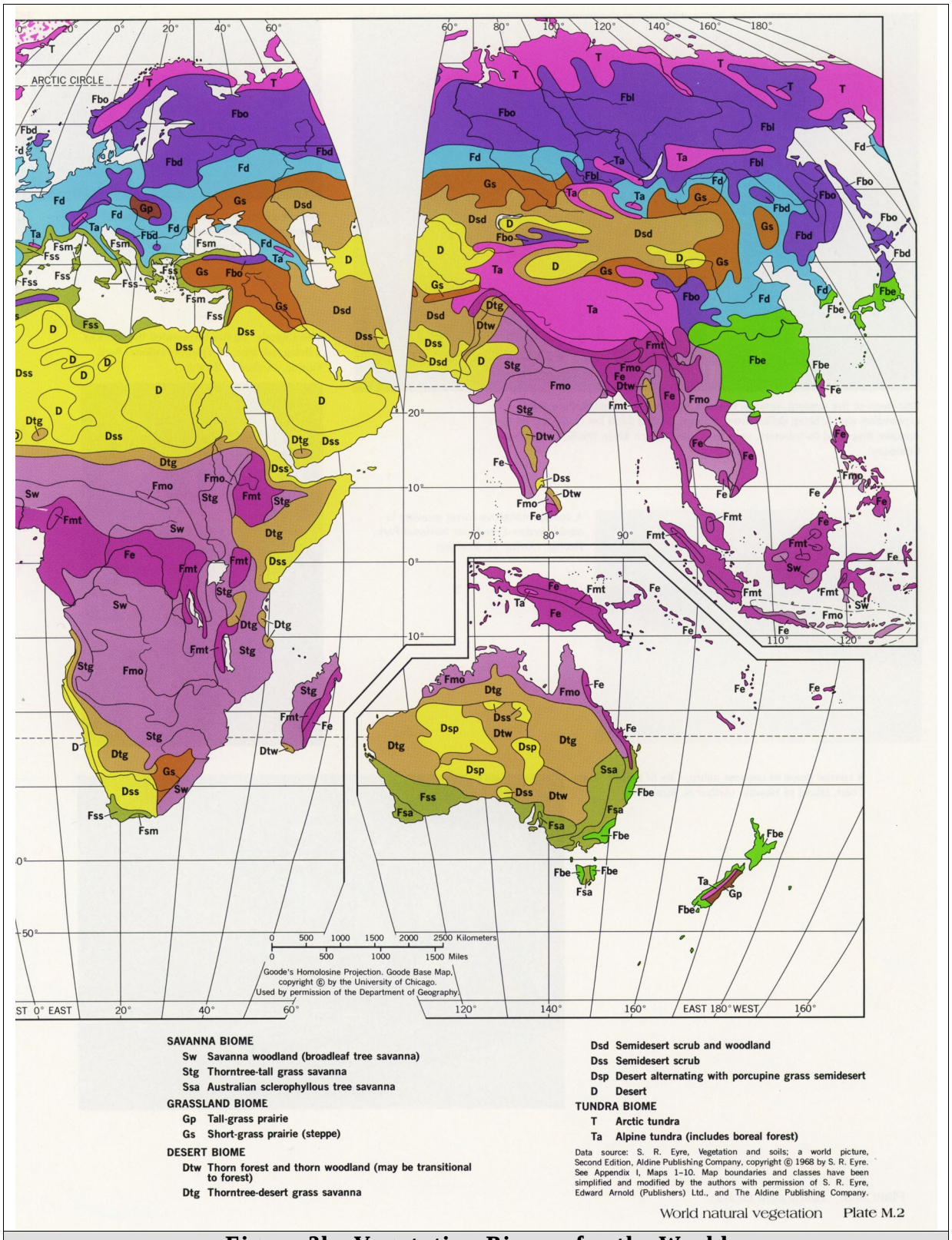

Figure 3b. Vegetation Biomes for the World

Fifteen geographic areas representing 13 sub-biomes were visited during the field data collection. Table 1 depicts the locations along with their sub-biome and climate definitions (if differentiated). Table 1 also offers a generalized or descriptive classification of the vegetation found in each of the sub-biome locations. Appendix B provides a detailed methodology about the selection of data collection locations (the general geographic area). It also provides detailed information about all of the data collection sites (the specific point on the ground from where data were collected) including data on canopy closure and undergrowth. Appendix C provides a general description of world climates with a link to each field collection location. Appendix D provides a description of the vegetation sub-biomes represented within the study.

Approximately two-thirds of the world's natural vegetation cover and all the major regional contingency (MRC) areas are represented in the regions selected for field collection. The remaining global sub-biomes were not evaluated because they fell into one of the following categories. First, several climates were void or nearly void of vegetation. These include several desert sub-biomes and several arctic sub-biomes. Second, small, unique areas located where the US Army is unlikely to deploy soldiers were excluded. These include the Great Lakes area and northern Siberia. Lastly, other sub-biomes that might be of future importance were eliminated due to prohibitive cost or restricted access.

The probable MRC locations were also used to select data collection locations. The Great Smoky Mountains National Park (referred to as Smoky Mountains throughout this report) and Willow Grove Naval Air Station (NAS) were selected because they are analogs to Korea. Natchaug State Forest (SF) and Fort Drum were selected because they are analogs to Bosnia. A detailed analysis describing how these analogs were selected can be found in appendix B.

Table 1. Vegetative Sub-Biome/Climate and Vegetation Definitions of Data Collection Locations		
Location	**Sub-Biome/Climate Type**	**Vegetation Description**
Panama - Gamboa	Monsoon Tropical/Tropical Wet-and-Dry	Monsoon (rainforest) - tropical deciduous forest
Panama - Fort Sherman	Tropical Rainforest/Tropic Wet	Monsoon (rainforest) - tropical deciduous forest
Panama - El Valle	Montane Forest/Tropic Upland	Equatorial and Tropical Rainforest - selva, broadleaf evergreen forest
Eglin Air Force Base (AFB), FL	Subtropical Broadleaf Evergreen Forest/Humid Subtropical	Oak and Pine Forest with some tropical vegetation
Fort Hood, TX	Dry Steppe (tall grass)	Tall Grass Prairie
Fort Carson, CO	Dry Steppe (short grass)	Short Grass Prairie
Fort Hunter-Liggett, CA	Sclerophyllus vegetation/Mediterranean	Old Oak Forest
Fort Lewis, WA	Coastal Forest/Temperate Oceanic (Marine)	Coastal Forest - largely needleleaf evergreen forest
Fort Benning, GA	Southern Pine Forest/Temperate (warm summer)	Southern Pine and Oak Forest
Great Smoky Mountains National Park, NC and TN	Midlatitude Deciduous Forest/Temperate (warm summer)	Mixed Deciduous Forest
Willow Grove Naval Air Station (NAS), PA	Midlatitude Deciduous Forest/Temperate (warm summer)	Mixed Deciduous Forest
Natchaug State Forest (SF), CT	Midlatitude Deciduous Forest/Temperate (cool summer)	Mixed Deciduous Forest
Fort Drum, NY	Mixed Boreal and Deciduous Forest/Temperate (cool summer)	Mixed Deciduous and Pine Forest
Canada - Gagetown Training Area (New Brunswick)	Mixed Boreal and Deciduous Forest/Temperate (cool summer)	Mixed Deciduous and Pine Forest
Fort Greely, AK	Boreal and Taiga	Mixed Spruce, Birch and Aspen

Site Selection

Once a primary geographic location within a sub-biome was selected, a data collection team visited the location. Typically, this visit consisted of 1 day of reconnaissance and 4 days of data collection. The reconnaissance was used to select potential sites for data collection. The field team assessed the potential sites and selected several (usually four) sites best representing the geographic area using the following three criteria for site selection. First, because disturbed vegetation would result in unrealistic LOS curves, the data collection team looked for areas with a minimum of damage due to traffic or natural disaster. Second, consistent with the third assumption of the study, only gently sloping and flat areas were considered for data collection. While it was not always possible to eliminate elevation changes in the site selection process, it was essential to find areas as level as possible in order to examine only the effects of vegetation. Lastly, the data collection team looked for vegetation typical of the locations in order to collect data representing a good cross section of the geographic area. After data collection and subsequent analysis of the four representative sites, the parameters of a "best" or recommended site were selected for model input.

Tactical Considerations for Data Collection

Once sites were selected for data collection, a location on the ground representing a tactical defensive position for a dismounted soldier was identified. The sites were selected based on terrain, tactics, mission, and enemy. The exact position within a vegetated area was selected by a career infantryman (noncommissioned officer) to represent a sound tactical position for a prone soldier.

A tactical field of view (FOV) was selected for data collection so the data would represent a potential real-world situation. Data were collected along azimuths (measured from grid north) within the tactical FOV. In every location visited, there were situations where the vegetation (either the undergrowth or a tree trunk) would block LOS at close range. At the other extreme, there were phenomena nicknamed "keyholes." These keyholes allowed visibility at long ranges where surrounding LOS was much shorter. For example, at one Fort Lewis location, the LOS along most azimuths was less than 50 meters. However, along one azimuth the LOS was over 90 meters. Rather than biasing the data collection by selecting or not selecting these extreme conditions, a stratified sampling technique was used. Magnetic north was determined (using a military compass) and then the offset to grid north was found using map information. A uniform spacing between azimuths, usually 10 degrees, was selected. This procedure allowed for the potential inclusion of these extreme conditions but data analysis treated them as outliers.

Data Collection Methodology

Introduction. The data collection methodology can be separated into four sections: the points of view from which data were collected, how the target silhouette was

designed for data collection, how the tactical field of view and azimuths were determined, and why humans were used to collect data.

Data Collection Points of View. Data were collected from both the defender and the attacker points of view. From both points of view, data were collected for both a prone (0.25 meter above the ground) and a crouching (1.5 meters above the ground) observer posture. For each posture (prone and crouching), data were collected to determine how much of the kneeling target was visible. The kneeling target was divided in such a manner that the visible portion of the prone target could also be calculated from the kneeling target (discussed next). This resulted in eight different defender/attacker viewpoint combinations.

The Target

The kneeling target silhouette (see figure 4) was 1.015 meters tall and divided into three nearly rectangular sections representing the head, torso (neck to waist), and the legs (waist to knees). The three sections of the silhouettes were painted with different ordered combinations of the three colors (e.g., pink head, orange torso, and yellow legs) and the silhouette with the highest contrast was selected for use. The torso and the legs were separated so the bottom section represented the height of a prone soldier. This allowed for data to be collected for a kneeling and prone soldier simultaneously. The rectangular areas made it easier for the data collection team to estimate the percentage of an area not obscured by vegetation.

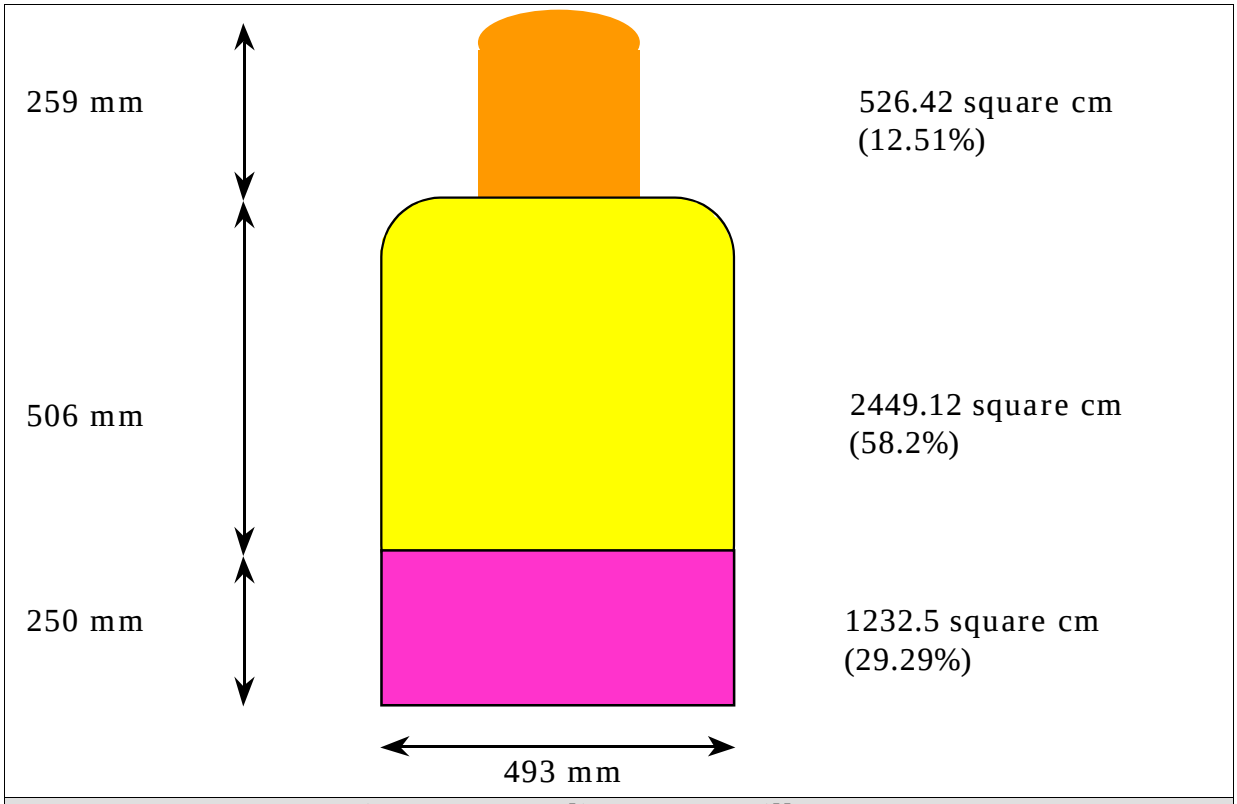

Figure 4. Kneeling Target Silhouette

cm - centimeter *mm - millimeter*

The local vegetation, sun angle, and the preference of the data collectors determined the silhouette used along each azimuth. The target silhouette was placed on the ground, facing the data collectors, at several locations along the azimuth. The silhouette was placed on the ground at locations where changes in vegetation affected LOS. For example, if a tree was in line with an azimuth, the target was placed in front of the tree and behind the tree. This allowed for the exact point where major changes in LOS were to be recorded. Figure 5 shows a sample azimuth and the location where the target would be placed.

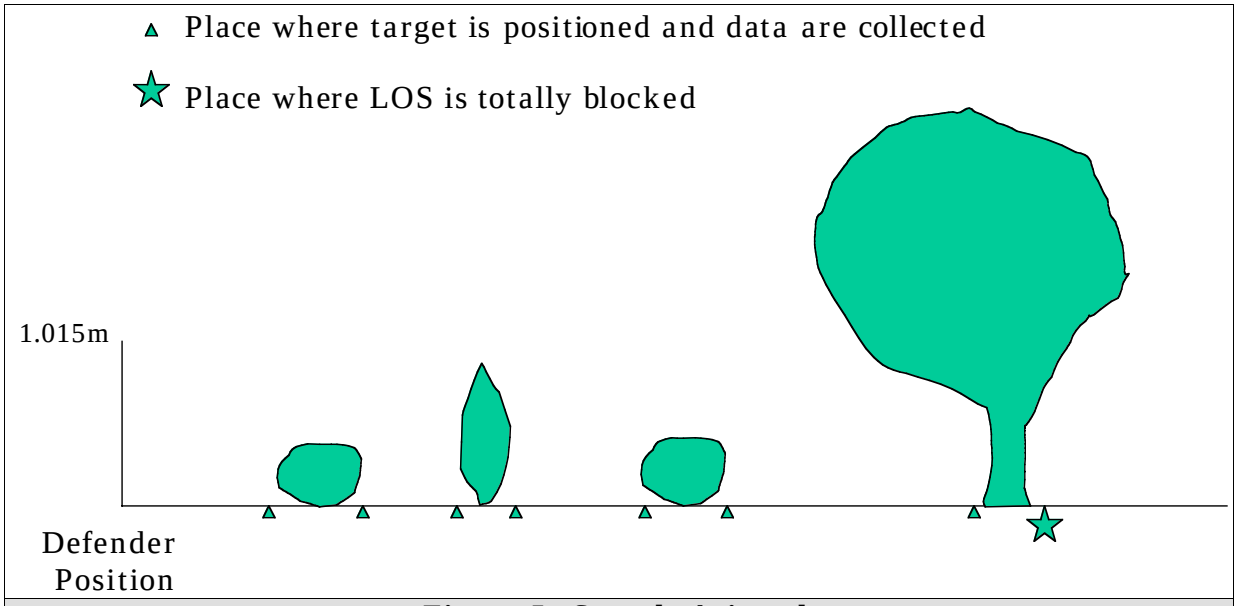

Figure 5. Sample Azimuth

A data collection problem occurred when vegetation was the same color as the target silhouette and, therefore, difficult to discriminate between the silhouette and the surrounding vegetation. This problem was overcome by moving the target up and down and relying on the observer to determine what was the target and what was vegetation.

Tactical Fields of View and Azimuth Selection

Data were collected at each site in the tactical field of view by moving the kneeling target silhouette away from the defensive position along several azimuths. Usually, these azimuths were 10 degrees apart. The percent of target visible at different distances was recorded. The silhouette was moved away from the defensive position until either the terrain began to interfere with the collection process (this rarely happened) or until the target was totally concealed by vegetation. A total survey station (TSS) was used to keep the target precisely on line to determine the exact distance between the defender location and the silhouette.

Survey flags were used to locate every point along each azimuth where data were collected. After the data were collected from the defender position, the silhouette was placed at the defender location and data were collected from the attacker point of view.

Human Data Collectors

Most of the data collected for this study were obtained using the unaided human eye. However, when ranges exceeded about 100 meters, the data collectors had the option to use binoculars. An example of a data sheet can be seen in figure 6.

Several methods were explored to analytically determine the percent of the target silhouette seen through vegetation. These included digital cameras, infrared photography, standard photography with telephoto lens, and human data collectors.

Two problems with digital cameras could not be overcome. First, currently available digital cameras did not produce enough resolution. In particular, at 140 meters, the target silhouette was 3 pixels wide and 5 pixels high. This number of pixels restricted the amount of target observed to a small range of values limiting meaningful analysis. Secondly, the digital camera blended colors. For example, if the target was orange and the background vegetation was green, pixels along the edge of the target would appear as different shades of brown. A digital camera could not separate colors on the target from the colors existing in the collection area, regardless of how brightly the target was painted or how much the target colors contrasted with the surrounding vegetation of any collection site.

Infrared (IR) photography was eliminated primarily because of cost and lack of a subject matter expert in IR photography. A means to produce a mobile, hand-held target silhouette, which could be heated in a field environment would have been time consuming, costly, and have unknown reliability. Another unknown was the cost of the IR film and its processing. The field collection effort was expensive and the data collectors needed to be sure all of the data were complete before leaving the area. If there was a problem with the film processing, all data would have been lost. Yet another problem with IR photography was the effects of the solar radiation on the vegetation. It was not known how the heat produced in vegetation from absorbing sunlight for several hours and the heat of the person holding the target could be separated from the artificially heated target silhouette.

Standard photography with a telephoto lens was also evaluated as a data collection technique. First, there was a problem with the enormous number of photographs required. The target was placed on the ground and evaluated over 5,000 times during this study. This would have required 5,000 photographs and each photograph would have had to be electronically scanned and analyzed. During the development of the data collection methodology, a second problem was discovered. Although the silhouette was brightly painted, contrasting colors assumed to exist only on the silhouette, were found in nature. These similar colors would have been counted as "visible" during the evaluation phase of these photographs.

OP: 8C	Azimuth: Nbr 6	Azimuth: Deg 280°	Date: 8-4	Time: 1230	Data Collector: LF

Check One: ☒ Defender looking at Attacker ☐ Attacker looking at Defender

OP Height: Crouching (1.5 meters)					OP Height: Prone (.21 meters)			
	Percent Visible				Percent Visible			
Distance (Meters)	Head	Body	Legs	Comments	Head	Body	Legs	Comments
1 13.6	80	75	85		95	90	65	
2 20.6	40	70	50		50	80	10	
3 27.2	0	17	5	Lg Tree	3	15	2	
4 28.2	0	5	0		1	8	0	
5 36.1	0	0	0		0	0	0	
6								
7								
8								
9								
10								
11								
12								
13								

Figure 6. Sample Data Collection Sheet

It was eventually decided the best readily available optical device was the human eye. Although the human eye is among the most discriminating sensors, it is the brain producing the images we perceive. The brain has a lifetime of biases built into it as evidenced by the fact that different people "see" things different ways.

A methodology was developed to measure and minimize other sources of observer bias and is discussed next.

Before the field collection began, all participants were tested to measure bias and accuracy of the estimations they would have to make. A test consisting of random black and white patterns was presented to the data collectors and they estimated the percentage of the pattern that was black. The average deviation between each observer's estimate and the actual values was between 5.4 and 9.7 percentage points. None of the data collectors were biased towards over-estimating or under-estimating the percentages. They were then retested with one additional set of information. Random patterns containing exactly 10, 20, 25, 30, 33.33, 40, and 50 percent black coverage were produced. The data collectors were asked to compare the unknown patterns to the known patterns. This reduced the average errors to between 2.7 and 5.7 percentage points. These random pattern plots were available to the field personnel during the collection process. A further analysis of the test results indicated these errors could be reduced to between 1.7 and 4.8 percentage points by using a second observer. Additional observers would have increased the accuracy of the estimates, but this improvement in accuracy would not justify the increased resources required.

Analysis

Introduction

The analysis begins by examining a sample of the raw data, and identifying the three functions to be used in attempting a curve fit of that data. As data were collected at more than 60 sites, the method of selecting the most representative site is discussed next. This is followed by a description of the method of selecting the best parameters for each of the selected functions. Ancillary to this, the correlations between the decay parameter of the exponential functions and various descriptors of the undergrowth are presented. Some comments on unexpected results in the Panama data, and insights of the data collection observers, conclude the analysis.

Appendix E provides a complete record of the raw data, further explanation of the three curve fits, and coefficients for the curve fits for each of the collection sites.

Raw Data

Figure 7 provides a sample of the raw data collected along each azimuth, the quartiles (the middle 50 percent of the data), and the median of the data. The analysis focuses on the median curve because it represents the most realistic representation of visibility in the field. The mean of the data was not used because outliers could skew the entire curve. Data were collected to represent looking at a kneeling target and a prone target. The kneeling target was 0.4206 square meter and the prone target was 0.12325 square meter. The y-axis of these plots is based on whether the target viewed was kneeling or prone. For example, if 100 percent of a kneeling target was seen, 0.4206 square meter was visible and if 100 percent of the prone target was seen, 0.12325 square meter was visible. The presented size of the target (number of square meters visible) is used in the detection equations.

The defensive positions selected for the field survey were selected as typical prone defensive positions. Data were collected between a crouching defender and a prone and kneeling attacker for comparison purposes only. This data is provided in the appendix but is not discussed in the analysis.

Curve Fits

The fits to three different curves were selected in this analysis to provide different approaches to represent the effects of vegetation on LOS. The three functions fitted to the raw data are an exponential decay curve, a field exponential decay curve, and a pole-zero fit.

The exponential function takes the form:

$$\mathbf{f} = \mathbf{e}^{-\frac{\mathbf{R}}{\mathbf{b}}},$$

where **f** is the visible fraction of the target, **R** is the range of LOS, and **b** represents the slope of the decay. A smaller value for **b** implies a steeper decay curve.

The field exponential equation takes the form:

$$\mathbf{f} = \mathbf{e}^{-\frac{\mathbf{R}-\mathbf{a}}{\mathbf{b}}},$$

where **a** represents the range at which the curve begins the decay. The value of **a** delays the decay until a certain range is exceeded. This second parameter in the exponential decay allows more flexibility in fitting the data.

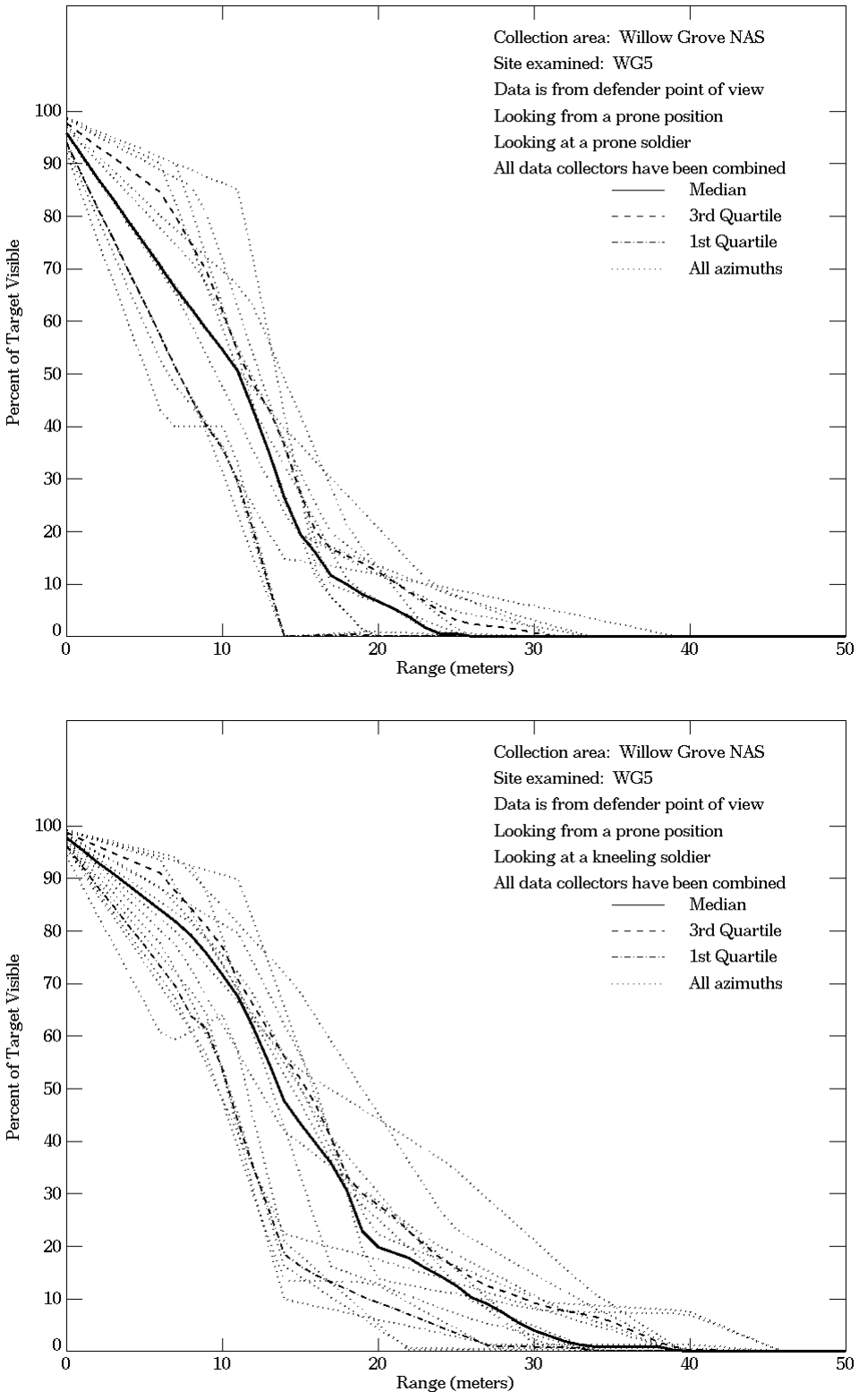

Figure 7. A Sample of the Plots Developed From the Field Collection

The pole-zero was included in the analysis because it was usually the best fit of the three curves. This equation is a version of the frequency response equation from electronic circuit analysis. It takes on the form:

$$\mathbf{f} = \alpha \left[\frac{\delta^{\gamma} + \mathbf{R}^{\gamma}}{\varepsilon^{\gamma} + \mathbf{R}^{\gamma}} \right],$$

where α is a scaling factor and δ represent the part of the curve where the decay is so gradual that is it insignificant. The ε parameter represents the range where the curve begins to turn downward. In other words, this is the distance where the target begins a significant degradation. The γ parameter, the exponent in the equation, is a measure of how quickly the signal degrades as range becomes larger than ε.

Representative Data Sites

Data were collected at several (between one and six) sites at each location. The parameters to all three curve fits and for each site are provided in appendix E. The sites at each location were analyzed and a site representative of a biome was selected by examining three different factors. First, the undergrowth data collected at each location was examined. The sites were subjectively ranked based on the most representative undergrowth type, median undergrowth height, and maximum undergrowth height. Second, the raw data curves, along with the field notes, were examined and the sites were subjectively ranked based on how well the site represented the location. Some of the sites were eliminated by this analysis because they were classified as outliers. Lastly, the data parameters for all three curves were examined and ranked based on the sum of squares (a measure of error between the raw and the fitted data). The best representative site at each location (table 2) was selected on the basis of these three approaches.

Table 2. Best Representative Sites for Each Location

Location	Site
Panama – Gamboa	gam2
Panama – Fort Sherman	mck1
Panama – El Valle	elv1
Eglin AFB	egl_B2
Fort Hood	hood1
Fort Carson	car28
Fort Hunter-Liggett	hl10
Fort Lewis	lew8
Fort Benning	ben_T4
Smoky Mountains	TN2
Willow Grove NAS	WG2
Natchaug SF	Nat4
Fort Drum	7G
Canada – Gagetown Training Area	Gage31
Fort Greely	G02

Parameter Selection

Tables 3 through 6 depict the exponential fits for four combinations of point of view, attacker posture, and defender posture. Tables 7 through 10 depict the field exponential fits and tables 11 through 14 depict the data fits for the pole-zero fits.

The sum of square error (SSE) for each fit is provided in the tables as a measure of error in the curve fit. Typically, as expected, the more parameters in a function, the smaller the SSE (and the better the fit). In every case, the field exponential fits (with two parameters) have smaller SSE than the exponential fits (with one parameter). The pole-zero fits (with four parameters) have a smaller SSE than all of the exponential fits and for about three-quarters of the field exponential fits. When the pole-zero SSE was higher than the field exponential SSE, the differences are either very close (i.e., 0.107 versus 0.113) or both of the SSEs were very small (i.e., 0.022 versus 0.038).

The **b** parameters in tables 3 through 6 describes how quickly the exponential curve decays. A small value (i.e., Panama and Eglin AFB) reflect a rapid decay and a larger value (i.e., Fort Carson and Fort Hunter-Liggett) depict a more gradual decay. The **a** and **b** parameters in tables 7 through 10 depict the beginning of the decay and the slope of the decay. For example, the fitted curve for Eglin AFB (from table 9) begins decaying at 1.598 meters and a decay factor of 3.73 indicates that the decay occurs very quickly. On the other hand, the decay for the Fort Hunter-Liggett curve fit begins at 15.427 meters and the decay factor of 16.385 indicates that the decay occurs very slowly.

Five of the sites from table 2 have been selected to depict how the different parameters are reflected in the graphs. Parameters for a prone defender looking at a kneeling attacker for Panama (gam2), Fort Greely (G02), Fort Drum (7G), Fort Carson (car28), and Fort Hunter-Liggett (hl10) were selected to provide a variety of biomes and to span the different values of the coefficients. Figures 8 through 11 depict the field measured data, the exponential fits, the field exponential fits, and the pole-zero fits, respectively. Data from tables 4, 8, and 12 were used to generate these figures.

Table 3. Data Fits for the Exponential Decay From a Prone Defender to a Prone Attacker

Collection Area	Site	SSE	Coeff b
Panama	gam2	0.199	7.163
Panama	mck1	0.067	8.492
Panama	elv1	0.273	9.311
Eglin AFB	egl_B2	0.123	5.233
Fort Hood	hood1	1.087	16.706
Fort Carson	car28	1.670	27.439
Fort Hunter-Liggett	hl10	0.975	33.978
Fort Lewis	lew8	0.194	9.691
Fort Benning	ben_T4	0.199	9.278
Smoky Mountains	TN2	0.992	12.020
Willow Grove NAS	WG2	0.057	4.673
Natchaug SF	Nat4	0.108	8.235
Fort Drum	7G	0.259	11.286
Canada – Gagetown	Gage31	0.226	6.085
Fort Greely	G02	0.201	7.796

Coeff - coefficient *SSE - sum of squares error*

Table 4. Data Fits for the Exponential Decay From a Prone Defender to a Kneeling Attacker

Collection Area	Site	SSE	Coeff b
Panama	gam2	0.224	8.314
Panama	mck1	0.181	14.836
Panama	elv1	0.262	11.032
Eglin AFB	egl_B2	0.174	9.189
Fort Hood	hood1	1.076	20.884
Fort Carson	car28	1.963	35.167
Fort Hunter-Liggett	hl10	1.140	40.437
Fort Lewis	lew8	0.317	2.480
Fort Benning	ben_T4	0.157	15.760
Smoky Mountains	TN2	0.753	16.379
Willow Grove NAS	WG2	0.072	8.947
Natchaug SF	Nat4	0.117	17.602
Fort Drum	7G	0.363	19.292
Canada – Gagetown	Gage31	0.195	9.814
Fort Greely	G02	0.081	14.670

Table 5. Data Fits for the Exponential Decay From a Prone Attacker to a Prone Defender			
Collection Area	**Site**	**SSE**	**Coeff b**
Panama	gam2	0.216	7.792
Panama	mck1	0.146	7.817
Panama	elv1	0.298	10.461
Eglin AFB	egl_B2	0.164	5.212
Fort Hood	hood1	0.566	16.816
Fort Carson	car28	1.869	30.661
Fort Hunter-Liggett	hl10	0.936	33.468
Fort Lewis	lew8	0.210	9.764
Fort Benning	ben_T4	0.252	10.583
Smoky Mountains	TN2	0.110	9.860
Willow Grove NAS	WG2	0.062	5.764
Natchaug SF	Nat4	0.173	6.190
Fort Drum	7G	0.166	8.089
Canada – Gagetown	Gage31	0.165	6.000
Fort Greely	G02	0.157	7.746

Table 6. Data Fits for the Exponential Decay From a Crouching Attacker to a Prone Defender			
Collection Area	**Site**	**SSE**	**Coeff b**
Panama	gam2	0.463	12.010
Panama	mck1	0.874	17.790
Panama	elv1	0.478	13.476
Eglin AFB	egl_B2	0.547	11.228
Fort Hood	hood1	0.768	20.871
Fort Carson	car28	2.480	29.048
Fort Hunter-Liggett	hl10	0.743	46.066
Fort Lewis	lew8	0.523	14.496
Fort Benning	ben_T4	0.753	19.109
Smoky Mountains	TN2	0.128	11.086
Willow Grove NAS	WG2	0.546	15.690
Natchaug SF	Nat4	0.051	9.913
Fort Drum	7G	0.074	9.702
Canada – Gagetown	Gage31	0.029	7.586
Fort Greely	G02	0.427	15.992

Table 7. Data Fits for the Field Exponential Decay From a Prone Defender to a Prone Attacker				
Collection Area	**Site**	**SSE**	**Coeff a**	**Coeff b**
Panama	gam2	0.095	2.347	5.008
Panama	mck1	0.021	1.446	7.084
Panama	elv1	0.080	3.378	6.127
Eglin AFB	egl_B2	0.053	1.496	3.843
Fort Hood	hood1	0.176	10.415	6.792
Fort Carson	car28	0.128	14.706	12.808
Fort Hunter-Liggett	hl10	0.498	9.597	25.161
Fort Lewis	lew8	0.056	2.632	7.184
Fort Benning	ben_T4	0.107	2.338	7.120
Smoky Mountains	TN2	0.075	7.732	4.008
Willow Grove NAS	WG2	0.025	0.766	3.935
Natchaug SF	Nat4	0.041	1.653	6.611
Fort Drum	7G	0.124	2.732	8.748
Canada – Gagetown	Gage31	0.086	2.470	3.809
Fort Greely	G02	0.091	2.399	5.582

Table 8. Data Fits for the Field Exponential Decay From a Prone Defender to a Kneeling Attacker				
Collection Area	**Site**	**SSE**	**Coeff a**	**Coeff b**
Panama	gam2	0.094	2.535	5.945
Panama	mck1	0.080	2.655	12.320
Panama	elv1	0.073	3.421	7.778
Eglin AFB	egl_B2	0.037	2.592	6.681
Fort Hood	hood1	0.143	11.288	9.921
Fort Carson	car28	0.468	16.463	19.288
Fort Hunter-Liggett	hl10	0.567	11.580	29.733
Fort Lewis	lew8	0.133	3.551	9.170
Fort Benning	ben_T4	0.090	2.359	13.531
Smoky Mountains	TN2	0.075	7.623	8.329
Willow Grove NAS	WG2	0.022	1.513	7.478
Natchaug SF	Nat4	0.053	2.379	15.323
Fort Drum	7G	0.119	5.402	13.948
Canada – Gagetown	Gage31	0.057	2.657	7.247
Fort Greely	G02	0.041	1.604	13.130

Table 9. Data Fits for the Field Exponential Decay From a Prone Attacker to a Prone Defender				
Collection Area	**Site**	**SSE**	**Coeff a**	**Coeff b**
Panama	gam2	0.102	2.421	5.567
Panama	mck1	0.065	1.717	6.201
Panama	elv1	0.099	3.532	7.154
Eglin AFB	egl_B2	0.075	1.598	3.730
Fort Hood	hood1	0.224	6.323	10.933
Fort Carson	car28	0.635	15.427	16.385
Fort Hunter-Liggett	hl10	0.474	9.491	24.748
Fort Lewis	lew8	0.054	2.740	7.141
Fort Benning	ben_T4	0.119	2.677	8.092
Smoky Mountains	TN2	0.048	1.685	8.258
Willow Grove NAS	WG2	0.029	0.834	4.970
Natchaug SF	Nat4	0.086	1.643	4.672
Fort Drum	7G	0.078	2.274	5.988
Canada – Gagetown	Gage31	0.081	1.619	4.503
Fort Greely	G02	0.078	1.688	6.172

Table 10. Data Fits for the Field Exponential Decay From a Crouching Attacker to a Prone Defender				
Collection Area	**Site**	**SSE**	**Coeff a**	**Coeff b**
Panama	gam2	0.097	5.397	6.886
Panama	mck1	0.159	9.427	8.770
Panama	elv1	0.122	5.366	8.405
Eglin AFB	egl_B2	0.050	5.591	5.706
Fort Hood	hood1	0.247	8.348	13.035
Fort Carson	car28	0.523	19.439	10.822
Fort Hunter-Liggett	hl10	0.310	10.493	36.141
Fort Lewis	lew8	0.153	5.608	9.233
Fort Benning	ben_T4	0.350	7.289	12.442
Smoky Mountains	TN2	0.050	2.304	8.886
Willow Grove NAS	WG2	0.097	6.422	9.538
Natchaug SF	Nat4	0.020	1.313	8.633
Fort Drum	7G	0.028	1.523	8.197
Canada – Gagetown	Gage31	0.013	0.696	6.885
Fort Greely	G02	0.169	4.725	11.564

Table 11. Data Fits for the Pole-Zero Decay From a Prone Defender to a Prone Attacker						
Collection Area	**Site**	**SSE**	**Coeff α**	**Coeff δ**	**Coeff ε**	**Coeff γ**
Panama	gam2	0.080	1.60e-13	1.89e+05	6.149	2.851
Panama	mck1	0.032	6.39e-14	3.88e+06	6.551	2.286
Panama	elv1	0.062	7.97e-14	2.14e+05	7.975	2.958
Eglin AFB	egl_B2	0.049	2.12e-13	1.78e+05	4.425	2.752
Fort Hood	hood1	0.094	1.38e-13	1.24e+04	15.481	4.430
Fort Carson	car28	0.087	5.58e-14	5.10e+04	24.404	3.992
Fort Hunter-Liggett	hl10	0.445	5.12e-14	1.50e+06	29.146	2.821
Fort Lewis	lew8	0.053	5.92e-14	6.86e+05	8.021	2.682
Fort Benning	ben_T4	0.113	6.26e-14	9.58e+05	7.682	2.591
Smoky Mountains	TN2	0.089	4.46e-04	4.76e+01	10.727	5.178
Willow Grove NAS	WG2	0.028	4.32e-14	1.23e+06	3.722	2.422
Natchaug SF	Nat4	0.033	2.31e-14	2.33e+06	6.531	2.456
Fort Drum	7G	0.117	7.64e-14	6.72e+05	9.495	2.705
Canada – Gagetown	Gage31	0.061	1.49e-13	5.37e+04	5.400	3.209
Fort Greely	G02	0.078	7.16e-14	3.12e-14	6.652	2.814

Table 12. Data Fits for the Pole-Zero Decay From a Prone Defender to a Kneeling Attacker						
Collection Area	**Site**	**SSE**	**Coeff α**	**Coeff δ**	**Coeff ε**	**Coeff γ**
Panama	gam2	0.072	5.63e-13	1.23e+05	7.124	2.891
Panama	mck1	0.124	7.94e-14	4.30e+06	11.706	2.354
Panama	elv1	0.067	4.60e-14	6.13e+05	9.236	2.766
Eglin AFB	egl_B2	0.030	7.91e-15	1.38e+06	7.538	2.680
Fort Hood	hood1	0.060	4.92e-14	4.85e+04	18.726	3.899
Fort Carson	car28	0.414	6.79e-14	1.84e+05	31.285	3.494
Fort Hunter-Liggett	hl10	0.486	6.56e-14	1.55e+06	34.653	2.835
Fort Lewis	lew8	0.123	4.53e-14	6.93e+05	10.569	2.770
Fort Benning	ben_T4	0.148	2.55e-14	1.34e+07	12.167	2.250
Smoky Mountains	TN2	0.075	2.83e-04	1.48e+02	13.713	3.435
Willow Grove NAS	WG2	0.038	5.97e-14	4.22e+06	6.905	2.286
Natchaug SF	Nat4	0.122	6.74e-14	1.46e+07	13.322	2.180
Fort Drum	7G	0.076	3.64e-14	1.96e+06	15.561	2.635
Canada – Gagetown	Gage31	0.048	2.93e-14	9.32e+05	8.047	2.672
Fort Greely	G02	0.105	1.11e-13	1.32e+07	10.977	2.130

Table 13. Data Fits for the Pole-Zero Decay From a Prone Attacker to a Prone Defender						
Collection Area	**Site**	**SSE**	**Coeff α**	**Coeff δ**	**Coeff ε**	**Coeff γ**
Panama	gam2	0.089	2.72e-14	4.00e+05	6.684	2.840
Panama	mck1	0.063	1.12e-13	5.73e+05	6.466	2.618
Panama	elv1	0.075	1.22e-13	2.15e+05	8.989	2.949
Eglin AFB	egl_B2	0.062	6.13e-14	1.30e+05	4.533	2.963
Fort Hood	hood1	0.160	3.26e-14	3.50e+05	14.642	3.081
Fort Carson	car28	0.398	1.83e-13	4.07e+04	28.778	4.043
Fort Hunter-Liggett	hl10	0.425	8.31e-14	1.30e+06	28.652	2.809
Fort Lewis	lew8	0.048	4.04e-14	6.51e+05	8.111	2.731
Fort Benning	ben_T4	0.107	8.48e-14	5.34e+05	8.939	2.737
Smoky Mountains	TN2	0.066	3.94e-14	3.40e+06	7.806	2.377
Willow Grove NAS	WG2	0.041	3.11e-14	2.54e+06	4.537	2.350
Natchaug SF	Nat4	0.078	8.53e-14	2.40e+05	5.298	2.807
Fort Drum	7G	0.075	6.68e-14	6.27e+05	6.743	2.652
Canada – Gagetown	Gage31	0.074	2.16e-13	1.67e+05	5.132	2.806
Fort Greely	G02	0.082	1.09e-13	6.28e+05	6.412	2.597

Table 14. Data Fits for the Pole-Zero Decay From a Crouching Attacker to a Prone Defender						
Collection Area	**Site**	**SSE**	**Coeff α**	**Coeff δ**	**Coeff ε**	**Coeff γ**
Panama	gam2	0.056	5.06e-14	1.04e+05	10.565	3.331
Panama	mck1	0.069	2.39e-14	5.54e+04	16.035	3.849
Panama	elv1	0.088	3.49e-14	2.26e+05	11.758	3.142
Eglin AFB	egl_B2	0.028	3.00e-14	4.71e+04	9.865	3.676
Fort Hood	hood1	0.188	2.85e-13	1.88e+05	18.214	3.126
Fort Carson	car28	0.280	6.34e-13	4.94e+03	28.172	5.437
Fort Hunter-Liggett	hl10	0.307	3.94e-14	6.81e+06	37.571	2.549
Fort Lewis	lew8	0.104	1.22e-14	2.94e+05	12.744	3.189
Fort Benning	ben_T4	0.260	1.27e-13	1.87e+05	17.048	3.193
Smoky Mountains	TN2	0.059	1.08e-13	2.06e+06	8.812	2.416
Willow Grove NAS	WG2	0.061	1.57e-13	1.47e+05	13.617	3.176
Natchaug SF	Nat4	0.047	4.26e-14	1.23e+07	7.418	2.150
Fort Drum	7G	0.033	3.13e-14	7.22e+06	7.438	2.255
Canada – Gagetown	Gage31	0.025	3.10e-14	2.10e+07	5.532	2.053
Fort Greely	G02	0.125	1.44e-13	3.66e+05	13.706	2.901

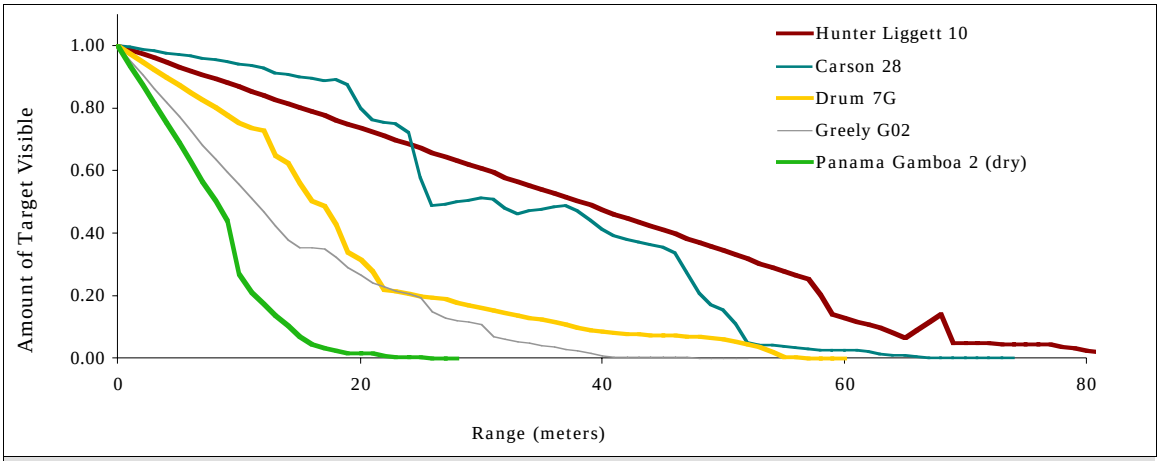

Figure 8. The Raw Data for Five Selected Sites Where a Prone Defender is Looking at a Kneeling Attacker

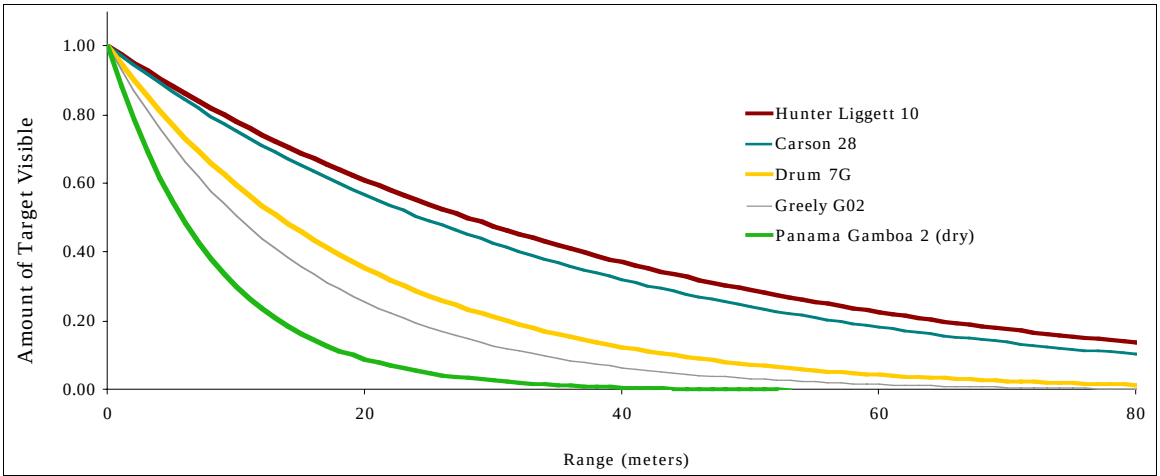

Figure 9. The Exponential Fits for Five Selected Sites Where a Prone Defender is Looking at a Kneeling Attacker

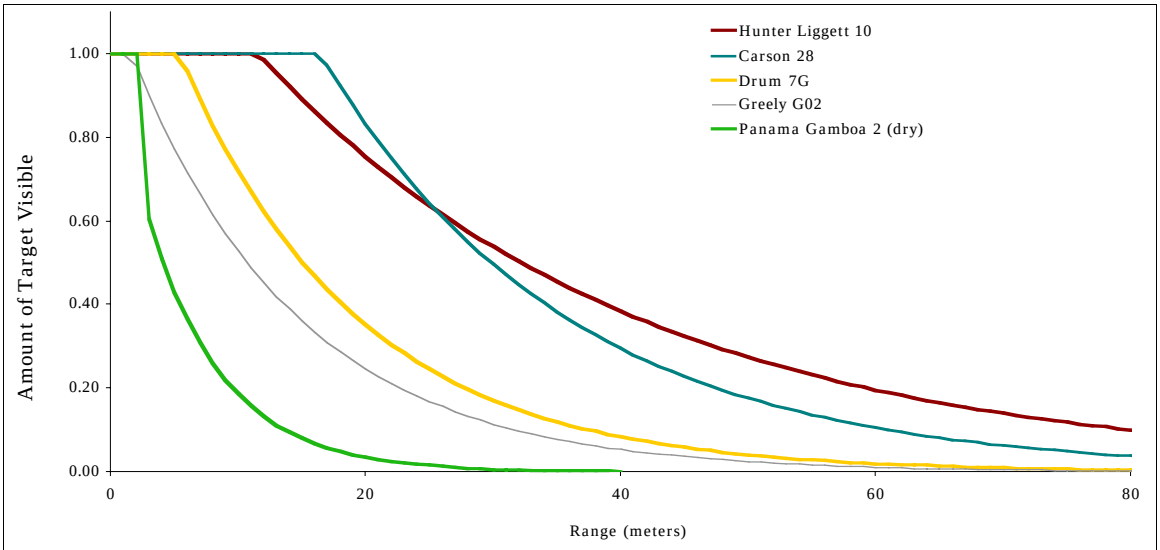

Figure 10. The Field Exponential Fits for Five Selected Sites Where a Prone Defender is Looking at a Kneeling Attacker

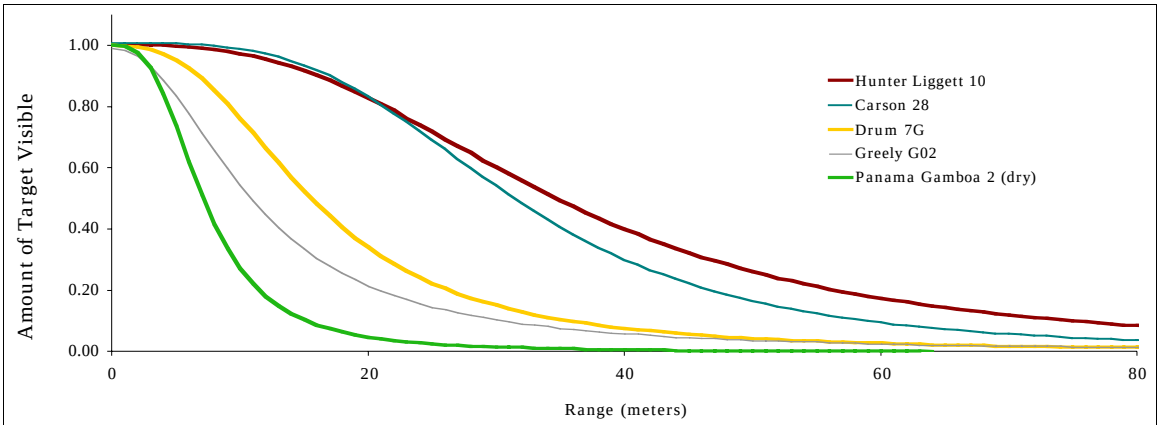

Figure 11. The Pole-Zero Fits for Five Selected Sites Where a Prone Defender is Looking at a Kneeling Attacker

Relationship of the Undergrowth to the LOS Parameters

It was expected that as a target moved farther from the observer, the target would eventually disappear behind a wall of trees. This was rarely the case. The major inhibitor of visibility for most places was the undergrowth, not the trees. Only three types of data were collected to measure the undergrowth of the collection sites. This data included a general description of the undergrowth (very sparse to very dense), the mean height of the undergrowth, and the maximum height of the undergrowth. This data is presented in table B-5, appendix B. The correlation between the exponential decay parameter and each of the undergrowth factors (along the with five other factors: annual rainfall, percent evergreen trees, elevation, percent canopy closure, and latitude) is included in table 15. An analysis of the data identified the Boreal and Mediterranean biomes as outliers. When these outliers were removed from the analysis, the correlation improved for the undergrowth density with the exponential decay parameter from -0.44 to -0.70.

Table 15. Correlation of Collected Data and Exponential Parameters for the Prone Defender Looking at the Kneeling Attacker

Factors	Correlation
Undergrowth Density	-0.44
Annual Rainfall	-0.39
Maximum Undergrowth Height	-0.34
Mean Undergrowth Height	-0.24
Percent Evergreen Trees	-0.24
Elevation	0.22
Percent Canopy Closure	-0.16
Latitude	-0.03

The subjective descriptions of undergrowth were given ordinal values between 1 and 7. The corresponding descriptions are:

1 - very sparse
2 - sparse
3 - sparse to medium
4 - medium
5 - medium to dense
6 - dense
7 - very dense

The three undergrowth parameters provide some of the stronger correlations, but they are the most subjective data in the table. The undergrowth patterns in Panama presented another problem. The data collection locations in Panama had few mature trees and the undergrowth was indistinguishable from the trees. It is possible that a more objective approach to collecting undergrowth information would provide a larger (absolute value) correlation. A better approach to collecting undergrowth data for the above table could be using regression equations that accurately predict the decay parameters which would, in turn, provide more realistic visibility in vegetation.

Panama Discussion

Data were collected in Panama twice. The first data collection coincided with the end of the worst drought in over 100 years. Because the vegetation appeared dry and sparse during the first data collection, data were collected a second time at the end of Panama's rainy season. Surprisingly, the visibility during the two trips was virtually equal. The differences in the fitted curves for the El Valle site for the two trips are less than one percent across all ranges. The vegetation parameters for the sites at Gamboa and Fort Sherman indicate that the vegetation was slightly denser the second trip. However, the difference was undistinguishable by the data collection team and was apparent only after the data were analyzed and plotted. The analysis showed that for the two visits, the difference between corresponding best fit curves, for any given range, was always less than 5 percent.

Data Collection Observations

As the study progressed, the data collection team developed insights as to how vegetation obscures visibility. These insights were gained post priori and are not included in the analysis section. Since the authors consider them important factors concerning how vegetation obscures visibility, they are discussed in the paragraphs below, and should be addressed in future data collection.

A priori, it was expected that the portion of the target silhouette visible would decrease steadily as a function of range; this was generally reflected in the data. For example, the medium value for the LOS had a downward trend. All of the curve fits presented a steady decrease in target visibility as range increased.

However, for one-third of the azimuths, the fraction of the target that was visible increased at longer ranges. But, when the median was calculated for the site, the data generally had a downward trend. All of the curve fits presented a steady decrease in target visible as range increased. There are two reasons why the portion of the target visible increased at longer ranges. First, the undergrowth blocking part of the target at close range does not block the target as much at longer ranges. For example, consider a bush obscuring the bottom part of the target at close range. Assuming no other obstructing features, the sensor looks over the bush and can see more of the target as the target is moved away along the azimuth line.

The second reason is a consequence of the discrepancy between the assumptions of the LOS problem and the sensors used in the experiments. When an observer uses both his eyes (aided and unaided) to observe, he is in conflict with the mathematical description of the problem. The image perceived by the observer is the brain's fusion of the scene presented by **each** of the observer's eyes, and depending on the geometry of the situation, some of the obscuration may be eliminated. The mathematical description of the problem assumes that the observer is a single point perceiving a single image. One can demonstrate this effect by holding a thumb in front of himself, and observing the scene one eye at a time, and then with both eyes. Clearly the obscured portion of the scene is different in all three cases.

A second insight into visibility in vegetation concerns how the different postures of the observers, whether prone or crouching, changed the view of the target. The fitted curve parameters all indicate that crouching soldiers have better visibility than prone soldiers. However, occasionally the undergrowth and crowns of trees blocking the view of the crouching soldier did not block the view of the prone soldier.

The final insight came from one of the infantry subject matter experts. Based on the collected field data, it was noticed that, in general, visibility from the point of view of the attacker declines faster than the visibility of the corresponding defender. This was especially true when they were both in their typical posture (prone defender, kneeling attacker). Therefore, a range exists where the defender has a significant advantage over the attacker. Further analysis of this aspect of visibility could lead to changes in dismounted infantry tactics by providing soldiers with a set of engagement ranges as a function of biome giving them the advantage over the attacker.

Conclusions

This study shows that LOS in vegetation can be accurately portrayed. Therefore, simulations representing LOS in vegetation should reflect the information in this report. Three equations have been developed allowing for the modification of LOS algorithms in combat models. These equations can be used to verify the vegetation density portrayed in simulators/simulations by comparing LOS in the simulators to the curves presented in this report.

Recommendations

This study examined the environment where trees were in full foliage. A follow-on study should be conducted examining the effects of trees without leaves.

The undergrowth played a very important part in blocking visibility. A more detailed analysis of the effects of undergrowth should be conducted.

Since the analysis required to select analog sites for the former Yugoslavia and Korea was not field checked outside the continental US (OCONUS), it is recommended that data actually be collected at these OCONUS sites.

Now that the analysis on dismounted infantry targets is complete, this work should be expanded to examine the effects of LOS on vehicle sized targets.

Appendix A. Probability of Detection (PDET)

Introduction

This appendix describes the empirical model, Acquire, used to determine probability of detection (PDET) for combat simulations. This model was developed by Night Vision Electronic Sensor Division based on extensive field tests. These tests were designed for long ranges (up to 10 kilometers) and for the use of forward looking infrared (FLIR) sights. These equations, however, have been extrapolated for direct view optics (DVO).

For the purpose of this study, the application of the Acquire model to determine PDET is only examined for sensors using DVO and dismounted infantry targets. DVO, for the purposes of this discussion, represents the unaided eye or binoculars.

Appendix A first describes the physics equations determining PDET. In order to visualize how the physics model works, a discussion of the inputs used by the Combined Arms and Support Task Force Evaluation Model (CASTFOREM) in a recent dismounted infantry study are also included.

Description of the Models

The models used to determine PDET can be separated into the following steps:

- Contrast (C)
- Apparent contrast (AC)
- Maximum resolvable frequency (MRF)
- Resolvable cycles (N)
- Target transfer probability function (TTPF)

Contrast (C)

Contrast (also called inherent contrast) is defined as the absolute value of the ratio of background brightness and target brightness. The equation is as follows:

$$\mathbf{C} = \left| \frac{\mathbf{BB} - \mathbf{TB}}{\mathbf{BB}} \right|,$$

where BB = background brightness

TB = target brightness

Apparent Contrast (AC)

The apparent contrast of a target requires several input parameters. This equation models the effects of the atmosphere on the transmission of contrast. The resulting equation is as follows:

$$\mathbf{AC} = \frac{\mathbf{C}}{\mathbf{1} + \mathbf{SOG}\left(\mathbf{e}^{\mathbf{ATTN*Range(Km)}} - \mathbf{1}\right)},$$

where SOG = sky over ground ratio

ATTN = atmospheric attenuation

Range (km) = Range to target in kilometers

SOG is defined as the ratio of sky over ground luminance. It is a function of ground reflectance, cloud cover, and solar geometry. A SOG of 1.0 is used for a night scenario. ATTN is defined as the atmospheric extinction coefficient.

Maximum Resolvable Frequency (MRF)

The MRF (also called the spatial frequency) is a lookup table considering the visible light and the AC. Nine light levels varying from a star-lit night to clear day are used by CASTFOREM.

AC values not found in the table are computed by a linear interpolation between values in the table. The MRF is then multiplied by the power of the optics used. The MRF is multiplied by 1.0 for an unaided eye and by 7.0 for seven power binoculars.

Resolvable Cycles (N)

Resolvable cycles (N) is defined as the number of black and white bars distinguishable in a target. It is a measure of the ability of the optic device in use to determine detail. As the value of N increases, targets become more distinguishable because the observer can see more detail. The resolvable cycles is computed as follows:

$$\mathbf{N} = \frac{\mathbf{MRF} \bullet \mathbf{CD}}{\mathbf{Range\ (km)}},$$

where CD = square root of the presented target area

Range (km) = distance to the target in kilometers

Target Transfer Probability Function (TTPF)

The TTPF is also the probability of detection given an infinite amount of time. It is defined as follows:

$$\mathbf{PDET} = \frac{\left(\frac{\mathbf{N}}{\mathbf{N50}}\right)^{\mathbf{E}}}{\mathbf{1} + \left(\frac{\mathbf{N}}{\mathbf{N50}}\right)^{\mathbf{E}}},$$

where E = 2.7 + 0.7 • N/N50

N50 = Resolvable cycles required to acquire at a specific acquisition

An N50 value of 0.75 is used to represent a man moving and standing and a value of 1.00 is used to represent a man kneeling and stationary. The existence of detection in CASTFOREM is determined by comparing PDET to a random number between zero and one.

Example

A typical European scenario in CASTFOREM is examined to illustrate how the inputs actually effect PDET. Since every target pairing in every simulation will have different input parameters, these numbers should only be viewed as an example and should not be used in combat simulations.

Contrast was defined as 0.36 for dismounted soldiers in a recent dismounted infantry scenario. This value approximates the contrast of a man in fatigues surrounded by growing deciduous trees. Different targets in different environments will yield different contrast values.

SOG is defined as 2.6 for a European type environment. In comparison, a SOG of 1.47 is used in Southwest Asia. An attenuation of 0.3566 was used for Europe.

Ranges up to 400 meters were used for this example because the field collection never encountered a visible target beyond 400 meters. Table A-1 gives the values of AC as a function of range.

Table A-1. Values of Apparent Contrast as a Function of Range in a European Scenario

Range (Meters)	AC
1	0.36
25	0.35
50	0.34
100	0.33
200	0.30
400	0.27

A close examination of the AC equation shows the maximum value for AC is C (0.36 in this case). The MRF table for AC values between 0.25 and 0.36 (the approximate values of AC between 0 and 400 meters) is in table A-2. Included in the table is the range for which the value of AC is associated. MRF is a function of AC and is not a function of range. Range was added to this table because it is easier to understand than contrast.

Table A-2. Minimum Resolvable Frequency for Different Light Levels and Different Values of AC

		Light Level Code*								
AC	**Associated Range (m)**	**9**	**8**	**7**	**6**	**5**	**4**	**3**	**2**	**1**
0.25	438	1.579	1.520	1.353	1.094	0.745	0.285	0.031	0.014	0.002
0.30	208	1.657	1.598	1.427	1.160	0.799	0.325	0.044	0.021	0.003
0.35	30	1.726	1.660	1.492	1.218	0.847	0.358	0.057	0.029	0.005
0.36**	0	1.787	1.726	1.550	1.270	0.889	0.389	0.071	0.037	0.008

**The light level codes are as follows: 1 - Clear - No Moon/Starlight, 2 - Starlight/Quarter Moon, 3 - Moonlight/Full Moon, 4 - Just After Twilight, 5 - Just Before Twilight, 6 - Sunset, 7 - Heavily Overcast Day, 8 - Overcast Day, 9 - Clear Day.*

*** The MRF values for 0.36 were interpolated from the actual CASTFOREM inputs.*

m - meters

Five of the nine light levels were examined: clear day, just before twilight, just after twilight, moonlight/full moon, and clear - no moon/starlight. Two sizes of moving targets are depicted in this example. The target sizes were for a fully exposed kneeling soldier (0.4206 square meter), and a fully exposed prone soldier (0.1233 square meter). However, the actual presented area of a soldier typically decreases as a function of range (in a vegetated environment) and vegetation density.

Table A-3 contains the MRF values for five light conditions. Table A-4 and table A-5 contain the values of N for different light conditions for a fully exposed kneeling and prone soldier, respectively. Figure A-1 and figure A-2 depict the PDET for different lighting conditions for a fully exposed kneeling and prone soldier, respectively. Values for AC have been replaced by range to make the example more straightforward. The actual equations require the AC values.

Table A-3. MRF Values for Five Light Conditions

Range (m)	**Light Conditions**				
	Clear Day	**Just Before Twilight**	**Just After Twilight**	**Moonlight/ Full Moon**	**Clear - No Moon/ Starlight**
1	1.787	0.889	0.389	0.071	0.008
25	1.736	0.854	0.363	0.059	0.006
50	1.718	0.839	0.354	0.056	0.005
100	1.695	0.825	0.345	0.052	0.004
200	1.654	0.801	0.324	0.044	0.003
400	1.592	0.754	0.292	0.033	0.002

Table A-4. Value of N for Different Light Conditions - Fully Exposed Kneeling Target on the Move

Range (m)	Light Conditions				
	Clear Day	Just Before Twilight	Just After Twilight	Moonlight/ Full Moon	Clear - No Moon/ Starlight
1	1158.935	576.549	252.281	46.046	5.188
25	45.034	22.154	9.417	1.531	0.156
50	22.284	10.882	4.592	0.726	0.065
100	10.993	5.350	2.237	0.337	0.026
200	5.363	2.597	1.051	0.143	0.010
400	2.581	1.222	0.473	0.054	0.003

Table A-5. Value of N for Different Light Conditions - Fully Exposed Prone Target on the Move

Range (m)	Light Conditions				
	Clear Day	Just Before Twilight	Just After Twilight	Moonlight/ Full Moon	Clear - No Moon/ Starlight
1	627.489	312.164	136.594	24.931	2.809
25	24.383	11.995	5.099	0.829	0.084
50	12.065	5.892	2.486	0.393	0.035
100	5.952	2.897	1.211	0.183	0.014
200	2.904	1.406	0.569	0.077	0.005
400	1.398	0.662	0.256	0.029	0.002

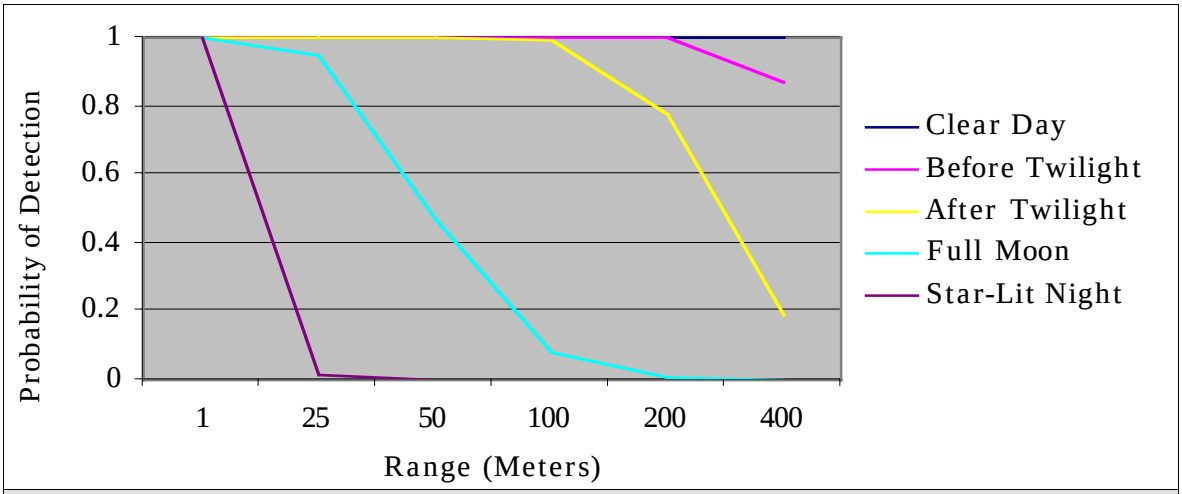

Figure A-1. Probability of Detection for Different Light Conditions - Fully Exposed Kneeling Target on the Move

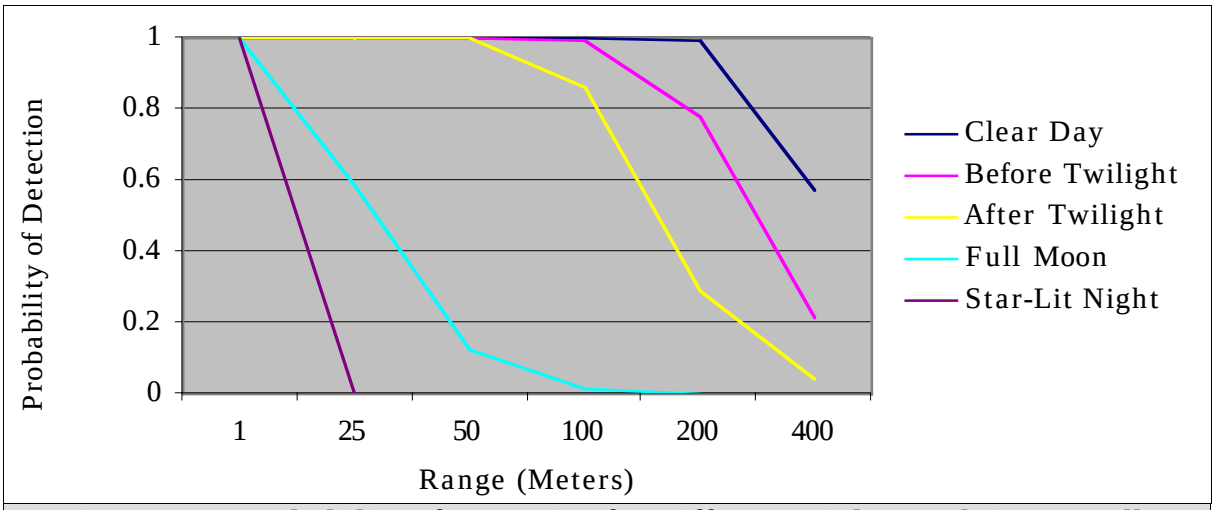

Figure A-2. Probability of Detection for Different Light Conditions - Fully Exposed Prone Target on the Move

Appendix B. Description of Data Collection Locations and Sites

Introduction

Fifteen geographic areas were selected for data collection. They represent a variety of vegetative sub-biomes, climates, latitudes, elevations, and therefore a variety of vegetation densities. This appendix provides a detailed description of the locations (general geographic area) and sites (specific point on the ground) where data were collected. It includes a discussion on how the sites were selected and detailed information about each location and site.

A compact disk-read only memory (CD-ROM) is included with this report. This CD-ROM provides two types of graphical information. Maps are included to represent the data collection locations. The actual sites selected for data collection are indicated by pink or red dots. Vegetation panoramas are included. Each of the data collection sites was photographed and provided.

Selection of Geographic Locations for Data Collection

Based on the initial scope and funding levels for the study, the TEC and TRAC-WSMR scientists decided to limit the field LOS investigations to the CONUS sites. The criteria used to select the study areas of interest were: (1) the probable locations of the US Army's future MRC, (2) world vegetative biome information, and (3) locations where field collections could be conducted.

All of the potential MRCs are located OCONUS and are often in unfriendly countries. The locations are Central America, the former Yugoslavia, and Korea. It was decided that areas with similar vegetation characteristics (based on vegetation, climate, elevation, and latitude) should be included in selecting collection locations. A climatologist from TEC developed a set of criteria enabling the field collectors to select CONUS areas best representing the former Yugoslavia and Korea. A detailed description of this methodology is described later in this section (see "Former Yugoslavia and Korea Analog Analysis").

While climates are better understood than biomes, biomes categorize vegetation types better than climate categories. A map (see figure B-1) depicting global vegetative biomes was consulted to identify US/world analogs (The CD-ROM included in this report depicts this picture in high resolution color.). The major vegetative biomes are delineated primarily on the basis of their specific vegetation types, i.e., forest, savanna, grassland, desert, and tundra. Each biome is further divided into smaller vegetation units or "sub-biomes" associated with vegetation structure, climate, soil types, soil moisture, and predominant species. In order to assure the best possible representation between CONUS locations and the rest of the world, the field collection sites for this study were selected from the sub-biome units identified in figure B-1. Eight CONUS sites were identified. Each site was situated in a corresponding sub-biome as follows:

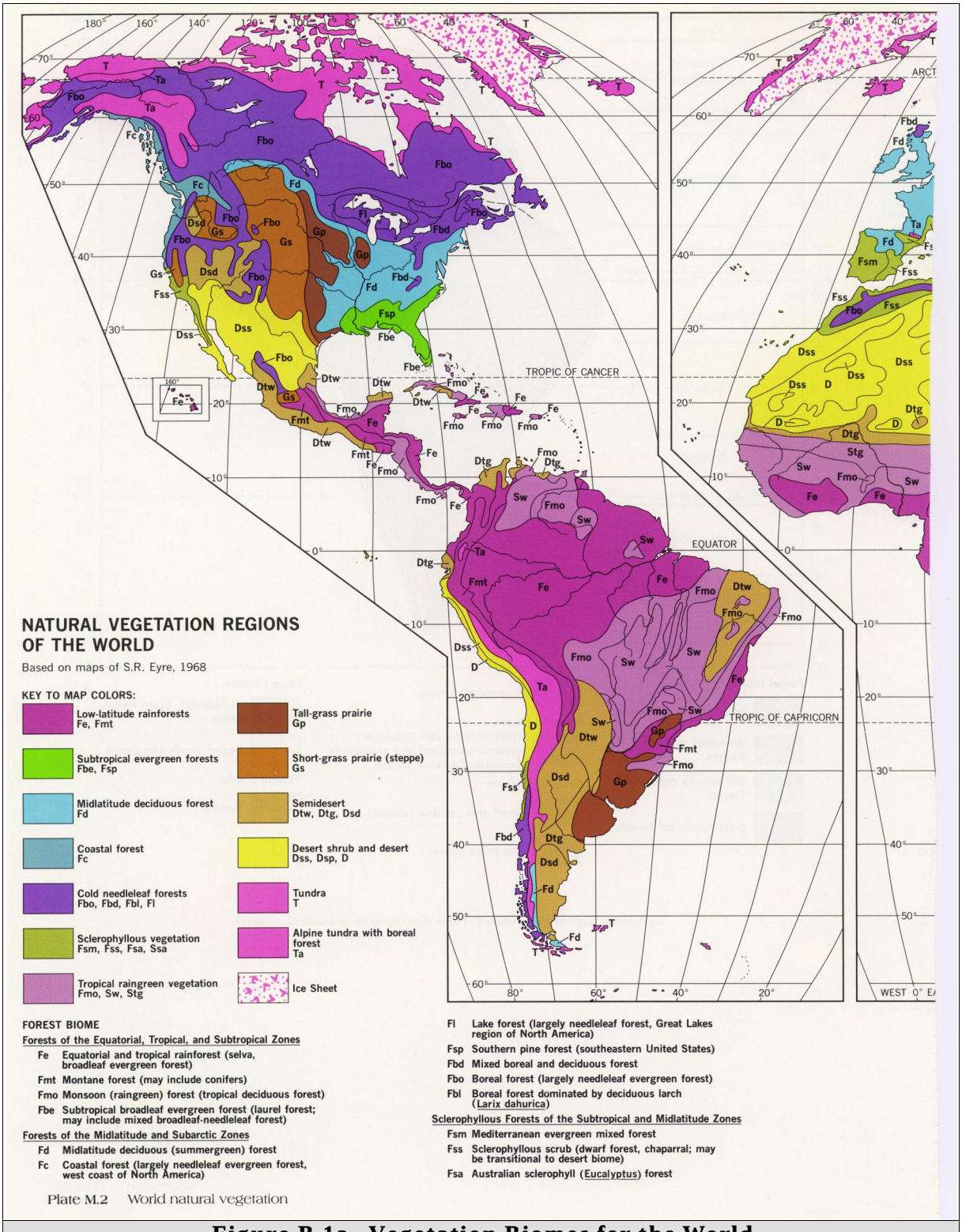

Figure B-1a. Vegetation Biomes for the World

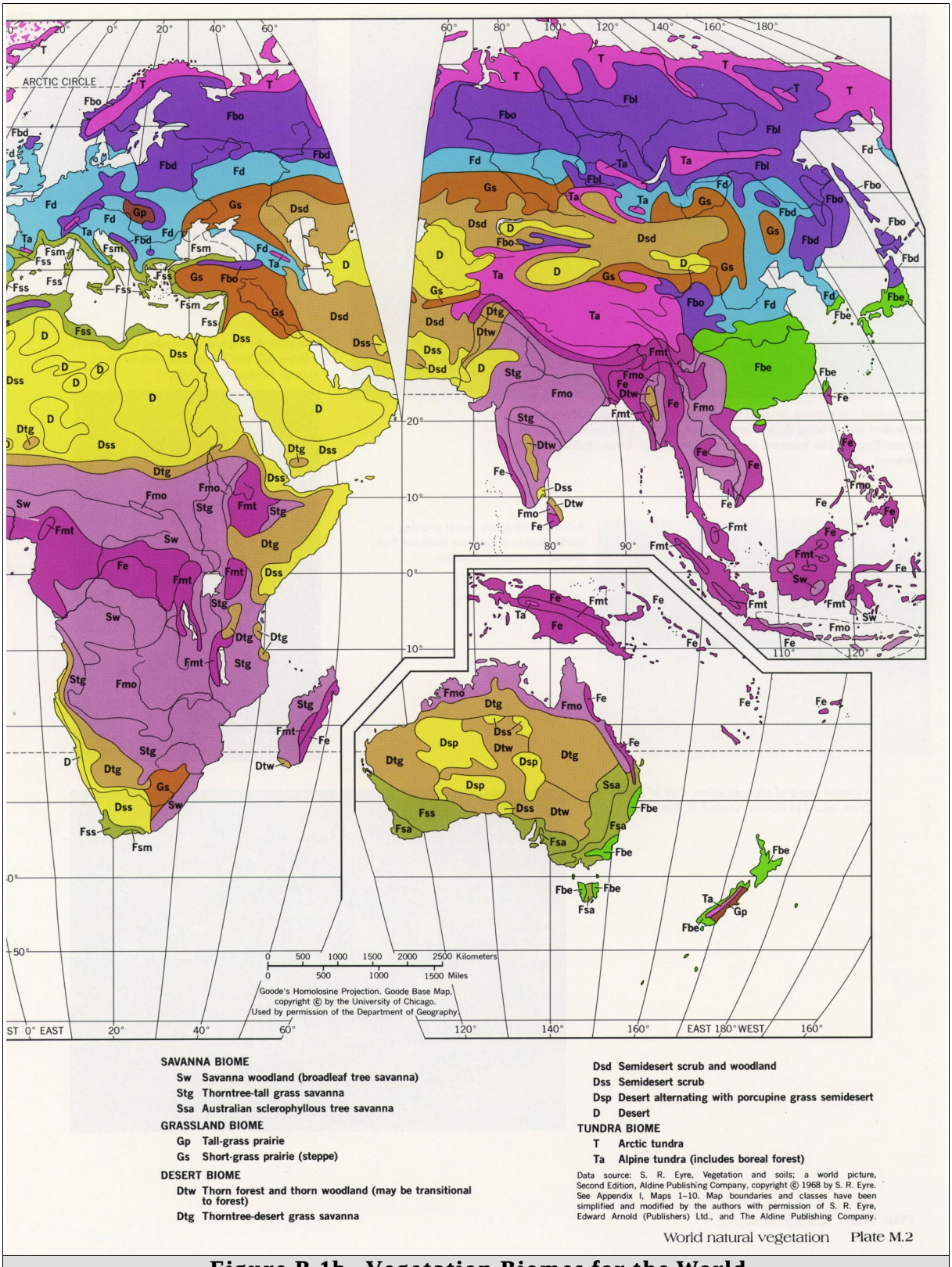

Figure B-1b. Vegetation Biomes for the World

- Coastal Forest (Marine West Coast)
- Sclerophyllous Vegetation (Mediterranean)
- Short Grass Prairie (Steppe)
- Tall Grass Prairie
- Mixed Boreal and Deciduous
- Midlatitude Deciduous
- Southern Pine Forest
- Subtropical Broadleaf Evergreen Forest

Figure B-1 shows the eight CONUS sub-biomes representing the natural vegetation of CONUS. These sub-biomes also represent most of Europe and Southwest Asia (excluding the Saudi Arabian Peninsula), the midlatitudes of Asia including a large portion of China, temperate latitudes of South America and Australia/New Zealand, and selected portions of North and South Africa.

As the study progressed, additional funding allowed the scope of the field collection to be expanded. The subsequent addition of the Boreal Forest, Tropical Rainforest, Montane Forest (a high-altitude tropical environment), and Wet and Dry (Monsoon) tropical sub-biomes to the study provided representative field information for the majority of equatorial and sub-polar vegetation types. When combined with the original eight sub-biomes, approximately two-thirds of the world's natural vegetation cover and all the major MRC areas are represented. The addition of Panama ensured the Central America MRCs would be accurately depicted. The remaining global sub-biomes were not evaluated in the study because they fell into one of the following categories:

- Climates void or nearly void of vegetation. These include several desert sub-biomes, and several arctic sub-biomes.
- Areas that are small, unique, and located where the US Army is unlikely to deploy soldiers. These include the Great Lakes area and northern Siberia.
- Sub-biomes of future importance were eliminated due to prohibitive cost or restricted access.

Military reservations, national parks, state parks, and private property were used for the field collection.

Thirteen sub-biomes and 15 geographic areas were visited during the field data collection. Table B-1 depicts the locations along with their sub-biome and climate definitions (if differentiated). Table B-1 also offers a generalized or descriptive classification of the vegetation found in each of the sub-biome locations. Appendix C provides a general description of world climates with a link to each field collection location. Appendix D provides a description of the vegetation sub-biomes represented within the study.

Table B-1. Vegetative Sub-Biome/Climate and Vegetation Definitions of Data Collection Locations		
Location	**Sub-Biome/Climate Type**	**Vegetation Description**
Panama - Gamboa	Monsoon Tropical/Tropical Wet-and-Dry	Monsoon (Rainforest) - Tropical Deciduous Forest
Panama - Fort Sherman	Tropical Rainforest/Tropic Wet	Monsoon (Rainforest) - Tropical Deciduous Forest
Panama - El Valle	Montane Forest/Tropic Upland	Equatorial and Tropical Rainforest - selva, broadleaf evergreen forest
Eglin AFB	Subtropical Broadleaf Evergreen Forest/Humid Subtropical	Oak and Pine Forest with some tropical vegetation
Fort Hood	Dry Steppe (tall grass)	Tall Grass Prairie
Fort Carson	Dry Steppe (short grass)	Short Grass Prairie
Fort Hunter-Liggett	Sclerophyllus vegetation/Mediterranean	Old Oak Forest
Fort Lewis	Coastal Forest/Temperate Oceanic (Marine)	Coastal Forest - largely needleleaf evergreen forest
Fort Benning	Southern Pine Forest/Temperate (warm summer)	Southern Pine and Oak Forest
Smoky Mountains	Midlatitude Deciduous Forest/Temperate (warm summer)	Mixed Deciduous Forest
Willow Grove NAS	Midlatitude Deciduous Forest/Temperate (warm summer)	Mixed Deciduous Forest
Natchaug SF	Midlatitude Deciduous Forest/Temperate (cool summer)	Mixed Deciduous Forest
Fort Drum	Mixed Boreal and Deciduous Forest/Temperate (cool summer)	Mixed Deciduous and Pine Forest
Canada - Gagetown	Mixed Boreal and Deciduous Forest/Temperate (cool summer)	Mixed Deciduous and Pine Forest
Fort Greely	Boreal and Taiga	Mixed Spruce, Birch and Aspen

Former Yugoslavia and Korea Analog Analysis

Based on current world situation, two potential areas for US deployment are the former Yugoslavia and Korea. Since the data collection team was not able to visit either place, US sites closely representing these areas were selected using climate-vegetation analog analysis.

The purpose of this analysis was to find, in CONUS, analogous climates for sites in Korea and former Yugoslavia. It was anticipated tree species could be inferred for locations OCONUS based on the vegetation existing in their US counterparts. Although this seems direct at first, a closer examination of the task revealed common climate classification schemes (e.g., Köeppen, Trewartha, etc.) were too broad and generalized in terms of the climatic variables to be used in selecting analogous CONUS sites. Therefore, individual variables used in the past to link climate and vegetation were employed. This is not to imply climate is the only variable regulating the existence of certain tree species at a particular location. Elements such as soils, solar radiation, local water table, competition from other species, latitude, and slope all play a role. However, climatic variables were used as an initial starting point.

The variables selected were: altitude, mean annual precipitation, mean annual temperature, potential evapotranspiration (PE), and moisture index (MI). The PE provides an indication of the evaporation (expressed in millimeters of water) based on temperature. The MI provides an indication of the moisture regime at a location. These two variables are derived from mean monthly precipitation and temperature. The PE and MI are used by a number of researchers to identify boundaries within which certain vegetation species exist.

The CONUS data set consisted of 176 meteorological stations in the eastern portion of the US. The entire data set containing the five variables for the CONUS stations was used to determine the most closely analogous OCONUS stations. In an optimal scenario, all variables for analogous stations would be compatible. However, during the analysis, it became clear this was not a realistic expectation. In a number of instances, candidate CONUS stations were selected for consideration although certain variables were not perfect matches. For example, in Korea, elevation and continentality were incompatible with many vegetated US stations. It was decided to use the more representative variables of temperature and precipitation in the selection process. Although somewhat subjective, a good deal of climatological reasoning was employed to ensure the candidate analogous CONUS stations were closely representative to the OCONUS stations.

Finally, an analysis of various anomalies was conducted. One difficulty encountered was that stations in Korea might experience a distinct summer monsoon season. Consequently, most Korean locations are especially influenced by either precipitation (pronounced monsoon) or temperature (less pronounced monsoon) criteria. Monthly precipitation values for the months of July through October at many Korean sites may

be more than three to four times the value of any non-monsoon month. On a monthly basis, there is no direct precipitation analog to any site in the entire US, although annual totals are comparable to certain eastern US sites. As previously mentioned, Korean stations also have high continentality indices comparable to those in the north central Great Plains of the US. This is due in part to the dominance of wintertime Siberian high pressure. Similar differences were noted between stations towards the coast of the former Yugoslavia and those further inland exhibiting more continental characteristics.

To better characterize these differences, two representative CONUS stations were chosen for both the former Yugoslavia and Korean sites. Further analysis of the OCONUS sites criteria revealed a good overall correlation to these dual eastern US locations. Figure B-2 depicts the results of the analysis used to determine the Korean analogs. Based on these findings, data were collected in the Smoky Mountains to represent the precipitation influence and at Willow Grove NAS to represent the temperature influence. Figure B-3 depicts the results of the former Yugoslavia analog analysis. Fort Drum was selected for collection to represent the continental influence and northeastern Connecticut was selected to represent the coastal influence.

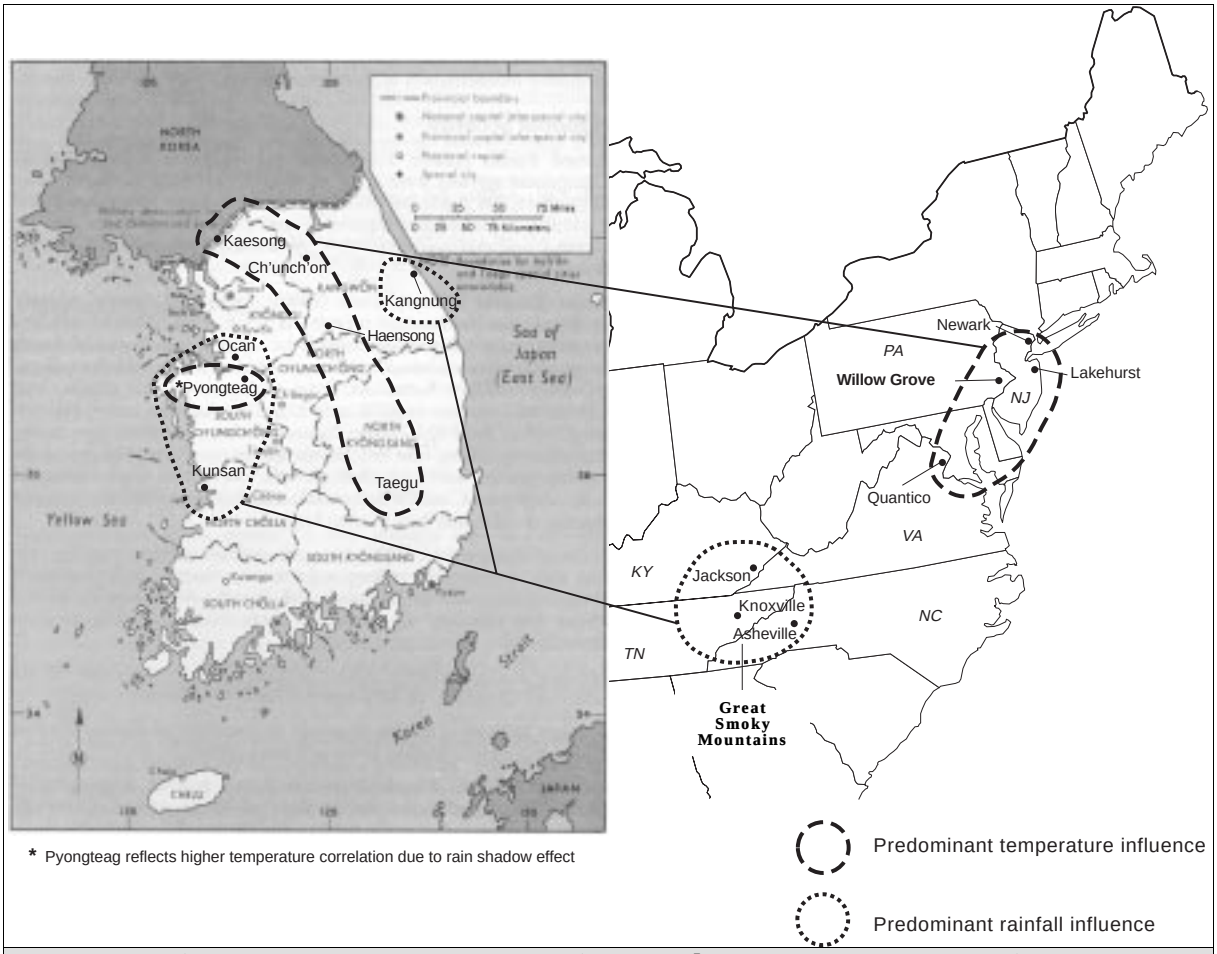

Figure B-2. CONUS Vegetation Analogs to Korea Vegetation

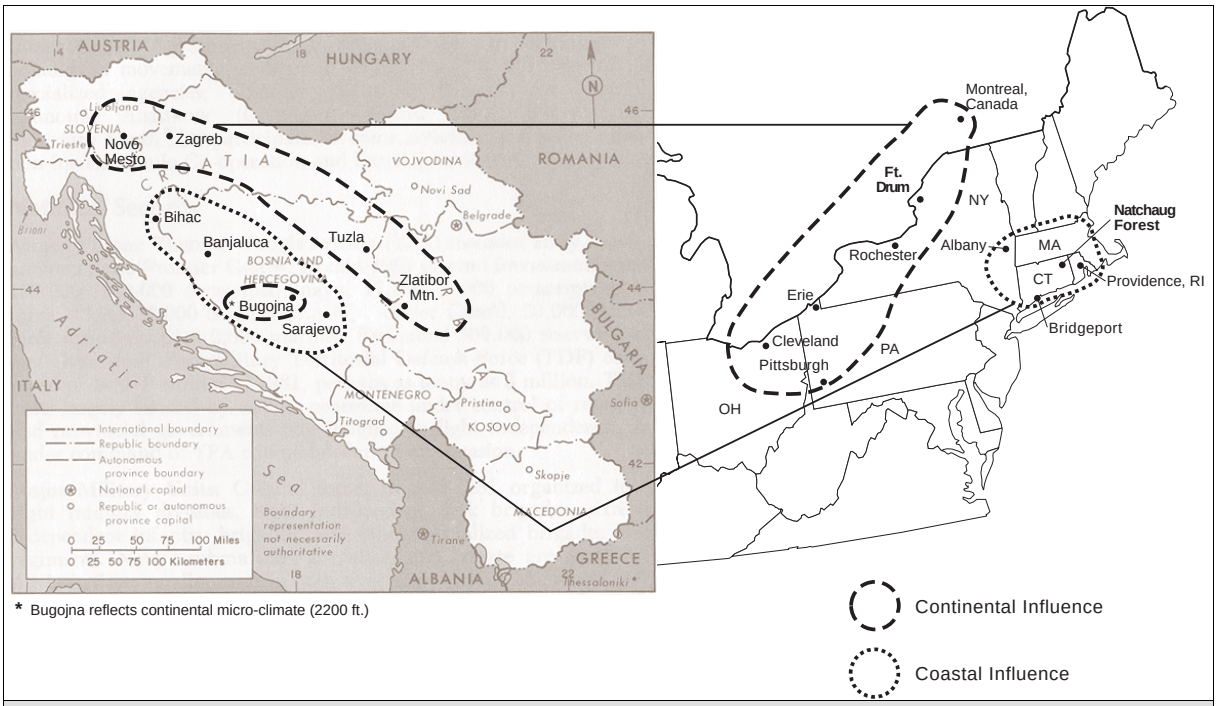

Figure B-3. CONUS Vegetation Analogs to the Former Yugoslavia

Location and Site Description

A general description of each geographic area is included for each data collection location. Places in the world with similar vegetation characteristics are also recorded for each collection location. The collection locations are subdivided into the individual collection sites. The data collected include a description of each data collection site, a description of the undergrowth, whether or not a tank could operate in the area, and the number of azimuths along which data were collected. The number of azimuths varied between four and nine depending on the tactical FOV, the distance along the azimuths, the time available to the data collectors, and weather conditions.

Table B-2 describes the location of the 15 sites to the nearest longitude and latitude and the horizontal datum.

Table B-2. Location of Field Collection Locations

	Approximate Latitude/Longitude	Horizontal Datum
Panama – Gamboa	79 W, 9 N	NAD 27
Panama – Fort Sherman	79 W, 9 N	NAD 27
Panama – El Valle	79 W, 9 N	NAD 27
Eglin AFB	86 W, 30 N	NAD 27
Fort Hood	98 W, 31 N	NAD 27
Fort Carson	105 W, 38 N	NAD 27
Fort Hunter-Liggett	121 W, 36 N	NAD 27
Fort Lewis	122 W, 47 N	WGS 84
Fort Benning	85 W, 32 N	NAD 27
Smoky Mountains	83 W, 36 N	NAD 27
Willow Grove NAS	75 W,40 N	NAD 27
Natchaug SF	72 W, 42 N	NAD 27
Fort Drum	75 W, 44 N	WGS 84
Canada - Gagetown	66 W, 46 N	WGS 84
Fort Greely	145 W, 64 N	NAD 27

Table B-3 provides the associated vegetative biome/climate, annual rainfall data, and the dates of the field collection for each geographic area evaluated for the study. A detailed description of the vegetative biomes and climates can be found in appendices C and D, respectively. The average rainfall was determined by examining and compiling data from a number of rainfall stations near each geographic location.

Table B-3. Climate Information About Data Collection Locations

Location	Climate	Annual Rainfall (Inches)	Collection Dates
Panama – Gamboa	Tropical Wet and Dry	50-60	10-12 March 1998 and 6-12 January 1999
Panama – Fort Sherman	Tropical Wet	110-120	13-16 March 1998 and 7-8 January 1999
Panama – El Valle	Tropical Upland	120-130	18 March 1998 and 5 January 1999
Eglin AFB	Subtropical Humid	60-65	22-25 June 1998
Fort Hood	Semiarid Tall Grass	30-35	30 Sep 97-3 October 1997
Fort Carson	Semiarid Short Grass (Steppe)	10-20	7-10 October 1997
Fort Hunter-Liggett	Mediterranean	5-10	4-7 November 1997
Fort Lewis	Temperate Oceanic (Marine)	35-40	9-12 November 1997
Fort Benning	Temperate Continental**	45-50	16-19 June 1998
Smoky Mountains	Temperate Continental**	40-50	14-18 September 1998
Willow Grove NAS	Temperate Continental**	40-45	22-25 September 1998
Natchaug SF	Temperate Continental*	40-45	11-14 August 1998
Fort Drum	Temperate Continental*	35-40	4-7 August 1998
Canada - Gagetown	Temperate Continental*	40-45	18-21 August 1998
Fort Greely	Boreal and Taiga	20-30	8-15 July 1998

*Note: * cool summer/cold winter*
*** warm summer/cool winter*

Several (usually four) different sites within each geographic area were selected for data collection. Table B-4 summarizes the individual collection sites. The site identification (ID) is typically an abbreviation of the geographic site and a training range identifier. The exceptions to this notation are Fort Hood, all the Panama locations, Natchaug State Forest, the Smoky Mountains, and Willow Grove NAS. These sites were given an abbreviation and a numerical designator. Table B-4 also includes a mapsheet series and number for each site along with its respective easting, northing, and elevation. The position information was collected in universal transverse mercator (UTM) coordinates using a precision lightweight Global Positioning System (GPS) receiver (precision lightweight GPS receiver (PLGR)) with a 5-7 meter absolute horizontal accuracy.

Table B-4. Exact Locations of Field Collection Sites Including Easting, Northing, and Elevation

Location	Mapsheets	Site ID	Easting	Northing	Elevation (Meters)
Panama – Gamboa	E762 4243 II	gam1	643009	1009123	50
	E762 4243 II	gam2	642959	1009193	70
	E762 4243 II	gam3	642963	1009135	65
Panama - Fort Sherman	E762 4243 IV	skh1	614610	1031326	90
	E762 4243 IV	mck1	611180	1031820	50
Panama - El Valle	E762 4040 II	elvl	595974	952690	735
Eglin AFB	V747 3645 III	egl_B2	513008	3383045	15
	V747 3744 IV	egl_X8	565583	3371785	10
	V747 36744 I	egl_X11	573012	3373589	0
	V747 3744 IV	egl_B12	568634	3374950	30
Fort Hood	V782 6446 II	hood1	634956	3447933	200
	V782 6446 IV	hood2	613053	3463615	300
	V782 6446 IV	hood3	611132	3468105	350
	V782 6446 II	hood4	634882	3447861	200
Fort Carson	V777 5061 III	car41	503646	4263333	2000
	V777 5060 IV	car43	507030	4256724	1800
	V777 5061 III	car28	503350	4267355	1900
	V777 5062 III	afa1	511932	4318862	2100
Fort Hunter-Liggett	V795 1756 III	hl2	652967	3992291	350
	V795 1756 III	hl5	652584	3990785	360
	V795 1756 II	hl10	664160	3987415	330
	V795 1755 IV	hl9	656824	3982800	330
Fort Lewis	V791 1578 III	lew10	538430	5209933	110
	V791 1477 I	lew19	536645	5203211	90
	V791 1477 I	lew3	524850	5209587	65
	V791 1578 III	lew8	539045	5212546	120
Fort Benning	V745 4048 IV	ben_T3	705258	3585925	140
	V745 4048 IV	ben_L3	709976	3591177	90
	V745 4048 IV	ben_T4	707977	3586537	180
	V745 4048 IV	ben_D12	709935	3586273	150
Smoky Mountains	V842 4355 II	NC1	307670	3945980	850
	V841 4355 III	TN1	282284	3956600	340
	V841 4255 II	TN2	270668	3952250	430
	V842 4255 II	TN3	251440	3943885	540
Willow Grove NAS	V831 5964 II	WG6	495527	4449610	110
	V831 5964 II	WG2	486691	4449202	100
	V831 5964 II	WG5	485991	4451554	80
	V831 5964 II	WG4	486737	4451412	80
Natchaug SF	V816 6567 I	Nat2	737646	4641602	230
	V816 6567 I	Nat1	733840	4640998	180
	V816 6567 I	Nat4	738667	4633070	180
	V816 6567 I	Nat5	742599	4633165	220
Fort Drum	V721 5872 II	8C	451100	4880171	210
	V721 5872 II	7G	450110	4874217	230
	V721 5872 II	7B	451600	4875950	240
	V721 5872 II	7E	452194	4875594	210

Table B-4. Exact Locations of Field Collection Sites including Easting, Northing, and Elevation (Continued)

Location	Mapsheets	Site ID	Easting	Northing	Elevation (Meters)
Canada - Gagetown	A702 21 G/9	Gage31	707665	5056363	110
	A702 21 G/9	Gage27	719194	5057459	80
	A702 21 G/9	Gage8	715896	5074298	65
	A702 21 G/9	Gage7	713958	5077119	40
Fort Greely	Q701 3648 IV	G22	561373	7089326	470
	Q701 3648 IV	G00	562483	7082880	560
	Q701 3648 IV	G25	562453	7092898	430
	Q701 3648 IV	G02	564988	7095640	400
	Q701 3648 IV	G24	563800	7094187	430
	Q701 3648 IV	G05	569169	7091552	430

Table B-5 shows the typical vegetation found at each geographic area. The vegetation/tree types at each area were delineated using a "Field Guide to Trees." A general description of the undergrowth, the undergrowth density, maximum and mean undergrowth height, and canopy closure were subjectively estimated by the data collection team. The canopy closure was the average of the canopy closure for all observers looking in five directions (straight up and looking up at 45-degree angles towards the north, south, east, and west). The overall average is presented in this appendix to the nearest 5 percent.

Table B-5. Canopy Closure, Tree Types, and Undergrowth Information for all Data Collection Sites

Location	Site ID	Canopy Closure (Percent)	Tree Types (Percent)	Under-growth Density	Maximum Height (Meters)	Mean Height (Meters)
Panama - Gamboa	gam1	85-90	Thick Tropical Vegetation (100)	Very Dense	*	*
	gam2	95-100	Thick Tropical Vegetation (100)	Very Dense	*	*
	gam3	95-100	Thick Tropical Vegetation (100)	Very Dense	*	*
Panama – Fort Sherman	skh1	90-95	Thick Tropical Vegetation (100)	Very Dense	*	*
	mck1	95-100	Thick Tropical Vegetation (100)	Very Dense	*	*
Panama - El Valle	elvl	90-95	Upland Tropical Vegetation (100)	Very Dense	*	*
Eglin AFB	egl_B2	25-30	Long Needle Pine (50), Post Oak (50)	Medium to Dense	1.80	1.50
	egl_X8	80-85	Oaks (70), Pines (30)	Dense	1.80	1.00
	egl_X11	65-70	Oaks (80), Pines (20)	Dense	1.25	0.80
	egl_B12	70-75	Oaks (50), Pines (50)	Sparse to Medium	1.25	1.00
Fort Hood	hood1	0	Juniper (100)	Very Sparse	0.75	0.50
	hood2	5	Elm (40), Scrub Oak (30), Juniper (20)	Sparse	1.00	0.75
	hood3	50-60	Juniper (75), Scrub Oak (25)	Very Dense	1.25	1.00
	hood4	0	Juniper (90), Scrub Oak (10)	Very Sparse	1.00	0.50

Table B-5. Canopy Closure, Tree Types, and Undergrowth Information for all Data Collection Sites (Continued)

Location	Site ID	Canopy Closure (Percent)	Tree Types (Percent)	Under-growth Density	Maximum Height (Meters)	Mean Height (Meters)
Fort Carson	car41	30-35	Juniper (65), Pinion Pine (35)	Very Sparse	1.00	0.50
	car43	0	Juniper (85), Pinion Pine (15)	Very Sparse	0.5	0.30
	car28	25	Pinion Pine (80), Juniper (20)	Very Sparse	0.5	0.25
	afa1	55-60	Ponderosa Pine (90), Scrub Oak (10)	Very Sparse	1.0	0.50
Fort Hunter-Liggett	hl2	60-65	Blue Oak (100)	Very Sparse	0.25	0.20
	hl5	50-55	Valley Oak (100)	Very Sparse	0.25	0.20
	hl10	65-70	Valley Oak (100)	Very Sparse	1.25	0.75
	hl9	60-65	Oaks (90), Coulter Pine (10)	Moderate	1.75	1.00
Fort Lewis	lew10	55-60	Douglas Fir (100)	Very Dense	3.0	2.00
	lew19	90-95	Douglas Fir (100)	Very Dense	3.0	1.00
	lew3	85-90	Douglas Fir (100)	Very Dense	3.5	1.00
	lew8	85-90	Douglas Fir (100)	Very Dense	4.0	2.00
Fort Benning	ben_T3	35-40	Loblolly Pine (65), Post and Blackjack Oak (35)	Medium	2.0	1.25
	ben_L3	90-95	Mixed Pine and Oak (100)	Medium	1.6	1.00
	ben_T4	70-75	Pine (95), Oaks (5)	Medium	1.8	1.00
	ben_D12	35-40	Loblolly Pine (85), Oaks (15)	Dense	2.5	1.50
Smoky Mountains	NC1	90-95	Oaks (35), Elm (25), Cypress (25), Sweetgum (15)	Medium	2.0	0.75
	TN1	85-90	Fir (25), Elm (25), Oak (20), Sweetgum (15), Other (15)	Dense	1.9	1.00
	TN2	70-75	Fir (20), Mixed Deciduous (80)	Very Sparse	1.0	0.10
	TN3	90-95	Mixed Deciduous (60), Fir (30), Longleaf Pine (10)	Sparse	1.0	0.50
Willow Grove NAS	WG6	75-80	Mixed Deciduous (90), Pine (10)	Medium	2.0	1.00
	WG2	80-85	Mixed Deciduous (90), Pine (10)	Medium to Dense	1.5	0.75
	WG5	75-80	Mixed deciduous (60), Mixed Evergreen (40)	Medium to Dense	2.0	1.00
	WG4	85-90	Elm (50), Sweetgum (40), Hickory (10)	Dense	2.0	1.00
Natchaug SF	Nat2	85-90	Oaks (80), Pines (20)	Medium	1.6	0.80
	Nat1	70-75	Mixed Deciduous Trees (100)	Medium	3.0	1.40
	Nat4	95-100	Mixed Deciduous Trees (100)	Sparse to Medium	1.3	0.70
	Nat5	85-90	Beech (50), Oak (50)	Sparse to Medium	0.75	0.40
Fort Drum	8C	80-85	White Pine (40), Red Maple (40), Aspen (20)	Medium	1.5	1.00
	7G	85-90	Red Maple (50), White Pine (35), Aspen (15)	Sparse	1.2	0.60
	7B	40-45	White Pine (100)	Sparse to Medium	2.0	1.00
	7E	90-95	Red Maple (50), Beech (45), White Pine (5)	Medium to Dense	2.0	0.80

Table B-5. Canopy Closure, Tree Types, and Undergrowth Information for all Data Collection Sites (Continued)

Location	Site ID	Canopy Closure (Percent)	Tree Types (Percent)	Under-growth Density	Maximum Height (Meters)	Mean Height (Meters)
Canada - Gagetown	Gage31	70-75	Red Maple (65), White Pine (35)	Medium	0.8	0.40
	Gage27	85-90	Red Maple (55), White Pine (25), White Birch (20)	Medium to Dense	2.0	0.75
	Gage8	80-85	White Pine (85), Red Maple (10), Birch (5)	Sparse	1.5	0.60
	Gage7	90-95	Red Maple (60), White Pine (40)	Sparse	0.6	0.30
Fort Greely	G22	10-15	Black Spruce (100)	Sparse to Medium	0.5	0.40
	G00	55-60	White Birch (100)	Sparse	0.6	0.30
	G25	35-40	Aspen (60), Black Spruce (40)	Medium	1	0.60
	G02	65-70	White Birch (50), Aspen (50)	Sparse	1	0.40
	G24	35-40	Black Spruce (100)	Very Sparse	0.4	0.20
	G05	55-60	Aspen (80), Black Spruce (20)	Medium	1	0.80

** The undergrowth in these areas is undistinguishable from the mature vegetation.*

Geographic Study Areas

The following sections describe each geographic study area visited during the study.

Panama

Six areas from Panama were selected for data collection. Three sites were located in Gamboa, two near Fort Sherman, and one site was in El Valle. Since these sites were all located in a tropical environment, they will be discussed under one heading (Panama) and divided into three separate vegetative/climate biomes.

The Gamboa and Fort Sherman sites were all very close to sea level, while the El Valle site was at a higher elevation (over 700 meters above sea level). Gamboa and Fort Sherman were divided into two different vegetation/climate types based on rainfall. The Fort Sherman area is designated as Tropical Rainforest in a Tropical Wet climate. This area receives rainfall throughout the year while Gamboa has a very distinct dry season (February to April). The vegetation/climate designation for the Gamboa area is Monsoon Forest in a Tropical Wet-and-Dry climate. The vegetation types found at Gamboa and Fort Sherman were similar.

The Fort Sherman sites receive more annual rainfall than the Gamboa sites and the rain is not interrupted by a dry season. However, the undergrowth at Fort Sherman was less dense. It is not completely understood why the undergrowth is thinner at Fort Sherman. One partial explanation is the thicker canopy at Fort Sherman may prevent sunlight to the undergrowth.

The vegetation/climate designation for El Valle is Montane Forest in a Tropical Upland climate. This area contained more broadleaf trees and fewer palms than the lowland sites. The El Valle site is of interest since it shows upland tropical climates (in

the 2,000 to 3,000 foot range) can present concealment rates approaching those of the jungle.

Data were collected from Panama twice. The first data collection coincided with the end of the worst drought in over 100 years. Because the vegetation appeared dry and sparse during the first data collection, data were collected a second time at the end of Panama's rainy season. Surprisingly, the visibility during the two trips was virtually equal. The differences in the fitted curves for the El Valle site for the two trips are less than 1 percent across all ranges. The vegetation parameters for the sites at Gamboa and Fort Sherman indicate that the vegetation was slightly denser the second trip. However, the difference was undistinguishable by the data collection team and was apparent only after the data were analyzed and plotted. The analysis showed that for the two visits, the difference between corresponding best fit curves, for any given range, was always less than 5 percent.

Panama (Monsoon Forest/Tropical Wet-Dry Climate). Three sites in close proximity, designated gam1, gam2, and gam3, were selected near the town of Gamboa. This is located on the Pacific Ocean side of Panama.

Other areas in the world with similar vegetation characteristics include the Pacific coasts of Honduras, Nicaragua, Costa Rica, and Panama; Haiti; the leeward portions of Puerto Rico and Cuba; northeast India, the border area between Viet Nam and China; northern Thailand, Laos, and Cambodia; northern Australia between 10 and 20 degrees south latitude; portions of eastern and southern Brazil, eastern Bolivia, and central Venezuela; and a large portion of subequatorial Africa including Angola, Zambia, northern Namibia, and Botswana.

- Number of Azimuths:

  gam1: 4

  gam2: 8

  gam3: 8

- Vegetation Types: Palms, vines, and some broadleaf trees
- Undergrowth Description: The undergrowth was not distinguishable from the trees
- Could a Tank Operate in This Area: No, very thick jungle vegetation

Panama (Tropical Rainforest/Tropical Wet Climate). The two sites at Fort Sherman are located on the Atlantic side of the country. The data were collected at sites named Skunk Hollow (skh1) and McKenzie Range (mck1).

Other areas in the world with similar vegetation characteristics include the Atlantic coasts of Honduras, Nicaragua, Costa Rica, and Panama; lowland portions of Guatemala, Belize, and portions of south-central Mexico; the Dominican Republic; the windward coasts of Puerto Rico and Cuba; northern Columbia, the interior and southeast coast of Brazil; Malaysia; most of Viet Nam; central Thailand; the

Philippines; most of Indonesia and southwest India; northeast coast of Australia; eastern Madagascar; the Congo; Gabon; and northern Zaire.

- Number of Azimuths:

  skh1: 5

  mck1: 7

- Undergrowth Description: The undergrowth was not distinguishable from the trees
- Could a Tank Operate in This Area: No, very thick jungle vegetation

Panama (Montane Forest/Tropical Uplands Climate). El Valle is a high altitude tropical environment located about 150 miles west of the Canal Zone. Data were collected at one site here.

Other areas in the world with similar vegetation characteristics include Nepal, Bhutan, southern China, inland New Guinea, and upland areas of Borneo and Sumatra; highlands of Kenya, Zaire, Tanzania, Malawi and central Ethiopia; central Peru and upland areas of Guatemala, Nicaragua, Costa Rica, and Honduras.

- Number of Azimuths: 6
- Vegetation Types: Mostly broadleaf trees. There were some evergreen trees in the general area, but none where the data were collected
- Undergrowth Description: The undergrowth was not distinguishable from the trees
- Could a Tank Operate in This Area: No, very thick jungle vegetation

Eglin Air Force Base (AFB), FL

Four sites from Eglin AFB were selected for data collection. The vegetation/climate designation for this area is Subtropical Broadleaf Evergreen Forest in a humid subtropical climate. The vegetation at Eglin AFB can be divided into two distinct types: Xeric and Baygall. Evergreen oaks with a thick canopy are typical of Xeric vegetation. Xeric vegetation is associated with dry, sandy soils. Baygall is characterized by dense, broadleafed evergreen shrubs and trees. Baygall typically occurs in wet soils such as depressions and floodplains. Sites representative of Xeric vegetation have been given an 'X' designation and sites representative of Baygall have been given a 'B' designation.

Other areas in the world with similar vegetation characteristics include the southern tip of South Korea, south Japan, and the southeast third of China; northern New Zealand, and portions of southeastern coastal Australia including the island of Tasmania.

egl_B2. This Baygall site was located on the northwest corner of Eglin AFB in a swampy area.

- Number of Azimuths: 8

- Undergrowth Description: Ferns, bushes, and tropical plants
- Could a Tank Operate in This Area: No, the trees are spaced too close together for a tank to operate

egl_X8. This Xeric site was located east of the main base in an area between state highway 20 and the Choctawhatchee Bay.

- Number of Azimuths: 7
- Undergrowth Description: Small bushes
- Could a Tank Operate in This Area: No, the trees are spaced too close together for a tank to operate

egl_X11. This Xeric site was located next to the Basin Bayou east of the Eglin AFB main base.

- Number of Azimuths: 7
- Undergrowth Description: Ferns, palms, vines, and tropical plants
- Could a Tank Operate in This Area: No, the trees are spaced too close together for a tank to operate

egl_B12. This Baygall site was located east of Eglin AFB in a swampy area south of a service road less than two miles north of the Choctawhatchee Bay.

- Number of Azimuths: 8
- Undergrowth Description: Small palms, small trees, and deadfall
- Could a Tank Operate in This Area: No, the trees are spaced too close together for a tank to operate

Fort Hood, TX

Four sites were selected on the Fort Hood military reservation. The vegetation/climate designation for this area is Tall Grass Prairie. There were three typical areas of sparse vegetation and one area with dense vegetation. The area of dense vegetation was selected to replicate a generic tropical environment. Data were collected at a time when it appeared funds would be unavailable to visit an actual tropical environment.

Other areas in the world with similar vegetation characteristics include Uruguay, eastern Argentina, eastern New Zealand, southeast Poland, eastern Hungary, and the Slovak Republic.

hood1. This site was located in the southeast portion of Fort Hood just south of Belton Reservoir. The vegetation is homogeneous and is representative of the majority of the post.

- Number of Azimuths: 6

- Undergrowth Description: Very sparse undergrowth made up of grasses and young trees (juniper)
- Could a Tank Operate in This Area: Yes, there is virtually no undergrowth and the trees are widely spaced

hood2. This site was located in the northwest portion of Fort Hood on some of the higher terrain on the post. There is a mix of vegetation common for Fort Hood.

- Number of Azimuths: 9
- Undergrowth Description: Sparse undergrowth made up of grasses
- Could a Tank Operate in This Area: Yes, there is virtually no undergrowth and the trees are widely spaced

hood3. This area was located in the northwest area of Fort Hood. It is an isolated area and is atypical because of the high density vegetation. There were places in the area so dense a soldier could not stand up straight. Data were collected early in the study when collecting data in a tropical climate seemed improbable. This site was selected to depict a tropical environment.

- Number of Azimuths: 6
- Undergrowth Description: Very thick. The undergrowth was made up of small trees and bushes
- Could a Tank Operate in This Area: No, the vegetation is too dense

hood4. The data collection team returned to the hood1 site and selected an area approximately 100 meters from hood1. This was done in order to attempt to replicate the data from the previous site.

- Number of Azimuths: 8
- Undergrowth Description: Very sparse undergrowth made up of grasses and young trees (scrub oak)
- Could a Tank Operate in This Area: Yes, there is virtually no undergrowth and the trees were widely spaced

Fort Carson, CO

Three areas from Fort Carson and one area from the Air Force Academy (AFA) were selected for data collection. The vegetation/climate designation for this area is Short Grass Prairie. The sites at Fort Carson contained medium density vegetation, while the AFA site provided a denser area of vegetation. All four sites were located at high altitudes (approximately 2,000 meters).

Other areas in the world with similar vegetation characteristics include parts of South Africa, interior Turkey, northern Iraq and Syria, parts of northern China, and in Russia from north of Mongolia west to the Black Sea at 50 degrees north latitude. The AFA site is similar to the higher elevations of north central China and the Caucasus area of northern Turkey.

car41. This site was along the western edge of Fort Carson in the foothills of the Rocky Mountains.

- Number of Azimuths: 9
- Undergrowth Description: Very sparse undergrowth made up of grasses
- Could a Tank Operate in This Area: Yes, there is virtually no undergrowth and the trees are widely spaced

car43. This site was along the southern part of Fort Carson on one of several plateaus.

- Number of Azimuths: 7
- Undergrowth Description: Very sparse undergrowth made up of grasses
- Could a Tank Operate in This Area: Yes, there is virtually no undergrowth and the trees are widely spaced

car28. This site was along the central portion of Fort Carson just west of the artillery impact area.

- Number of Azimuths: 8
- Undergrowth Description: Very sparse undergrowth made up of grasses and some deadfall
- Could a Tank Operate in This Area: Yes, but there would be limited mobility due to the density of low-branching trees (average "height of lowest branch" is 2 to 3 meters above the ground)

afa1. This area was located north of North-Gate Boulevard in the northeast portion of the AFA. All of the previous three sites represent Fort Carson vegetation very well. However, the AFA site provided a different vegetation type. Although Fort Carson and the AFA are located less than 10 miles apart and elevations are comparable, they exhibit very different vegetation and climate characteristics. While Fort Carson can be described as a Short Grass Prairie climate (or Steppe), the AFA is in an area which transitions to a boreal vegetation and climate zone. This is the result of the unique geography in the area causing increased rainfall and cooler temperatures.

- Number of Azimuths: 7
- Undergrowth Description: Very sparse undergrowth made up of grasses and small scrub oaks
- Could a Tank Operate in This Area: No, too many large trees are spaced closely together

Fort Hunter-Liggett, CA

Four sites from Fort Hunter-Liggett were selected for data collection. The vegetation/climate designation for this area is Sclerophyllous forest (better known as "chaparral") with a Mediterranean climate. The sites were primarily populated with old, widely scattered live oak, some grasses, and scrub.

Other areas in the world with similar vegetation characteristics include the Mediterranean region of Europe (southeast Spain, southern France (Riviera), Sicily, Corsica, Sardinia, all of coastal Italy inland to the Appenines, Greece and coastal Turkey), the North African coast from Libya to Morocco, and southwest Australia.

hl2. This site was located at the northern edge of Fort Hunter-Liggett at the boundary with the Los Padres National Forest.

- Number of Azimuths: 8
- Undergrowth Description: Very sparse undergrowth made up of grasses
- Could a Tank Operate in This Area: Yes, there is virtually no undergrowth and the trees are widely spaced; however, mobility would be impaired because tree limbs are about 2 meters above the ground

hl5. This site was located at the northwest part of Fort Hunter-Liggett.

- Number of Azimuths: 8
- Undergrowth Description: Very sparse undergrowth made up of grasses
- Could a Tank Operate in This Area: Yes, there is virtually no undergrowth and the trees are widely spaced; however, mobility would be impaired because tree limbs are about 2 meters above the ground

hl10. This site was located at the northeast edge of Fort Hunter-Liggett.

- Number of Azimuths: 8
- Undergrowth Description: Sparse undergrowth made up of grasses
- Could a Tank Operate in This Area: Yes, there is virtually no undergrowth and the trees are widely spaced; however, mobility would be impaired because tree limbs are about 2 meters above the ground

hl9. This site was located near the center of Fort Hunter-Liggett about 4 kilometers south of the main post area.

- Number of Azimuths: 6
- Undergrowth Description: Moderate undergrowth made up of grasses and several dead trees.
- Could a Tank Operate in This Area: Yes, there is some undergrowth but the trees are widely spaced. Mobility would be impaired because dead trees and tree limbs are about 2 meters above the ground

Fort Lewis, WA

Four areas from Fort Lewis were selected for data collection. The vegetation/climate designation for this area is Coastal Forest/Marine West Coast climate. All sites were densely vegetated.

Other areas in the world with similar vegetation characteristics include portions of the northwestern US, southern British Columbia, the western coast of Canada, and southeastern Alaska.

lew10. This site was along the east edge of Fort Lewis.

- Number of Azimuths: 6
- Undergrowth Description: Very dense undergrowth made up of small trees, ferns, shrubs, and deadfall
- Could a Tank Operate in This Area: No, the undergrowth is too thick for any type of vehicles; even dismounted units would have trouble with mobility in this area

lew19. This site was along the southwest corner of Fort Lewis just to the southwest of the artillery impact area.

- Number of Azimuths: 8
- Undergrowth Description: Very dense undergrowth made up of small trees, ferns, shrubs, and deadfall
- Could a Tank Operate in This Area: No, the undergrowth is too thick for any type of vehicles. Even dismounted units would have trouble with mobility in this area

lew3. This site was in the western part of Fort Lewis just east of the Nisqually River.

- Number of Azimuths: 8
- Undergrowth Description: Very dense undergrowth made up of small trees, ferns, shrubs, and deadfall
- Could a Tank Operate in This Area: No, the undergrowth is too thick for any type of vehicles. Even dismounted units would have trouble with mobility in this area

lew8. This site was along the east edge of Fort Lewis 2 kilometers north of lew10.

- Number of Azimuths: 8
- Undergrowth Description: Very dense undergrowth made up of small trees, ferns, shrubs, and deadfall
- Could a Tank Operate in This Area: No, the undergrowth is too thick for any type of vehicles. Even dismounted units would have trouble with mobility in this area

Fort Benning, GA

Four areas from Fort Benning were selected for data collection and are representative of the entire area. The vegetation/climate designation for this area is Southern Pine Forest in a temperate (warm summer/cool winter) climate. All of these

sites were selected in the central part of the training ranges to avoid impact areas and Army Training and Evaluation Program (ARTEP) training.

Other areas in the world with similar vegetation characteristics include the southeast and gulf coast regions of the US.

ben_T3. This site was located in a flat area between Selby Hill and Wadsworth Hill.

- Number of Azimuths: 5
- Undergrowth Description: Scrub oak, small trees and bushes, vines
- Could a Tank Operate in This Area: No, the trees are spaced too close together for a tank to operate

ben_L3. This site was located in a large flat area west of the Upatoi River.

- Number of Azimuths: 8
- Undergrowth Description: Small trees and bushes, deadfall
- Could a Tank Operate in This Area: No, the trees are spaced too close together for a tank to operate

ben_T4. This site was located south of Rockwell Hill just off First Division Road.

- Number of Azimuths: 8
- Undergrowth Description: Small trees and bushes
- Could a Tank Operate in this Area: No, the trees are spaced too close together for a tank to operate

ben_D12. This site was along the east edge of Fort Benning near the intersection of Hourglass Road and Buffalo Road.

- Number of Azimuths: 8
- Undergrowth Description: Small trees and bushes
- Could a Tank Operate in This Area: No, the trees are spaced too close together for a tank to operate

Great Smoky Mountains National Park, NC and TN

Four areas from the Smoky Mountains were selected for data collection. The vegetation/climate designation for this area is Midlatitude Deciduous Forest in a temperate (warm summer/cool winter) climate. The Smoky Mountains are located along the NC/TN border. This park was selected for data collection because its vegetation/climate are similar to those regions of Korea with pronounced monsoon (predominant rainfall influence) characteristics.

Other areas in the world with similar vegetation characteristics include most of South Korea, North Korea, the country of Georgia, portions of central Russia between

50 and 55 degrees north latitude, northern Iran, the Caucasus Mountains, England, Ireland, Wales, most of Scotland, France, northern Spain, most of Germany, most of the Czech Republic, western Hungary, Bulgaria, and southern Romania.

NC1. This site was to the northwest of the Cataloochee Divide. It is behind a gated area southwest of the ranger station and at the end of a long open field.

- Number of Azimuths: 7
- Undergrowth Description: Bushes, deadfall, and small elms and pines
- Could a Tank Operate in This Area: No, the trees are spaced too close together for a tank to operate

TN1. This site was located in the Greenbriar State Recreation Area of the Smoky Mountains approximately 8 miles east of Gatlinburg, TN. It is next to the Little Pigeon River and close to the ranger station.

- Number of Azimuths: 8
- Undergrowth Description: Ferns, deadfall, and small trees
- Could a Tank Operate in This Area: No, the trees are spaced too close together for a tank to operate

TN2. This area was to the southeast of Sugarlands on the northeast side of an old rock wall. This area was an agricultural area before the national park was established. The agriculture was abandoned and the area has been forested since the 1940s.

- Number of Azimuths: 7
- Undergrowth Description: Ferns, deadfall, and small trees
- Could a Tank Operate in This Area: No, the trees are spaced too close together for a tank to operate

TN3. This area was located at the northeast end of Big Springs Cove. It is located east of Laurel Creek Road in a recreational area.

- Number of Azimuths: 6
- Undergrowth Description: Deadfall and widely scattered small trees
- Could a Tank Operate in This Area: No, the trees are spaced too close together for a tank to operate

Willow Grove NAS, PA

Willow Grove NAS is located north of Philadelphia, PA. Four areas from Willow Grove NAS were selected for data collection. The vegetation/climate designation for this area is Midlatitude Deciduous Forest in a temperate (warm summer/cool winter) climate. This area was selected for data collection because its vegetation/climate are similar to those regions of Korea with less pronounced monsoon (predominant temperature influence) characteristics.

Other areas in the world with similar vegetation characteristics include most of South Korea, North Korea, the country of Georgia, portions of central Russia between 50 and 55 degrees north latitude, northern Iran, the Caucasus Mountains, England, Ireland, Wales, most of Scotland, France, northern Spain, most of Germany, most of the Czech Republic, western Hungary, and southern Romania.

WG6. This site was located at the former US Naval Air Development Center. It is located in a wooded area south of the eastern end of the runway.

- Number of Azimuths: 6
- Undergrowth Description: Bushes, vines, and thick grass
- Could a Tank Operate in This Area: Probably, the trees are spaced far enough apart for a tank to operate in this area

WG2. This site was located at a corner near the picnic area at Willow Grove NAS.

- Number of Azimuths: 7
- Undergrowth Description: Bushes and vines
- Could a Tank Operate in This Area: No, the trees are spaced too close together for a tank to operate

WG5. This area belongs to the town of Willow Grove. The site selected was just north of the police firing range.

- Number of Azimuths: 7
- Undergrowth Description: Bushes, vines, small trees, and thick grass
- Could a Tank Operate in This Area: No, the trees are spaced too close together for a tank to operate

WG4. This area belongs to the city of Willow Grove. It was located southwest of the Graeme Historical Site.

- Number of Azimuths: 6
- Undergrowth Description: Bushes and vines
- Could a Tank Operate in This Area: No, the trees are spaced too close together for a tank to operate

Natchaug State Forest, CT

Four areas from Natchaug State Forest were selected for collection. Natchaug State Forest is made up of small, disjointed parcels of land scattered about the northeast portion of the state. The vegetation/climate designation for this area is Midlatitude Deciduous Forest in a temperate (cool summer/cold winter) climate. This park was selected for data collection because its vegetation/climate are similar to those regions of Bosnia and the former Yugoslavia which are closer to the Adriatic coast.

Other areas in the world with similar vegetation characteristics include most of South Korea, North Korea, the country of Georgia, portions of central Russia between 50 and 55 degrees north latitude, northern Iran, the Caucasus Mountains, England, Ireland, Wales, most of Scotland, France, northern Spain, most of Germany, most of the Czech Republic, western Hungary, Bulgaria, and southern Romania.

Nat2. This site was located north of Summer Lane west of an old rock wall.

- Number of Azimuths: 4
- Undergrowth Description: Ferns, small shrubs, and deadfall
- Could a Tank Operate in This Area: No, the trees are spaced too close together for a tank to operate

Nat1. This site was located at the end of Laurel Lane to southwest of a recreational vehicle park.

- Number of Azimuths: 6
- Undergrowth Description: Ferns, mountain laurel, and deadfall
- Could a Tank Operate in This Area: No, the trees are spaced too close together for a tank to operate

Nat4. This site was located west of Pumpkin Road.

- Number of Azimuths: 8
- Undergrowth Description: Ferns, scattered small shrubs, and deadfall
- Could a Tank Operate in This Area: No, the trees are spaced too close together for a tank to operate

Nat5. This site was located north of Station Road.

- Number of Azimuths: 5
- Undergrowth Description: Mostly ferns with some small trees
- Could a Tank Operate in This Area: No, the trees are spaced too close together for a tank to operate

Fort Drum, NY

Four areas from Fort Drum were selected for data collection. The vegetation/climate designation for this area is Mixed Boreal and Deciduous Forest in a temperate (cool summer/cold winter) climate. Fort Drum was selected as a data collection location because its vegetation/climate are similar to those regions in the interior of Bosnia and adjacent portions of former Yugoslavia. The data collection was limited to the southern portion of Fort Drum because a large ice storm in January 1998 destroyed or changed the typical vegetation for most of the fort.

Other areas in the world with similar vegetation characteristics include southern Chile, northeast China, northern Japan, Estonia, Latvia, Lithuania, most of

Switzerland, western Austria, southeastern Germany, western regions of the Czech Republic, southern Poland, and northern Romania.

8C. This site was located near Lake School Road.

- Number of Azimuths: 8
- Undergrowth Description: Ferns, small trees, and deadfall
- Could a Tank Operate in This Area: No, the trees are spaced too close together for a tank to operate

7G. This site was located in a large flat area just north of Ward Hill.

- Number of Azimuths: 8
- Undergrowth Description: Ground cover, small trees, and deadfall
- Could a Tank Operate in This Area: No, the trees are spaced too close together for a tank to operate

7B. This site was located north of a park north of state highway 3A.

- Number of Azimuths: 8
- Undergrowth Description: Bushes and small trees
- Could a Tank Operate in This Area: No, the trees are spaced too close together for a tank to operate

7E. This site was located north of Barr Hill just south of state highway 3A.

- Number of Azimuths: 6
- Undergrowth Description: Ferns, small trees, deadfall, and ground cover
- Could a Tank Operate in this Area: No, the trees are spaced too close together for a tank to operate

Gagetown Canadian Forces Base, New Brunswick, Canada

Four areas from Gagetown were selected for data collection in order to assist the Canadian modeling and simulation program. The vegetation/climate designation for this area is Mixed Boreal and Deciduous Forest in a temperate (cool summer/cold winter) climate.

Other areas in the world with similar vegetation characteristics include southern Chile, northeast China, northern Japan, Estonia, Latvia, Lithuania, most of Switzerland, western Austria, southeastern Germany, western regions of the Czech Republic, southern Poland, and northern Romania.

Gage31. This site was located on McCutcheon Road south of the impact area.

- Number of Azimuths: 5
- Undergrowth Description: Mostly ferns with some deadfall

- Could a Tank Operate in This Area: No, the trees are spaced too close together for a tank to operate

Gage27. This site was located on the southeast corner of the post near the Saint John River.

- Number of Azimuths: 7
- Undergrowth Description: Ferns, small trees, and deadfall
- Could a Tank Operate in This Area: No, the trees are spaced too close together for a tank to operate

Gage8. This site was located along Shirley Road in the northeast portion of post.

- Number of Azimuths: 8
- Undergrowth Description: Small trees and ferns
- Could a Tank Operate in This Area: No, the trees are spaced too close together for a tank to operate

Gage7. This site was located along Shirley Road in the northeast portion of post.

- Number of Azimuths: 6
- Undergrowth Description: Small trees
- Could a Tank Operate in This Area: Possibly, the trees are scattered in spots and thin

Fort Greely, AK

Six areas from the eastern half of Fort Greely were selected for data collection. The vegetation/climate designation for this area is Boreal Forest/Taiga. The vegetation at Fort Greely can be equally divided into three distinct types: evergreen, deciduous, and mixed. The evergreen areas are exclusively black spruce. The deciduous areas are white birch or aspen. There were also areas at Fort Greely with a mixture of evergreen and deciduous trees. Data were collected at two areas for each of the three vegetation types. Sites G05 and G02 were located along 33 Mile Loop, sites G22 and G00 were located along the main supply route (MSR), and sites G24 and G25 were located close to the main post.

Other areas in the world with similar vegetation characteristics include northern Canada, mountainous areas of the western US, central Alaska, Finland, Sweden, the Swiss/Italian Alps, coastal Norway, northern Japan, western and central Russia between 55 and 65 degrees north latitude, the pacific coast of Russia, portions of western China (including Tibet and the Himalayan region), high altitude areas of Indonesia, upland areas of northern Peru, northern Chile, Bolivia, Argentina, and the Atlas mountains of Africa.

G22. This site was located south of the main post near a pumping station and next to the MSR road.

- Number of Azimuths: 6
- Undergrowth Description: Small deciduous bushes
- Could a Tank Operate in This Area: No, the trees are spaced too close together for a tank to operate

G00. This site was located at the southern portion of Fort Greely next to the MSR road.

- Number of Azimuths: 7
- Undergrowth Description: Small black spruce and deadfall
- Could a Tank Operate in This Area: No, the trees are spaced too close together for a tank to operate

G25. This site was located about 1 kilometer south of the main housing area at Fort Greely.

- Number of Azimuths: 8
- Undergrowth Description: Small spruce, deadfall, and small bushes
- Could a Tank Operate in This Area: No, the trees are spaced too close together for a tank to operate

G02. This site was located east of Jarvis Creek and west of Buffalo Drop Zone.

- Number of Azimuths: 8
- Undergrowth Description: Small spruce, shrubs, and deadfall
- Could a Tank Operate in This Area: No, the trees are spaced too close together for a tank to operate

G24. This site was located east of the housing area and west of Jarvis Creek.

- Number of Azimuths: 8
- Undergrowth Description: Small spruce and deadfall
- Could a Tank Operate in This Area: No, the trees are spaced too close together for a tank to operate

G05. This site was located along 33 Mile Loop north of the Eddy Landing Zone/Drop Zone.

- Number of Azimuths: 8
- Undergrowth Description: Small spruce and deadfall
- Could a Tank Operate in This Area: No, the trees are spaced too close together for a tank to operate

Appendix C. Climates

Introduction

Climate may be defined as a composite of the long-term prevailing weather occurring at a location. It is the normal reoccurring weather pattern, with some small variations perhaps, from year to year. This appendix discusses the different climate types evaluated in this study. It is not the intent within this section to provide a climate primer with very detailed climate definitions but rather to offer a general guide to facilitate ease of use by model developers.

Climate Types

The earliest climatic classification schemes were based solely on temperature. The early Greeks divided the world into three zones – torrid, temperate, and frigid. Throughout the centuries this scheme was modified by others to reflect seasonal variations of temperature – e.g., cool summers, warm summers, warm winters, cold winters, etc. Precipitation was then added to the classification to reflect the moisture characteristics of regions. This was especially true in the differentiation of arid climates. Classifications based on these two elements, temperature and precipitation (moisture), are the most numerous in the literature; the schemes of Köppen and Trewartha are the dominant ones in use today. Other classifications have added additional elements (e.g., solar radiation, air mass frequencies, evaporation, etc.) to further define and subdivide regions based on similar climate characteristics. Many classification schemes have as their basis the regional distribution of natural vegetation. Listed from the equator to the poles, they are: tropical, dry, subtropical, temperate, boreal, and polar. Most have significant subdivisions, which are also discussed.

Tropical Climates

Tropical climates (sometimes referred to as ***Equatorial*** climates) are found straddling the equator generally between 23.5 degrees north (N) latitude (Tropic of Cancer) and 23.5 degrees south (S) latitude (Tropic of Capricorn). They tend to be somewhat wider on the eastern side of continents than on the western side. These climates cover about 25 percent of the surface of the land. Areas within the tropical climates experience frost-free conditions year-round and each month has an average temperature of over 65° Fahrenheit (F) (18° Celsius (C)). In addition to warm temperatures, the yearly rainfall is generally over 70 inches and can be substantially more (over 100 inches). The tropical climates can be divided into two subtypes: ***tropical wet*** and ***tropical wet-and-dry***.

The ***tropical wet*** climate (sometimes referred to as the *tropical rainforest* climate) is located primarily between 10°N and 10°S latitude and resides in the region

under the influence of the *intertropical convergence zone* (ITCZ). The ITCZ represents the boundary between the northeast and southeast trade winds. Areas experiencing the tropical wet regime account for about 10 percent of the land surface of the earth. Temperatures within this region exhibit little variation from day to day and from month to month. Although the region as a whole has abundant precipitation throughout the year (greater than 70 inches), there are locations experiencing short dry seasons that last for less than 2 months.

The ***tropical wet-and-dry*** climate is found poleward of the tropical wet climate, extends to approximately 20°N and 20°S, and accounts for approximately 15 percent of the land surface of the earth. Regions with this type climate alternate throughout the year between the influences of the wetter ITCZ and the more stable, drier subtropical anticyclones (areas of high pressure). The tropical wet-and-dry region has a dry season of more than 2 months and the typical annual rainfall is usually between 40 and 60 inches. Temperatures are similar to those experienced in the tropical wet climatic regions. In addition to the two major divisions of the tropical climate, the tropical wet-and-dry subdivision can be further divided into a ***tropical upland wet-and-dry*** climate. This climate is defined as having elevations of greater than 610 meters (2,000 feet). This differs from tropical wet-and-dry because its higher elevations typically produce lower temperatures.

The data collected in Panama represent all three of the tropical climates. Gamboa is a tropical wet-and-dry climate, Fort Sherman is a tropical wet climate, and El Valle is a tropical upland wet-and-dry climate.

Dry Climates

Dry climates are defined as areas where the annual water loss through evaporation exceeds the annual water gain through precipitation. These climates can be found at almost every latitude and make up approximately 25 percent of the land surface of the earth. They extend from north of the tropical wet-and-dry up to the vicinity of the Arctic Circle (66.5°N latitude). At lower latitudes, dry climates are caused by the dominance of the subtropical anticyclones, which produce generally clear skies. Moving northward, they are found in the interior of continents far away from moisture sources. Dryness here may also be accentuated by mountain ranges producing a rainshadow effect. These more northerly dry areas typically have warmer summers and colder winters than other climates at the same latitude. Dry climates can be subdivided into ***desert*** and ***semiarid*** (***steppe)*** subclimates. Desert climates experience an annual rainfall of 10 inches or less, whereas areas of semiarid climate have annual amounts in the range of 15-25 inches. Semiarid climates (also referred to as ***grassland*** climates) can also be further broken down into tall-grass and short-grass varieties (steppe).

Data collected at Fort Hood (tall-grass) and Fort Carson (short-grass/steppe) represent a dry climate. No data were collected for a desert climate.

Subtropical Climates

Subtropical climates are characterized as having definite seasonal rhythms creating a summer and a winter. Most of the subtropics are subject to an occasional killing frost. Eight months will have an average temperature of over 50 degrees. The subtropics can be divided into two sub-climates: ***subtropical dry-summer*** climate, often called a ***Mediterranean*** climate and ***subtropical humid*** climate, which is also known as ***humid subtropical***. The Mediterranean climate is typically located in the middle latitudes at approximately 30-40° latitude and along the western sides of continents. This is a transitional climate, lying between the low-latitude dry climates to the south and the cool, moist marine climates further north. This climate has almost no severe cold weather during the winter season. Average winter temperature are generally between 40 and 50°F (4.5 and 10°C). Summers can be hot, with average summer temperatures between 65 and 80°F (18 and 21°C). The average annual rainfall is usually 15-25 inches with the bulk falling during the winter months.

The subtropical humid climate differs from the Mediterranean climate because it is located on the eastern side of continents, has more annual rainfall (30-60 inches), and the rain falls throughout the year with a maximum occurring during the summer months. The average winter temperature is between 40 and 55°F (4.5 and 12.8°C) and average summer temperatures range from 75 to 80°F (24 to 26.6°C).

Data collected at Fort Hunter-Liggett represents a Mediterranean climate and data collected at Eglin AFB represents a subtropical humid climate.

Temperate Climates

A ***temperate*** climate is defined as an area where average temperatures are over 50 degrees for four to eight months. There are two subclimates: the ***temperate oceanic*** and the ***temperate continental***. The temperate oceanic, often referred to as ***Marine West Coast***, exhibits milder temperature conditions than does the temperate continental. Winters are warmer and summers are cooler than for more continental locations at the same latitude. All months average above freezing. The average rainfall in the temperate oceanic climate varies widely (between 20 and 150 inches), but it is considered to have adequate rainfall for all seasons.

Locations with a temperate continental climate have most of their annual rainfall (20 to 60 inches) during the summer months. This climate can be further subdivided into two more groups: a) temperate continental with warm summer and cool winter and b) temperate continental with a cool summer and a cold winter. An average summer temperature of 72°F (22°C) is used to distinguish between the two subgroups.

Fort Lewis was used to represent the temperate oceanic climate. The temperate continental (warm summer and cool winter) data were collected at the Smoky Mountains, Willow Grove NAS, and Fort Benning. The temperate continental (cool

summer and cold winter) data were collected at Fort Drum, Natchaug State Forest, and Gagetown (Canada).

Boreal Climate

Boreal climates, sometimes referred to as ***Continental Subarctic*** or ***Subpolar*** climates, are normally restricted to between 50 and 65 degrees latitude (or high elevations at lower latitudes). They will have an average monthly temperature of at least 50°F (10°C) for 1 to 3 months. The average annual rainfall is usually less than 20 inches and falls during the short summer. The transition zone at which large woody vegetation can no longer exist is known as the "tree line." These zones (also referred to a taiga or alpine tundra) usually occur within the fringes of the boreal climate.

Data were collected at Fort Greely to represent boreal and taiga climates.

Polar Climate

Polar climates, sometimes referred to as ***Ice*** climates or ***Tundra*** climates, exist when the average monthly temperature never reaches 50°F (10°C). The average annual precipitation is meager; most stations receive less than 8 to 10 inches. This climate type is usually divided into an area possessing tundra vegetation (mosses, lichen, and small plants) and one possessing a permanent ice cap.

The absence of a growing season dictated data would not be collected in a polar climate.

Appendix D. Vegetative Sub-Biome Descriptions

This appendix contains definitions and descriptions of the vegetative sub-biomes representing the 15 field data collection locations. Each sub-biome is usually linked to a specific climate (although some occur in multiple climates) with a unique set of vegetation types and patterns. This appendix provides a general guide to typical vegetation and characteristics expected to occur at each vegetative sub-biome location. It is intended to facilitate ease of use by model developers. Figure D-1 (found at the end of this appendix) provides a world map delineated by sub-biome type. The abbreviations after each section heading represent the sub-biome designations identified in figure D-1. While the world is divided into 27 sub-biomes, this appendix concentrates on only the 13 where data were collected. Table D-1 (found at the end of this appendix) provides an alphabetized list of global locations (by continent and country), their corresponding vegetative sub-biomes, and a short discussion regarding the 14 sub-biomes omitted from the study.

Tropical Rainforest (Fe)

Tropical Rainforest consists of closely set trees whose crowns form a continuous canopy of foliage and provide dense shade for the ground and lower layers. The floor of the tropical rainforest is usually densely shaded and plant foliage is often sparse close to the ground. Further up, tree leaves are large and evergreen. Crowns of the trees tend to form into two or three layers, of which the highest layer consists of scattered emergent crowns rising to 40 meters and protruding conspicuously above a second layer, 15 to 30 meters high, which is continuous. A third, lower layer consists of small, slender trees 5 to 15 meters in height with narrow crowns. Typical in this vegetation are thick, woody vines and epiphytes (ferns, orchids, mosses, etc.) supported by the trunks, branches, and foliage of the trees. These vines and ferns often occur in the lower layers of vegetation near the ground, hampering movement and visibility. Another particularly important characteristic of the tropical rainforest is the large number of tree species coexisting; as many as 1,000 species may be found in a square kilometer.

Monsoon Forest (Fmo)

Monsoon Forest presents a more open tree growth than the tropical rainforest. Consequently, there is a greater development of vegetation in the lower layers. Maximum tree heights range from 12 to 35 meters and tree trunks are massive. Branching starts at low levels (compared to the tropical forest) and produces large, round crowns. Many tree species are present and may number 30 to 40 in a small tract. One of the most important aspects of the monsoon forest is the deciduous nature of the tree species present. The shedding of leaves results from the stress of a pronounced dry season occurring at a time of low sun and cooler temperatures. Thus, the monsoon forest in the dry season has a somewhat dormant appearance. Vines and ferns are locally abundant but are fewer and smaller than in the tropical rainforest.

Undergrowth is often a dense shrub thicket. However, where second growth vegetation has formed, the undergrowth is typically jungle.

Montane Forest (Fmt)

Montane Forest exists in regions of tropical rainforest where island-like highlands of cooler climate are found. Between 600 meters and 2,000 meters above sea level, the rainforest gradually changes in structure. Montane Forest has lower tree heights and a less dense canopy than tropical rainforests of adjacent lowlands. Due to the sparse canopy, undergrowth can be very dense and tree ferns and bamboo are numerous.

Broadleaf Evergreen Forest (Fbe)

Broadleaf Evergreen Forest differs from tropical rainforests in having relatively few species of trees. Thus, there are large populations of individuals of a species. Trees are shorter than in the tropical rainforests, the leaves tend to be smaller and more leathery, and the leaf canopy is less dense. Broadleaf evergreen forests tend to have a well-developed lower stratum of vegetation including tree ferns, small palms, bamboo, shrubs, and herbaceous plants. Vines, ferns, and mosses are abundant. An example is the "spanish moss" draping many oak and cypress trees on the Gulf Coast of the southeastern US.

Tall Grass Prairie (Gp)

Tall Grass Prairie consists of tall grasses comprised of dominant herbs and subdominant herbaceous plants. Trees and shrubs are generally sparse, but may occur as forest or woodland patches in valley bottoms or other locations. The grasses are deeply rooted and may form a continuous and dense cover. The grasses peak in spring and the herbaceous plants peak in late summer. In North America, areas of deciduous forest are mixed with areas of tall grass prairie over a large transition belt from the Dakotas to central Texas. The Pampa region of Argentina in South America and the Puszta region of eastern Europe (eastern Hungary/Slovak Republic) are other examples of tall grass prairie.

Short Grass Prairie (Gs)

Short Grass Prairie (also known as Steppe) is comprised of many species of short grasses and herbs occurring in sparsely distributed clumps or bunches. Scattered shrubs and low trees may also be found in the steppe. Ground coverage is small and much bare soil is exposed. Steppe grades into semi-desert in dry environments, into tall grass prairie where rainfall is more abundant, or may give way to deciduous/coniferous forest at higher elevations or latitudes. Steppe vegetation is largely concentrated in vast mid-latitude areas of North America (western plains to the front range of the Rocky Mountains) and Eurasia. Steppe grasses peak in early summer and are usually dormant by mid-summer, although occasional summer rainstorms may cause periods of revived growth.

Sclerophyllous Forest (Also Called Mediterranean/Chaparral Vegetation) (Fss)

Sclerophyllous Forest consists of low trees with small, hard, leathery leaves. Typically, the trees are low-branched and gnarled, with thick bark and canopy coverage of only 25 to 60 percent. Some of this is woodland consisting of "live oak," "white oak," and other similar species. There may also be extensive areas of Sclerophyllous scrub or "dwarf forest/chaparral" having a canopy closure of under 50 percent. This chaparral varies in composition with elevation and exposure. The trees and shrubs are predominantly evergreen; their thickened leaves being retained despite a severe annual drought. There is little stratification in the Sclerophyllous forest and scrub, although there may be a significant grass layer providing substantial ground cover.

Needleleaf/Coniferous Forests

Needleleaf or Coniferous Forests are composed of largely straight-trunked, conical trees with relatively short branches and small, needlelike leaves. Usually evergreen, the coniferous forest provides continuous and deep shade to the ground so lower layers of vegetation are often sparse, except for a thick layer of mosses or ferns in many places. Species are few and large tracts of forest may consist almost entirely of one or two species. Three sub-biomes of the coniferous forest were evaluated during the course of this study. They are described below.

Southern Pine Forest (Fsp)

The Southern Pine Forest consists of a number of different pine species. It is found in the sandy soils comprising much of the coastal fringe of the southeastern US. It is a specialized vegetation type thriving on fast-draining soils and frequent fires. The incidence of fire plays a major role in the stratification of the forest. Undergrowth can range from very thick in areas where fire has significantly opened the canopy to sparse in areas untouched by fire.

Coastal Forest (Fc)

This forest is found in the coastal regions of southeastern Alaska, western Canada, and the northwestern US. Under a heavy regimen of rainfall and prevailing high humidity, these areas have the densest of all coniferous forests. Coastal Redwood, Sequoia, and Douglas Fir predominate and are remarkable in their size and girth. Individual trees can attain heights over 100 meters and girths of over 20 meters. Although canopy closures average over 80 percent, high moisture budgets may result in a thick understory of ferns and mosses. These are especially prevalent on the myriad deadfall often littering the forest floor.

Boreal and Mixed Deciduous/Boreal Forest (Fbo/Fbd)

Boreal forest predominates in two great continental belts, one in North America and one in Eurasia between the latitudes of 45 and 75 degrees. It is predominantly composed of evergreen conifers such as spruce, fir, and pine. Deciduous trees such as aspen, poplar, willow, and birch tend to take over rapidly in stream beds or open areas and in portions of the boreal forest which have been burned. These open areas may have a well-developed shrub and/or moss layer. Mixed forest is common in the transition zones between the midlatitude and northern forest types and occurs partly in response to a cool summer season.

Midlatitude Deciduous Forest (Fd)

Midlatitude Forests are dominated by tall, broadleaf trees typically providing a continuous and dense canopy in summer, but shedding their leaves completely in the winter. Lower layers of small trees and shrubs are weakly developed. Predominant species are oak, beech, birch, and elm. Undergrowth is usually thick early in the growing season but is later reduced depending on the amount of tree foliage and subsequent shade. Undergrowth may be much more prominent in poorly drained areas and conifers readily develop as dense second growth vegetation once deciduous forests have been cleared. The deciduous forest is almost entirely limited to the midlatitude landmasses of the northern hemisphere.

World Vegetative Sub-Biomes by Continent and Country

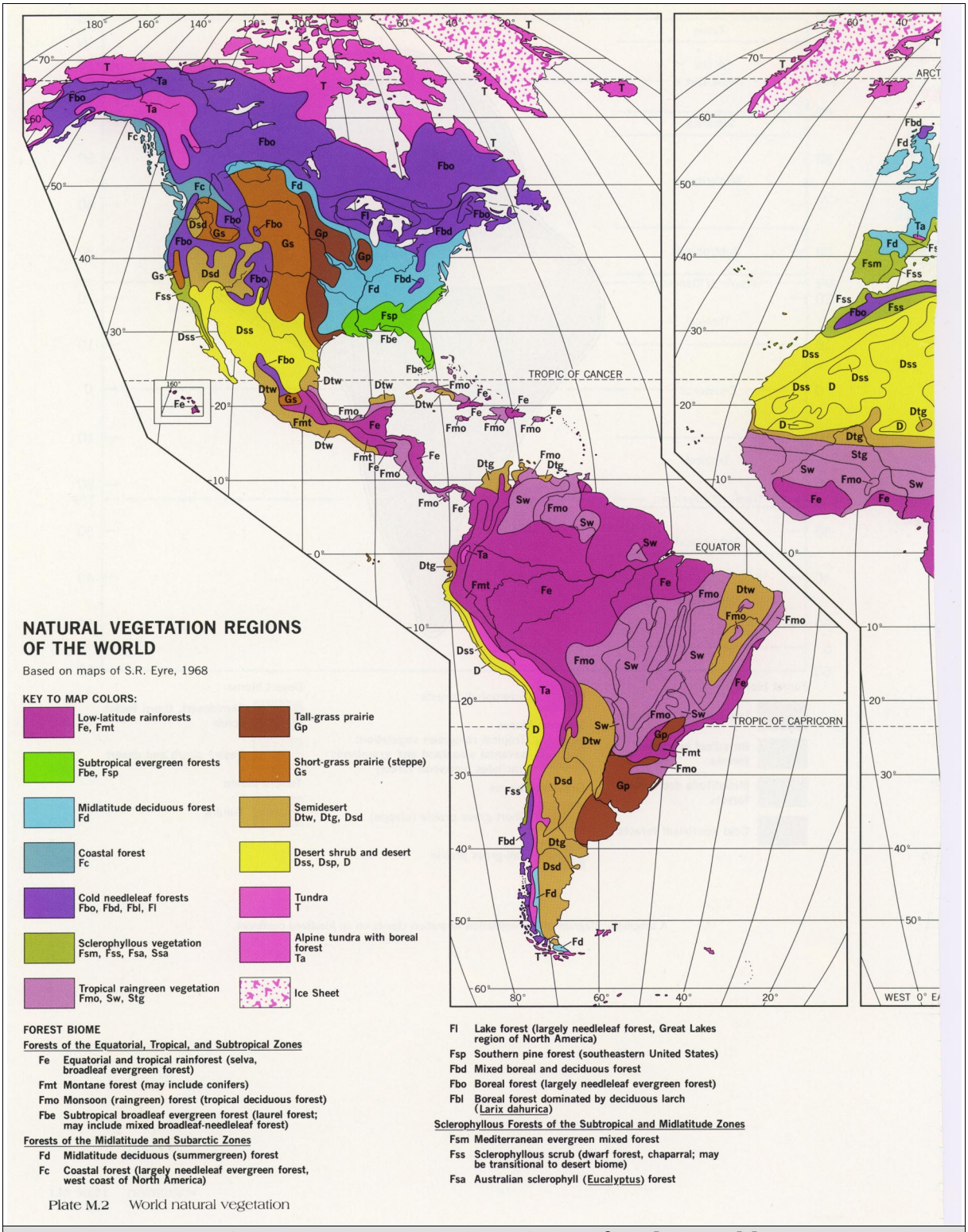

Figure D-1a. Vegetation Biomes for the World

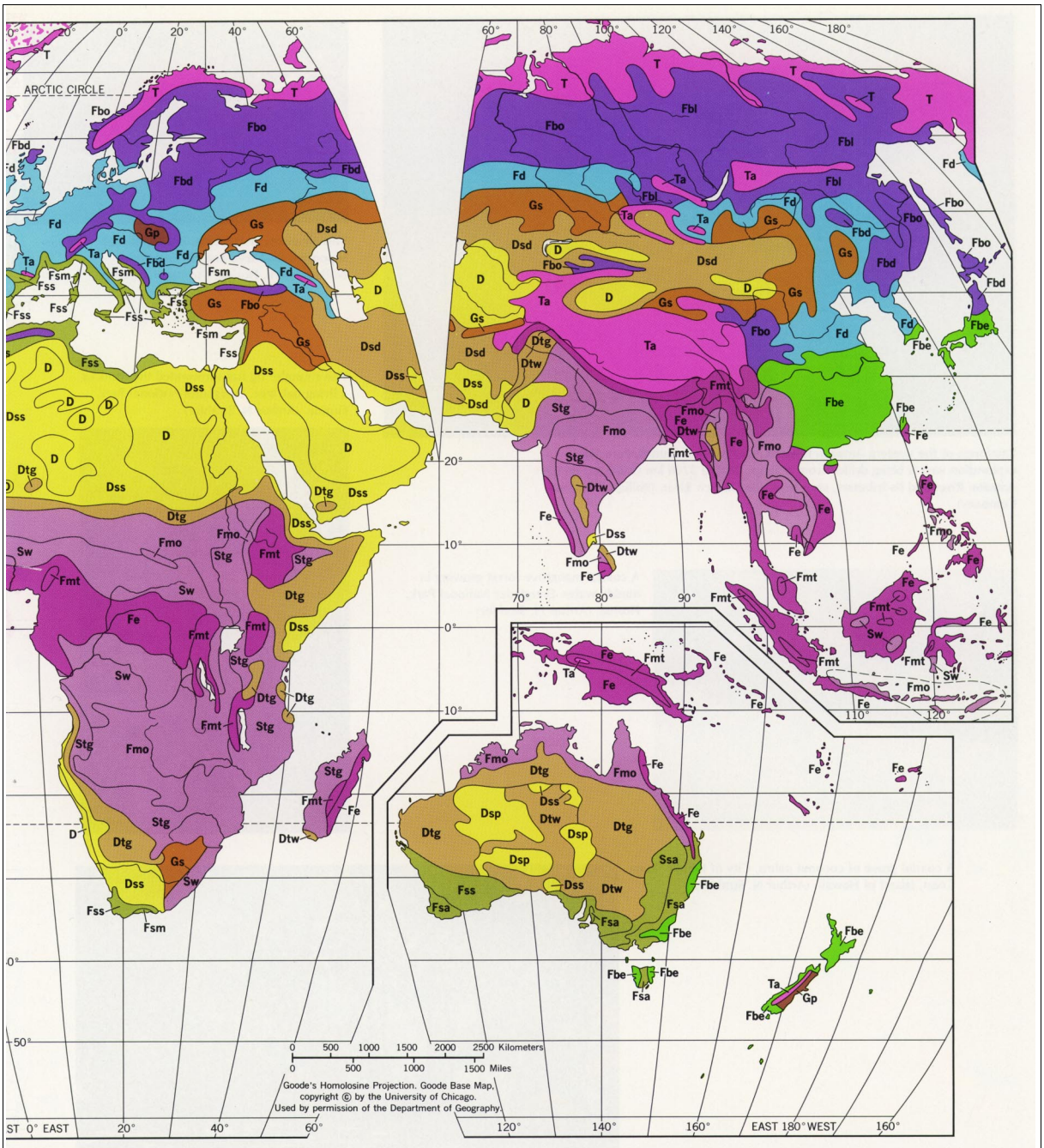

Figure D-1b. Vegetation Biomes for the World

key: (* - not evaluated in study; **represented in study**)

D – Desert*
Dsd – Semidesert scrub and woodland*
Dsp – Desert alternating with grass semidesert*
Dss – Semidesert scrub*
Dtg – Thorntree-desert grass savanna*
Dtw – Thorn forest and woodland (transitional to forest)*
Fbd – Mixed boreal and deciduous forest
Fbe – Subtropical broadleaf evergreen forest
Fbo/Fbl **– Boreal forest**/Boreal forest (larch dominant)
Fc – Coastal forest
Fd – Midlatitude deciduous forest
Fe – Tropical rainforest
Fl – Lake forest*
Fmo – Monsoon forest
Fmt – Montane forest
Fsa – Australian eucalyptus forest*
Fsm – Mediterranean evergreen mixed forest*
Fsp – Southern pine forest
Fss – Sclerophyllous scrub (dwarf forest/chaparral)
Gp – Tall-grass prairie
Gs – Short-grass prairie (steppe)
Ssa – Australian Sclerophyllous tree savanna*
Stg – Thorntree-tall grass savanna*
Sw – Savanna woodland*
T – Arctic tundra*
Ta – Alpine tundra (includes boreal forest); also known as taiga

The following biomes were not evaluated because of lack of vegetation: D, Dsd, Dss, Dsp, and T. The Fl and Fbl were not evaluated because they exist in unique areas (the Great Lakes area and northern Siberia) where the US Army is unlikely to deploy soldiers. The remainder of the unevaluated areas exist only in OCONUS and were not evaluated because of cost.

Table D-1. World Vegetative Sub-Biomes by Continent and Country

Asia

Country	**Sub-Biome(s)**
Afghanistan	D, Dsd, **Gs**
Bahrain	Dss
Bangladesh	**Fe, Fmo**
Bhutan	**Fmt, Ta**
Brunei	**Fe**
Burma	**Fe, Fmt, Fmo**, Dtw
Cambodia	**Fe, Fmo**
Ceylon	**Fe, Fmo**, Dtw
China	D, Dsd, Fbl, **Fbo**, **Gs, Fbd, Fbe**, **Fe, Fmo, Fmt, Ta**
Cyprus	Fsm
India	D, Dss, Dtw, Stg, **Fmt, Fmo, Fe**
Indonesia	Sw, **Fe, Fmo, Fmt, Ta**
Iran	Dss, Dsd, **Fd**
Iraq	Dss, **Gs**
Israel	Dss, **Fss**
Japan	**Fbe, Fbd, Fbo**
Jordan	Dss
North Korea	**Fd, Fbd**

Table D-1. World Vegetative Sub-Biomes by Continent and Country (Continued)

Asia

Country	Sub-Biome(s)
South Korea	**Fd, Fbe**
Kuwait	Dss
Laos	**Fe, Fmo**
Lebanon	**Fss, Gs**
Malaysia	**Fe, Fmt**
Maldives	**Fe**
Mongolia	**Fd, Ta, Gs**, D, Dsd
Nepal	**Fmt, Ta**
Oman	D, Dss
Pakistan	D, Dss, Dsd, Dtw, Dtg, **Fmt, Ta**
Philippines	**Fe, Fmo**
Qatar	Dss
Saudi Arabia	D, Dss
Syria	Dss, **Gs, Fss**
Taiwan	**Fe, Fbe**
Thailand	**Fe, Fmo**
Turkey	Fsm, **Fss, Fbo, Fd, Gs**
Former USSR (east of Ural Mountains)	D, Dsd, **Gs, Fd**, Fbl, **Fbd, Fbo, Ta,** T
United Arab Emirates	D, Dss
Vietnam	**Fe, Fmo, Fbe**
Yemen	Dss, Dtg

Africa

Country	Sub-Biome(s)
Algeria	D, Dss, **Fss, Fbo**
Angola	D, Dss, Dtg, Stg, Sw, **Fmo**
Benin	**Fe, Fmo**, Sw
Botswana	Dtg, Stg, **Fmo**
Burundi	**Fmt**, Sw
Cameroon	**Fmt, Fe**, Sw
Central African Republic	**Fmo, Fe**, Sw, Stg
Chad	D, Dss, Dtg, Stg, Sw
Congo	**Fe**, Sw
Djibouti	Dss
Egypt	D, Dss
Ethiopia	Dss, Dtg, Stg, **Fmt, Fmo**
Gabon	**Fe**, Sw
Gambia	Sw
Ghana	**Fe**, Sw
Guinea	Sw
Ivory Coast	**Fe**, Sw
Kenya	Dss, Dtg, Stg, **Fmt**
Lesotho	**Gs**, Sw
Liberia	**Fe**, Sw
Libya	**Fss**, D, Dss
Madagascar	Dtw, **Fe, Fmt**, Stg
Malawi	**Fmt**, Stg
Mali	D, Dss, Dtg, Stg, Sw
Mauritania	D, Dss, Dtg, Stg
Morocco	Dss, **Fbo, Fss**
Mozambique	**Fmo**, Stg
Namibia	D, Dss, Dtg, Stg, **Fmo**
Niger	D, Dss, Dtg, Stg

Table D-1. World Vegetative Sub-Biomes by Continent and Country (Continued)

Africa

Country	Sub-Biome(s)
Nigeria	**Fe**, Sw, Stg
Rwanda	**Fmt**, Sw
Senegal	Dtg, Sw
Sierra Leone	**Fe**, Sw
Somalia	Dtg, Dss, Stg
South Africa	D, Dss, Dtg, Fsm, **Fss, Gs**, Stg, Sw
Sudan	D, Dss, Dtg, Stg, Sw
Swaziland	**Gs**, Sw
Tanzania	Dtg, Stg, **Fmt**
Togo	**Fe, Fmo**, Sw
Tunisia	D, **Fss**
Uganda	**Fmt**, Stg, Sw
Upper Volta	**Fmo**, Stg
Zaire	**Fe, Fmo, Fmt**, Sw
Zambia	**Fmo, Fmt**
Zimbabwe	**Fmo**, Stg

Europe

Country	Sub-Biome(s)
Albania	Fsm, **Fd, Fbd**
Andorra	**Ta**
Austria	**Fd, Fbd**
Belgium	**Fd**
Bulgaria	**Fd, Fbd**
Czech Republic	**Fd, Fbd**
Denmark	**Fd**
Finland	**Fbd, Fbo**, T
France	Fsm, **Fd, Ta**
Germany	**Fd, Fbd**
Gibraltar	Fsm
Greece	**Fss, Fd**
Hungary	**Gp, Fd**
Iceland	T
Ireland	**Fd**
Italy	Fsm, **Fss, Fd, Fbd, Ta**
Liechtenstein	**Fbd**
Luxembourg	**Fd**
Malta	**Fss**
Monaco	**Fss**
Netherlands	**Fd**
Norway	**Fbo**, T
Poland	**Fd, Fbd**
Portugal	Fsm
Romania	**Gs, Gp, Fd, Fbd**
San Marino	Fsm
Spain	Fsm, **Fss, Fd, Ta**
Sweden	**Fd, Fbd, Fbo, T**
Switzerland	**Fbd, Ta**
United Kingdom	**Fd, Fbd**
Former USSR (west of Ural Mountains)	Dsd, **Gs, Gp, Fd, Fbd, Fbo, Ta**, T
Former Yugoslavia	Fsm, **Fd, Fbd**

Table D-1. World Vegetative Sub-Biomes by Continent and Country (Continued)	
North America (Including Central America)	
Country	**Sub-Biome(s)**
Belize	**Fe**
Bahamas	**Fe, Fmo**
Canada	**Gs, Fc, Fd, Fbd**, Fl, **Fbo, Ta**, T
Costa Rica	**Fe, Fmo, Fmt**
Cuba	Dtw, **Fe, Fmo**
Dominican Republic	**Fe, Fmo**
El Salvador	Dtw, **Fe**
Guatemala	Dtw, **Fe, Fmt**
Haiti	**Fmo**
Honduras	**Fe, Fmo, Fmt**
Jamaica	**Fe, Fmo**
Lesser Antilles	**Fe, Fmo**
Mexico	Dss, Dtw, **Fss, Gs, Fe, Fmo, Fmt, Fbo**
Nicaragua	**Fe, Fmo, Fmt**
Panama	**Fe, Fmo, Fmt**
United States (including Puerto Rico)	Dss, Dsd, **Fss, Gp, Gs, Fe, Fmo, Fc, Fbe, Fsp, Fd, Fbd,** Fl**, Fbo, Ta,** T
Oceania	
Country	**Sub-Biome(s)**
Australia	Dsp, Dss, Dtg, Dtw, **Fbe**, Fsa, **Fss**, **Fe, Fmo**, Ssa
Melanesia	**Fe**
Micronesia	**Fe**
New Zealand	**Fbe, Gp, Ta**
Polynesia	**Fe**
South America	
Country	**Sub-Biome(s)**
Argentina	Dsd, Dtg, Dtw, **Gp, Fd, Fe, Fmt, Ta,** T (Falkland Islands)
Bolivia	Dtw, **Fe, Fmo, Fmt, Ta**
Brazil	Dtw, Sw, **Gp, Fe, Fmo, Fmt**
Chile	D, Dss, **Fss, Fd, Fbd, Ta**, T
Columbia	Dtg, Sw, **Fe, Fmt, Ta**
Equador	Dss, Dtg, **Fe, Fmt, Ta**
French Guiana	**Fe**
Guyana	Sw, **Fe, Fmo**
Netherlands Antilles	**Fe, Fmo**
Paraguay	Dtw, Sw, **Fmo**
Peru	D, Dss, **Fe, Fmt, Ta**
Suriname	**Fe**
Trinidad and Tobago	**Fmo**
Uruguay	**Gp**
Venezuela	Dtg, Sw, **Fe, Fmo, Fmt**

Appendix E. Analysis

Introduction

Fifteen diverse geographic locations were selected for data collection. They represent a variety of vegetative sub-biomes, climates, latitudes, elevations, and therefore a variety of vegetation densities. At each geographic location, several (usually four) sites were selected for data collection. Table E-1 describes the geographic locations, the individual sites, the grid coordinates, and the elevation of each site. Appendix B provides a detailed description of the locations where data were collected.

Table E-1. Exact Locations of Field Collection Sites Including Easting, Northing, and Elevation

Location	Mapsheets	Site ID	Easting	Northing	Elevation (Meters)
Fort Hood	V782 6446 II	hood1	634956	3447933	200
	V782 6446 IV	hood2	613053	3463615	300
	V782 6446 IV	hood3	611132	3468105	350
	V782 6446 II	hood4	634882	3447861	200
Fort Carson	V777 5061 III	car41	503646	4263333	2000
	V777 5060 IV	car43	507030	4256724	1800
	V777 5061 III	car28	503350	4267355	1900
	V777 5062 III	afa1	511932	4318862	2100
Fort Hunter-Liggett	V795 1756 III	hl2	652967	3992291	350
	V795 1756 III	hl5	652584	3990785	360
	V795 1756 II	hl10	664160	3987415	330
	V795 1755 IV	hl9	656824	3982800	330
Fort Lewis	V791 1578 III	lew10	538430	5209933	110
	V791 1477 I	lew19	536645	5203211	90
	V791 1477 I	lew3	524850	5209587	65
	V791 1578 III	lew8	539045	5212546	120
Panama – Gamboa	E762 4243 II	gam1	643009	1009123	50
	E762 4243 II	gam2	642959	1009193	70
	E762 4243 II	gam3	642963	1009135	65
Panama - Fort Sherman	E762 4243 IV	skh1	614610	1031326	90
	E762 4243 IV	mck1	611180	1031820	50
Panama - El Valle	E762 4040 II	elval	595974	952690	735
Fort Benning	V745 4048 IV	ben_T3	705258	3585925	140
	V745 4048 IV	ben_L3	709976	3591177	90
	V745 4048 IV	ben_T4	707977	3586537	180
	V745 4048 IV	ben_D12	709935	3586273	150
Eglin AFB	V747 3645 III	egl_B2	513008	3383045	15
	V747 3744 IV	egl_X8	565583	3371785	10
	V747 36744 I	egl_X11	573012	3373589	0
	V747 3744 IV	egl_B12	568634	3374950	30
Fort Greely	Q701 3648 IV	G22	561373	7089326	470
	Q701 3648 IV	G00	562483	7082880	560
	Q701 3648 IV	G25	562453	7092898	430
	Q701 3648 IV	G02	564988	7095640	400
	Q701 3648 IV	G24	563800	7094187	430
	Q701 3648 IV	G05	569169	7091552	430
Fort Drum	V721 5872 II	8C	451100	4880171	210
	V721 5872 II	7G	450110	4874217	230
	V721 5872 II	7B	451600	4875950	240
	V721 5872 II	7E	452194	4875594	210
Natchaug SF	V816 6567 I	Nat2	737646	4641602	230
	V816 6567 I	Nat1	733840	4640998	180
	V816 6567 I	Nat4	738667	4633070	180
	V816 6567 I	Nat5	742599	4633165	220

Table E-1. Exact Locations of Field Collection Sites including Easting, Northing, and Elevation (Continued)					
Location	**Mapsheets**	**Site ID**	**Easting**	**Northing**	**Elevation (Meters)**
Canada - Gagetown	A702 21 G/9	Gage31	707665	5056363	110
	A702 21 G/9	Gage27	719194	5057459	80
	A702 21 G/9	Gage8	715896	5074298	65
	A702 21 G/9	Gage7	713958	5077119	40
Smoky Mountains	V842 4355 II	NC1	307670	3945980	850
	V841 4355 III	TN1	282284	3956600	340
	V841 4255 II	TN2	270668	3952250	430
	V842 4255 II	TN3	251440	3943885	540
Willow Grove NAS	V831 5964 II	WG6	495527	4449610	110
	V831 5964 II	WG2	486691	4449202	100
	V831 5964 II	WG5	485991	4451554	80
	V831 5964 II	WG4	486737	4451412	80
Fort Greely	Q701 3648 IV	G22	561373	7089326	470
	Q701 3648 IV	G00	562483	7082880	560
	Q701 3648 IV	G25	562453	7092898	430
	Q701 3648 IV	G02	564988	7095640	400
	Q701 3648 IV	G24	563800	7094187	430
	Q701 3648 IV	G05	569169	7091552	430

Raw Data

Figures E-1 through E-124 (provided at the end of this appendix) provide a visual description of the raw data. Each figure show the raw data collected along each azimuth, the quartiles (the middle 50 percent of the data), and the median of the data. The analysis will focus on the median curve.

The defensive positions selected for the field survey were selected as typical prone defensive positions. Data were collected from a crouching defender and towards a prone and kneeling defender for comparison purposes only. There data are provided in tables, but are not discussed in the analysis.

A CD-ROM is provided with this report. The CD-ROM provides maps depicting the exact locations of the each data collection site. Also included are panoramas of every tactical field of view. These panoramas provide the user with a visual image of where data were collected.

Analysis

Introduction

The analysis focuses on the median curve because it represents the most realistic representation of visibility in the field. The mean of the data were not used because outliers could skew the entire curve. Data were collected to represent looking at a kneeling target and a prone target. The kneeling target was 0.4206 square meter and the prone target was 0.12325 square meter. The y-axis of these plots is based on weather the target viewed was kneeling or prone. For example, if 100 percent of a kneeling target was seen, 0.4206 square meter was visible and if 100 percent of the prone target was seen, 0.12325 square meter was visible. The presented size of the target (number of square meters visible) is used in the detection equations.

Curve Fits

The fits to three different curves were selected in this analysis to provide different approaches to represent the effects of vegetation on LOS. The three functions fitted to the raw data are exponential, a field exponential, and a pole-zero.

The exponential function takes the form:

$$\mathbf{f} = \mathbf{e}^{\frac{-\mathbf{R}}{\mathbf{b}}},$$

where **f** is the visible fraction of the target, **R** is the length of LOS, and **b** is a parameter of the function. A smaller value for **b** implies a steeper decay curve.

The field exponential equation takes the form:

$$\mathbf{f} = \mathbf{e}^{\frac{-\mathbf{R}-\mathbf{a}}{\mathbf{b}}},$$

where **a** represents the range at which the curve begins the decay.

The pole-zero plot, an equation usually associated with the frequency response of electronic circuits was included in the analysis because often it was the best fit of the data. This was to be expected, as there are twice as many parameters as in the other equations. It takes the form

$$\mathbf{f} = \alpha\left[\frac{\delta^{\gamma} + \mathbf{R}^{\gamma}}{\varepsilon^{\gamma} + \mathbf{R}^{\gamma}}\right],$$

where α is a scaling factor and δ represents the part of the curve where the decay is so gradual that it is insignificant. The ε parameter represents the range where the curve begins to turn downward. In other words, this is the distance where the target begins a significant degradation. The γ parameter, the exponent in the equation, is a measure of how quickly the signal degrades as range becomes larger than ε.

Tables E-2 through E-9 depict the data fits for the exponential fits based for all eight combinations of POV, attacker posture, and defender posture. Tables E-10 through E-17 depict the data fits for the field exponential fits and tables E-18 through E-25 depict the data fits for the pole-zero fits. Along with the fits is the sum of squares error for each fit.

Table E-2. Data Fits for the Exponential Decay From a Prone Defender to a Prone Attacker			
Collection Area	**Site**	**SSE**	**Coeff b**
Panama	gam1	0.042	4.994
	gam2	0.199	7.163
	gam3	1.027	10.350
	skh1	0.191	8.921
	mck1	0.067	8.492
	elv1	0.273	9.311
Panama - Wet	gam1w	0.056	4.205
	gam2w	0.635	8.725
	gam3w	0.204	7.375
	shk1w	0.073	6.926
	mck1w	0.124	7.453
	elv1w	0.216	8.389
Eglin AFB	egl_B2	0.123	5.233
	egl_X8	0.187	7.135
	egl_X11	0.272	7.103
	egl_B12	1.004	24.271
Fort Hood	hood1	1.087	16.706
	hood2	0.293	10.576
	hood3	0.073	6.188
	hood4	0.800	18.839
Fort Carson	car28	1.670	27.439
	car41	2.043	24.407
	car43	0.737	24.578
	afa1	2.343	26.985
Fort Hunter-Liggett	hl2	6.310	81.070
	hl5	9.122	120.313
	hl9	0.288	13.140
	hl10	0.975	33.978
Fort Lewis	lew3	0.214	5.774
	lew8	0.194	9.691
	lew10	0.586	13.800
	lew19	0.166	5.840
Fort Benning	ben_T3	0.175	6.248
	ben_L3	0.282	9.206
	ben_T4	0.199	9.278
	ben_D12	0.152	5.942
Smoky Mountains	NC1	0.890	15.932
	TN1	0.061	4.855
	TN2	0.992	12.020
	TN3	1.045	21.671
Willow Grove NAS	WG4	0.288	8.457
	WG6	0.100	5.756
	WG2	0.057	4.673
	WG5	0.398	11.849
Natchaug SF	Nat2	0.226	11.258
	Nat1	0.371	11.368
	Nat4	0.108	8.235
	Nat5	0.174	7.261
Fort Drum	8C	0.704	12.210
	7G	0.259	11.286
	7B	0.369	10.432
	7E	0.072	8.405
Canada - Gagetown	Gage31	0.226	6.085
	Gage27	0.113	5.320
	Gage08	0.183	7.940
	Gage07	0.517	10.035
Fort Greely	G22	0.180	6.916
	G00	0.077	9.144
	G25	0.088	5.296
	G02	0.201	7.796
	G24	0.359	9.723
	G05	0.125	6.158

Table E-3. Data Fits for the Exponential Decay From a Prone Defender to a Kneeling Attacker			
Collection Area	**Site**	**SSE**	**Coeff b**
Panama	gam1	0.118	7.900
	gam2	0.224	8.314
	gam3	0.988	11.985
	skh1	0.261	12.722
	mck1	0.181	14.836
	elv1	0.262	11.032
Panama - Wet	gam1w	0.191	6.446
	gam2w	0.511	10.478
	gam3w	0.235	10.164
	shk1w	0.212	10.572
	mck1w	0.035	9.372
	elv1w	0.267	11.241
Eglin AFB	egl_B2	0.174	9.189
	egl_X8	0.421	11.881
	egl_X11	0.495	10.198
	egl_B12	1.544	32.910
Fort Hood	hood1	1.076	20.884
	hood2	0.527	18.429
	hood3	0.069	7.745
	hood4	1.835	28.831
Fort Carson	car28	1.963	35.167
	car41	3.596	31.002
	car43	2.782	39.557
	afa1	1.836	31.408
Fort Hunter-Liggett	hl2	6.131	129.506
	hl5	13.150	142.157
	hl9	0.740	20.939
	hl10	1.140	40.437
Fort Lewis	lew3	0.144	9.075
	lew8	0.317	12.480
	lew10	1.061	18.079
	lew19	0.113	7.369
Fort Benning	ben_T3	0.179	8.978
	ben_L3	0.339	13.321
	ben_T4	0.157	15.760
	ben_D12	0.158	6.793
Smoky Mountains	NC1	1.221	22.762
	TN1	0.205	8.989
	TN2	0.753	16.379
	TN3	1.605	30.273
Willow Grove NAS	WG4	0.433	11.588
	WG6	0.242	12.666
	WG2	0.072	8.947
	WG5	0.624	16.303
Natchaug SF	Nat2	0.474	17.348
	Nat1	0.331	23.767
	Nat4	0.117	17.602
	Nat5	0.069	19.012
Fort Drum	8C	0.874	16.067
	7G	0.363	19.292
	7B	0.422	12.940
	7E	0.194	19.231
Canada - Gagetown	Gage31	0.195	9.814
	Gage27	0.187	8.294
	Gage08	0.154	10.193
	Gage07	0.550	14.109
Fort Greely	G22	0.297	13.129
	G00	0.099	14.990
	G25	0.026	7.348
	G02	0.081	14.670
	G24	0.469	14.066
	G05	0.127	8.785

Table E-4. Data Fits for the Exponential Decay From a Crouching Defender to a Prone Attacker			
Collection Area	**Site**	**SSE**	**Coeff b**
Panama	gam1	0.330	7.498
	gam2	0.283	9.082
	gam3	0.768	11.286
	skh1	0.237	11.477
	mck1	0.412	13.938
	elv1	0.369	11.239
Panama - Wet	gam1w	0.166	6.532
	gam2w	0.520	10.345
	gam3w	1.017	12.943
	shk1w	0.211	12.133
	mck1w	0.278	12.261
	elv1w	0.333	11.686
Eglin AFB	egl_B2	0.594	8.388
	egl_X8	0.845	13.934
	egl_X11	1.006	11.495
	egl_B12	0.881	27.670
Fort Hood	hood1	1.646	19.703
	hood2	0.200	12.890
	hood3	0.100	7.878
	hood4	1.870	27.801
Fort Carson	car28	3.213	33.619
	car41	3.271	43.013
	car43	0.903	31.023
	afa1	1.668	34.246
Fort Hunter-Liggett	hl2	5.813	86.439
	hl5	8.956	134.178
	hl9	2.186	27.085
	hl10	1.308	37.861
Fort Lewis	lew3	0.195	9.112
	lew8	0.352	12.418
	lew10	1.858	19.672
	lew19	0.268	7.221
Fort Benning	ben_T3	0.103	6.995
	ben_L3	0.350	15.816
	ben_T4	0.268	12.604
	ben_D12	0.139	6.743
Smoky Mountains	NC1	1.601	23.119
	TN1	0.512	10.125
	TN2	1.015	15.529
	TN3	2.165	28.896
Willow Grove NAS	WG4	1.020	13.467
	WG6	0.507	10.230
	WG2	0.186	12.759
	WG5	1.116	16.419
Natchaug SF	Nat2	1.189	18.409
	Nat1	0.883	22.720
	Nat4	0.477	22.284
	Nat5	0.139	14.627
Fort Drum	8C	1.177	14.960
	7G	0.852	18.141
	7B	2.447	17.737
	7E	1.085	20.605
Canada - Gagetown	Gage31	0.465	10.029
	Gage27	0.583	9.853
	Gage08	0.406	13.335
	Gage07	0.896	16.034
Fort Greely	G22	0.842	12.997
	G00	0.935	19.776
	G25	0.314	11.668
	G02	0.214	12.766
	G24	0.590	12.622
	G05	0.348	9.336

Table E-5. Data Fits for the Exponential Decay From a Crouching Defender to a Kneeling Attacker			
Collection Area	**Site**	**SSE**	**Coeff b**
Panama	gam1	0.183	9.390
	gam2	0.186	11.266
	gam3	0.882	13.283
	skh1	0.494	17.330
	mck1	0.433	15.732
	elv1	0.473	12.646
Panama - Wet	gam1w	0.324	7.647
	gam2w	0.507	12.275
	gam3w	0.935	13.749
	shk1w	0.277	14.902
	mck1w	0.368	15.145
	elv1w	0.515	13.373
Eglin AFB	egl_B2	0.539	11.053
	egl_X8	0.804	14.925
	egl_X11	1.099	13.407
	egl_B12	2.159	35.897
Fort Hood	hood1	1.615	26.545
	hood2	0.507	27.880
	hood3	0.165	10.139
	hood4	3.043	38.057
Fort Carson	car28	2.835	32.630
	car41	5.263	50.808
	car43	4.267	64.160
	afa1	1.894	38.749
Fort Hunter-Liggett	hl2	9.613	131.209
	hl5	18.174	165.260
	hl9	2.013	50.502
	hl10	2.229	79.345
Fort Lewis	lew3	0.639	16.027
	lew8	0.642	20.833
	lew10	1.925	24.953
	lew19	0.431	13.304
Fort Benning	ben_T3	0.292	23.499
	ben_L3	0.802	28.102
	ben_T4	0.181	26.385
	ben_D12	0.159	10.812
Smoky Mountains	NC1	2.008	28.475
	TN1	0.455	15.450
	TN2	0.836	16.739
	TN3	1.833	29.992
Willow Grove NAS	WG4	0.990	15.630
	WG6	0.409	32.984
	WG2	1.137	25.835
	WG5	1.198	18.114
Natchaug SF	Nat2	1.240	21.936
	Nat1	1.384	32.789
	Nat4	0.573	33.389
	Nat5	0.465	30.453
Fort Drum	8C	1.051	19.758
	7G	0.838	23.636
	7B	2.218	20.387
	7E	1.120	26.902
Canada - Gagetown	Gage31	0.332	17.998
	Gage27	0.467	12.761
	Gage08	0.550	14.205
	Gage07	0.768	17.810
Fort Greely	G22	0.771	17.019
	G00	1.189	21.489
	G25	0.598	14.179
	G02	0.333	20.488
	G24	0.525	14.174
	G05	0.463	11.751

Table E-6. Data Fits for the Exponential Decay From a Prone Attacker to a Prone Defender			
Collection Area	**Site**	**SSE**	**Coeff b**
Panama	gam1	0.076	5.871
	gam2	0.216	7.792
	gam3	1.115	11.445
	skh1	0.165	8.846
	mck1	0.146	7.817
	elv1	0.298	10.461
Panama - Wet	gam1w	0.037	4.616
	gam2w	0.352	9.302
	gam3w	0.108	6.710
	shk1w	0.049	6.818
	mck1w	0.098	6.764
	elv1w	0.333	10.739
Eglin AFB	egl_B2	0.164	5.212
	egl_X8	0.257	8.075
	egl_X11	0.237	7.153
	egl_B12	1.457	28.175
Fort Hood	hood1	0.566	16.816
	hood2	0.296	10.565
	hood3	0.492	10.052
	hood4	0.331	16.848
Fort Carson	car28	1.869	30.661
	car41	0.949	24.266
	car43	0.683	24.342
	afa1	1.751	27.385
Fort Hunter-Liggett	hl2	0.408	53.724
	hl5	7.021	138.022
	hl9	0.255	12.709
	hl10	0.936	33.468
Fort Lewis	lew3	0.122	5.785
	lew8	0.210	9.764
	lew10	0.355	12.106
	lew19	0.164	5.816
Fort Benning	ben_T3	0.139	6.403
	ben_L3	0.399	10.960
	ben_T4	0.252	10.583
	ben_D12	0.150	5.796
Smoky Mountains	NC1	0.224	14.076
	TN1	0.078	3.469
	TN2	0.110	9.860
	TN3	0.430	22.028
Willow Grove NAS	WG4	0.113	7.818
	WG6	0.184	7.628
	WG2	0.062	5.764
	WG5	0.091	7.036
Natchaug SF	Nat2	0.080	7.922
	Nat1	0.183	6.628
	Nat4	0.173	6.190
	Nat5	0.082	9.740
Fort Drum	8C	0.384	11.114
	7G	0.166	8.089
	7B	0.177	9.640
	7E	0.083	7.340
Canada - Gagetown	Gage31	0.165	6.000
	Gage27	0.118	5.200
	Gage08	0.066	6.573
	Gage07	0.821	12.830
Fort Greely	G22	0.221	8.216
	G00	0.157	7.456
	G25	0.125	5.014
	G02	0.157	7.746
	G24	0.323	10.931
	G05	0.122	5.887

Table E-7. Data Fits for the Exponential Decay From a Prone Attacker to a Kneeling Defender			
Collection Area	**Site**	**SSE**	**Coeff b**
Panama	gam1	0.232	8.968
	gam2	0.176	9.506
	gam3	0.956	13.221
	skh1	0.299	12.148
	mck1	0.231	15.251
	elv1	0.413	14.098
Panama - Wet	gam1w	0.174	6.673
	gam2w	0.592	12.030
	gam3w	0.147	10.712
	shk1w	0.068	9.223
	mck1w	0.099	9.795
	elv1w	0.321	12.663
Eglin AFB	egl_B2	0.202	9.698
	egl_X8	0.307	13.297
	egl_X11	0.507	10.283
	egl_B12	1.768	34.888
Fort Hood	hood1	0.639	23.050
	hood2	0.387	14.438
	hood3	0.347	11.905
	hood4	0.945	27.748
Fort Carson	car28	2.898	38.581
	car41	1.704	34.787
	car43	1.012	32.206
	afa1	1.268	34.212
Fort Hunter-Liggett	hl2	4.416	142.809
	hl5	13.062	186.153
	hl9	0.981	25.729
	hl10	0.974	37.049
Fort Lewis	lew3	0.250	11.534
	lew8	0.324	12.249
	lew10	0.803	17.280
	lew19	0.107	6.662
Fort Benning	ben_T3	0.243	9.632
	ben_L3	0.311	13.113
	ben_T4	0.361	19.608
	ben_D12	0.135	6.821
Smoky Mountains	NC1	1.145	24.455
	TN1	0.104	9.027
	TN2	0.419	16.673
	TN3	0.887	33.182
Willow Grove NAS	WG4	0.259	11.426
	WG6	0.386	12.155
	WG2	0.101	9.829
	WG5	0.199	13.991
Natchaug SF	Nat2	0.237	15.772
	Nat1	0.064	21.314
	Nat4	0.160	16.604
	Nat5	0.286	20.989
Fort Drum	8C	0.795	16.366
	7G	0.233	19.278
	7B	0.070	14.444
	7E	0.156	17.562
Canada - Gagetown	Gage31	0.091	10.966
	Gage27	0.074	8.315
	Gage08	0.165	12.848
	Gage07	0.772	16.180
Fort Greely	G22	0.398	14.502
	G00	0.072	17.040
	G25	0.033	9.079
	G02	0.097	14.075
	G24	0.532	17.248
	G05	0.159	9.155

Table E-8. Data Fits for the Exponential Decay From a Crouching Attacker to a Prone Defender			
Collection Area	**Site**	**SSE**	**Coeff b**
Panama	gam1	0.914	11.709
	gam2	0.463	12.010
	gam3	1.582	17.684
	skh1	0.734	15.477
	mck1	0.874	17.790
	elv1	0.478	13.476
Panama - Wet	gam1w	0.303	7.216
	gam2w	0.957	14.324
	gam3w	0.449	11.246
	shk1w	0.510	14.038
	mck1w	0.544	11.707
	elv1w	0.377	12.366
Eglin AFB	egl_B2	0.547	11.228
	egl_X8	0.221	10.288
	egl_X11	0.338	11.717
	egl_B12	3.089	41.556
Fort Hood	hood1	0.768	20.871
	hood2	0.727	16.185
	hood3	0.245	10.996
	hood4	2.265	34.020
Fort Carson	car28	2.480	29.048
	car41	2.322	36.707
	car43	0.893	29.979
	afa1	1.493	35.096
Fort Hunter-Liggett	hl2	5.232	116.136
	hl5	10.556	135.370
	hl9	1.129	32.163
	hl10	0.743	46.066
Fort Lewis	lew3	0.436	15.054
	lew8	0.523	14.496
	lew10	0.550	14.482
	lew19	0.225	9.537
Fort Benning	ben_T3	0.427	12.280
	ben_L3	0.534	17.025
	ben_T4	0.753	19.109
	ben_D12	0.202	9.320
Smoky Mountains	NC1	0.259	19.493
	TN1	0.036	4.452
	TN2	0.128	11.086
	TN3	0.221	23.960
Willow Grove NAS	WG4	0.697	14.825
	WG6	0.930	23.147
	WG2	0.546	15.690
	WG5	0.466	12.846
Natchaug SF	Nat2	0.034	9.546
	Nat1	0.152	7.148
	Nat4	0.051	9.913
	Nat5	0.091	24.614
Fort Drum	8C	2.127	21.112
	7G	0.074	9.702
	7B	0.080	16.278
	7E	0.485	16.530
Canada - Gagetown	Gage31	0.029	7.586
	Gage27	0.071	9.034
	Gage08	0.099	8.506
	Gage07	1.020	20.118
Fort Greely	G22	1.206	17.801
	G00	0.147	8.383
	G25	0.132	5.046
	G02	0.427	15.992
	G24	0.719	17.626
	G05	0.373	12.421

Table E-9. Data Fits for the Exponential Decay From a Crouching Attacker to a Kneeling Defender			
Collection Area	**Site**	**SSE**	**Coeff b**
Panama	gam1	0.663	13.638
	gam2	0.376	14.206
	gam3	1.272	17.693
	skh1	0.607	19.495
	mck1	0.886	19.992
	elv1	0.898	17.012
Panama - Wet	gam1w	0.460	8.600
	gam2w	0.972	16.373
	gam3w	0.448	13.546
	shk1w	0.416	16.346
	mck1w	0.678	14.365
	elv1w	0.724	15.065
Eglin AFB	egl_B2	0.762	15.825
	egl_X8	0.557	13.651
	egl_X11	0.758	17.247
	egl_B12	2.095	43.068
Fort Hood	hood1	0.881	25.360
	hood2	0.922	28.999
	hood3	0.223	12.095
	hood4	1.712	37.096
Fort Carson	car28	2.314	38.751
	car41	3.026	42.610
	car43	1.618	62.329
	afa1	0.976	48.820
Fort Hunter-Liggett	hl2	16.293	169.264
	hl5	12.854	185.701
	hl9	2.935	68.273
	hl10	0.993	118.241
Fort Lewis	lew3	1.824	23.062
	lew8	0.712	24.152
	lew10	1.216	27.287
	lew19	0.371	16.810
Fort Benning	ben_T3	0.107	26.357
	ben_L3	0.955	25.409
	ben_T4	0.859	45.724
	ben_D12	0.448	14.018
Smoky Mountains	NC1	1.182	27.527
	TN1	0.212	15.536
	TN2	0.258	18.249
	TN3	0.604	32.196
Willow Grove NAS	WG4	0.453	21.326
	WG6	1.208	40.062
	WG2	0.822	24.940
	WG5	0.691	18.682
Natchaug SF	Nat2	0.428	23.866
	Nat1	0.473	30.850
	Nat4	0.318	30.855
	Nat5	0.735	46.781
Fort Drum	8C	1.880	23.785
	7G	0.568	24.423
	7B	0.237	34.108
	7E	0.475	25.292
Canada - Gagetown	Gage31	0.232	19.916
	Gage27	0.177	15.329
	Gage08	0.163	12.913
	Gage07	0.944	22.777
Fort Greely	G22	0.935	22.244
	G00	0.257	20.985
	G25	0.077	14.868
	G02	0.674	28.715
	G24	0.640	18.858
	G05	0.520	14.887

Table E-10. Data Fits for the Field Exponential Decay From a Prone Defender to a Prone Attacker				
Collection Area	**Site**	**SSE**	**Coeff a**	**Coeff b**
Panama	gam1	0.017	0.706	4.309
	gam2	0.095	2.347	5.008
	gam3	0.119	7.677	3.001
	skh1	0.089	2.391	6.707
	mck1	0.021	1.446	7.084
	elv1	0.080	3.378	6.127
Panama - Wet	gam1w	0.025	0.726	3.511
	gam2w	0.075	5.597	3.308
	gam3w	0.087	2.415	5.143
	shk1w	0.033	1.322	5.678
	mck1w	0.057	1.583	5.970
	elv1w	0.035	2.734	5.698
Eglin AFB	egl_B2	0.053	1.496	3.843
	egl_X8	0.072	2.396	4.905
	egl_X11	0.130	2.524	4.796
	egl_B12	0.324	9.683	15.222
Fort Hood	hood1	0.176	10.415	6.792
	hood2	0.149	2.741	8.045
	hood3	0.031	1.319	4.941
	hood4	0.356	7.473	12.012
Fort Carson	car28	0.128	14.706	12.808
	car41	0.438	15.507	9.755
	car43	0.359	7.472	17.716
	afa1	0.065	16.590	10.239
Fort Hunter-Liggett	hl2	2.548	55.483	28.407
	hl5	3.747	68.502	57.566
	hl9	0.134	3.448	9.944
	hl10	0.498	9.597	25.161
Fort Lewis	lew3	0.087	2.416	3.563
	lew8	0.056	2.632	7.184
	lew10	0.253	5.518	8.736
	lew19	0.082	1.602	4.360
Fort Benning	ben_T3	0.087	1.653	4.720
	ben_L3	0.129	2.697	6.702
	ben_T4	0.107	2.338	7.120
	ben_D12	0.072	1.588	4.472
Smoky Mountains	NC1	0.217	8.445	8.007
	TN1	0.027	0.791	4.100
	TN2	0.075	7.732	4.008
	TN3	1.019	-1.594	23.040
Willow Grove NAS	WG4	0.114	2.749	5.889
	WG6	0.041	1.447	4.395
	WG2	0.025	0.766	3.935
	WG5	0.179	4.331	7.873
Natchaug SF	Nat2	0.106	2.629	8.810
	Nat1	0.165	3.634	8.013
	Nat4	0.041	1.653	6.611
	Nat5	0.083	1.736	5.646
Fort Drum	8C	0.274	5.715	6.961
	7G	0.124	2.732	8.748
	7B	0.190	3.456	7.277
	7E	0.030	1.389	7.077
Canada - Gagetown	Gage31	0.086	2.470	3.809
	Gage27	0.050	1.456	3.969
	Gage08	0.083	2.336	5.778
	Gage07	0.140	5.449	4.960
Fort Greely	G22	0.072	2.357	4.727
	G00	0.048	1.299	7.811
	G25	0.037	1.377	4.001
	G02	0.091	2.399	5.582
	G24	0.067	3.679	6.161
	G05	0.055	1.533	4.729

Table E-11. Data Fits for the Field Exponential Decay From a Prone Defender to a Kneeling Attacker				
Collection Area	**Site**	**SSE**	**Coeff a**	**Coeff b**
Panama	gam1	0.056	1.571	6.426
	gam2	0.094	2.535	5.945
	gam3	0.058	7.775	4.304
	skh1	0.114	3.392	9.549
	mck1	0.080	2.655	12.320
	elv1	0.073	3.421	7.778
Panama - Wet	gam1w	0.089	1.752	4.817
	gam2w	0.059	5.443	5.214
	gam3w	0.055	3.398	6.911
	shk1w	0.113	2.446	8.306
	mck1w	0.016	0.839	8.555
	elv1w	0.079	3.298	8.085
Eglin AFB	egl_B2	0.037	2.592	6.681
	egl_X8	0.156	4.439	7.750
	egl_X11	0.161	4.643	5.895
	egl_B12	0.320	15.355	18.304
Fort Hood	hood1	0.143	11.288	9.921
	hood2	0.254	5.493	13.339
	hood3	0.041	1.193	6.619
	hood4	0.370	16.796	12.871
Fort Carson	car28	0.468	16.463	19.288
	car41	0.454	27.535	3.914
	car43	1.242	21.562	20.022
	afa1	0.181	14.732	16.793
Fort Hunter-Liggett	hl2	2.338	50.611	78.929
	hl5	3.155	107.485	41.505
	hl9	0.206	8.492	12.895
	hl10	0.567	11.580	29.733
Fort Lewis	lew3	0.055	2.307	6.896
	lew8	0.133	3.551	9.170
	lew10	0.228	10.476	8.153
	lew19	0.047	1.587	5.859
Fort Benning	ben_T3	0.086	2.336	6.810
	ben_L3	0.069	4.336	9.130
	ben_T4	0.090	2.359	13.531
	ben_D12	0.074	1.667	5.240
Smoky Mountains	NC1	0.133	11.549	11.529
	TN1	0.053	2.685	6.40
	TN2	0.075	7.623	8.329
	TN3	0.877	17.203	14.998
Willow Grove NAS	WG4	0.104	4.693	7.121
	WG6	0.105	3.320	9.568
	WG2	0.022	1.513	7.478
	WG5	0.131	7.381	9.280
Natchaug SF	Nat2	0.207	5.398	12.356
	Nat1	0.083	5.543	18.378
	Nat4	0.053	2.379	15.323
	Nat5	0.057	1.104	17.930
Fort Drum	8C	0.153	8.583	7.873
	7G	0.119	5.402	13.948
	7B	0.192	4.418	8.879
	7E	0.115	2.646	16.728
Canada - Gagetown	Gage31	0.057	2.657	7.247
	Gage27	0.066	2.471	5.972
	Gage08	0.062	2.372	7.956
	Gage07	0.067	6.517	7.705
Fort Greely	G22	0.122	3.571	9.770
	G00	0.046	1.848	13.173
	G25	0.011	0.679	6.677
	G02	0.041	1.604	13.130
	G24	0.054	5.474	8.709
	G05	0.059	1.667	7.218

Table E-12. Data Fits for the Field Exponential Decay From a Crouching Defender to a Prone Attacker				
Collection Area	**Site**	**SSE**	**Coeff a**	**Coeff b**
Panama	gam1	0.137	3.408	4.395
	gam2	0.113	3.371	5.931
	gam3	0.117	7.453	4.117
	skh1	0.116	2.646	9.016
	mck1	0.155	4.395	9.818
	elv1	0.083	3.788	7.589
Panama - Wet	gam1w	0.091	1.589	5.067
	gam2w	0.069	5.459	5.101
	gam3w	0.085	7.779	5.317
	shk1w	0.076	3.218	9.076
	mck1w	0.149	2.754	9.702
	elv1w	0.108	3.700	8.196
Eglin AFB	egl_B2	0.050	5.375	3.124
	egl_X8	0.355	6.580	7.894
	egl_X11	0.101	6.838	4.726
	egl_B12	0.499	7.643	20.660
Fort Hood	hood1	0.159	12.339	7.363
	hood2	0.094	2.642	10.349
	hood3	0.086	0.650	7.258
	hood4	0.198	16.415	11.397
Fort Carson	car28	0.493	20.516	13.483
	car41	1.243	20.622	22.664
	car43	0.443	9.433	22.052
	afa1	0.361	13.411	21.148
Fort Hunter-Liggett	hl2	1.900	53.408	36.197
	hl5	2.361	72.284	65.462
	hl9	0.372	19.365	6.681
	hl10	0.700	11.601	27.251
Fort Lewis	lew3	0.104	2.295	6.980
	lew8	0.145	3.651	9.004
	lew10	0.180	13.807	6.242
	lew19	0.115	2.582	4.838
Fort Benning	ben_T3	0.045	1.493	5.592
	ben_L3	0.107	4.490	11.546
	ben_T4	0.107	3.475	9.336
	ben_D12	0.062	1.620	5.230
Smoky Mountains	NC1	0.384	12.340	11.403
	TN1	0.026	5.247	4.851
	TN2	0.023	8.552	6.725
	TN3	0.385	17.636	12.023
Willow Grove NAS	WG4	0.215	8.466	5.446
	WG6	0.134	5.434	5.168
	WG2	0.130	1.802	10.870
	WG5	0.029	9.367	6.914
Natchaug SF	Nat2	0.306	10.474	8.650
	Nat1	0.074	9.608	12.994
	Nat4	0.301	4.457	17.928
	Nat5	0.088	1.797	12.870
Fort Drum	8C	0.142	9.440	5.832
	7G	0.143	9.419	8.708
	7B	0.074	13.674	3.939
	7E	0.152	10.496	10.525
Canada - Gagetown	Gage31	0.070	4.648	5.310
	Gage27	0.143	5.370	4.806
	Gage08	0.147	4.486	9.146
	Gage07	0.039	8.253	7.597
Fort Greely	G22	0.326	7.295	6.312
	G00	0.145	10.284	9.819
	G25	0.104	3.651	8.235
	G02	0.084	3.266	9.689
	G24	0.067	5.636	7.098
	G05	0.091	3.693	5.832

Table E-13. Data Fits for the Field Exponential Decay From a Crouching Defender to a Kneeling Attacker				
Collection Area	**Site**	**SSE**	**Coeff a**	**Coeff b**
Panama	gam1	0.086	2.385	7.167
	gam2	0.069	2.619	8.774
	gam3	0.080	7.717	5.757
	skh1	0.174	5.672	11.979
	mck1	0.129	5.305	10.719
	elv1	0.120	4.740	8.123
Panama - Wet	gam1w	0.083	3.527	4.335
	gam2w	0.105	5.410	7.104
	gam3w	0.087	8.365	5.642
	shk1w	0.138	3.417	11.716
	mck1w	0.165	4.375	11.070
	elv1w	0.174	5.461	8.298
Eglin AFB	egl_B2	0.012	5.380	5.572
	egl_X8	0.236	8.285	7.279
	egl_X11	0.108	8.324	5.234
	egl_B12	0.645	18.453	18.694
Fort Hood	hood1	0.152	12.878	13.595
	hood2	0.208	6.613	21.534
	hood3	0.157	0.564	9.627
	hood4	0.333	24.360	14.431
Fort Carson	car28	0.282	19.535	13.266
	car41	2.270	26.209	25.694
	car43	3.185	20.294	43.478
	afa1	0.435	15.558	23.680
Fort Hunter-Liggett	hl2	2.583	69.415	63.495
	hl5	1.682	133.582	34.638
	hl9	0.373	19.464	30.970
	hl10	1.066	23.275	56.427
Fort Lewis	lew3	0.210	6.511	9.848
	lew8	0.252	6.611	14.636
	lew10	0.093	14.812	10.029
	lew19	0.084	5.363	8.082
Fort Benning	ben_T3	0.287	0.691	22.816
	ben_L3	0.344	8.389	20.082
	ben_T4	0.108	3.145	23.339
	ben_D12	0.067	2.404	8.550
Smoky Mountains	NC1	0.244	16.327	12.654
	TN1	0.025	5.505	9.875
	TN2	0.073	8.432	7.858
	TN3	0.399	17.351	13.610
Willow Grove NAS	WG4	0.089	9.338	6.241
	WG6	0.408	0.352	32.622
	WG2	0.857	5.762	20.654
	WG5	0.023	9.755	8.124
Natchaug SF	Nat2	0.258	11.465	11.104
	Nat1	0.425	11.732	21.613
	Nat4	0.350	5.839	27.977
	Nat5	0.344	4.273	26.497
Fort Drum	8C	0.150	10.450	9.667
	7G	0.067	9.567	13.884
	7B	0.154	14.295	4.944
	7E	0.372	11.407	16.318
Canada - Gagetown	Gage31	0.086	4.411	13.650
	Gage27	0.115	5.341	7.656
	Gage08	0.185	5.577	9.014
	Gage07	0.023	8.143	9.565
Fort Greely	G22	0.130	8.453	8.786
	G00	0.060	11.487	9.899
	G25	0.090	6.572	7.819
	G02	0.105	4.789	15.894
	G24	0.042	5.615	8.604
	G05	0.124	4.686	7.326

Table E-14. Data Fits for the Field Exponential Decay From a Prone Attacker to a Prone Defender				
Collection Area	**Site**	**SSE**	**Coeff a**	**Coeff b**
Panama	gam1	0.030	1.355	4.586
	gam2	0.102	2.421	5.567
	gam3	0.054	8.417	3.170
	skh1	0.074	2.316	6.688
	mck1	0.065	1.717	6.201
	elv1	0.099	3.532	7.154
Panama - Wet	gam1w	0.018	0.611	4.032
	gam2w	0.128	3.588	5.976
	gam3w	0.053	1.458	5.350
	shk1w	0.030	0.715	6.136
	mck1w	0.042	1.462	5.389
	elv1w	0.040	4.281	6.519
Eglin AFB	egl_B2	0.075	1.598	3.730
	egl_X8	0.129	2.499	5.784
	egl_X11	0.119	2.418	4.946
	egl_B12	0.424	13.650	15.478
Fort Hood	hood1	0.224	6.323	10.933
	hood2	0.151	2.745	8.032
	hood3	0.097	4.701	5.581
	hood4	0.151	4.318	12.823
Fort Carson	car28	0.635	15.427	16.385
	car41	0.423	9.388	15.623
	car43	0.346	6.689	18.186
	afa1	0.271	16.356	11.833
Fort Hunter-Liggett	hl2	0.169	8.260	45.610
	hl5	3.555	52.656	89.060
	hl9	0.115	3.344	9.594
	hl10	0.474	9.491	24.748
Fort Lewis	lew3	0.052	1.525	4.361
	lew8	0.054	2.740	7.141
	lew10	0.178	3.529	8.863
	lew19	0.081	1.601	4.338
Fort Benning	ben_T3	0.063	1.592	4.915
	ben_L3	0.173	3.704	7.531
	ben_T4	0.119	2.677	8.092
	ben_D12	0.072	1.568	4.346
Smoky Mountains	NC1	0.167	1.818	12.404
	TN1	0.036	0.745	2.768
	TN2	0.048	1.685	8.258
	TN3	0.382	2.268	19.977
Willow Grove NAS	WG4	0.053	1.538	6.376
	WG6	0.090	1.785	5.965
	WG2	0.029	0.834	4.970
	WG5	0.036	1.467	5.648
Natchaug SF	Nat2	0.032	1.445	6.545
	Nat1	0.091	1.698	5.056
	Nat4	0.086	1.643	4.672
	Nat5	0.030	1.574	8.216
Fort Drum	8C	0.172	3.645	7.752
	7G	0.078	2.274	5.988
	7B	0.078	2.410	7.388
	7E	0.035	1.433	5.936
Canada - Gagetown	Gage31	0.081	1.619	4.503
	Gage27	0.053	1.461	3.846
	Gage08	0.025	1.324	5.308
	Gage07	0.131	7.646	5.540
Fort Greely	G22	0.074	2.605	5.766
	G00	0.073	1.716	5.846
	G25	0.058	1.470	3.658
	G02	0.078	1.688	6.172
	G24	0.065	3.690	7.339
	G05	0.053	1.515	4.475

Table E-15. Data Fits for the Field Exponential Decay From a Prone Attacker to a Kneeling Defender				
Collection Area	**Site**	**SSE**	**Coeff a**	**Coeff b**
Panama	gam1	0.128	2.403	6.753
	gam2	0.085	2.353	7.292
	gam3	0.021	7.754	5.294
	skh1	0.143	3.410	8.994
	mck1	0.095	3.436	12.000
	elv1	0.133	4.607	9.747
Panama - Wet	gam1w	0.072	1.768	5.014
	gam2w	0.132	5.667	6.655
	gam3w	0.082	1.751	9.075
	shk1w	0.051	0.773	8.492
	mck1w	0.038	1.656	8.212
	elv1w	0.045	4.403	8.362
Eglin AFB	egl_B2	0.046	3.243	6.580
	egl_X8	0.099	3.711	9.784
	egl_X11	0.174	4.625	5.999
	egl_B12	0.648	16.369	19.801
Fort Hood	hood1	0.265	7.278	16.257
	hood2	0.194	4.301	10.451
	hood3	0.213	2.779	9.371
	hood4	0.345	10.314	18.138
Fort Carson	car28	1.139	23.551	17.214
	car41	0.236	17.357	17.883
	car43	0.518	9.613	23.332
	afa1	0.302	14.351	20.572
Fort Hunter-Liggett	hl2	2.616	39.355	106.191
	hl5	4.234	111.487	79.599
	hl9	0.589	8.493	16.695
	hl10	0.515	9.660	28.146
Fort Lewis	lew3	0.101	3.320	8.435
	lew8	0.137	3.559	8.937
	lew10	0.348	7.410	10.461
	lew19	0.044	1.532	5.186
Fort Benning	ben_T3	0.114	2.601	7.200
	ben_L3	0.117	3.685	9.654
	ben_T4	0.150	4.639	15.232
	ben_D12	0.060	1.614	5.307
Smoky Mountains	NC1	0.358	11.505	13.795
	TN1	0.056	1.484	7.620
	TN2	0.144	5.429	11.513
	TN3	0.634	6.678	27.165
Willow Grove NAS	WG4	0.087	3.459	8.150
	WG6	0.174	3.724	8.686
	WG2	0.045	1.650	8.153
	WG5	0.091	2.709	11.422
Natchaug SF	Nat2	0.138	2.692	13.265
	Nat1	0.063	0.306	21.014
	Nat4	0.070	2.663	14.070
	Nat5	0.174	3.458	17.778
Fort Drum	8C	0.131	8.401	8.350
	7G	0.079	3.805	15.566
	7B	0.024	1.713	12.766
	7E	0.112	1.781	15.897
Canada - Gagetown	Gage31	0.048	1.525	9.463
	Gage27	0.031	1.415	6.963
	Gage08	0.066	2.559	10.420
	Gage07	0.168	7.625	8.965
Fort Greely	G22	0.133	4.590	10.159
	G00	0.068	0.464	16.579
	G25	0.014	0.810	8.280
	G02	0.041	2.192	11.899
	G24	0.084	6.371	11.072
	G05	0.073	2.285	7.022

Table E-16. Data Fits for the Field Exponential Decay From a Crouching Attacker to a Prone Defender				
Collection Area	**Site**	**SSE**	**Coeff a**	**Coeff b**
Panama	gam1	0.125	7.668	4.343
	gam2	0.097	5.397	6.886
	gam3	0.087	11.643	6.188
	skh1	0.225	7.497	8.500
	mck1	0.159	9.427	8.770
	elv1	0.122	5.366	8.405
Panama - Wet	gam1w	0.109	3.389	4.104
	gam2w	0.112	8.588	6.072
	gam3w	0.135	4.641	6.891
	shk1w	0.155	5.434	8.937
	mck1w	0.049	5.660	6.165
	elv1w	0.075	4.523	7.989
Eglin AFB	egl_B2	0.050	5.591	5.706
	egl_X8	0.082	2.694	7.751
	egl_X11	0.129	3.668	8.298
	egl_B12	0.642	26.553	16.653
Fort Hood	hood1	0.247	8.348	13.035
	hood2	0.351	6.445	10.318
	hood3	0.113	3.321	7.929
	hood4	0.907	18.500	17.144
Fort Carson	car28	0.523	19.439	10.822
	car41	0.451	20.500	17.258
	car43	0.456	8.620	22.062
	afa1	0.404	14.698	21.243
Fort Hunter-Liggett	hl2	1.724	49.289	69.865
	hl5	2.874	96.593	43.731
	hl9	0.243	13.521	19.146
	hl10	0.310	10.493	36.141
Fort Lewis	lew3	0.155	5.295	10.123
	lew8	0.153	5.608	9.233
	lew10	0.227	5.510	9.399
	lew19	0.088	2.644	7.047
Fort Benning	ben_T3	0.174	4.483	8.150
	ben_L3	0.217	5.592	11.843
	ben_T4	0.350	7.289	12.442
	ben_D12	0.086	2.504	6.980
Smoky Mountains	NC1	0.201	2.363	17.320
	TN1	0.013	0.664	3.799
	TN2	0.050	2.304	8.886
	TN3	0.204	1.354	22.704
Willow Grove NAS	WG4	0.080	7.286	7.650
	WG6	0.131	10.326	13.162
	WG2	0.097	6.422	9.538
	WG5	0.115	5.489	7.640
Natchaug SF	Nat2	0.014	0.862	8.683
	Nat1	0.069	1.682	5.573
	Nat4	0.020	1.313	8.633
	Nat5	0.086	0.656	23.987
Fort Drum	8C	0.203	15.613	6.079
	7G	0.028	1.523	8.197
	7B	0.033	1.806	14.505
	7E	0.158	5.633	11.235
Canada - Gagetown	Gage31	0.013	0.696	6.885
	Gage27	0.029	1.427	7.666
	Gage08	0.044	1.538	7.050
	Gage07	0.277	9.649	11.098
Fort Greely	G22	0.162	10.777	7.423
	G00	0.066	1.759	6.709
	G25	0.062	1.485	3.676
	G02	0.169	4.725	11.564
	G24	0.104	7.168	10.621
	G05	0.182	3.614	9.087

Table E-17. Data Fits for the Field Exponential Decay From a Crouching Attacker to a Kneeling Defender				
Collection Area	**Site**	**SSE**	**Coeff a**	**Coeff b**
Panama	gam1	0.144	6.422	7.537
	gam2	0.132	4.522	9.974
	gam3	0.080	10.446	7.333
	skh1	0.164	7.488	12.360
	mck1	0.079	9.576	10.531
	elv1	0.165	9.197	8.291
Panama - Wet	gam1w	0.072	4.597	4.205
	gam2w	0.132	9.463	7.316
	gam3w	0.145	5.317	8.589
	shk1w	0.188	4.515	12.119
	mck1w	0.080	6.670	7.881
	elv1w	0.186	7.345	8.191
Eglin AFB	egl_B2	0.079	7.346	8.641
	egl_X8	0.167	5.577	8.417
	egl_X11	0.342	6.632	11.175
	egl_B12	0.773	20.397	24.358
Fort Hood	hood1	0.354	9.250	16.802
	hood2	0.249	10.703	18.719
	hood3	0.057	3.401	8.810
	hood4	0.648	16.357	21.993
Fort Carson	car28	0.497	22.598	17.530
	car41	0.575	23.556	20.003
	car43	0.648	18.664	44.931
	afa1	0.434	11.698	37.861
Fort Hunter-Liggett	hl2	2.612	127.613	45.937
	hl5	4.844	103.318	86.794
	hl9	1.266	23.700	46.195
	hl10	0.472	17.508	101.429
Fort Lewis	lew3	0.297	15.483	8.448
	lew8	0.240	7.714	16.895
	lew10	0.227	12.497	15.273
	lew19	0.110	4.749	12.299
Fort Benning	ben_T3	0.033	3.179	23.172
	ben_L3	0.223	11.320	14.560
	ben_T4	0.245	11.770	34.469
	ben_D12	0.161	4.727	9.608
Smoky Mountains	NC1	0.208	13.267	14.825
	TN1	0.184	1.428	14.236
	TN2	0.120	3.590	14.863
	TN3	0.439	5.410	27.248
Willow Grove NAS	WG4	0.079	6.195	15.187
	WG6	0.128	14.584	25.574
	WG2	0.333	8.420	17.115
	WG5	0.125	7.565	11.419
Natchaug SF	Nat2	0.223	5.319	18.923
	Nat1	0.461	1.255	29.716
	Nat4	0.243	3.329	27.774
	Nat5	0.493	7.515	39.838
Fort Drum	8C	0.202	15.612	8.675
	7G	0.263	6.556	18.334
	7B	0.134	4.229	30.024
	7E	0.200	6.343	19.336
Canada - Gagetown	Gage31	0.216	1.218	18.802
	Gage27	0.094	2.508	12.946
	Gage08	0.060	2.592	10.430
	Gage07	0.236	10.382	13.030
Fort Greely	G22	0.081	10.250	12.153
	G00	0.202	2.358	18.801
	G25	0.074	0.415	14.475
	G02	0.150	9.433	19.575
	G24	0.075	6.777	12.138
	G05	0.194	5.509	9.777

Table E-18. Data Fits for the Pole-Zero Decay From a Prone Defender to a Prone Attacker						
Collection Area	**Site**	**SSE**	**Coeff α**	**Coeff δ**	**Coeff ε**	**Coeff γ**
Panama	gam1	0.027	1.30e-13	1.77e+06	3.851	2.275
	gam2	0.080	1.60e-13	1.89e+05	6.149	2.851
	gam3	0.055	5.29e-14	8.29e+02	10.111	6.938
	skh1	0.087	1.72e-14	1.07e+06	7.463	2.669
	mck1	0.032	6.39e-14	3.88e+06	6.551	2.286
	elv1	0.062	7.97e-14	2.14e+05	7.975	2.958
Panama - Wet	gam1w	0.030	1.30e-14	1.65e+06	3.364	2.440
	gam2w	0.033	2.73e-13	2.53e+03	8.156	5.044
	gam3w	0.073	3.36e-14	3.19e+05	6.317	2.865
	shk1w	0.051	8.01e-14	2.21e+06	5.433	2.335
	mck1w	0.066	1.10e-13	8.44e+05	6.075	2.519
	elv1w	0.030	3.25e-14	4.06e+05	6.977	2.831
Eglin AFB	egl_B2	0.049	2.12e-13	1.78e+05	4.425	2.752
	egl_X8	0.057	6.01e-14	2.48e+05	6.094	2.869
	egl_X11	0.102	1.02e-13	8.81e+04	6.319	3.134
	egl_B12	0.220	2.68e-13	1.33e+05	21.649	3.319
Fort Hood	hood1	0.094	1.38e-13	1.24e+04	15.481	4.430
	hood2	0.133	1.16e-13	3.71e+05	9.047	2.804
	hood3	0.041	2.17e-14	2.54e+06	4.903	2.391
	hood4	0.251	1.22e-13	1.30e+05	17.007	3.327
Fort Carson	car28	0.087	5.58e-14	5.10e+04	24.404	3.992
	car41	0.272	7.59e-14	9.54e+03	23.359	5.025
	car43	0.304	1.85e-13	5.40e+05	21.243	2.891
	afa1	0.025	3.53e-14	1.09e+04	24.711	5.090
Fort Hunter-Liggett	hl2	1.712	6.78e-13	2.51e+04	75.757	4.827
	hl5	2.532	1.97e-13	7.30e+04	115.912	4.539
	hl9	0.127	1.55e-13	6.38e+05	11.023	2.689
	hl10	0.445	5.12e-14	1.50e+06	29.146	2.821
Fort Lewis	lew3	0.062	2.92e-13	4.24e+04	5.132	3.200
	lew8	0.053	5.92e-14	6.86e+05	8.021	2.682
	lew10	0.173	3.04e-14	1.29e+05	12.463	3.367
	lew19	0.076	2.38e-13	1.53e+05	5.004	2.814
Fort Benning	ben_T3	0.079	1.34e-13	2.04e+05	5.349	2.810
	ben_L3	0.107	1.70e-13	1.91e+05	7.956	2.914
	ben_T4	0.113	6.26e-14	9.58e+05	7.682	2.591
	ben_D12	0.068	1.07e-13	2.49e+05	5.049	2.764
Smoky Mountains	NC1	0.118	1.74e-13	2.41e+04	14.701	3.969
	TN1	0.032	5.17e-14	1.14e+06	3.879	2.430
	TN2	0.089	4.46e-04	4.76e+01	10.727	5.178
	TN3	1.523	5.91e-13	1.52e+08	14.658	1.743
Willow Grove NAS	WG4	0.074	1.09e-13	9.47e+04	7.452	3.158
	WG6	0.042	1.26e-13	4.61e+05	4.731	2.586
	WG2	0.028	4.32e-14	1.23e+06	3.722	2.422
	WG5	0.131	7.20e-14	1.94e+05	10.419	3.077
Natchaug SF	Nat2	0.108	2.55e-14	1.42e+06	9.348	2.624
	Nat1	0.128	1.14e-13	1.94e+05	9.939	3.017
	Nat4	0.033	2.31e-14	2.33e+06	6.531	2.456
	Nat5	0.077	6.30e-14	4.14e+05	6.138	2.733
Fort Drum	8C	0.173	7.81e-14	2.53e+04	11.440	3.918
	7G	0.117	7.64e-14	6.72e+05	9.495	2.705
	7B	0.158	3.17e-13	1.36e+05	9.153	2.995
	7E	0.053	1.70e-14	7.38e+06	6.493	2.274
Canada - Gagetown	Gage31	0.061	1.49e-13	5.37e+04	5.400	3.209
	Gage27	0.050	1.44e-13	2.84e+05	4.450	2.672
	Gage08	0.077	8.05e-14	4.51e+05	6.673	2.711
	Gage07	0.072	1.66e-13	1.70e+04	9.227	3.913
Fort Greely	G22	0.057	2.25e-14	3.53e+05	5.891	2.856
	G00	0.037	1.87e-13	7.24e+06	6.790	2.111
	G25	0.038	1.00e-13	5.18e+05	4.333	2.560
	G02	0.078	7.16e-14	3.12e+05	6.652	2.814
	G24	0.039	5.74e-14	1.08e+05	8.467	3.225
	G05	0.057	2.43e-13	3.04e+05	5.127	2.643

Table E-19. Data Fits for the Pole-Zero Decay From a Prone Defender to a Kneeling Attacker						
Collection Area	**Site**	**SSE**	**Coeff α**	**Coeff δ**	**Coeff ε**	**Coeff γ**
Panama	gam1	0.069	1.30e-13	1.06e+06	6.385	2.468
	gam2	0.072	5.63e-13	1.23e+05	7.124	2.891
	gam3	0.019	2.06e-13	2.35e+03	11.180	5.462
	skh1	0.102	4.05e-14	1.05e+06	10.619	2.680
	mck1	0.124	7.94e-14	4.30e+06	11.706	2.354
	elv1	0.067	4.60e-14	6.13e+05	9.236	2.766
Panama - Wet	gam1w	0.070	7.87e-14	1.65e+05	5.585	2.931
	gam2w	0.026	3.06e-14	3.89e+04	9.364	3.735
	gam3w	0.043	8.08e-14	4.09e+05	8.484	2.796
	shk1w	0.120	4.78e-14	1.30e+06	8.741	2.576
	mck1w	0.052	4.24e-14	1.82e+07	6.912	2.083
	elv1w	0.090	3.63e-14	9.76e+05	9.316	2.677
Eglin AFB	egl_B2	0.030	7.91e-15	1.38e+06	7.538	2.680
	egl_X8	0.105	3.65e-14	1.76e+05	10.487	3.180
	egl_X11	0.094	2.81e-13	2.35e+04	9.350	3.692
	egl_B12	0.179	6.58e-15	2.74e+05	29.532	3.575
Fort Hood	hood1	0.060	4.92e-14	4.85e+04	18.726	3.899
	hood2	0.207	1.23e-13	4.84e+05	15.850	2.878
	hood3	0.075	5.01e-14	6.79e+06	5.893	2.194
	hood4	0.194	8.26e-14	2.35e+04	26.750	4.443
Fort Carson	car28	0.414	6.79e-14	1.84e+05	31.285	3.494
	car41	0.303	1.15e-03	5.67e+01	30.159	0.705
	car43	0.827	2.76e-13	2.88e+04	38.053	4.363
	afa1	0.110	1.34e-13	7.05e+04	28.023	3.785
Fort Hunter-Liggett	hl2	2.433	5.74e-13	1.64e+06	107.554	2.925
	hl5	1.854	5.52e-13	1.26e+04	139.002	6.267
	hl9	0.121	5.07e-14	2.46e+05	18.335	3.221
	hl10	0.486	6.56e-14	1.55e+06	34.653	2.835
Fort Lewis	lew3	0.058	8.55e-14	1.05e+06	7.375	2.536
	lew8	0.123	4.53e-14	6.93e+05	10.569	2.770
	lew10	0.117	2.96e-14	2.71e+04	16.651	4.212
	lew19	0.048	4.66e-13	4.53e+05	5.988	2.528
Fort Benning	ben_T3	0.086	2.39e-14	1.21e+06	7.443	2.614
	ben_L3	0.062	2.82e-14	7.09e+05	11.160	2.821
	ben_T4	0.148	2.55e-14	1.34e+07	12.167	2.250
	ben_D12	0.069	7.67e-14	3.77e+05	5.729	2.722
Smoky Mountains	NC1	0.050	6.60e-14	5.12e+04	20.452	3.878
	TN1	0.035	6.62e-14	3.52e+05	7.516	2.822
	TN2	0.075	2.83e-04	1.48e+02	13.713	3.435
	TN3	0.563	6.88e-14	6.70e+04	28.495	3.904
Willow Grove NAS	WG4	0.054	1.37e-13	7.35e+04	10.214	3.335
	WG6	0.100	1.06e-13	8.79e+05	10.505	2.636
	WG2	0.038	5.97e-14	4.22e+06	6.905	2.286
	WG5	0.063	8.46e-15	2.09e+05	14.365	3.381
Natchaug SF	Nat2	0.166	9.65e-14	4.86e+05	14.911	2.884
	Nat1	0.115	4.16e-14	5.74e+06	18.780	2.439
	Nat4	0.122	6.74e-14	1.46e+07	13.322	2.180
	Nat5	0.158	4.48e-14	1.11e+08	13.353	1.929
Fort Drum	8C	0.066	1.01e-13	2.38e+04	14.680	4.049
	7G	0.076	3.64e-14	1.96e+06	15.561	2.635
	7B	0.148	9.48e-14	2.35e+05	11.321	3.017
	7E	0.193	4.10e-14	1.47e+07	14.779	2.232
Canada - Gagetown	Gage31	0.048	2.93e-14	9.32e+05	8.047	2.672
	Gage27	0.056	4.41e-14	4.77e+05	6.972	2.762
	Gage08	0.069	3.77e-14	1.83e+06	8.256	2.512
	Gage07	0.030	4.39e-14	1.06e+05	12.212	3.391
Fort Greely	G22	0.101	1.26e-14	1.22e+06	11.046	2.757
	G00	0.071	6.05e-14	1.25e+07	11.319	2.187
	G25	0.034	1.46e-13	8.85e+06	5.374	2.065
	G02	0.105	1.11e-13	1.32e+07	10.977	2.130
	G24	0.040	2.27e-14	3.33e+05	11.982	3.070
	G05	0.073	1.78e-13	1.08e+06	7.083	2.459

Table E-20. Data Fits for the Pole-Zero Decay From a Crouching Defender to a Prone Attacker						
Collection Area	**Site**	**SSE**	**Coeff α**	**Coeff δ**	**Coeff ε**	**Coeff γ**
Panama	gam1	0.091	3.01e-13	2.95e+04	6.817	3.444
	gam2	0.077	7.33e-14	1.61e+05	7.867	3.047
	gam3	0.053	8.41e-14	5.12e+03	10.516	4.866
	skh1	0.119	1.57e-13	7.36e+05	9.536	2.620
	mck1	0.145	4.50e-14	5.79e+05	11.900	2.848
	elv1	0.074	2.95e-14	3.32e+05	9.627	2.982
Panama - Wet	gam1w	0.092	1.05e-14	8.94e+05	5.508	2.683
	gam2w	0.031	1.57e-14	4.03e+04	9.312	3.796
	gam3w	0.025	1.07e-13	4.85e+03	12.038	4.979
	shk1w	0.088	5.78e-14	1.74e+06	9.799	2.522
	mck1w	0.139	6.33e-14	8.57e+05	10.287	2.682
	elv1w	0.083	1.90e-14	4.82e+05	10.012	2.931
Eglin AFB	egl_B2	0.014	2.97e-14	5.41e+03	7.716	4.754
	egl_X8	0.232	3.08e-13	1.93e+04	13.094	3.948
	egl_X11	0.074	3.02e-13	4.00e+03	10.686	4.865
	egl_B12	0.469	8.74e-14	1.11e+06	23.696	2.795
Fort Hood	hood1	0.128	2.09e-13	6.56e+03	18.022	4.952
	hood2	0.090	2.33e-14	3.17e+06	10.382	2.486
	hood3	0.141	3.69e-14	2.55e+07	5.713	2.020
	hood4	0.117	2.77e-13	1.46e+04	24.992	4.542
Fort Carson	car28	0.284	6.35e-14	9.69e+03	31.771	5.312
	car41	1.298	4.51e-13	1.50e+05	37.522	3.428
	car43	0.343	8.66e-14	1.03e+06	26.310	2.845
	afa1	0.311	7.77e-14	2.77e+05	30.085	3.307
Fort Hunter-Liggett	hl2	1.162	1.82e-13	4.83e+04	81.059	4.590
	hl5	1.386	4.54e-13	8.80e+04	125.234	4.335
	hl9	0.261	5.24e-03	5.29e+01	24.302	6.757
	hl10	0.602	1.45e-13	7.73e+05	33.012	2.938
Fort Lewis	lew3	0.119	8.81e-14	1.11e+06	7.436	2.523
	lew8	0.136	6.96e-14	5.15e+05	10.554	2.806
	lew10	0.137	1.74e-12	1.93e+03	18.719	5.840
	lew19	0.083	1.61e-13	6.61e+04	6.421	3.188
Fort Benning	ben_T3	0.055	1.43e-13	8.56e+05	5.654	2.479
	ben_L3	0.097	6.46e-14	8.93e+05	13.194	2.731
	ben_T4	0.088	8.82e-14	6.34e+05	10.547	2.732
	ben_D12	0.061	2.29e-13	3.14e+05	5.629	2.663
Smoky Mountains	NC1	0.221	1.02e-13	2.46e+04	21.581	4.250
	TN1	0.021	1.17e-13	2.93e+04	8.810	3.672
	TN2	0.035	2.27e-13	1.54e+04	13.624	4.142
	TN3	0.186	1.39e-13	1.46e+04	27.060	4.708
Willow Grove NAS	WG4	0.101	8.28e-14	5.26e+03	12.779	5.004
	WG6	0.067	1.89e-14	3.59e+04	9.371	3.829
	WG2	0.133	3.24e-14	2.88e+07	9.140	2.076
	WG5	0.027	1.66e-13	1.34e+04	14.614	4.312
Natchaug SF	Nat2	0.162	1.56e-13	1.49e+04	17.355	4.367
	Nat1	0.077	4.24e-14	3.00e+05	19.123	3.188
	Nat4	0.349	1.55e-13	5.80e+06	17.135	2.317
	Nat5	0.125	5.82e-14	1.41e+07	10.959	2.166
Fort Drum	8C	0.059	3.54e-14	6.23e+03	14.059	5.082
	7G	0.069	6.30e-05	2.05e+02	15.861	3.779
	7B	0.022	5.39e-14	4.77e+02	17.004	9.163
	7E	0.066	5.95e-14	4.95e+04	18.653	3.863
Canada - Gagetown	Gage31	0.042	7.82e-13	1.95e+04	8.660	3.611
	Gage27	0.079	1.87e-13	1.20e+04	9.131	4.079
	Gage08	0.117	1.31e-13	2.60e+05	11.507	2.959
	Gage07	0.058	4.99e-13	2.82e+04	13.874	3.719
Fort Greely	G22	0.189	7.29e-13	9.85e+03	12.240	4.177
	G00	0.073	2.42e-14	8.67e+04	17.540	3.686
	G25	0.081	9.35e-14	3.11e+05	9.974	2.899
	G02	0.084	5.26e-14	1.55e+06	10.436	2.568
	G24	0.053	4.03e-14	9.10e+04	11.060	3.421
	G05	0.052	8.51e-14	7.42e+04	8.221	3.304

Table E-21. Data Fits for the Pole-Zero Decay From a Crouching Defender to a Kneeling Attacker						
Collection Area	**Site**	**SSE**	**Coeff α**	**Coeff δ**	**Coeff ε**	**Coeff γ**
Panama	gam1	0.082	2.42e-13	4.76e+05	7.799	2.636
	gam2	0.069	7.92e-14	1.18e+06	9.164	2.563
	gam3	0.030	4.97e-14	1.08e+04	12.212	4.514
	skh1	0.110	1.34e-14	6.01e+05	14.935	3.013
	mck1	0.090	4.94e-14	4.45e+05	13.465	2.944
	elv1	0.086	1.97e-13	1.11e+05	11.048	3.176
Panama - Wet	gam1w	0.047	9.30e-14	3.63e+04	6.861	3.500
	gam2w	0.071	1.04e-13	8.58e+04	10.809	3.329
	gam3w	0.030	1.26e-14	1.44e+04	12.688	4.551
	shk1w	0.150	1.70e-13	1.23e+06	12.242	2.552
	mck1w	0.153	2.23e-14	1.32e+06	12.691	2.721
	elv1w	0.104	7.89e-14	1.04e+05	11.924	3.325
Eglin AFB	egl_B2	0.012	5.79e-14	4.73e+04	9.521	3.582
	egl_X8	0.124	4.56e-14	3.46e+04	13.817	3.925
	egl_X11	0.039	9.81e-14	4.59e+03	12.488	5.071
	egl_B12	0.380	4.09e-13	3.77e+04	33.501	4.061
Fort Hood	hood1	0.164	1.66e-13	6.46e+04	23.334	3.713
	hood2	0.229	4.32e-14	4.79e+06	22.370	2.507
	hood3	0.258	1.37e-13	1.19e+07	7.654	2.078
	hood4	0.133	6.93e-13	8.60e+03	35.636	5.103
Fort Carson	car28	0.150	2.21e-13	1.02e+04	30.298	5.006
	car41	1.911	3.17e-13	3.20e+04	48.252	4.429
	car43	3.134	3.22e-13	2.74e+06	50.536	2.638
	afa1	0.271	9.42e-14	1.89e+05	34.479	3.483
Fort Hunter-Liggett	hl2	2.259	9.14e-13	1.32e+05	118.967	3.953
	hl5	1.000	9.33e-14	6.35e+03	160.235	8.153
	hl9	0.380	6.60e-14	8.27e+05	42.531	3.073
	hl10	1.013	2.23e-13	4.38e+06	63.646	2.615
Fort Lewis	lew3	0.156	2.80e-13	1.14e+05	13.956	3.208
	lew8	0.204	1.19e-14	1.01e+06	17.896	2.930
	lew10	0.047	8.47e-14	1.08e+04	22.739	4.885
	lew19	0.066	8.50e-14	2.38e+05	11.242	3.021
Fort Benning	ben_T3	0.425	1.13e-13	1.63e+08	16.035	1.848
	ben_L3	0.333	8.31e-14	1.49e+06	23.387	2.722
	ben_T4	0.216	1.02e-13	2.80e+07	19.607	2.111
	ben_D12	0.075	4.24e-14	1.94e+06	8.764	2.501
Smoky Mountains	NC1	0.105	1.51e-13	2.11e+04	26.285	4.415
	TN1	0.023	2.61e-14	5.48e+05	12.806	2.933
	TN2	0.065	6.03e-04	1.06e+02	14.144	3.687
	TN3	0.196	7.66e-14	3.59e+04	27.781	4.215
Willow Grove NAS	WG4	0.039	7.39e-05	1.19e+02	13.963	4.446
	WG6	0.550	1.03e-13	7.76e+08	21.160	1.717
	WG2	0.822	3.80e-13	4.74e+05	22.841	2.877
	WG5	0.033	5.05e-14	2.59e+04	15.952	4.142
Natchaug SF	Nat2	0.125	9.58e-14	3.65e+04	20.191	3.997
	Nat1	0.325	1.82e-14	5.32e+05	28.964	3.222
	Nat4	0.432	1.86e-13	4.43e+06	27.048	2.441
	Nat5	0.515	3.14e-13	8.98e+06	23.721	2.242
Fort Drum	8C	0.072	3.62e-14	5.25e+04	17.775	3.873
	7G	0.077	9.62e-14	3.50e+05	19.654	3.062
	7B	0.104	3.29e-03	3.73e+01	18.291	8.009
	7E	0.238	5.36e-14	2.05e+05	24.142	3.378
Canada - Gagetown	Gage31	0.136	6.95e-14	3.32e+06	14.238	2.451
	Gage27	0.063	9.36e-14	1.03e+05	11.149	3.284
	Gage08	0.127	5.08e-14	1.54e+05	12.616	3.253
	Gage07	0.026	8.01e-14	1.17e+05	15.212	3.371
Fort Greely	G22	0.054	4.33e-14	6.67e+04	15.026	3.664
	G00	0.032	7.53e-14	3.78e+04	18.902	3.976
	G25	0.040	4.97e-14	7.70e+04	12.489	3.510
	G02	0.106	5.05e-14	2.55e+06	16.664	2.564
	G24	0.036	3.17e-14	2.39e+05	12.079	3.142
	G05	0.085	1.45e-13	8.87e+04	10.372	3.265

Table E-22. Data Fits for the Pole-Zero Decay From a Prone Attacker to a Prone Defender						
Collection Area	**Site**	**SSE**	**Coeff α**	**Coeff δ**	**Coeff ε**	**Coeff γ**
Panama	gam1	0.035	4.34e-14	1.29e+06	4.702	2.457
	gam2	0.089	2.72e-14	4.00e+05	6.684	2.840
	gam3	0.020	1.50e-13	1.04e+03	10.861	6.469
	skh1	0.073	4.62e-14	9.44e+05	7.310	2.609
	mck1	0.063	1.12e-13	5.73e+05	6.466	2.618
	elv1	0.075	1.22e-13	2.15e+05	8.989	2.949
Panama - Wet	gam1w	0.037	4.33e-14	3.87e+06	3.528	2.213
	gam2w	0.084	5.04e-14	9.56e+04	8.285	3.273
	gam3w	0.065	2.00e-14	1.80e+06	5.439	2.481
	shk1w	0.063	2.86e-14	1.08e+07	5.122	2.141
	mck1w	0.051	7.99e-14	1.07e+06	5.459	2.474
	elv1w	0.037	2.92e-14	3.22e+05	8.995	2.972
Eglin AFB	egl_B2	0.062	6.13e-14	1.30e+05	4.533	2.963
	egl_X8	0.113	2.01e-13	1.67e+05	7.000	2.900
	egl_X11	0.100	9.79e-14	1.58e+05	6.241	2.954
	egl_B12	0.250	6.24e-14	8.42e+04	25.888	3.760
Fort Hood	hood1	0.160	3.26e-14	3.50e+05	14.642	3.081
	hood2	0.135	1.13e-13	3.67e+05	9.046	2.809
	hood3	0.051	1.80e-13	2.59e+04	9.084	3.688
	hood4	0.144	2.93e-13	7.91e+05	13.988	2.637
Fort Carson	car28	0.398	1.83e-13	4.07e+04	28.778	4.043
	car41	0.285	3.55e-14	2.73e+05	21.695	3.281
	car43	0.311	1.15e-13	8.39e+05	20.843	2.810
	afa1	0.112	5.19e-13	1.56e+04	25.448	4.409
Fort Hunter-Liggett	hl2	0.219	1.38e-13	2.28e+07	41.059	2.239
	hl5	2.901	1.12e-13	1.07e+06	124.114	3.290
	hl9	0.108	4.46e-14	1.13e+06	10.579	2.654
	hl10	0.425	8.31e-14	1.30e+06	28.652	2.809
Fort Lewis	lew3	0.049	5.79e-14	4.04e+05	4.842	2.690
	lew8	0.048	4.04e-14	6.51e+05	8.111	2.731
	lew10	0.156	2.56e-13	2.71e+05	10.423	2.852
	lew19	0.075	1.14e-13	1.98e+05	4.983	2.814
Fort Benning	ben_T3	0.061	3.59e-13	2.33e+05	5.359	2.683
	ben_L3	0.121	1.53e-13	1.04e+05	9.724	3.179
	ben_T4	0.107	8.48e-14	5.34e+05	8.939	2.737
	ben_D12	0.069	4.42e-14	3.36e+05	4.926	2.763
Smoky Mountains	NC1	0.229	1.60e-13	3.52e+06	11.213	2.328
	TN1	0.056	7.65e-06	9.70e+01	2.807	3.325
	TN2	0.066	3.94e-14	3.40e+06	7.806	2.377
	TN3	0.540	8.74e-14	1.31e+07	17.248	2.221
Willow Grove NAS	WG4	0.069	4.43e-14	1.83e+06	6.287	2.443
	WG6	0.081	1.81e-13	2.92e+05	6.450	2.737
	WG2	0.041	3.11e-14	2.54e+06	4.537	2.350
	WG5	0.045	1.07e-13	1.13e+06	5.644	2.448
Natchaug SF	Nat2	0.049	1.97e-13	1.62e+06	6.221	2.345
	Nat1	0.083	8.28e-14	2.64e+05	5.668	2.802
	Nat4	0.078	8.53e-14	2.40e+05	5.298	2.807
	Nat5	0.045	4.91e-14	4.58e+06	7.553	2.301
Fort Drum	8C	0.133	3.06e-13	1.22e+05	9.765	3.055
	7G	0.075	6.68e-14	6.27e+05	6.743	2.652
	7B	0.078	8.71e-14	8.19e+05	7.962	2.605
	7E	0.035	1.84e-13	1.40e+06	5.755	2.364
Canada - Gagetown	Gage31	0.074	2.16e-13	1.67e+05	5.132	2.806
	Gage27	0.052	6.70e-14	3.23e+05	4.374	2.706
	Gage08	0.034	3.58e-14	2.58e+06	5.168	2.360
	Gage07	0.059	5.23e-14	1.02e+04	11.932	4.531
Fort Greely	G22	0.055	9.31e-14	2.03e+05	7.035	2.921
	G00	0.067	8.58e-14	4.83e+05	6.229	2.672
	G25	0.056	5.37e-14	2.78e+05	4.254	2.756
	G02	0.082	1.09e-13	6.28e+05	6.412	2.597
	G24	0.059	3.00e-13	1.91e+05	9.227	2.901
	G05	0.053	1.81e-13	3.00e+05	4.914	2.662

Table E-23. Data Fits for the Pole-Zero Decay From a Prone Attacker to a Kneeling Defender						
Collection Area	**Site**	**SSE**	**Coeff α**	**Coeff δ**	**Coeff ε**	**Coeff γ**
Panama	gam1	0.126	1.96e-13	4.07e+05	7.548	2.685
	gam2	0.081	8.15e-14	9.18e+05	7.811	2.582
	gam3	0.016	1.72e-05	1.22e+02	11.816	4.692
	skh1	0.129	1.88e-13	4.32e+05	10.290	2.752
	mck1	0.097	9.12e-14	1.78e+06	12.388	2.528
	elv1	0.121	6.81e-14	4.69e+05	11.982	2.867
Panama - Wet	gam1w	0.056	4.22e-14	2.70e+05	5.703	2.860
	gam2w	0.070	1.60e-14	5.48e+04	10.917	3.728
	gam3w	0.105	2.35e-14	3.81e+06	8.602	2.414
	shk1w	0.106	5.09e-14	1.54e+07	6.888	2.093
	mck1w	0.058	6.72e-14	3.13e+06	7.686	2.348
	elv1w	0.045	8.87e-15	1.04e+06	10.503	2.813
Eglin AFB	egl_B2	0.034	3.18e-14	6.75e+05	8.012	2.740
	egl_X8	0.094	4.81e-14	8.20e+05	11.134	2.736
	egl_X11	0.114	1.94e-13	3.24e+04	9.383	3.593
	egl_B12	0.411	3.12e-13	8.17e+04	32.062	3.671
Fort Hood	hood1	0.244	1.51e-14	1.74e+06	19.488	2.792
	hood2	0.166	8.84e-14	5.77e+05	12.288	2.794
	hood3	0.185	1.03e-13	3.92e+05	10.301	2.836
	hood4	0.260	1.02e-13	4.20e+05	24.188	3.064
Fort Carson	car28	0.739	8.59e-14	2.35e+04	37.407	4.671
	car41	0.145	1.42e-13	1.02e+05	30.770	3.650
	car43	0.433	8.89e-14	8.76e+05	27.860	2.902
	afa1	0.166	5.49e-14	3.27e+05	30.048	3.285
Fort Hunter-Liggett	hl2	2.269	5.83e-13	2.70e+06	122.345	2.816
	hl5	2.459	2.05e-13	8.50e+04	175.318	4.725
	hl9	0.410	5.18e-03	1.31e+02	20.765	2.857
	hl10	0.489	1.64e-13	1.52e+06	31.365	2.730
Fort Lewis	lew3	0.092	6.09e-14	7.29e+05	9.661	2.709
	lew8	0.123	8.95e-14	4.73e+05	10.422	2.802
	lew10	0.258	7.24e-14	1.25e+05	15.525	3.365
	lew19	0.039	7.24e-14	7.93e+05	5.409	2.544
Fort Benning	ben_T3	0.097	4.00e-14	5.49e+05	8.163	2.775
	ben_L3	0.093	1.58e-13	4.00e+05	11.100	2.810
	ben_T4	0.153	1.27e-13	1.55e+06	16.122	2.588
	ben_D12	0.059	9.79e-14	4.75e+05	5.670	2.642
Smoky Mountains	NC1	0.212	1.21e-13	8.38e+04	22.284	3.613
	TN1	0.081	1.18e-13	2.78e+06	7.079	2.311
	TN2	0.093	2.98e-14	6.69e+05	14.100	2.893
	TN3	0.629	2.42e-13	1.51e+06	28.203	2.668
Willow Grove NAS	WG4	0.067	3.94e-14	6.26e+05	9.604	2.785
	WG6	0.128	3.30e-14	3.12e+05	10.596	3.017
	WG2	0.031	2.26e-14	7.17e+06	7.528	2.282
	WG5	0.095	3.67e-14	2.80e+06	11.307	2.491
Natchaug SF	Nat2	0.186	1.03e-13	3.50e+06	12.598	2.385
	Nat1	0.209	5.91e-14	2.56e+08	14.474	1.825
	Nat4	0.108	1.38e-13	4.41e+06	13.015	2.326
	Nat5	0.236	8.72e-14	5.34e+06	16.748	2.373
Fort Drum	8C	0.060	1.29e-13	4.13e+04	14.734	3.739
	7G	0.084	5.20e-14	4.90e+06	15.149	2.411
	7B	0.060	1.36e-14	2.99e+07	10.821	2.153
	7E	0.218	1.18e-13	1.33e+07	13.339	2.155
Canada - Gagetown	Gage31	0.071	1.05e-13	7.79e+06	8.193	2.171
	Gage27	0.049	6.57e-14	3.33e+06	6.487	2.309
	Gage08	0.084	1.84e-14	4.55e+06	10.253	2.432
	Gage07	0.098	4.73e-14	7.14e+04	14.591	3.611
Fort Greely	G22	0.096	1.94e-13	2.70e+05	12.409	2.931
	G00	0.161	5.65e-14	1.78e+08	11.596	1.844
	G25	0.042	2.46e-14	2.63e+07	6.635	2.063
	G02	0.048	2.44e-14	1.65e+07	10.661	2.199
	G24	0.061	7.91e-15	7.25e+05	14.683	3.005
	G05	0.081	5.06e-14	1.34e+06	7.458	2.530

Table E-24. Data Fits for the Pole-Zero Decay From a Crouching Attacker to a Prone Defender						
Collection Area	**Site**	**SSE**	**Coeff α**	**Coeff δ**	**Coeff ε**	**Coeff γ**
Panama	gam1	0.053	3.28e-13	2.34e+03	11.095	5.371
	gam2	0.056	5.06e-14	1.04e+05	10.565	3.331
	gam3	0.024	8.17e-14	3.79e+03	16.543	5.545
	skh1	0.120	1.40e-13	3.96e+04	14.136	3.728
	mck1	0.069	2.39e-14	5.54e+04	16.035	3.849
	elv1	0.088	3.49e-14	2.26e+05	11.758	3.142
Panama - Wet	gam1w	0.069	6.16e-14	4.82e+04	6.502	3.414
	gam2w	0.045	9.29e-15	1.56e+04	13.308	4.571
	gam3w	0.076	1.29e-13	5.97e+04	10.046	3.415
	shk1w	0.117	9.55e-14	1.77e+05	12.289	3.130
	mck1w	0.020	6.98e-14	4.26e+04	10.349	3.640
	elv1w	0.070	6.46e-14	3.39e+05	10.416	2.923
Eglin AFB	egl_B2	0.028	3.00e-14	4.71e+04	9.865	3.676
	egl_X8	0.072	4.00e-14	7.27e+05	8.597	2.719
	egl_X11	0.097	6.73e-14	2.90e+05	10.118	2.955
	egl_B12	0.328	5.82e-14	1.86e+04	39.697	4.956
Fort Hood	hood1	0.188	2.85e-13	1.88e+05	18.214	3.126
	hood2	0.258	1.25e-14	2.12e+05	14.669	3.342
	hood3	0.090	5.61e-14	5.82e+05	9.280	2.762
	hood4	0.594	2.38e-13	3.17e+04	32.373	4.221
Fort Carson	car28	0.280	6.34e-13	4.94e+03	28.172	5.437
	car41	0.261	6.21e-14	5.07e+04	33.928	4.160
	car43	0.400	1.36e-13	8.38e+05	25.823	2.852
	afa1	0.275	4.70e-14	3.00e+05	31.195	3.346
Fort Hunter-Liggett	hl2	1.211	8.85e-14	7.45e+05	103.878	3.385
	hl5	1.982	1.83e-13	4.35e+04	127.569	5.029
	hl9	0.124	2.37e-14	4.23e+05	27.870	3.258
	hl10	0.307	3.94e-14	6.81e+06	37.571	2.549
Fort Lewis	lew3	0.122	1.09e-13	3.45e+05	12.933	2.929
	lew8	0.104	1.22e-14	2.94e+05	12.744	3.189
	lew10	0.155	1.70e-13	1.12e+05	12.895	3.243
	lew19	0.068	2.79e-14	5.31e+05	8.066	2.813
Fort Benning	ben_T3	0.126	8.49e-14	1.67e+05	10.830	3.122
	ben_L3	0.169	5.08e-14	4.14e+05	14.808	2.990
	ben_T4	0.260	1.27e-13	1.87e+05	17.048	3.193
	ben_D12	0.077	9.80e-14	4.92e+05	7.803	2.710
Smoky Mountains	NC1	0.307	1.40e-13	7.97e+06	15.234	2.247
	TN1	0.018	3.14e-14	2.89e+06	3.431	2.279
	TN2	0.059	1.08e-13	2.06e+06	8.812	2.416
	TN3	0.420	1.41e-13	4.37e+07	17.528	2.009
Willow Grove NAS	WG4	0.023	6.82e-14	4.86e+04	13.067	3.688
	WG6	0.059	2.03e-14	2.17e+05	20.275	3.397
	WG2	0.061	1.57e-13	1.47e+05	13.617	3.176
	WG5	0.058	2.35e-13	7.14e+04	11.294	3.323
Natchaug SF	Nat2	0.030	5.06e-14	1.90e+07	6.991	2.066
	Nat1	0.065	4.62e-14	5.72e+05	5.977	2.677
	Nat4	0.047	4.26e-14	1.23e+07	7.418	2.150
	Nat5	0.294	4.87e-14	1.93e+08	17.211	1.888
Fort Drum	8C	0.081	1.81e-13	1.57e+03	20.481	6.763
	7G	0.033	3.13e-14	7.22e+06	7.438	2.255
	7B	0.073	1.36e-14	3.70e+07	12.169	2.139
	7E	0.102	9.13e-14	2.87e+05	14.298	3.030
Canada - Gagetown	Gage31	0.025	3.10e-14	2.10e+07	5.532	2.053
	Gage27	0.052	4.21e-14	5.61e+06	6.966	2.265
	Gage08	0.062	1.67e-13	1.59e+06	6.745	2.379
	Gage07	0.158	7.32e-14	5.82e+04	18.427	3.754
Fort Greely	G22	0.064	1.67e-13	7.92e+03	16.572	4.768
	G00	0.060	6.31e-14	8.90e+05	6.877	2.582
	G25	0.059	1.03e-13	2.04e+05	4.296	2.777
	G02	0.125	1.44e-13	3.66e+05	13.706	2.901
	G24	0.082	1.50e-14	2.93e+05	15.257	3.228
	G05	0.162	4.02e-14	5.38e+05	10.676	2.848

Table E-25. Data Fits for the Pole-Zero Decay From a Crouching Attacker to a Kneeling Defender						
Collection Area	**Site**	**SSE**	**Coeff α**	**Coeff δ**	**Coeff ε**	**Coeff γ**
Panama	gam1	0.077	3.75e-14	5.69e+04	12.302	3.663
	gam2	0.101	1.39e-13	3.38e+05	12.147	2.892
	gam3	0.041	5.36e-14	1.44e+04	16.071	4.497
	skh1	0.090	1.04e-12	1.15e+05	16.816	3.125
	mck1	0.044	3.48e-14	1.16e+05	17.407	3.521
	elv1	0.070	1.29e-13	3.24e+04	15.481	3.882
Panama - Wet	gam1w	0.031	5.10e-13	9.35e+03	7.842	3.995
	gam2w	0.056	4.92e-14	2.16e+04	15.039	4.216
	gam3w	0.095	4.14e-14	2.26e+05	11.848	3.126
	shk1w	0.178	2.40e-13	5.72e+05	13.771	2.733
	mck1w	0.039	1.68e-14	8.46e+04	12.761	3.605
	elv1w	0.099	4.08e-14	6.17e+04	13.683	3.664
Eglin AFB	egl_B2	0.039	4.88e-14	7.38e+04	14.001	3.576
	egl_X8	0.107	1.62e-13	7.97e+04	12.175	3.352
	egl_X11	0.246	1.55e-13	1.07e+05	15.600	3.340
	egl_B12	0.459	1.09e-13	1.31e+05	39.617	3.683
Fort Hood	hood1	0.279	1.04e-13	4.02e+05	22.183	3.049
	hood2	0.179	4.78e-14	6.29e+05	24.691	3.023
	hood3	0.062	1.35e-13	9.37e+05	9.787	2.584
	hood4	0.446	1.21e-13	1.87e+05	33.523	3.447
Fort Carson	car28	0.244	1.62e-13	3.43e+04	36.063	4.294
	car41	0.347	1.70e-13	3.51e+04	39.601	4.333
	car43	0.539	6.65e-14	2.41e+06	53.040	2.830
	afa1	0.486	1.27e-13	4.20e+06	40.090	2.569
Fort Hunter-Liggett	hl2	1.361	1.19e-13	1.68e+04	162.200	6.410
	hl5	3.101	2.71e-13	1.22e+05	173.672	4.416
	hl9	1.011	4.86e-13	4.50e+05	60.723	3.182
	hl10	0.770	1.67e-13	5.58e+07	90.708	2.207
Fort Lewis	lew3	0.136	2.46e-14	8.87e+03	22.074	5.227
	lew8	0.178	4.44e-14	6.55e+05	20.823	2.969
	lew10	0.140	2.79e-13	9.78e+04	24.150	3.480
	lew19	0.101	4.80e-14	1.08e+06	14.009	2.726
Fort Benning	ben_T3	0.090	1.84e-14	8.33e+07	19.215	2.069
	ben_L3	0.100	5.28e-14	1.85e+05	22.312	3.389
	ben_T4	0.255	6.51e-14	4.06e+06	37.502	2.619
	ben_D12	0.109	1.23e-13	1.91e+05	12.244	3.079
Smoky Mountains	NC1	0.136	7.22e-14	1.62e+05	24.296	3.436
	TN1	0.269	1.43e-13	5.77e+06	12.265	2.264
	TN2	0.143	2.93e-13	1.89e+06	14.655	2.453
	TN3	0.462	3.09e-14	6.11e+06	26.532	2.519
Willow Grove NAS	WG4	0.125	4.45e-14	2.81e+06	17.077	2.560
	WG6	0.083	2.67e-14	1.15e+06	33.574	2.993
	WG2	0.284	4.22e-14	7.32e+05	21.588	2.952
	WG5	0.078	2.01e-14	2.80e+05	16.301	3.234
Natchaug SF	Nat2	0.230	1.17e-14	5.28e+06	19.670	2.566
	Nat1	0.806	1.72e-13	4.79e+07	22.876	2.019
	Nat4	0.427	1.29e-13	1.87e+07	23.714	2.186
	Nat5	0.614	1.44e-13	8.11e+06	37.711	2.408
Fort Drum	8C	0.072	3.07e-14	8.04e+03	22.387	5.288
	7G	0.220	8.41e-14	1.10e+06	20.637	2.766
	7B	0.253	3.24e-14	4.95e+07	25.515	2.145
	7E	0.207	9.40e-14	2.24e+06	20.746	2.588
Canada - Gagetown	Gage31	0.391	6.35e-14	3.21e+07	15.026	2.085
	Gage27	0.147	3.39e-14	9.73e+06	11.864	2.278
	Gage08	0.073	3.56e-14	3.43e+06	10.286	2.435
	Gage07	0.129	4.33e-14	1.50e+05	20.357	3.455
Fort Greely	G22	0.040	1.07e-14	2.32e+05	19.342	3.425
	G00	0.336	5.09e-14	2.12e+07	16.071	2.172
	G25	0.208	1.59e-13	5.84e+07	10.437	1.897
	G02	0.087	3.38e-14	1.27e+06	24.015	2.852
	G24	0.075	4.01e-14	4.59e+05	15.929	3.004
	G05	0.144	1.08e-13	1.98e+05	13.058	3.101

Representative Data Sites

Data were collected at several (between one and six) sites at each location. The sites at each location were analyzed and a site representative of the biome was selected by examining three different factors. First, the undergrowth data collected at each location was examined. The sites were subjectively ranked based on the most representative undergrowth type, median undergrowth height, and maximum undergrowth height. Second, the raw data curves along with the field notes were examined and the sites were subjectively ranked based on how well the site represented the location. Some of the sites were eliminated by this analysis because they were classified as outliers. Lastly, the data parameters for all three curves were examined and ranked based on parameters and sum of squares (a measure of error between the raw and the fitted data). Sites were ranked and preference given to those with parameters similar to the rest of the sites. The sum of squares was used as a discriminating factor when ranking sites with similar parameters. The most representative site at each location was selected based on these three approaches and presented in table E-26.

Table E-26. Best Representative Sites for Each Location

Location	Site
Panama – Gamboa	gam2
Panama – Fort Sherman	mck1
Panama – El Valle	elv1
Eglin AFB	egl_B2
Fort Hood	hood1
Fort Carson	car28
Fort Hunter-Liggett	hl10
Fort Lewis	lew8
Fort Benning	ben_T4
Smoky Mountains	TN2
Willow Grove NAS	WG2
Natchaug State Forest	Nat4
Fort Drum	7G
Canada - Gagetown	Gage 31
Fort Greely	G2

Panama Discussion

Data was collected from Panama twice. The first data collection coincided with the end of the worst drought in over 100 years. Because the vegetation appeared dry and sparse during the first data collection, data was collected a second time at the end of Panama's rainy season. Surprisingly, the visibility during the two trips was virtually equal. The differences in the fitted curves for the El Valle site for the two trips are less than 1 percent across all ranges. The vegetation parameters for the sites at Gamboa and Fort Sherman indicate that the vegetation was slightly denser the second trip. However, the difference was undistinguishable by the data collection team and was apparent only after the data was analyzed and plotted. The analysis showed that for the two visits, the difference between corresponding best fit curves, for any given range, was always less than 5 percent.

This page intentionally left blank.

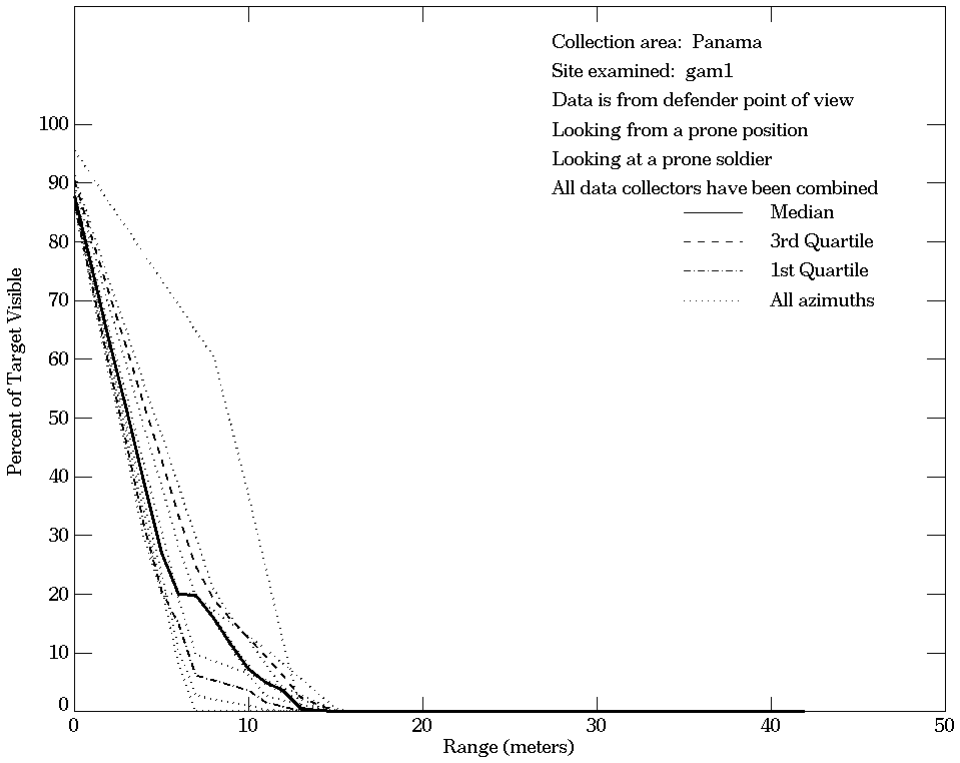

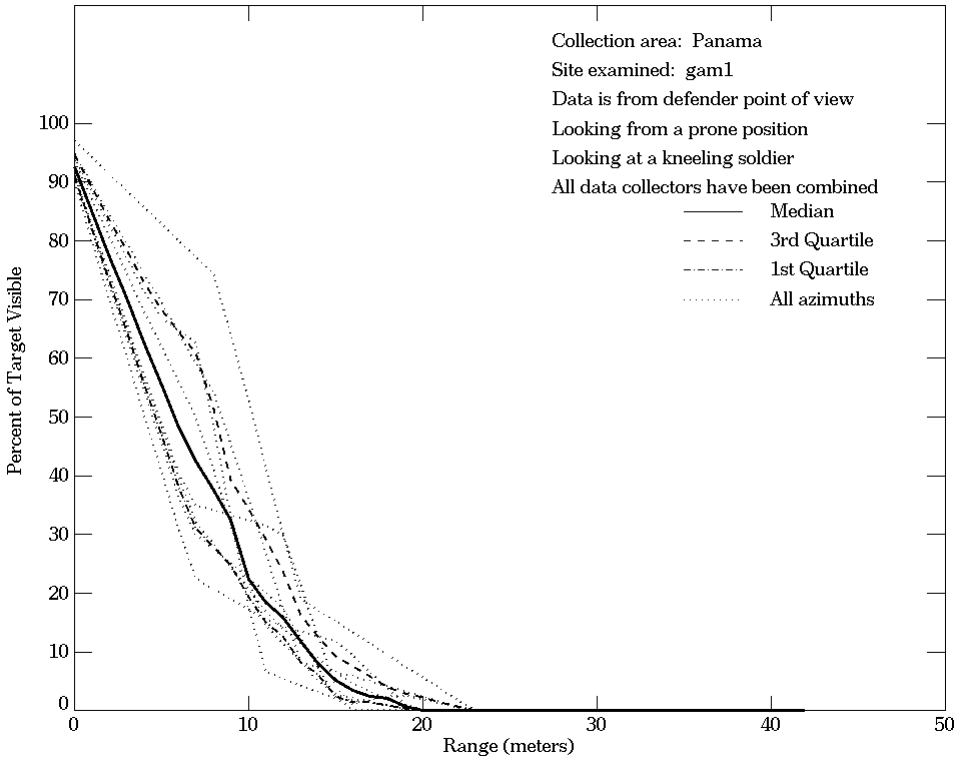

Figure E-1. Panama, From Defender Point of View, Site gam1

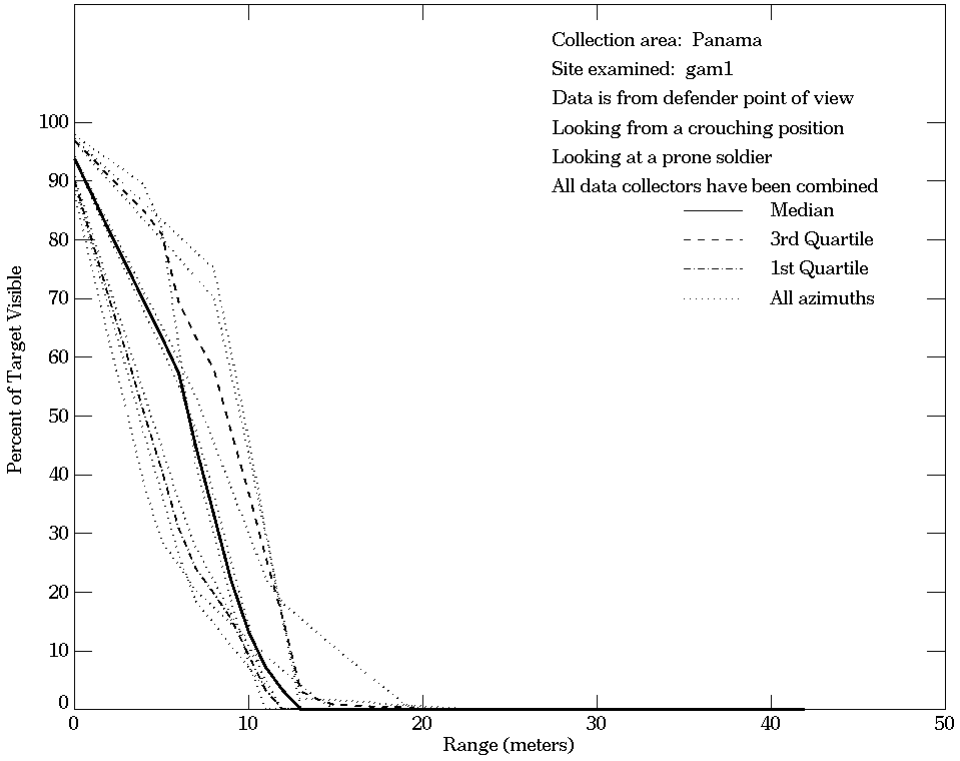

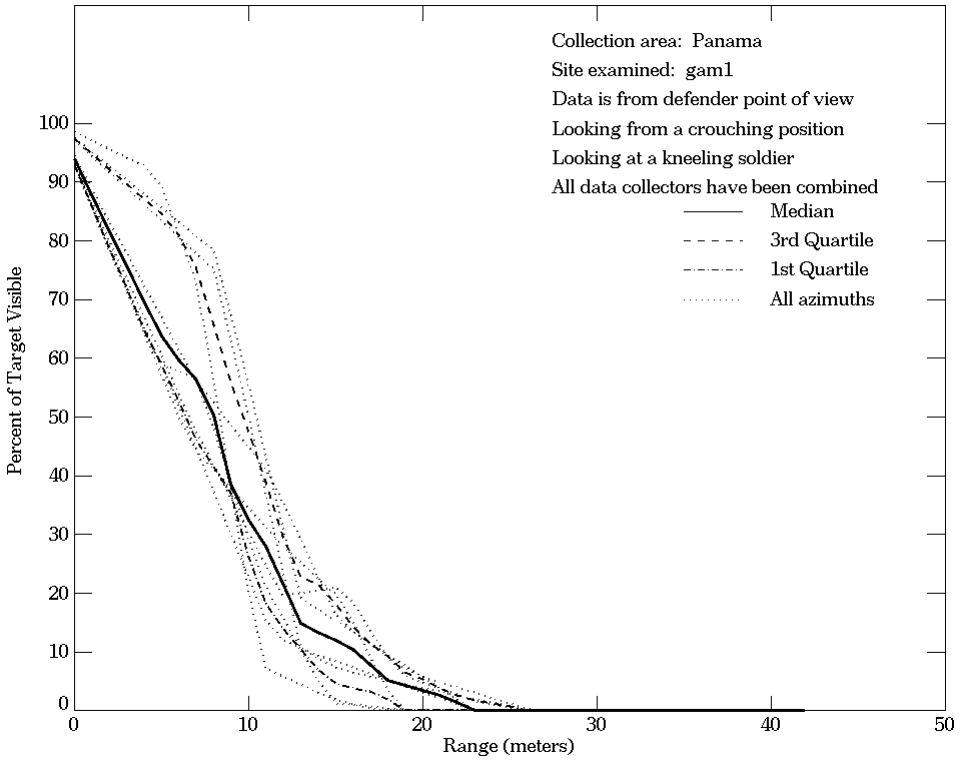

Figure E-1. Panama, From Defender Point of View, Site gam1 (Continued)

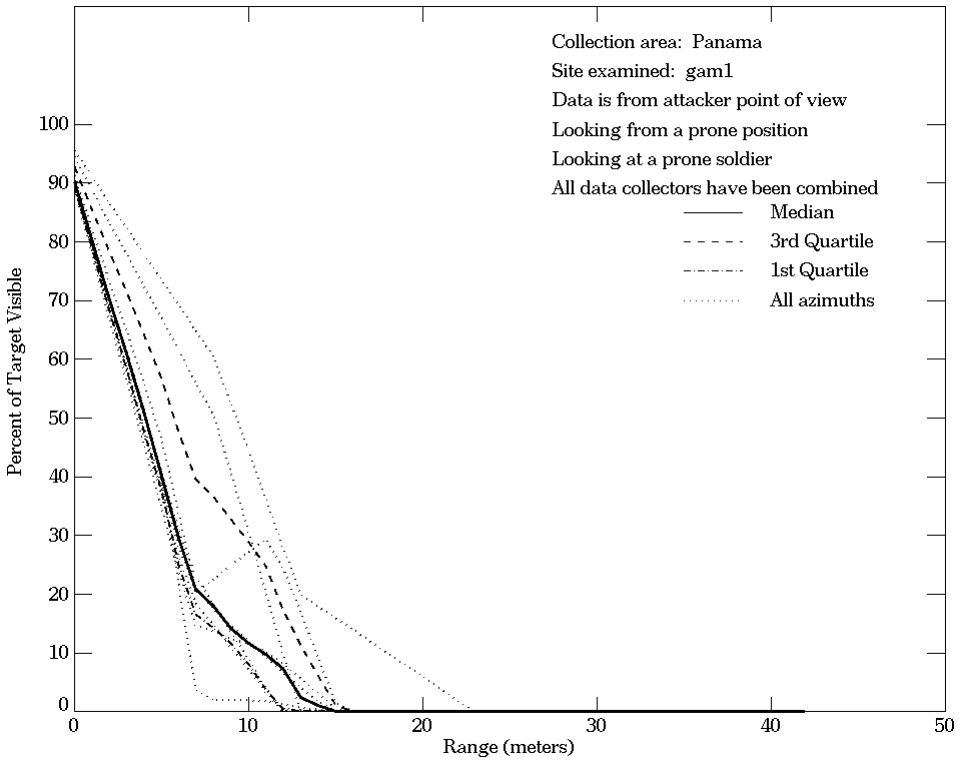

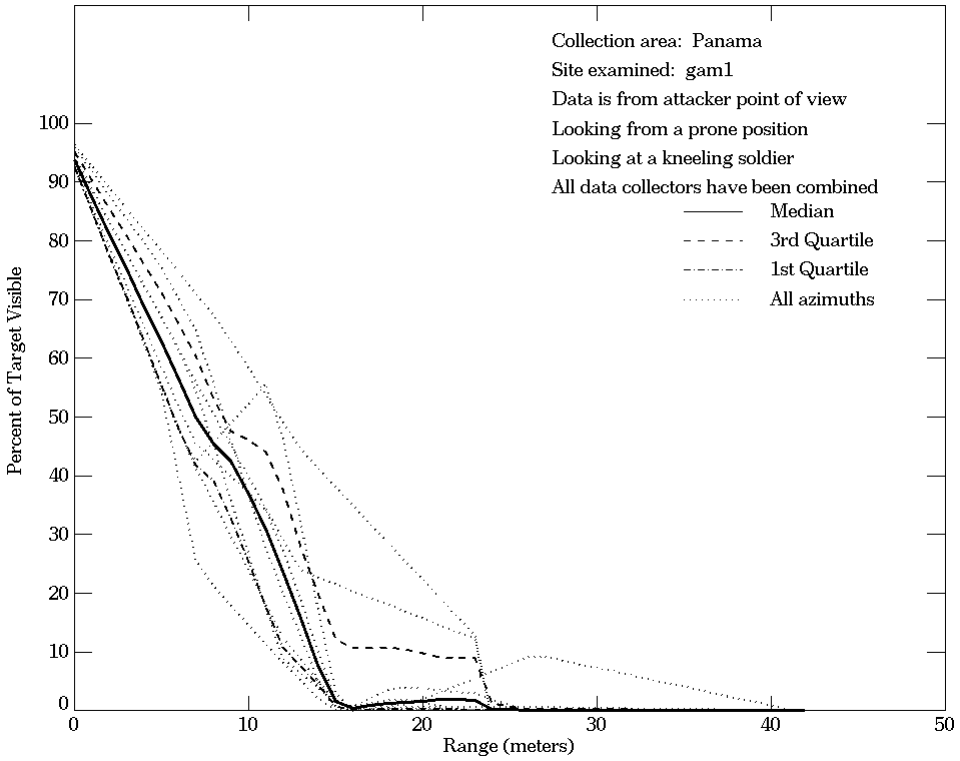

Figure E-2. Panama, From Attacker Point of View, Site gam1

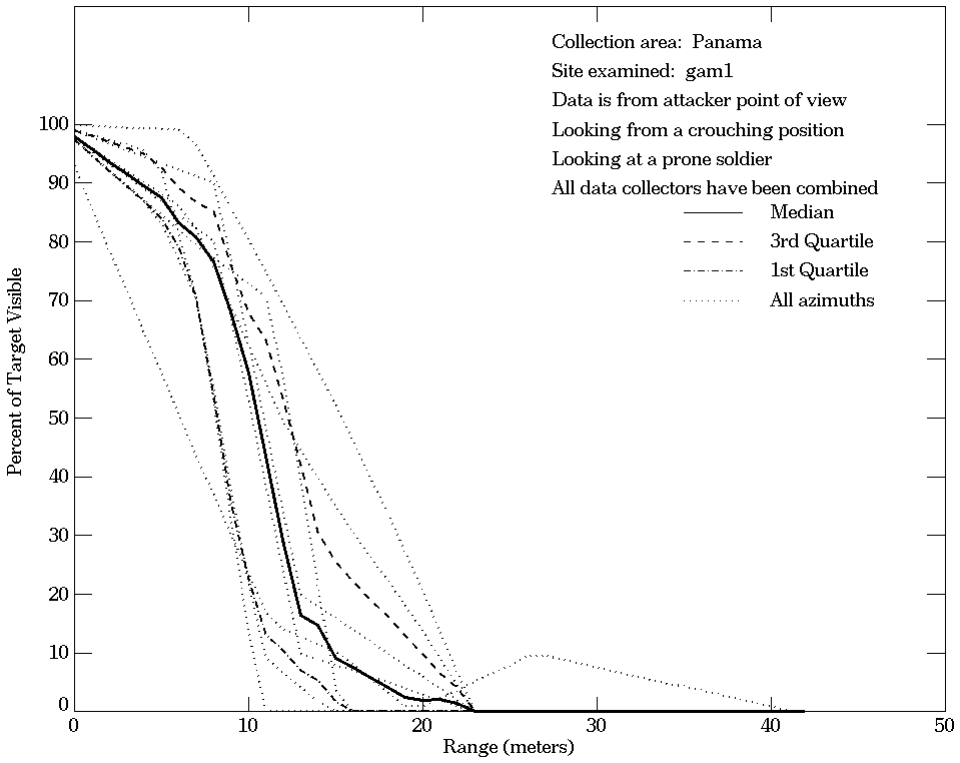

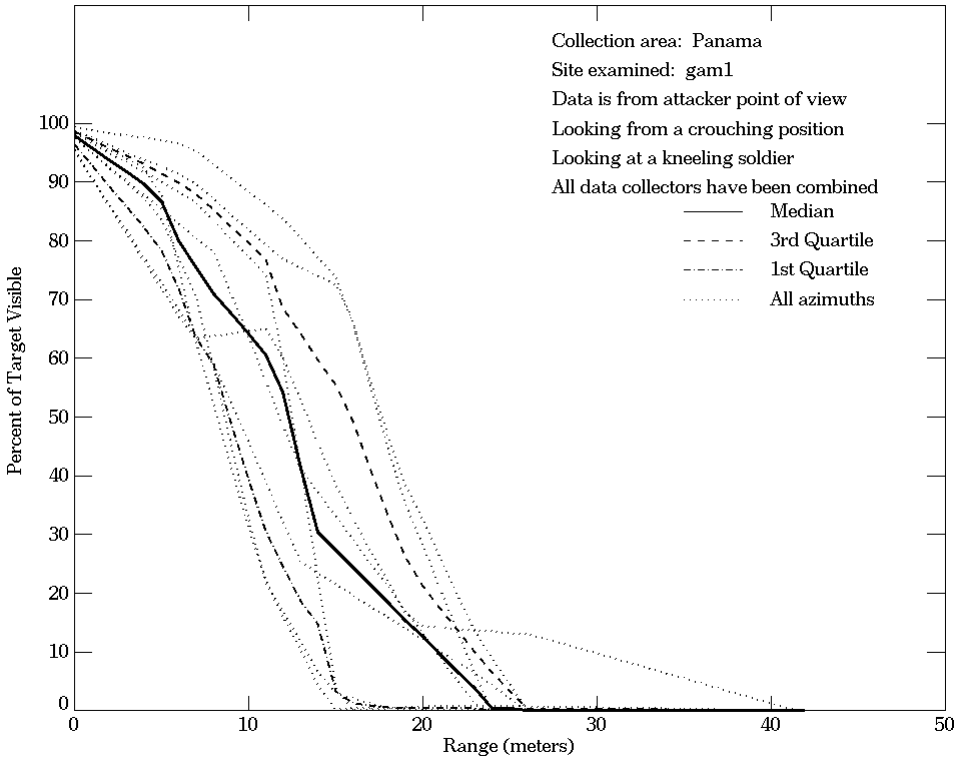

Figure E-2. Panama, From Attacker Point of View, Site gam1 (Continued)

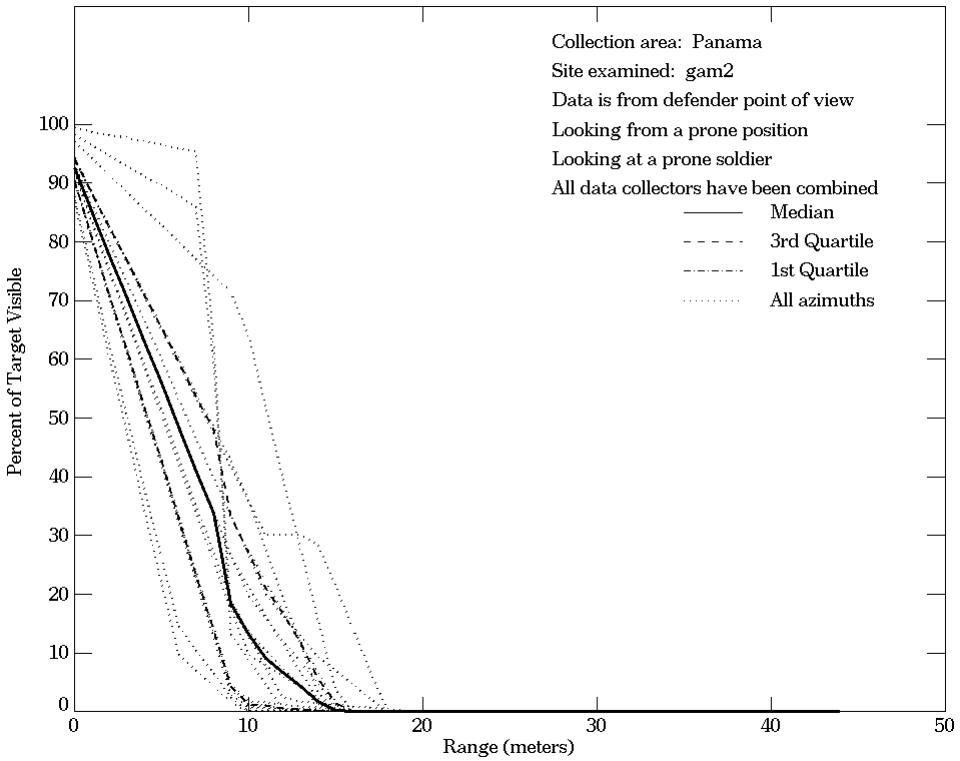

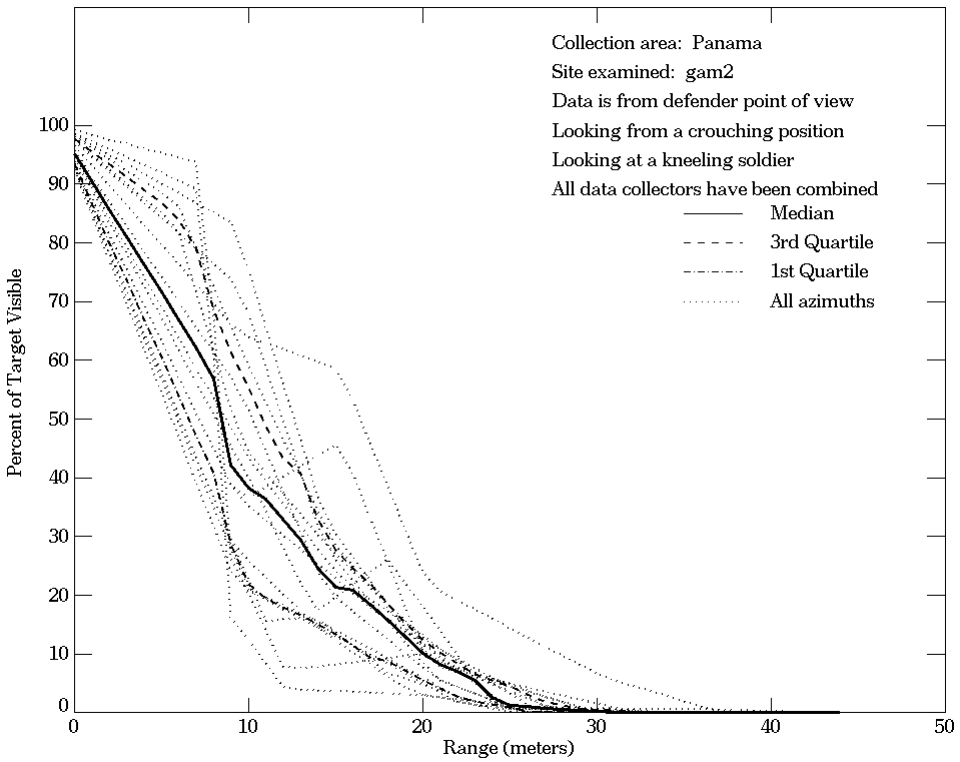

Figure E-3. Panama, From Defender Point of View, Site gam2

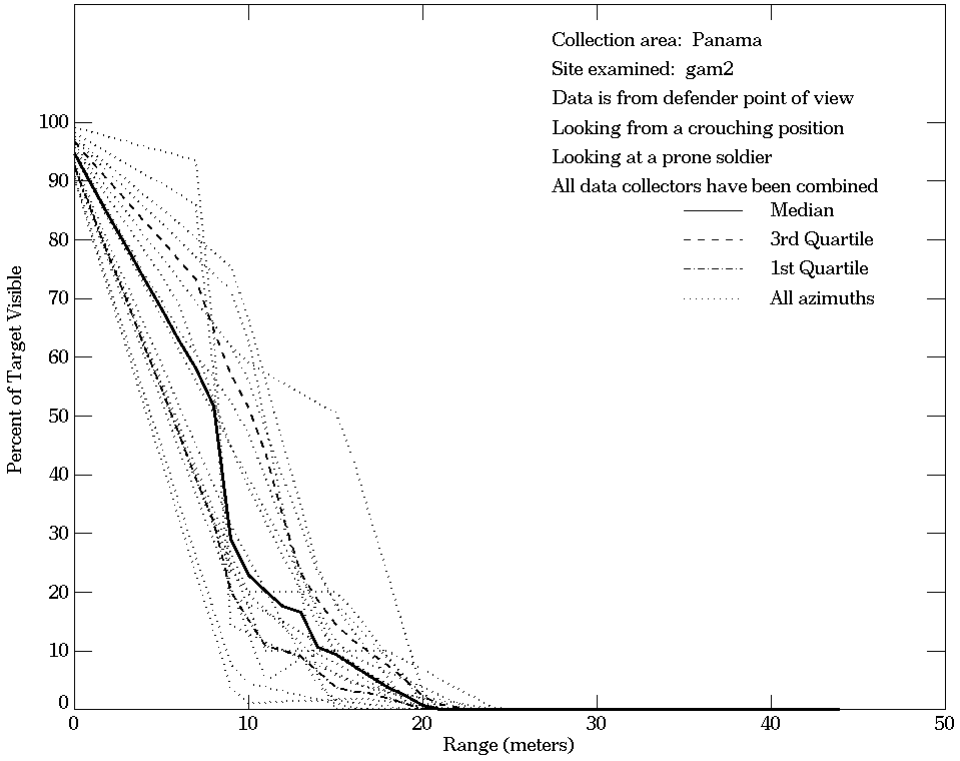

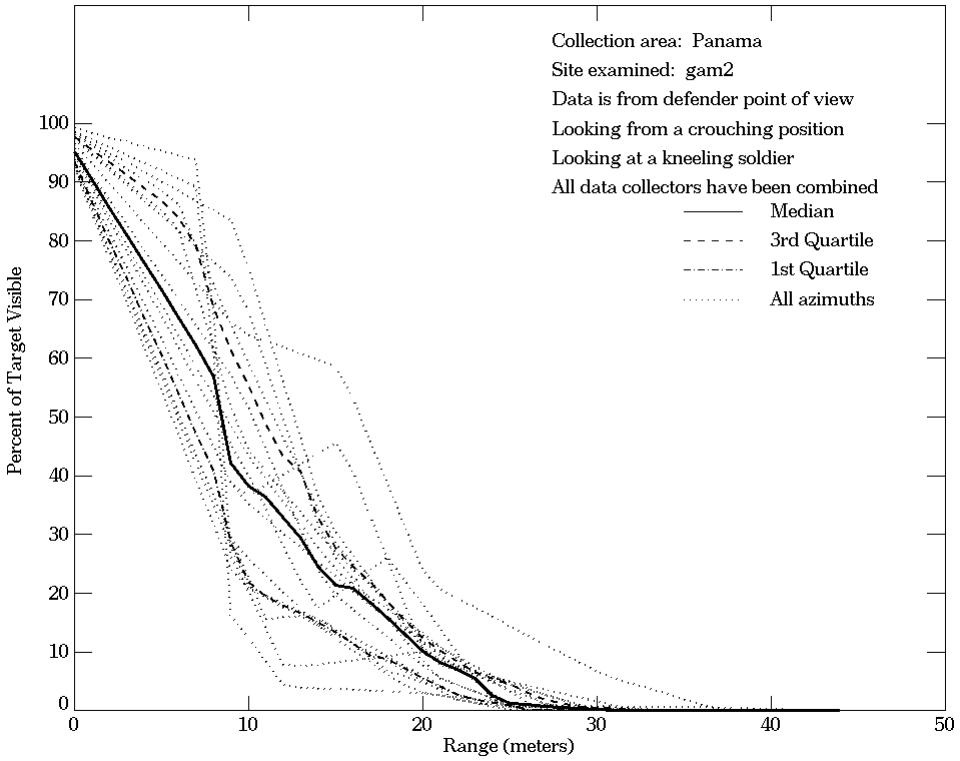

Figure E-3. Panama, From Defender Point of View, Site gam2 (Continued)

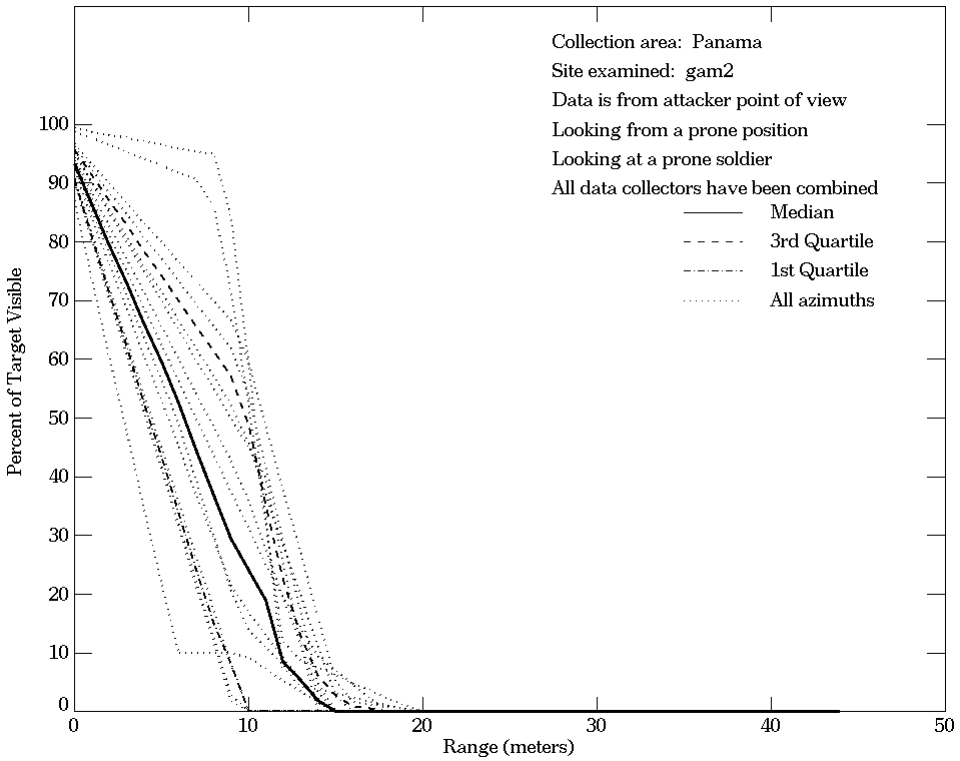

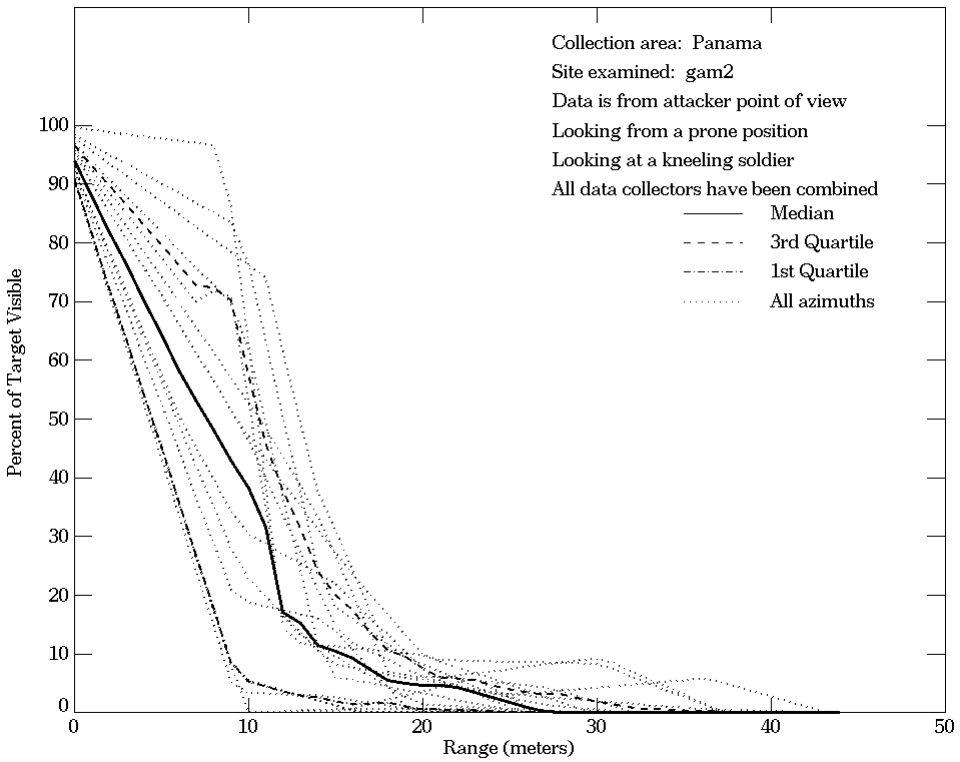

Figure E-4. Panama, From Attacker Point of View, Site gam2

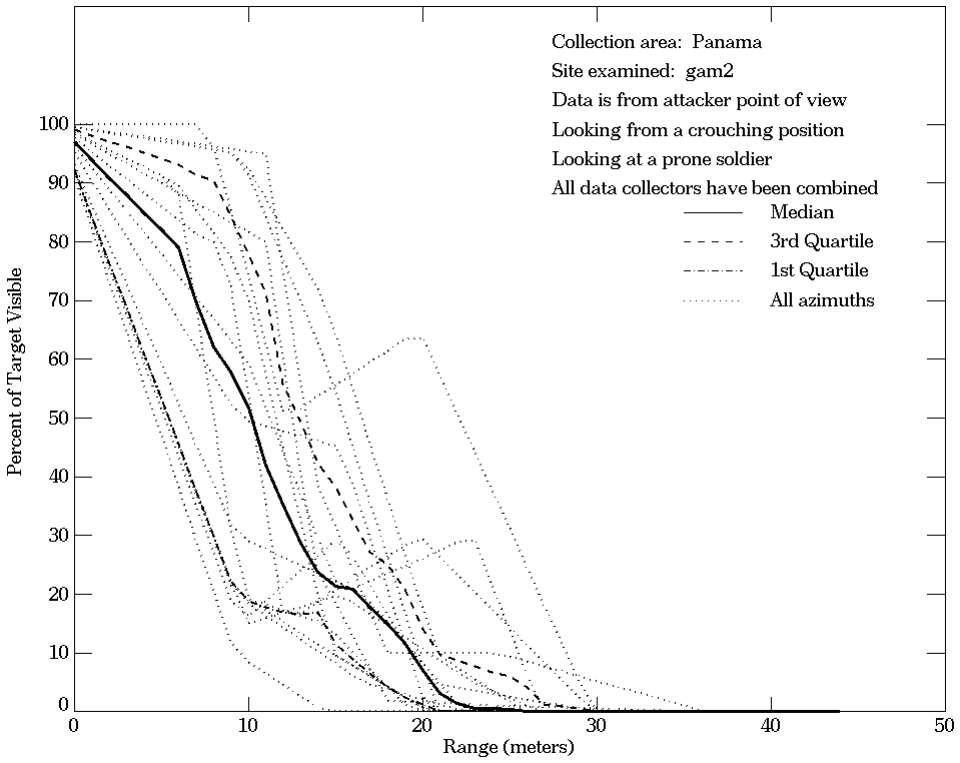

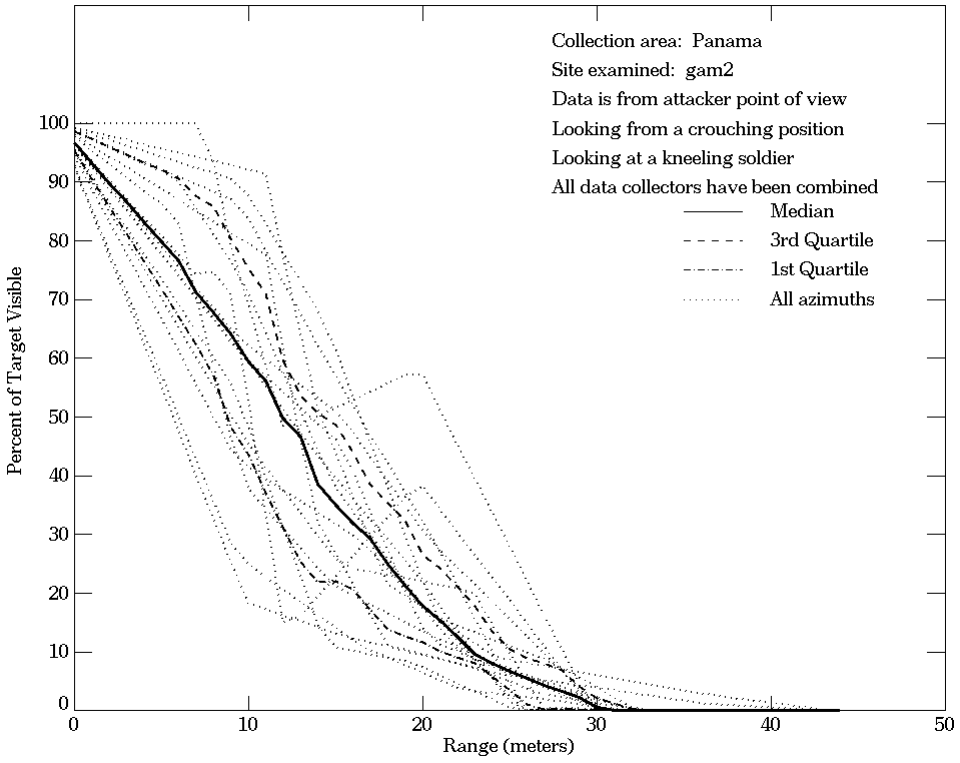

Figure E-4. Panama, From Attacker Point of View, Site gam2 (Continued)

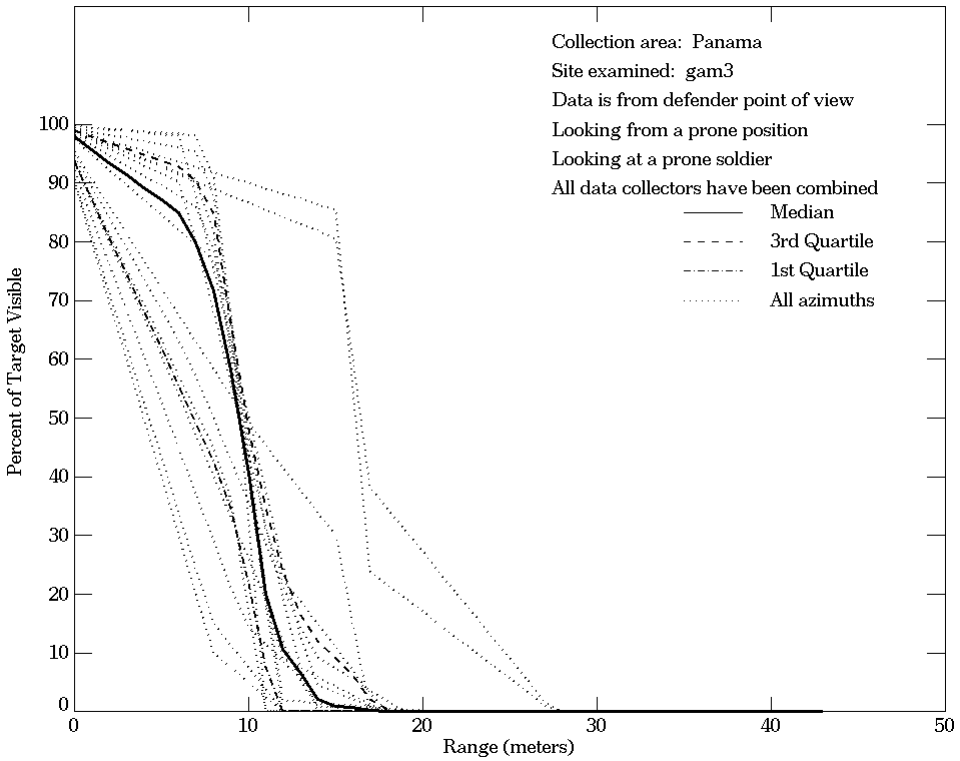

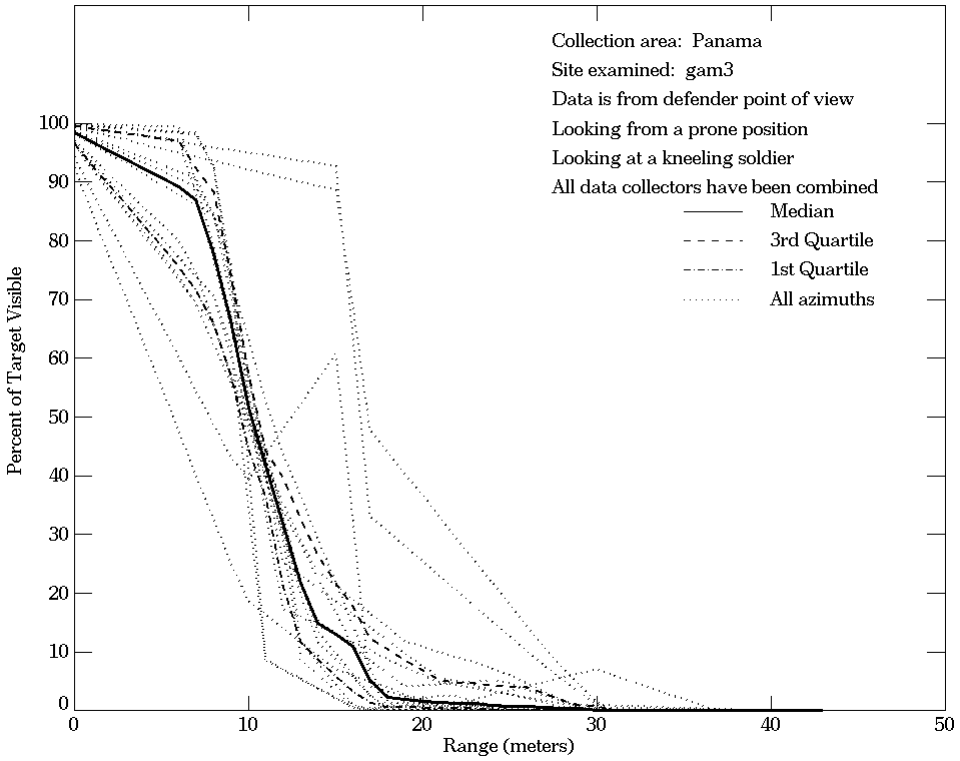

Figure E-5. Panama, From Defender Point of View, Site gam3

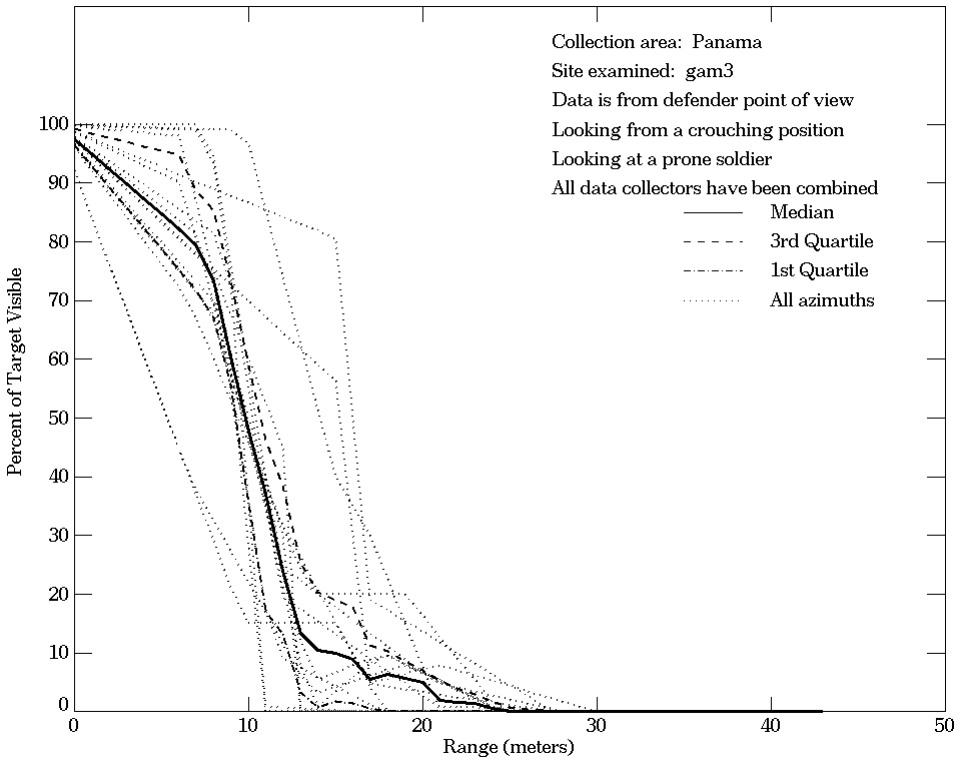

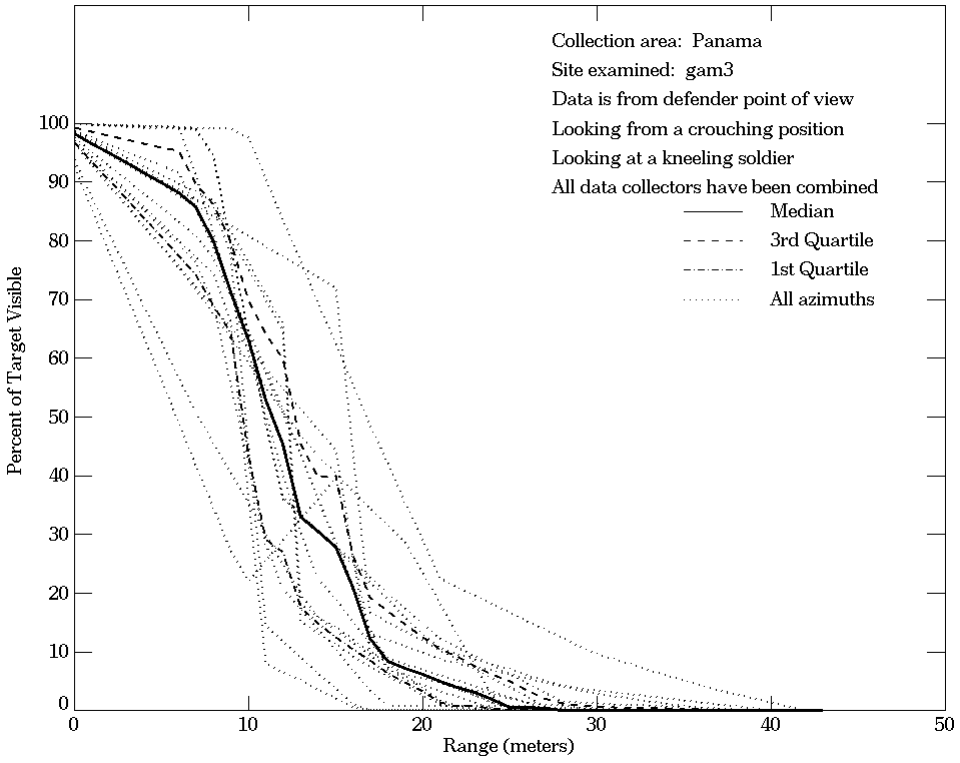

Figure E-5. Panama, From Defender Point of View, Site gam3 (Continued)

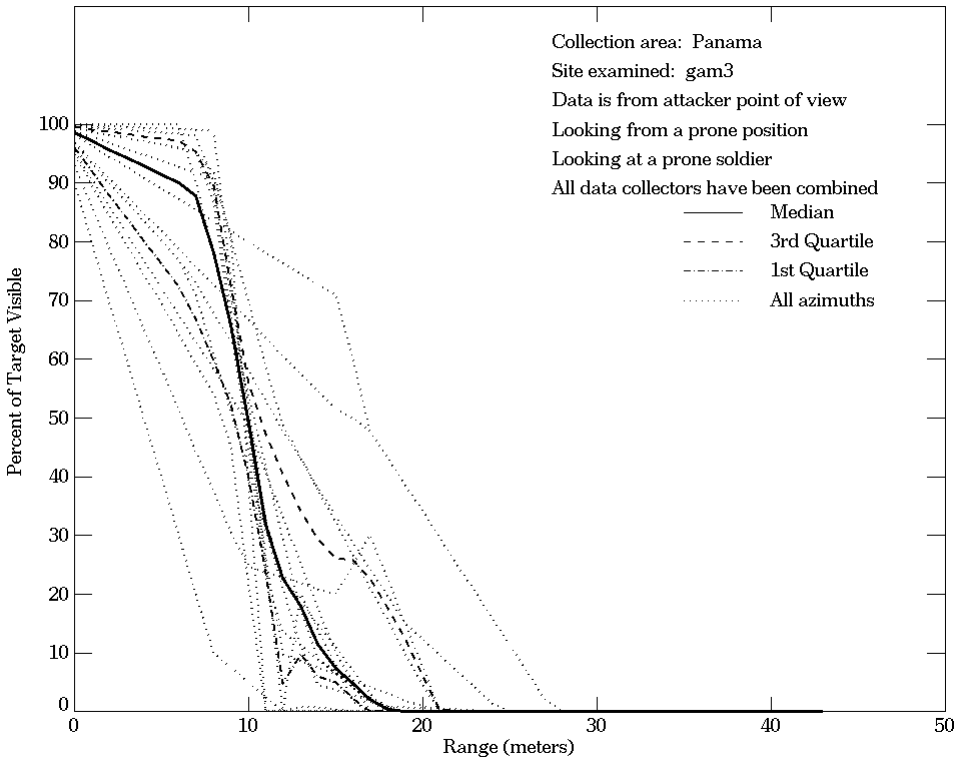

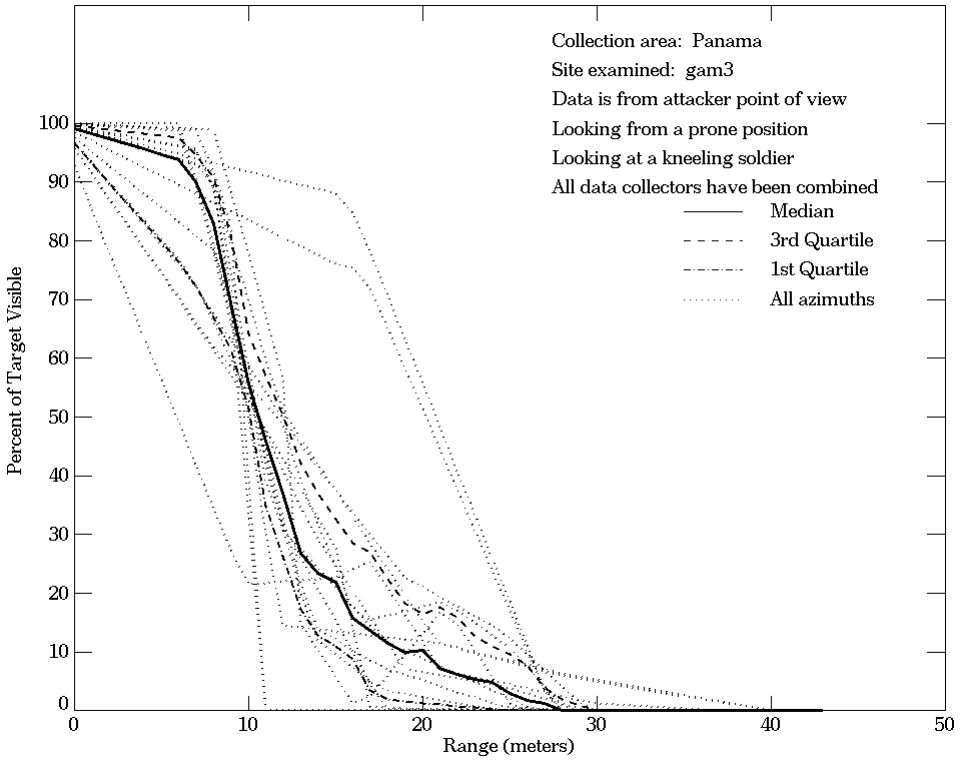

Figure E-6. Panama, From Attacker Point of View, Site gam3

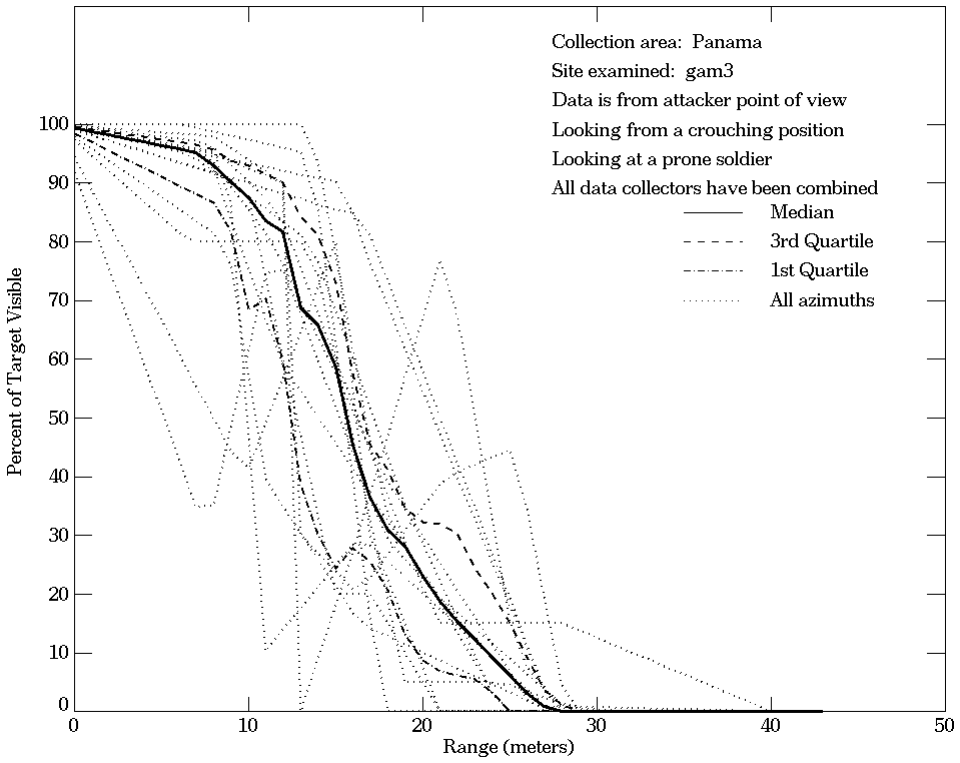

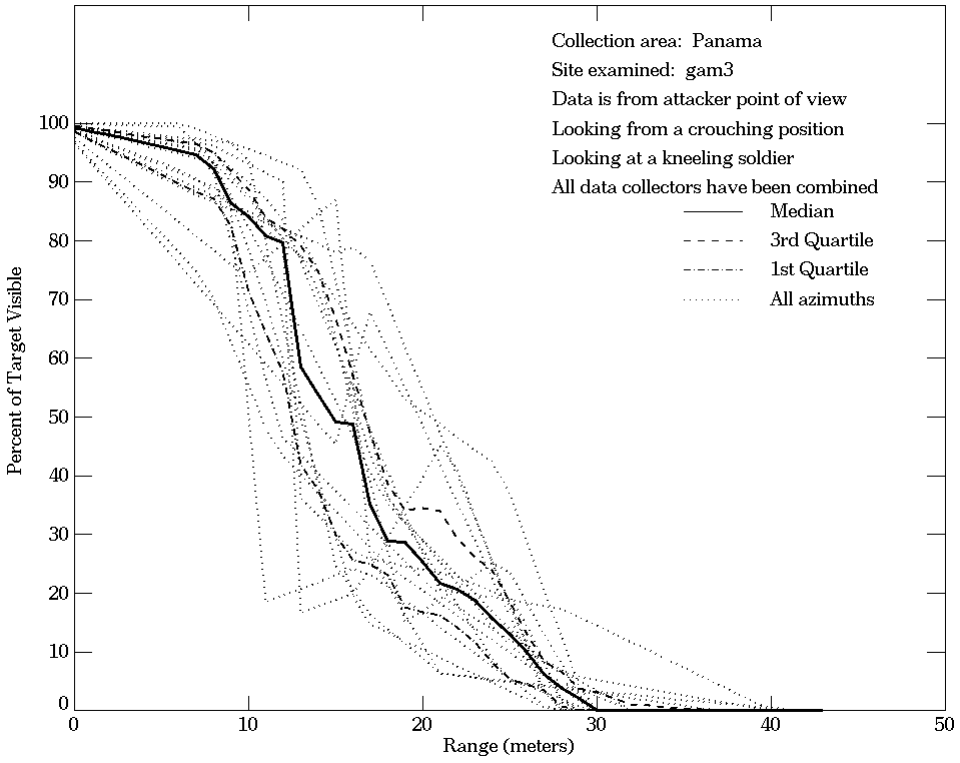

Figure E-6. Panama, From Attacker Point of View, Site gam3 (Continued)

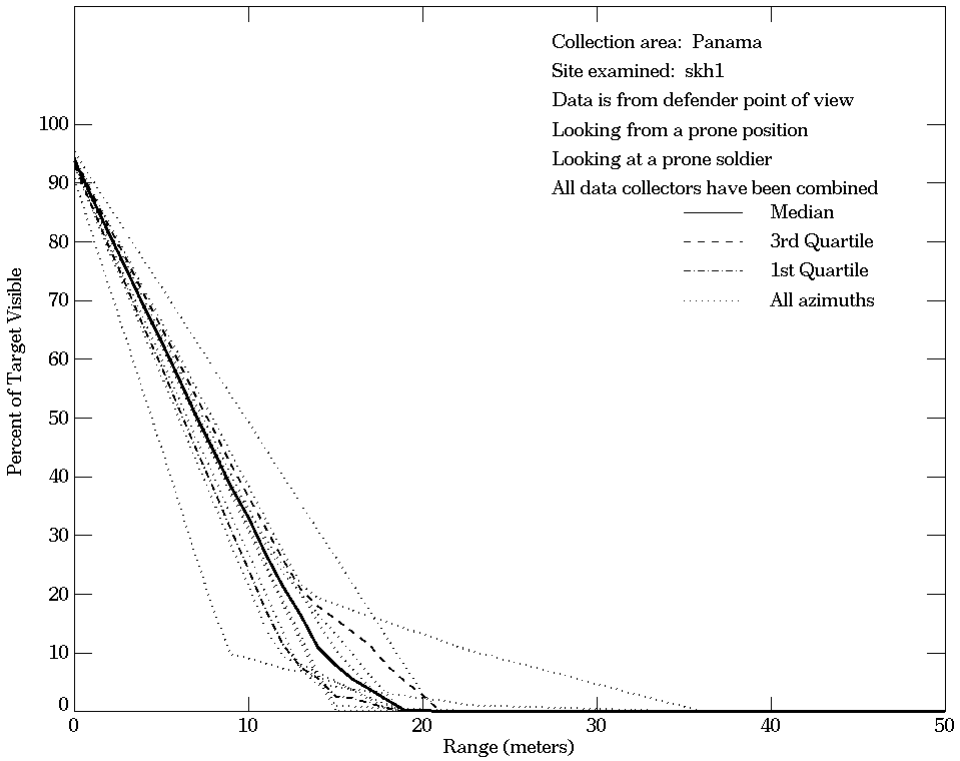

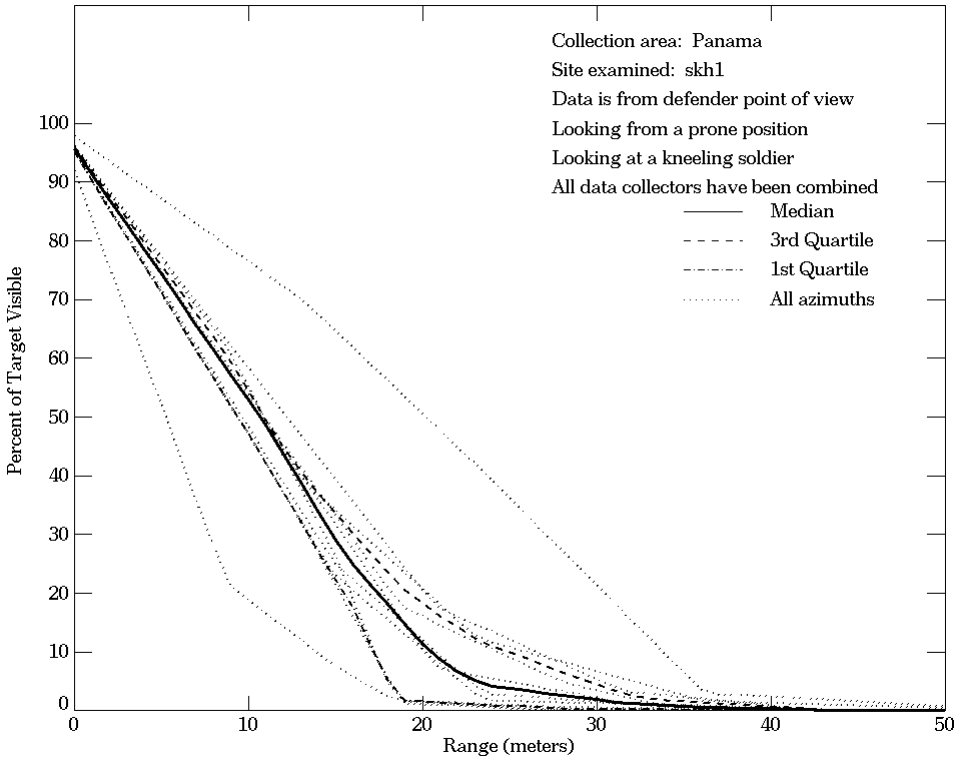

Figure E-7. Panama, From Defender Point of View, Site skh1

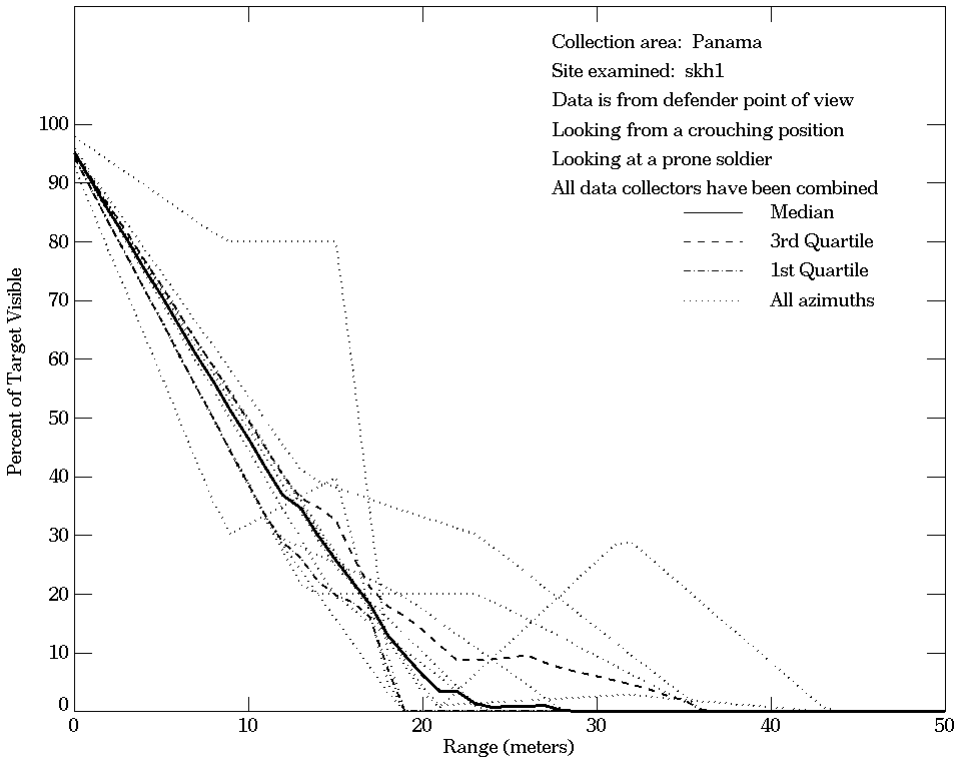

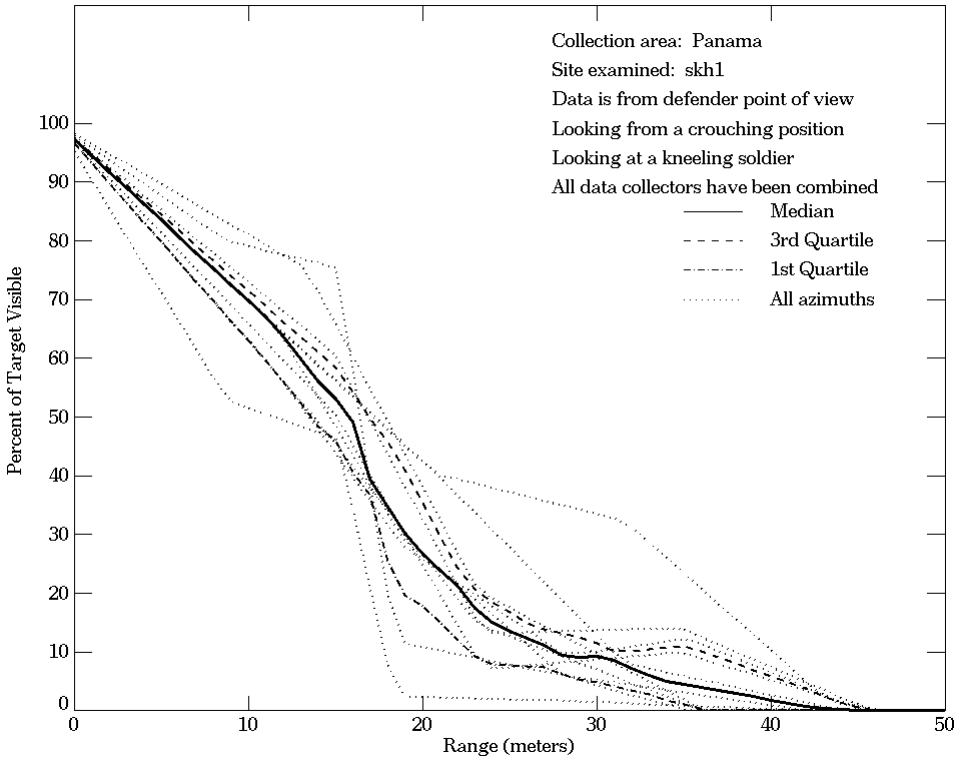

Figure E-7. Panama, From Defender Point of View, Site skh1 (Continued)

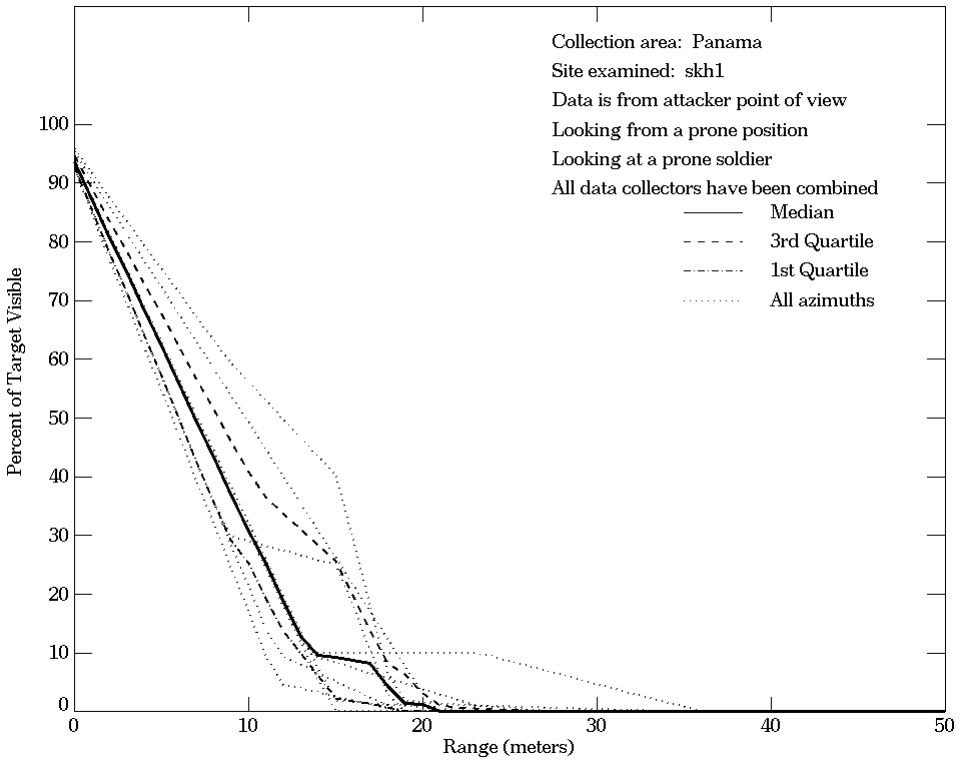

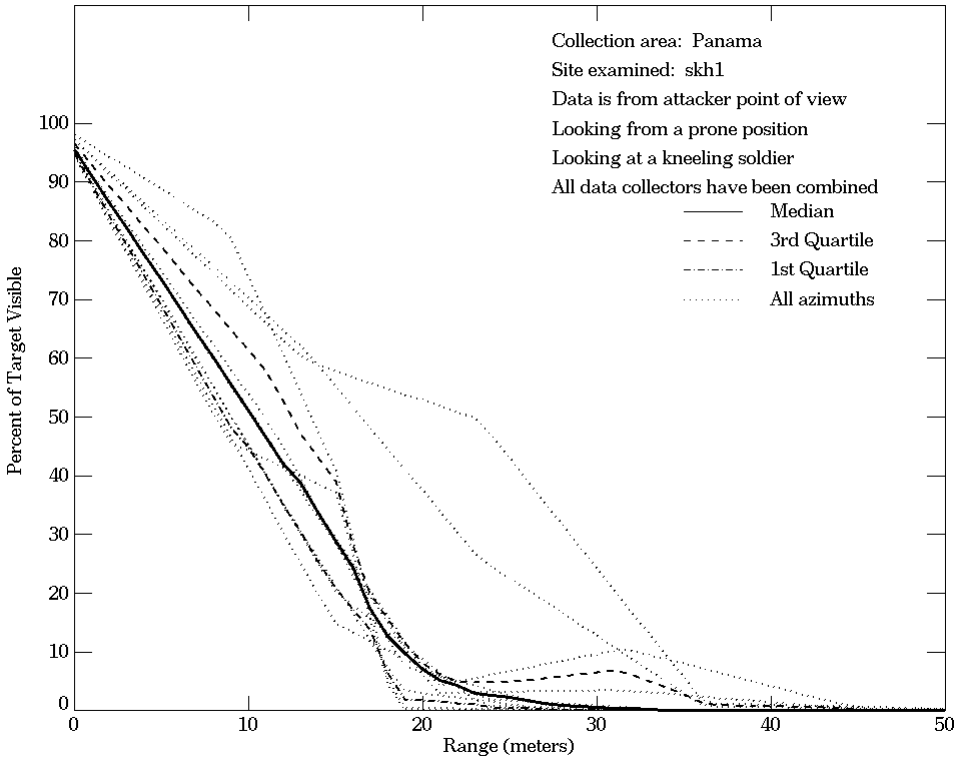

Figure E-8. Panama, From Attacker Point of View, Site skh1

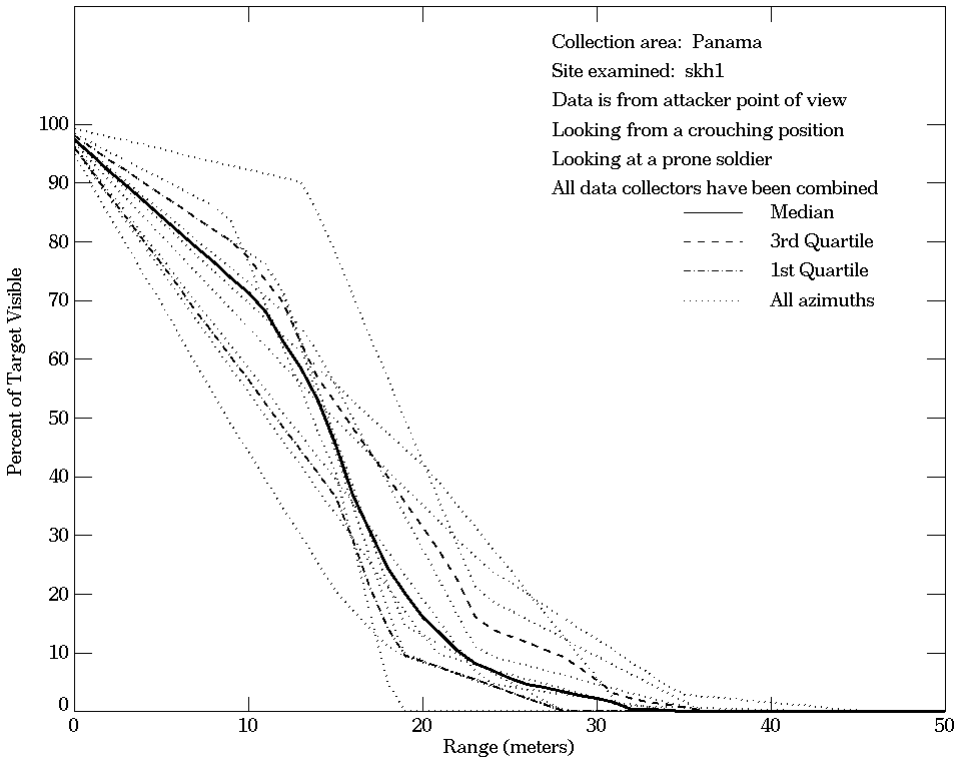

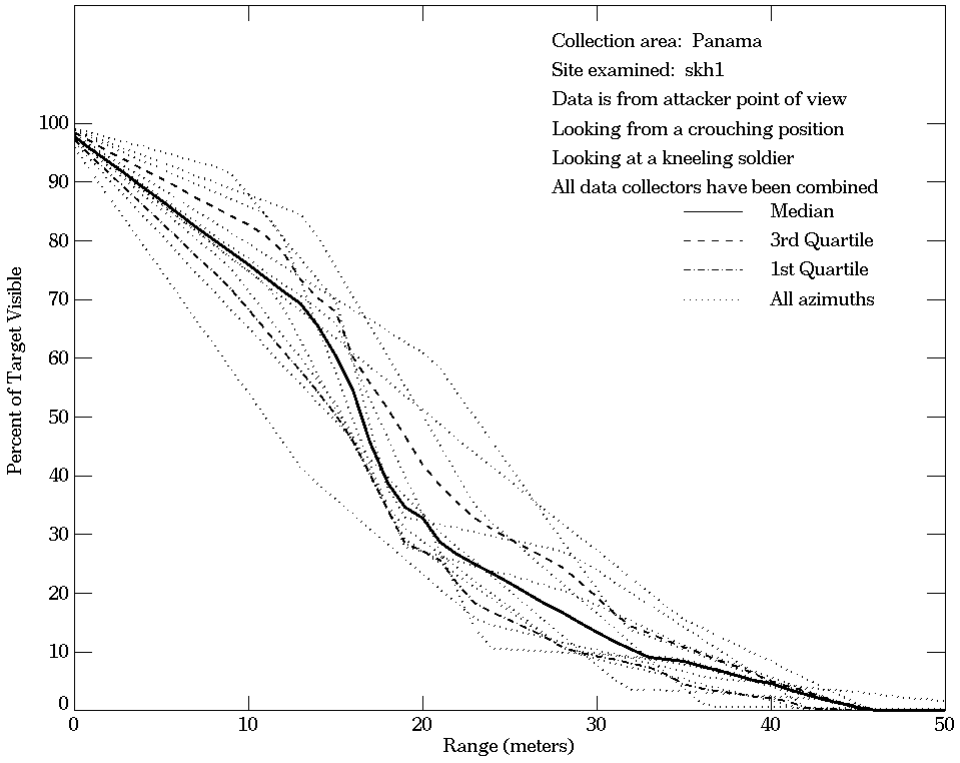

Figure E-8. Panama, From Attacker Point of View, Site skh1 (Continued)

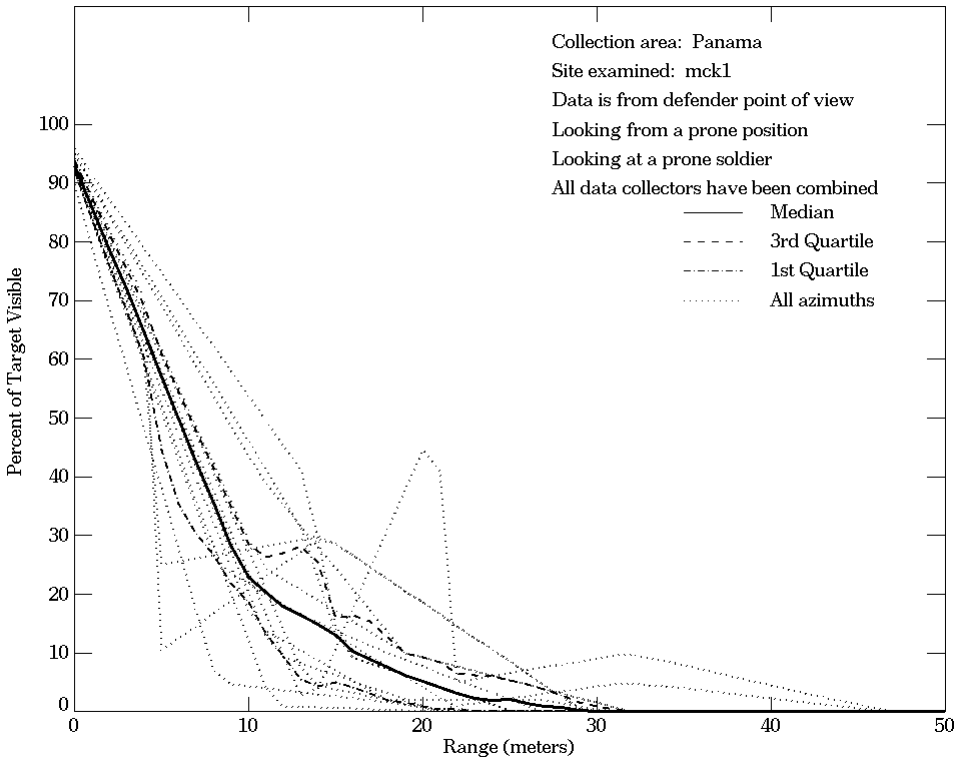

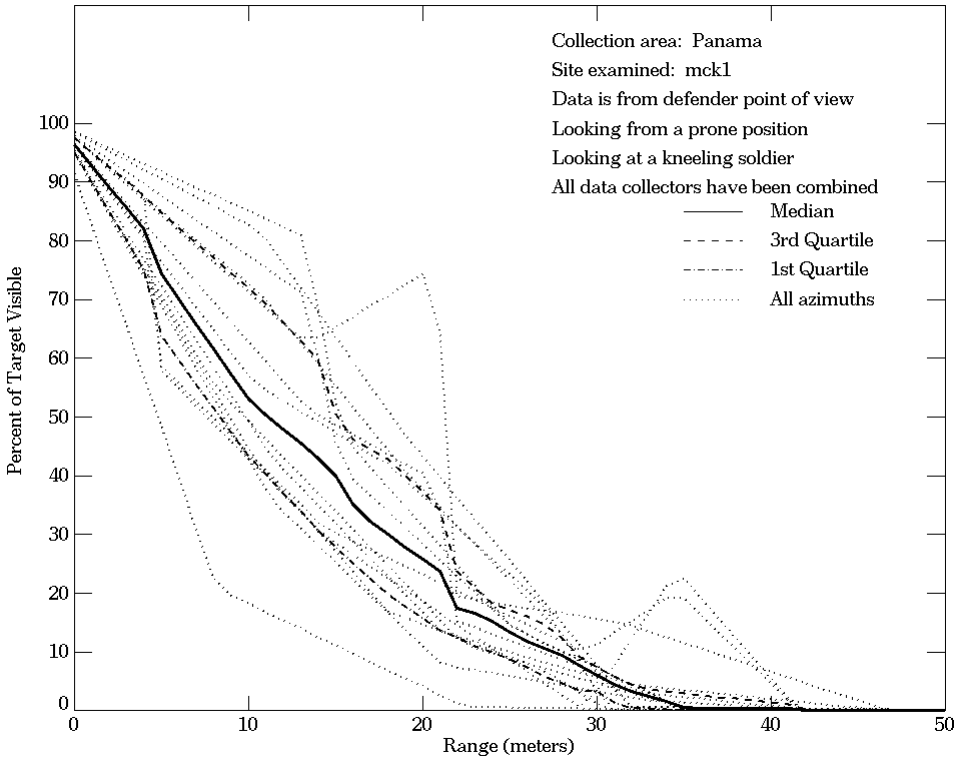

Figure E-9. Panama, From Defender Point of View, Site mck1

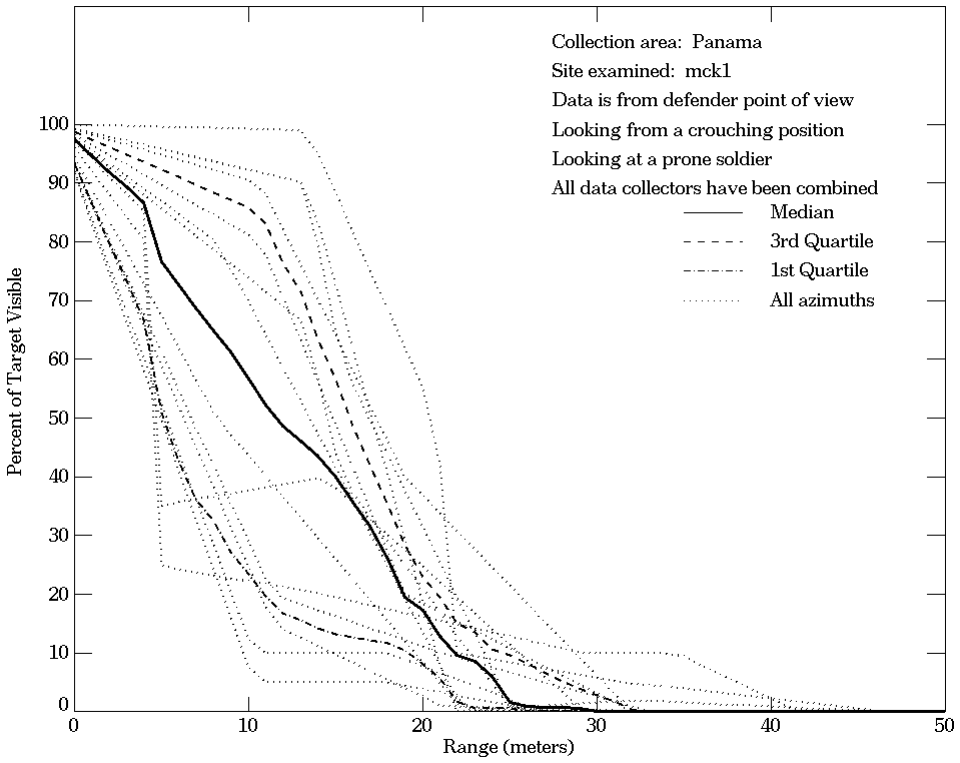

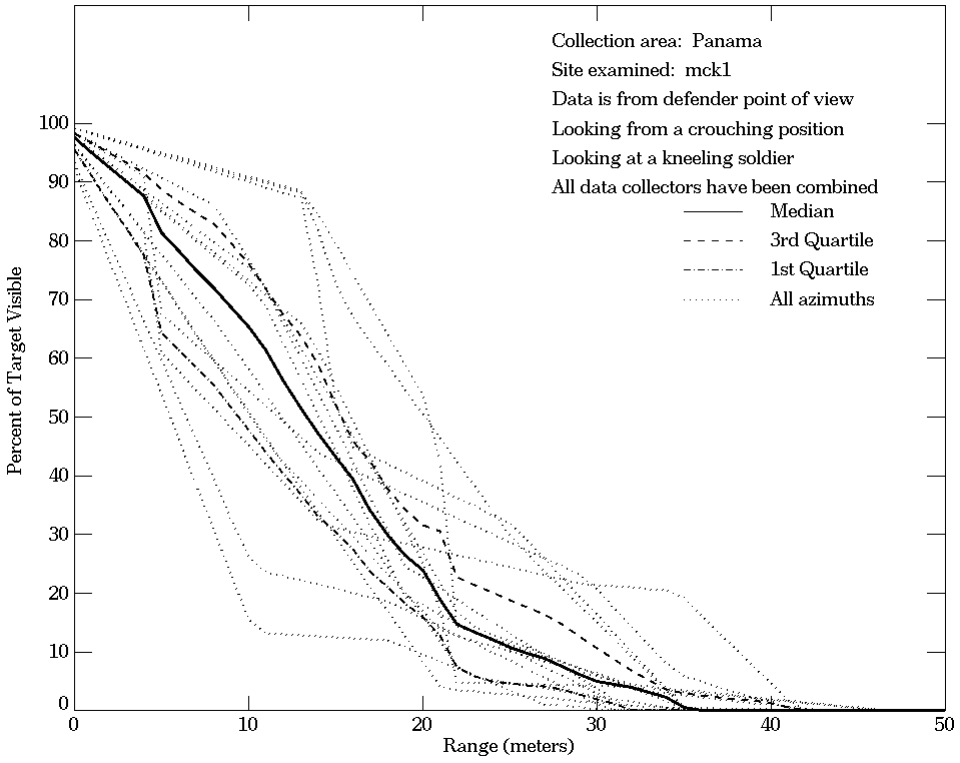

Figure E-9. Panama, From Defender Point of View, Site mck1 (Continued)

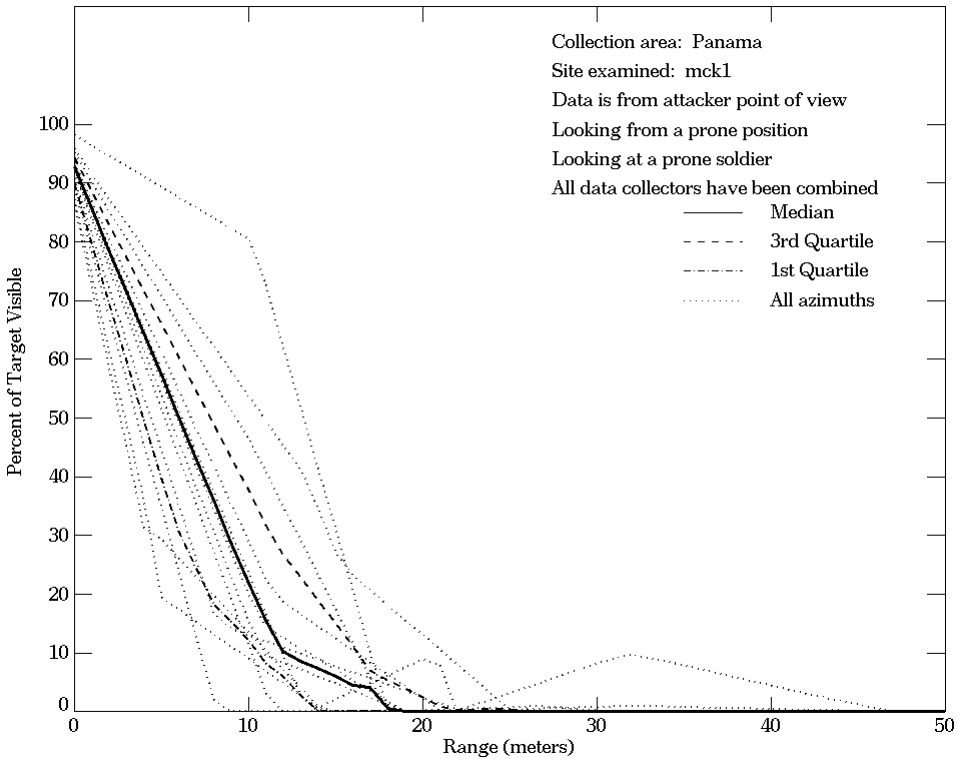

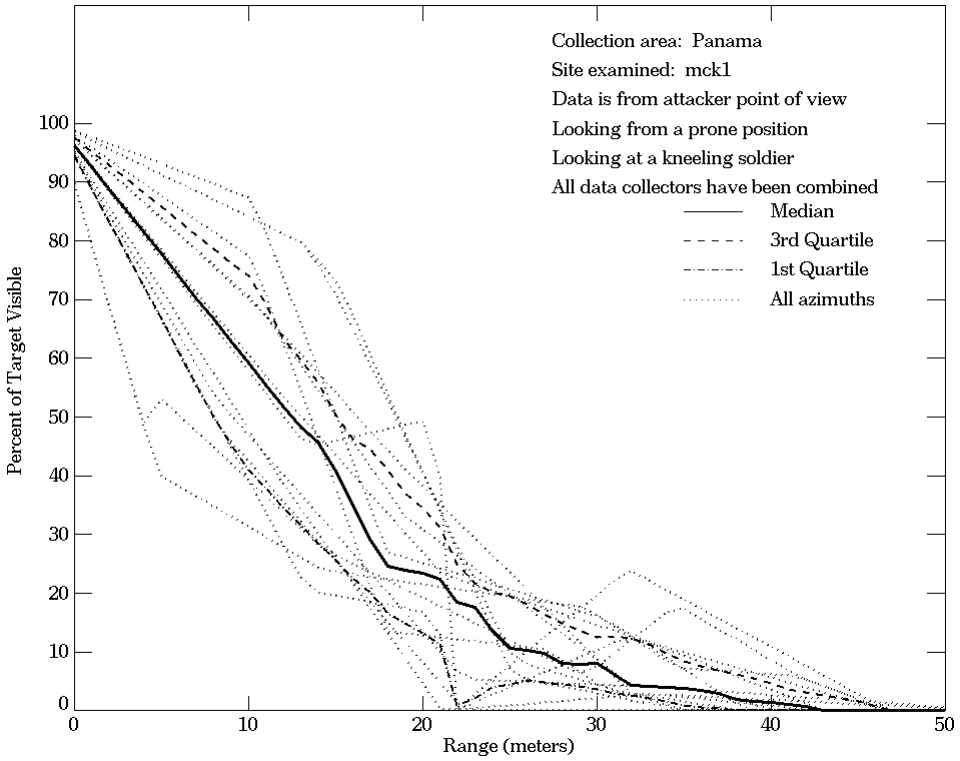

Figure E-10. Panama, From Attacker Point of View, Site mck1

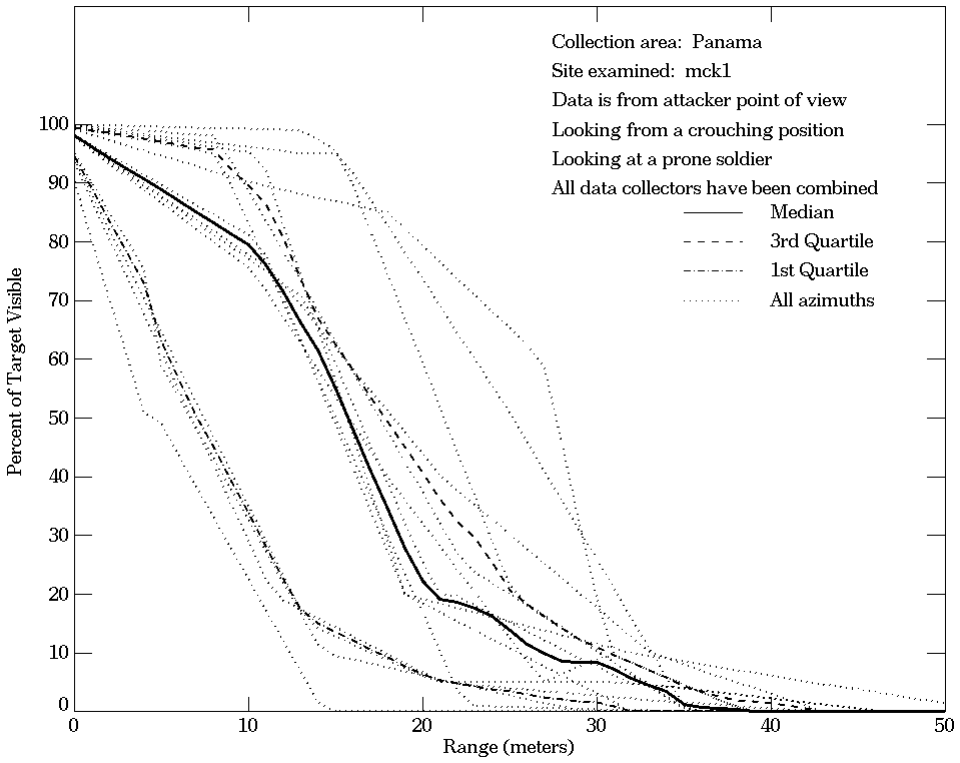

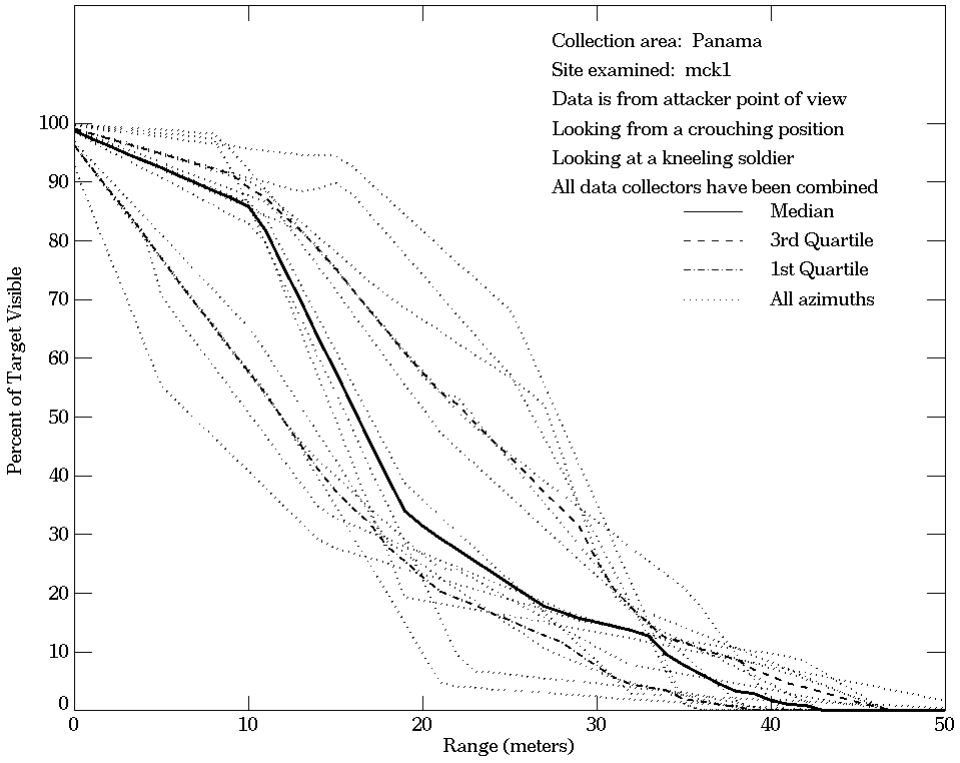

Figure E-10. Panama, From Attacker Point of View, Site mck1 (Continued)

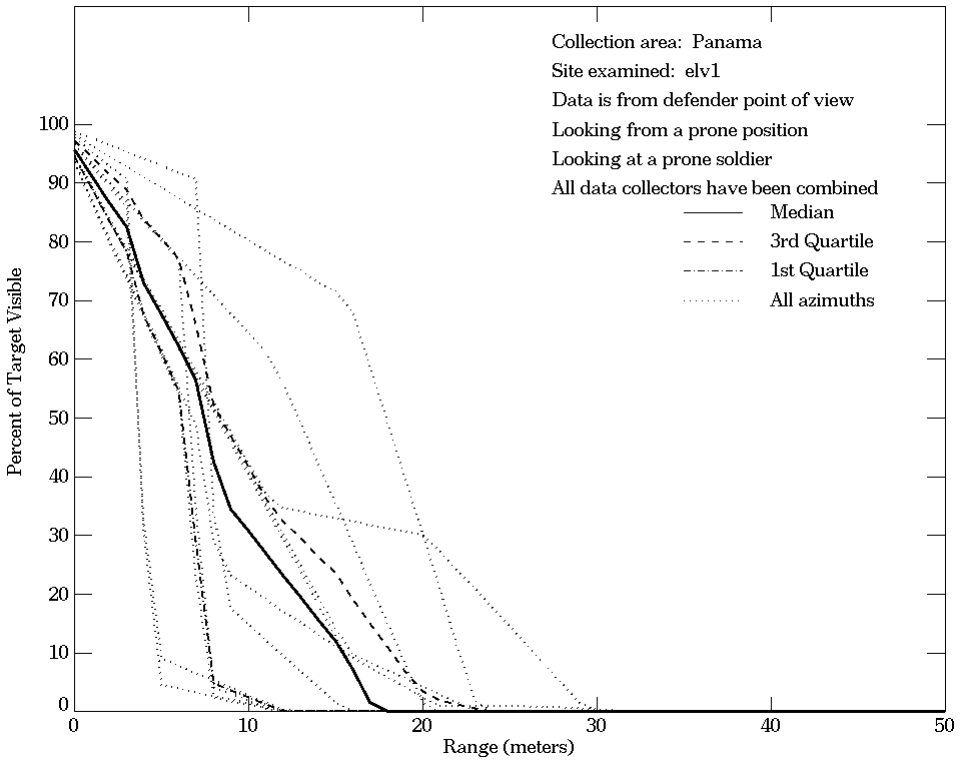

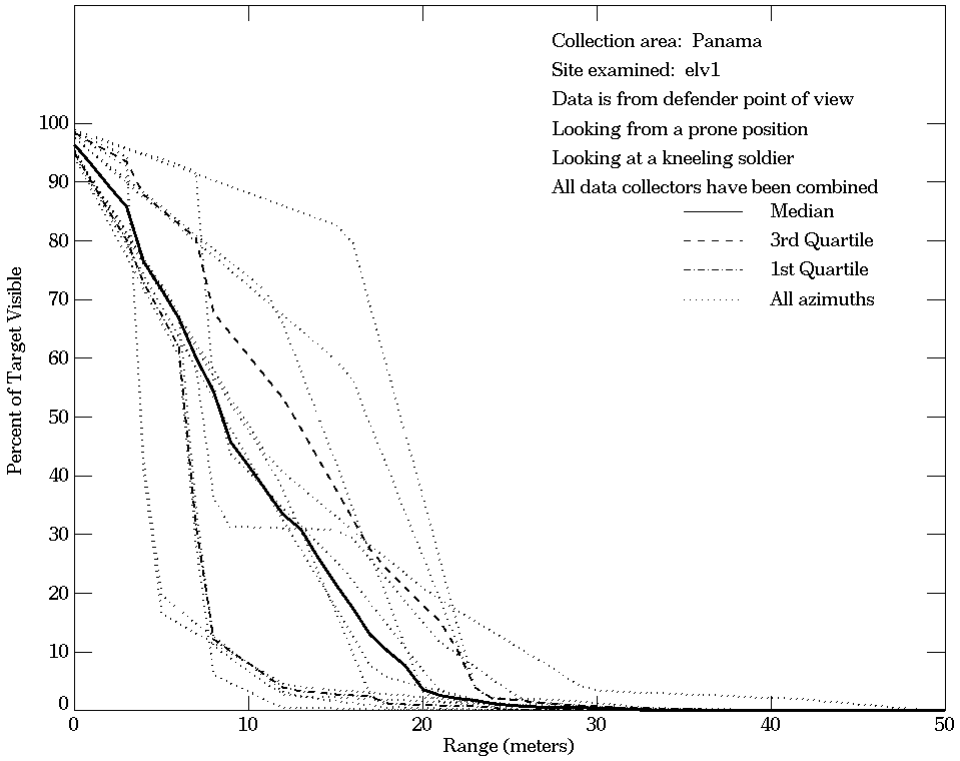

Figure E-11. Panama, From Defender Point of View, Site elv1

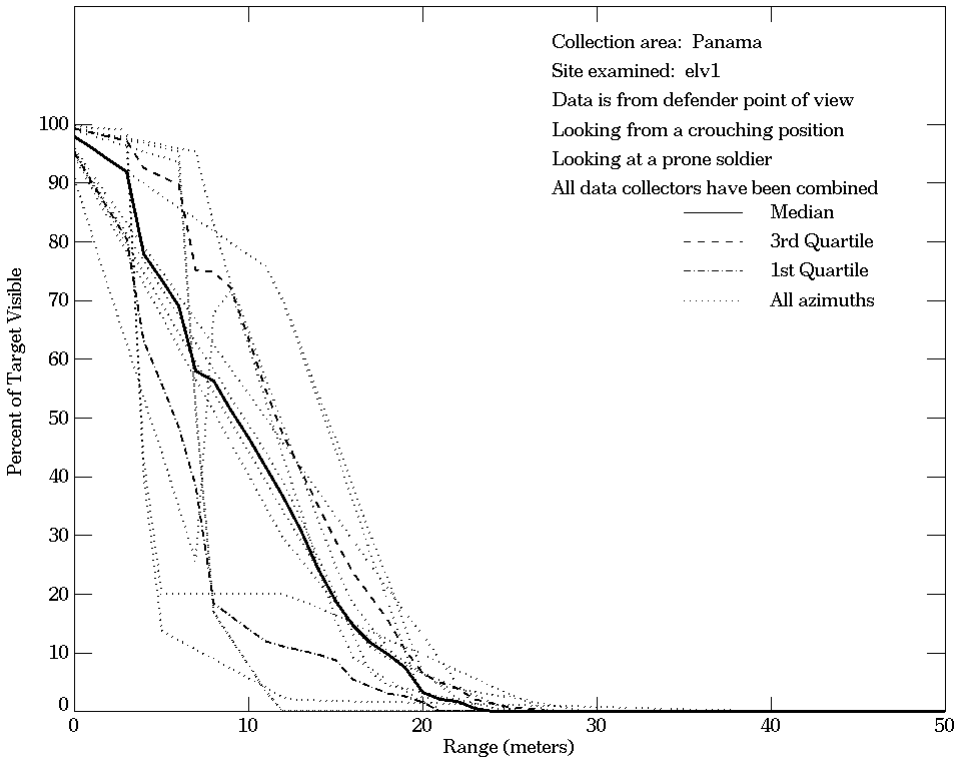

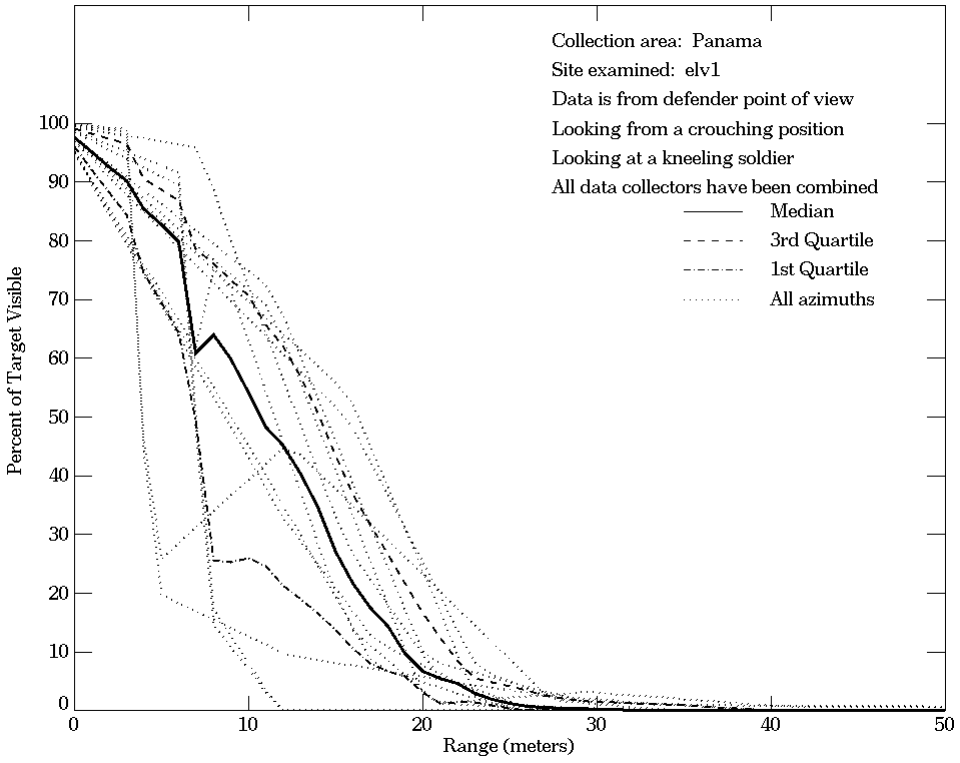

Figure E-11. Panama, From Defender Point of View, Site elv1 (Continued)

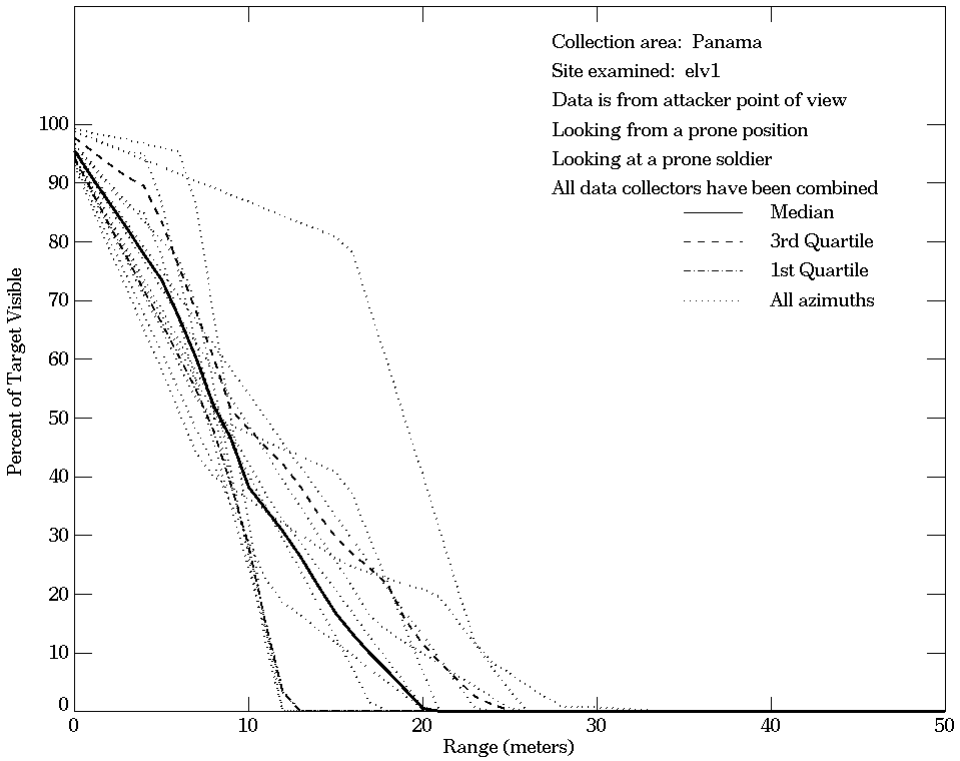

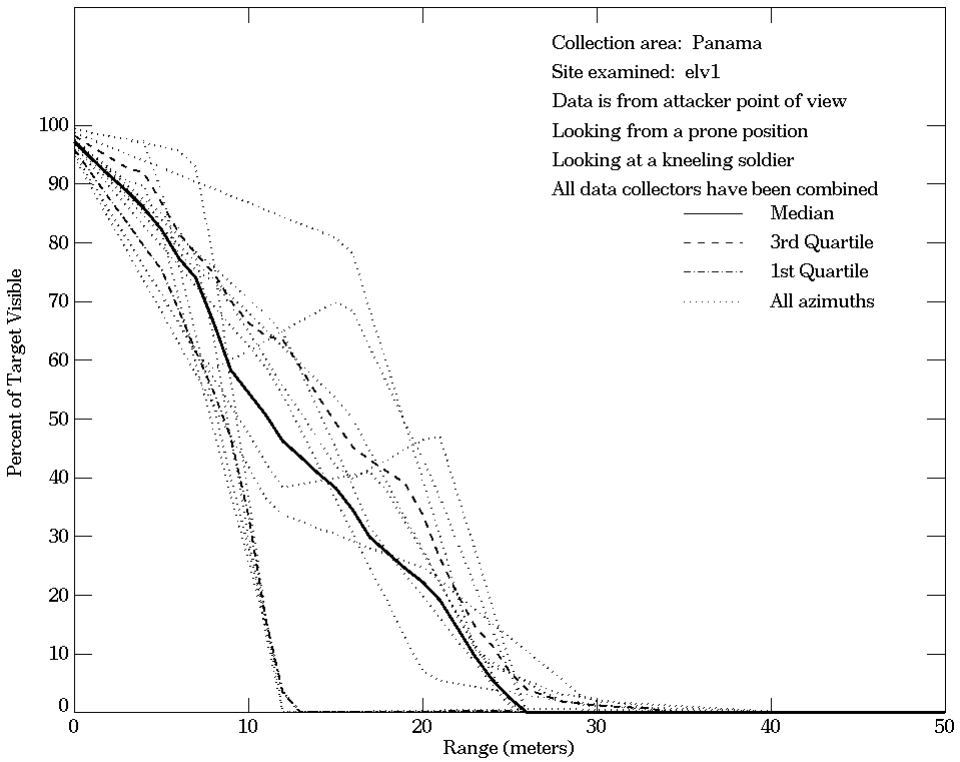

Figure E-12. Panama, From Attacker Point of View, Site elv1

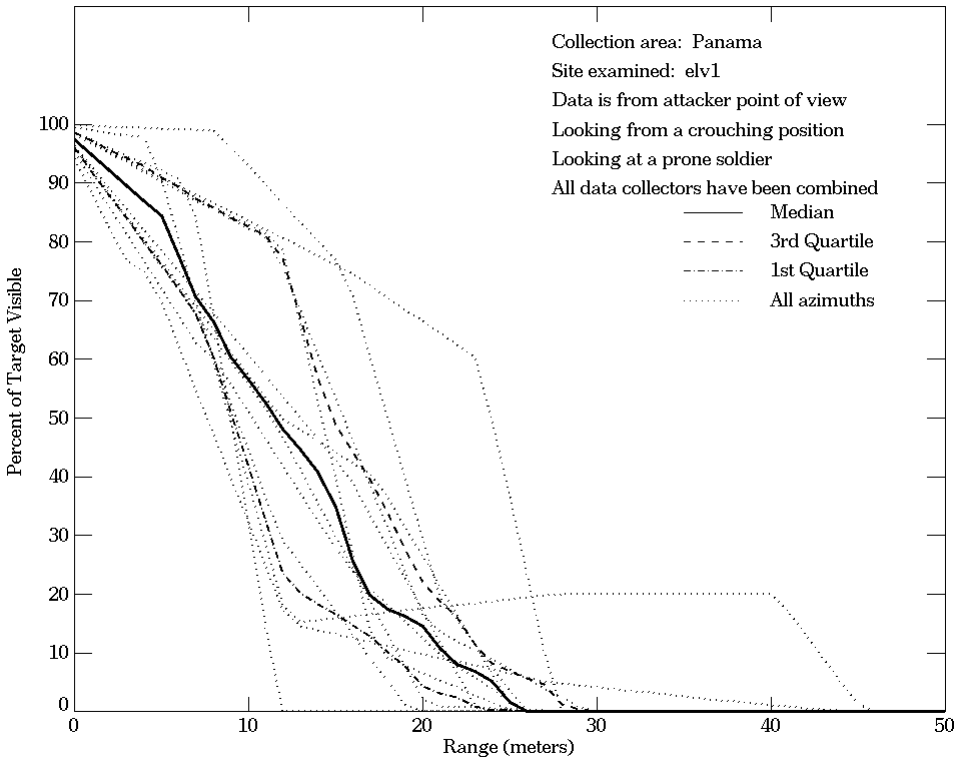

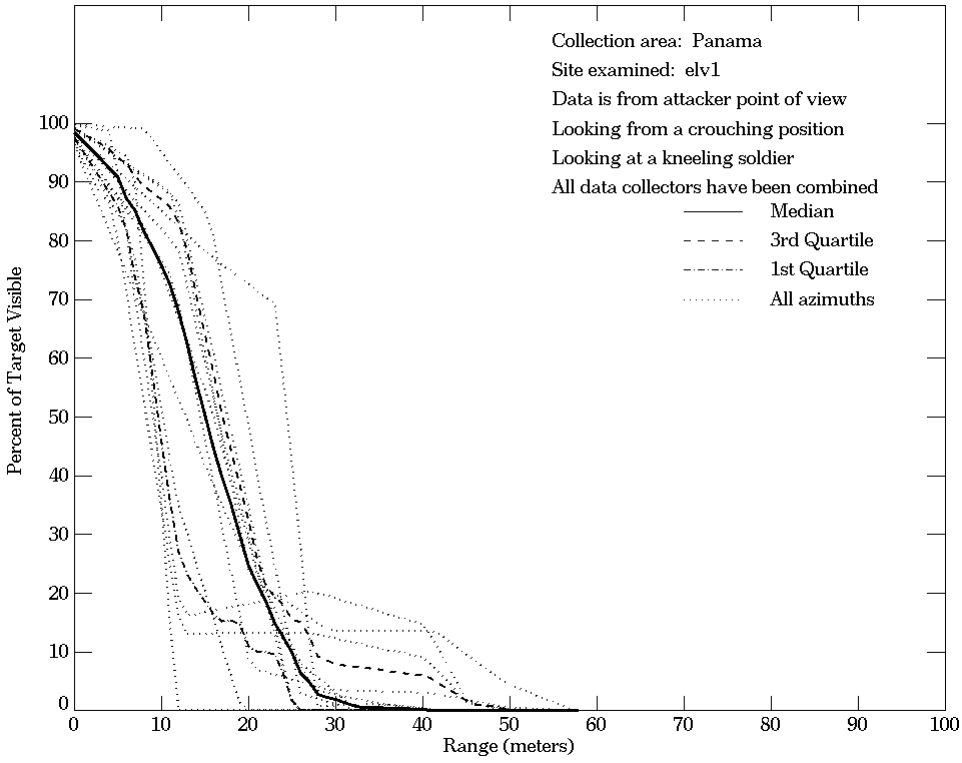

Figure E-12. Panama, From Attacker Point of View, Site elv1 (Continued)

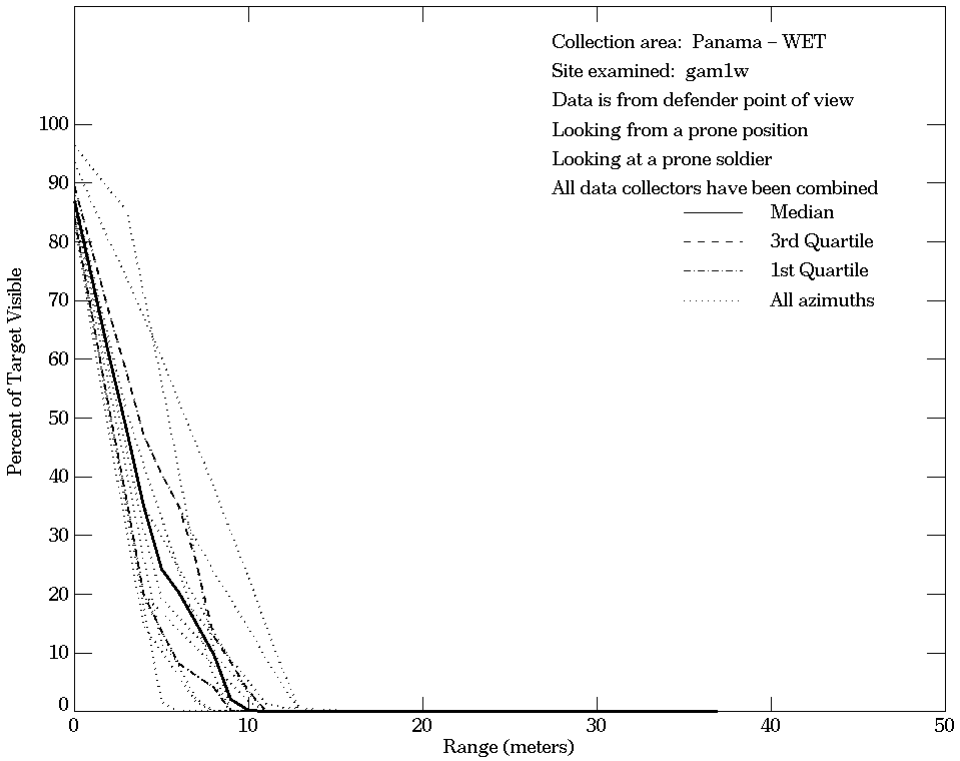

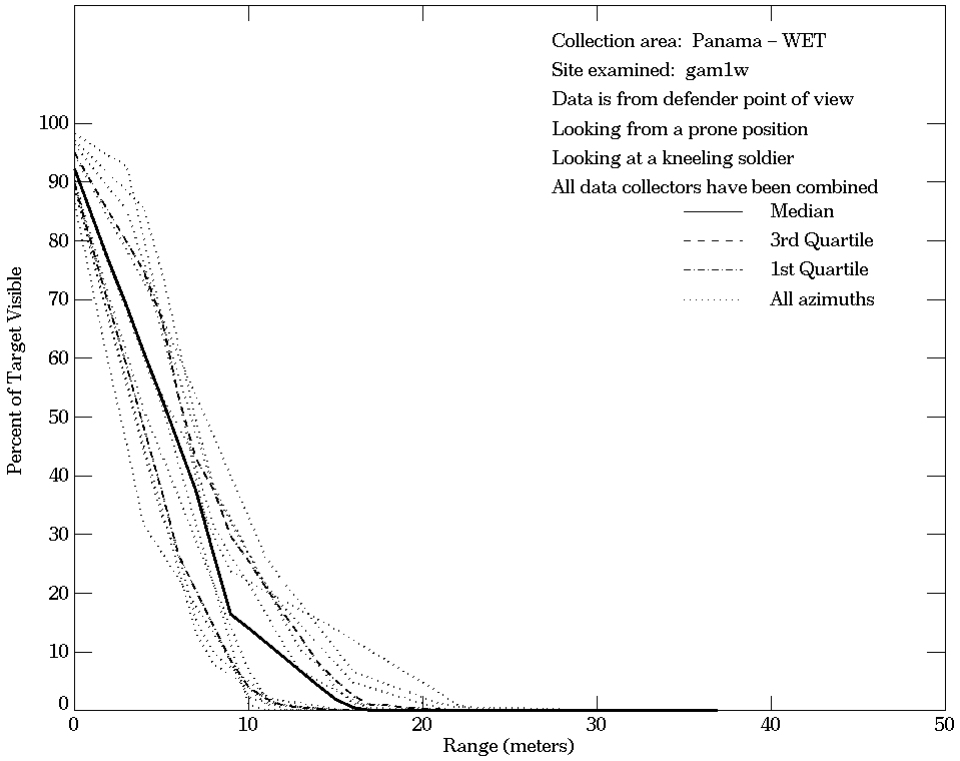

Figure E-13. Panama - Wet, From Defender Point of View, Site gam1w

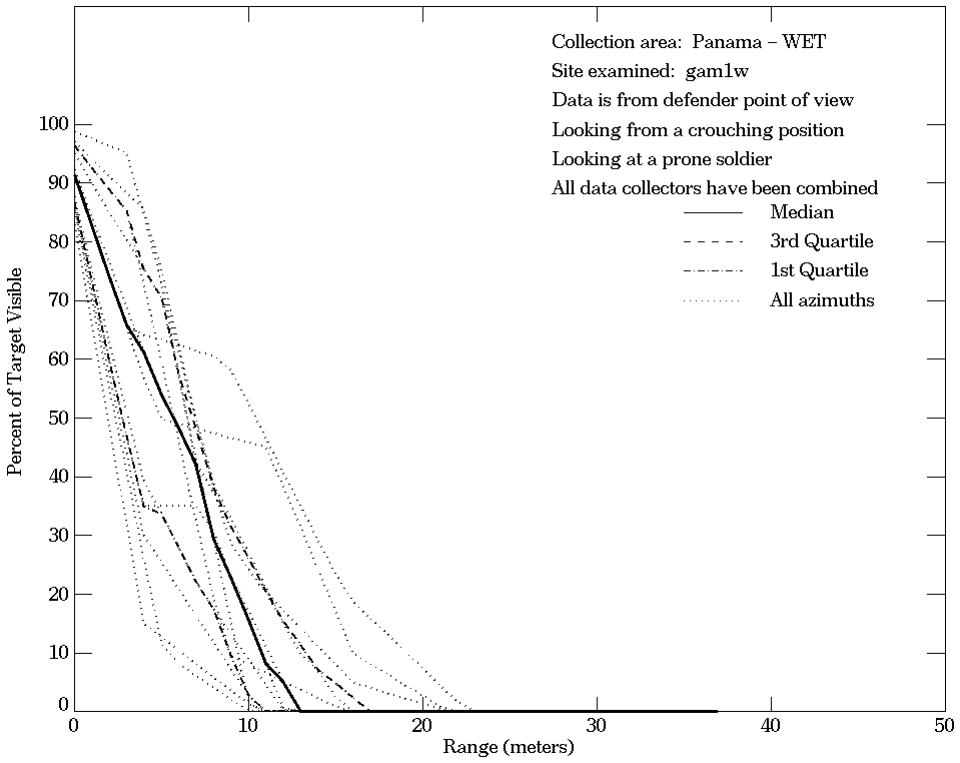

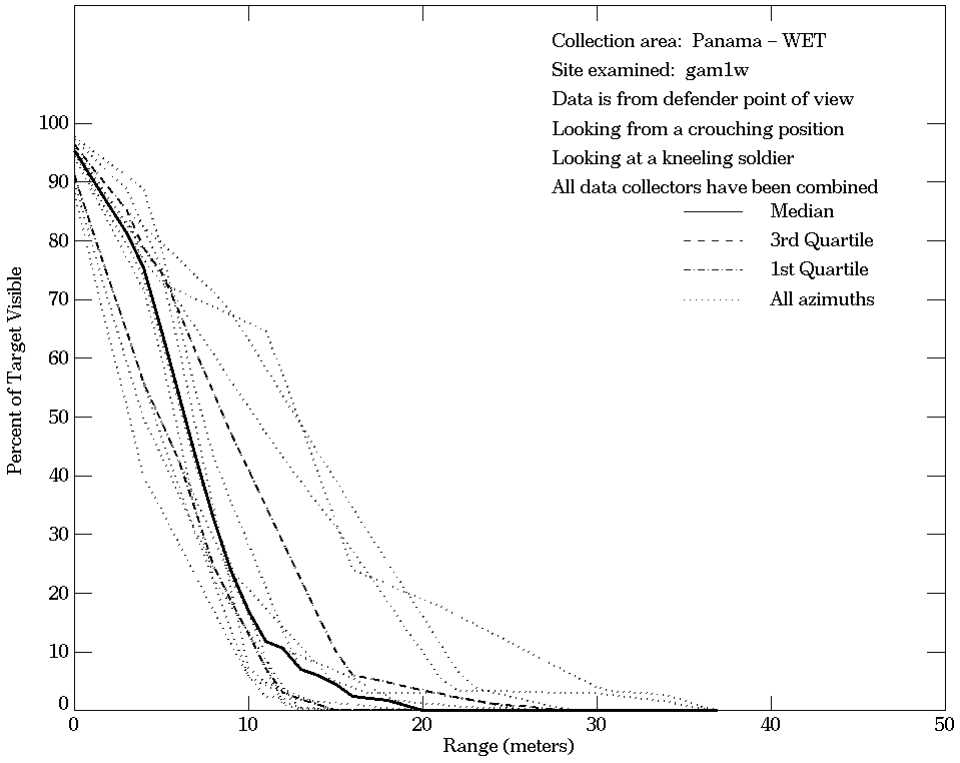

Figure E-13. Panama - Wet, From Defender Point of View, Site gam1w (Continued)

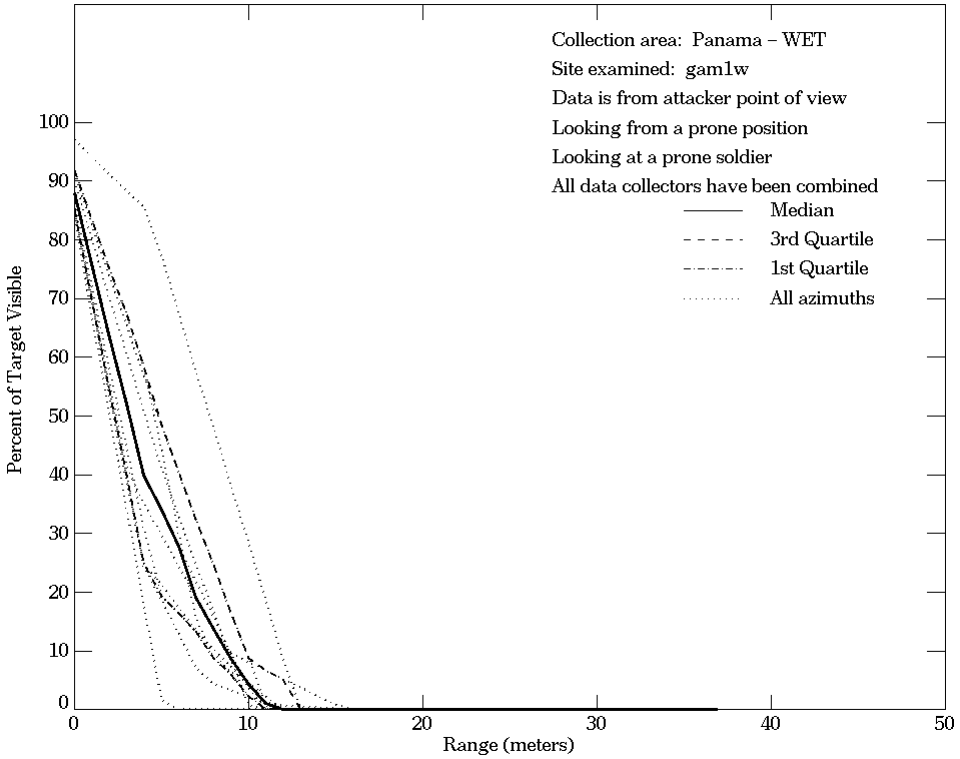

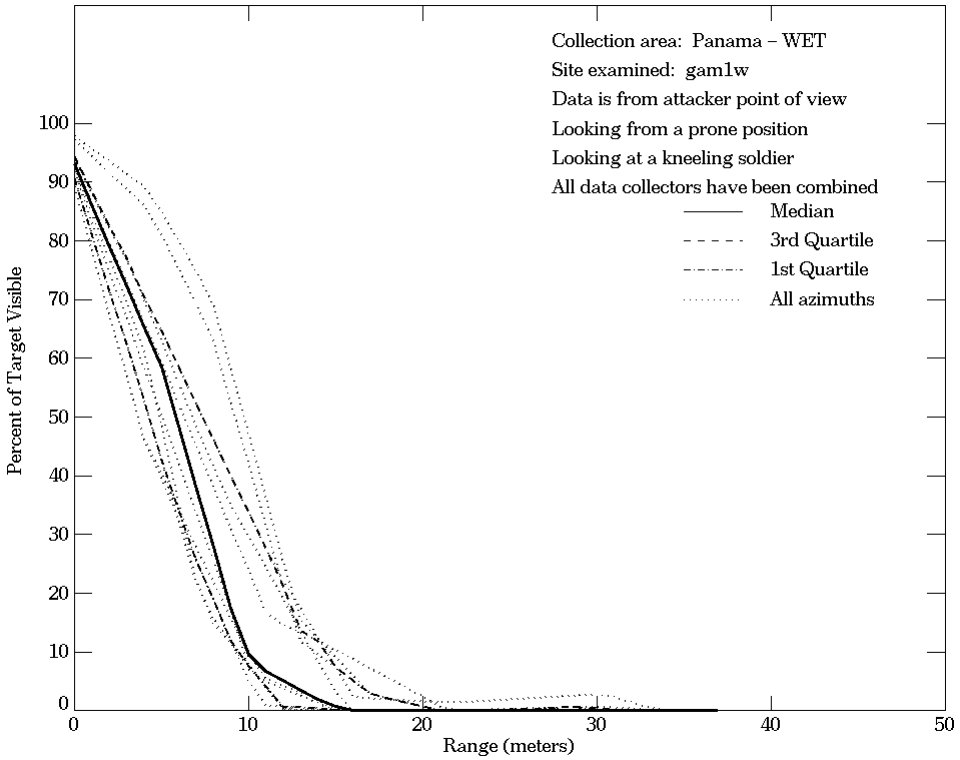

Figure E-14. Panama - Wet, From Attacker Point of View, Site gam1w

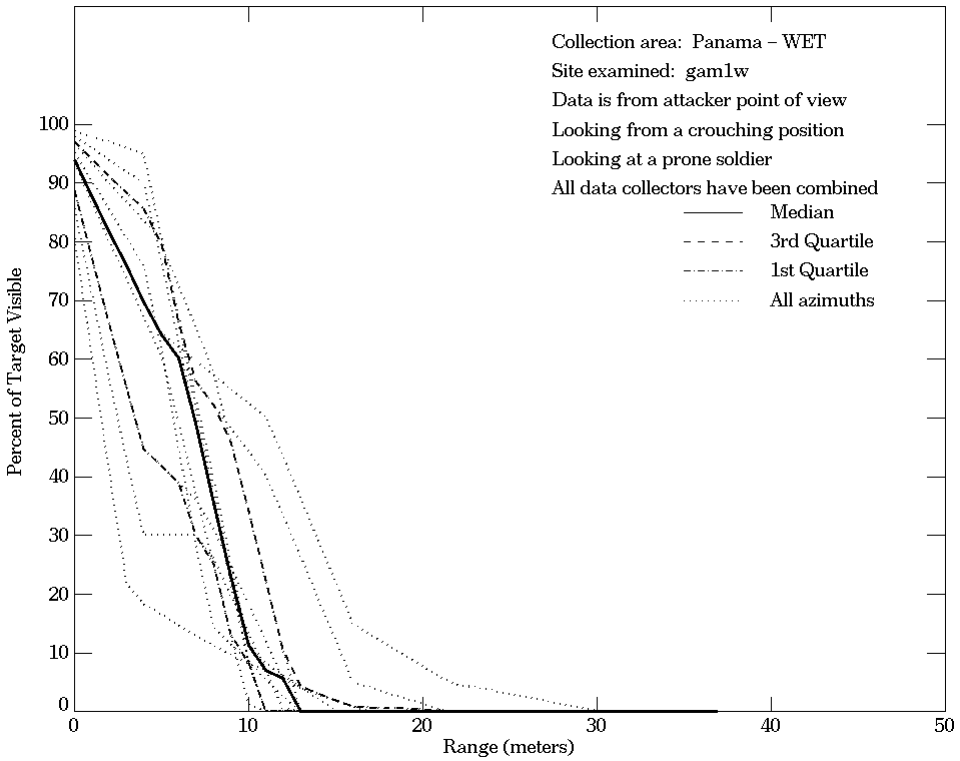

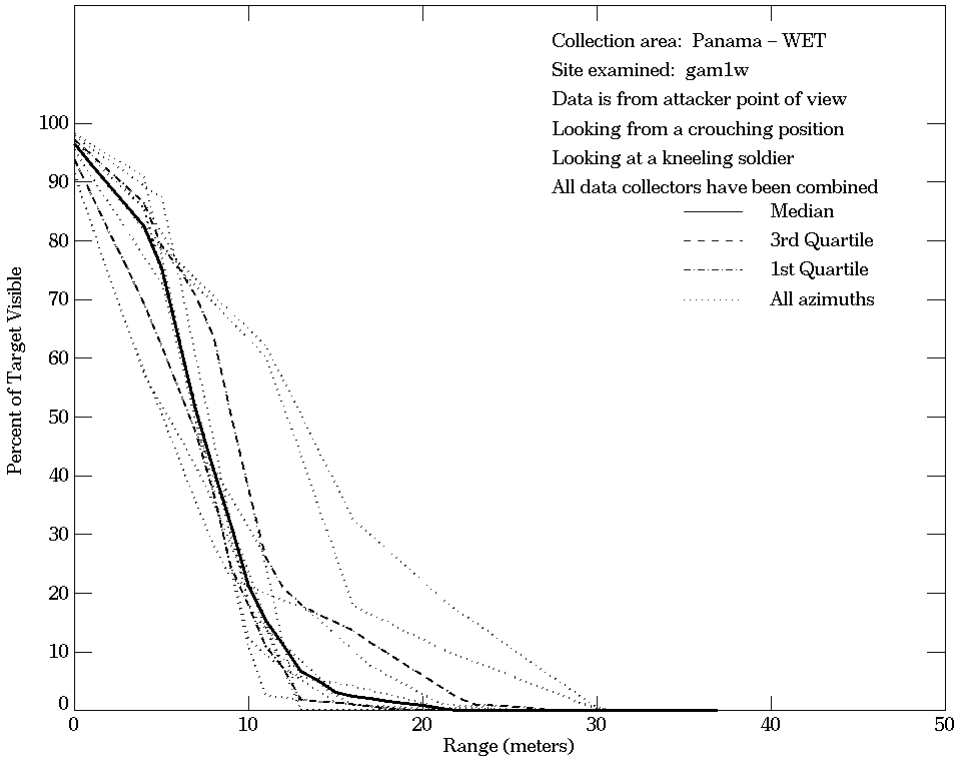

Figure E-14. Panama - Wet, From Attacker Point of View, Site gam1w (Continued)

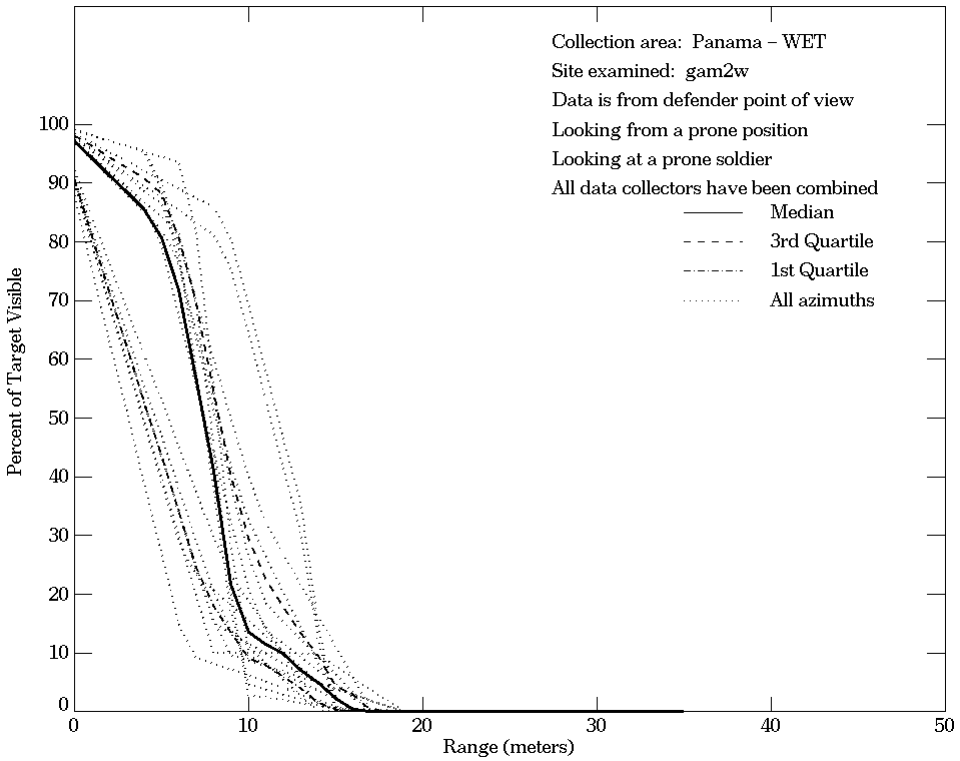

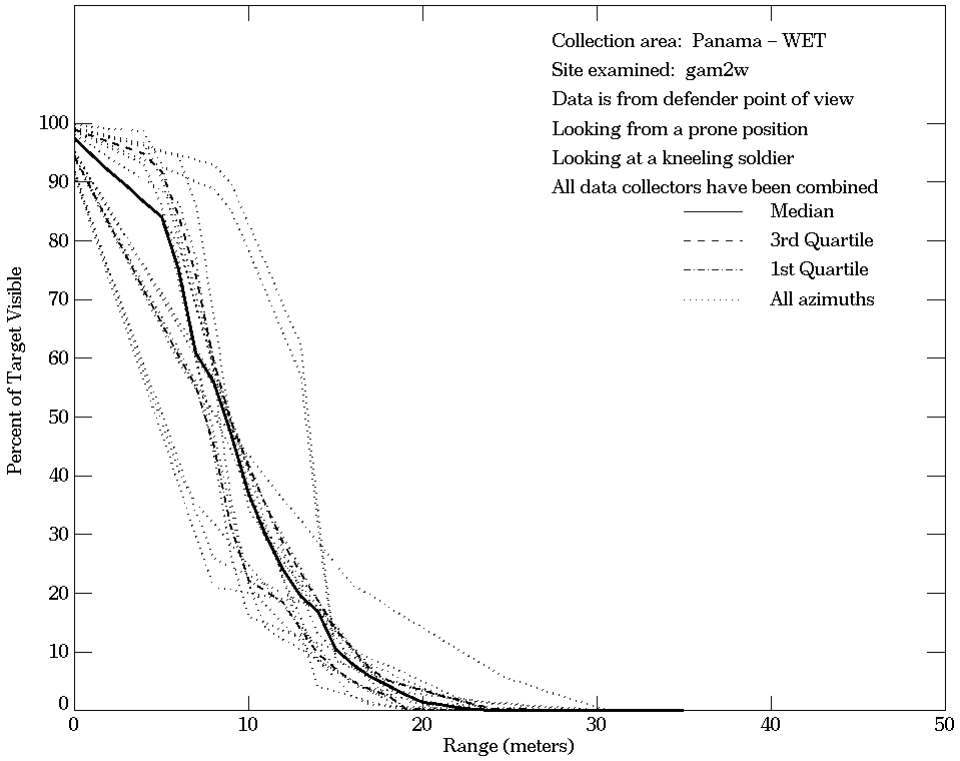

Figure E-15. Panama - Wet, From Defender Point of View, Site gam2w

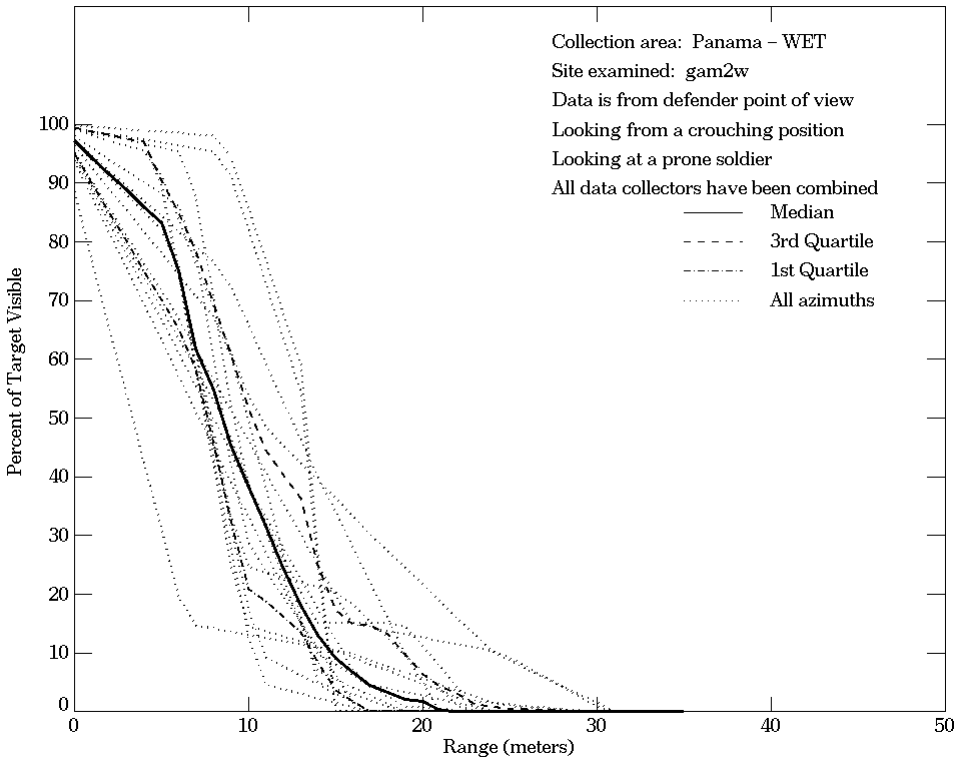

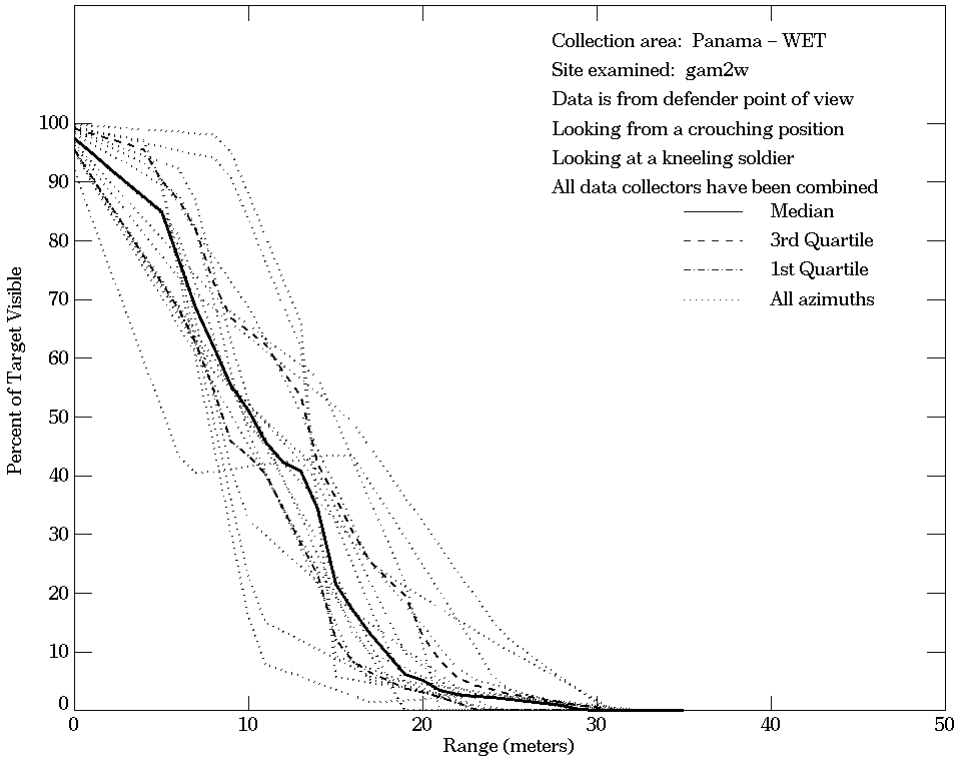

Figure E-15. Panama - Wet, From Defender Point of View, Site gam2w (Continued)

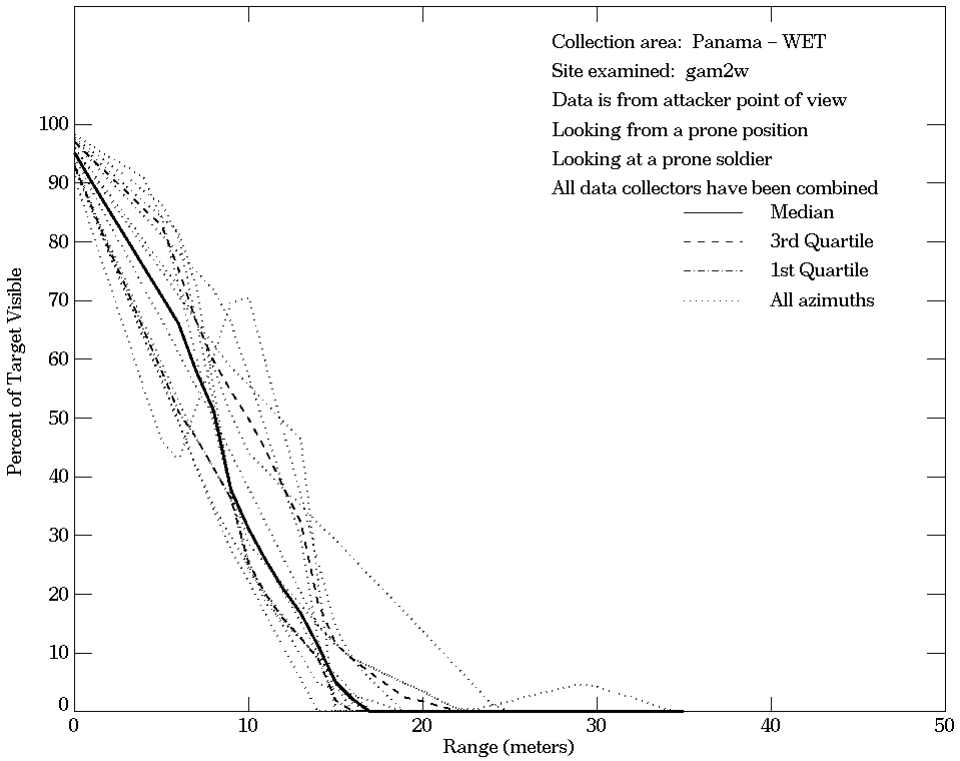

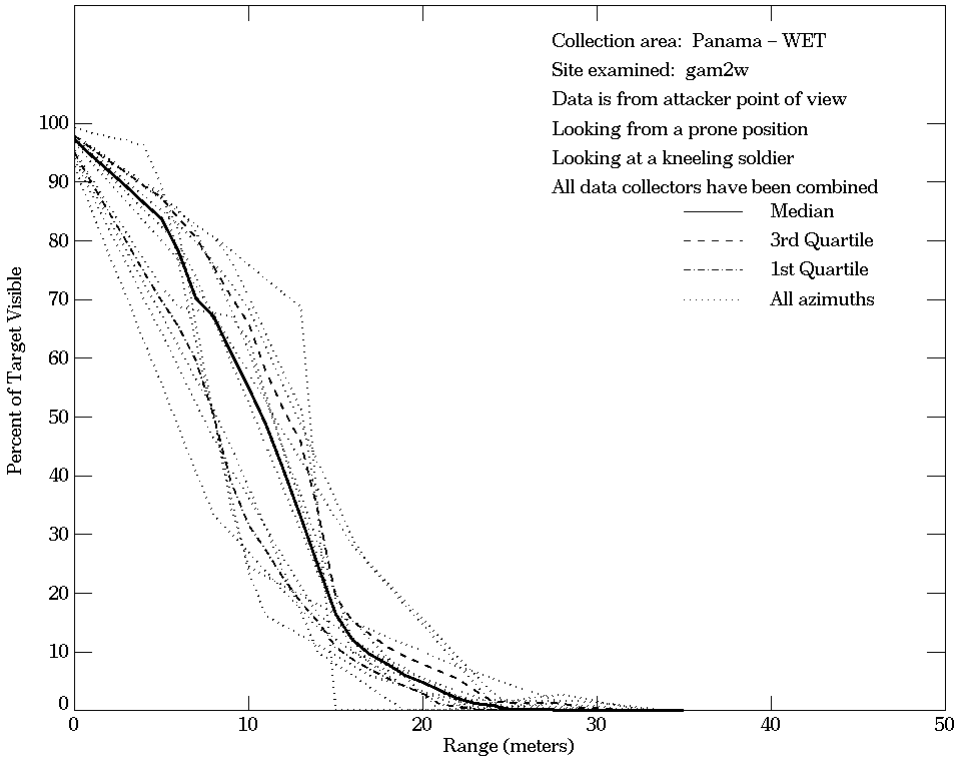

Figure E-16. Panama - Wet, From Attacker Point of View, Site gam2w

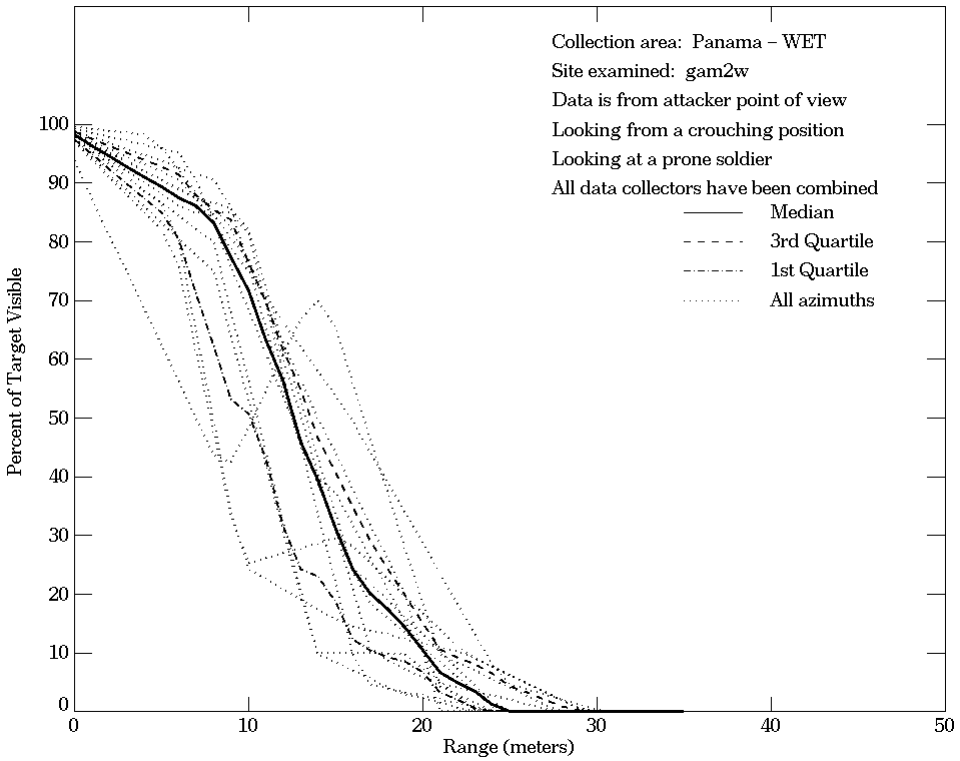

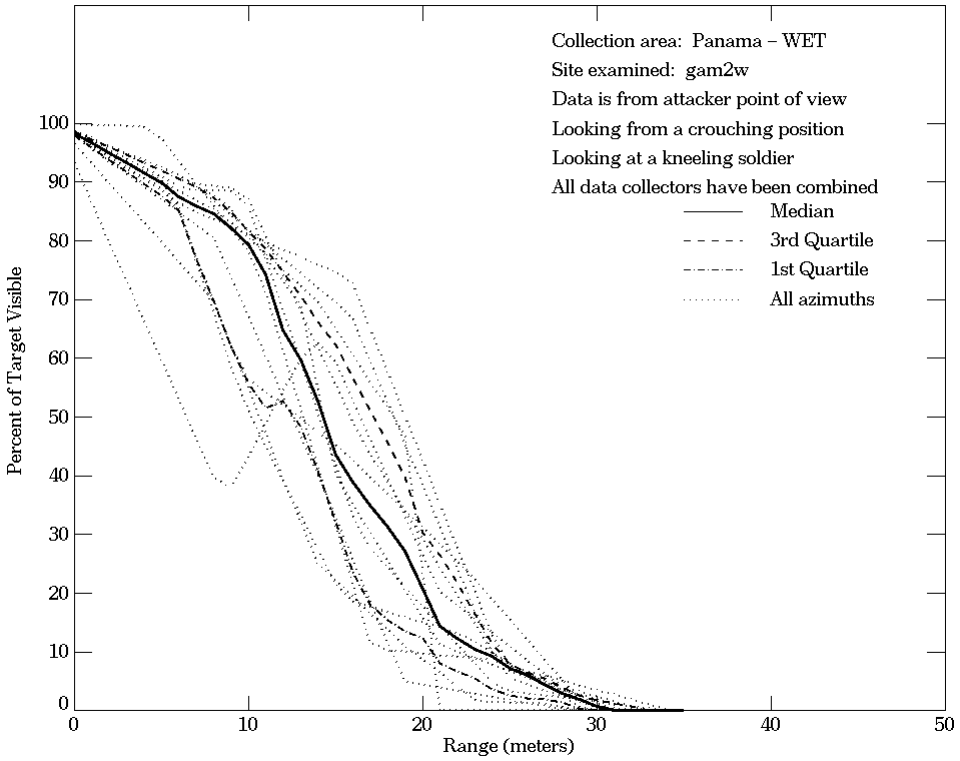

Figure E-16. Panama - Wet, From Attacker Point of View, Site gam2w (Continued)

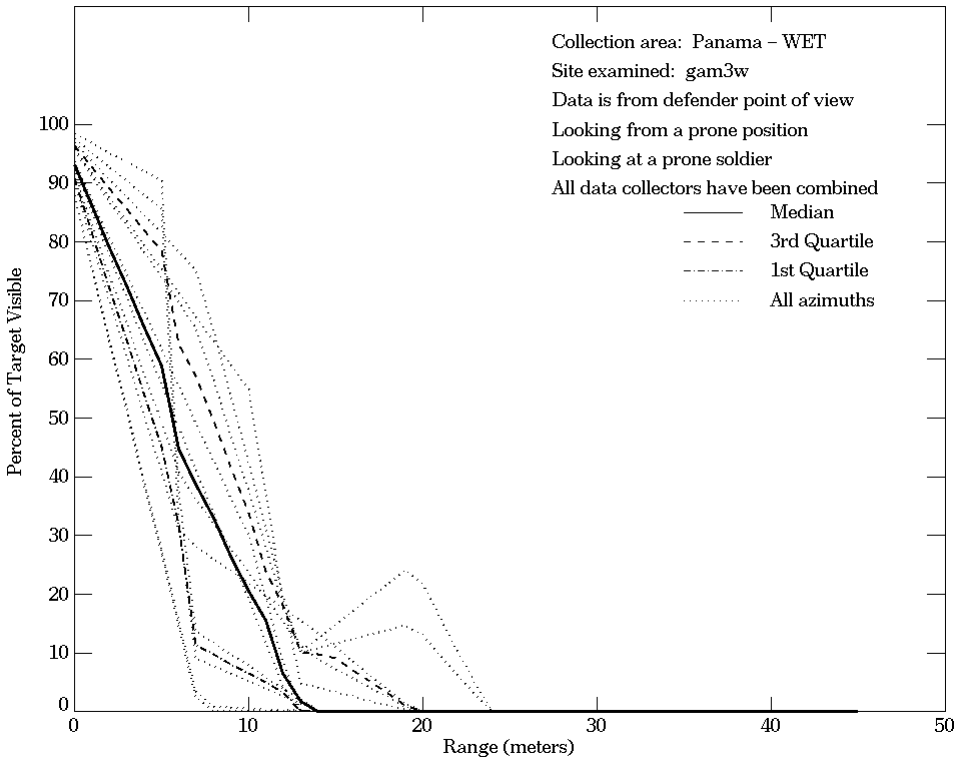

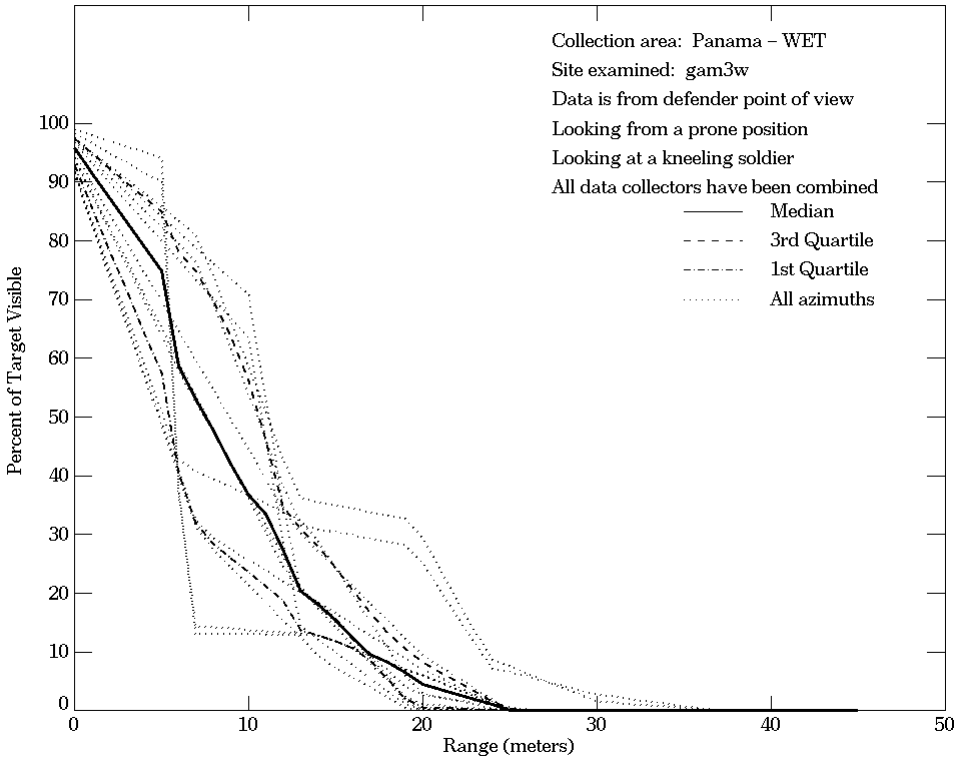

Figure E-17. Panama - Wet, From Defender Point of View, Site gam3w

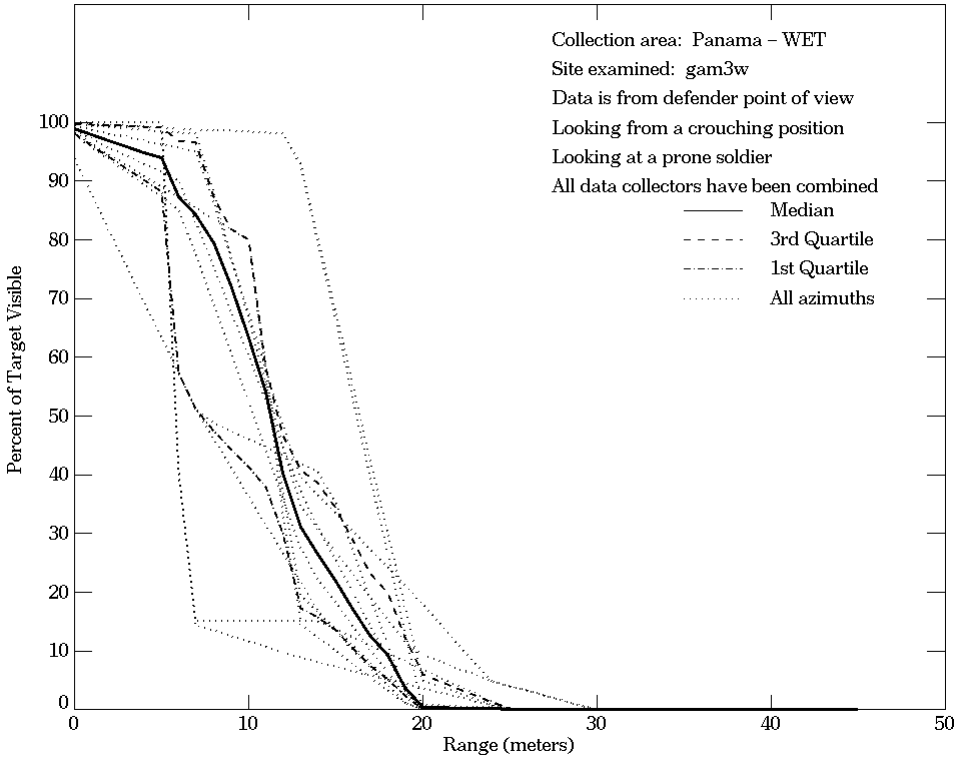

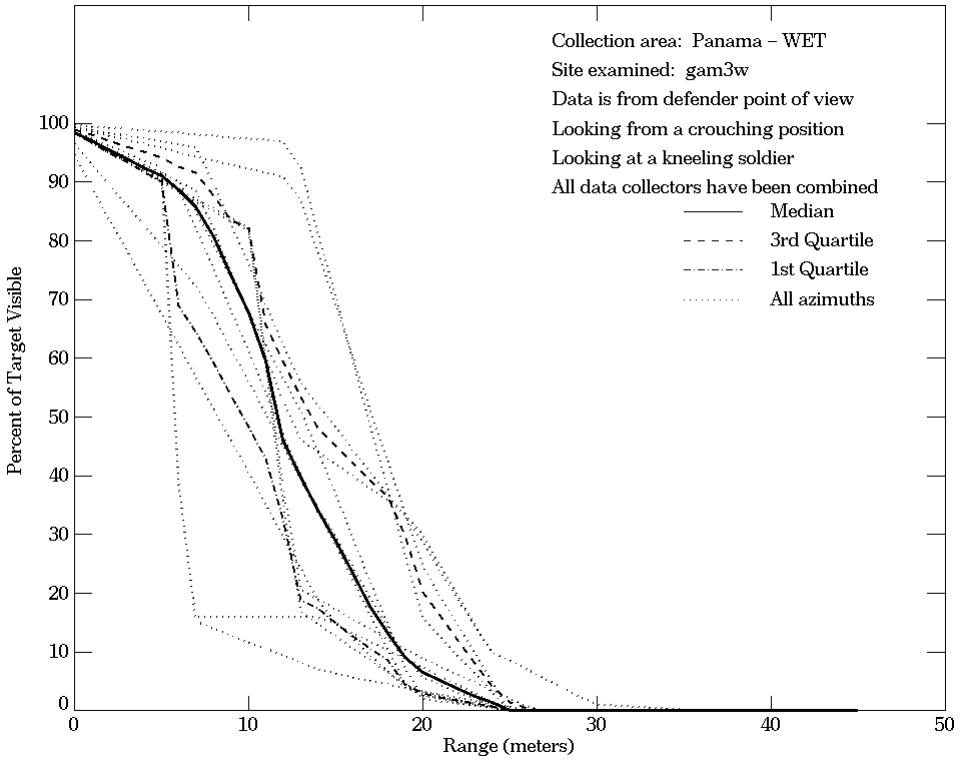

Figure E-17. Panama - Wet, From Defender Point of View, Site gam3w (Continued)

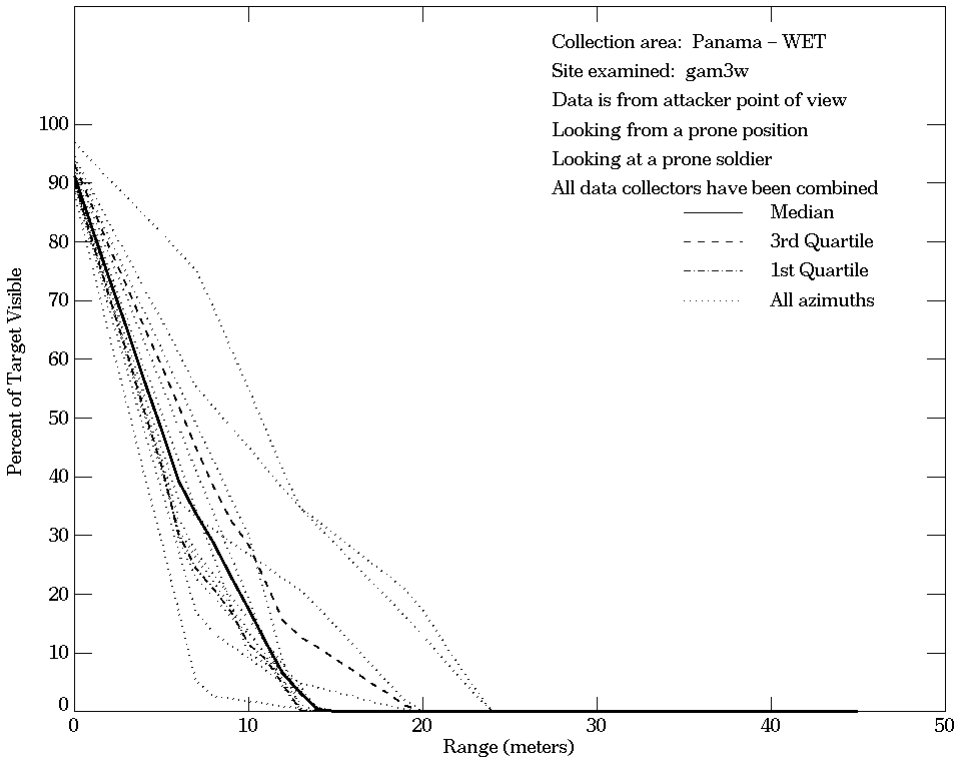

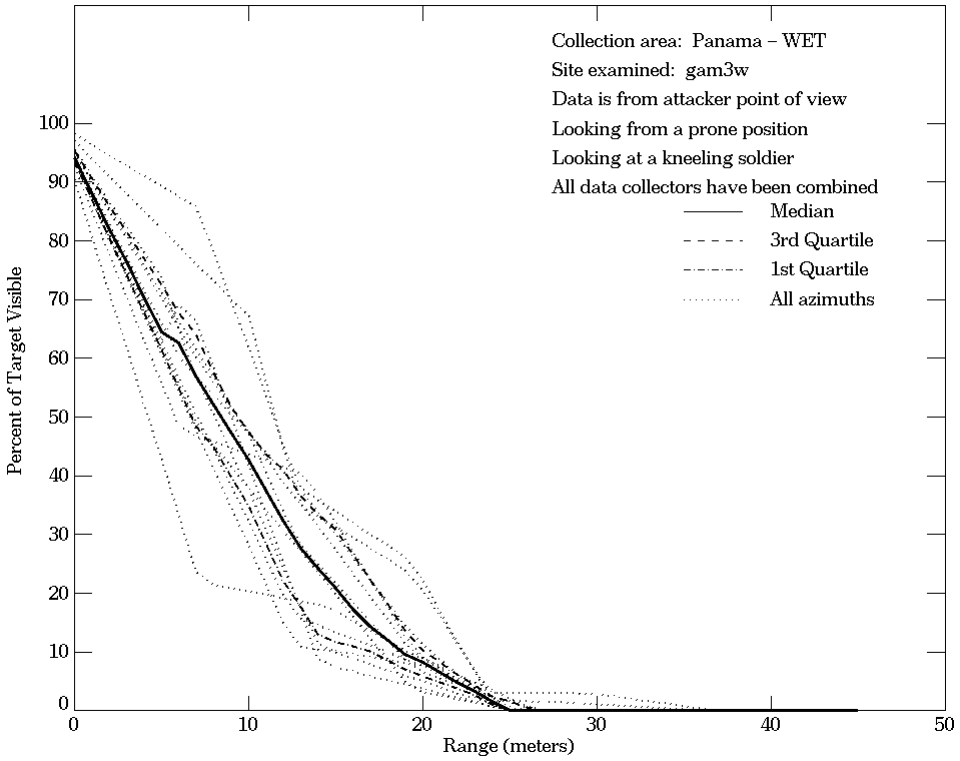

Figure E-18. Panama - Wet, From Attacker Point of View, Site gam3w

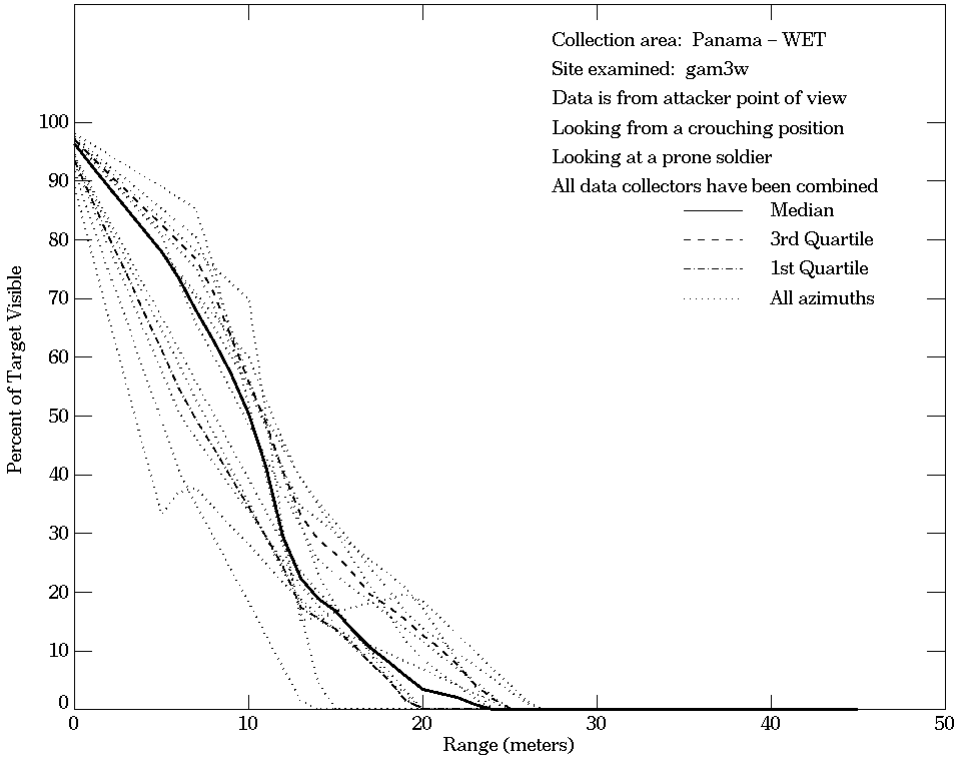

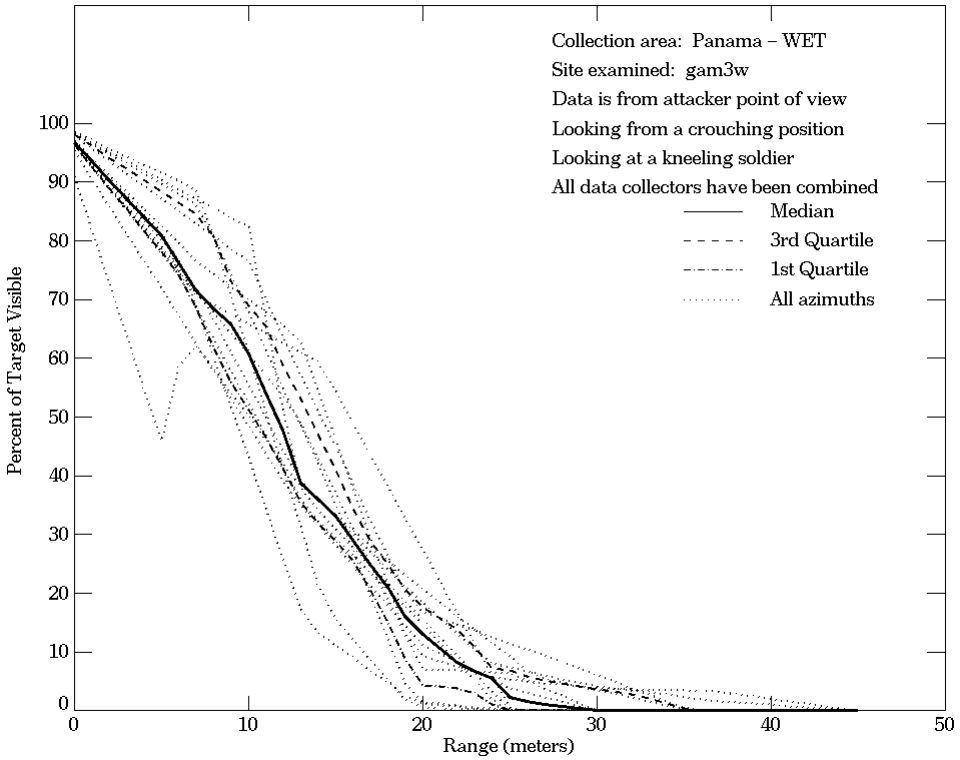

Figure E-18. Panama - Wet, From Attacker Point of View, Site gam3w (Continued)

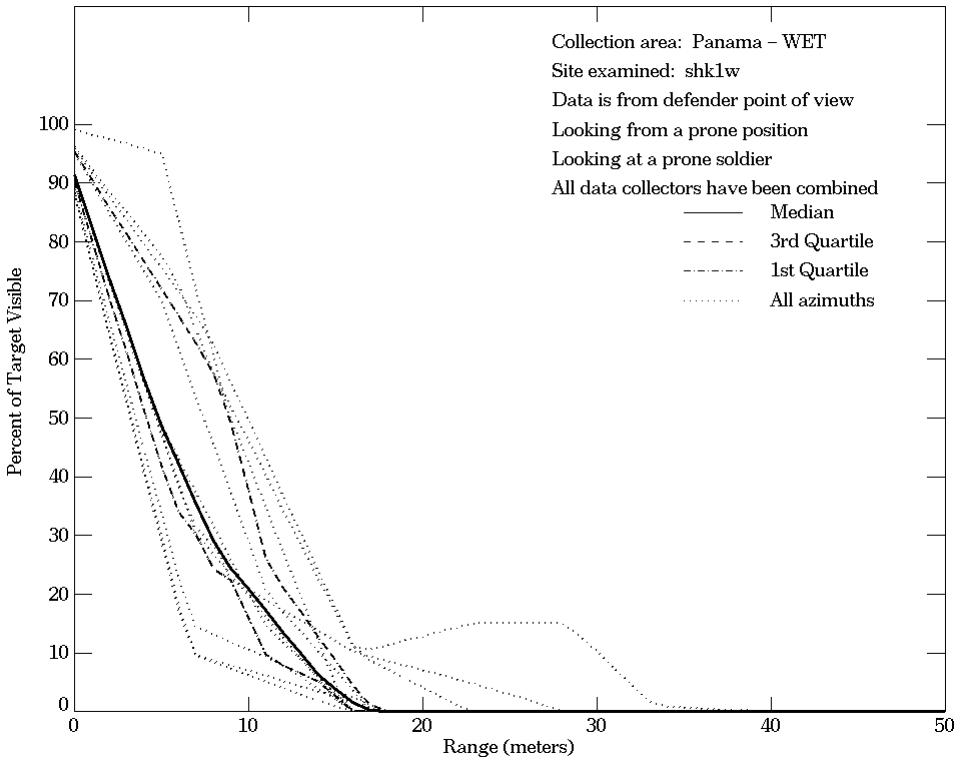

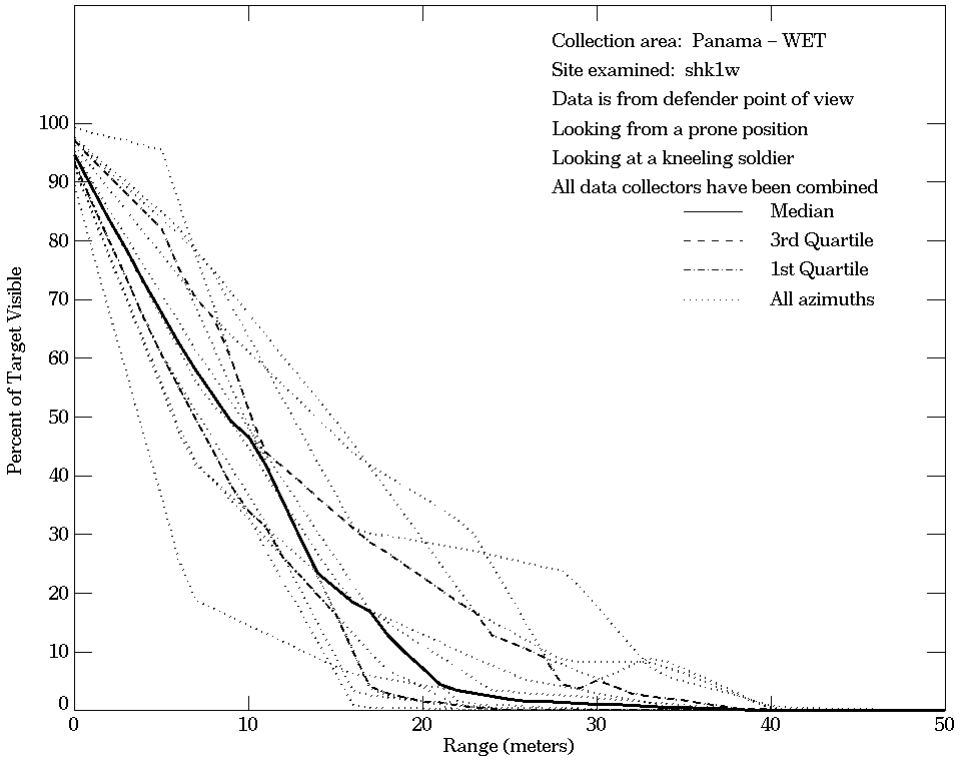

Figure E-19. Panama - Wet, From Defender Point of View, Site shk1w

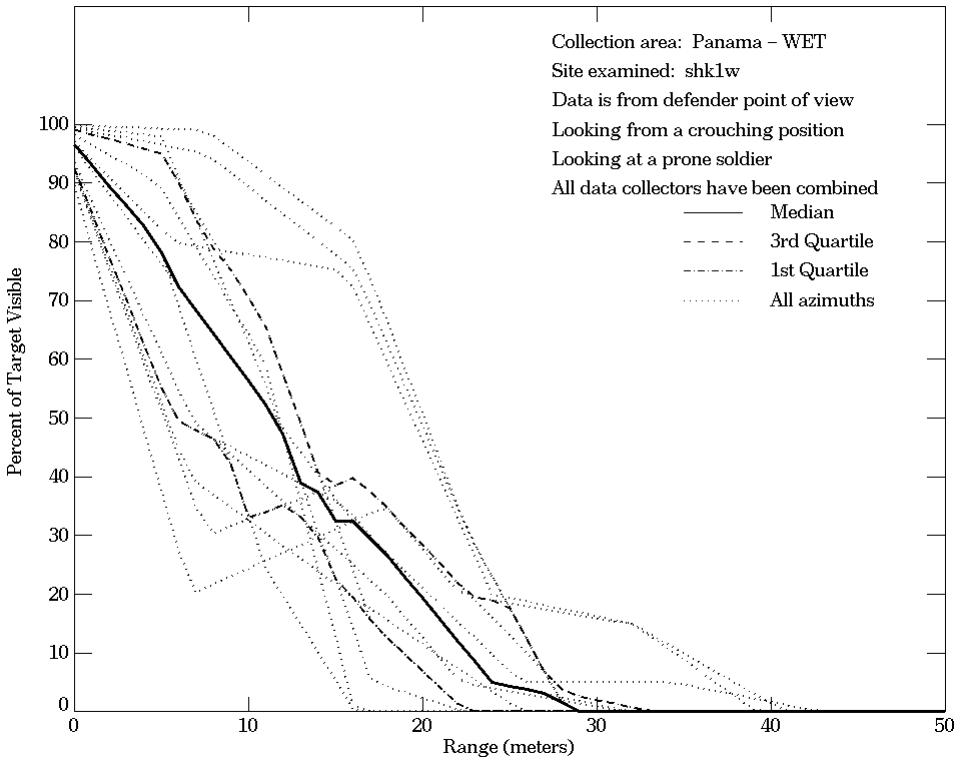

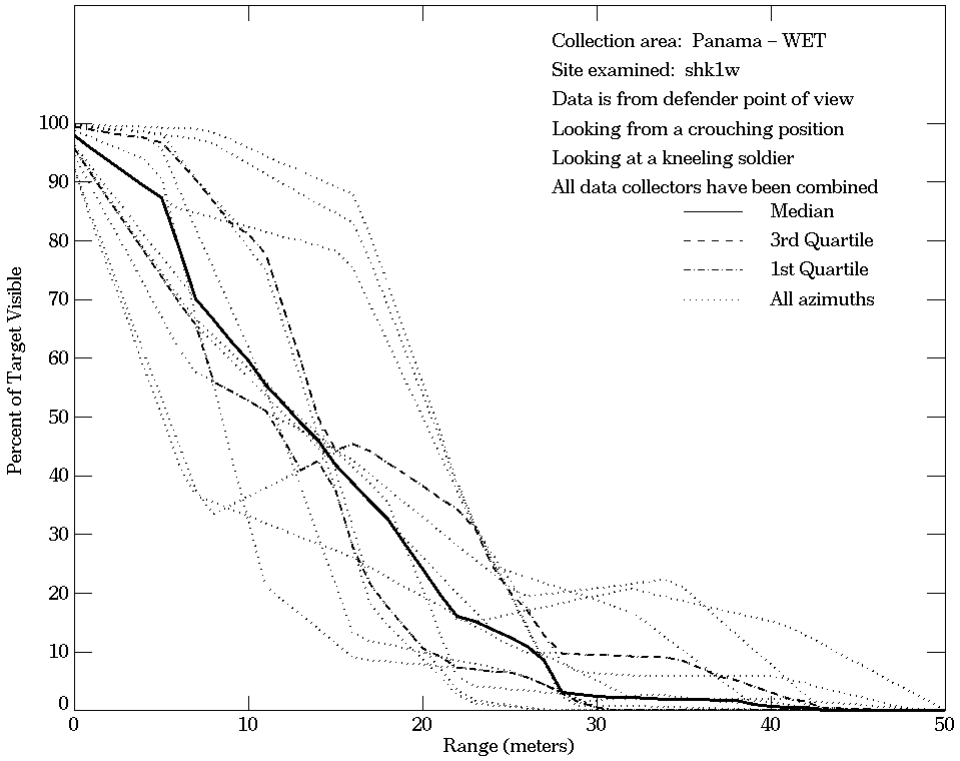

Figure E-19. Panama - Wet, From Defender Point of View, Site shk1w (Continued)

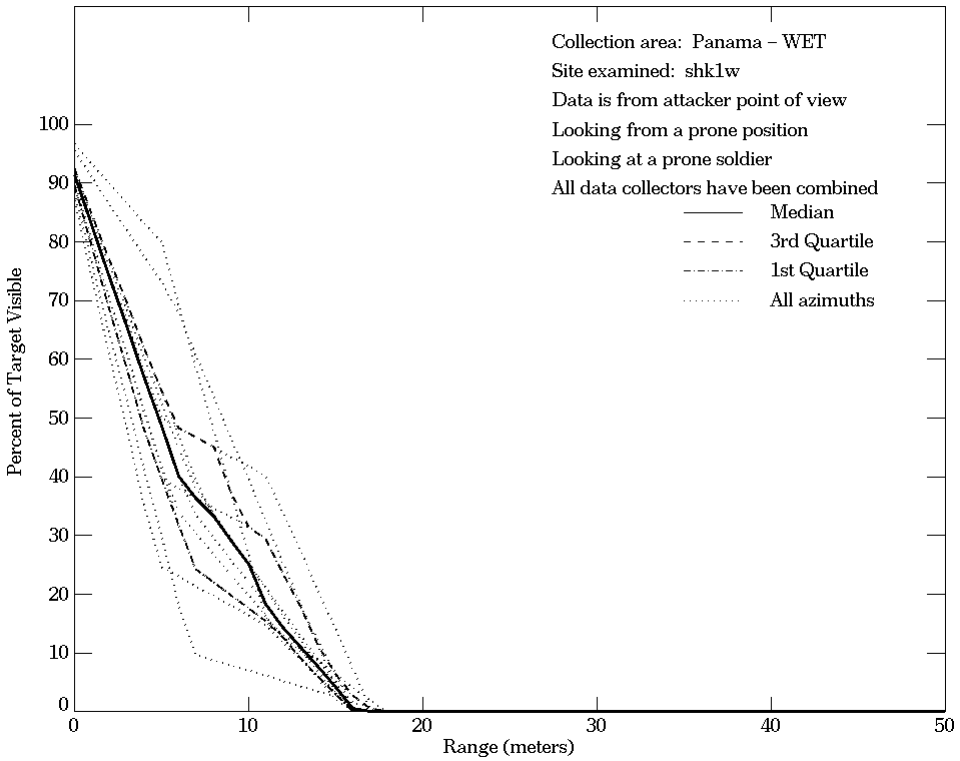

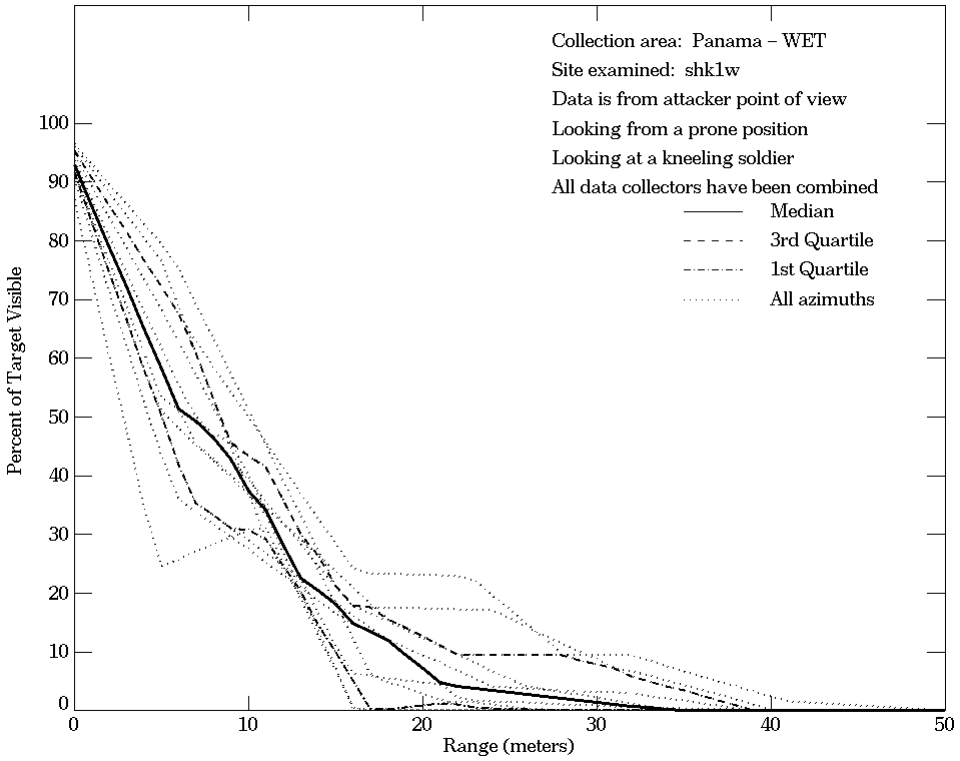

Figure E-20. Panama - Wet, From Attacker Point of View, Site shk1w

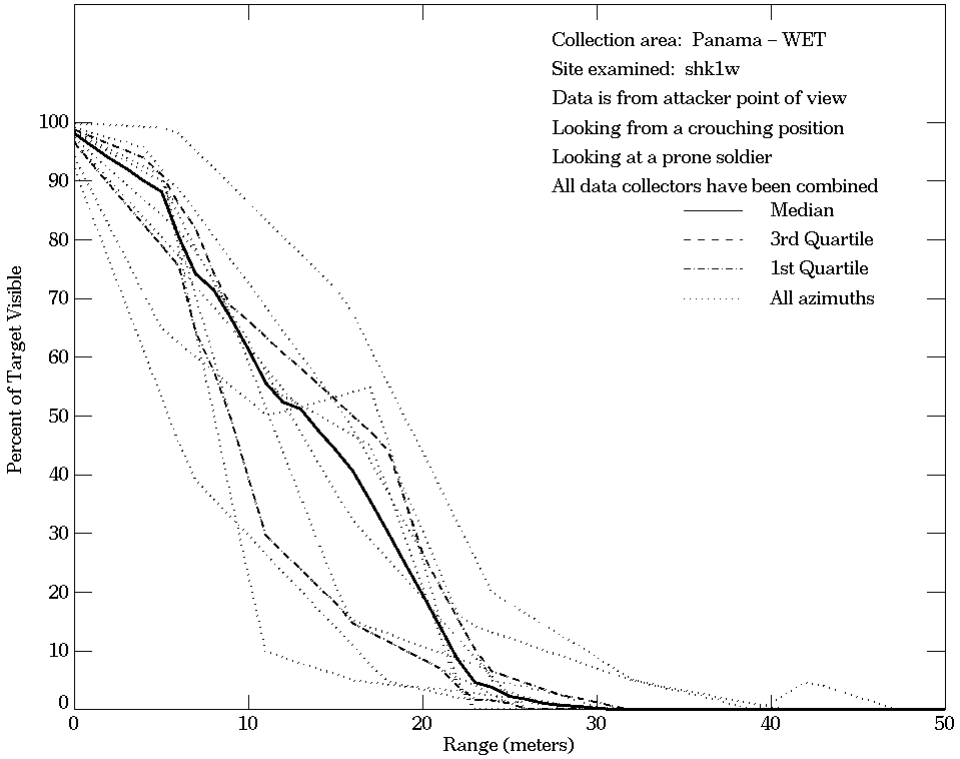

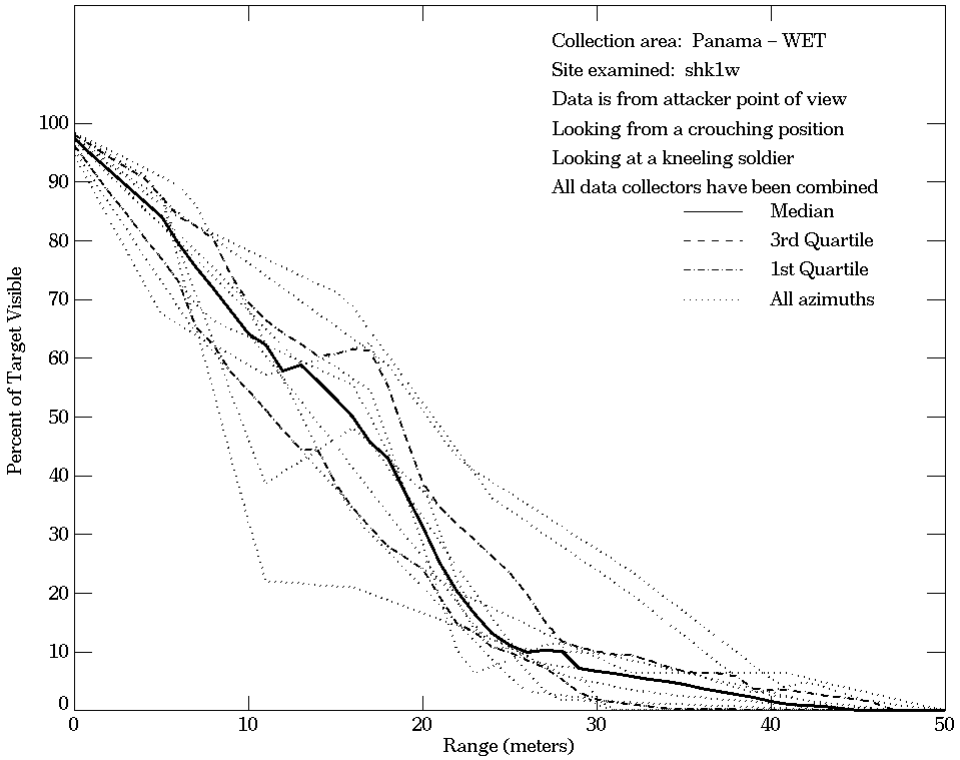

Figure E-20. Panama - Wet, From Attacker Point of View, Site shk1w (Continued)

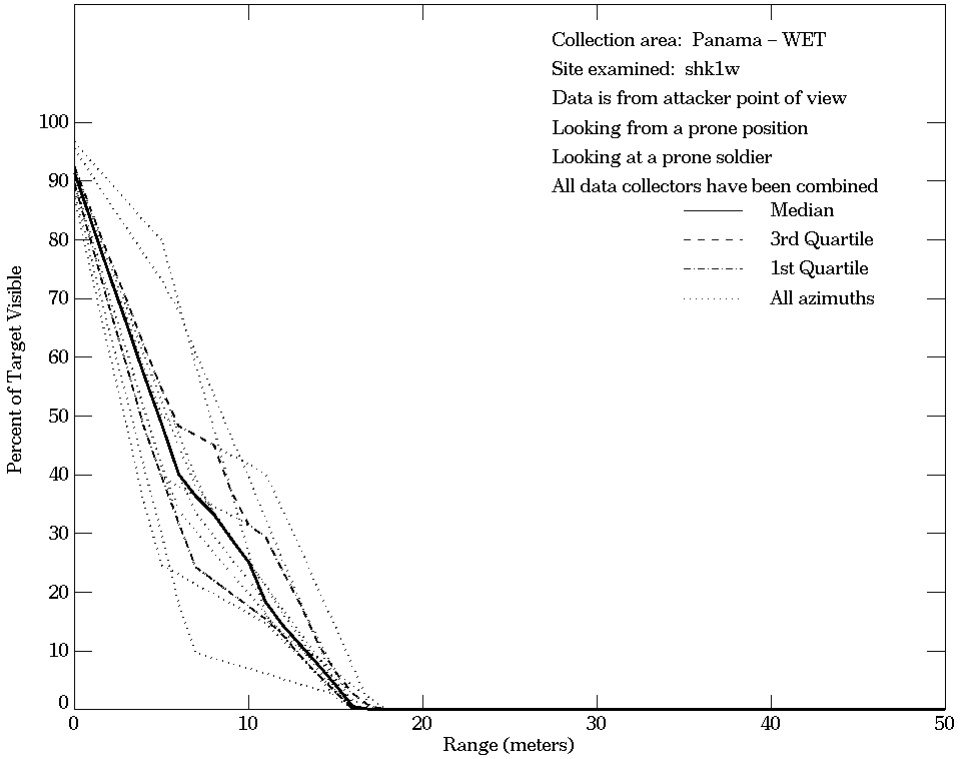

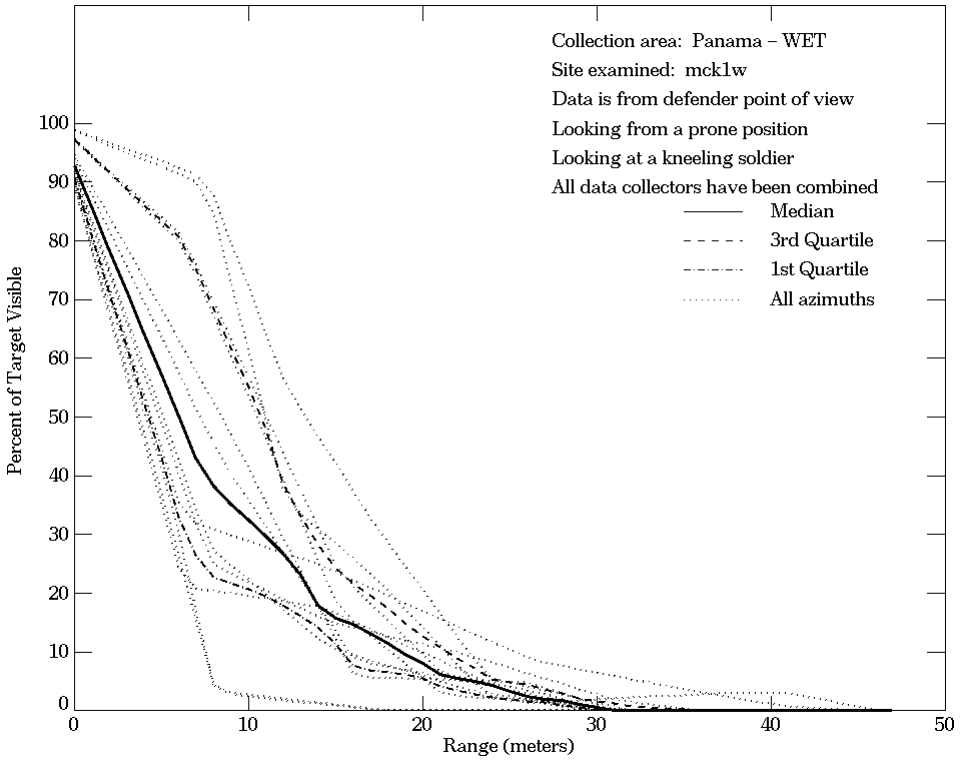

Figure E-21. Panama - Wet, From Defender Point of View, Site mck1w

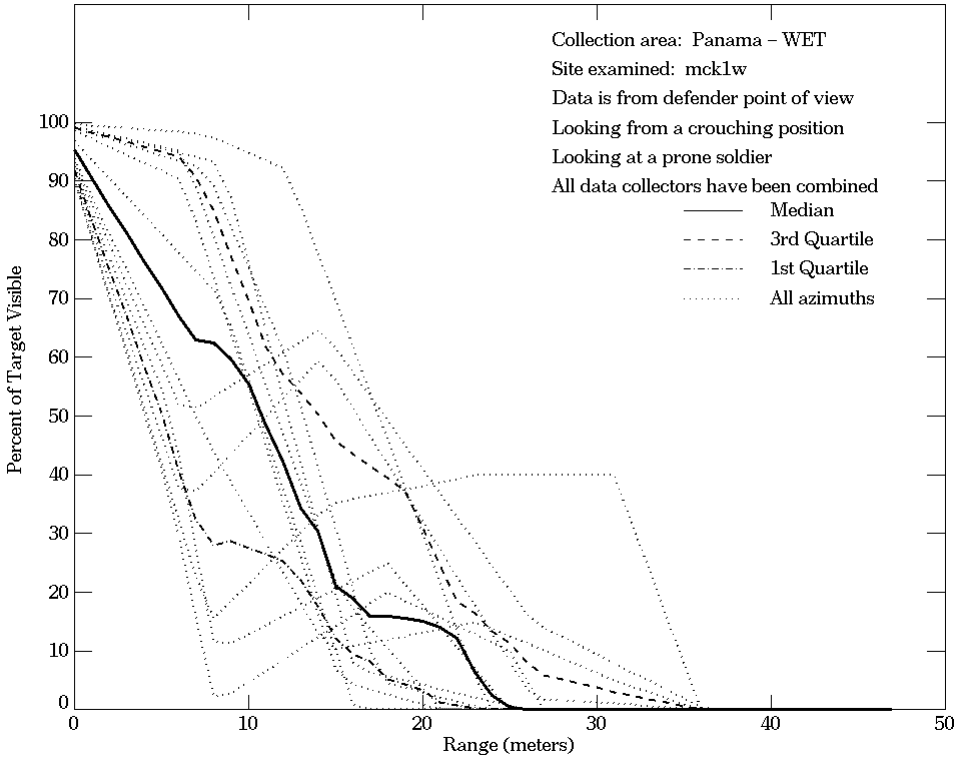

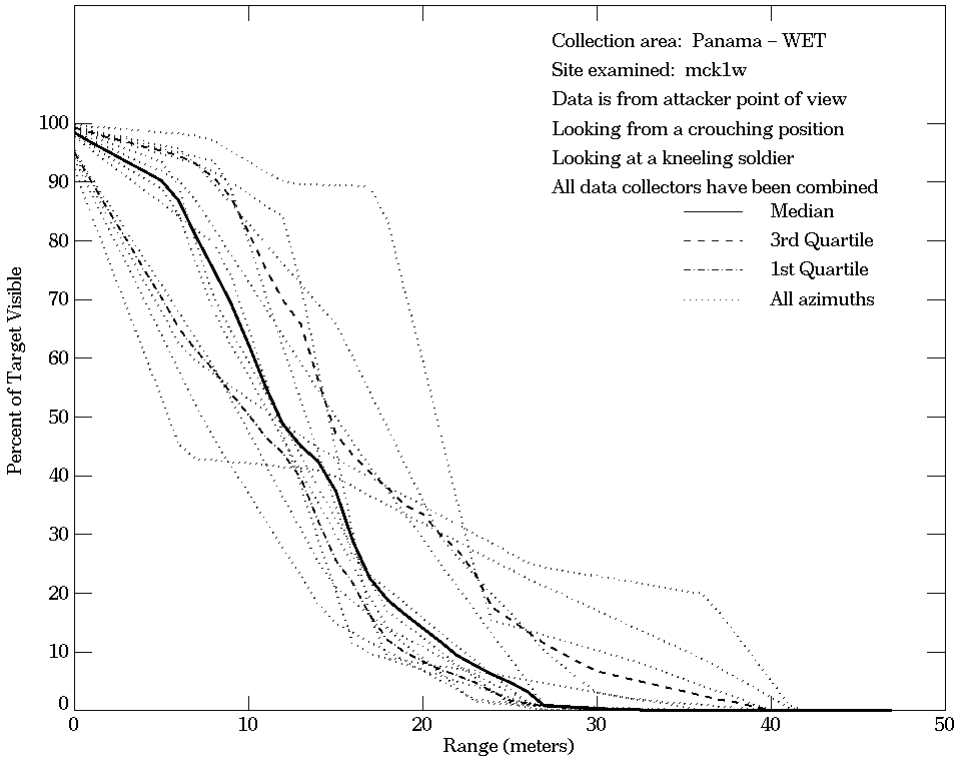

Figure E-21. Panama - Wet, From Defender Point of View, Site mck1w (Continued)

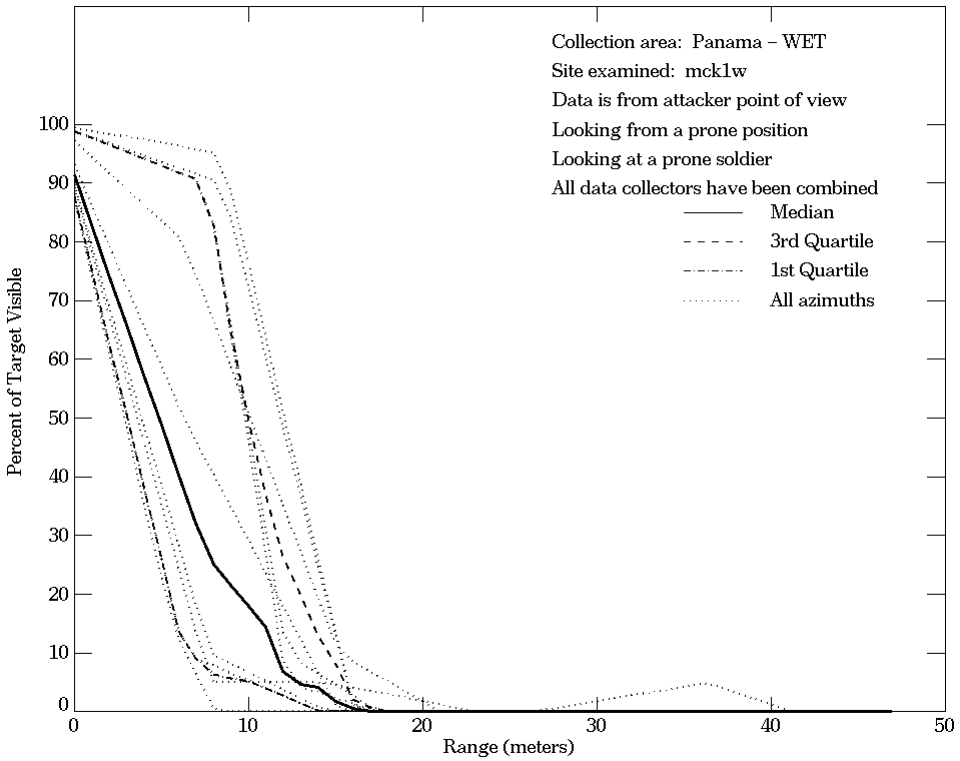

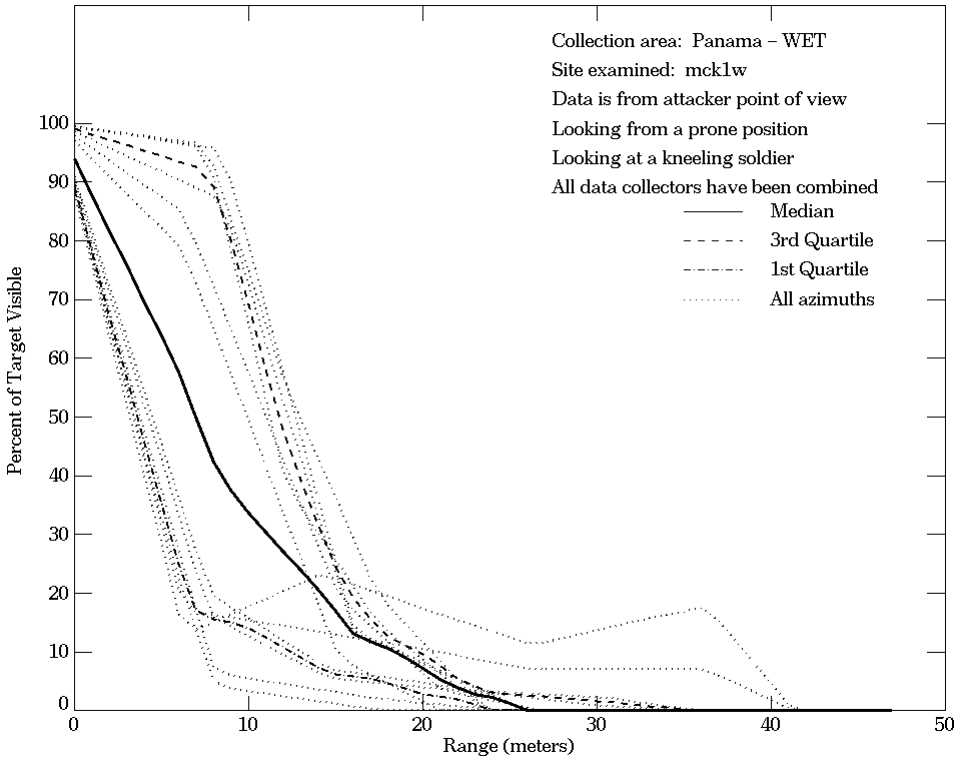

Figure E-22. Panama - Wet, From Attacker Point of View, Site mck1w

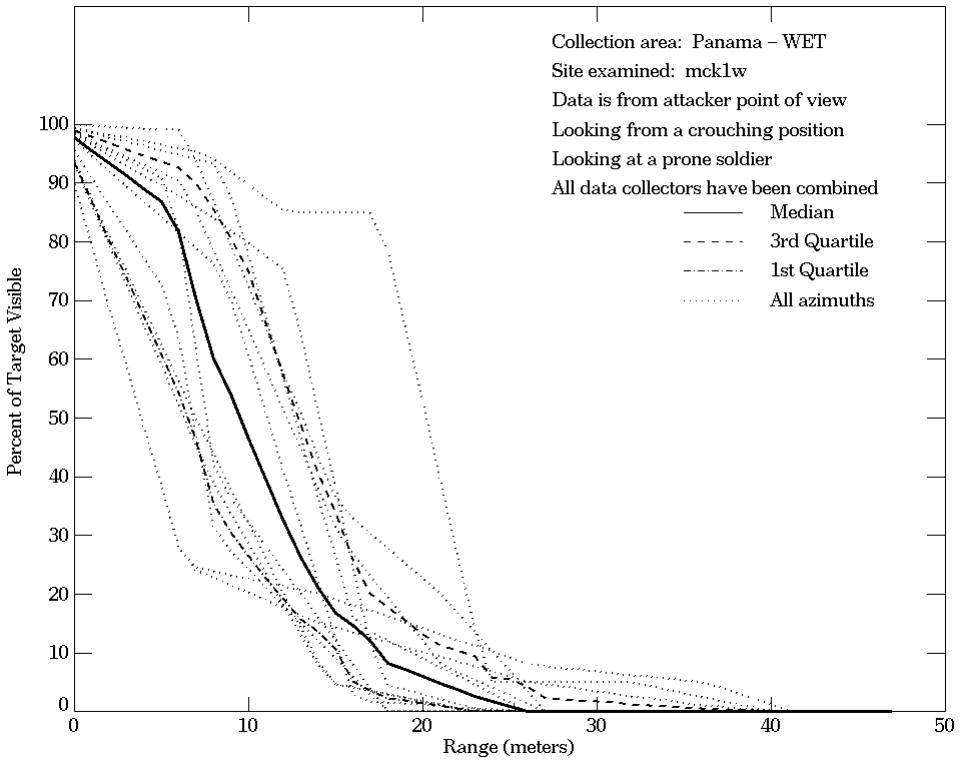

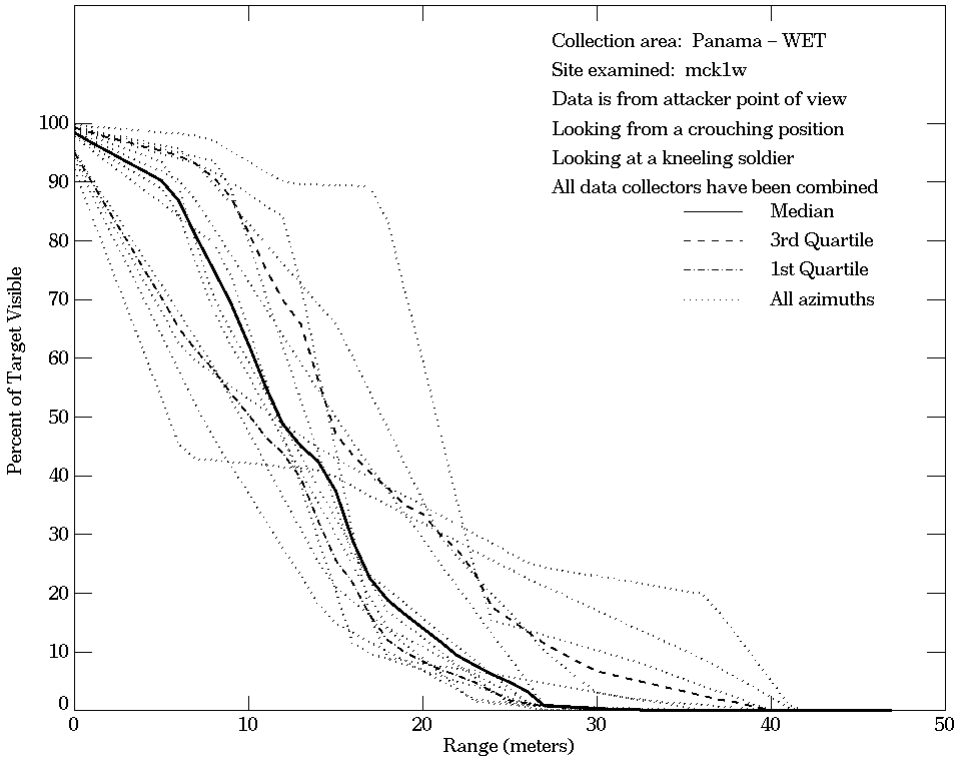

Figure E-22. Panama - Wet, From Attacker Point of View, Site mck1w (Continued)

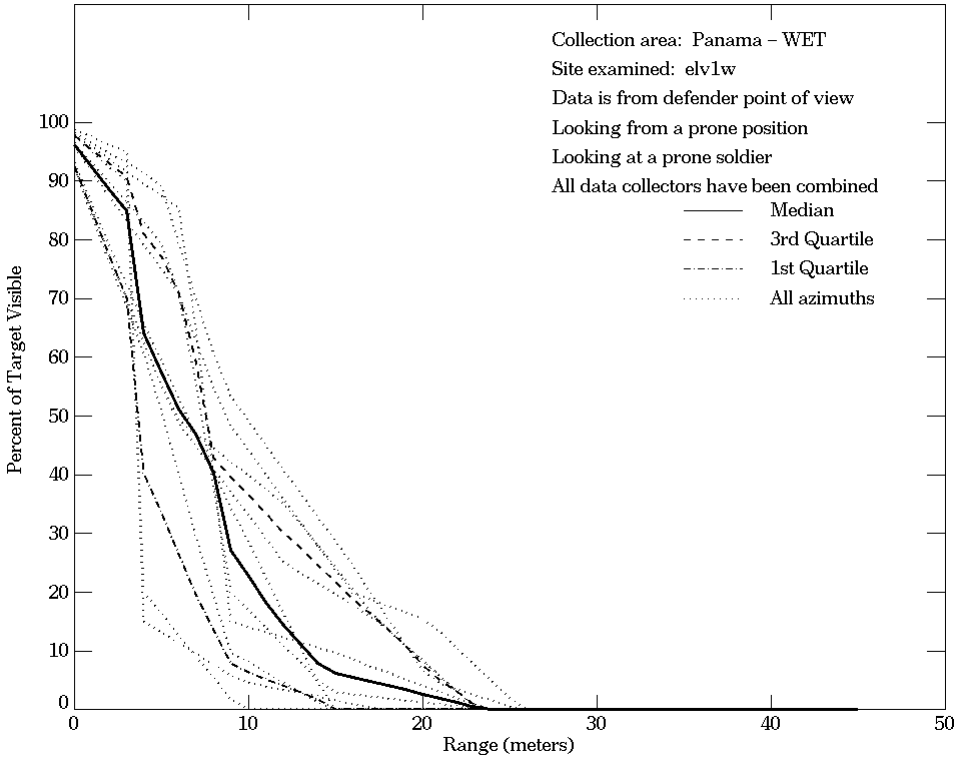

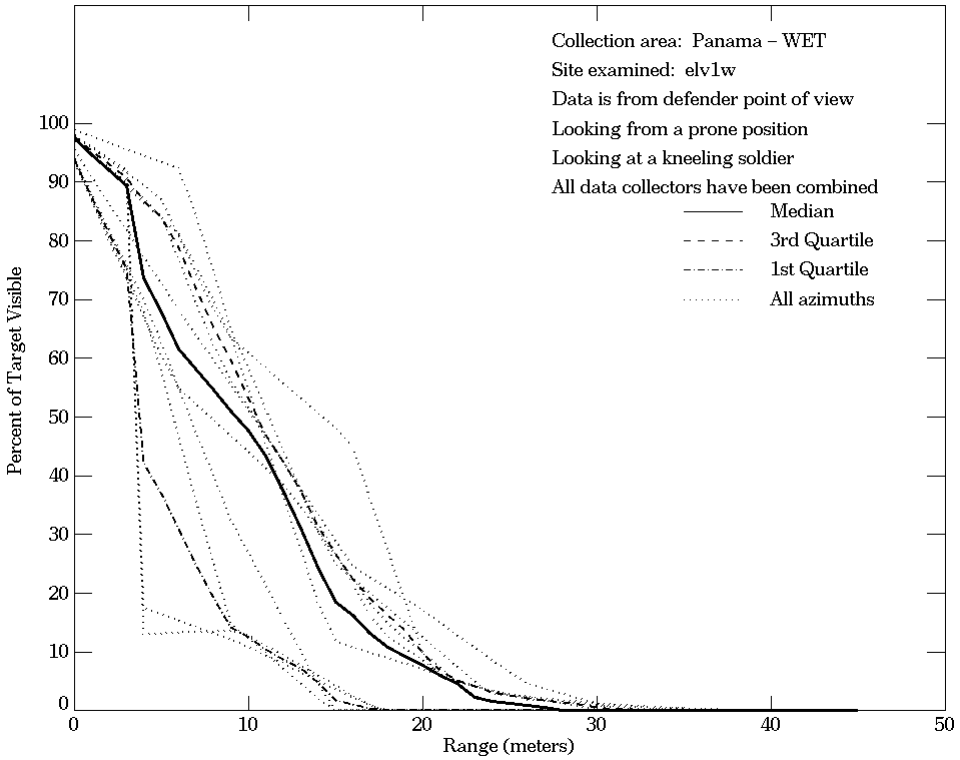

Figure E-23. Panama - Wet, From Defender Point of View, Site elv1w

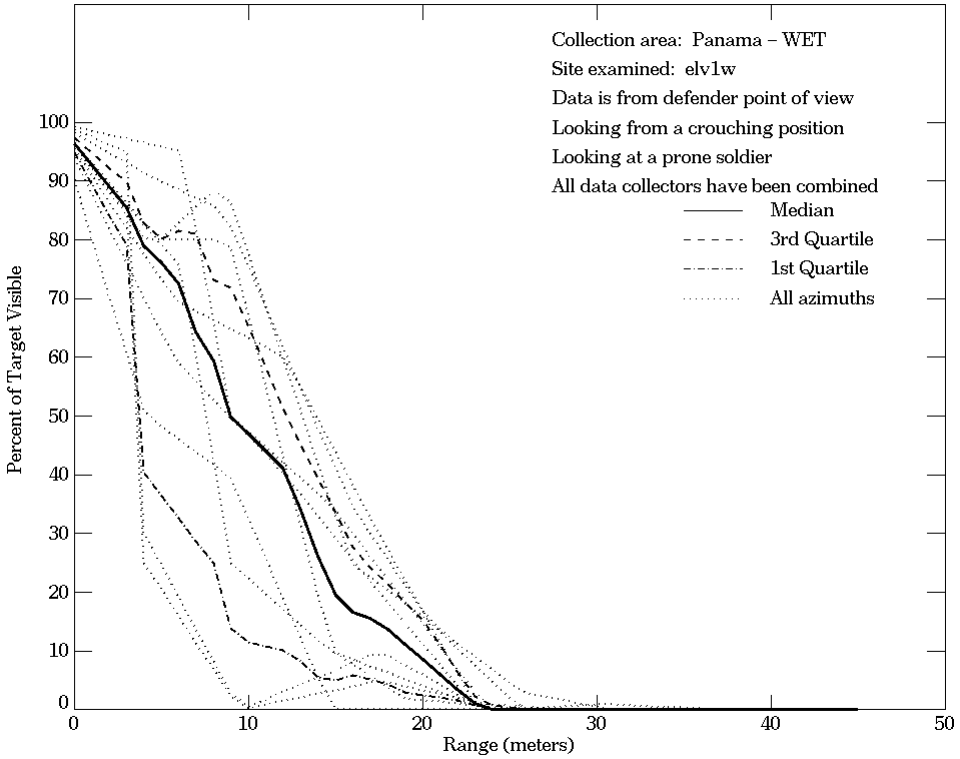

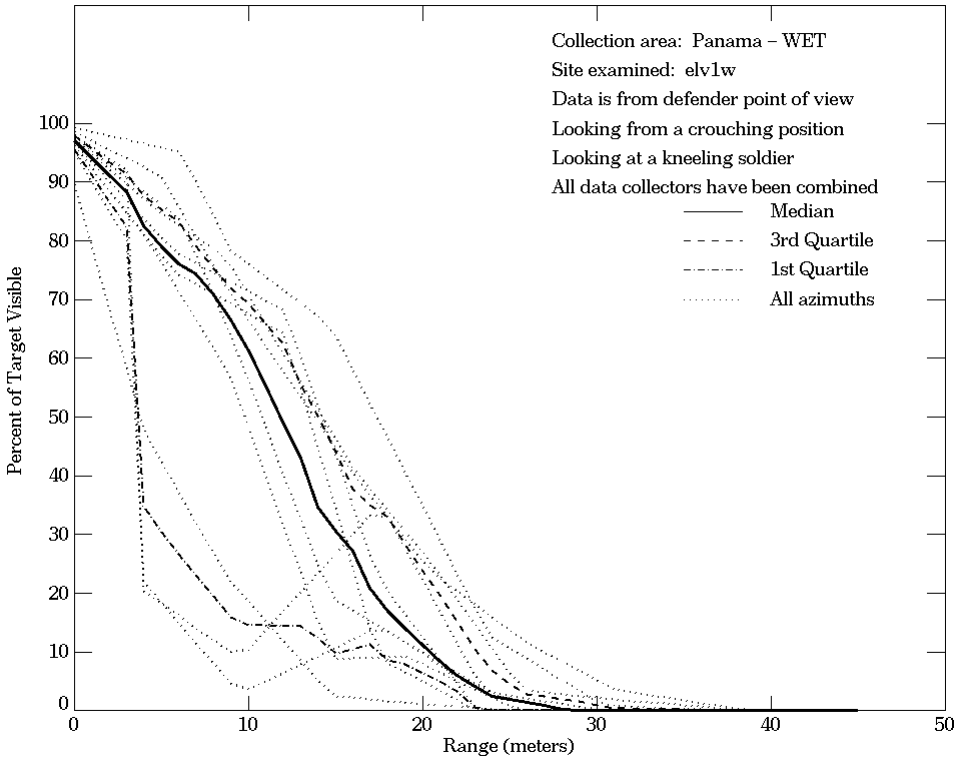

Figure E-23. Panama - Wet, From Defender Point of View, Site elv1w (Continued)

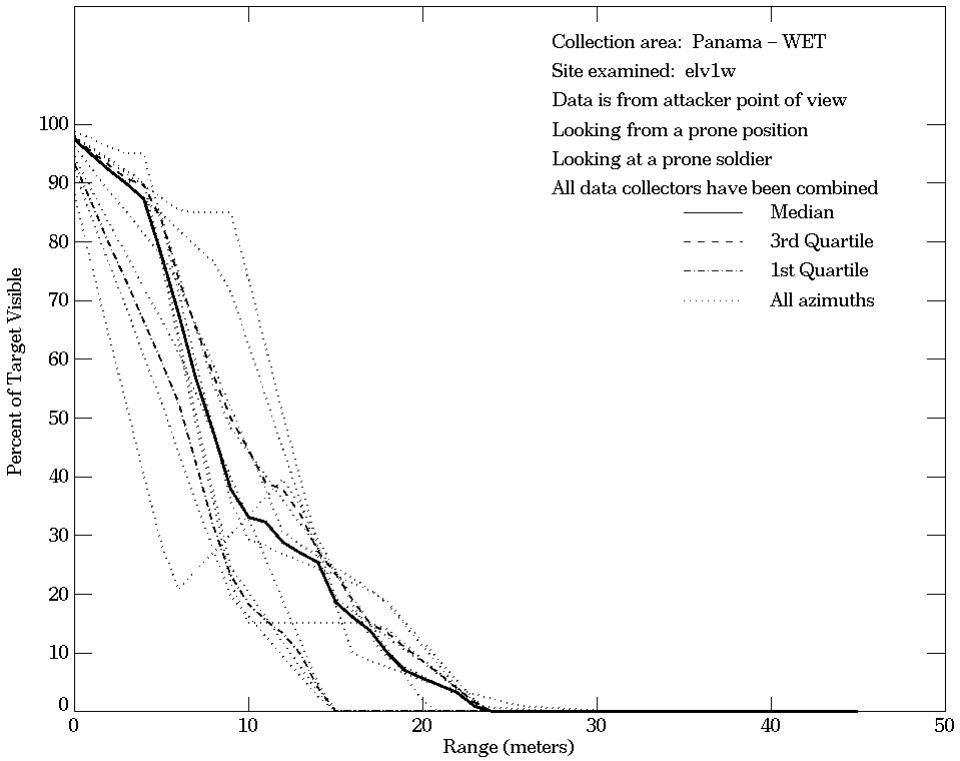

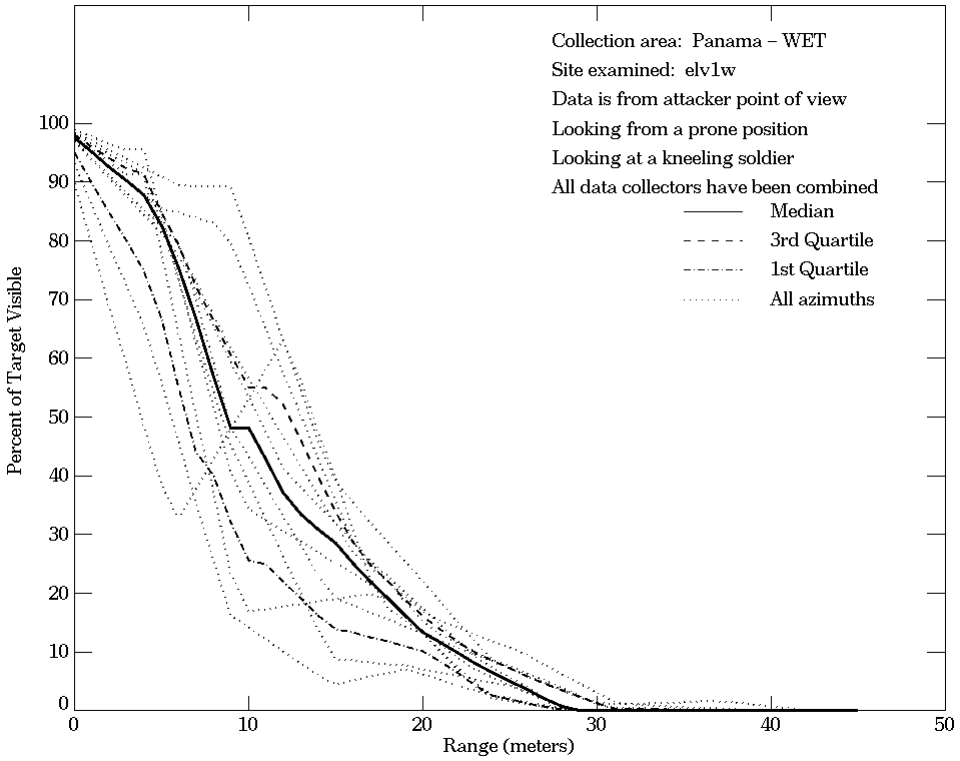

Figure E-24. Panama - Wet, From Attacker Point of View, Site elv1w

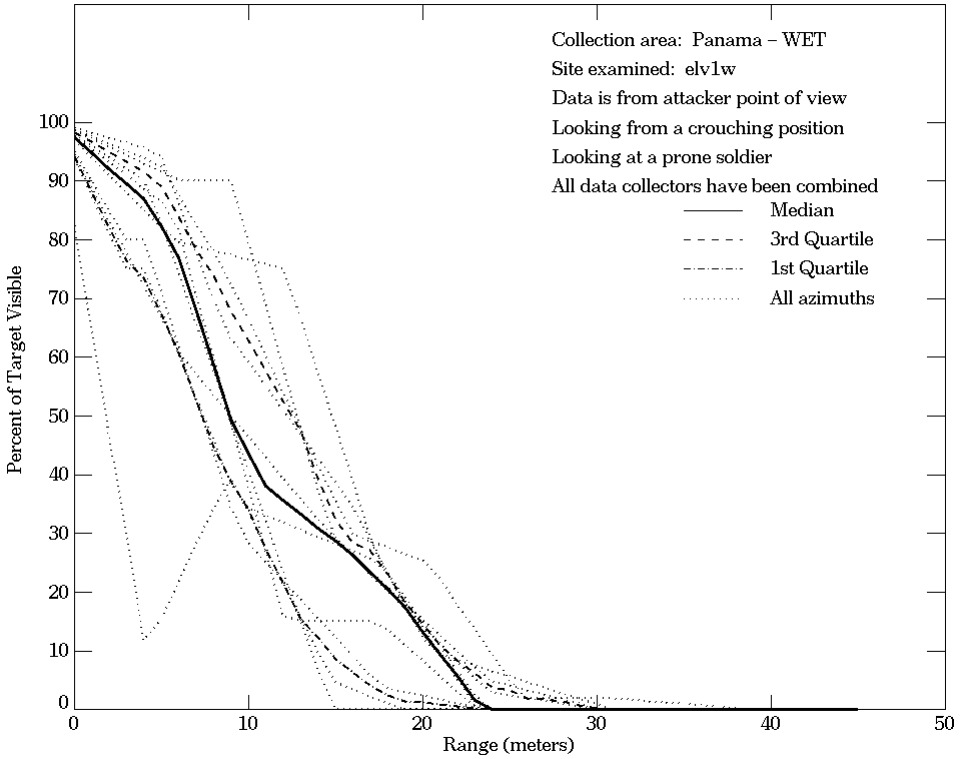

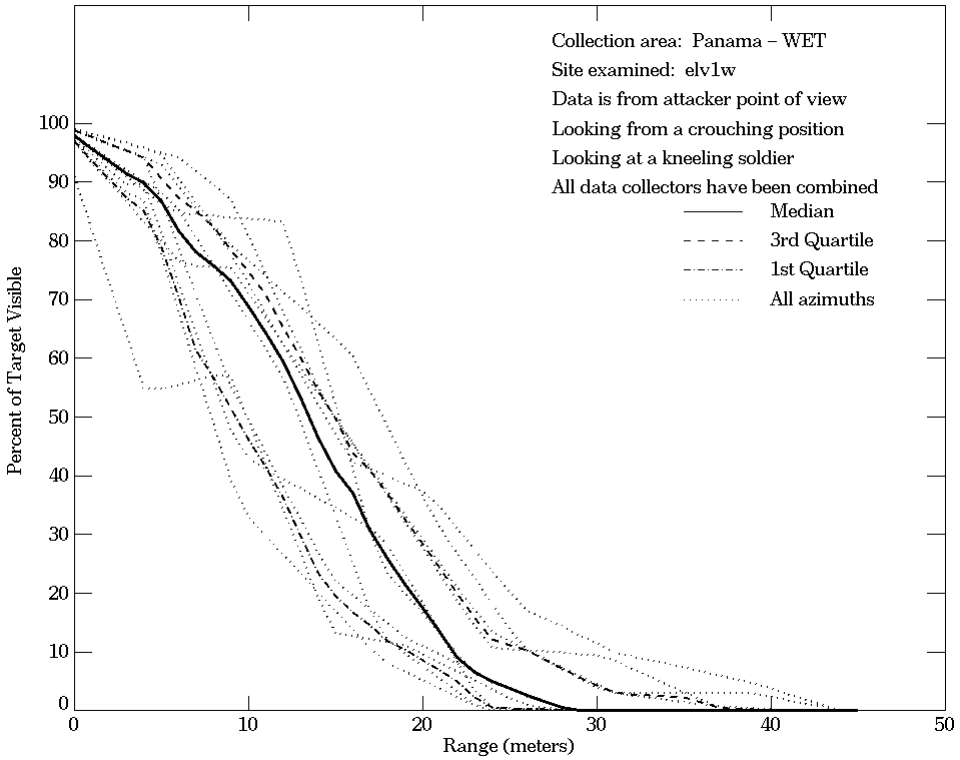

Figure E-24. Panama - Wet, From Attacker Point of View, Site elv1w (Continued)

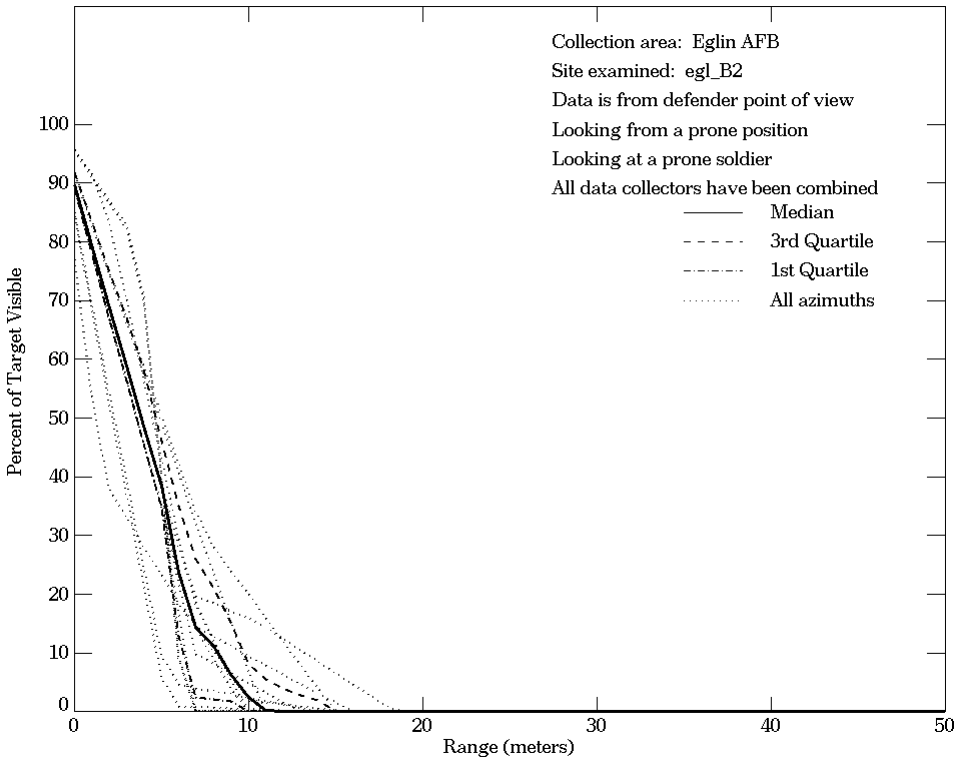

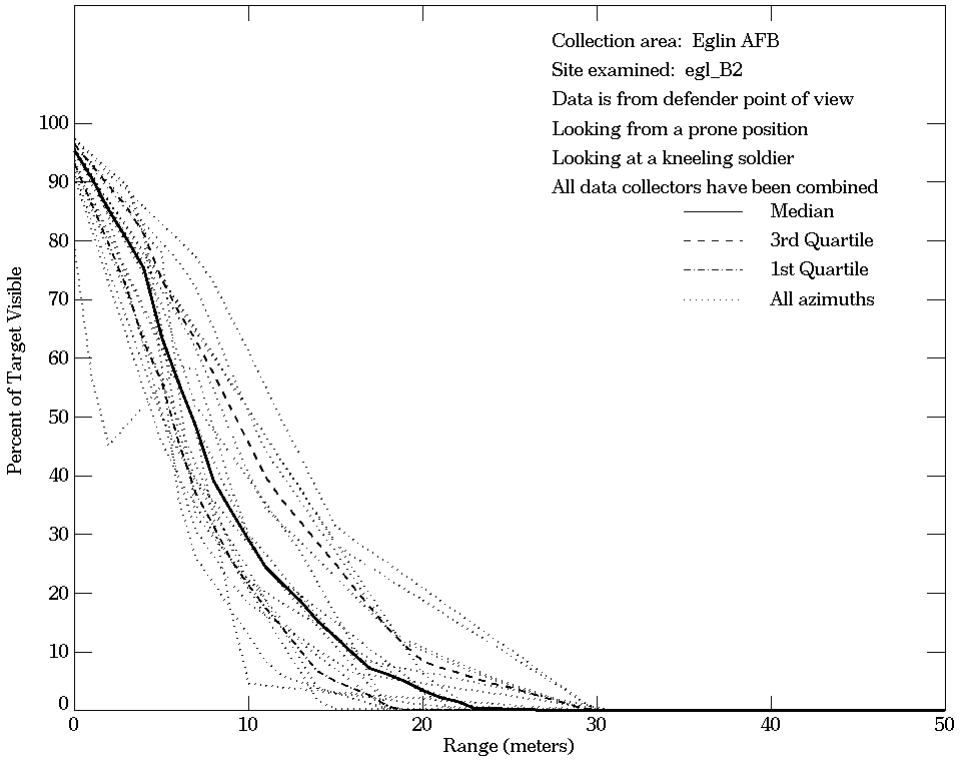

Figure E-25. Eglin AFB, From Defender Point of View, Site egl_B2

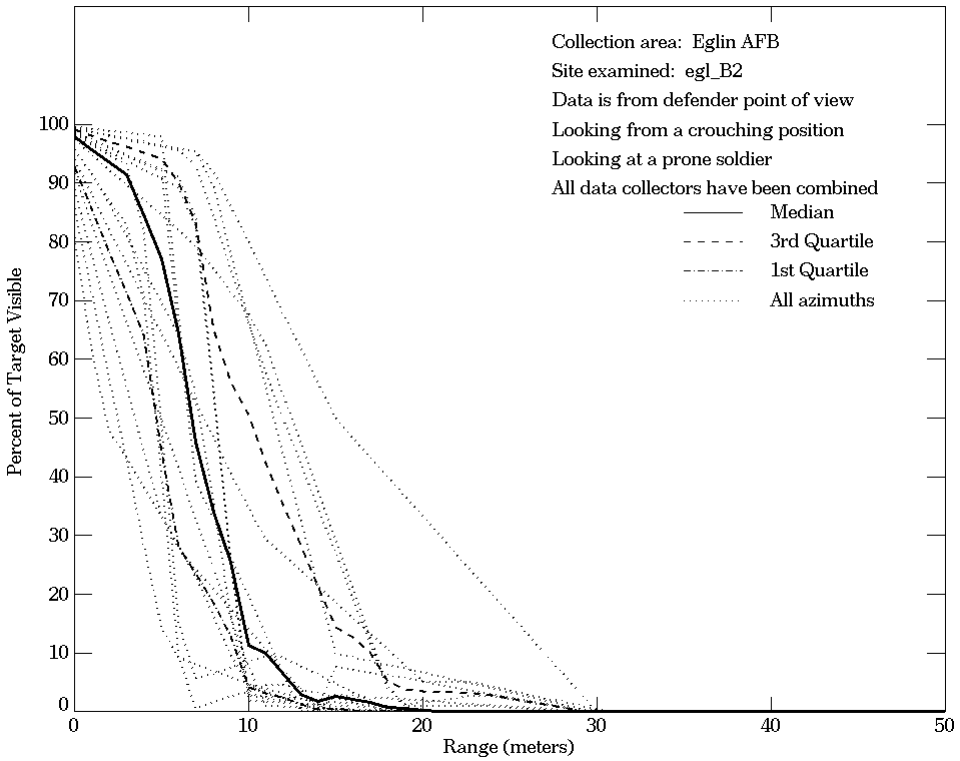

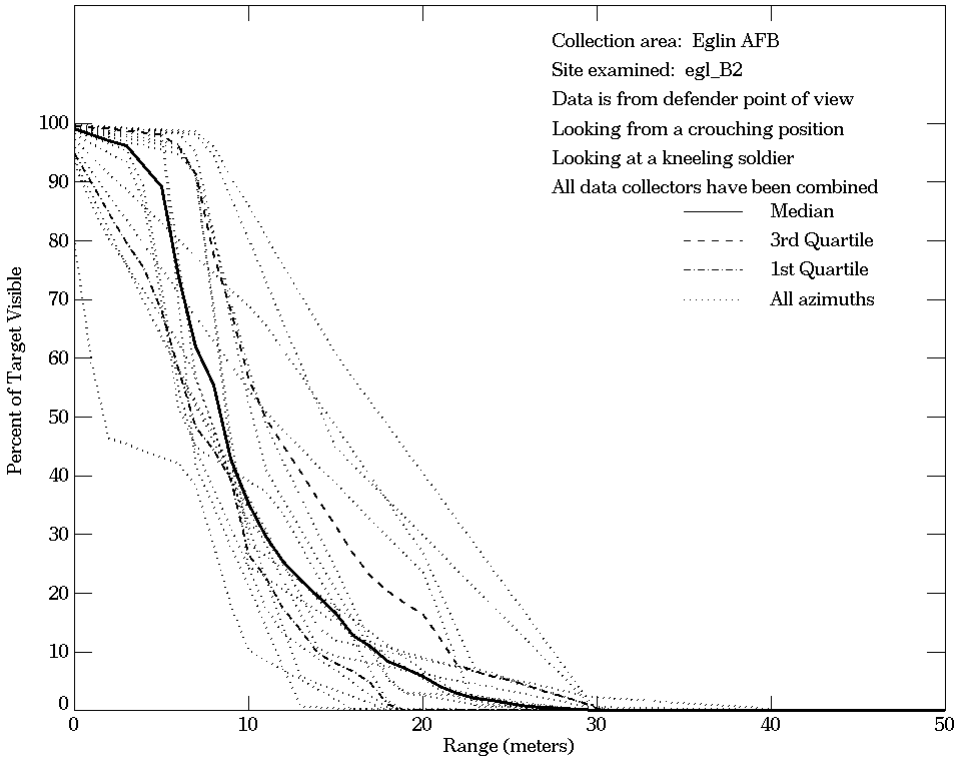

Figure E-25. Eglin AFB, From Defender Point of View, Site egl_B2 (Continued)

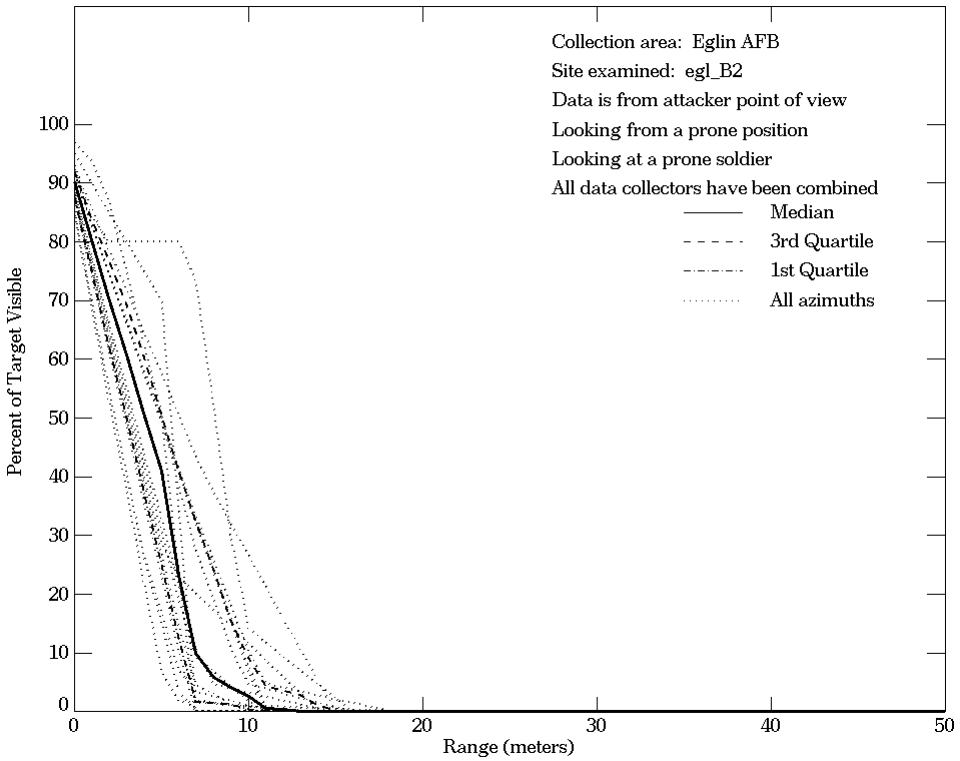

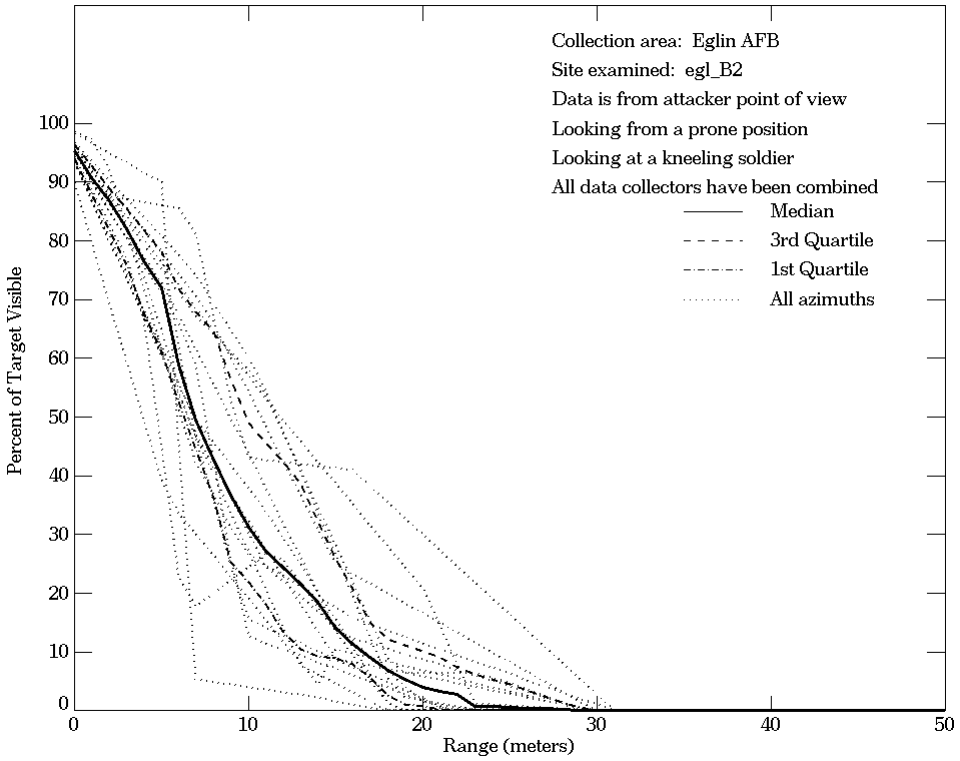

Figure E-26. Eglin AFB, From Attacker Point of View, Site egl_B2

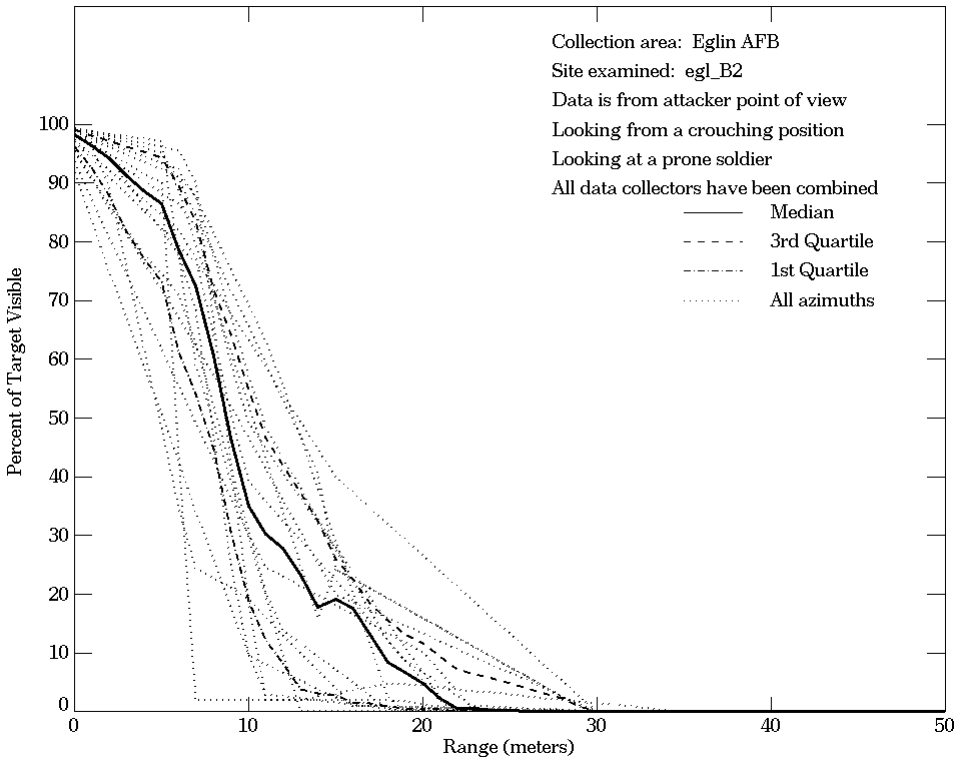

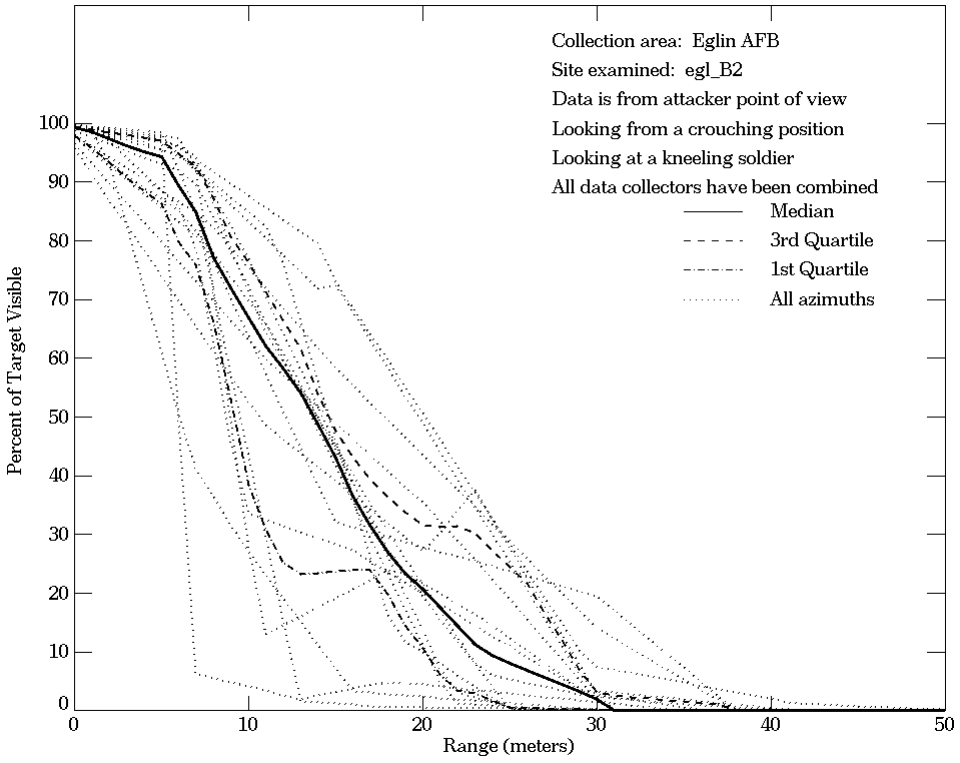

Figure E-26. Eglin AFB, From Attacker Point of View, Site egl_B2 (Continued)

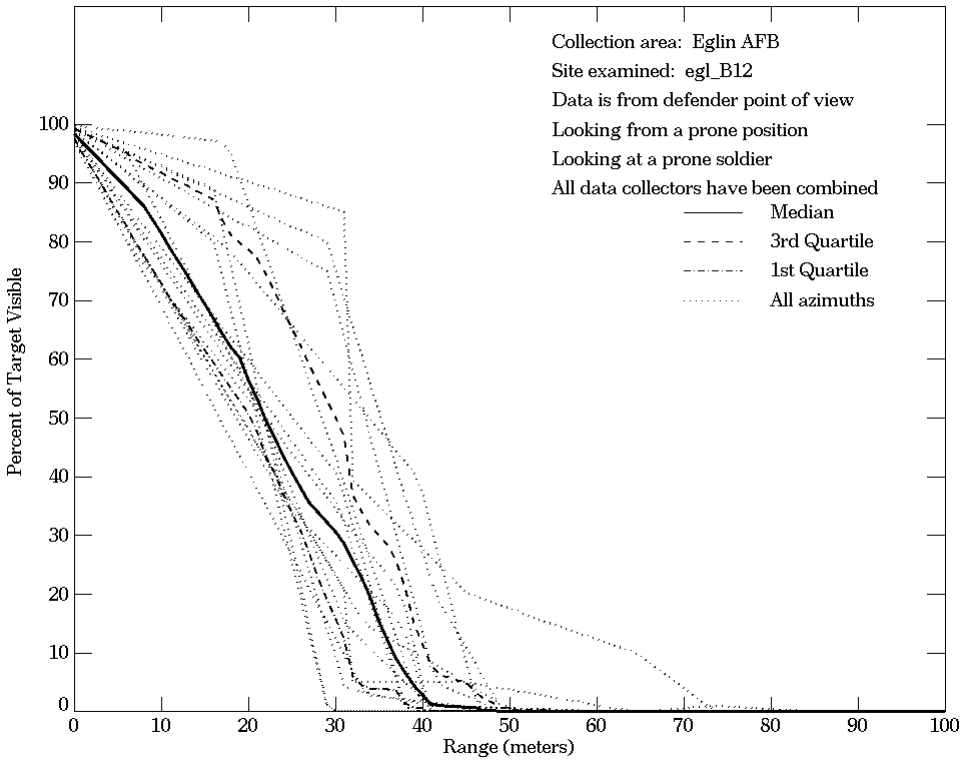

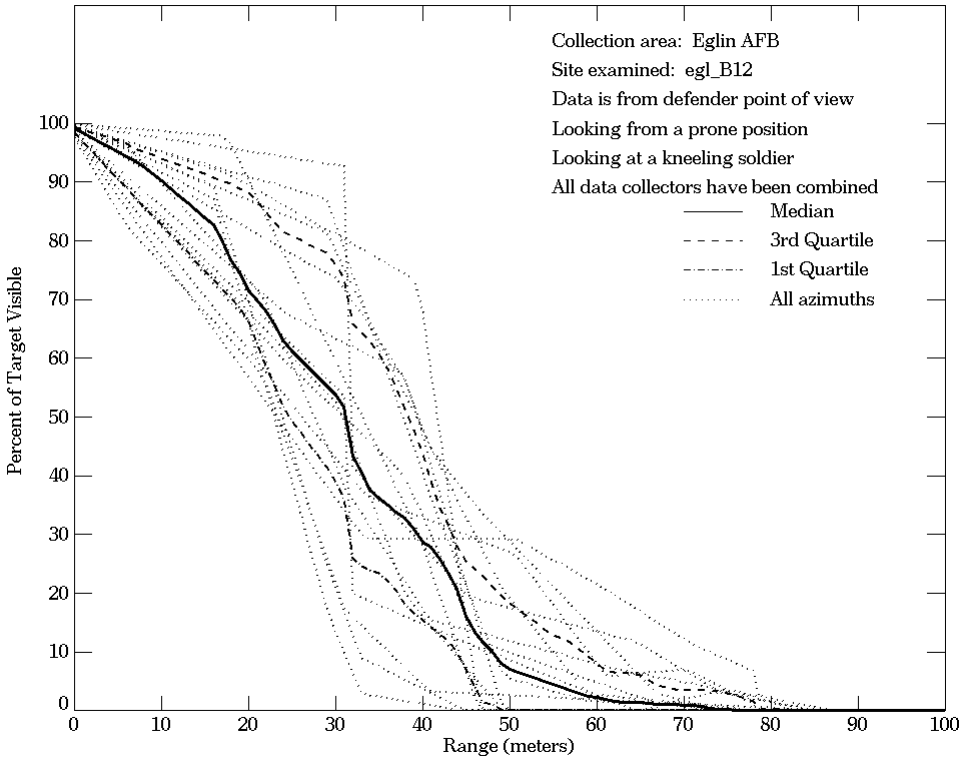

Figure E-27. Eglin AFB, From Defender Point of View, Site egl_B12

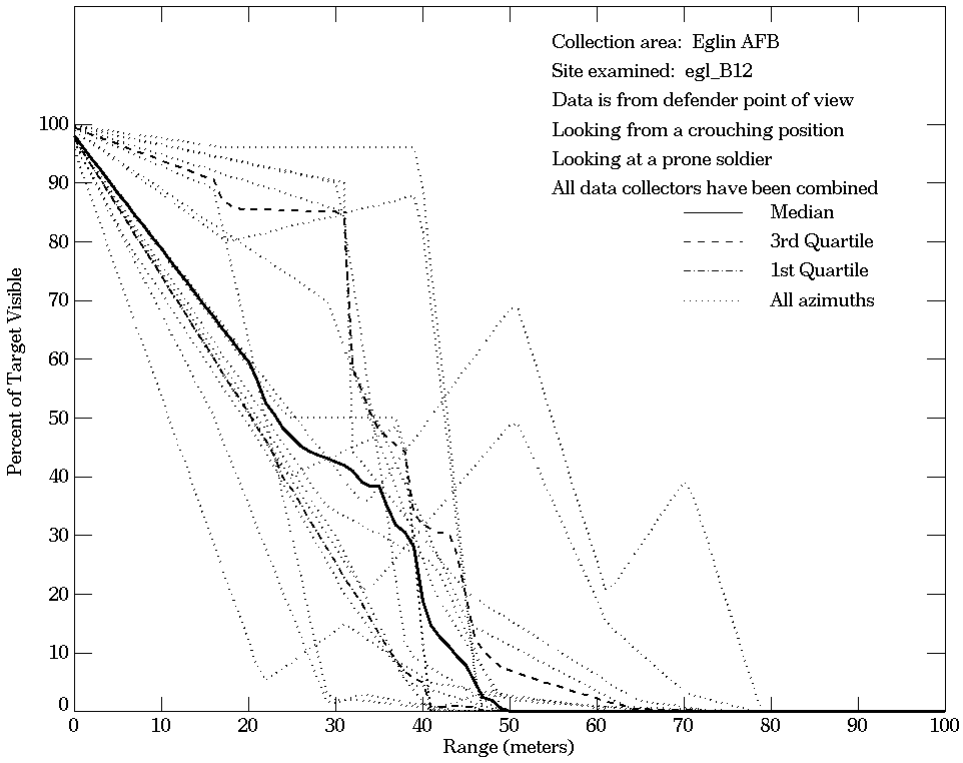

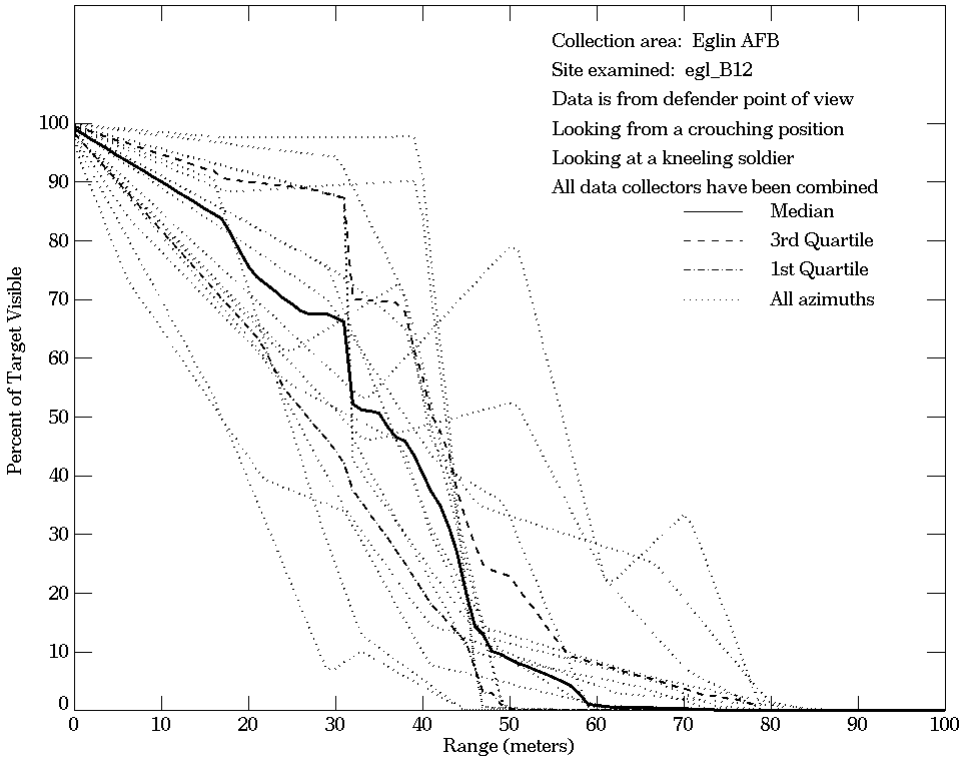

Figure E-27. Eglin AFB, From Defender Point of View, Site egl_B12 (Continued)

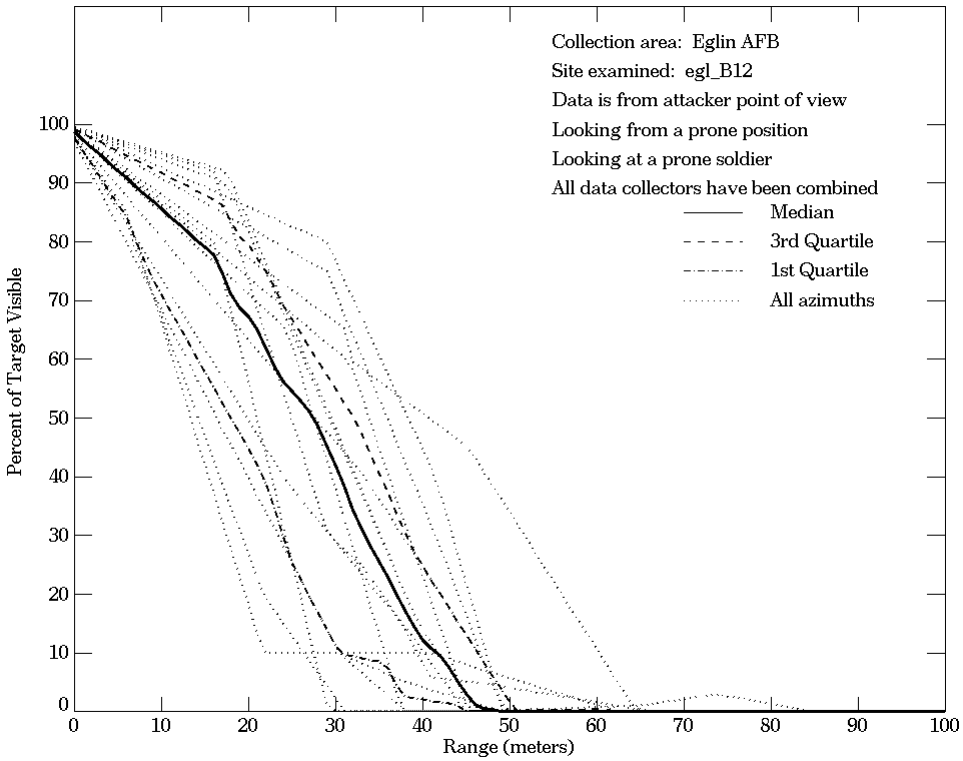

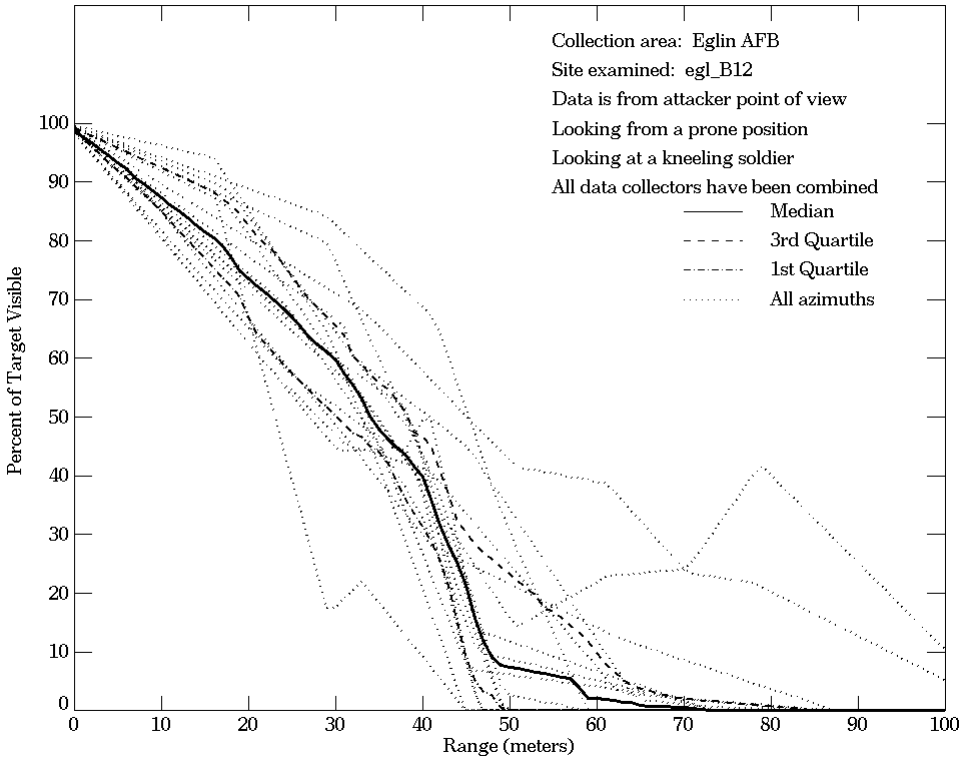

Figure E-28. Eglin AFB, From Attacker Point of View, Site egl_B12

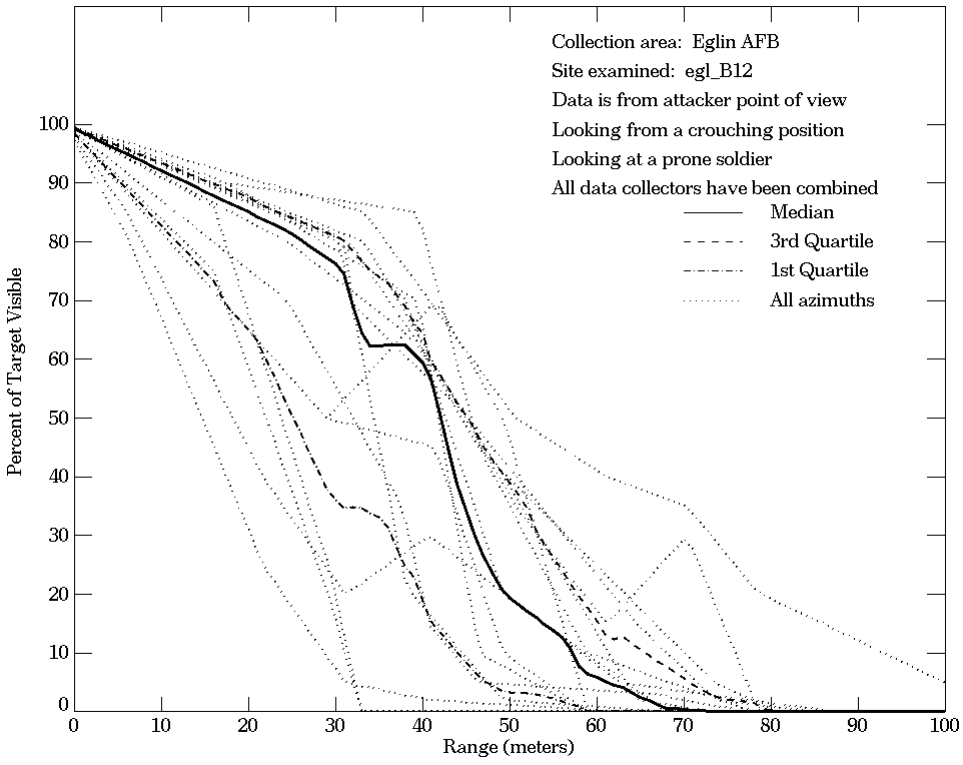

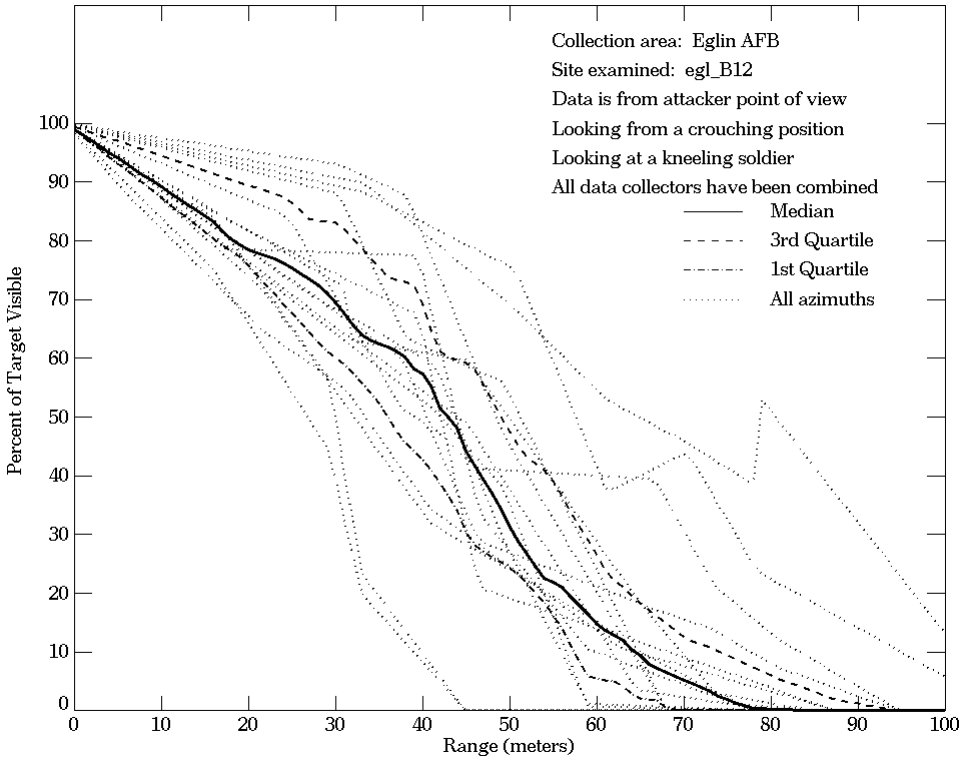

Figure E-28. Eglin AFB, From Attacker Point of View, Site egl_B12 (Continued)

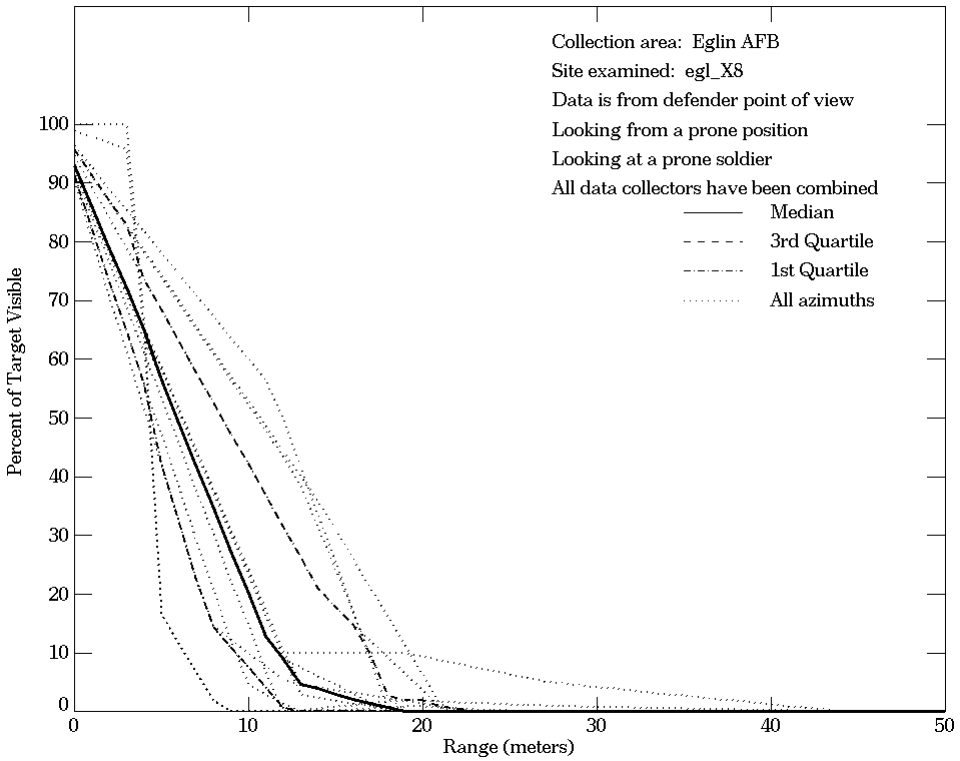

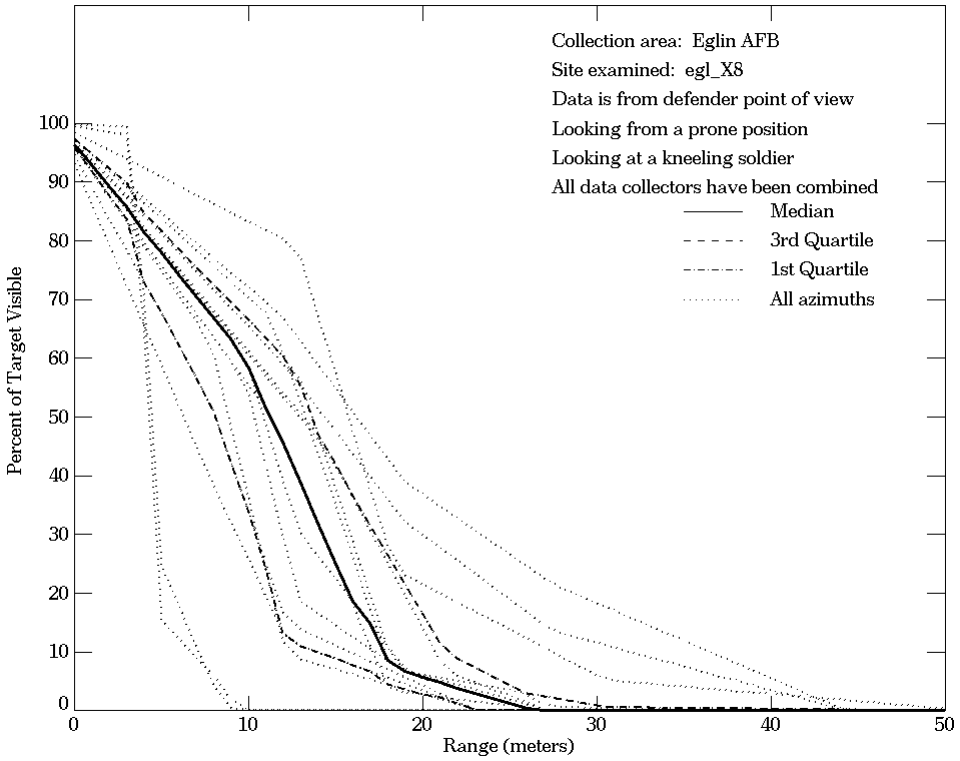

Figure E-29. Eglin AFB, From Defender Point of View, Site egl_X8

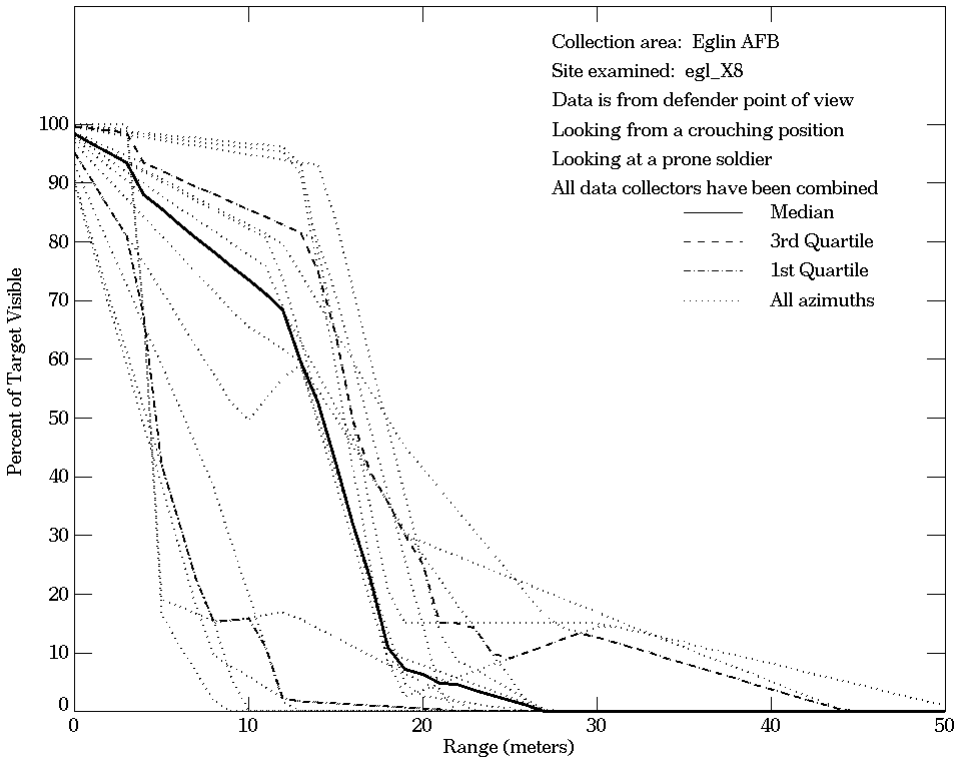

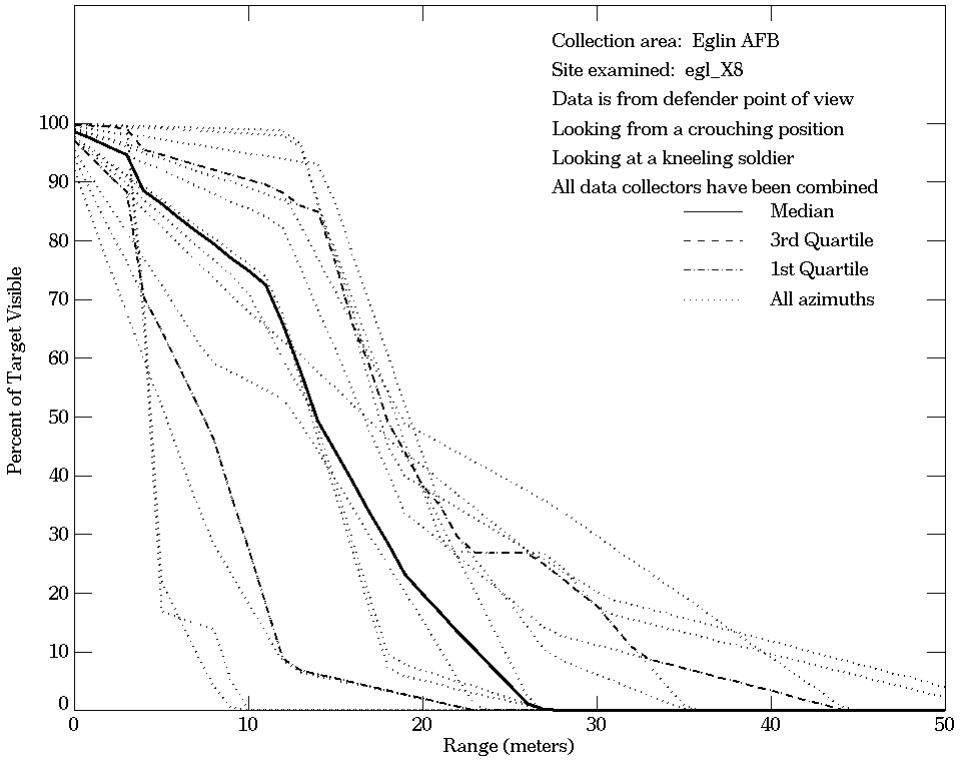

Figure E-29. Eglin AFB, From Defender Point of View, Site egl_X8 (Continued)

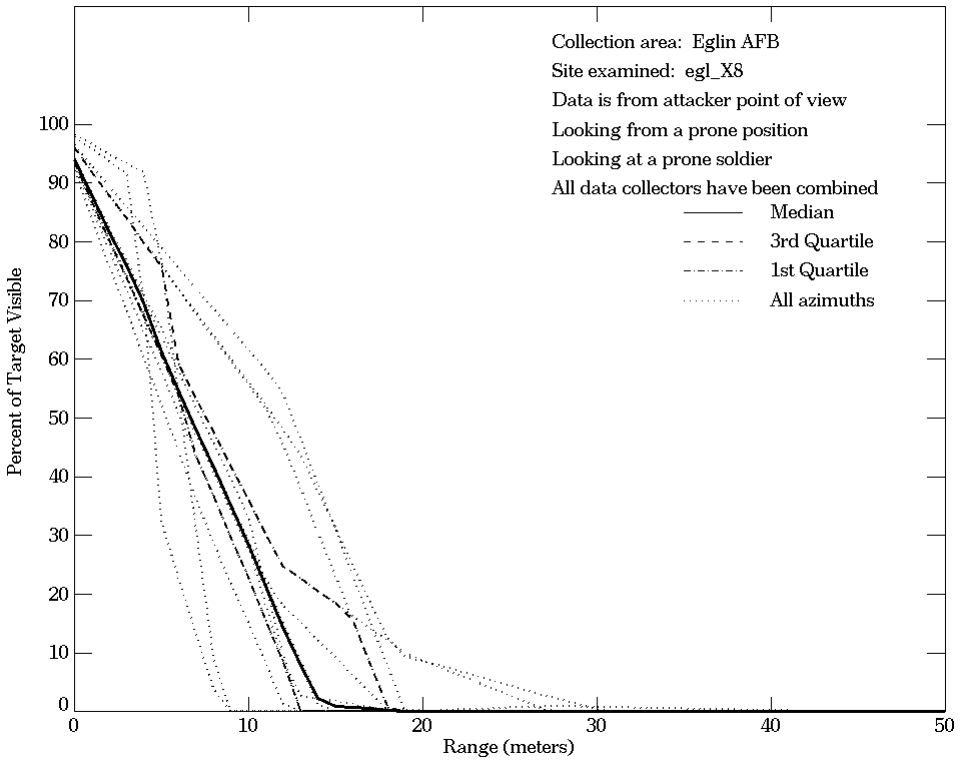

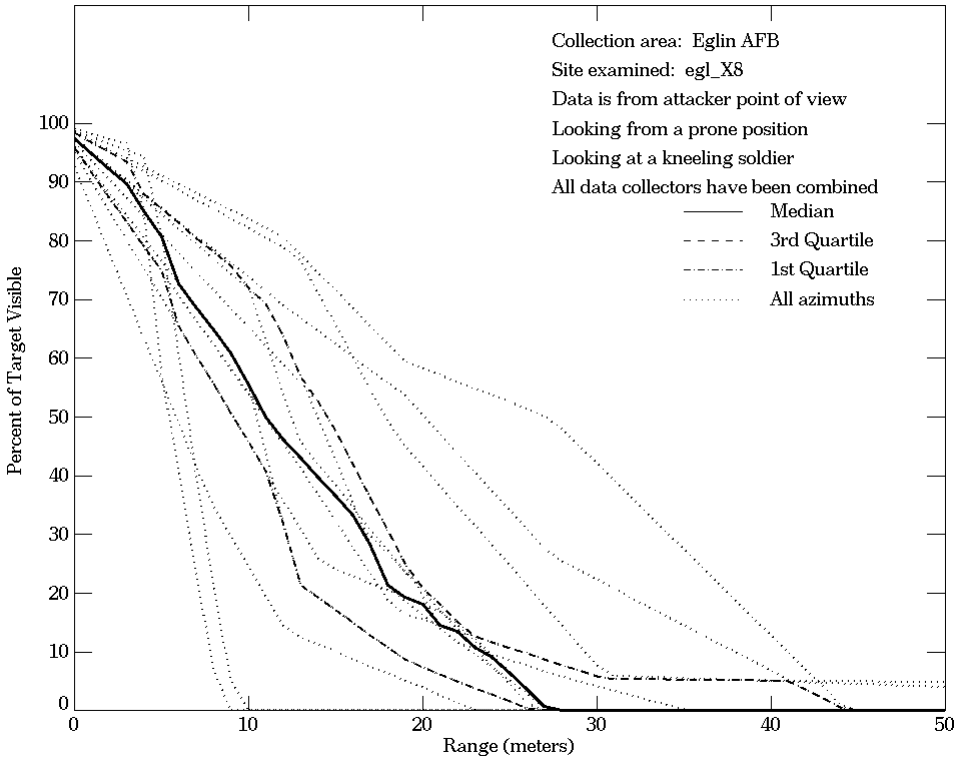

Figure E-30. Eglin AFB, From Attacker Point of View, Site egl_X8

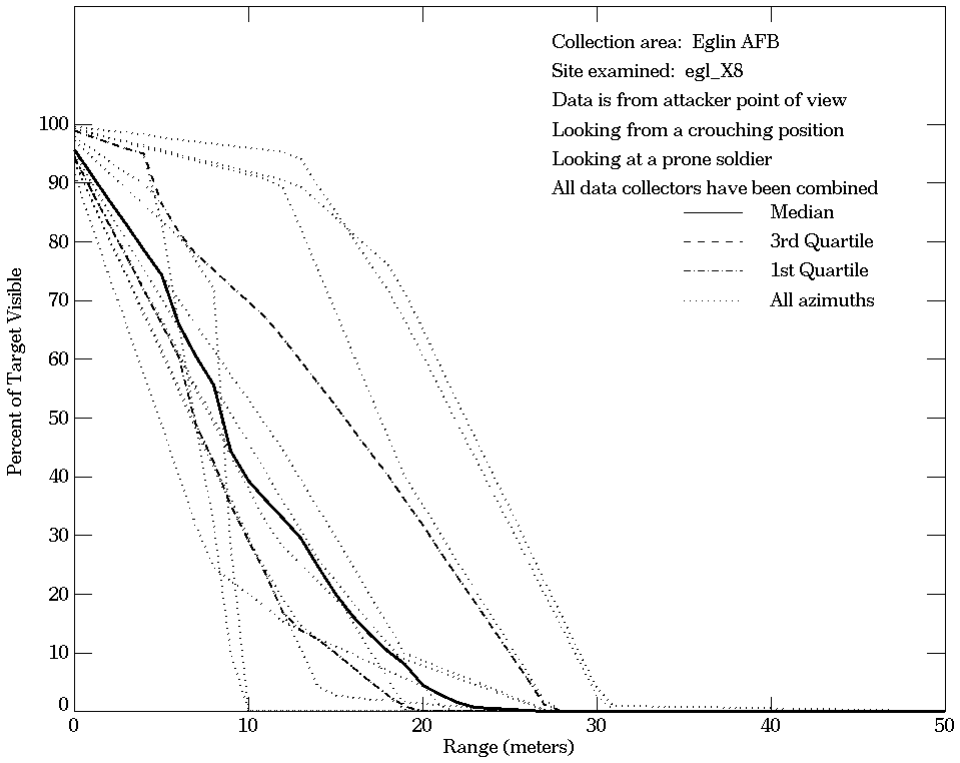

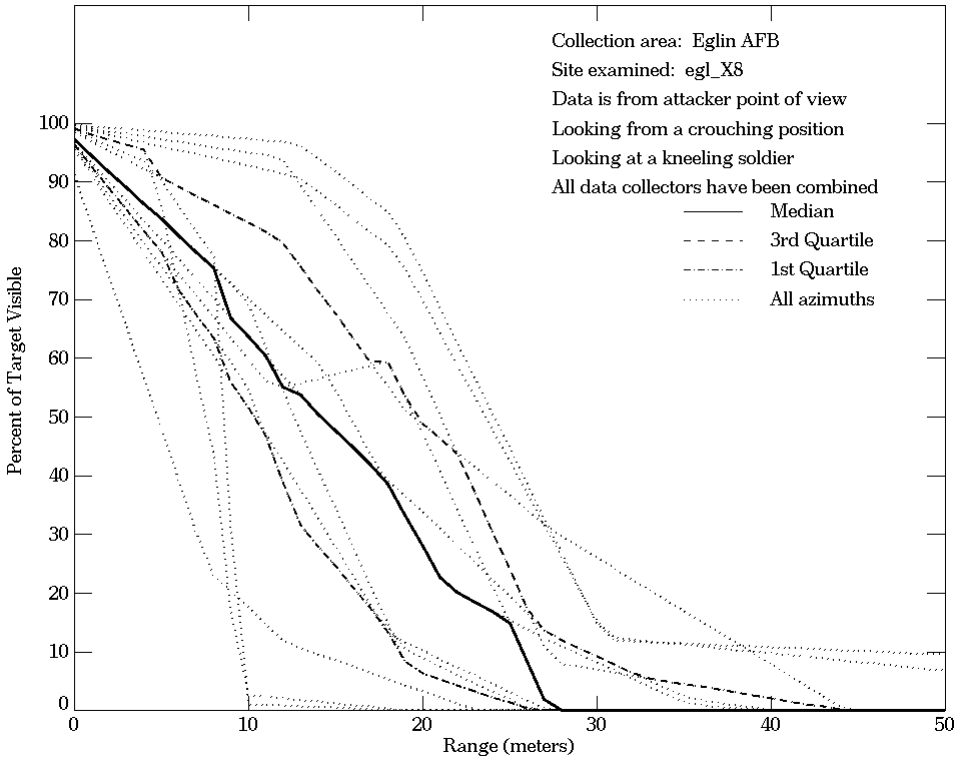

Figure E-30. Eglin AFB, From Attacker Point of View, Site egl_X8 (Continued)

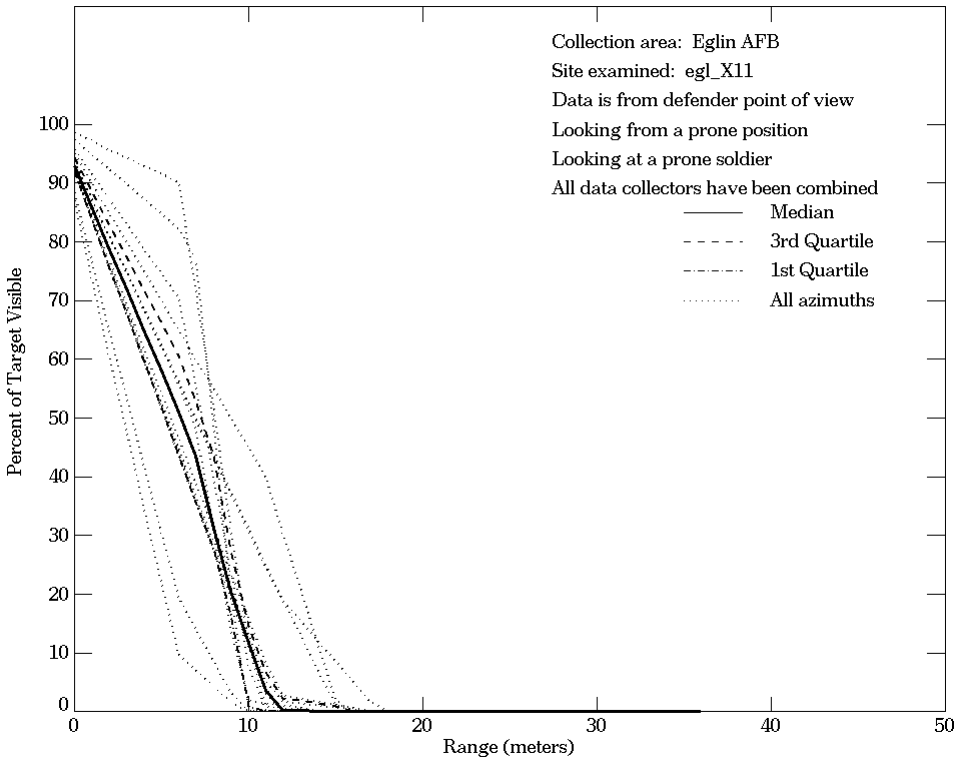

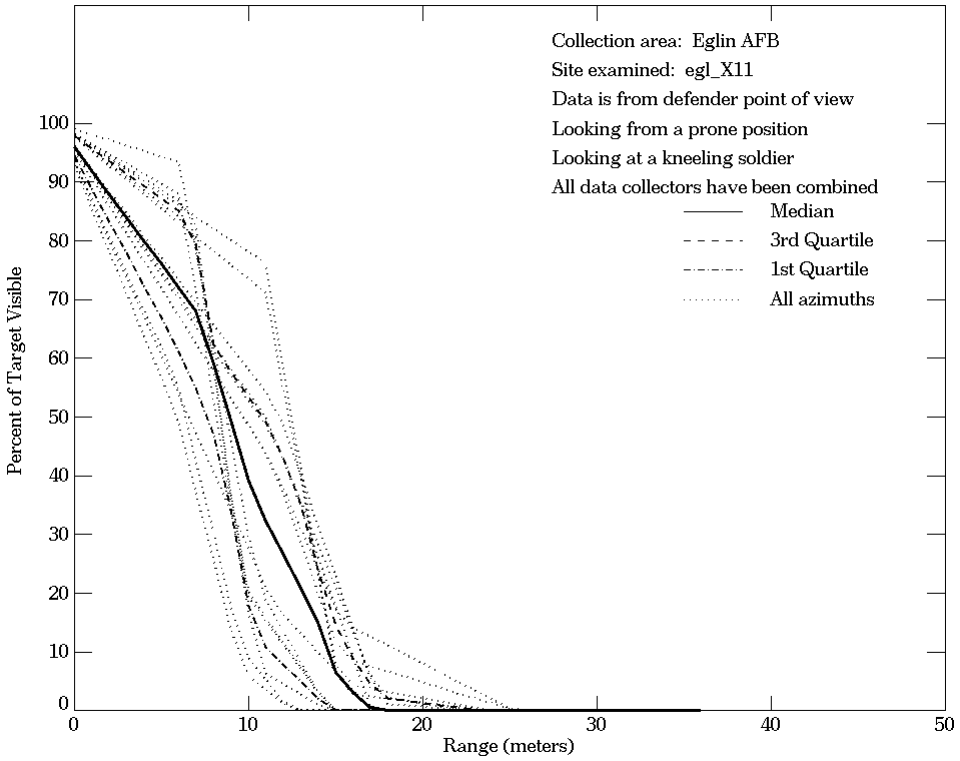

Figure E-31. Eglin AFB, From Defender Point of View, Site egl_X11

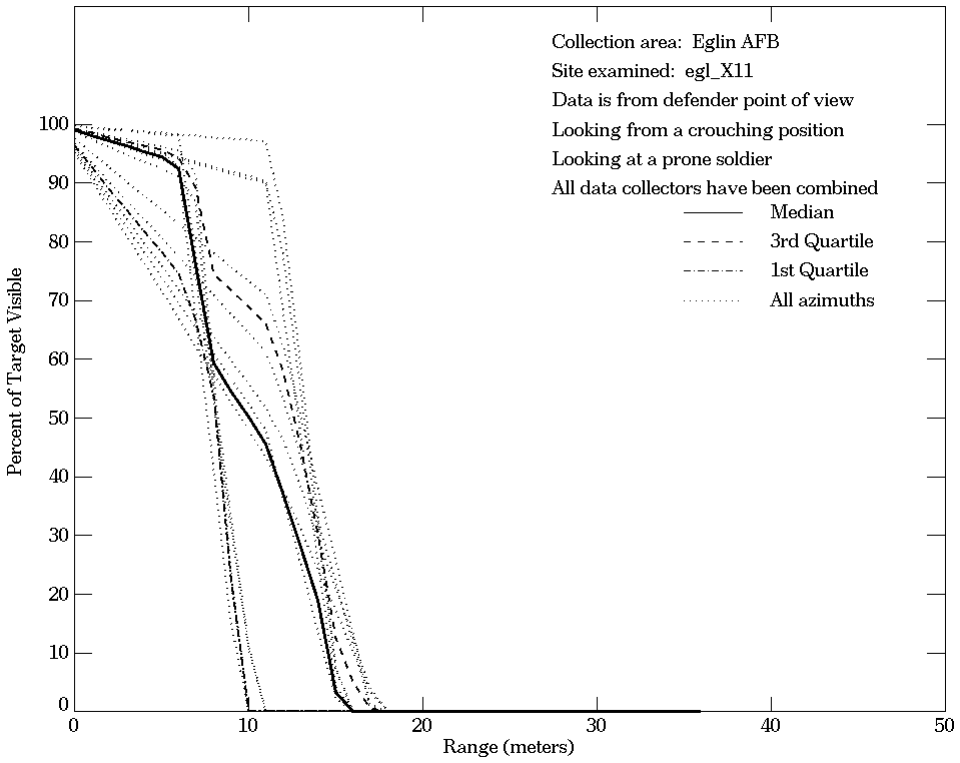

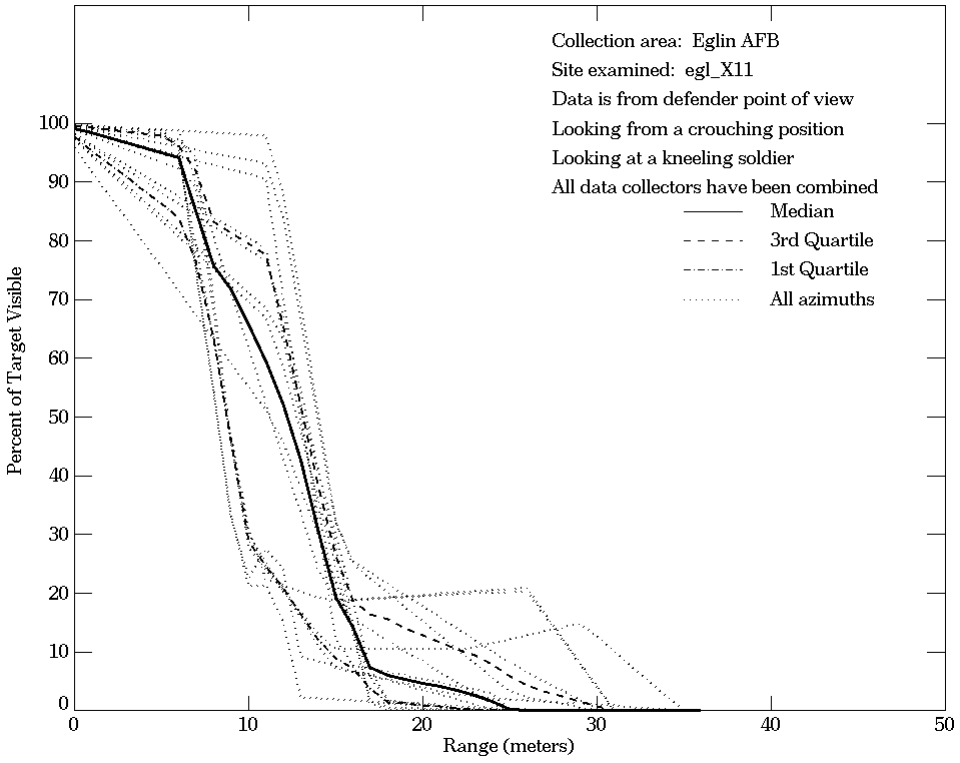

Figure E-31. Eglin AFB, From Defender Point of View, Site egl_X11 (Continued)

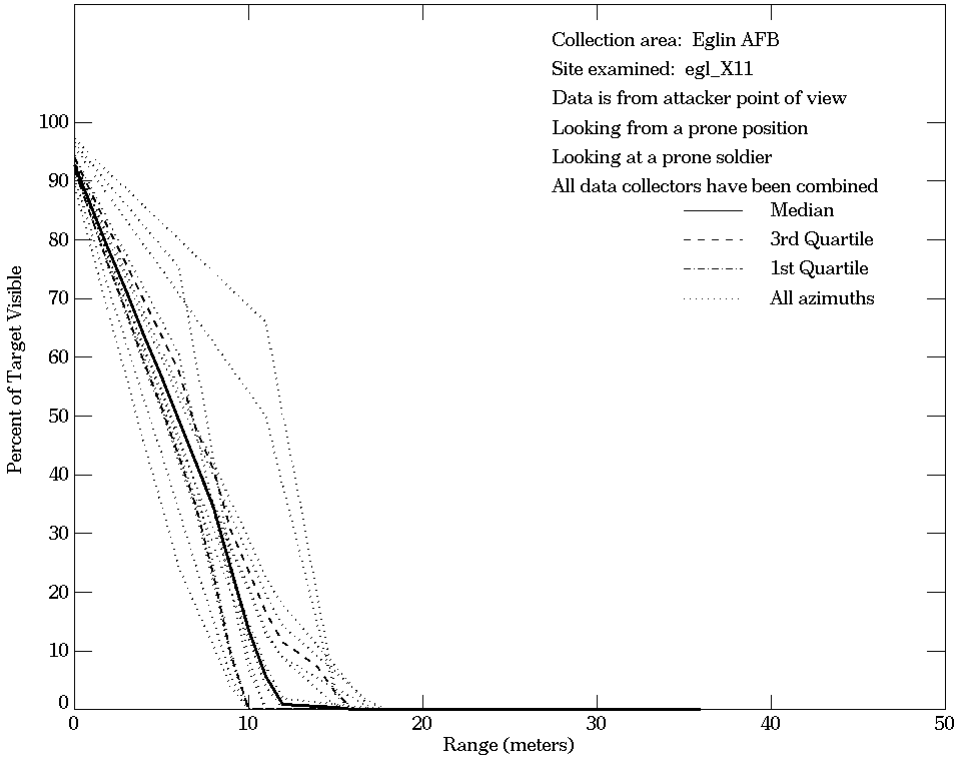

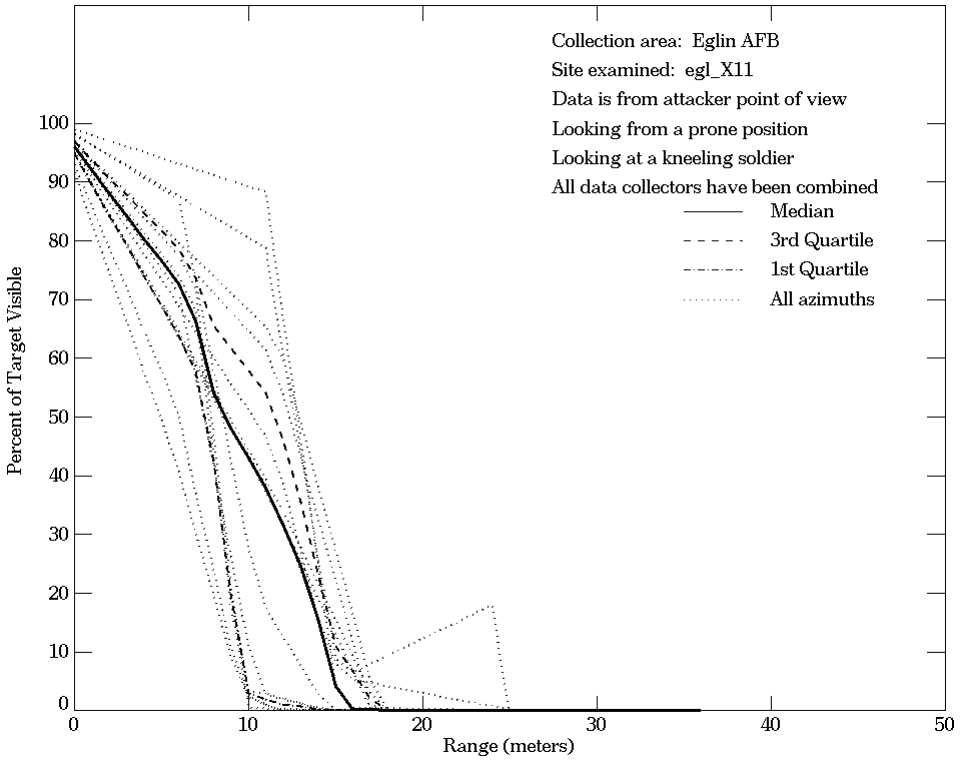

Figure E-32. Eglin AFB, From Attacker Point of View, Site egl_X11

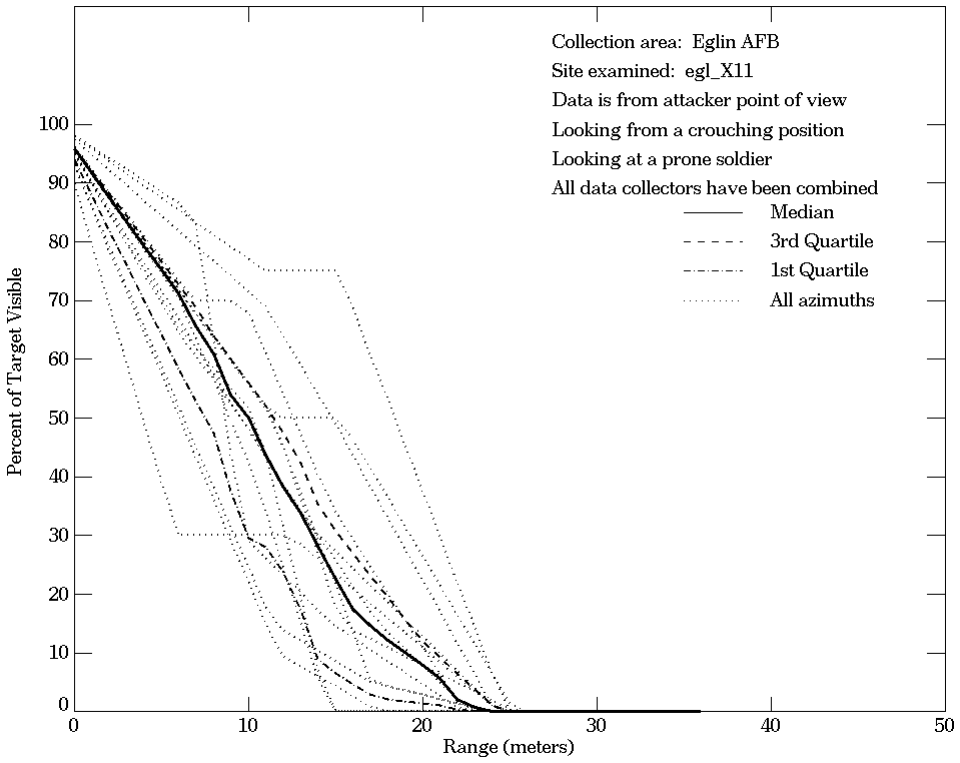

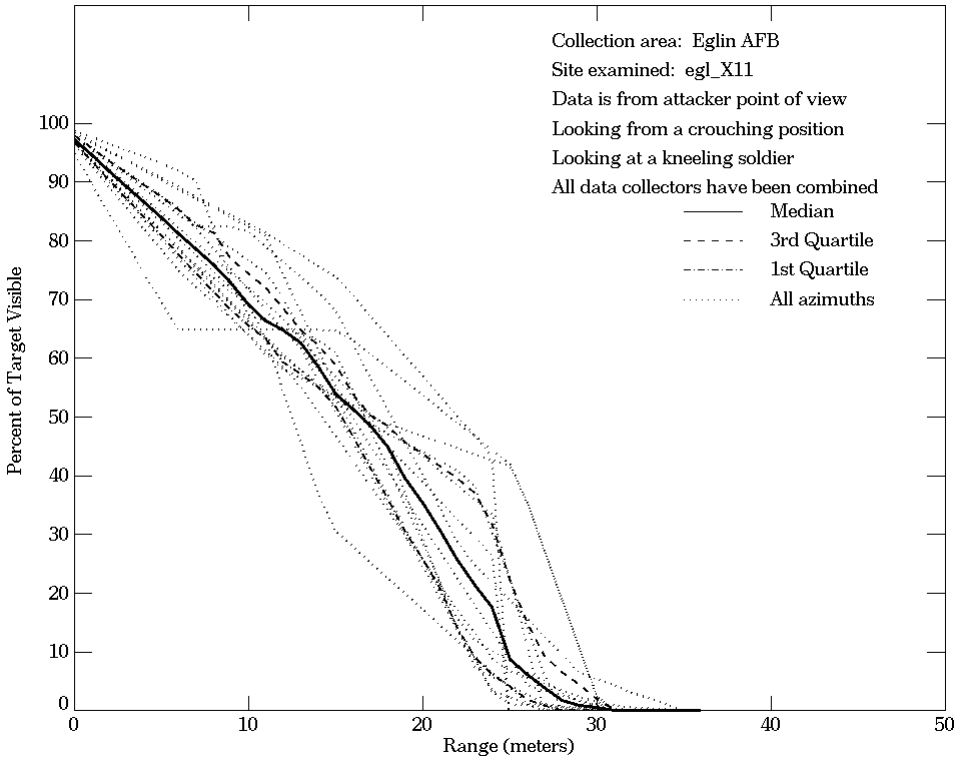

Figure E-32. Eglin AFB, From Attacker Point of View, Site egl_X11 (Continued)

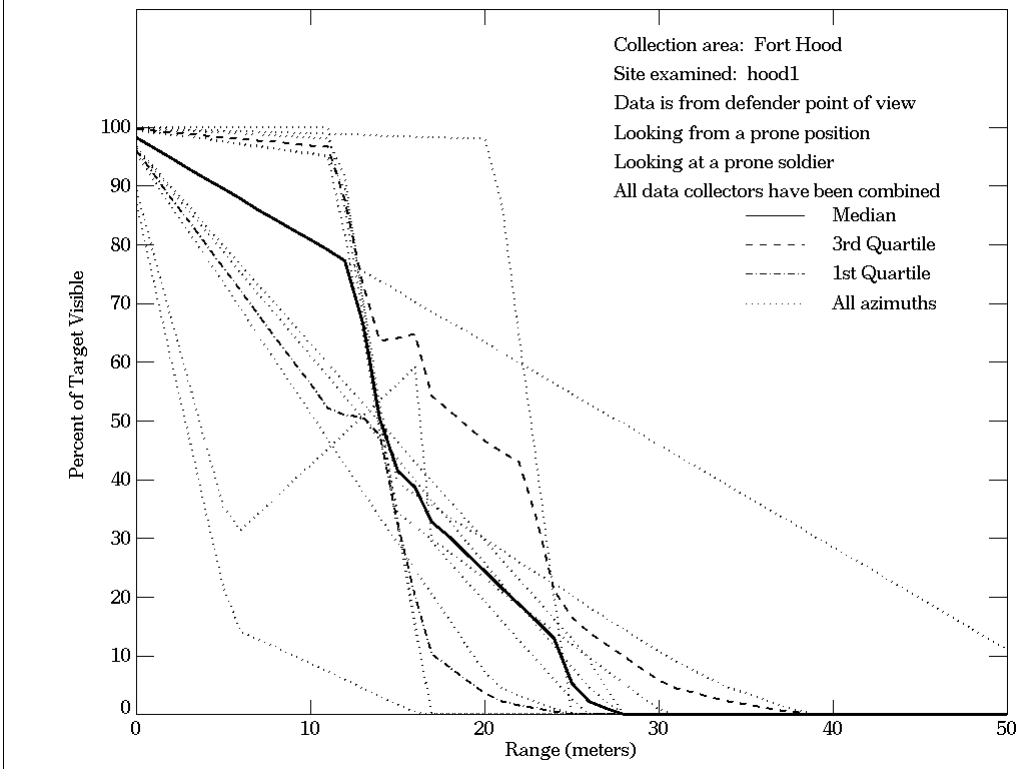

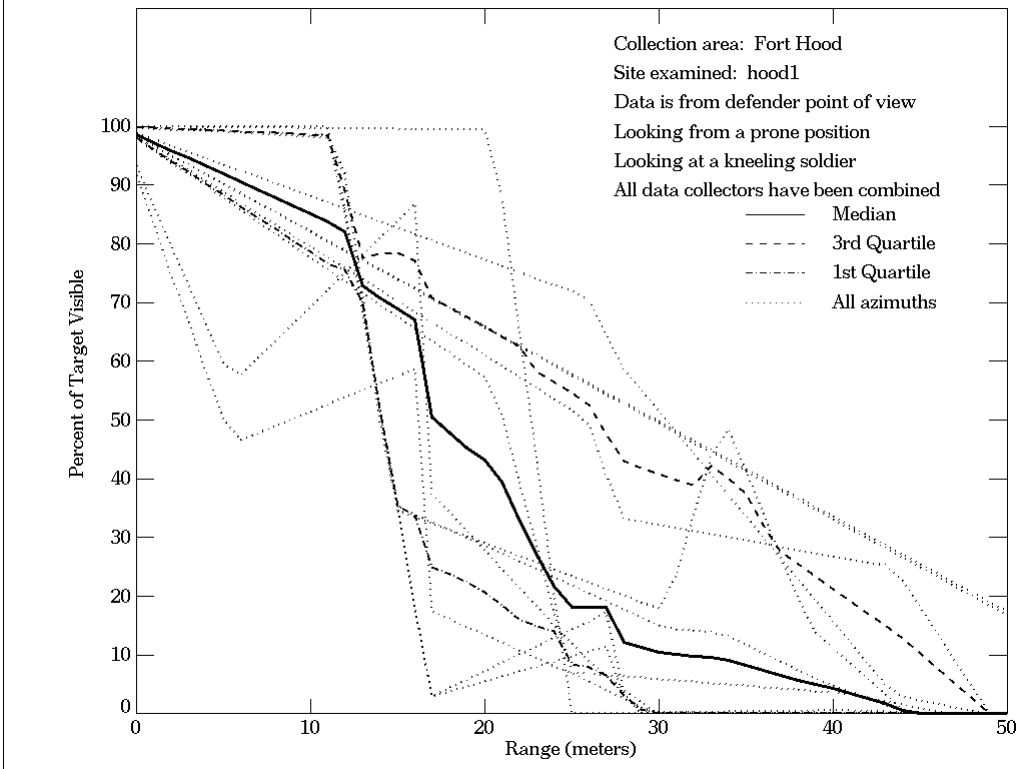

Figure E-33. Fort Hood, From Defender Point of View, Site hood1

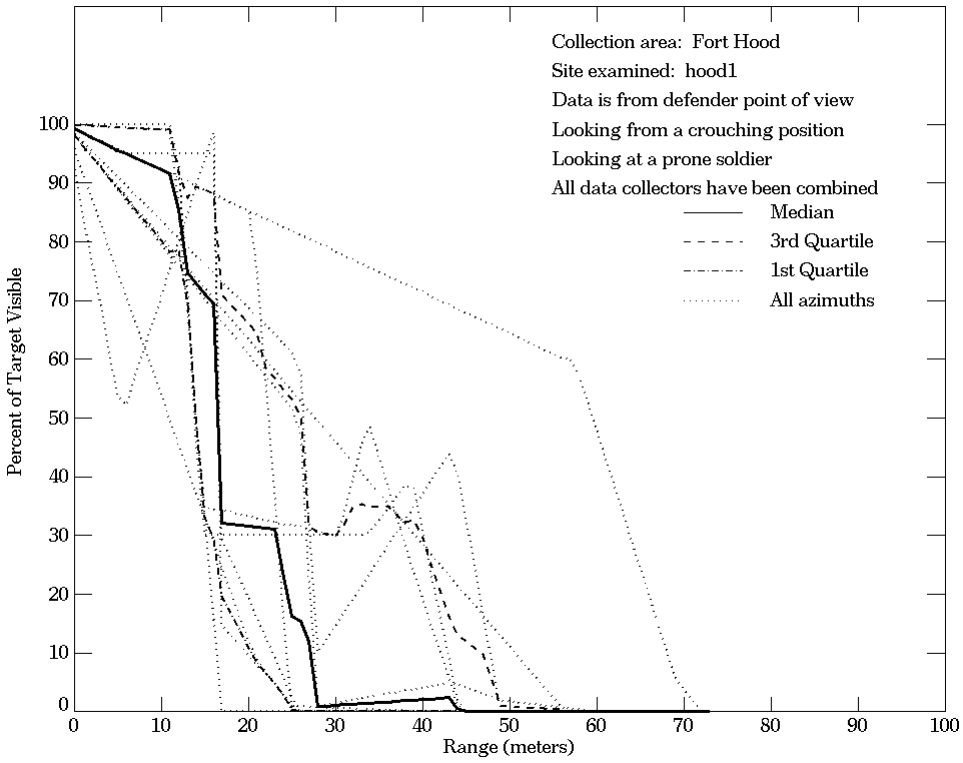

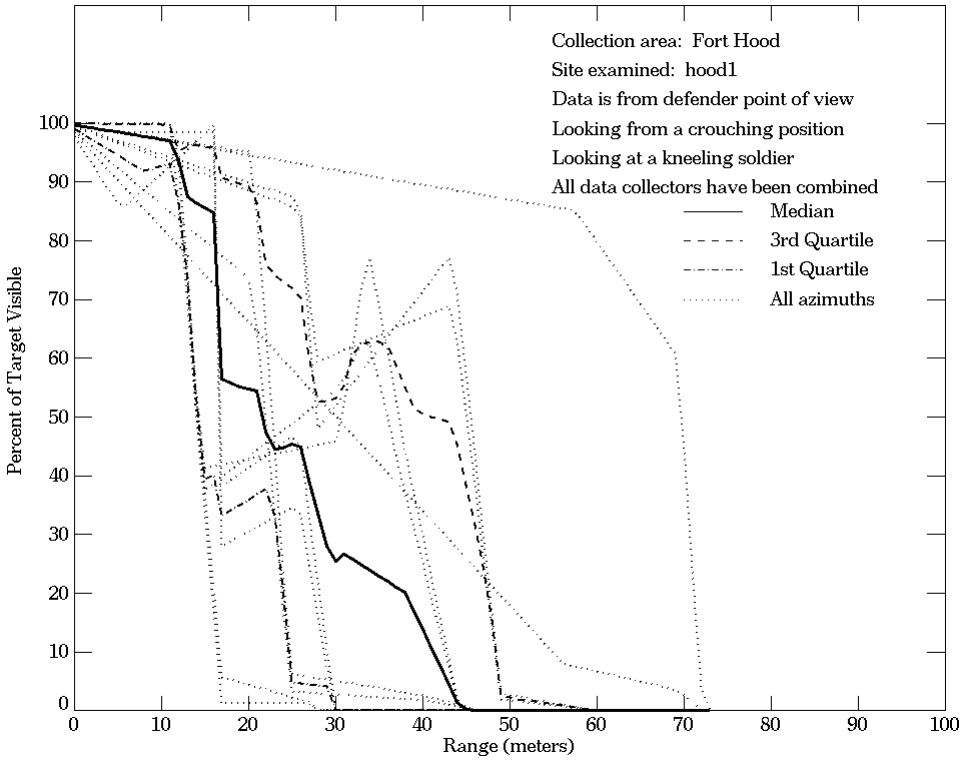

Figure E-33. Fort Hood, From Defender Point of View, Site hood1 (Continued)

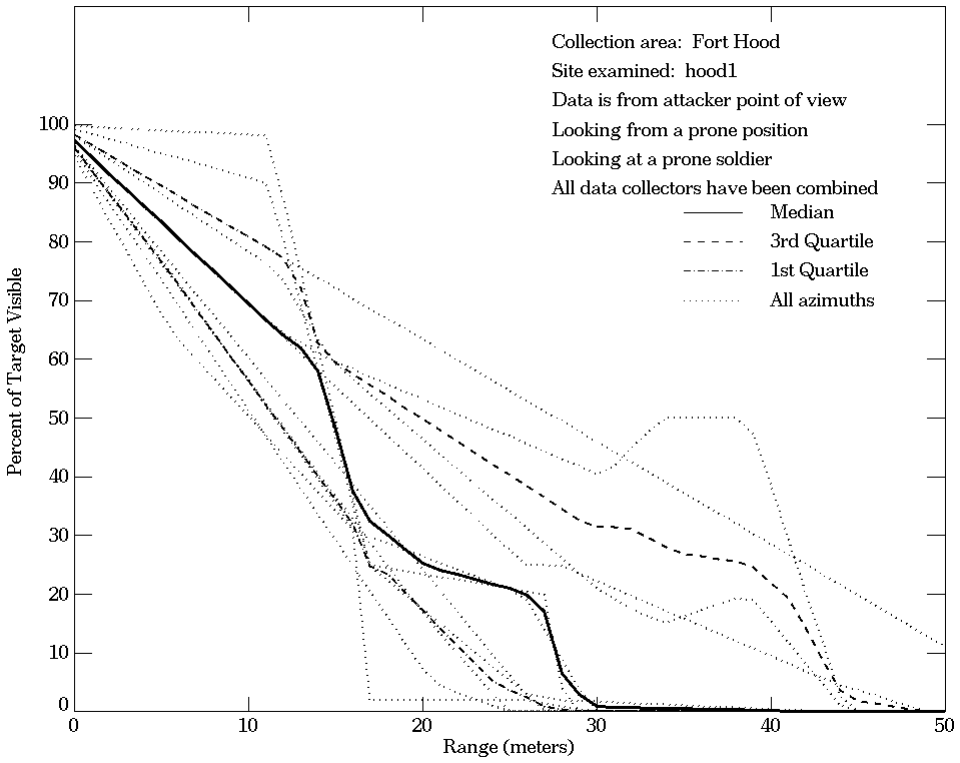

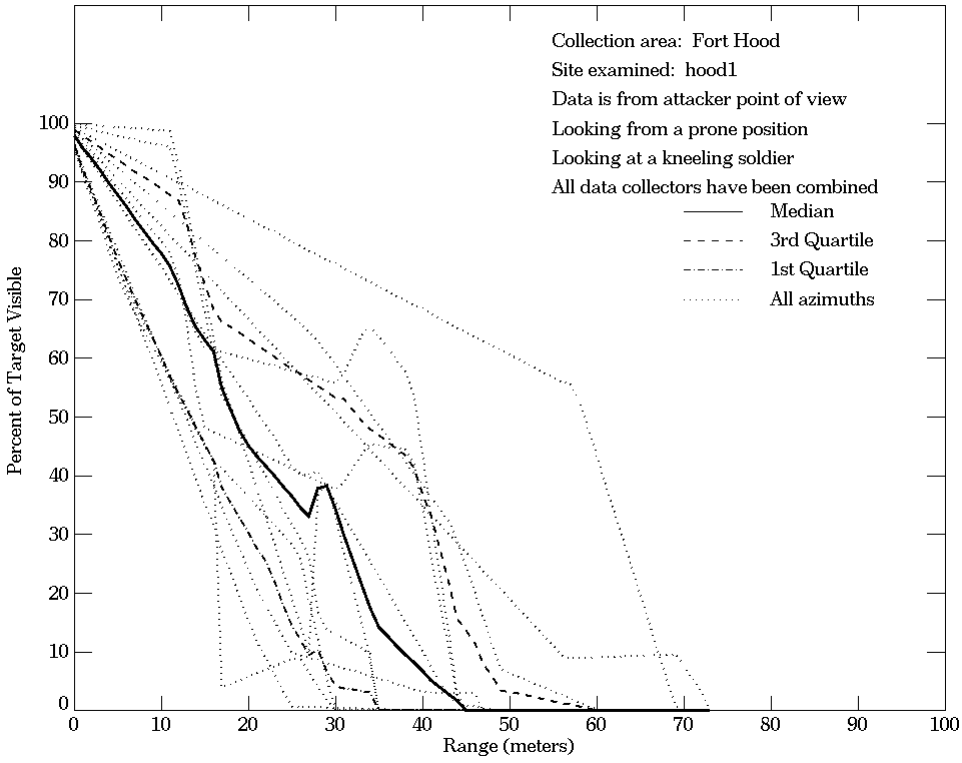

Figure E-34. Fort Hood, From Attacker Point of View, Site hood1

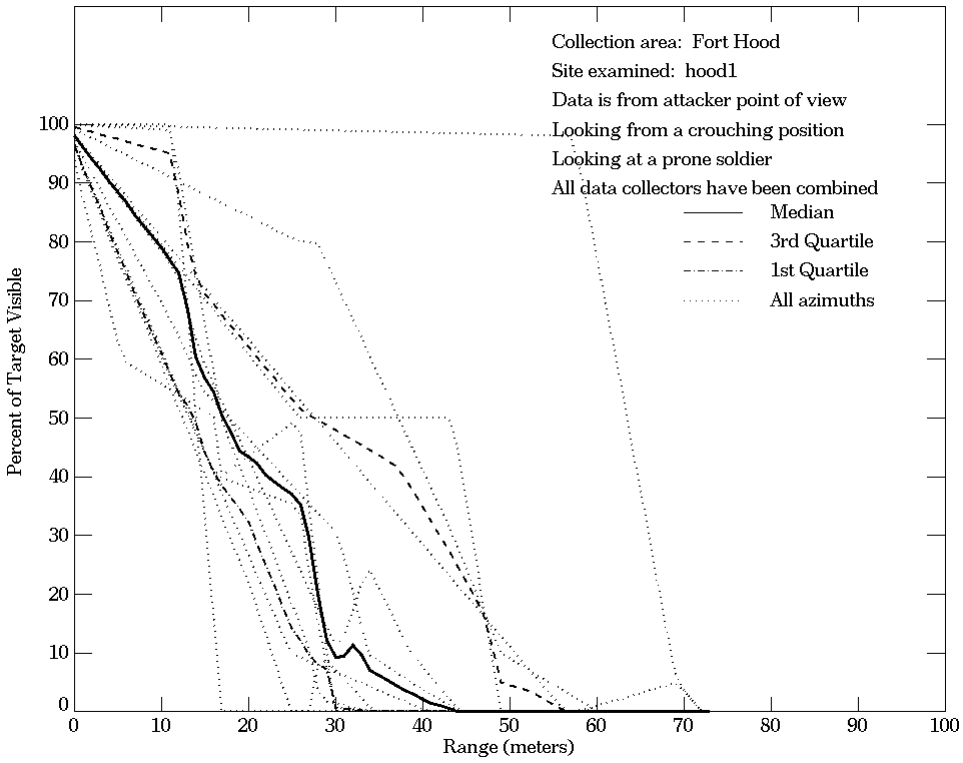

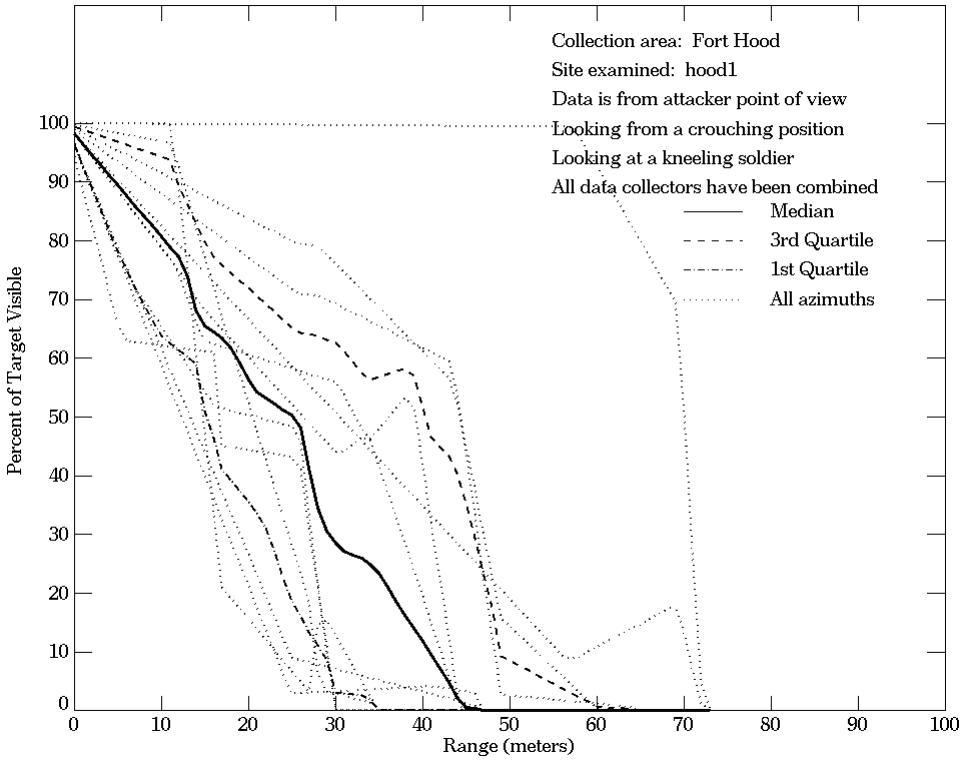

Figure E-34. Fort Hood, From Attacker Point of View, Site hood1 (Continued)

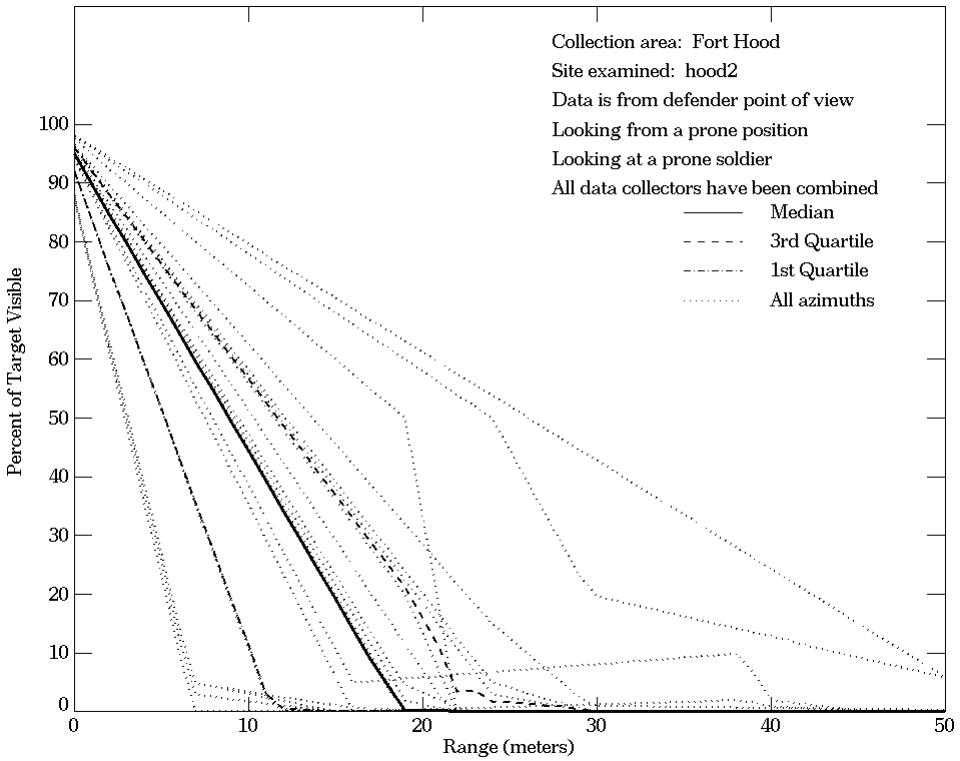

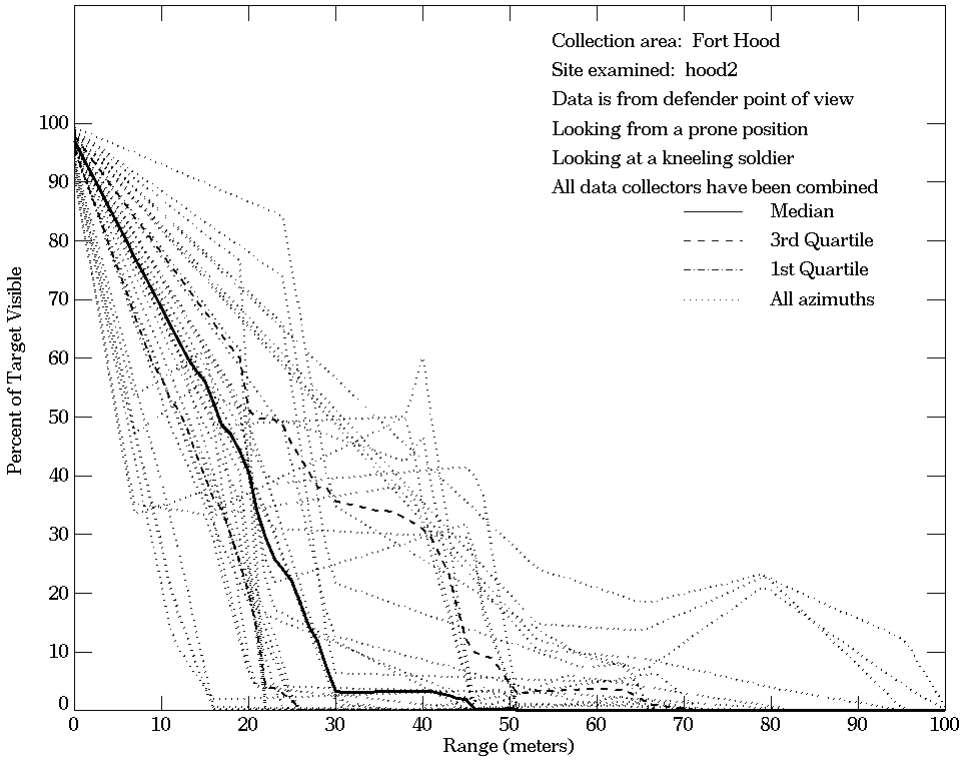

Figure E-35. Fort Hood, From Defender Point of View, Site hood2

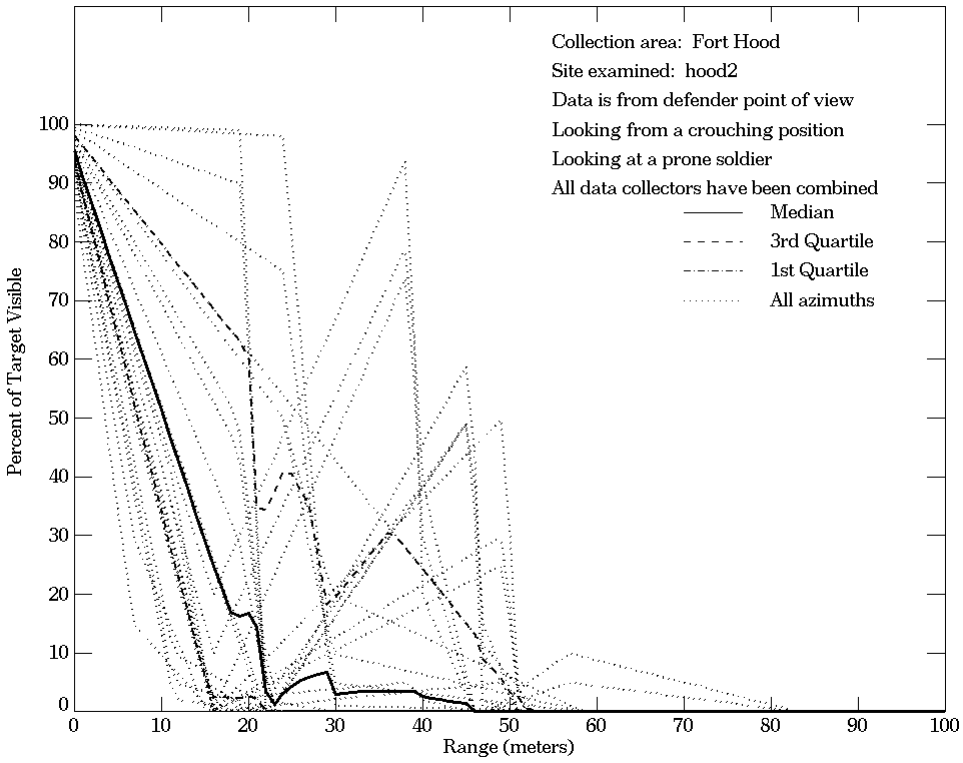

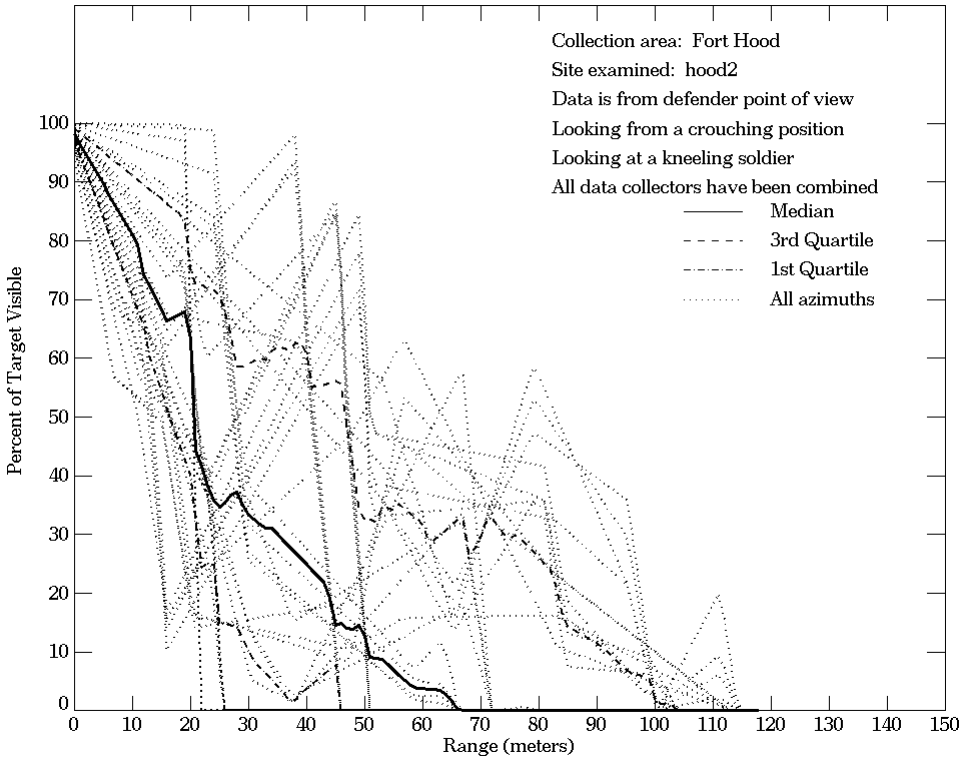

Figure E-35. Fort Hood, From Defender Point of View, Site hood2 (Continued)

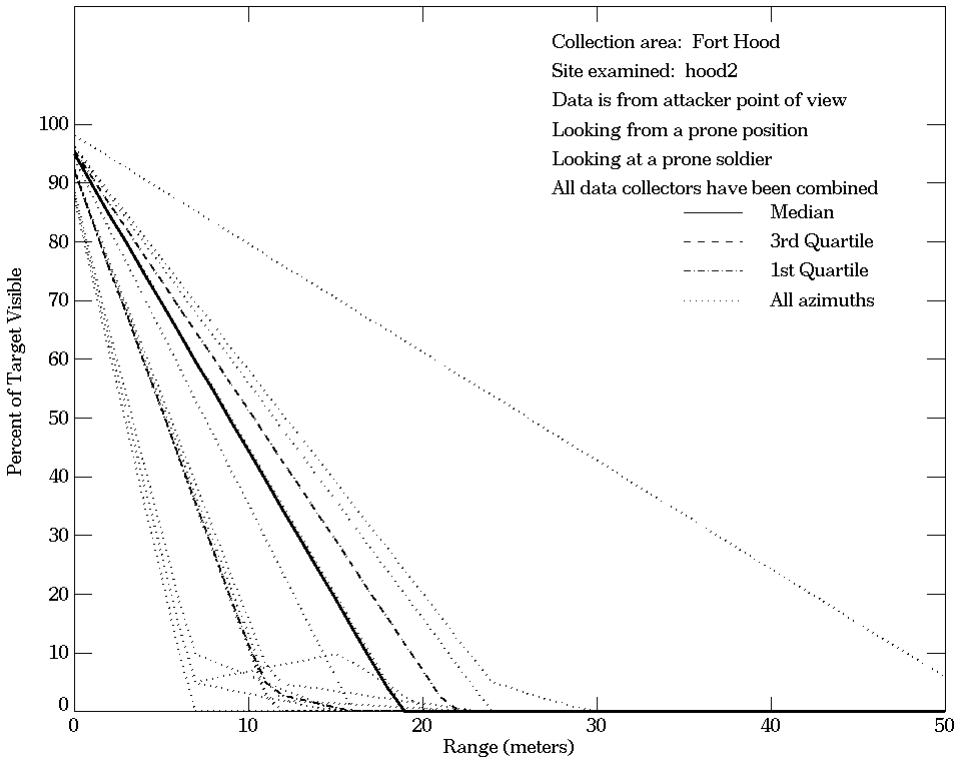

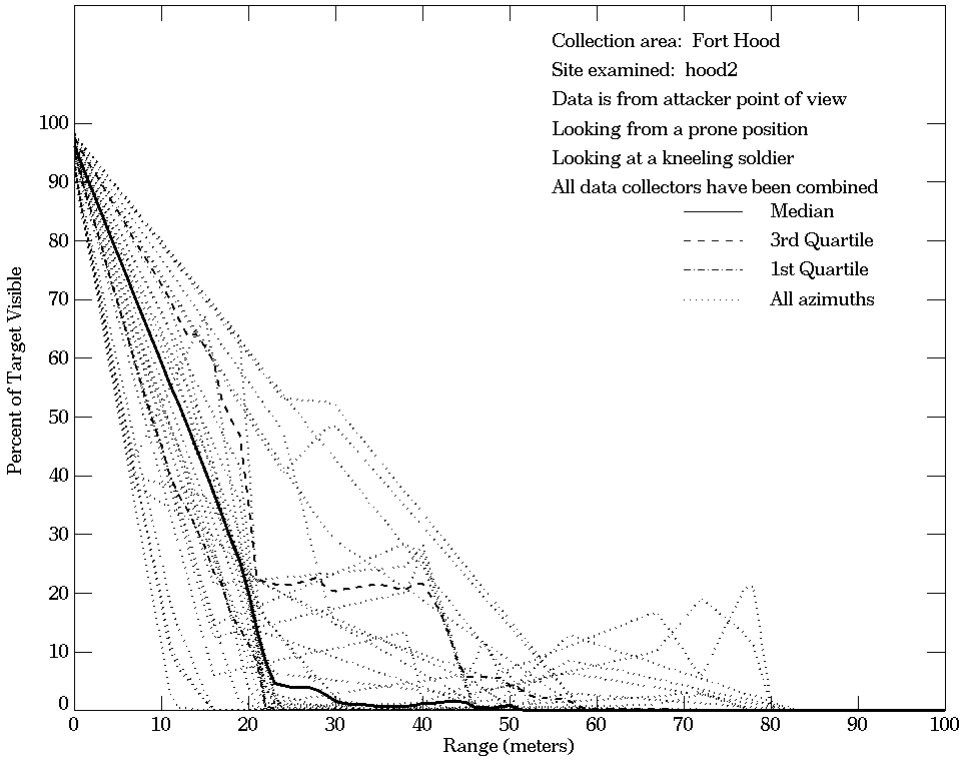

Figure E-36. Fort Hood, From Attacker Point of View, Site hood2

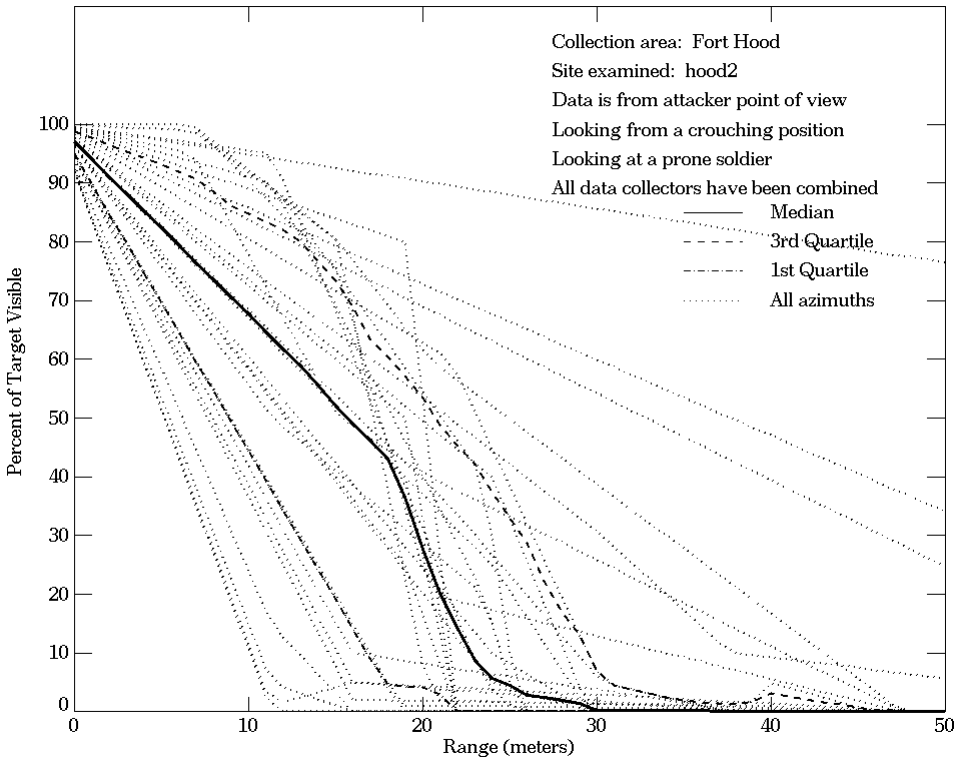

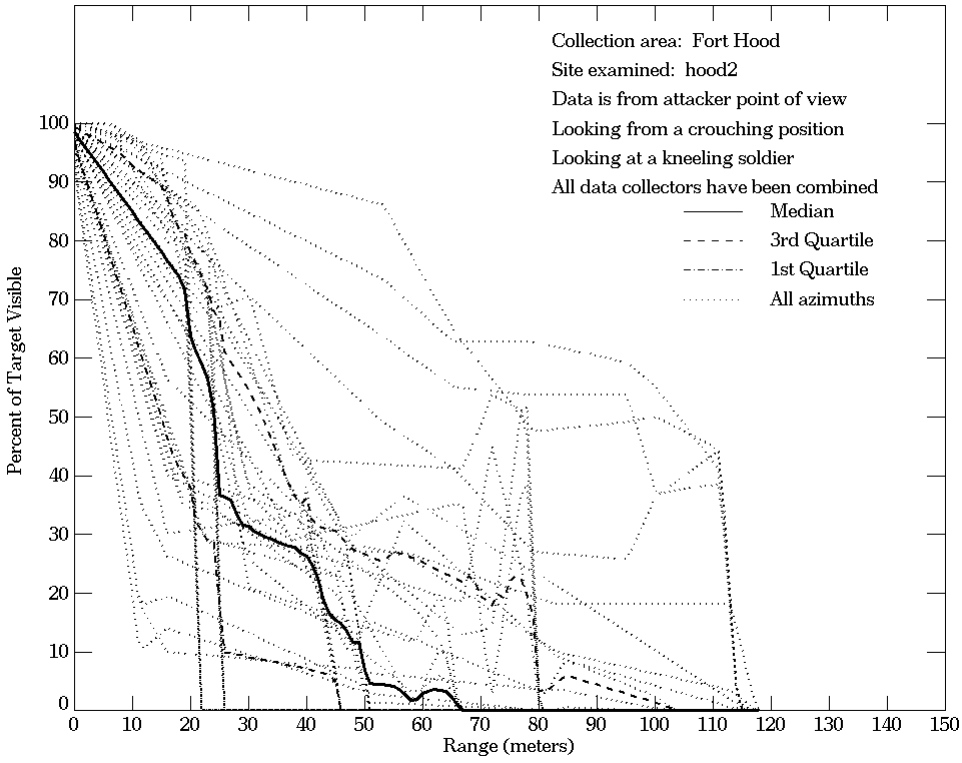

Figure E-36. Fort Hood, From Attacker Point of View, Site hood2 (Continued)

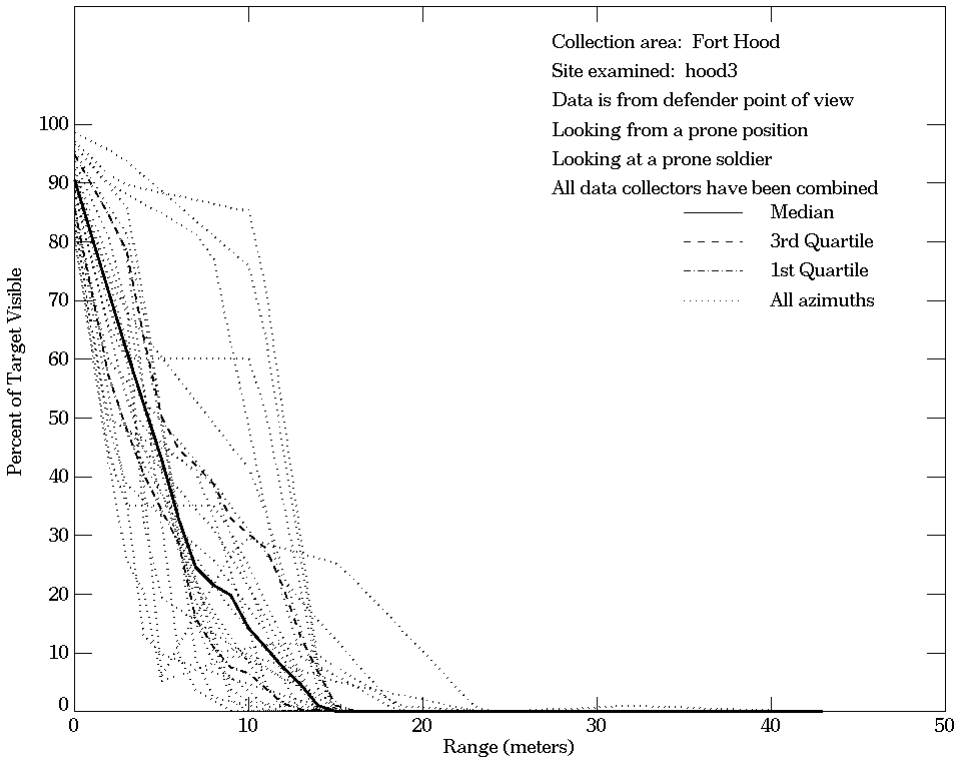

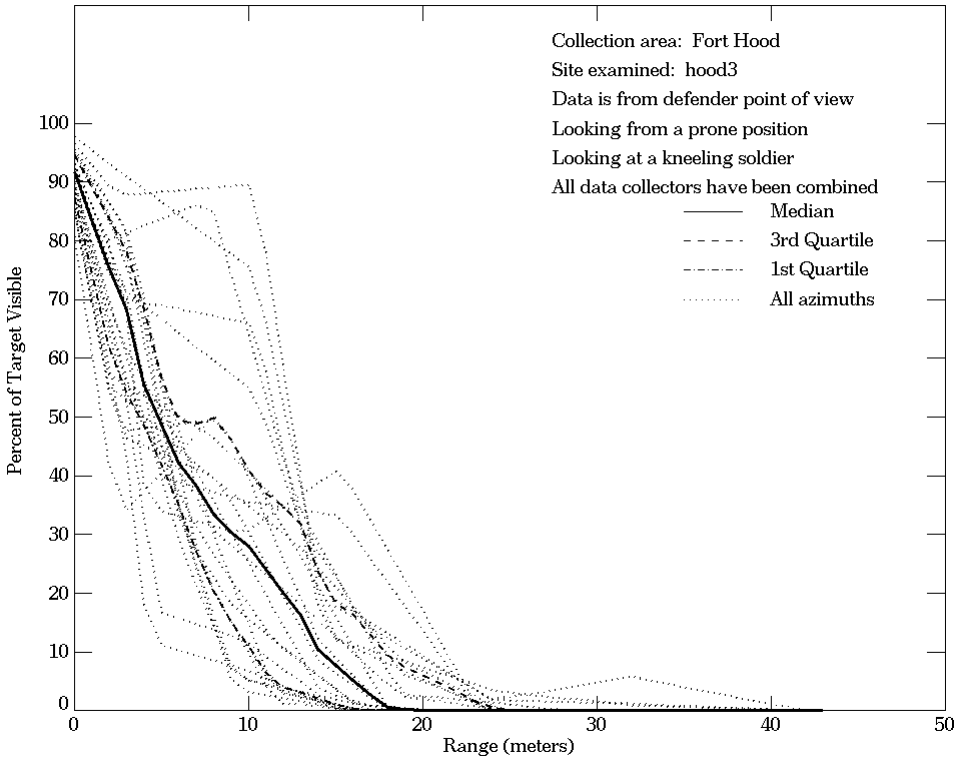

Figure E-37. Fort Hood, From Defender Point of View, Site hood3

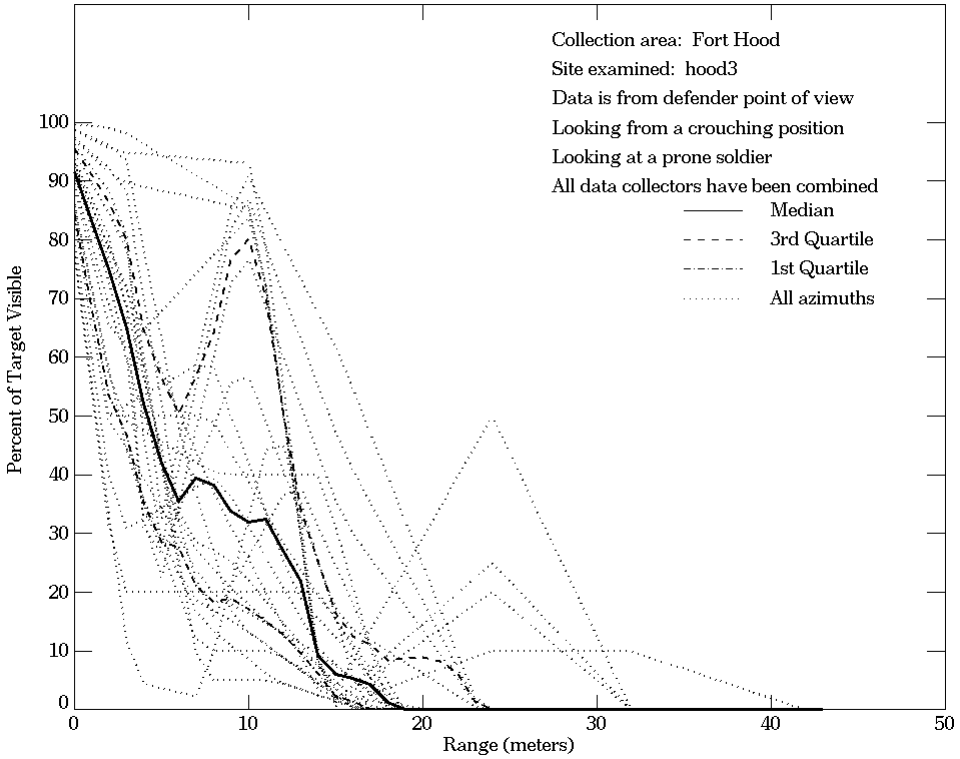

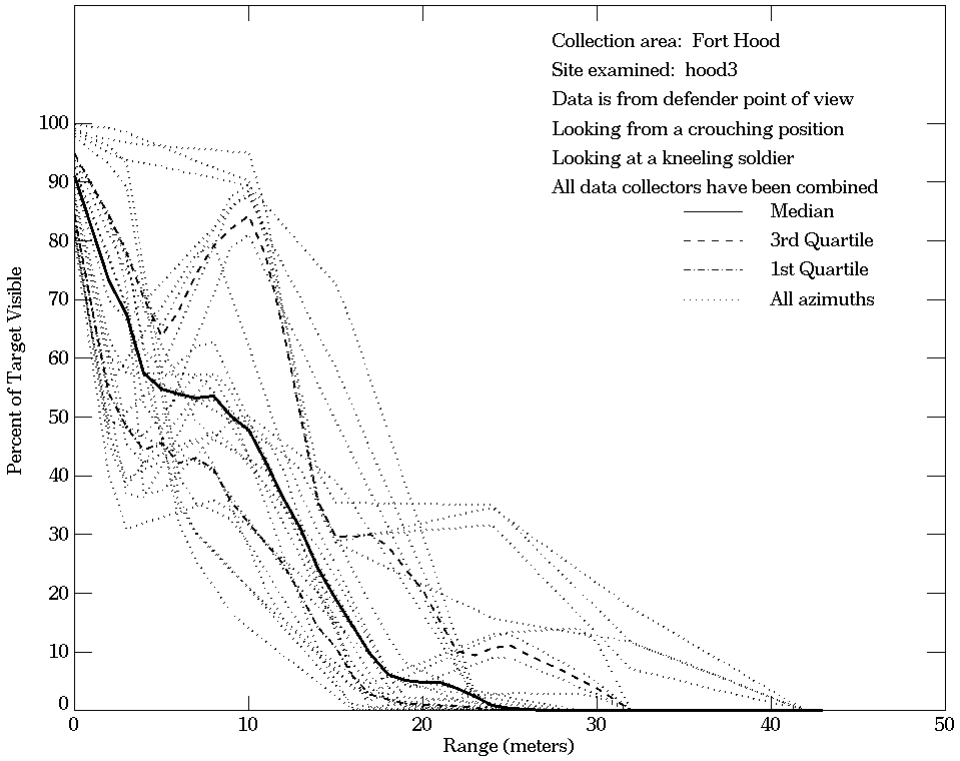

Figure E-37. Fort Hood, From Defender Point of View, Site hood3 (Continued)

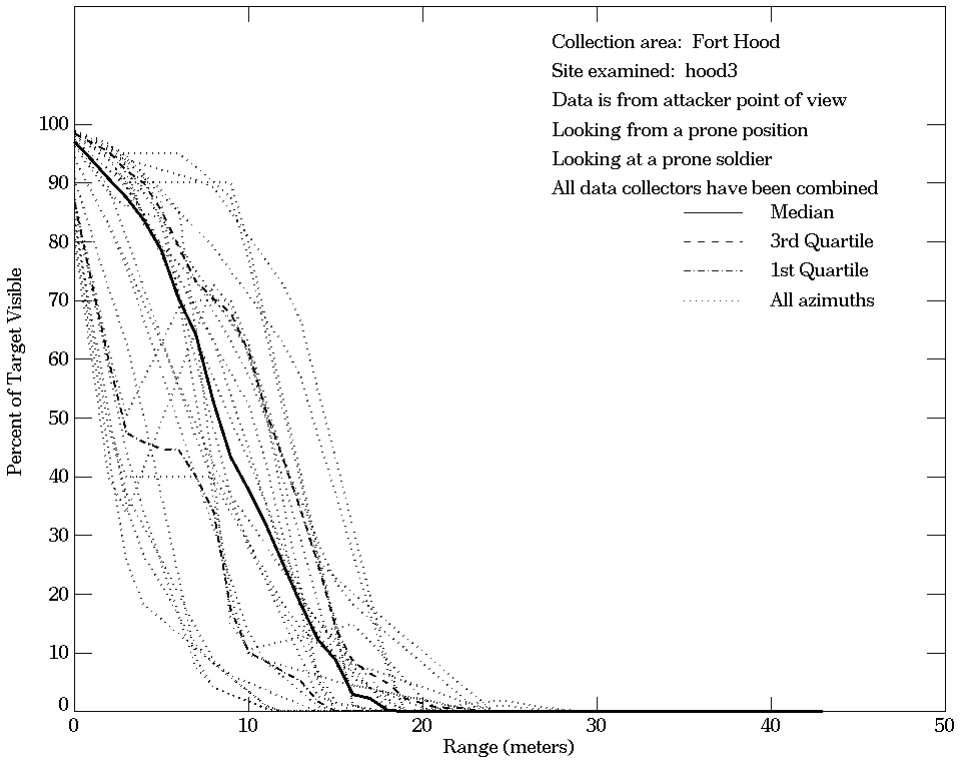

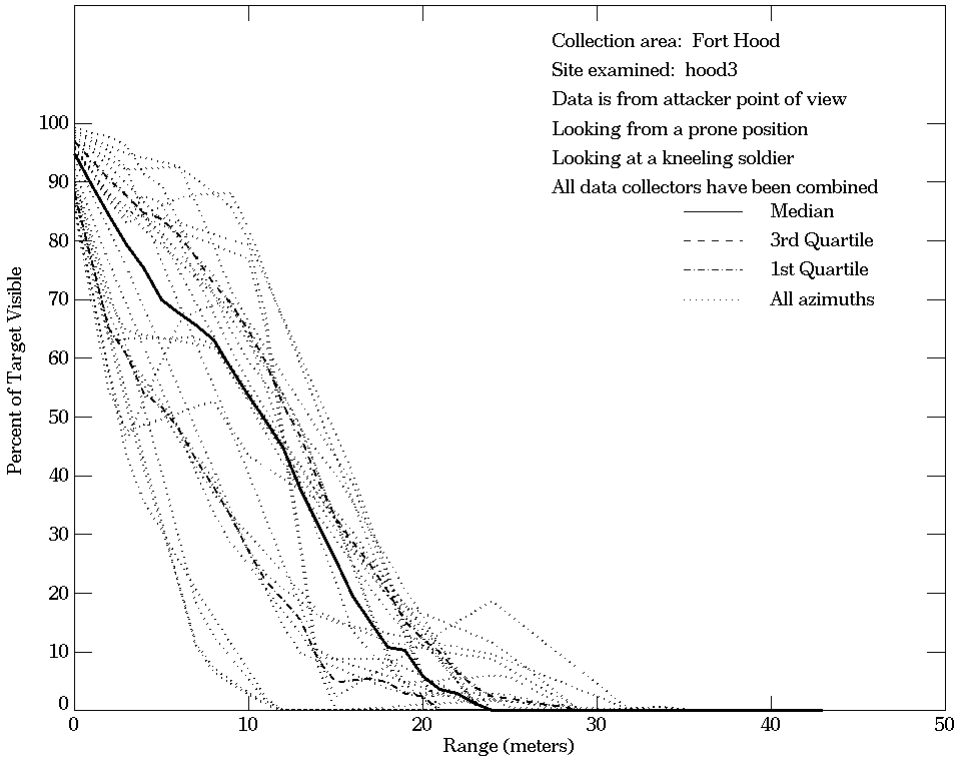

Figure E-38. Fort Hood, From Attacker Point of View, Site hood3

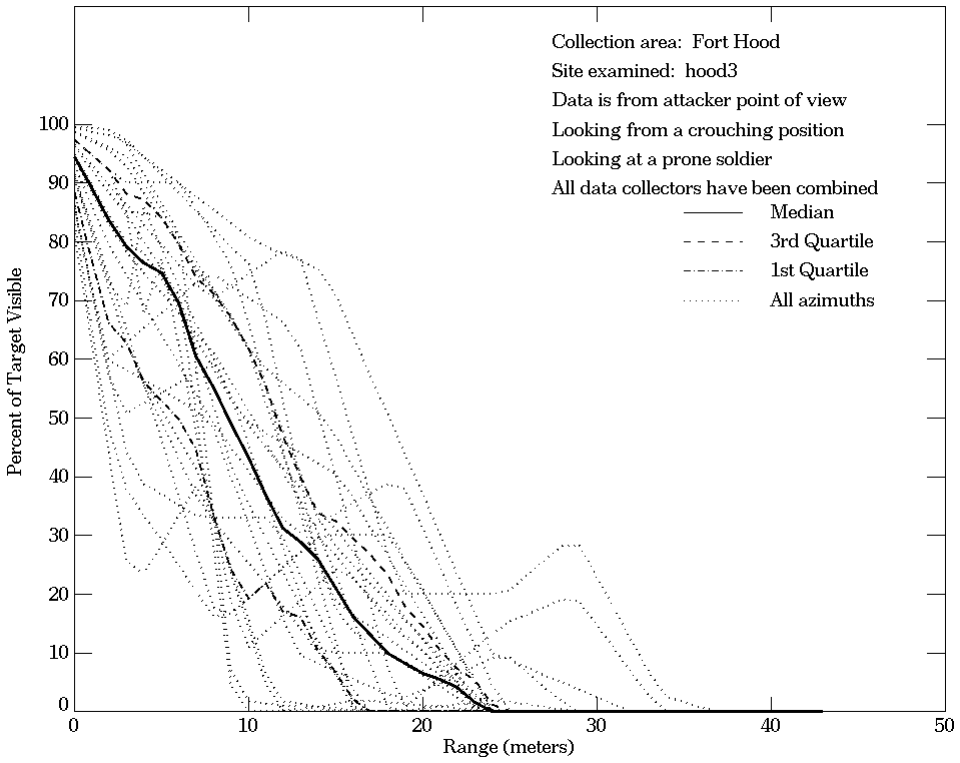

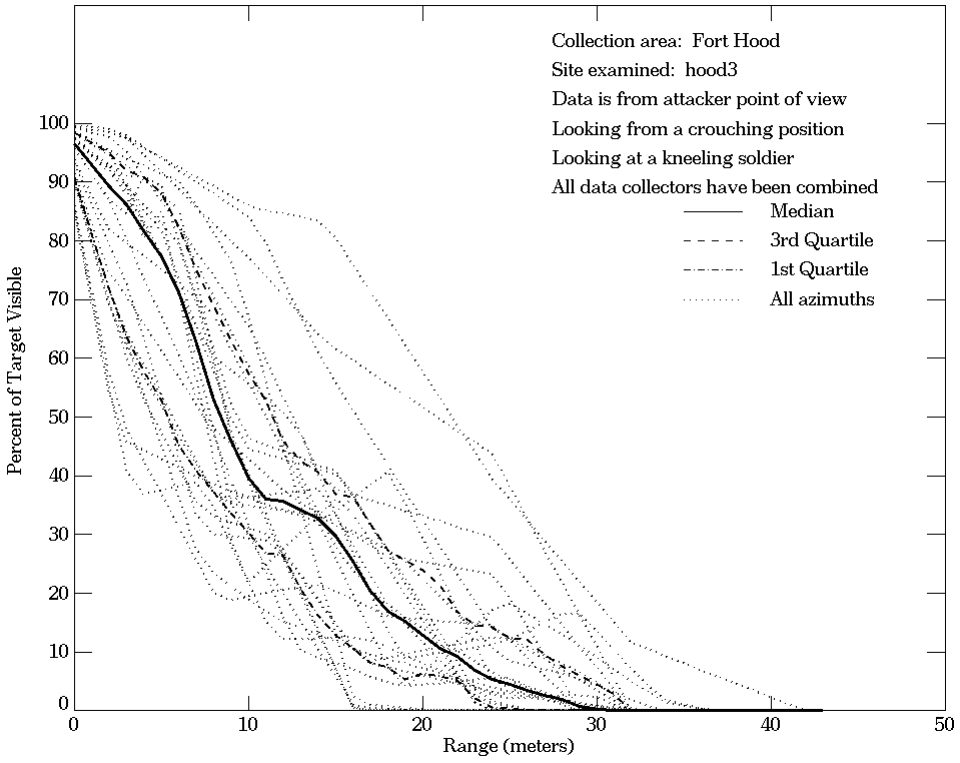

Figure E-38. Fort Hood, From Attacker Point of View, Site hood3 (Continued)

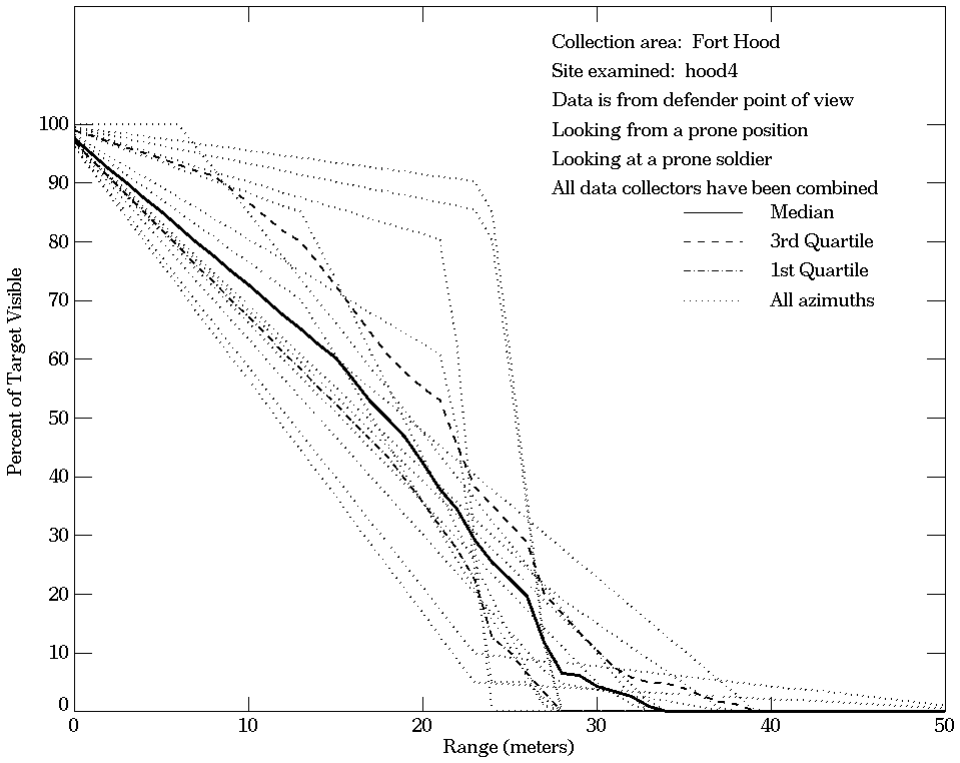

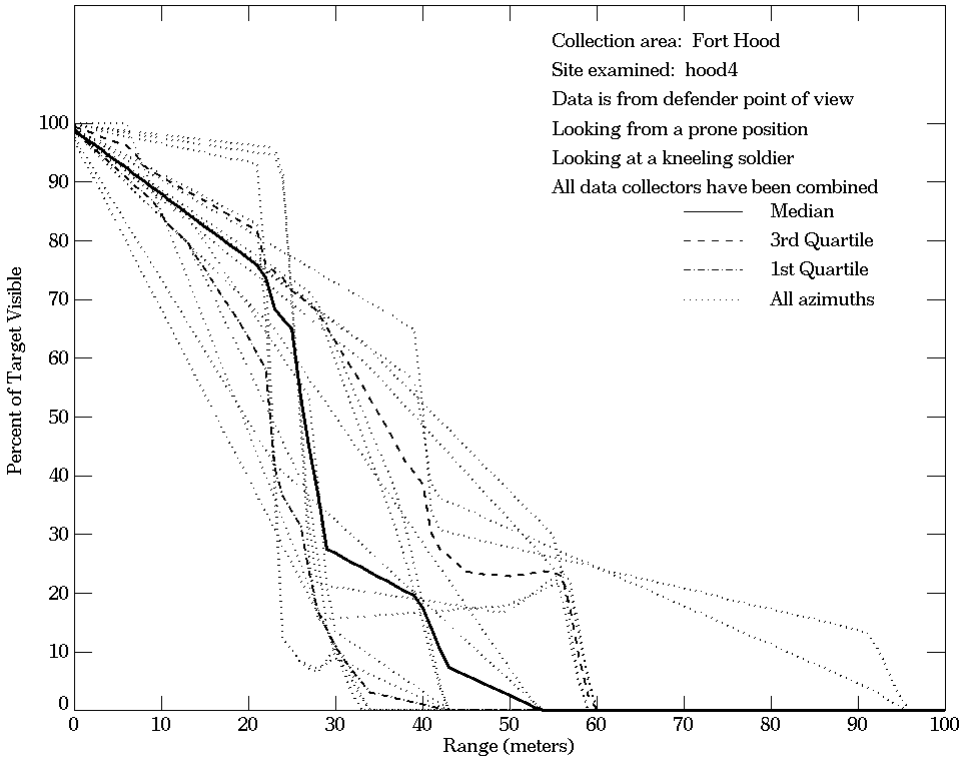

Figure E-39. Fort Hood, From Defender Point of View, Site hood4

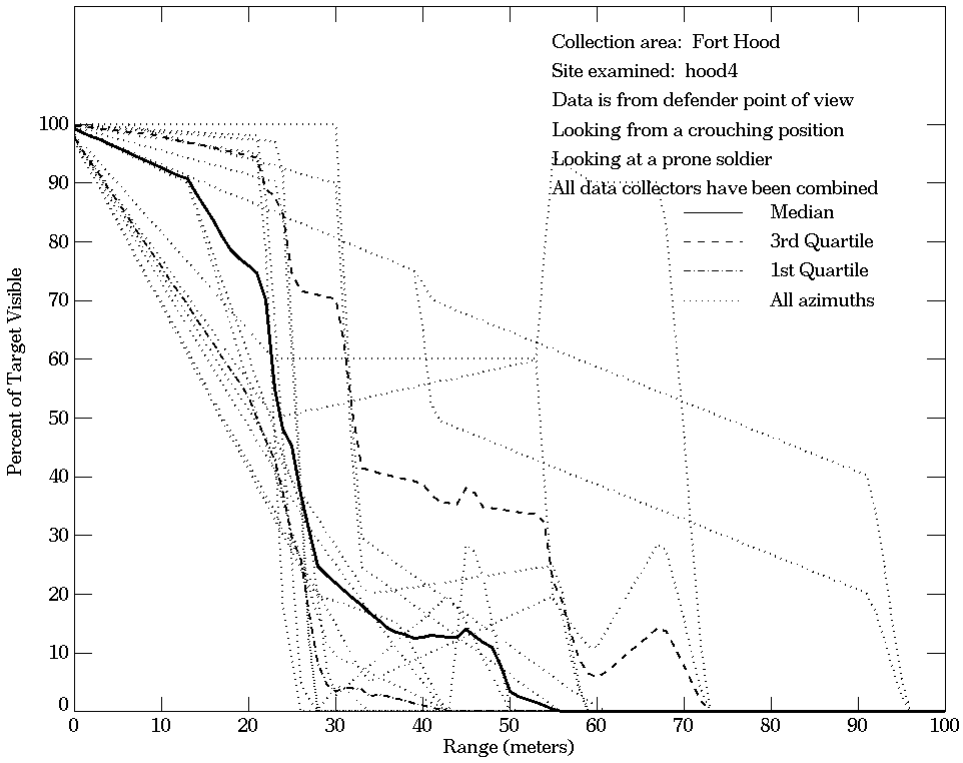

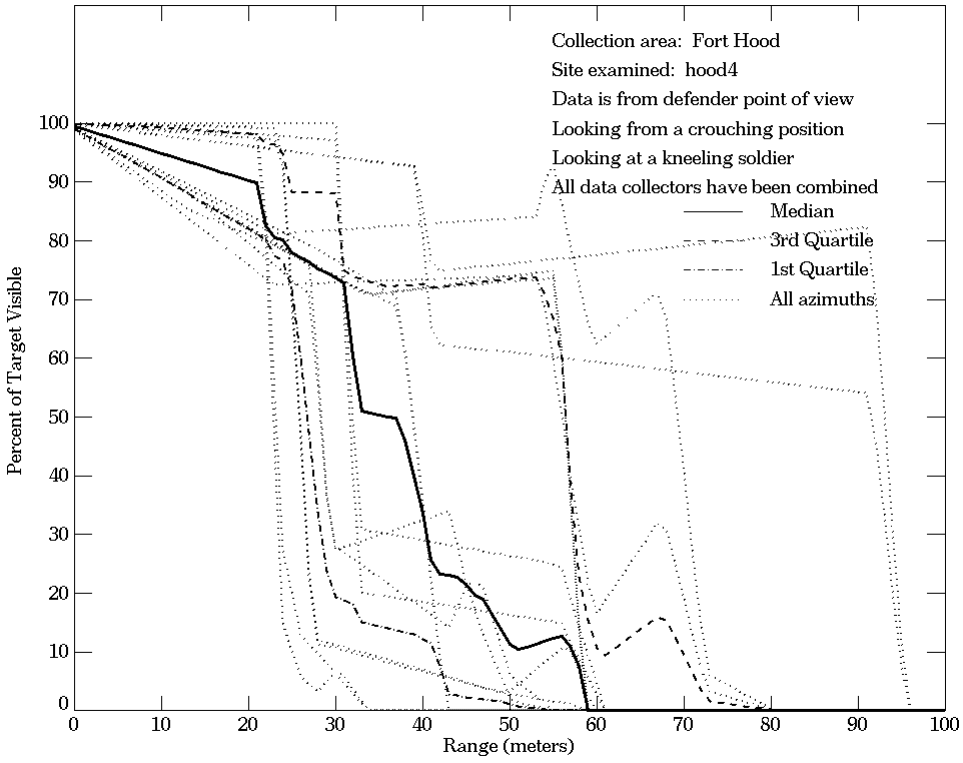

Figure E-39. Fort Hood, From Defender Point of View, Site hood4 (Continued)

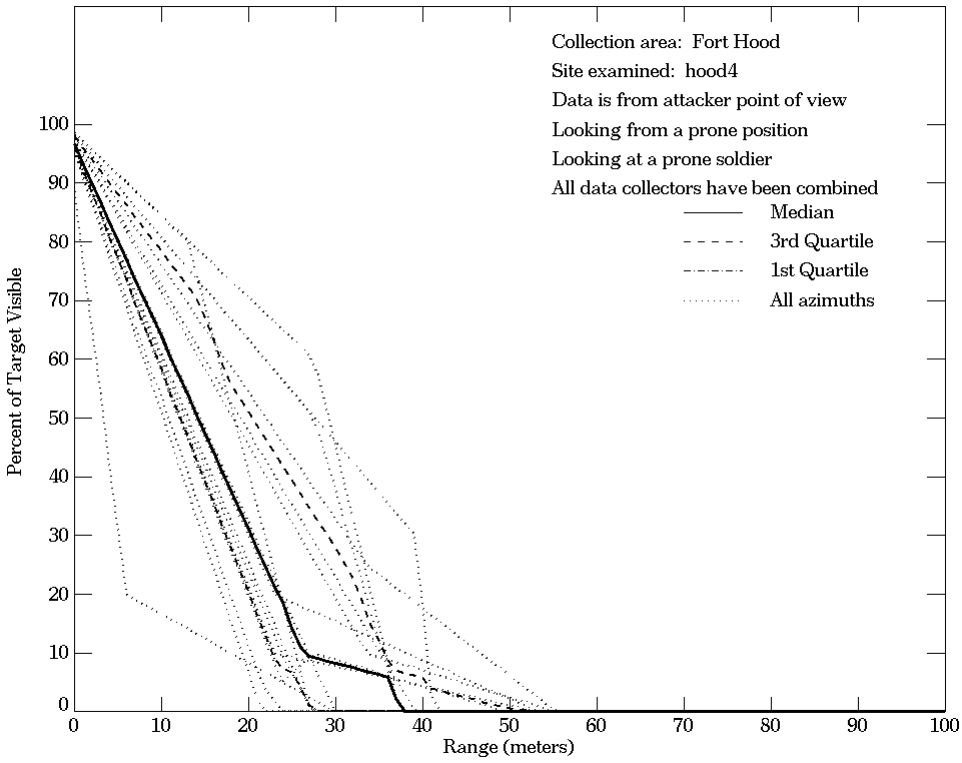

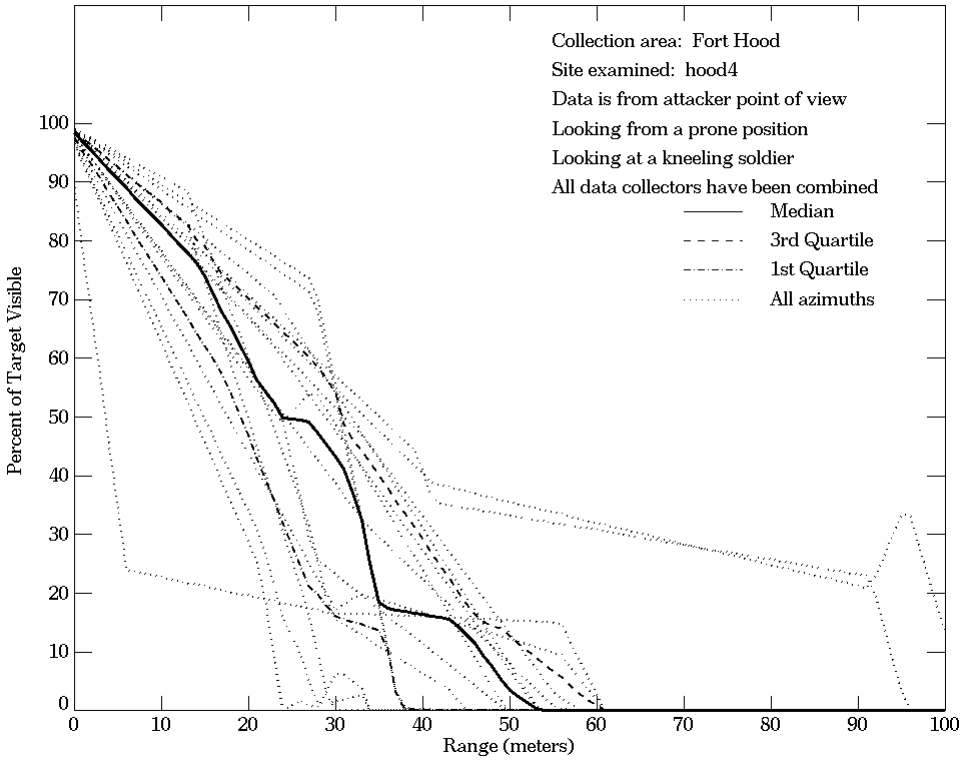

Figure E-40. Fort Hood, From Attacker Point of View, Site hood4

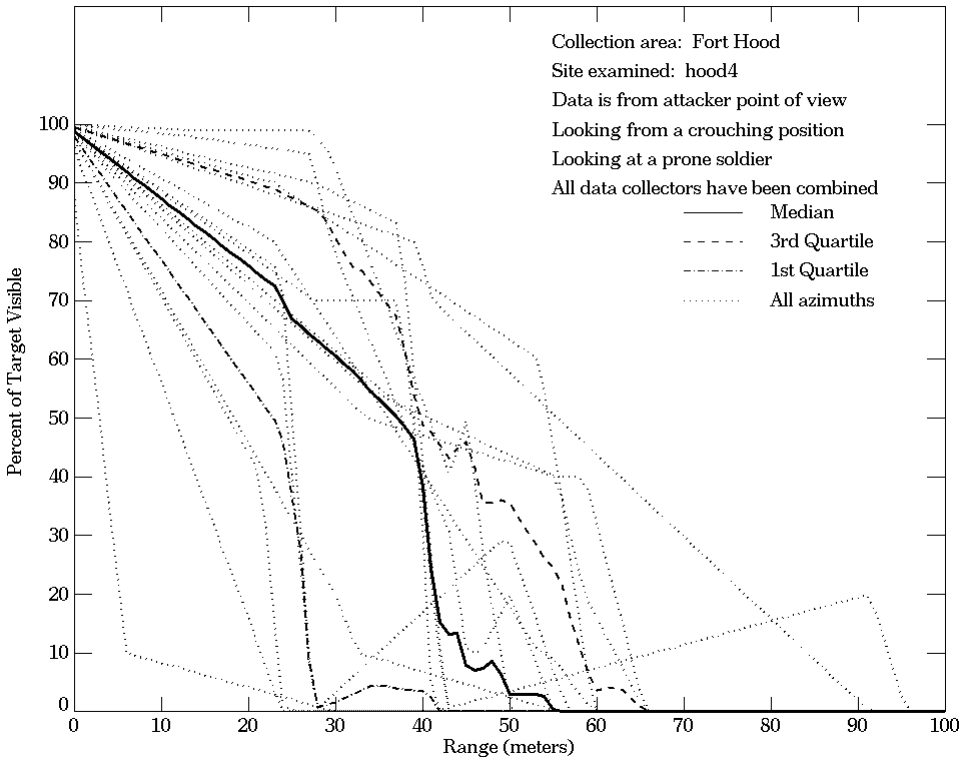

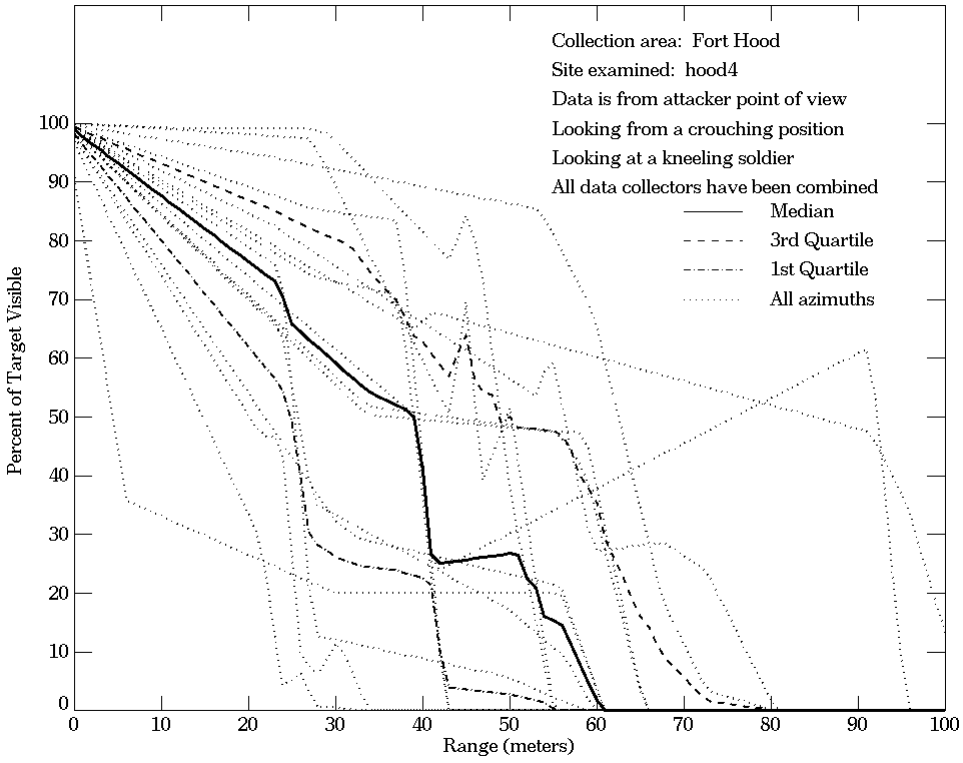

Figure E-40. Fort Hood, From Attacker Point of View, Site hood4 (Continued)

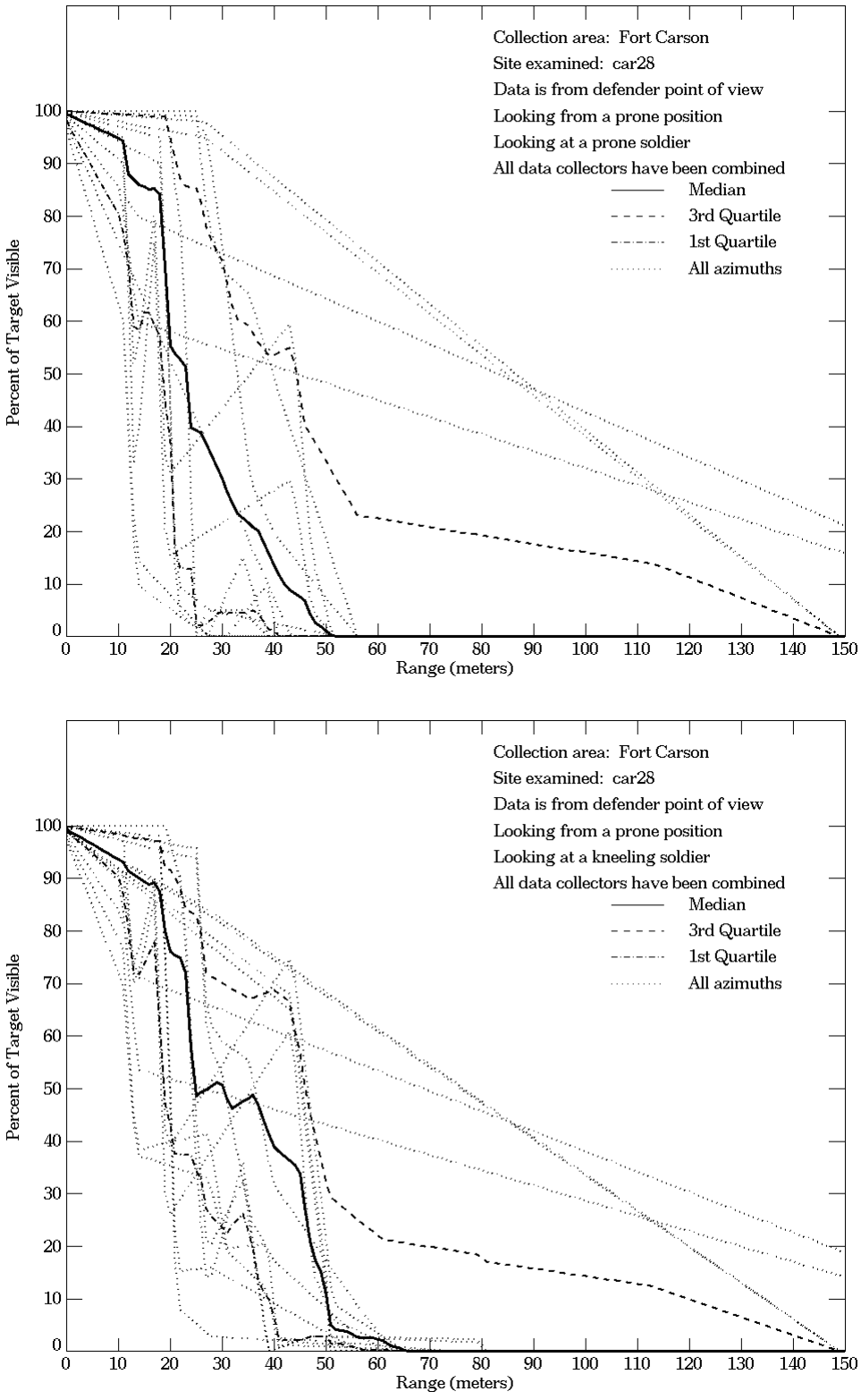

Figure E-41. Fort Carson, From Defender Point of View, Site car28

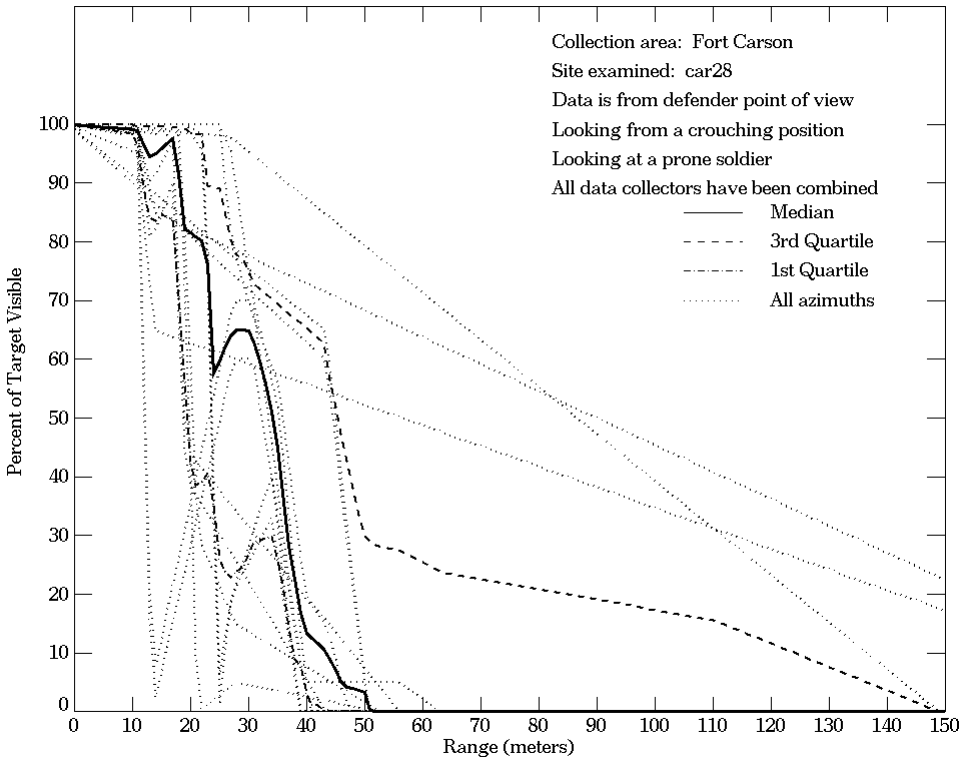

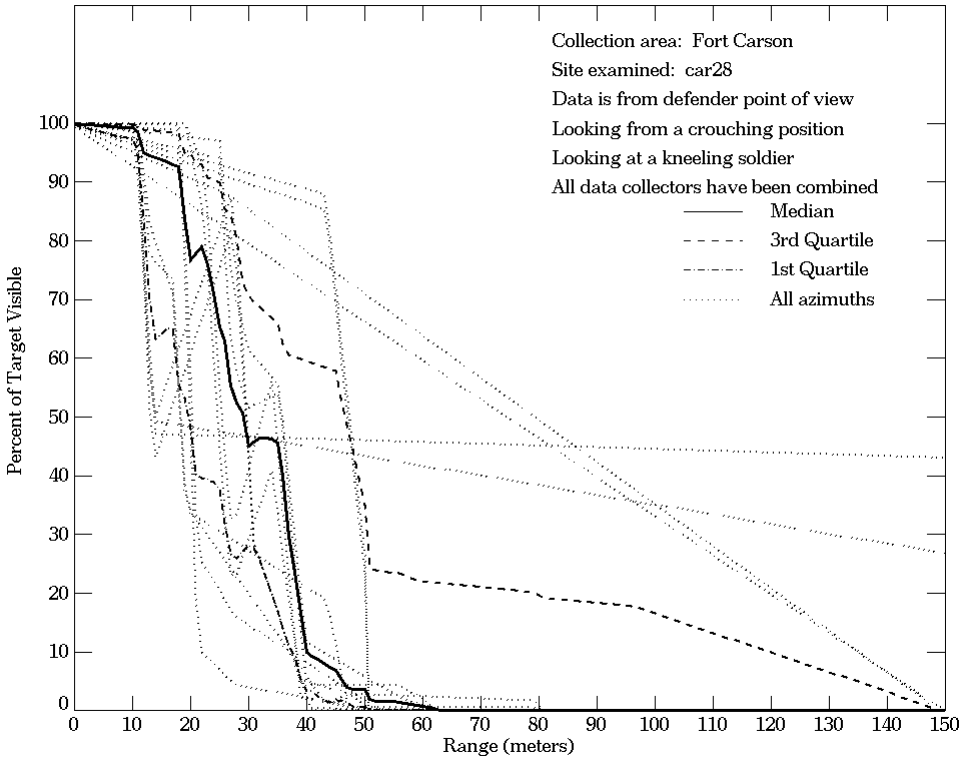

Figure E-41. Fort Carson, From Defender Point of View, Site car28 (Continued)

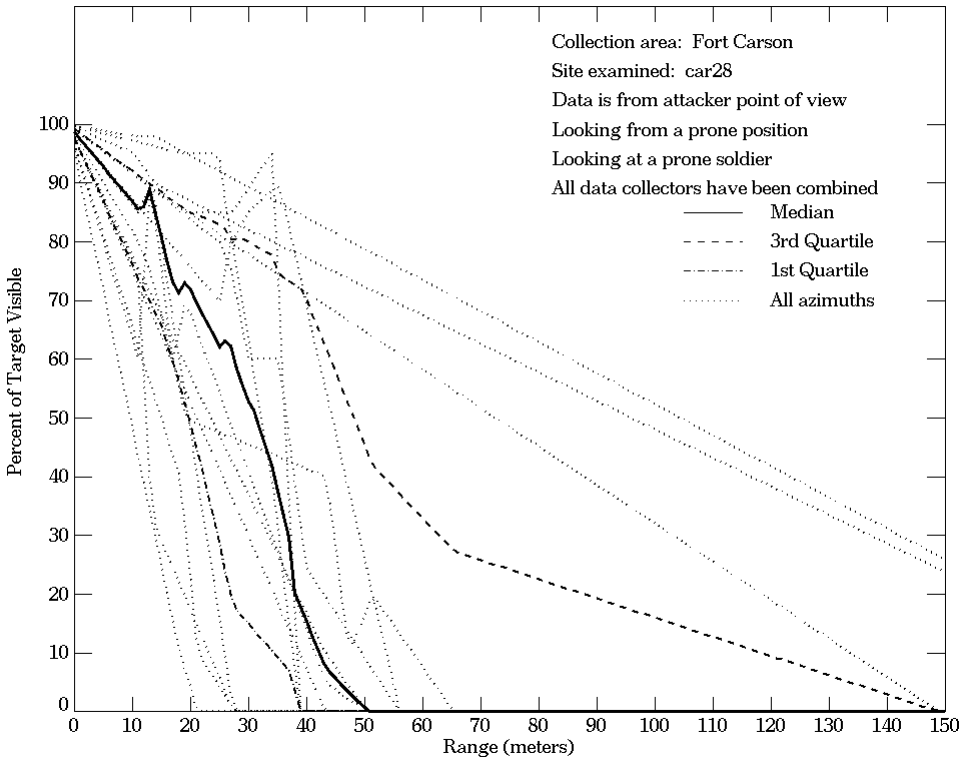

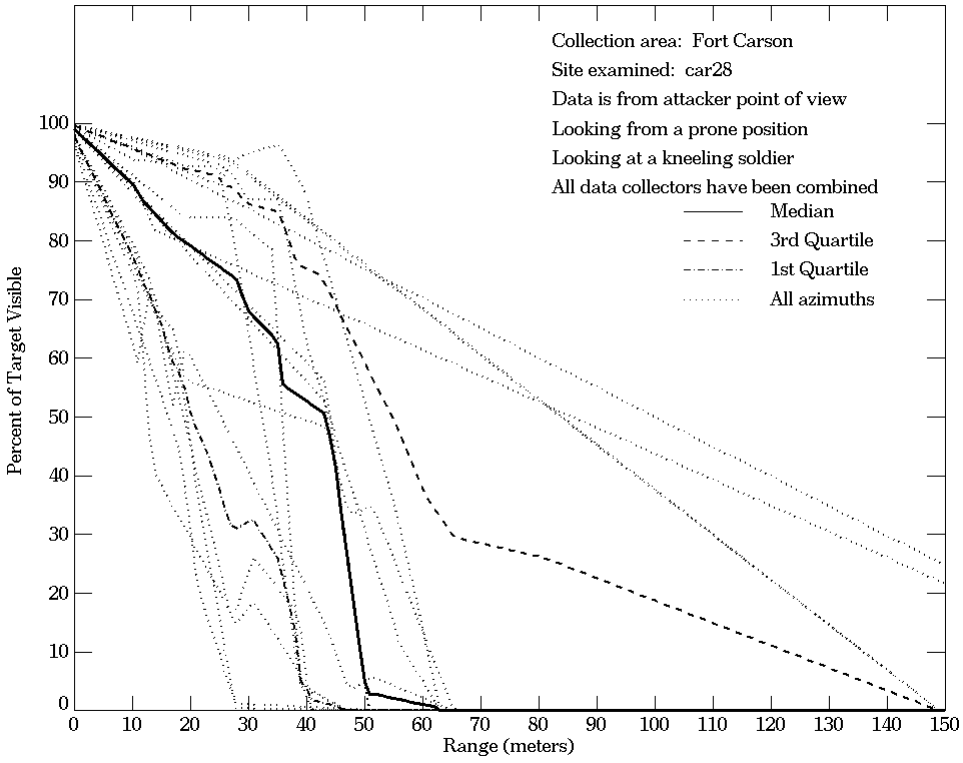

Figure E-42. Fort Carson, From Attacker Point of View, Site car28

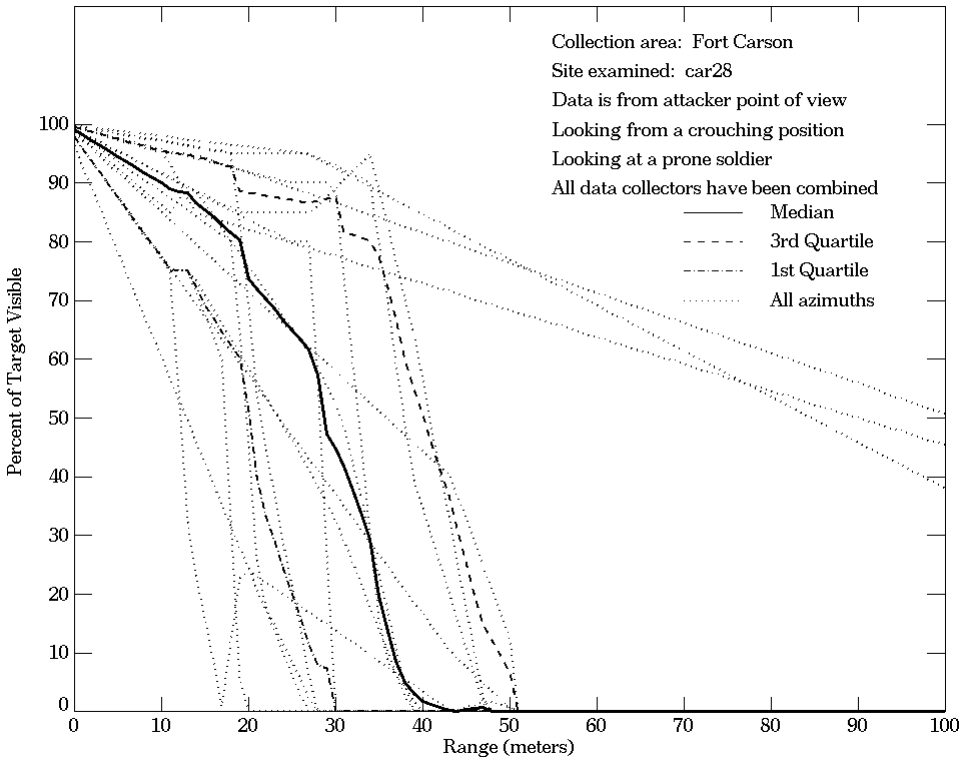

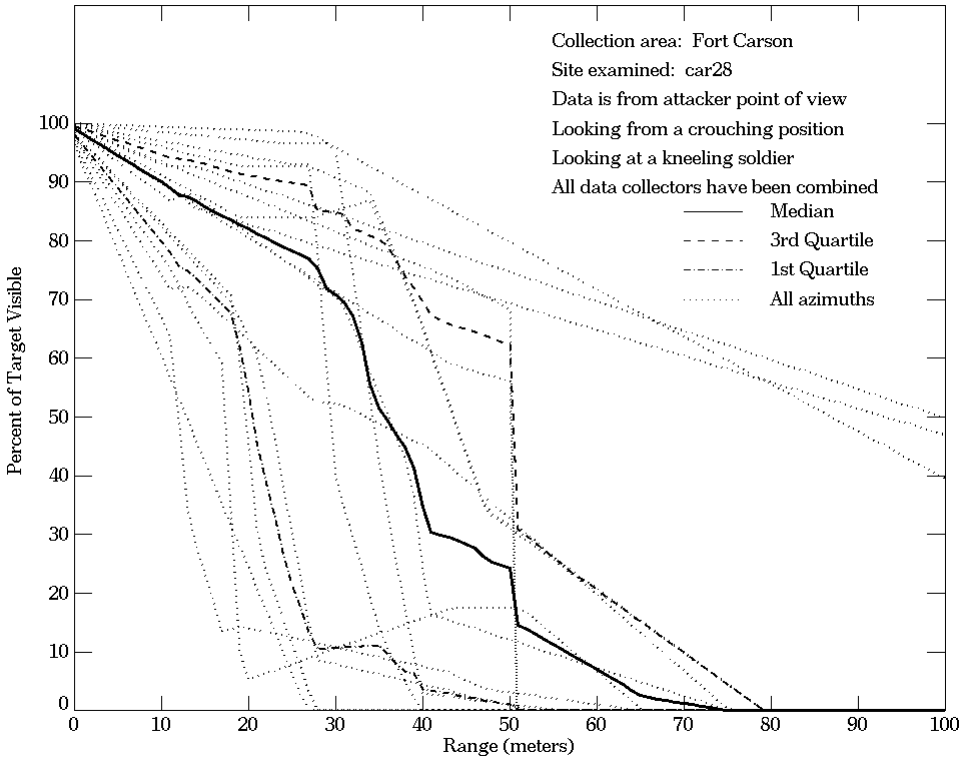

Figure E-42. Fort Carson, From Attacker Point of View, Site car28 (Continued)

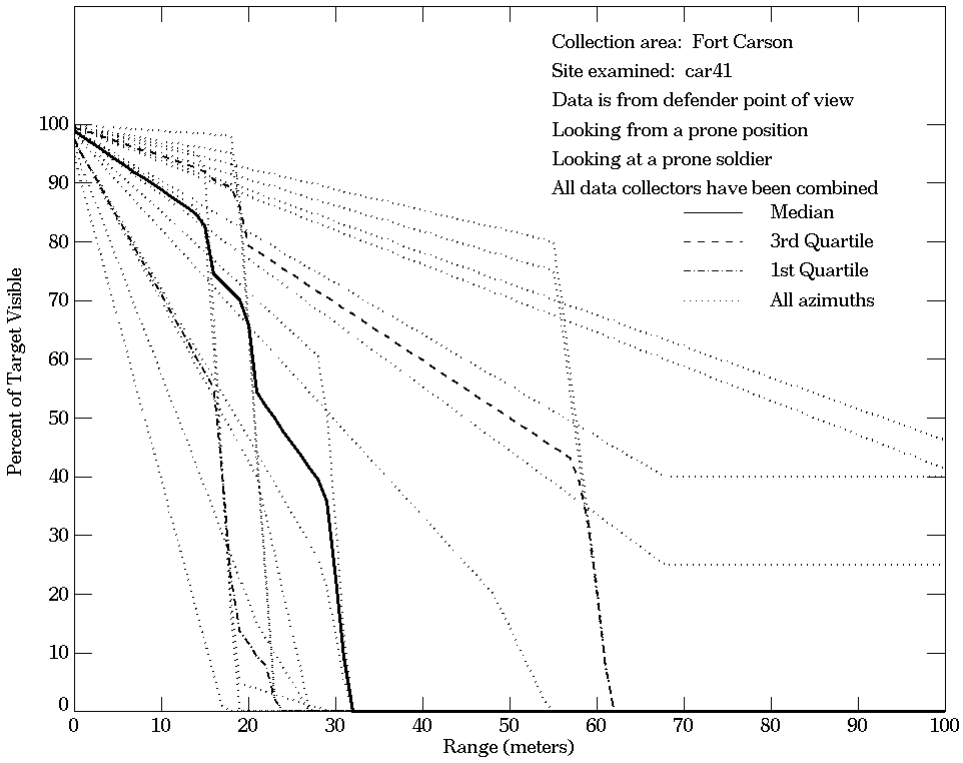

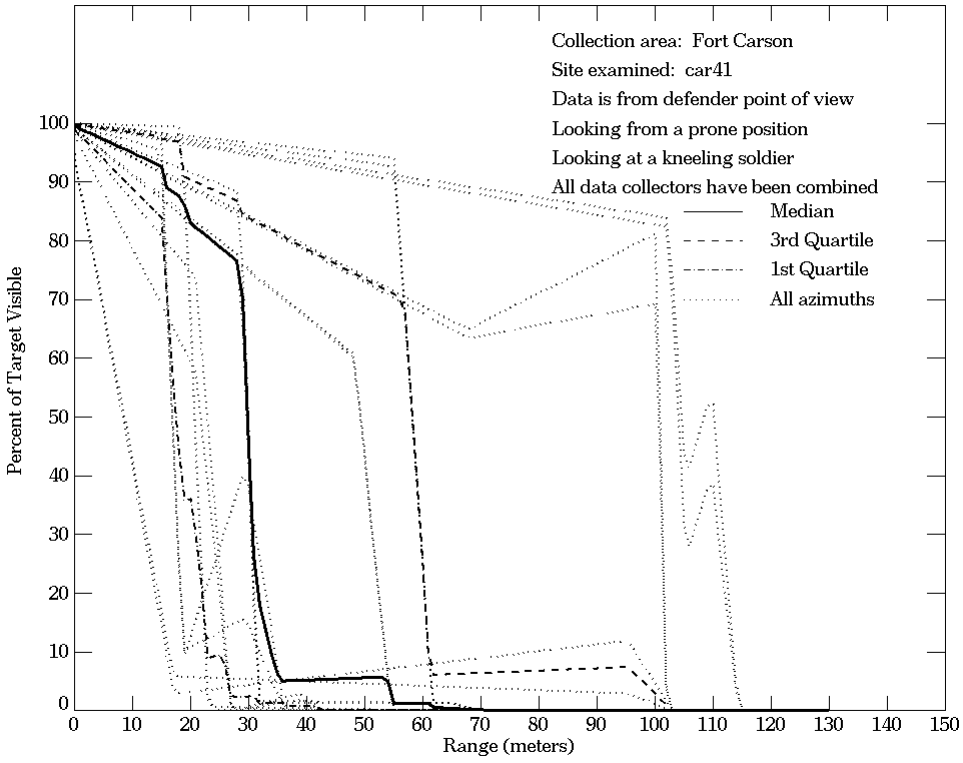

Figure E-43. Fort Carson, From Defender Point of View, Site car41

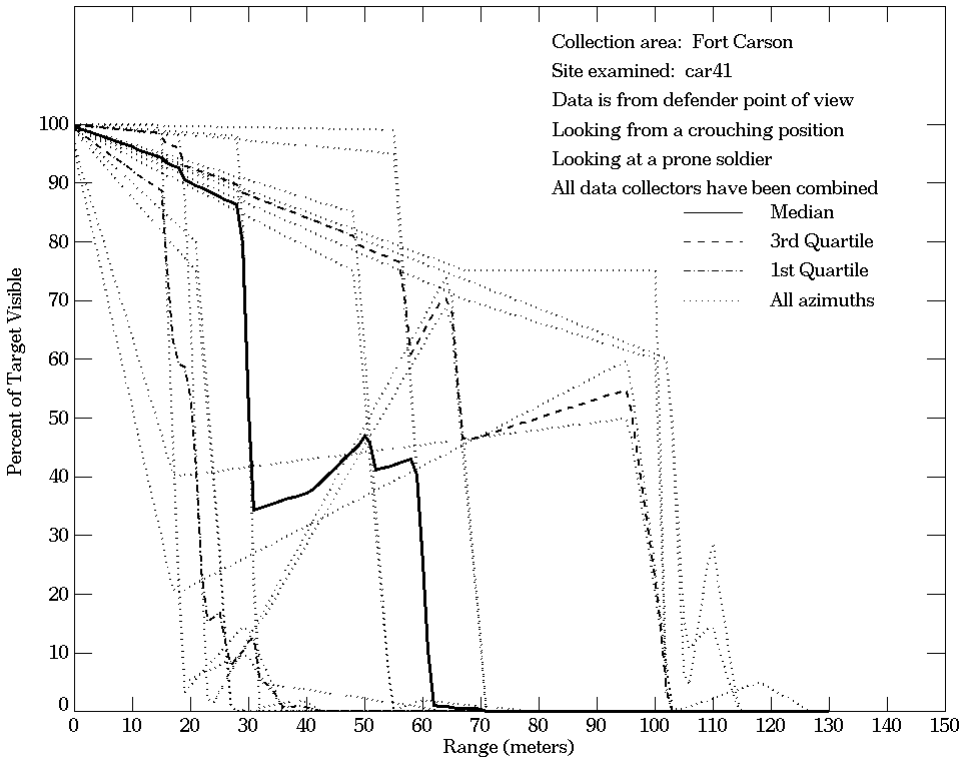

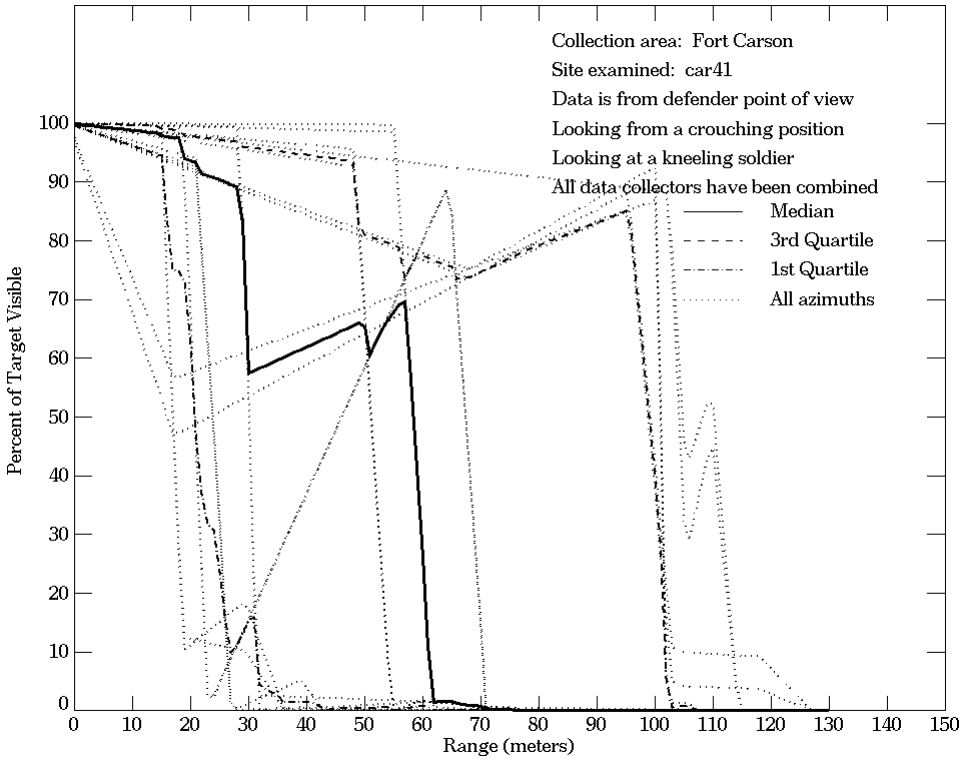

Figure E-43. Fort Carson, From Defender Point of View, Site car41 (Continued)

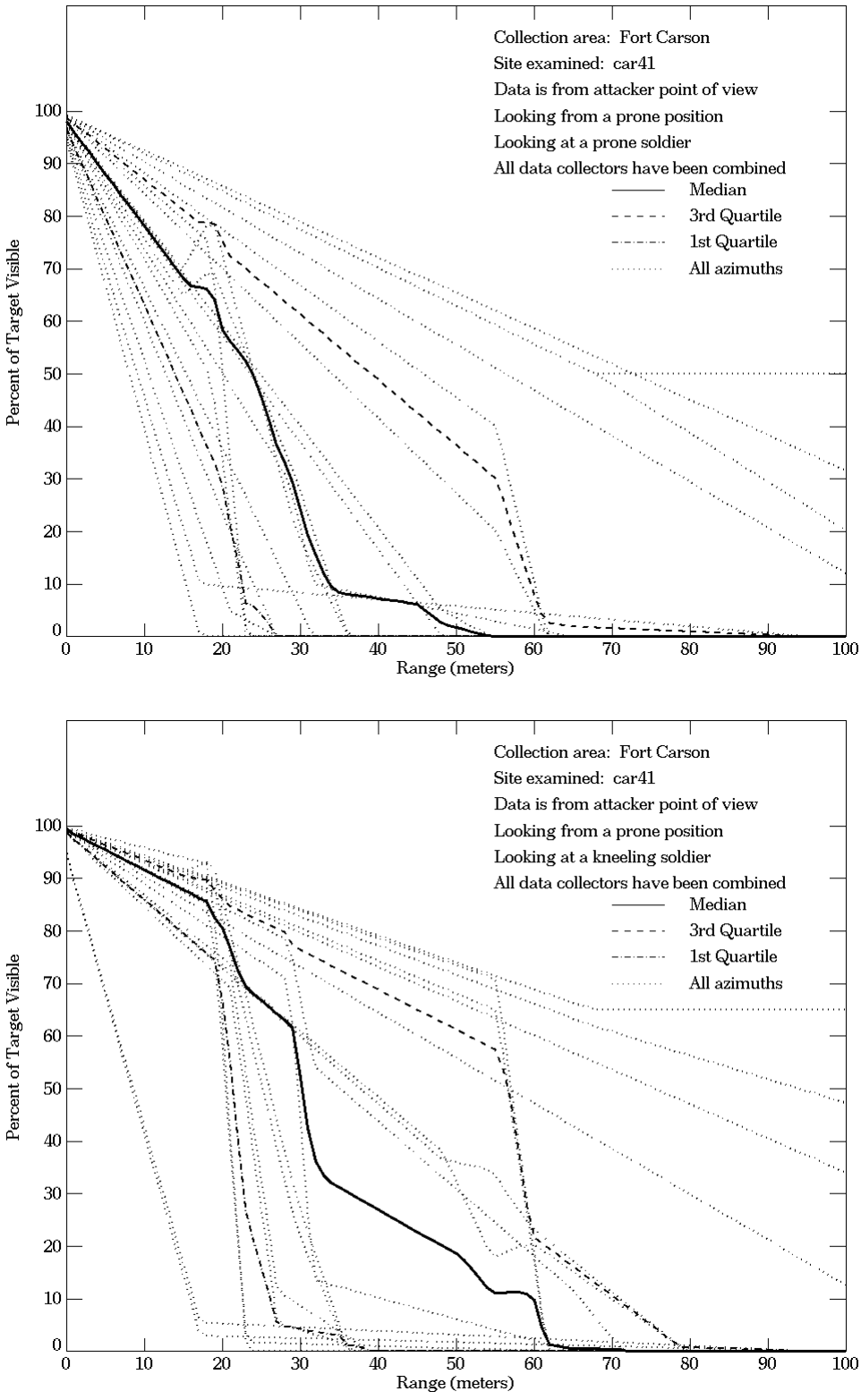

Figure E-44. Fort Carson, From Attacker Point of View, Site car41

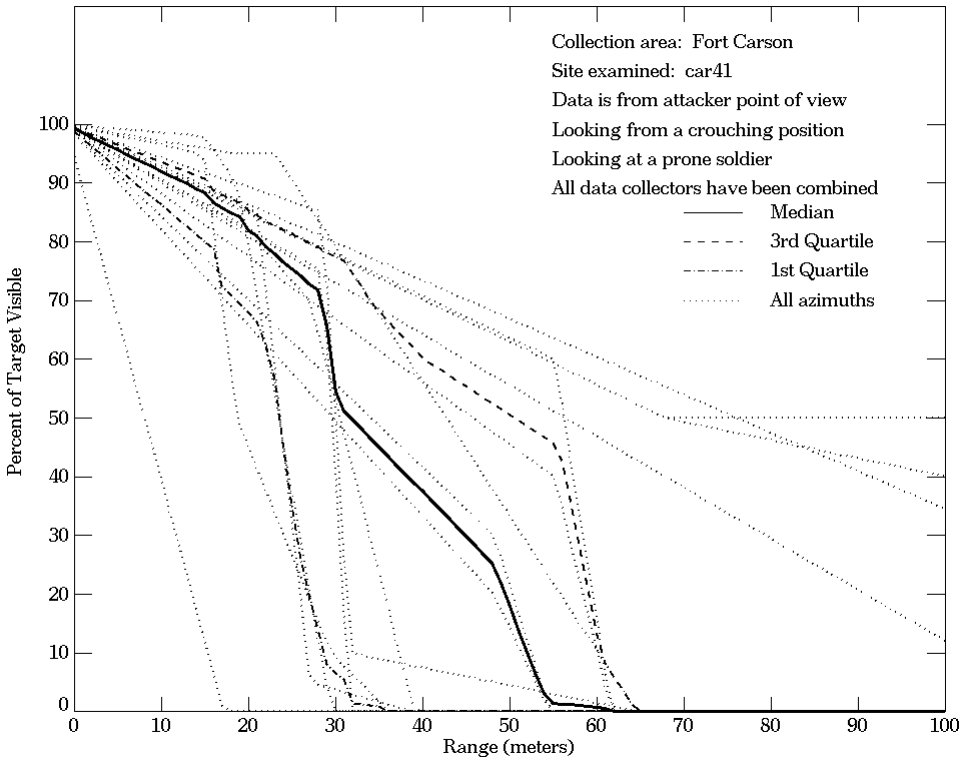

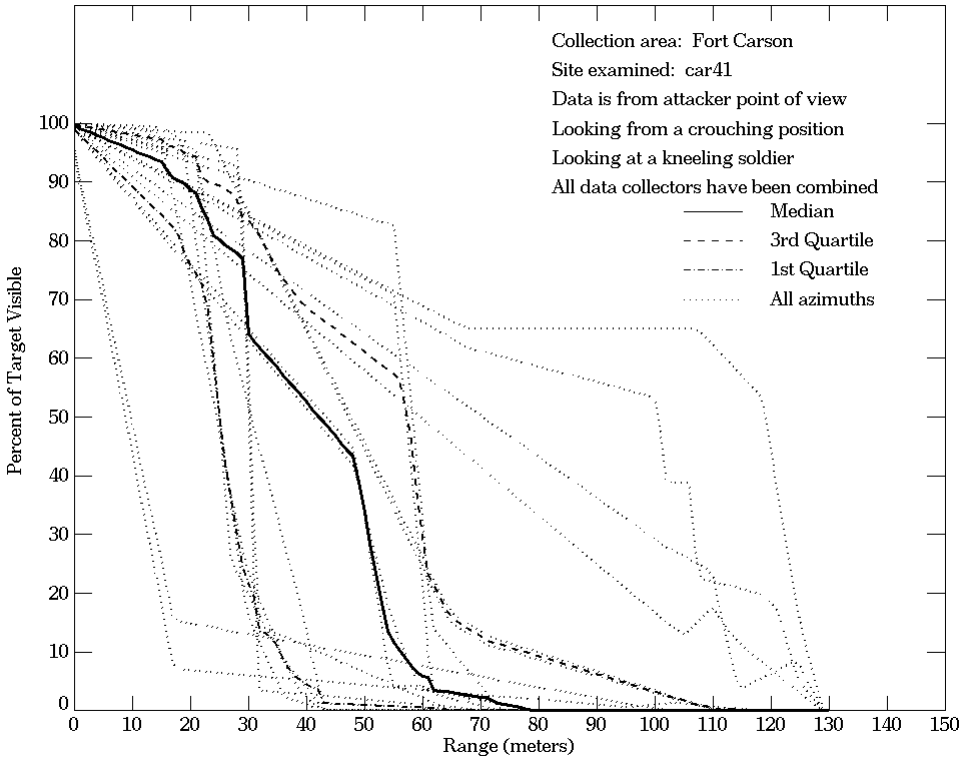

Figure E-44. Fort Carson, From Attacker Point of View, Site car41 (Continued)

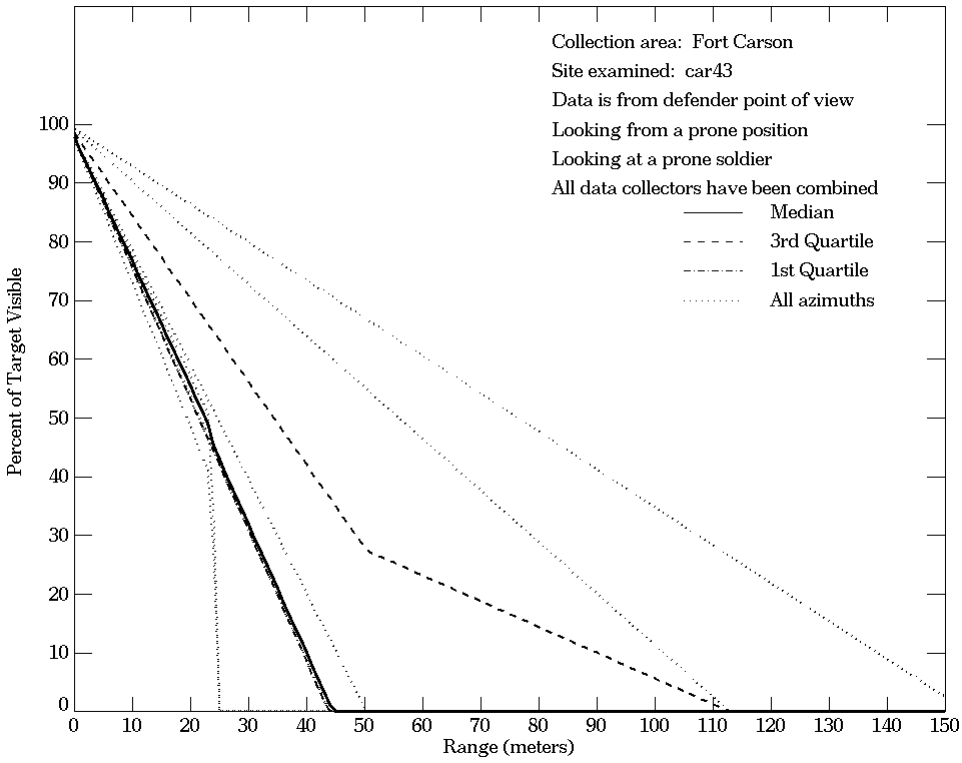

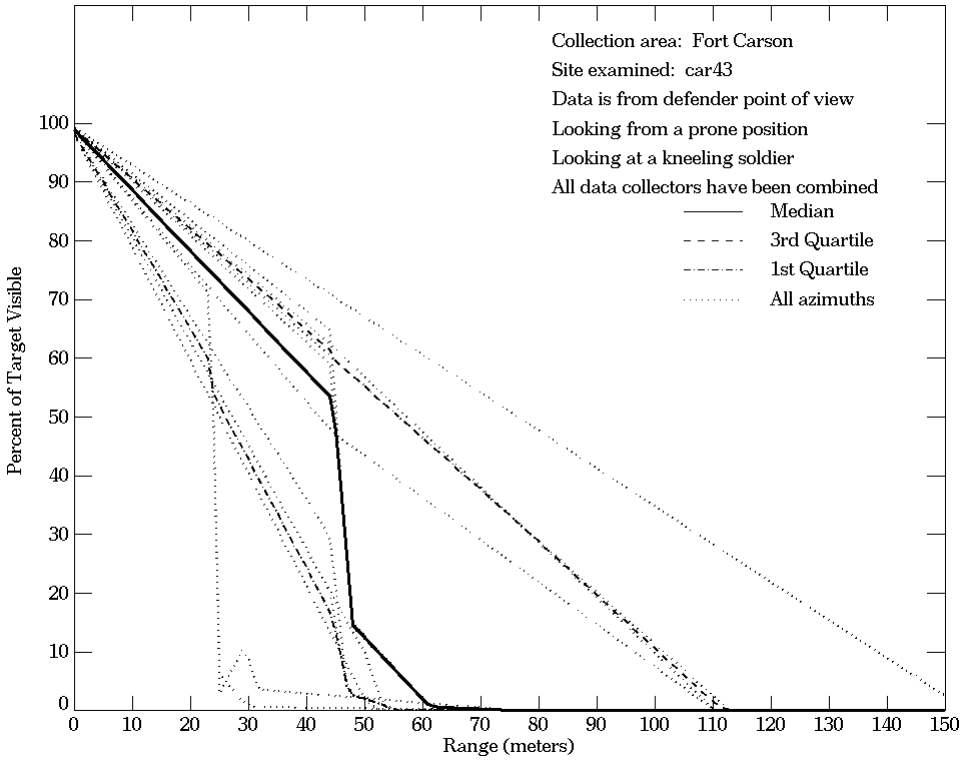

Figure E-45. Fort Carson, From Defender Point of View, Site car43

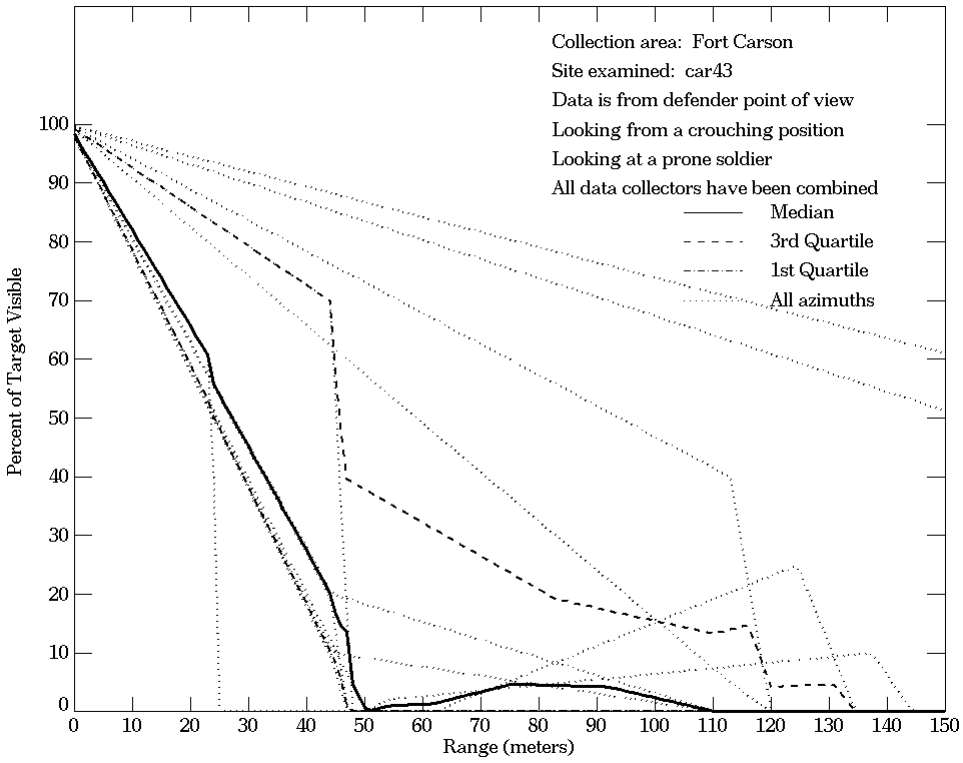

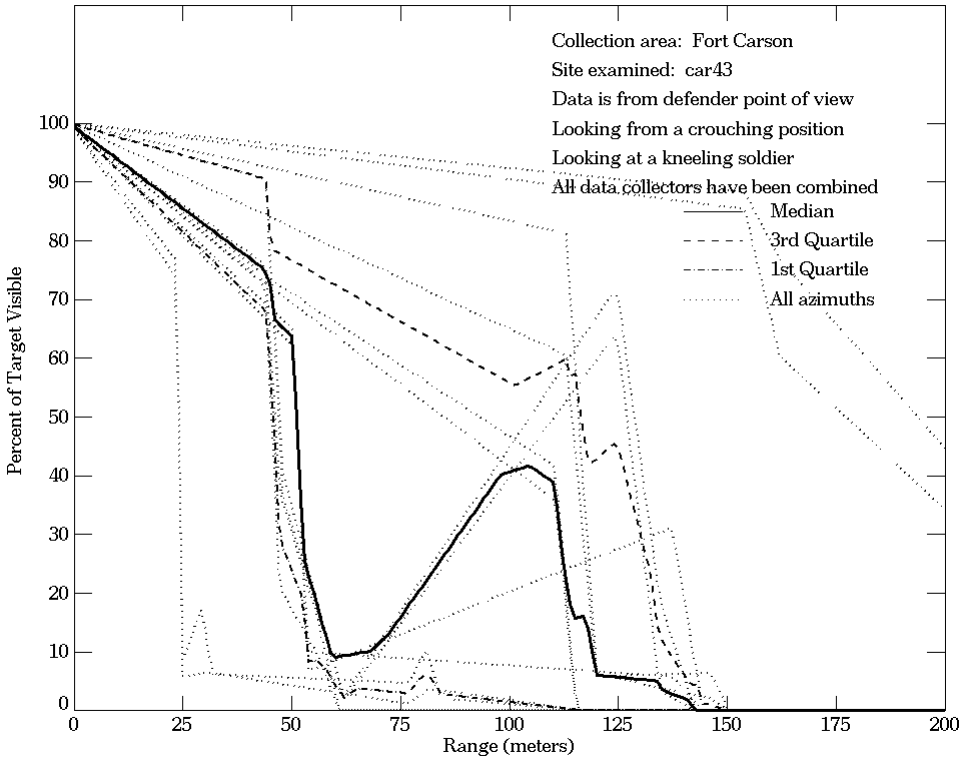

Figure E-45. Fort Carson, From Defender Point of View, Site car43 (Continued)

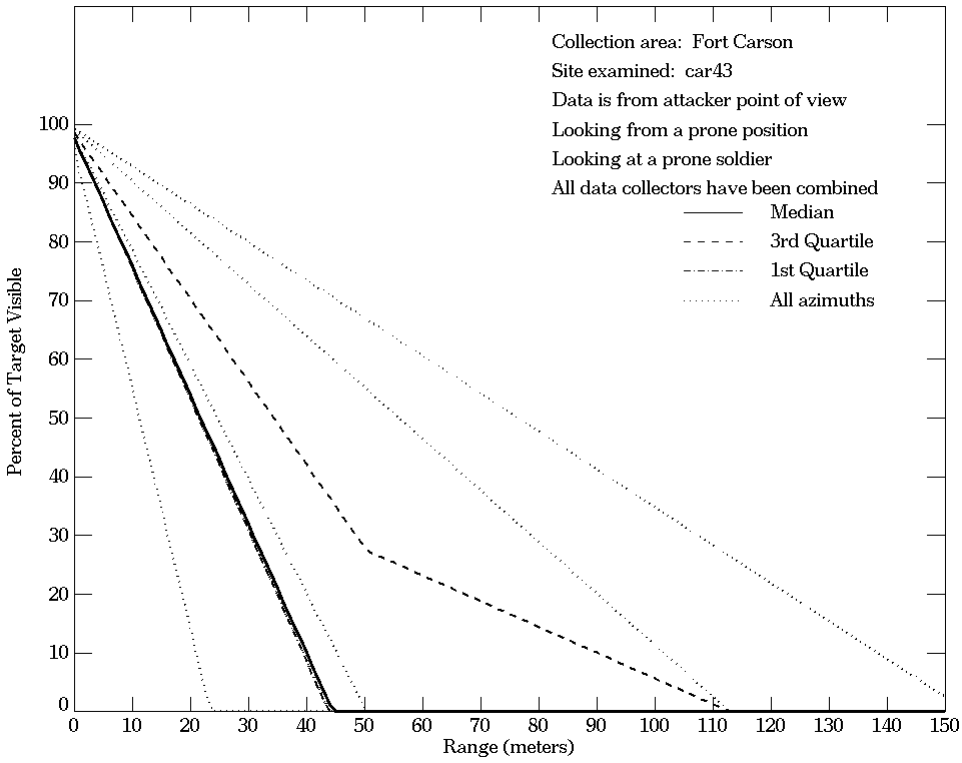

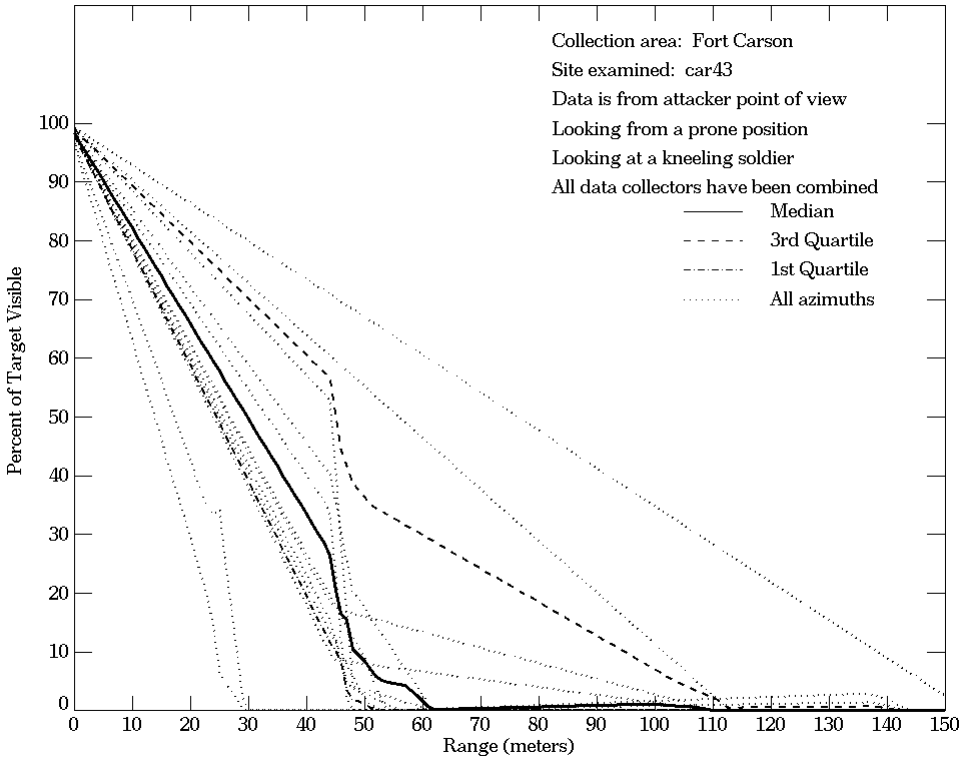

Figure E-46. Fort Carson, From Attacker Point of View, Site car43

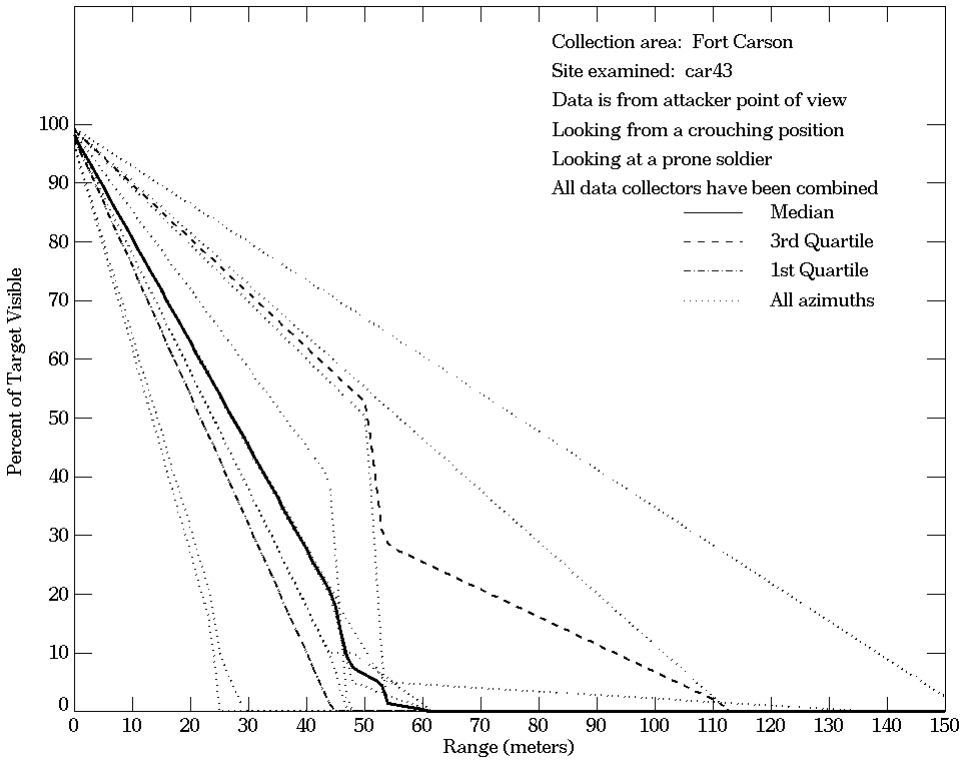

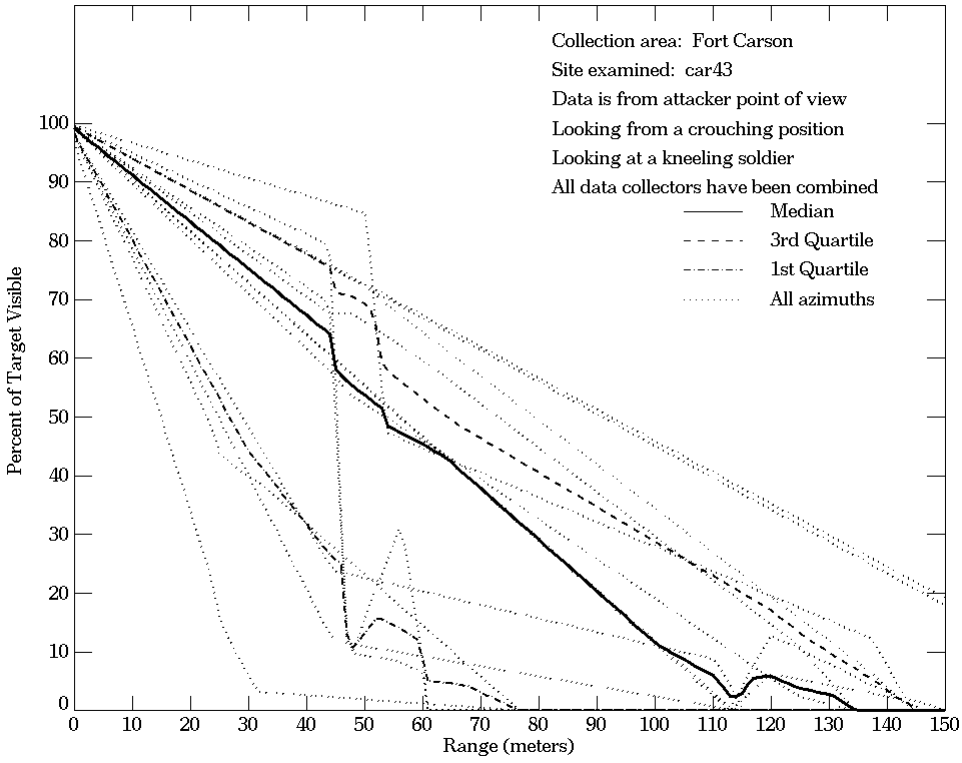

Figure E-46. Fort Carson, From Attacker Point of View, Site car43 (Continued)

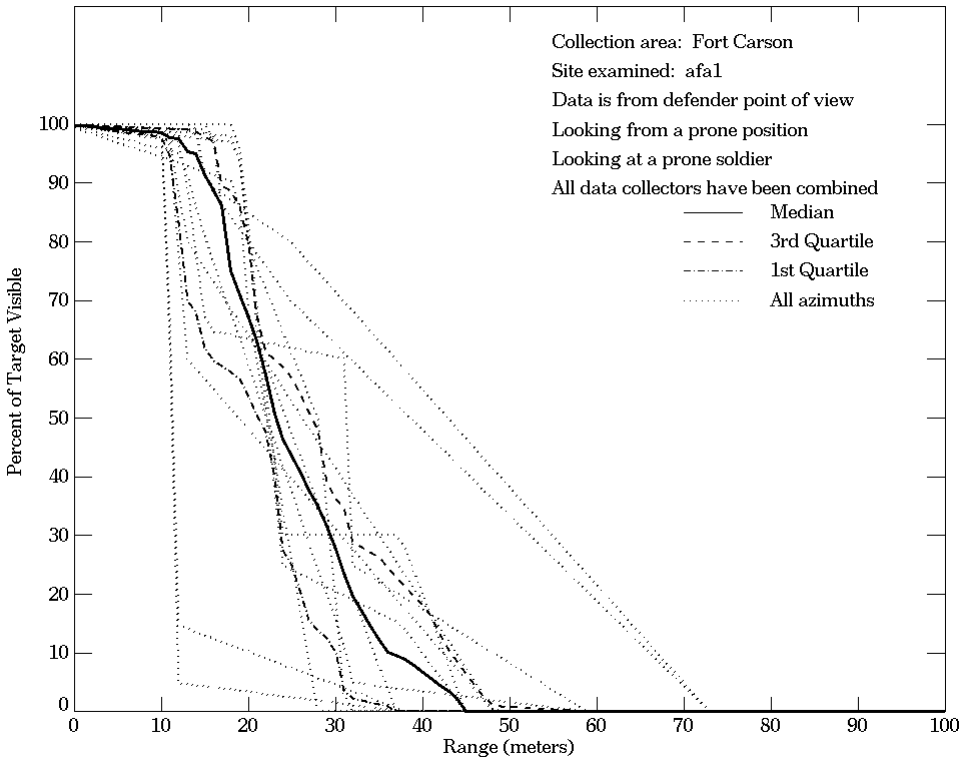

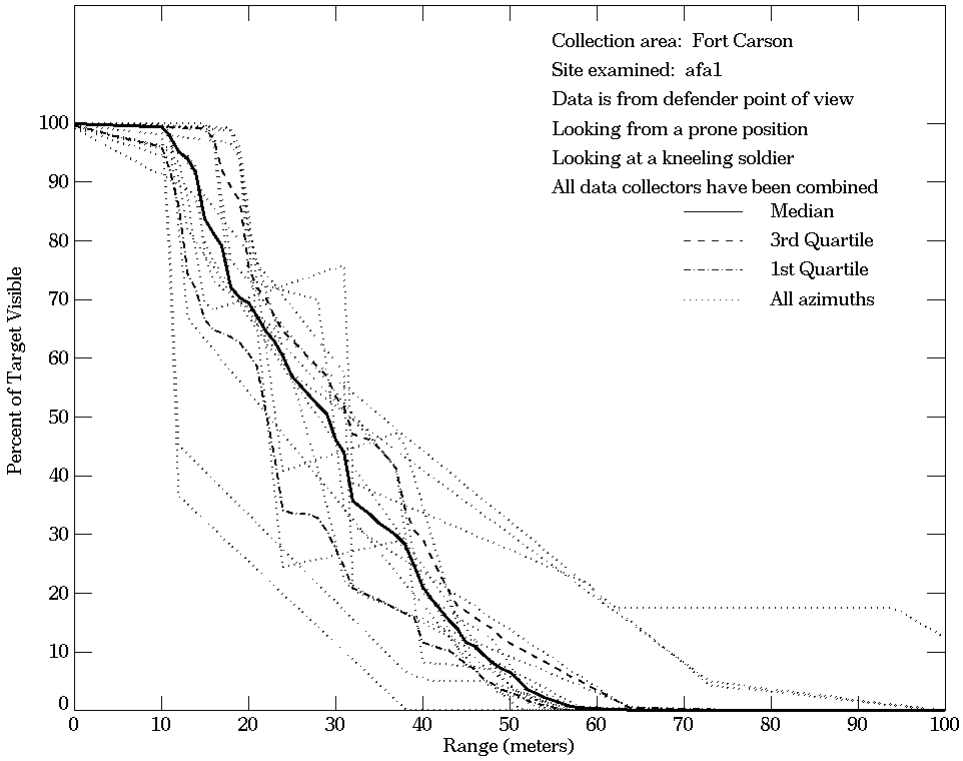

Figure E-47. Fort Carson, From Defender Point of View, Site afa1

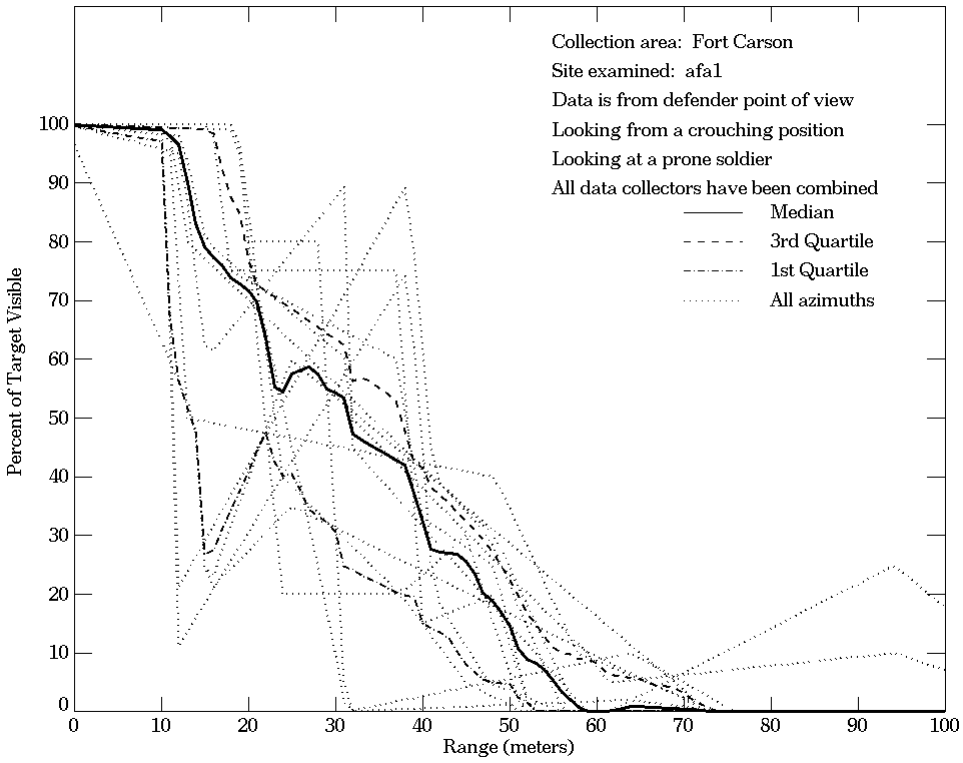

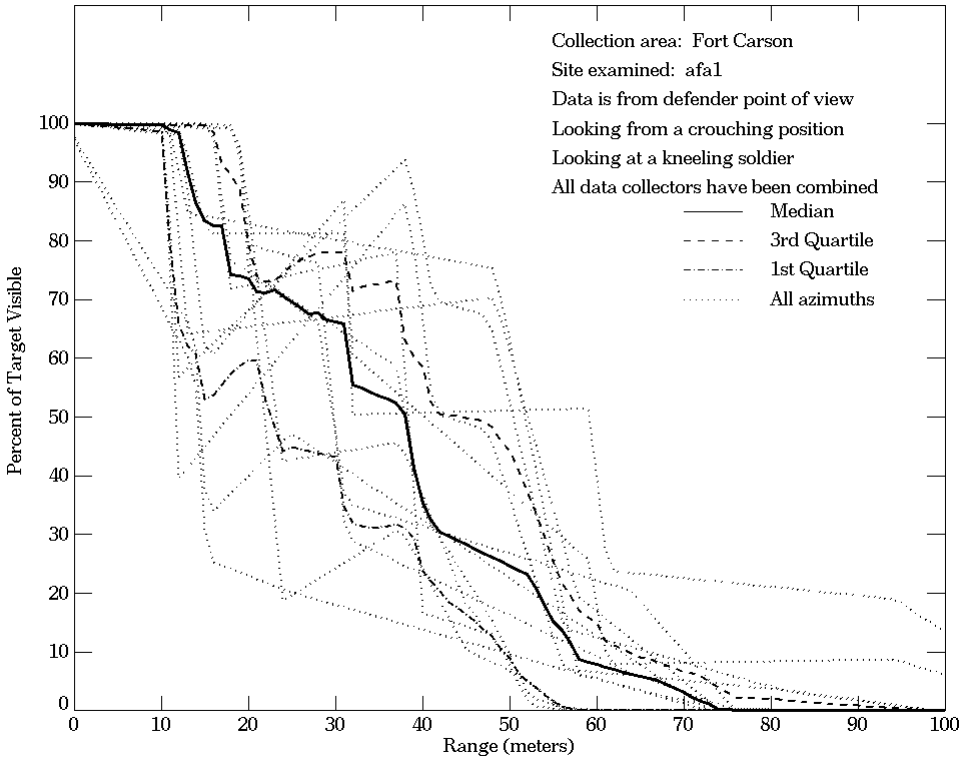

Figure E-47. Fort Carson, From Defender Point of View, Site afa1 (Continued)

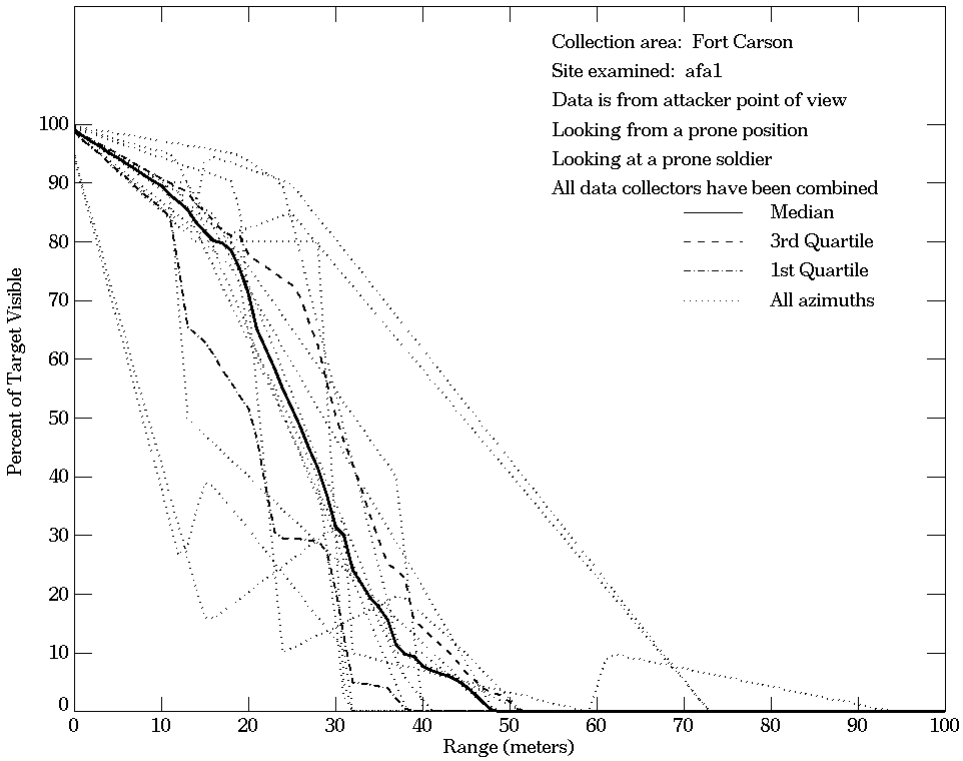

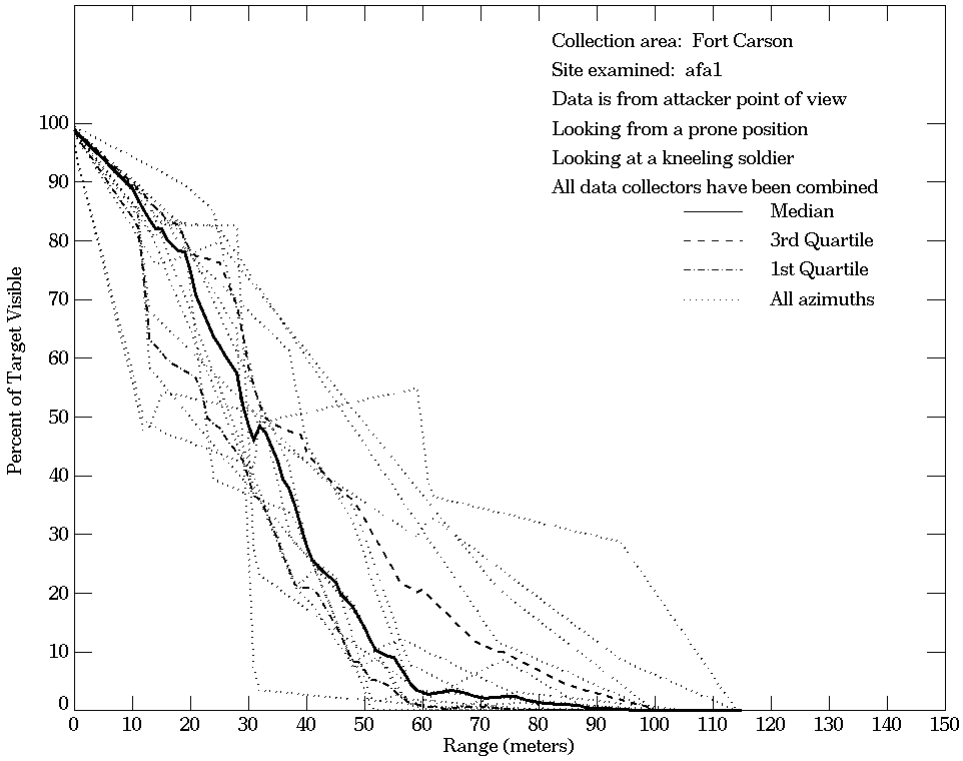

Figure E-48. Fort Carson, From Attacker Point of View, Site afa1

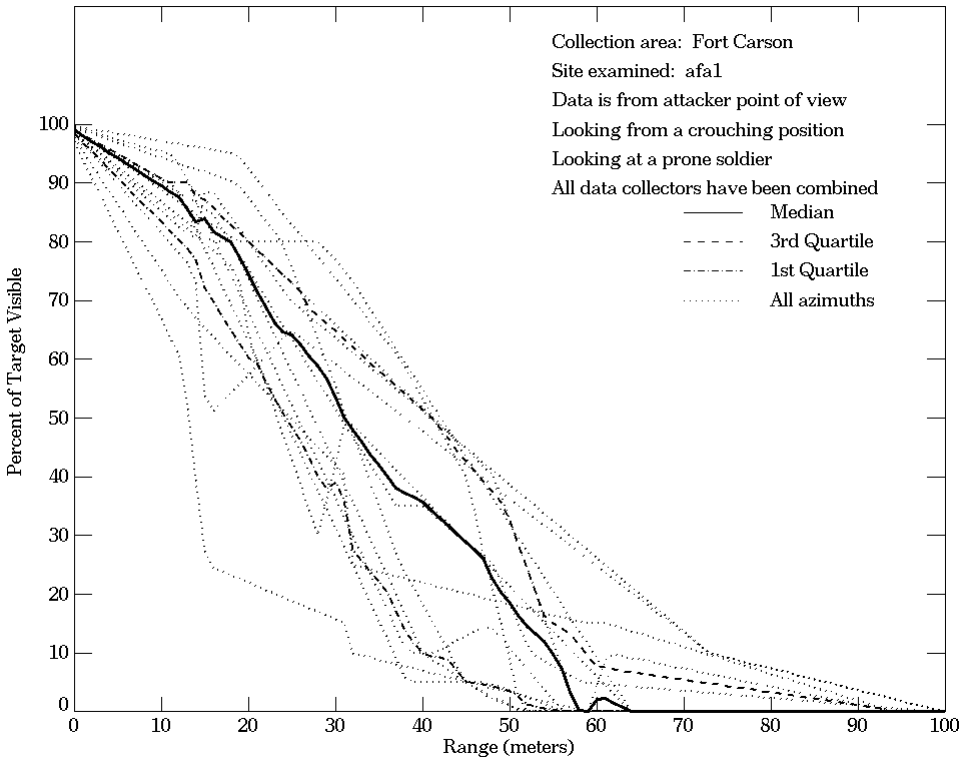

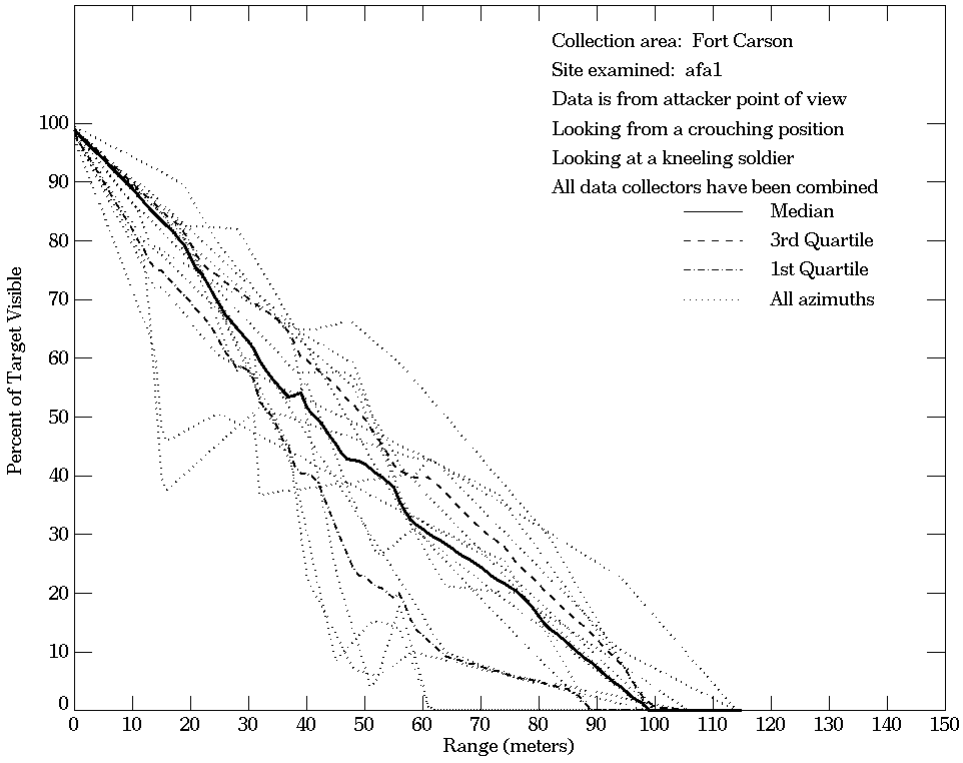

Figure E-48. Fort Carson, From Attacker Point of View, Site afa1 (Continued)

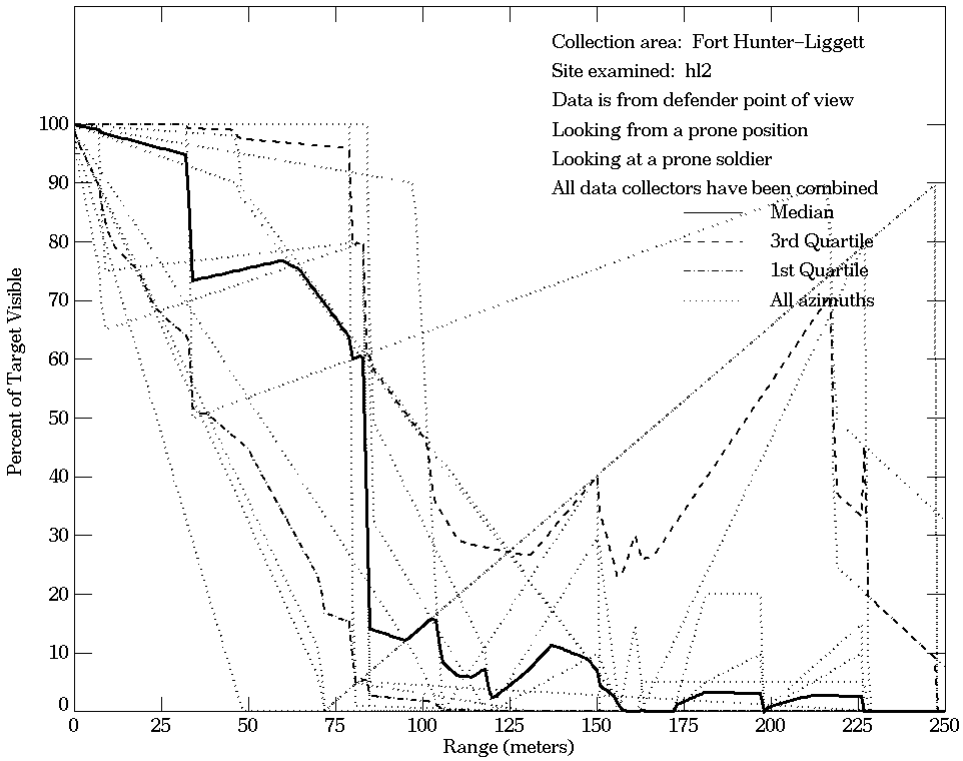

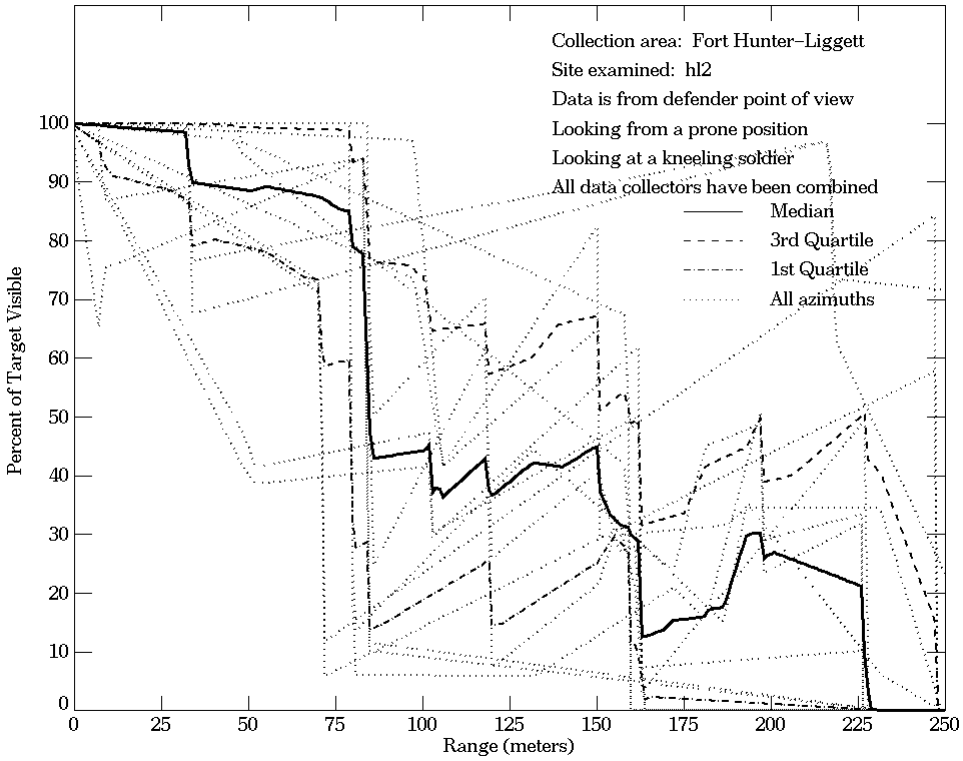

Figure E-49. Fort Hunter-Liggett, From Defender Point of View, Site hl2

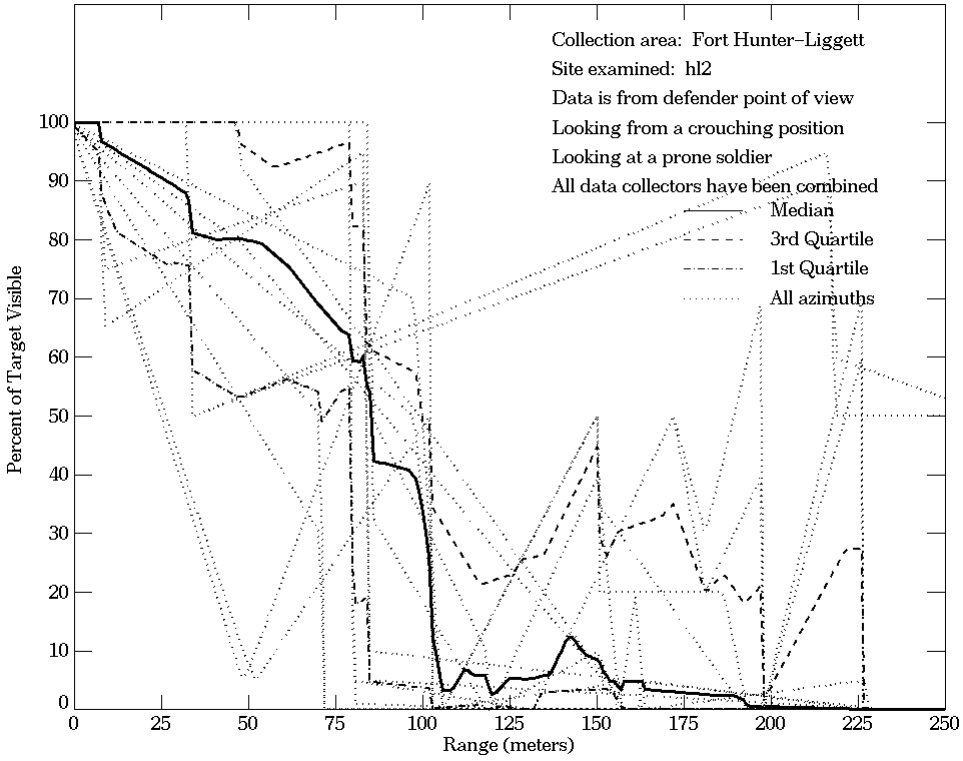

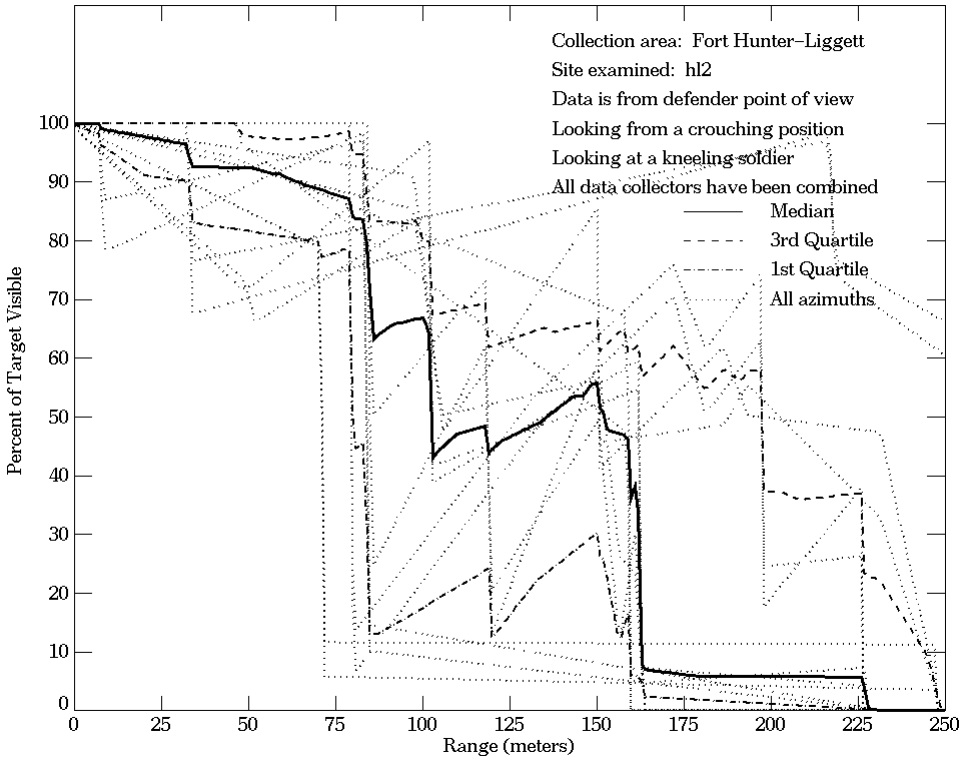

Figure E-49. Fort Hunter-Liggett, From Defender Point of View, Site hl2 (Continued)

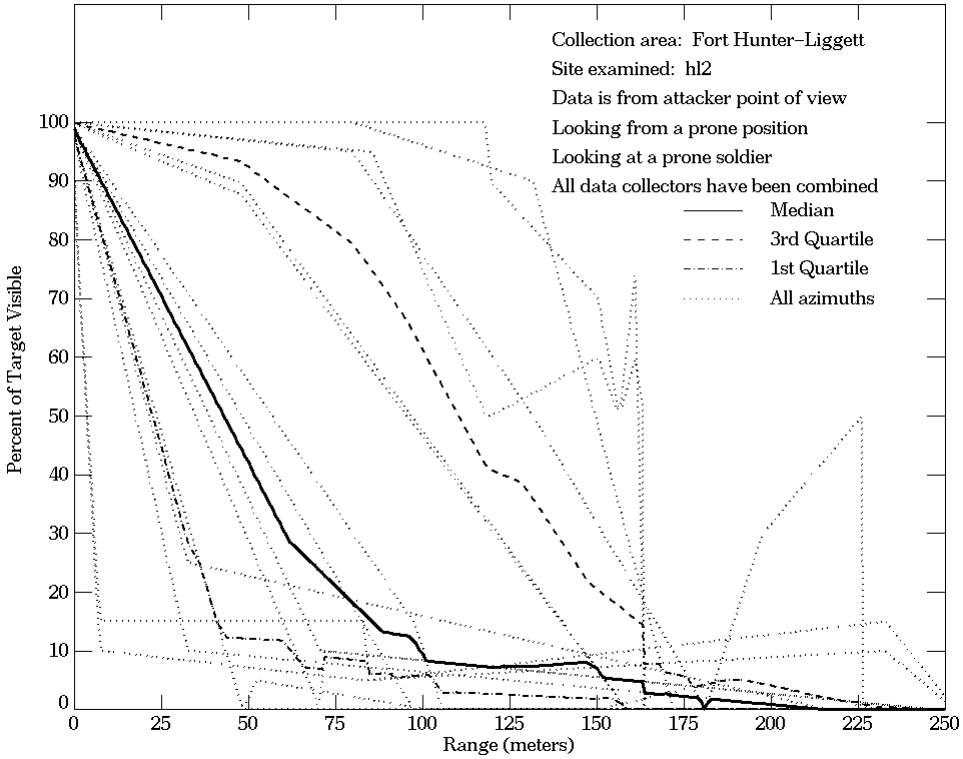

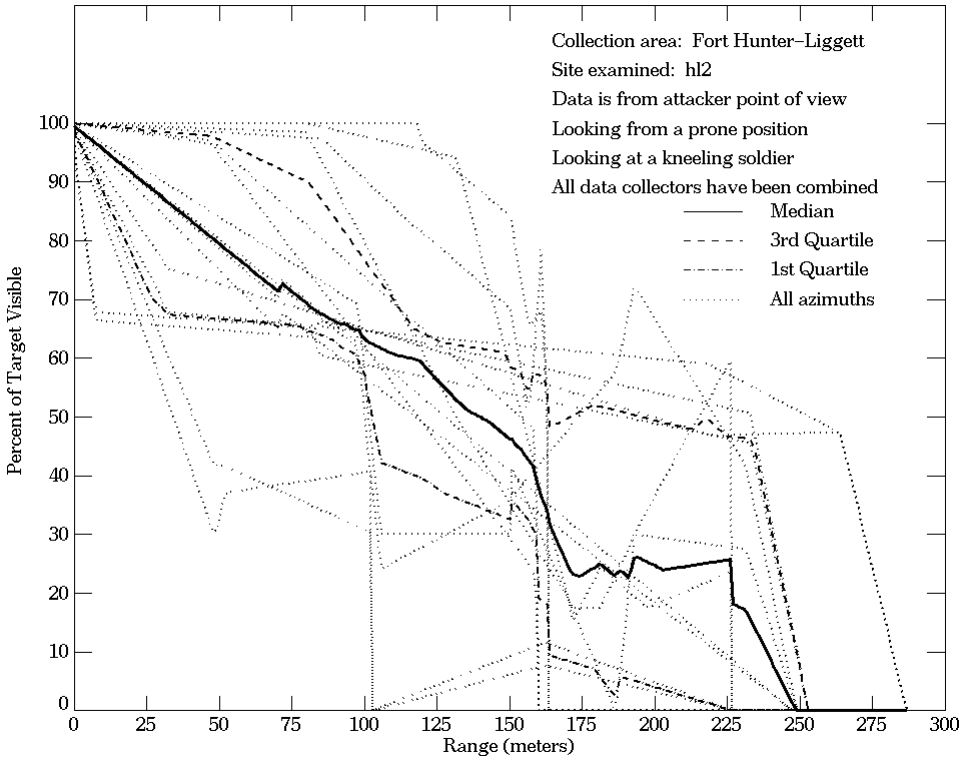

Figure E-50. Fort Hunter-Liggett, From Attacker Point of View, Site hl2

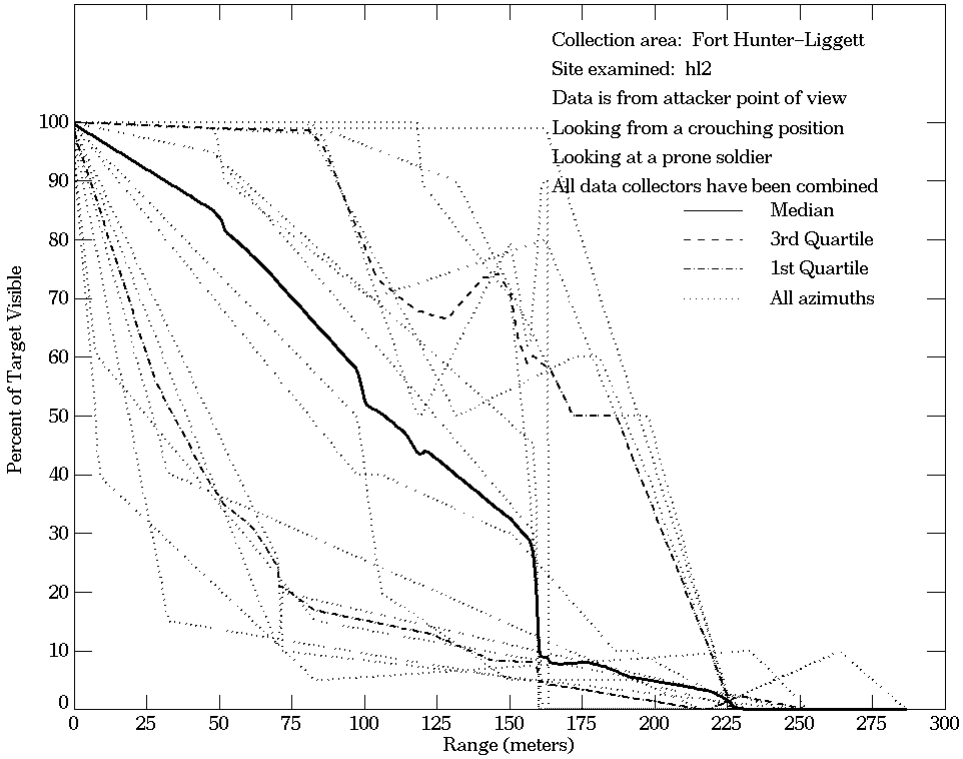

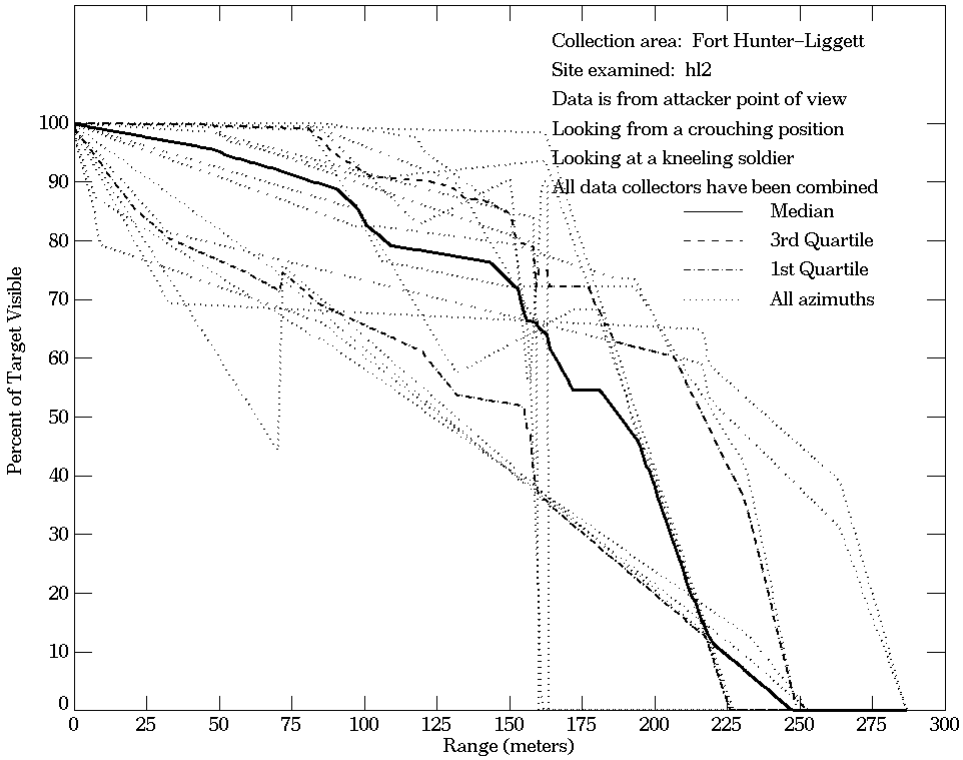

Figure E-50. Fort Hunter-Liggett, From Attacker Point of View, Site hl2 (Continued)

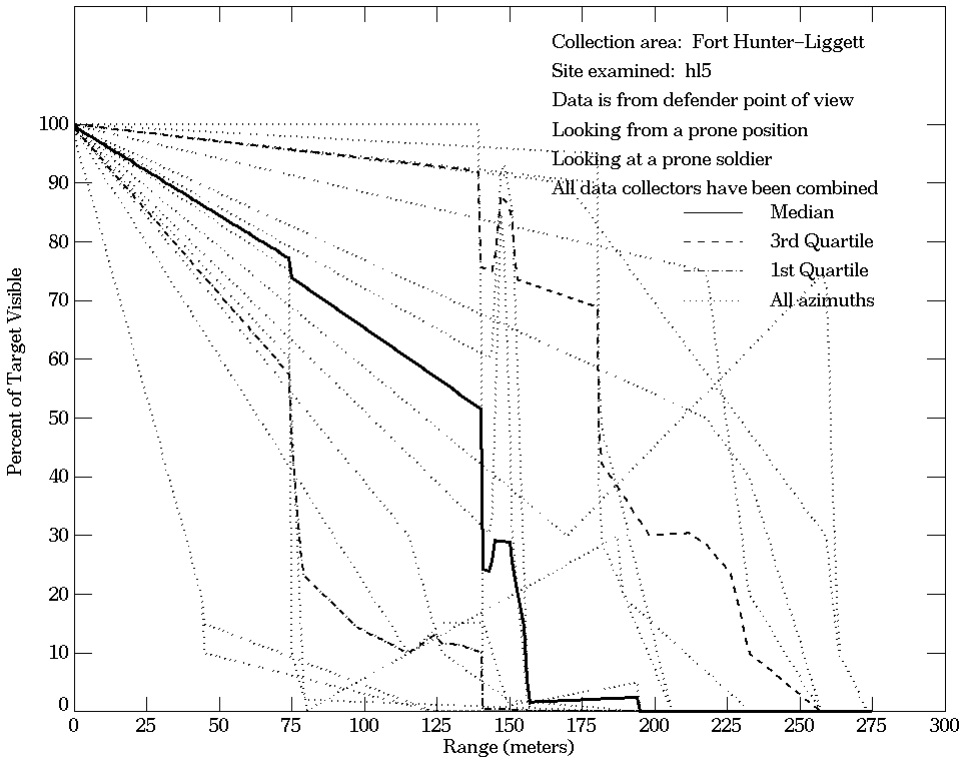

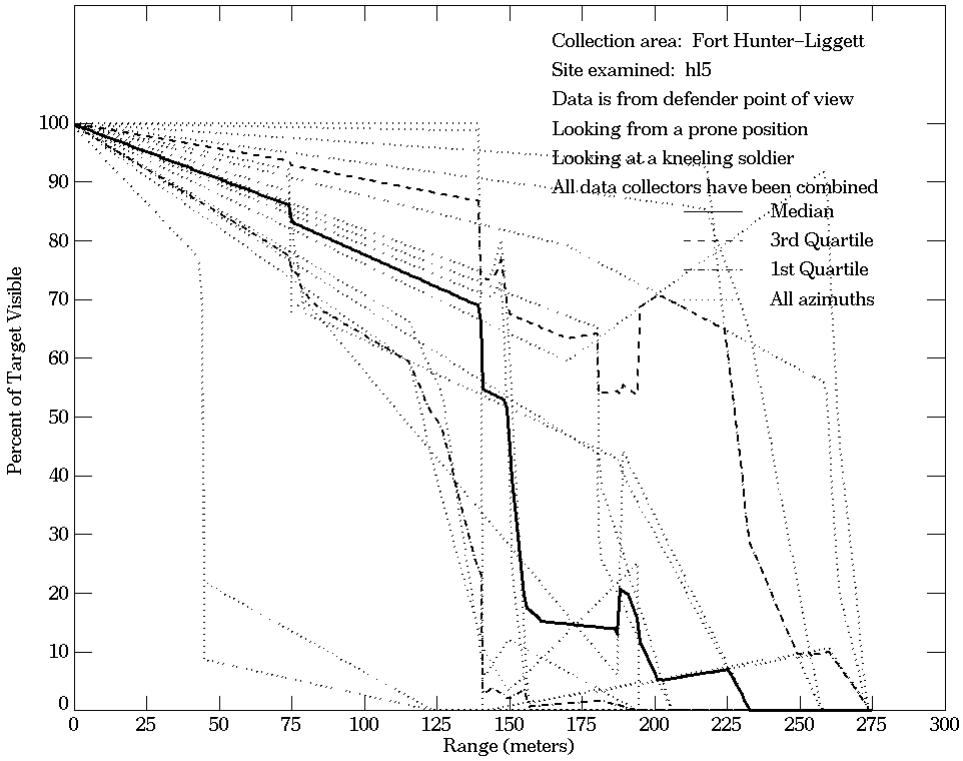

Figure E-51. Fort Hunter-Liggett, From Defender Point of View, Site hl5

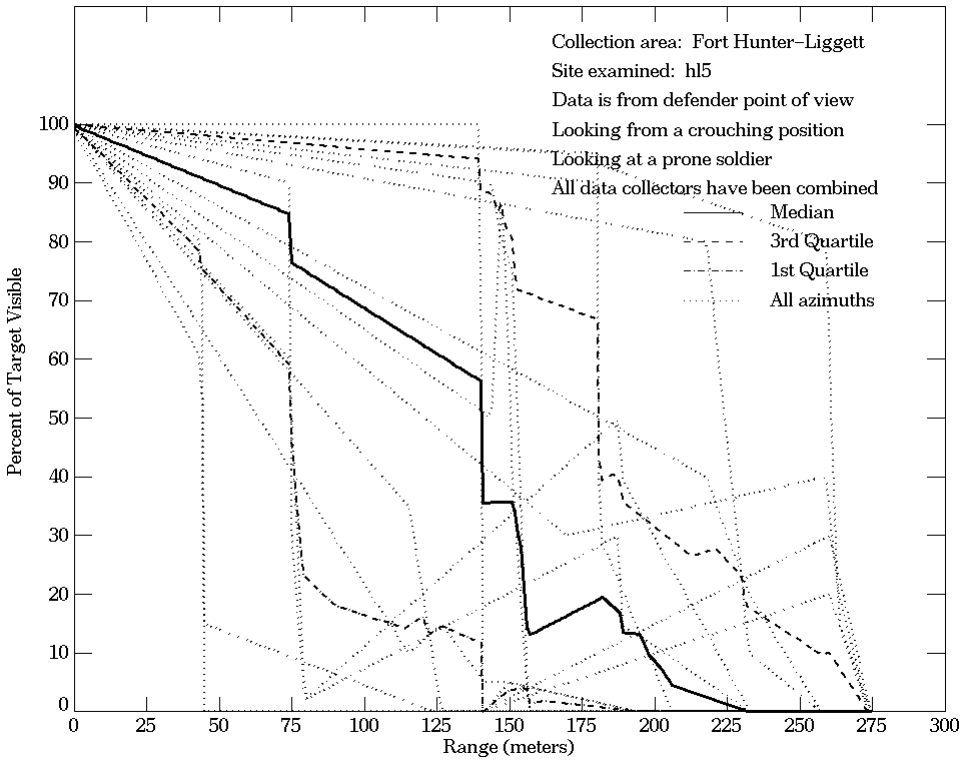

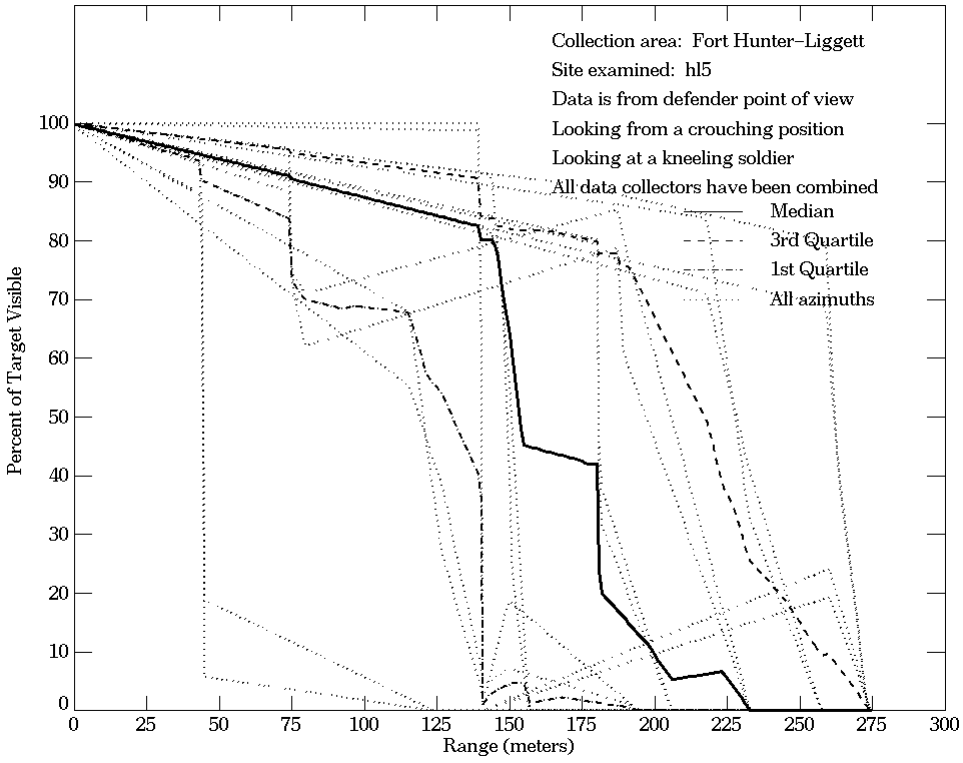

Figure E-51. Fort Hunter-Liggett, From Defender Point of View, Site hl5 (Continued)

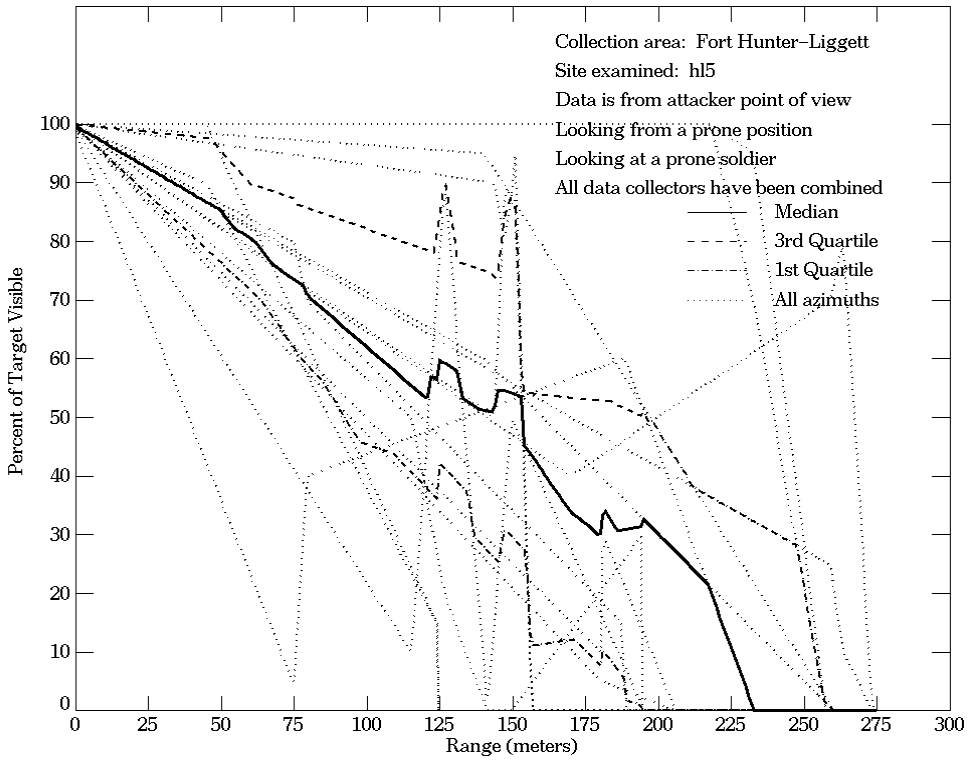

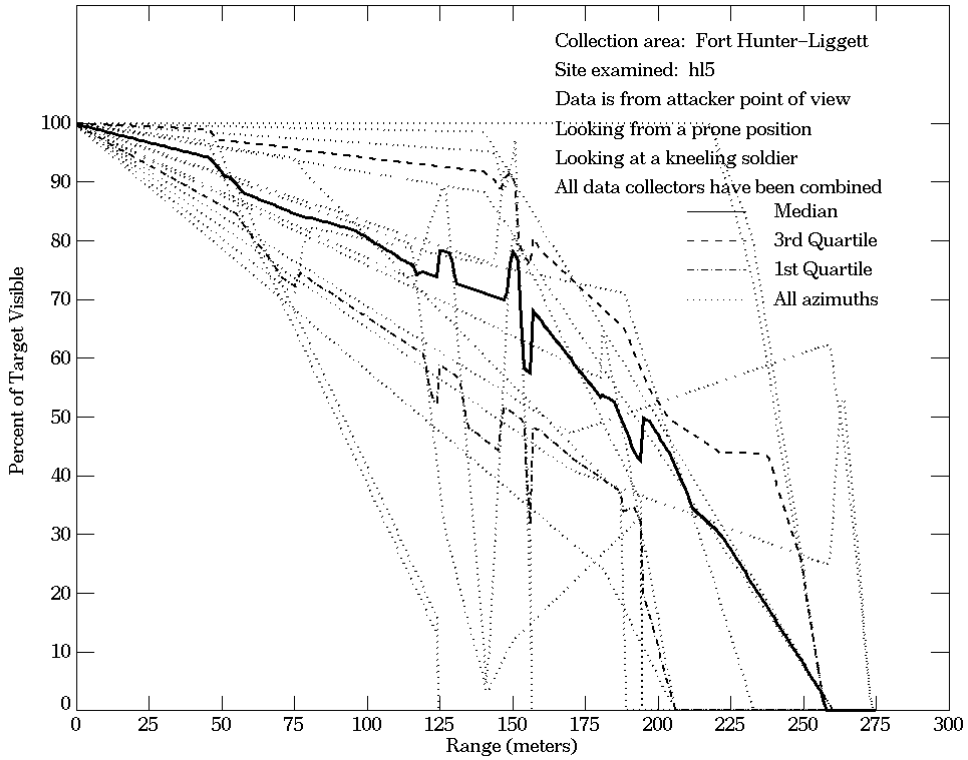

Figure E-52. Fort Hunter-Liggett, From Attacker Point of View, Site hl5

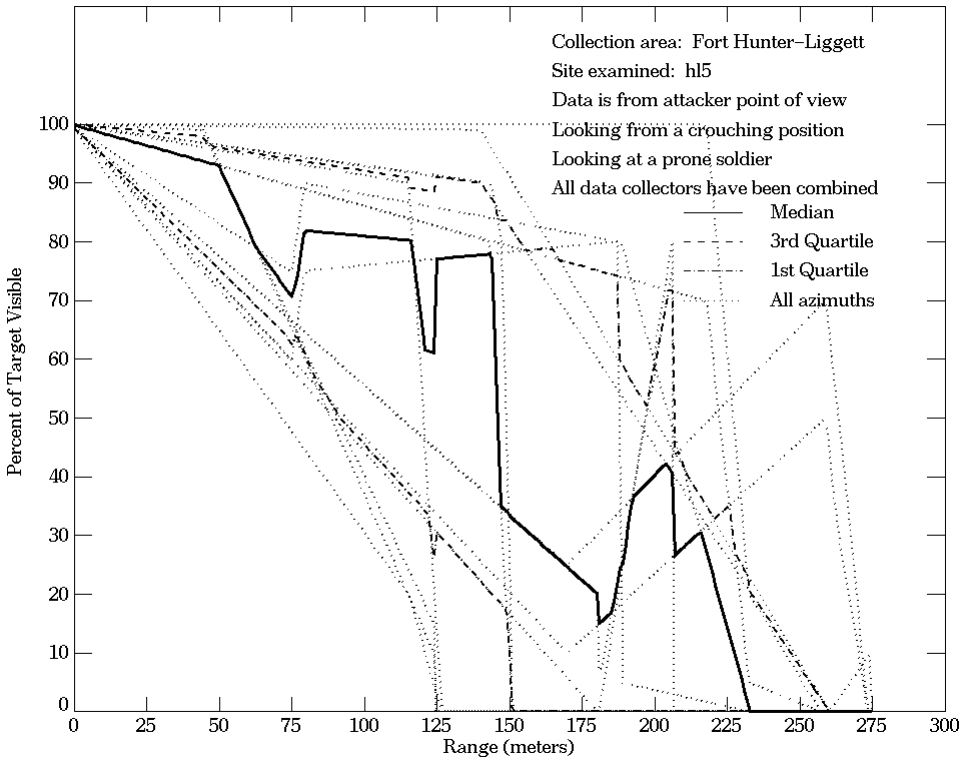

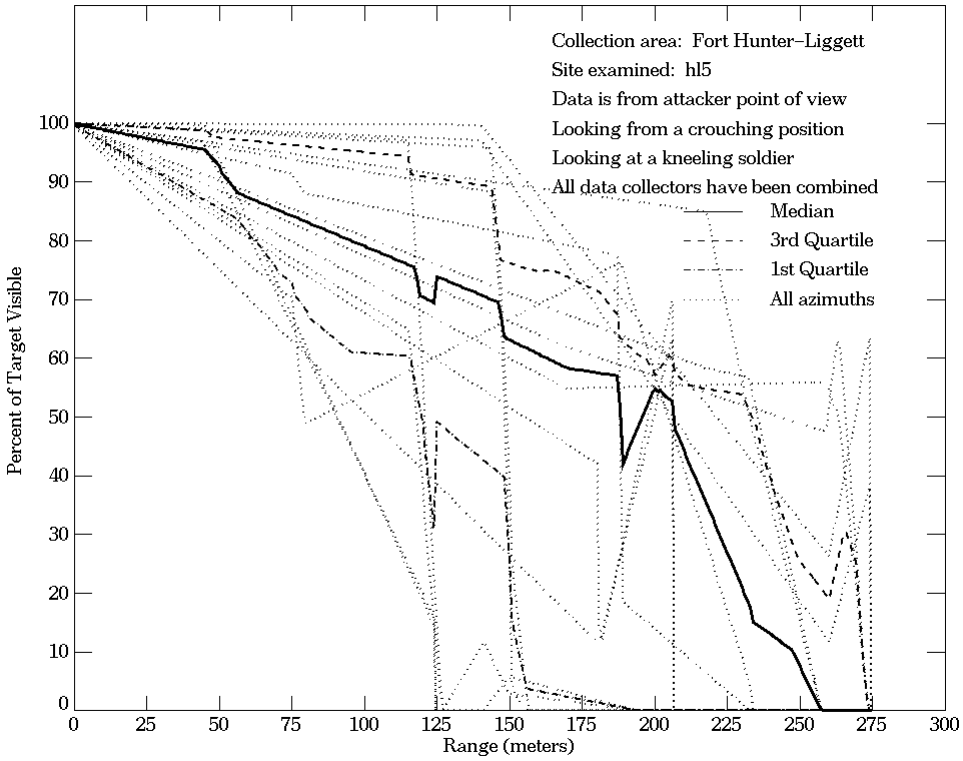

Figure E-52. Fort Hunter-Liggett, From Attacker Point of View, Site hl5 (Continued)

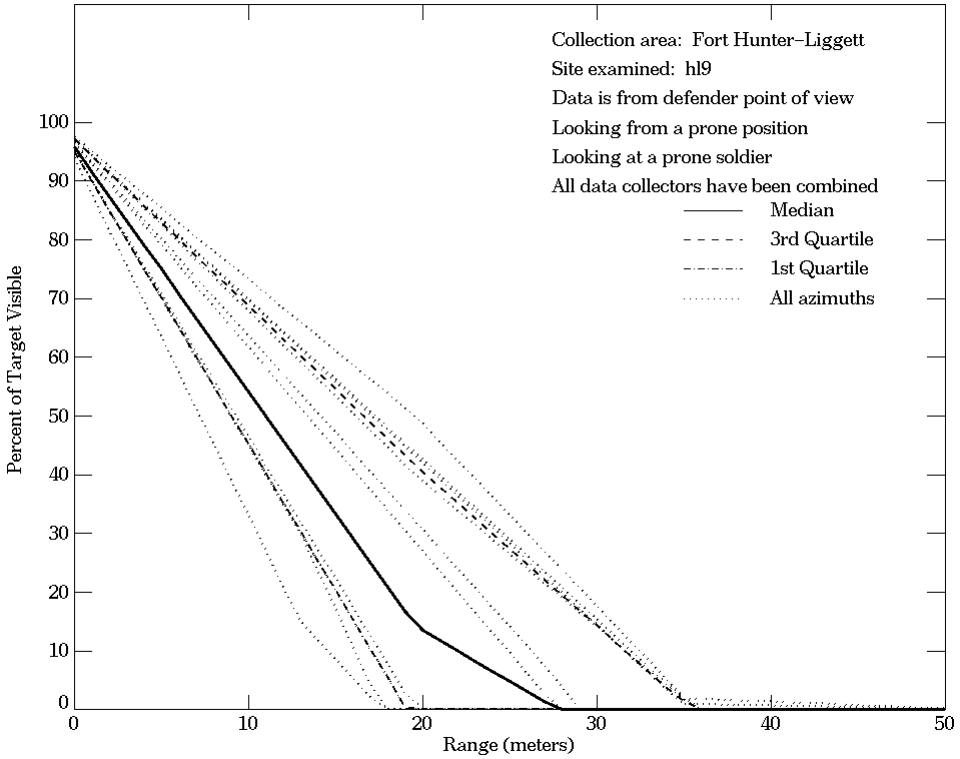

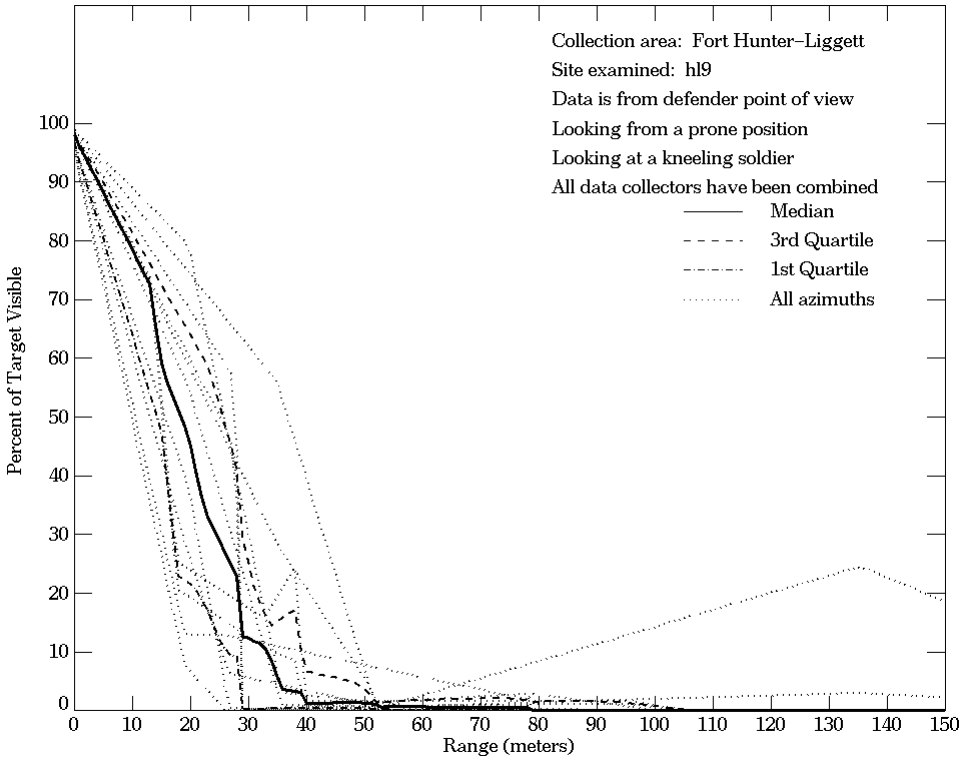

Figure E-53. Fort Hunter-Liggett, From Defender Point of View, Site hl9

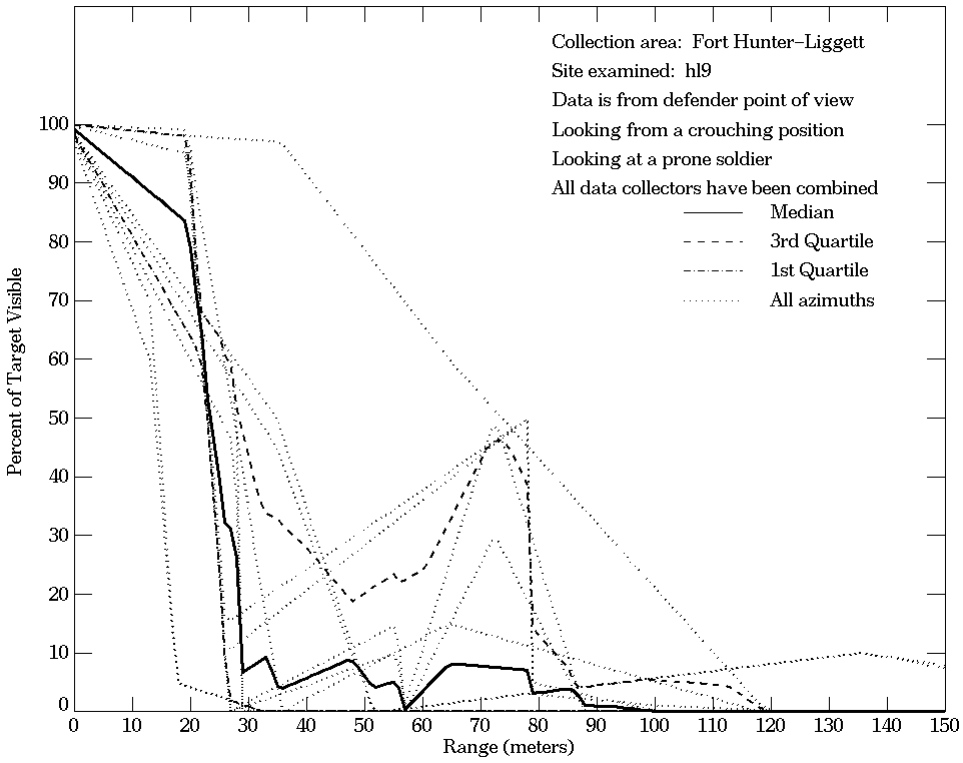

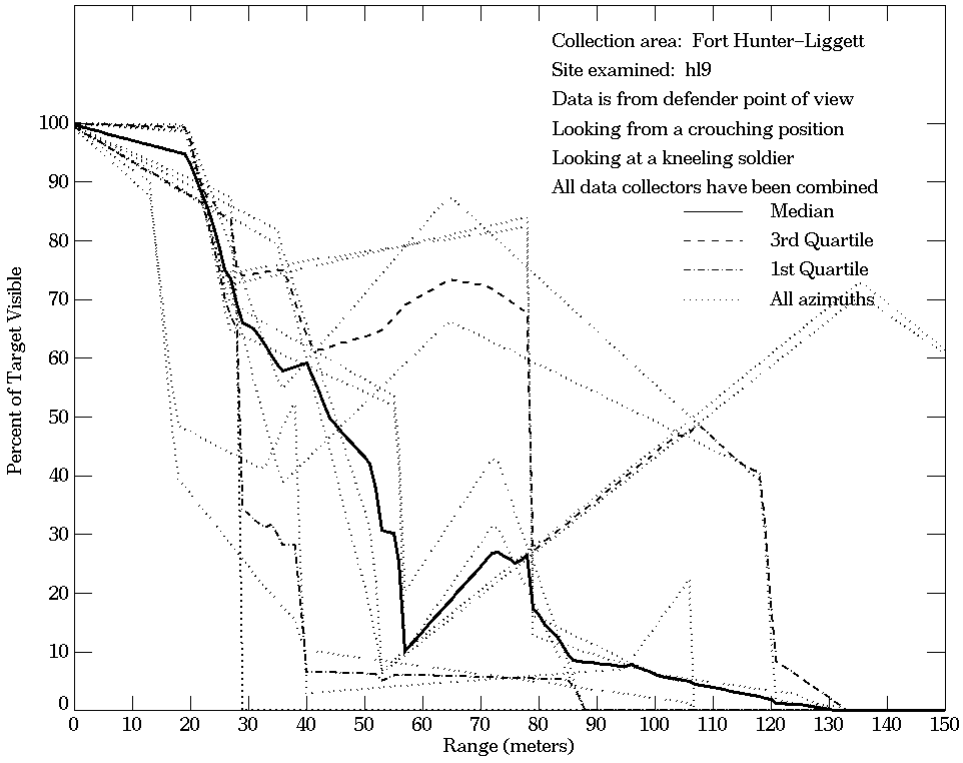

Figure E-53. Fort Hunter-Liggett, From Defender Point of View, Site hl9 (Continued)

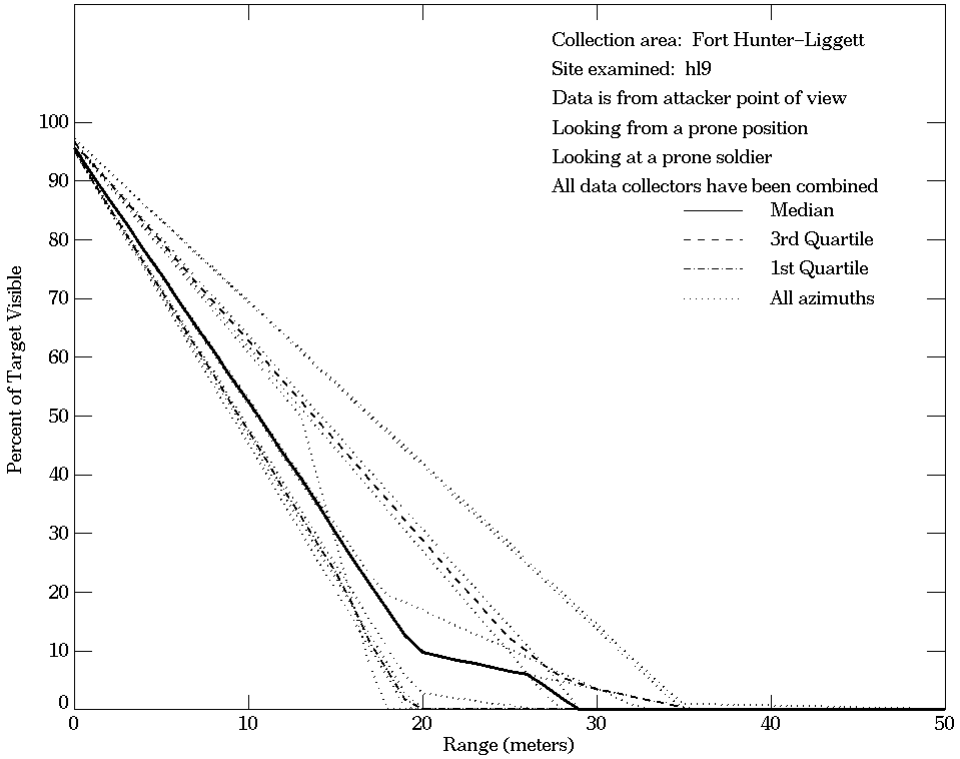

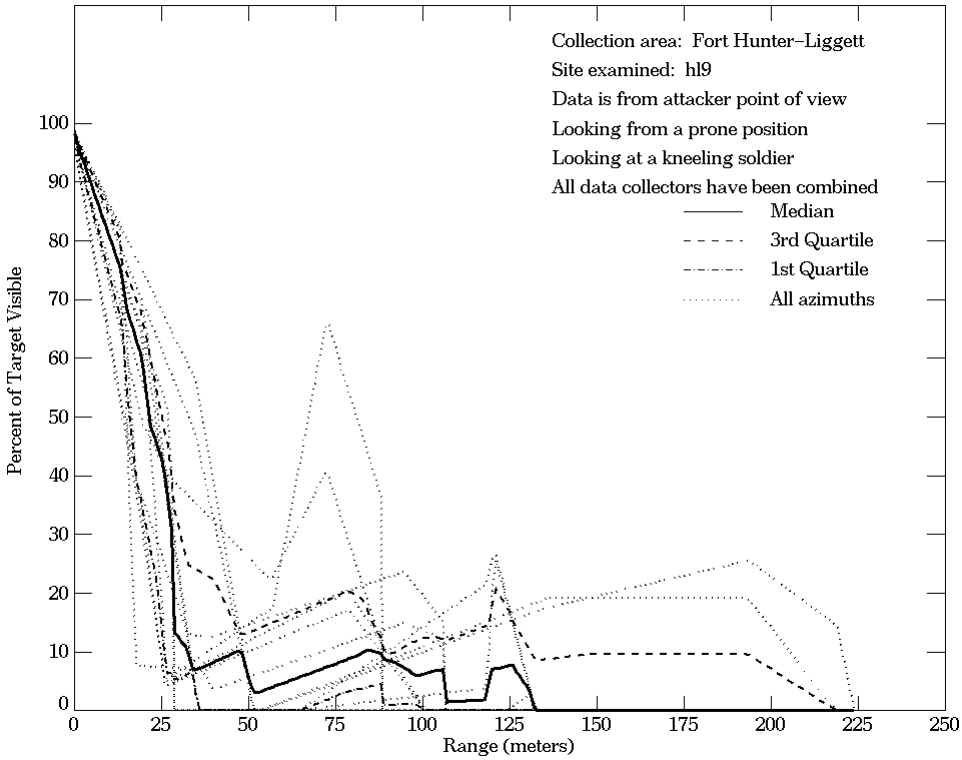

Figure E-54. Fort Hunter-Liggett, From Attacker Point of View, Site hl9

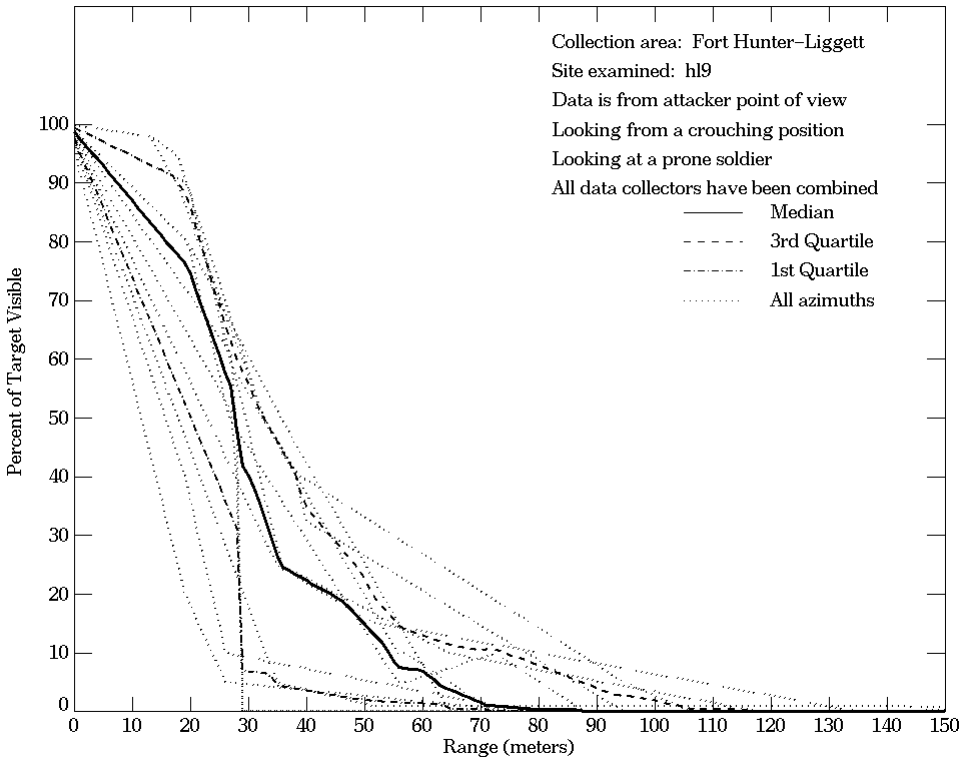

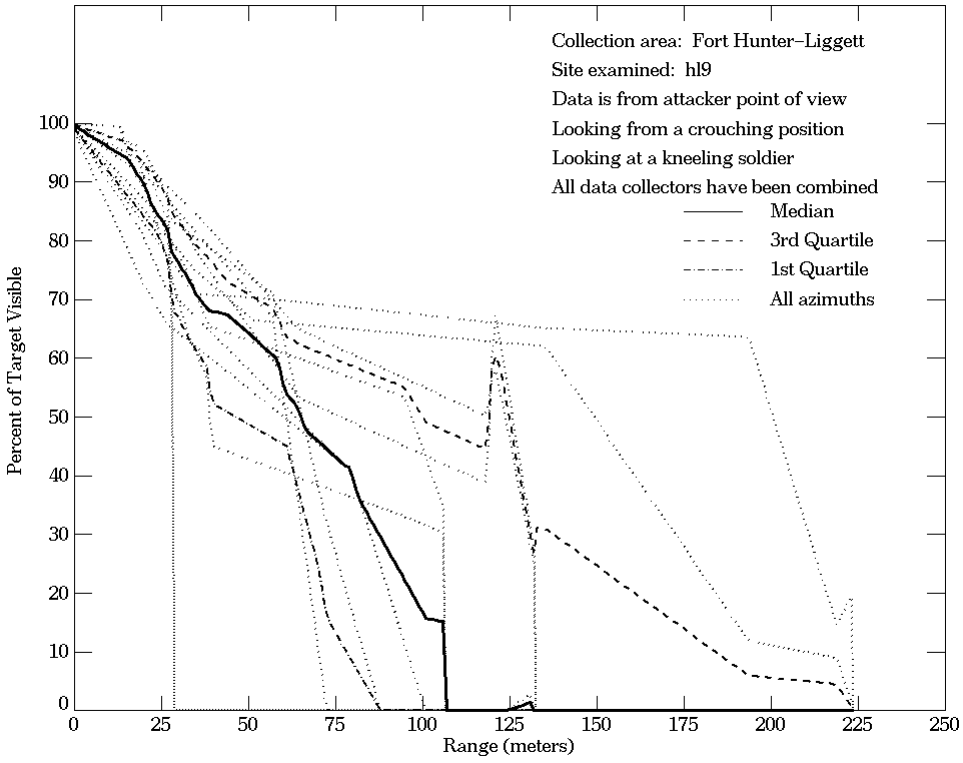

Figure E-54. Fort Hunter-Liggett, From Attacker Point of View, Site hl9 (Continued)

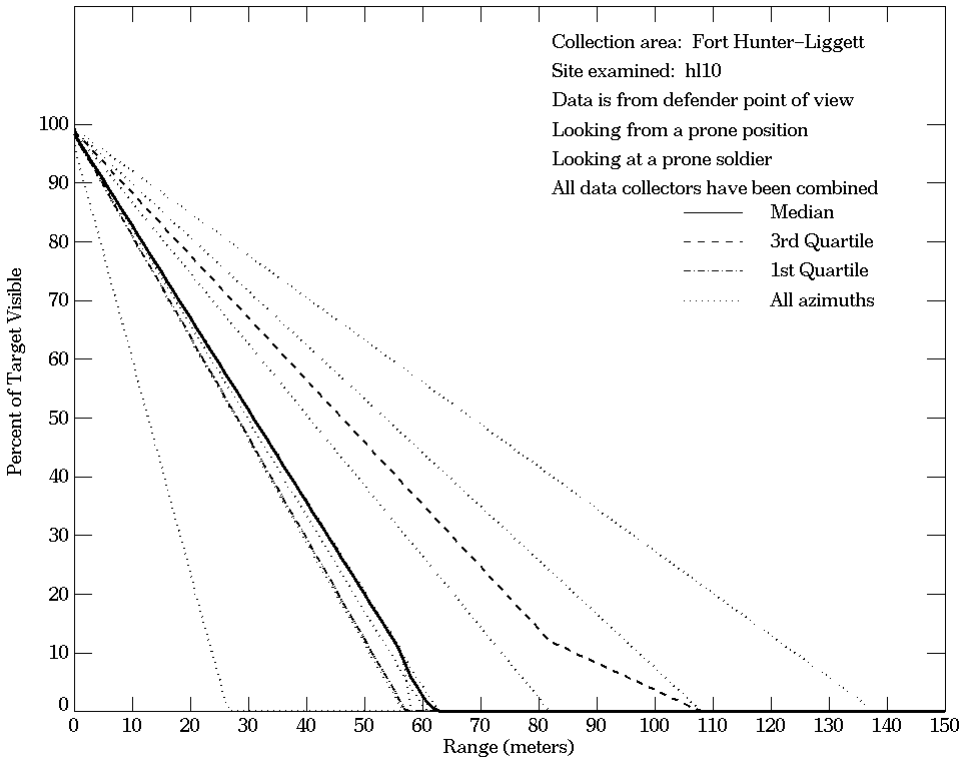

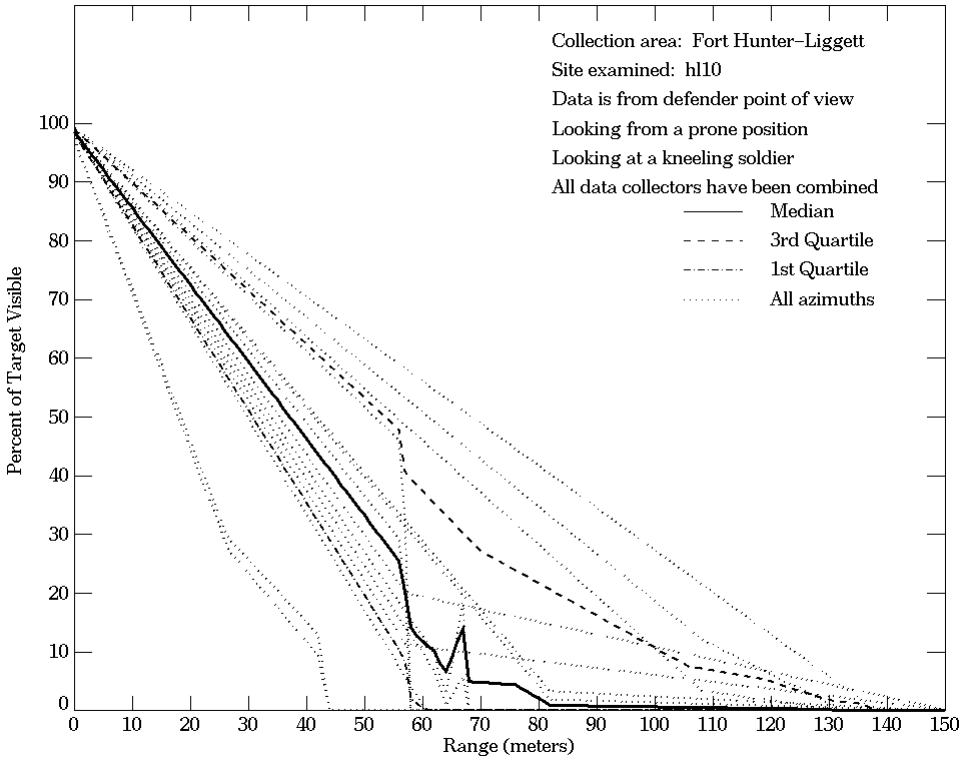

Figure E-55. Fort Hunter-Liggett, From Defender Point of View, Site hl10

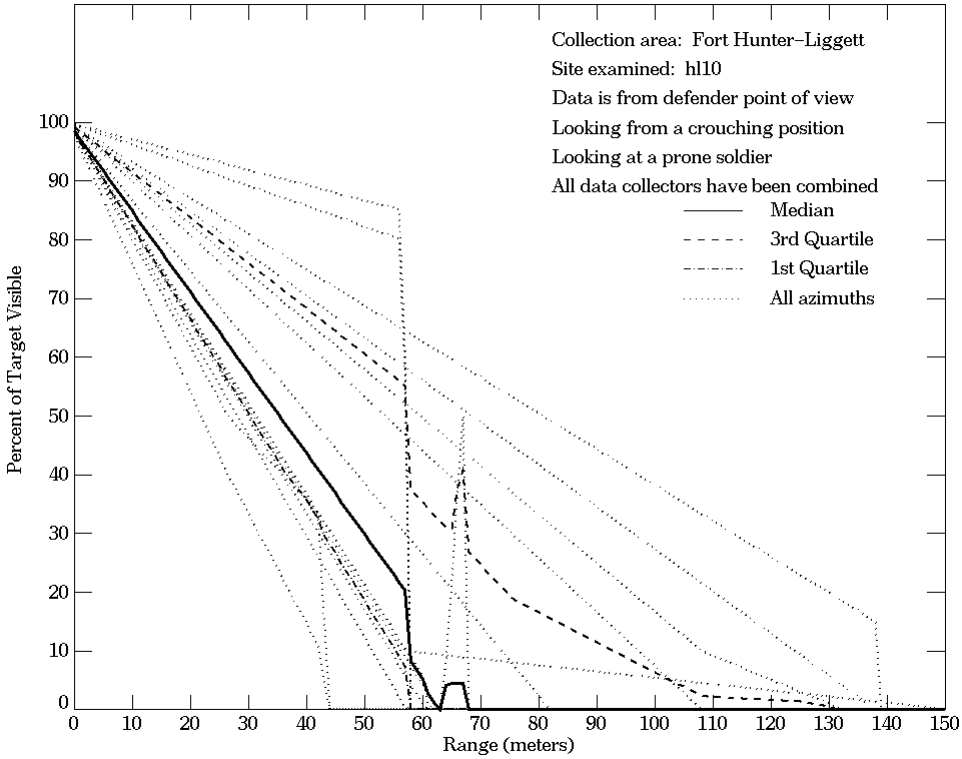

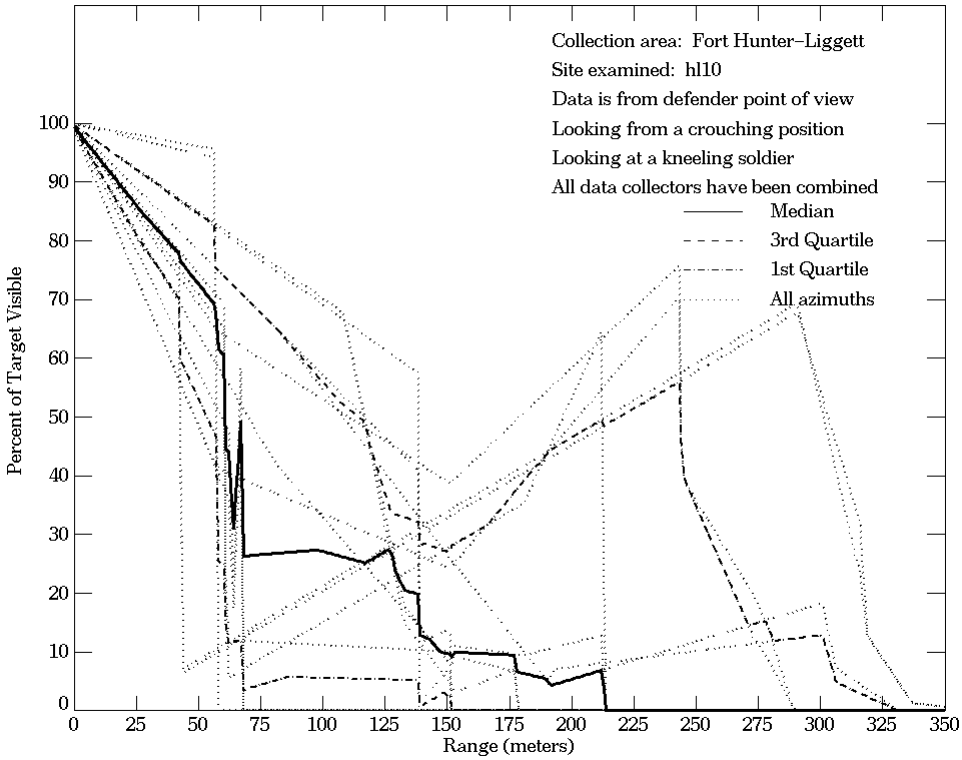

Figure E-55. Fort Hunter-Liggett, From Defender Point of View, Site hl10 (Continued)

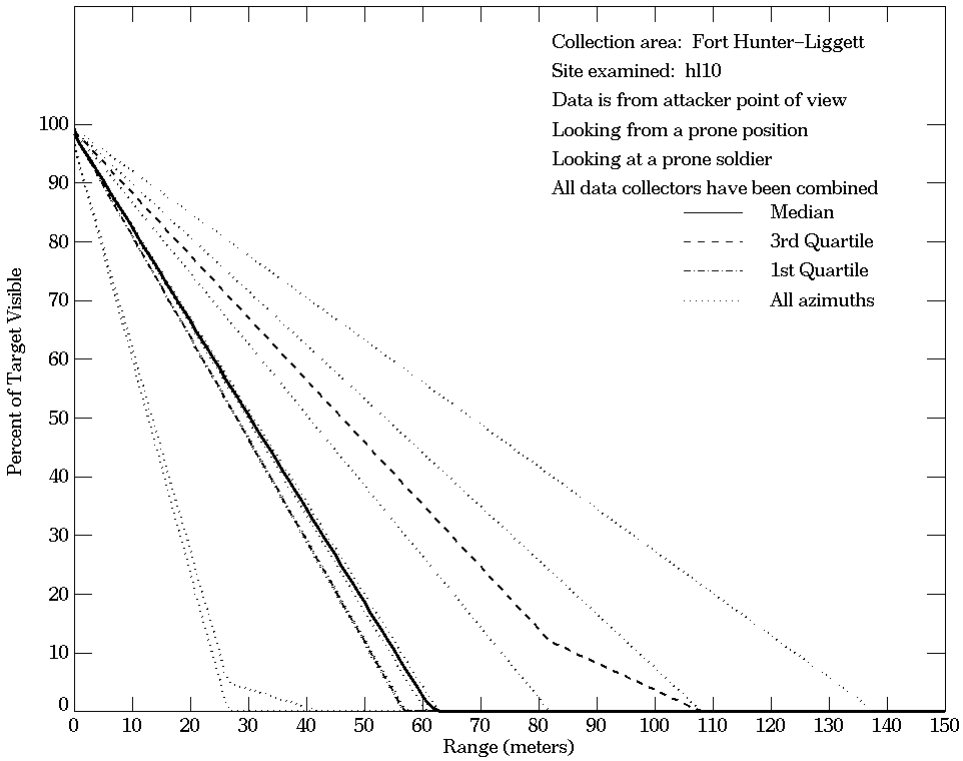

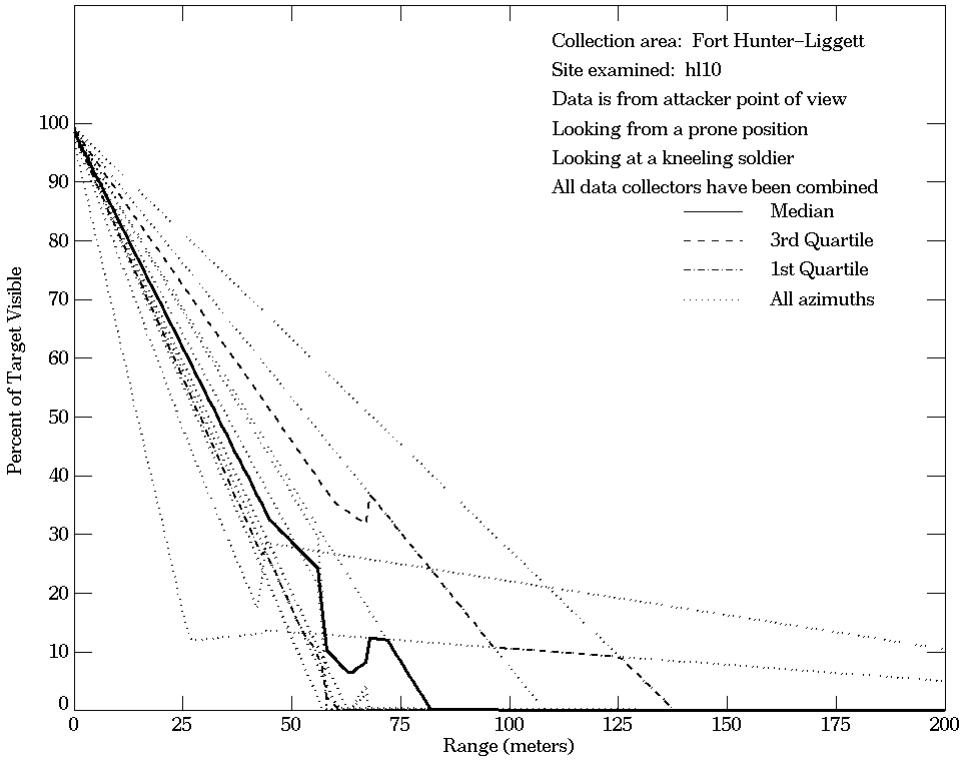

Figure E-56. Fort Hunter-Liggett, From Attacker Point of View, Site hl10

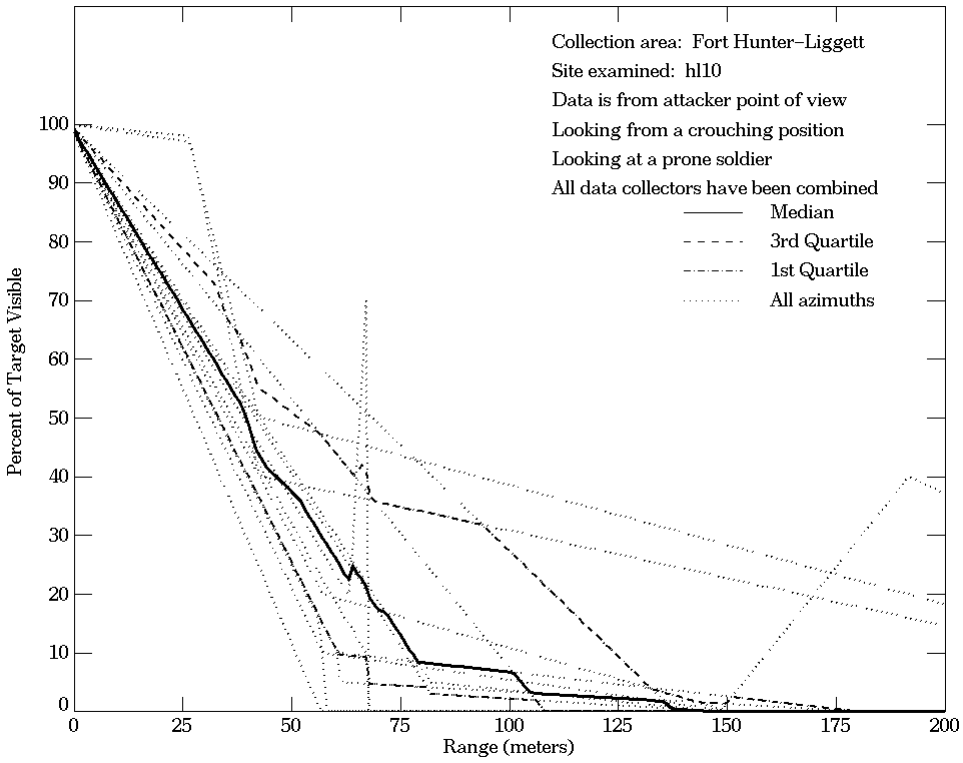

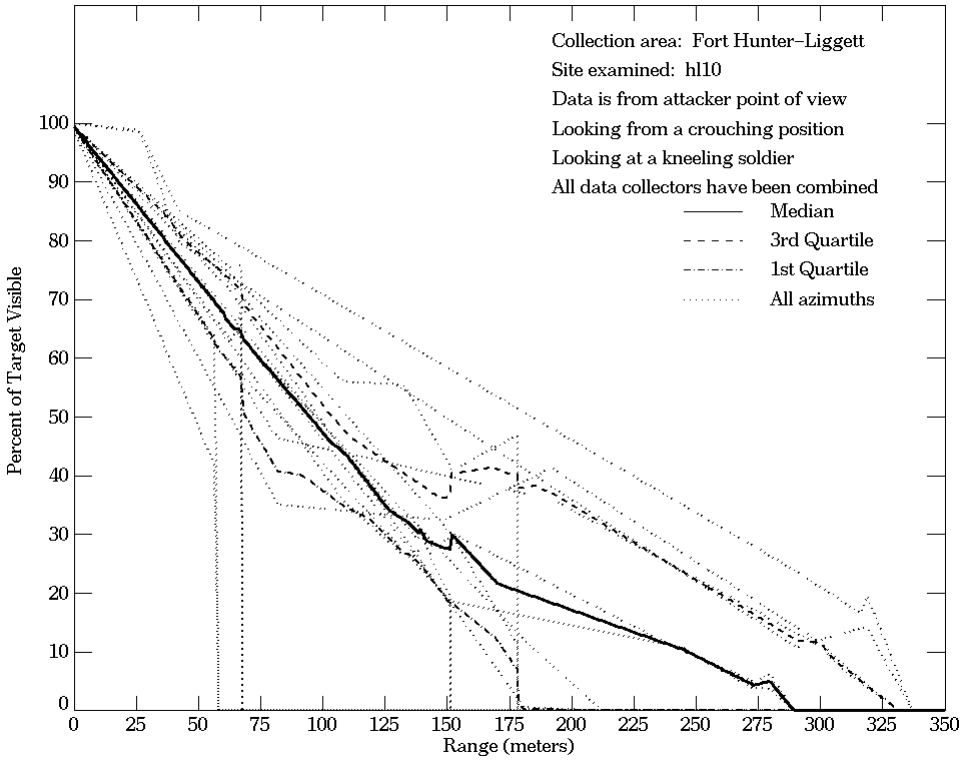

Figure E-56. Fort Hunter-Liggett, From Attacker Point of View, Site hl10 (Continued)

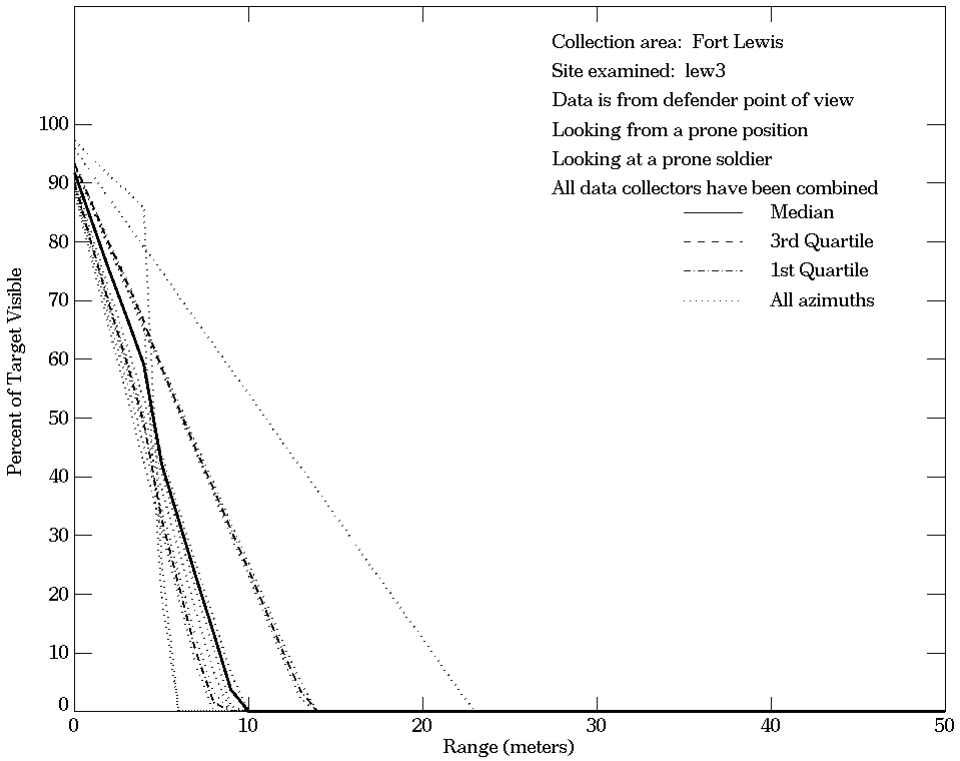

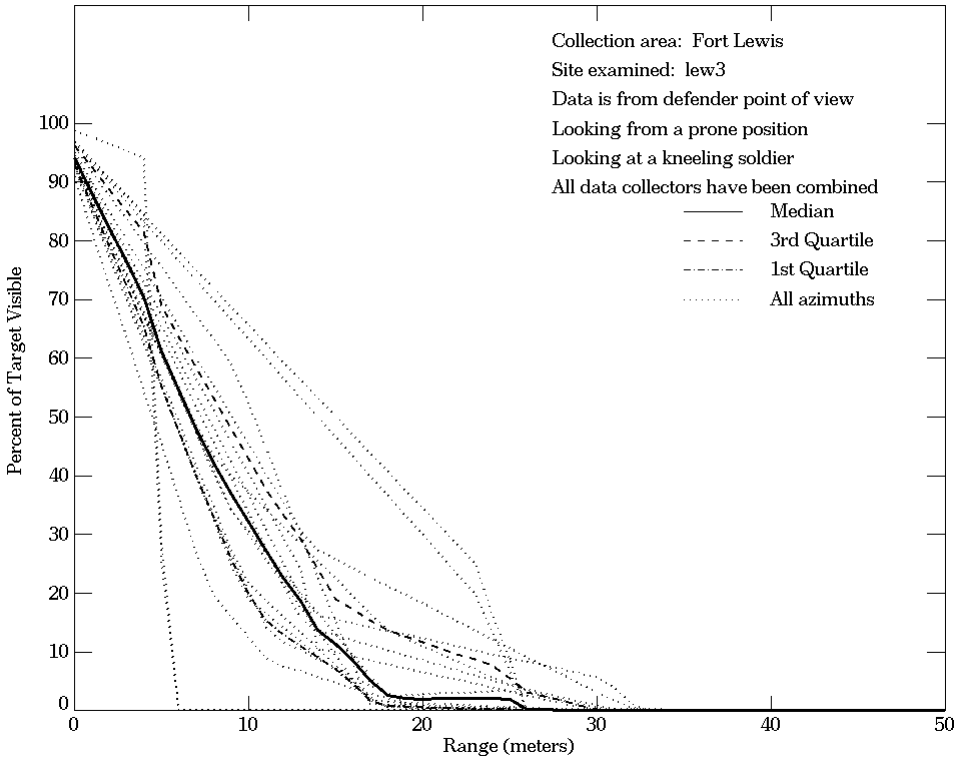

Figure E-57. Fort Lewis, From Defender Point of View, Site lew3

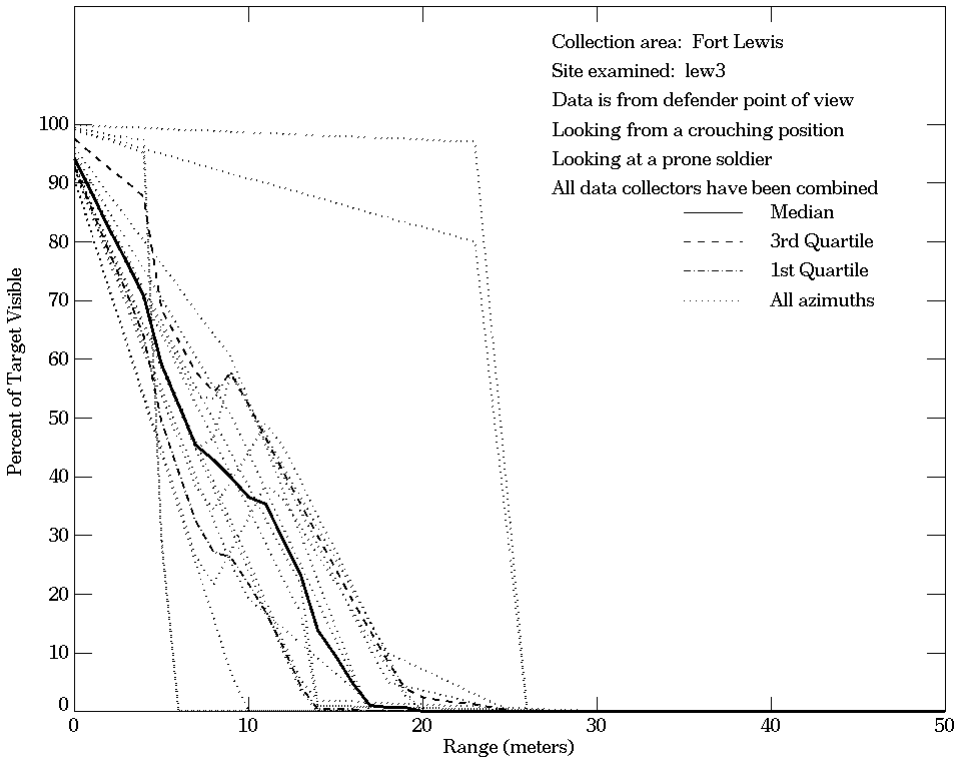

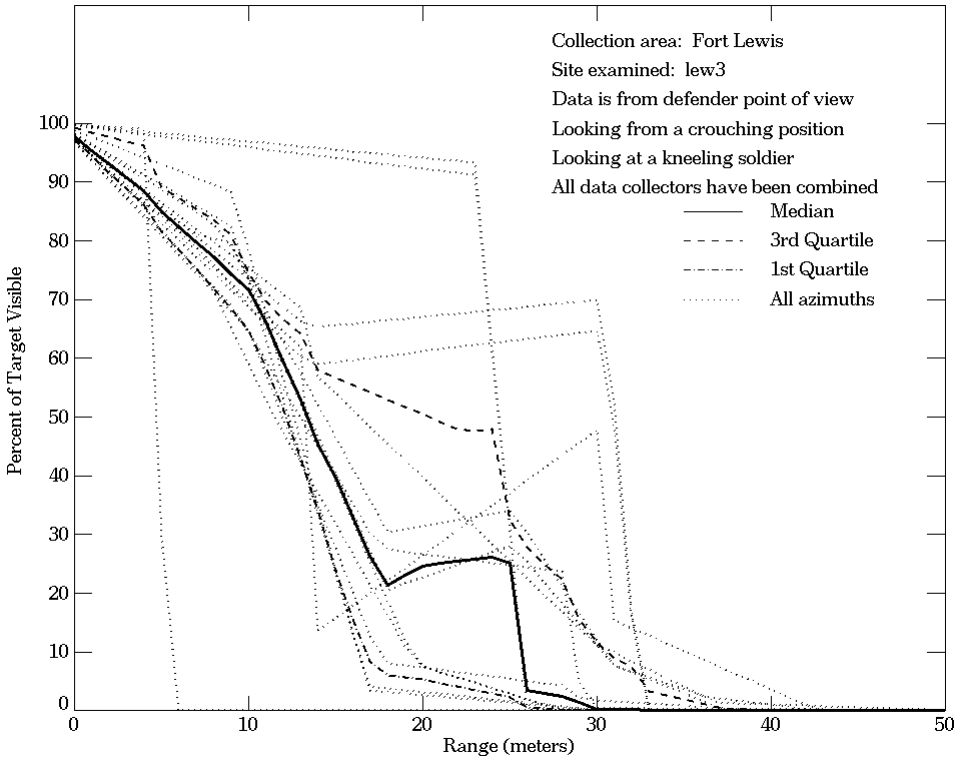

Figure E-57. Fort Lewis, From Defender Point of View, Site lew3 (Continued)

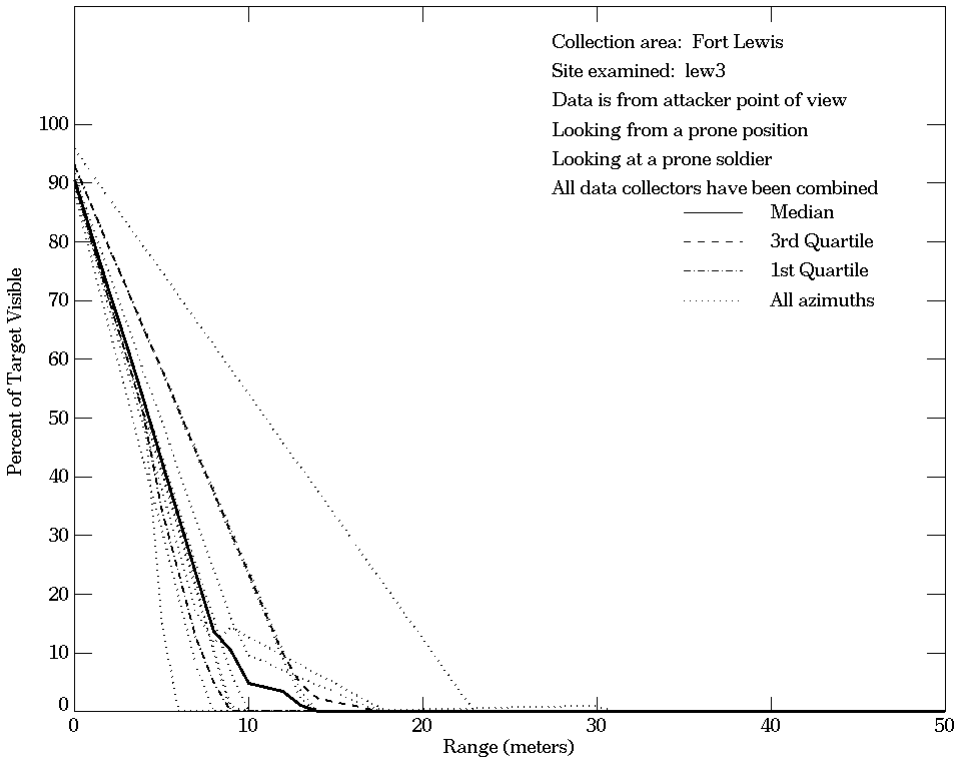

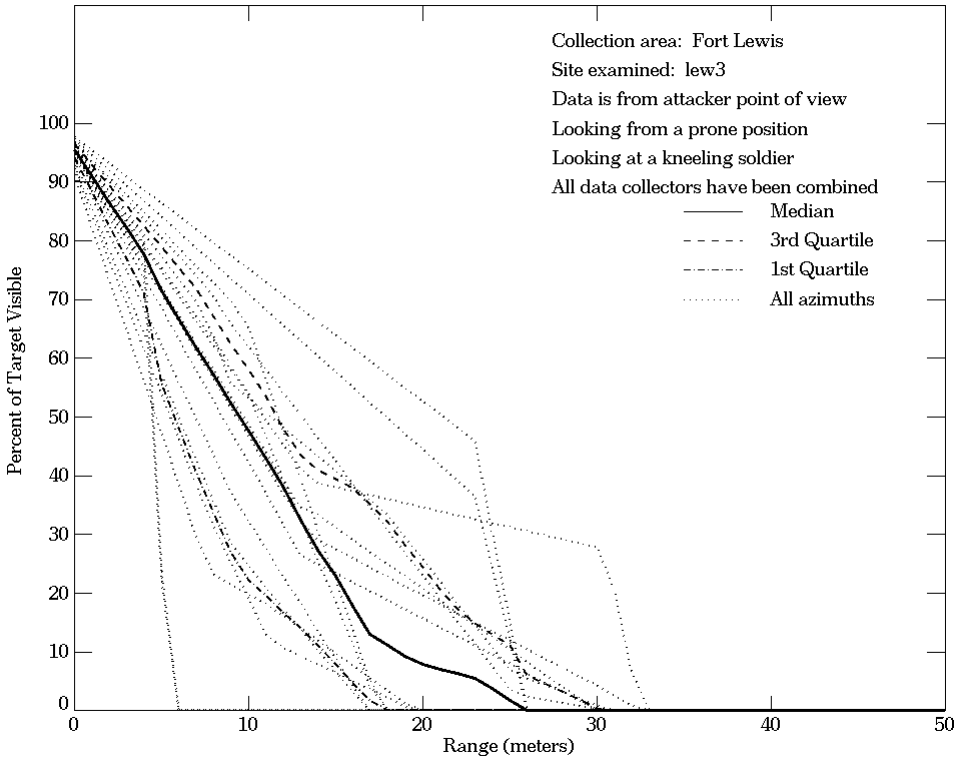

Figure E-58. Fort Lewis, From Attacker Point of View, Site lew3

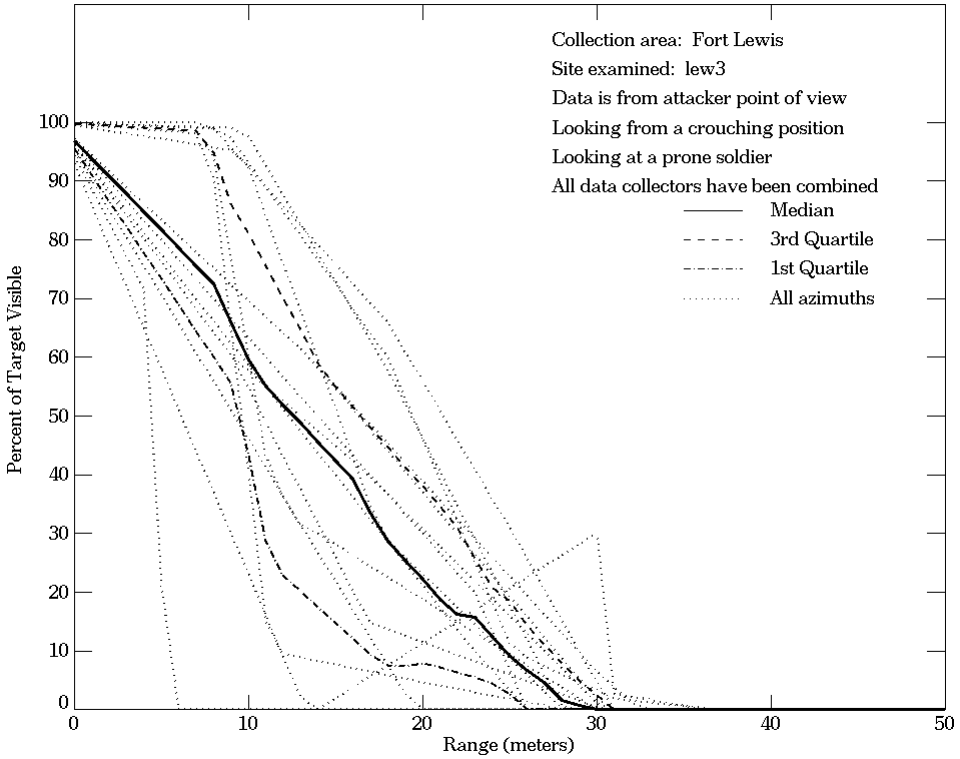

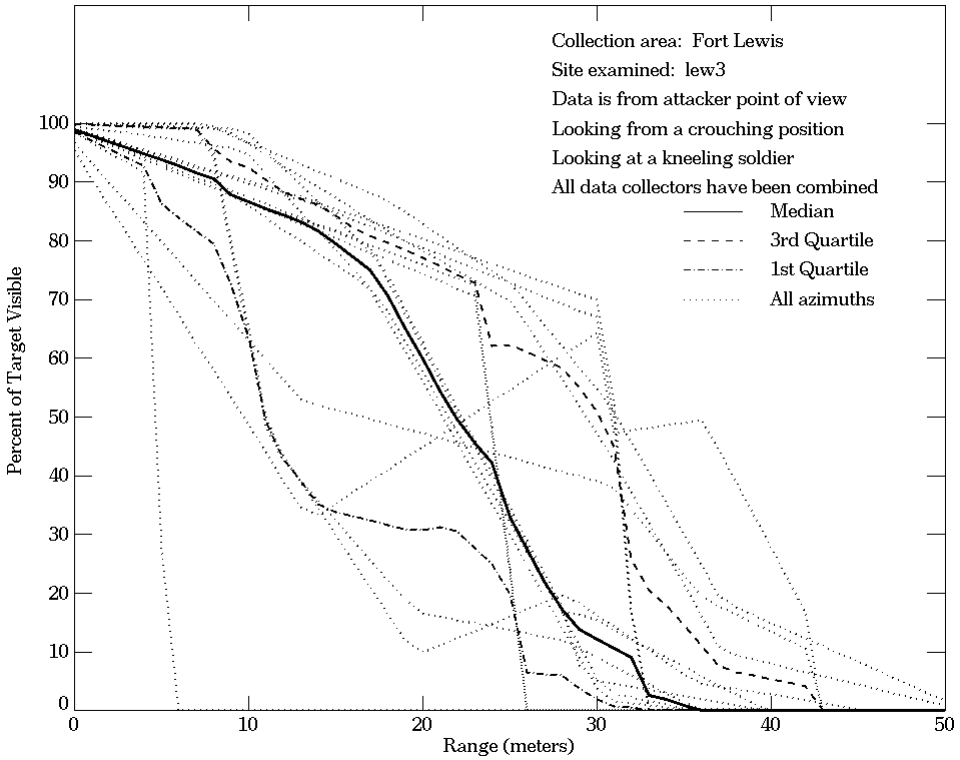

Figure E-58. Fort Lewis, From Attacker Point of View, Site lew3 (Continued)

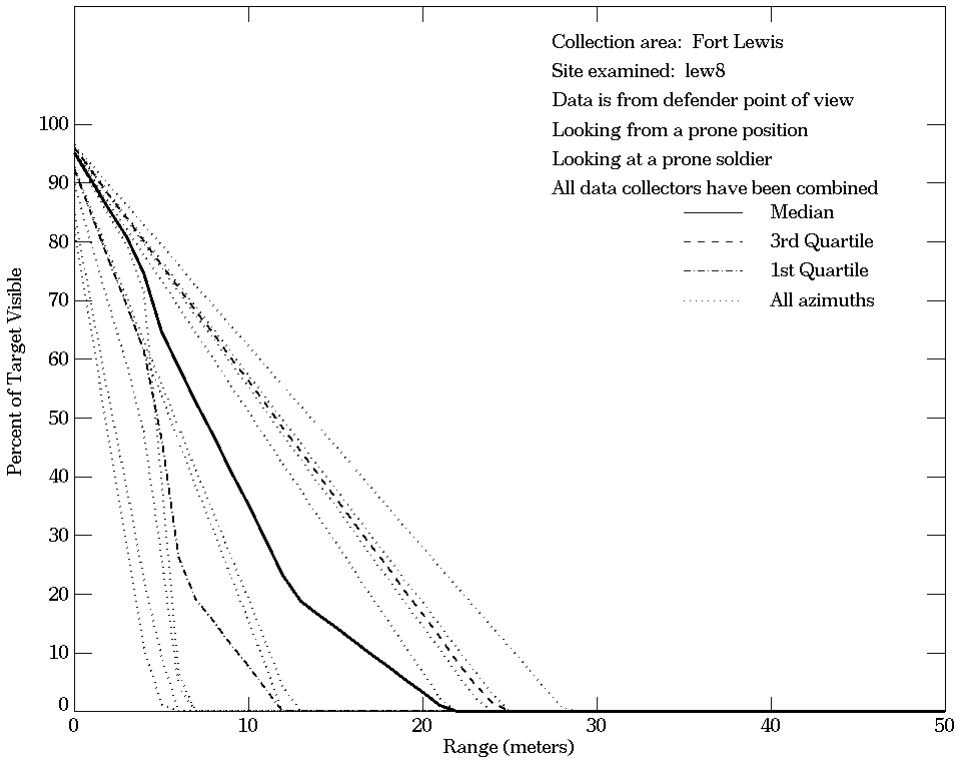

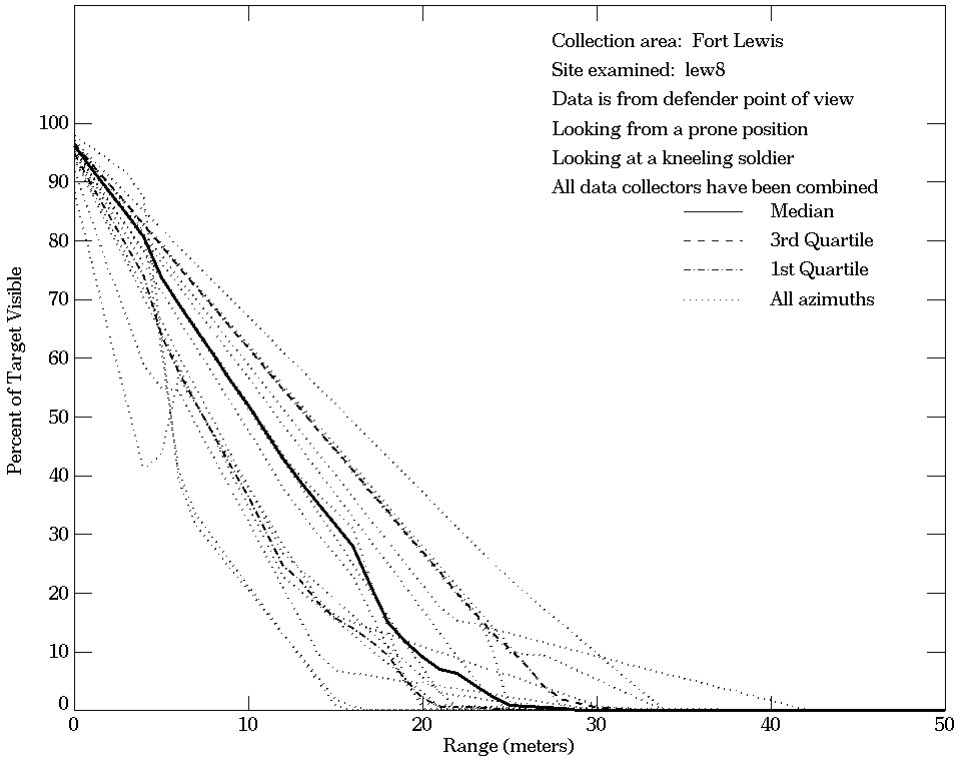

Figure E-59. Fort Lewis, From Defender Point of View, Site lew8

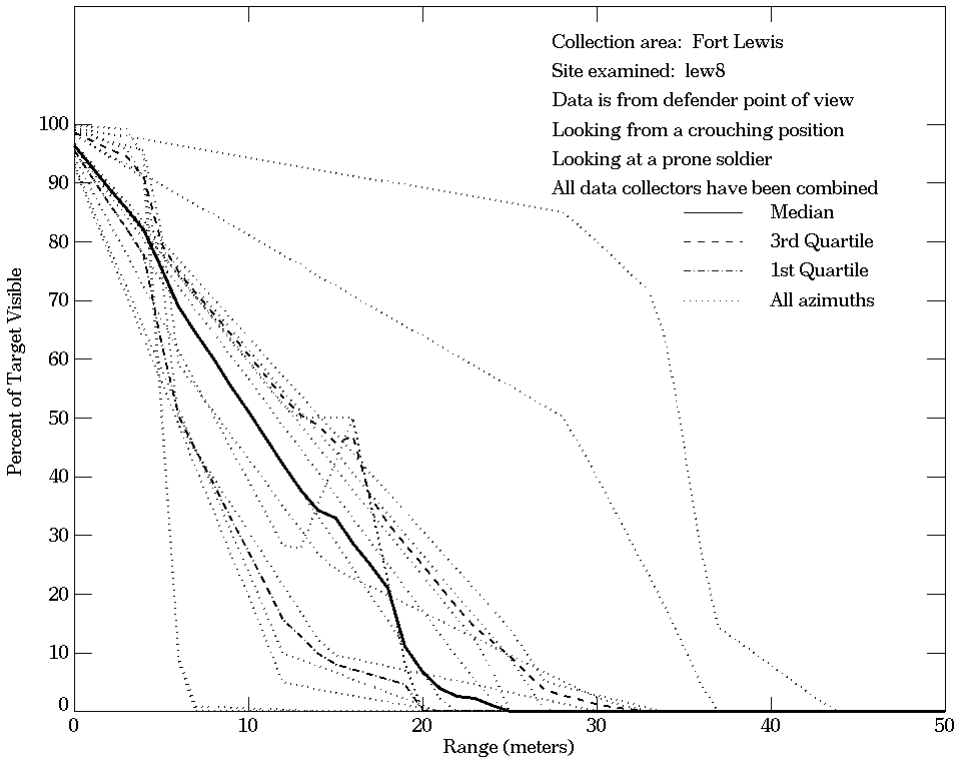

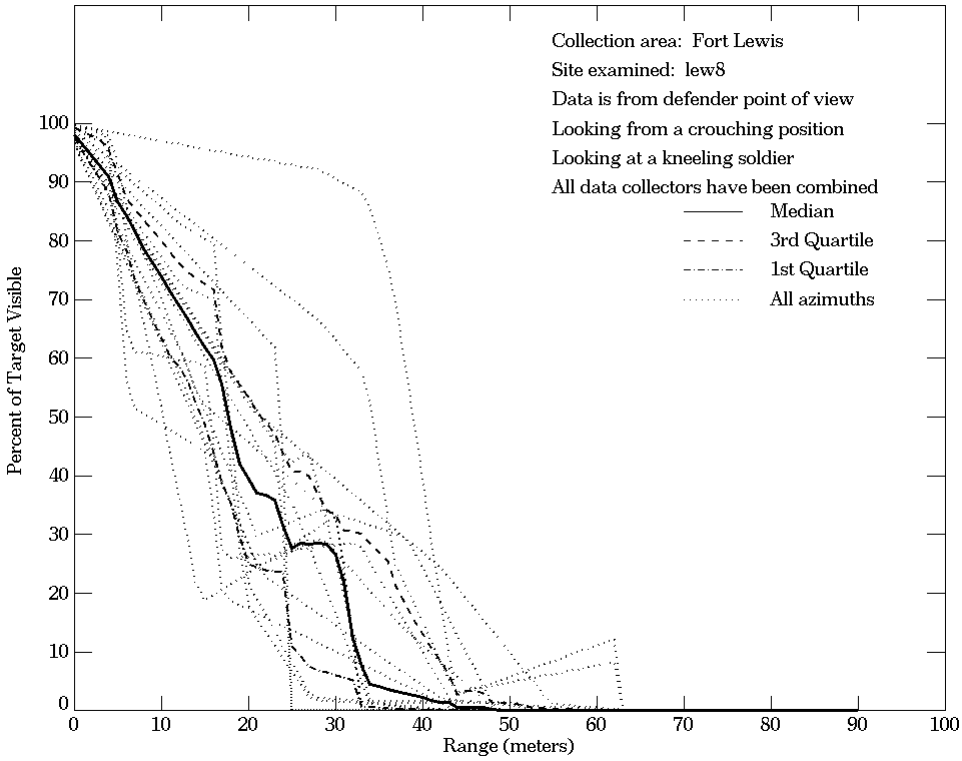

Figure E-59. Fort Lewis, From Defender Point of View, Site lew8 (Continued)

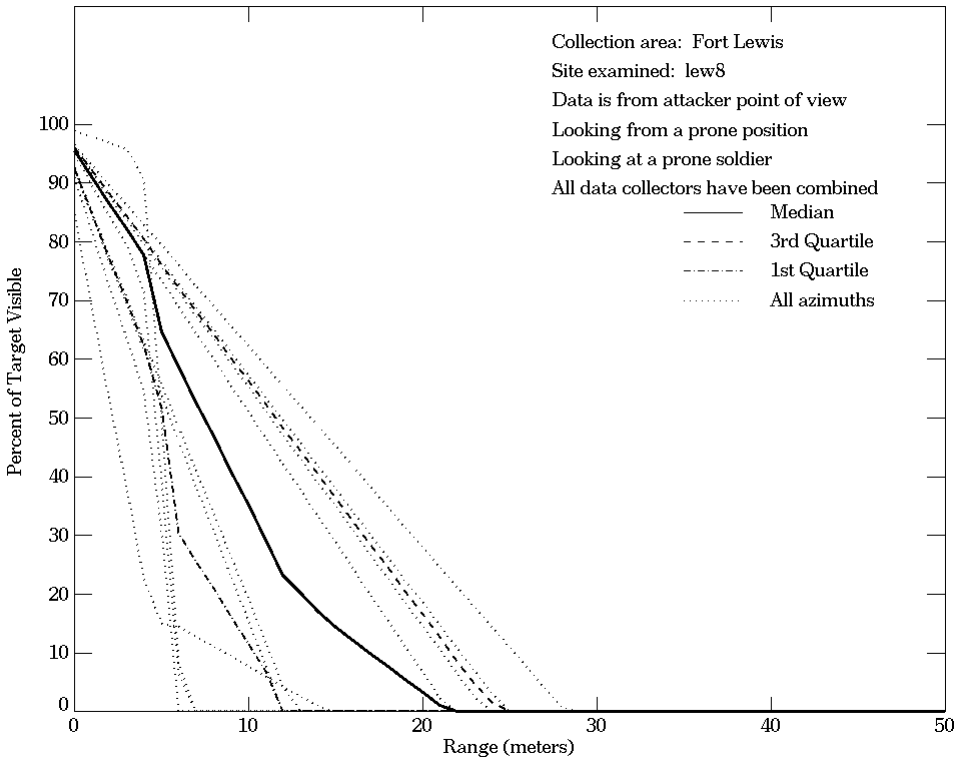

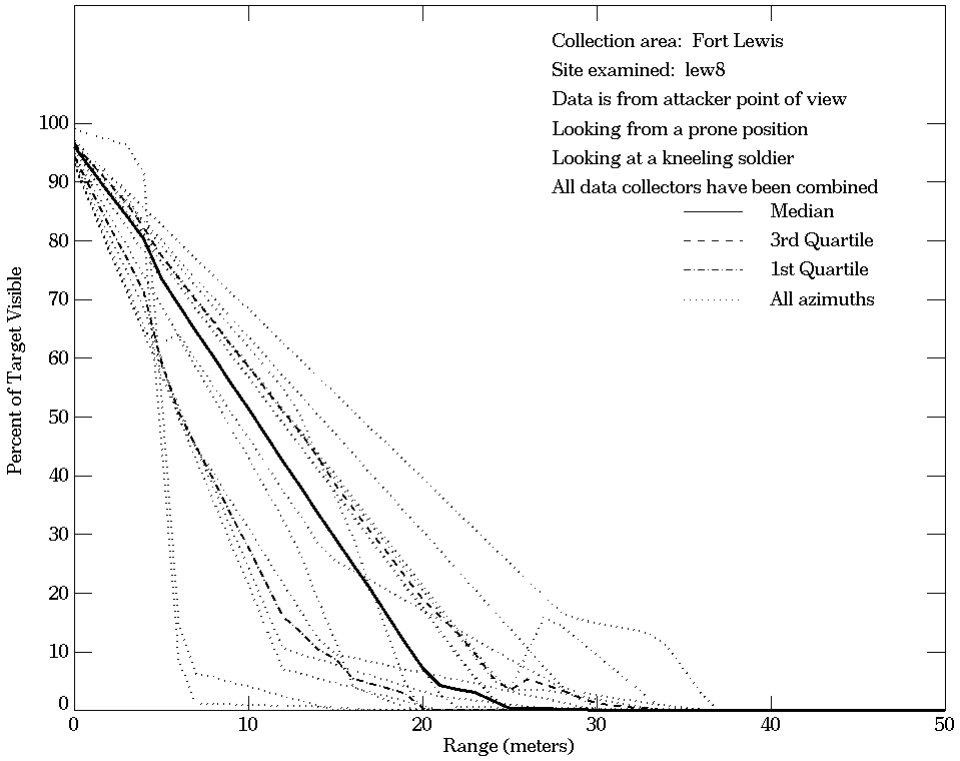

Figure E-60. Fort Lewis, From Attacker Point of View, Site lew8

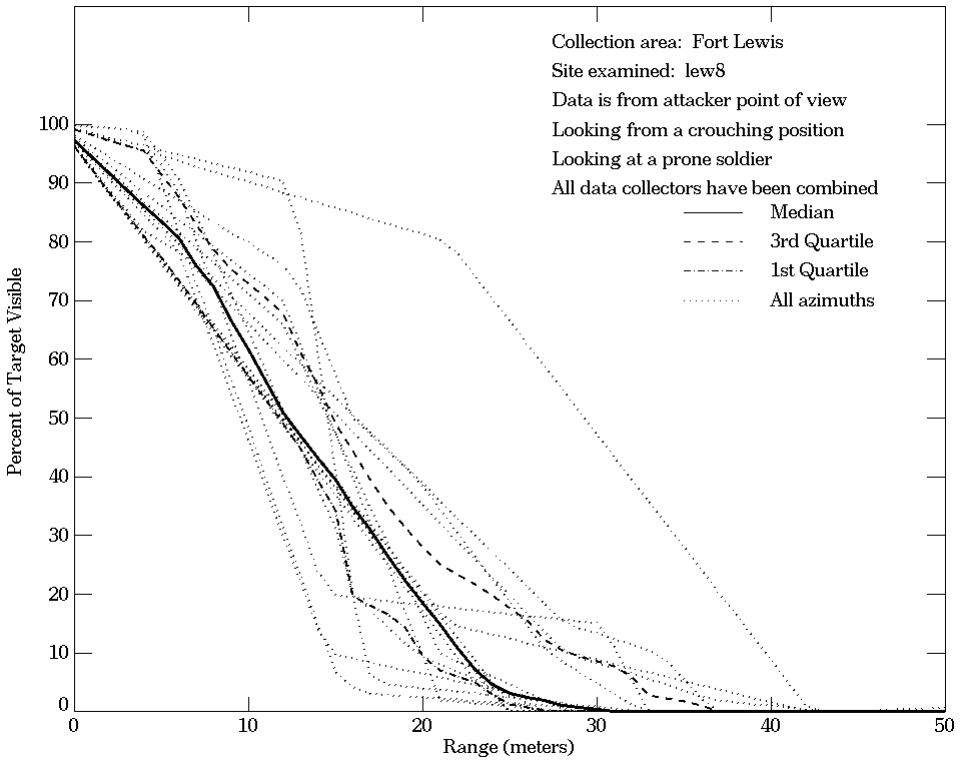

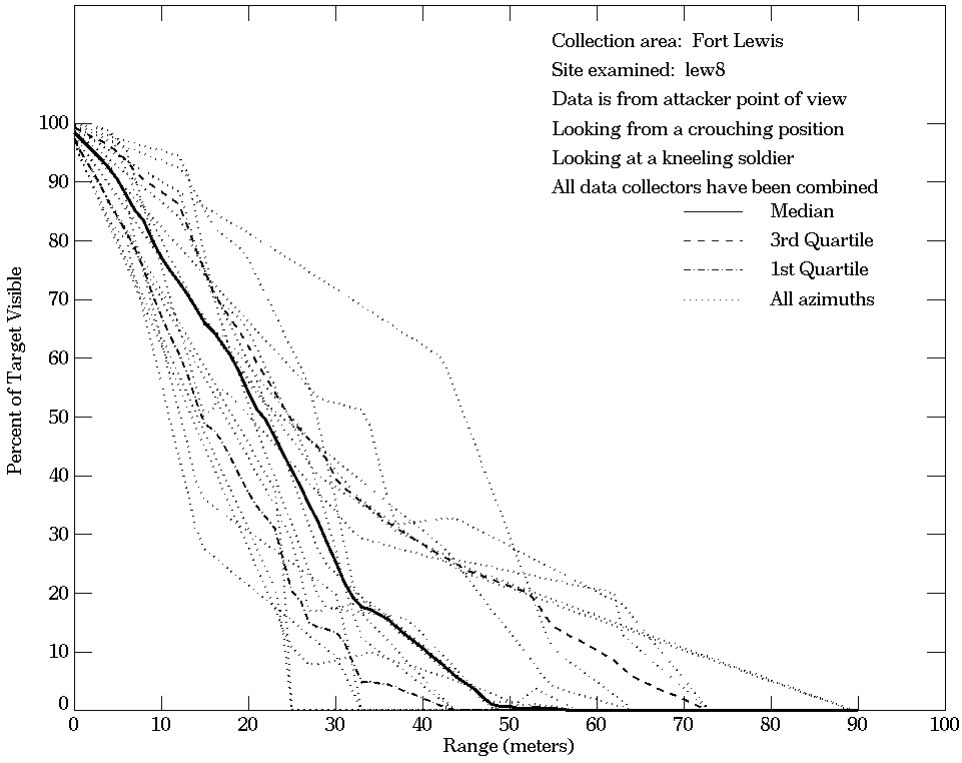

Figure E-60. Fort Lewis, From Attacker Point of View, Site lew8 (Continued)

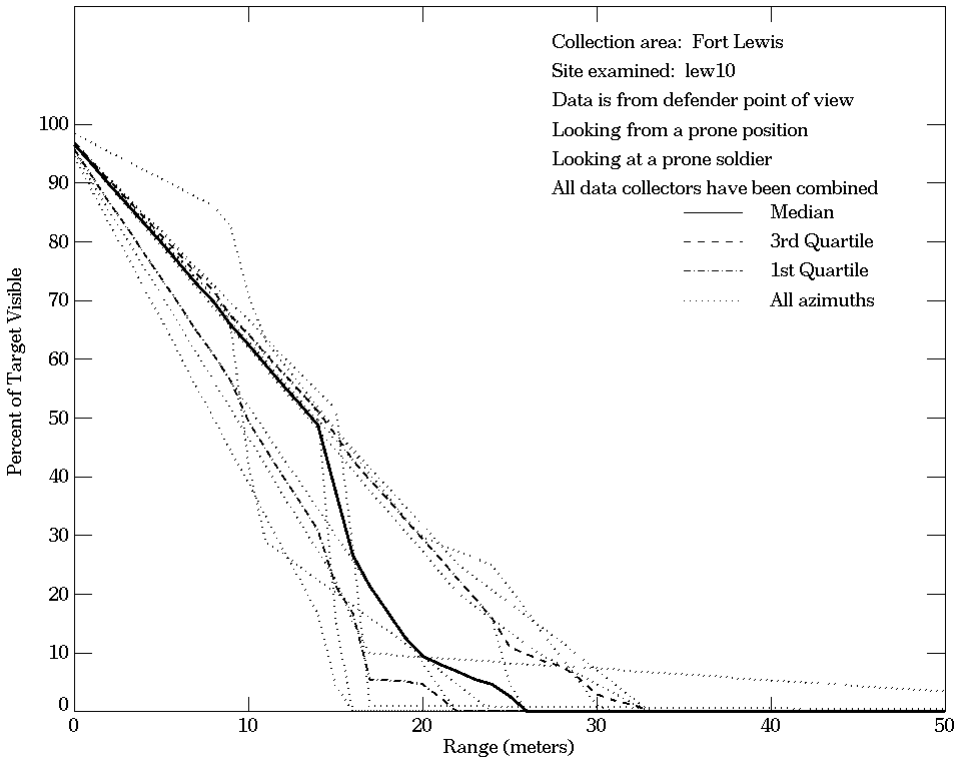

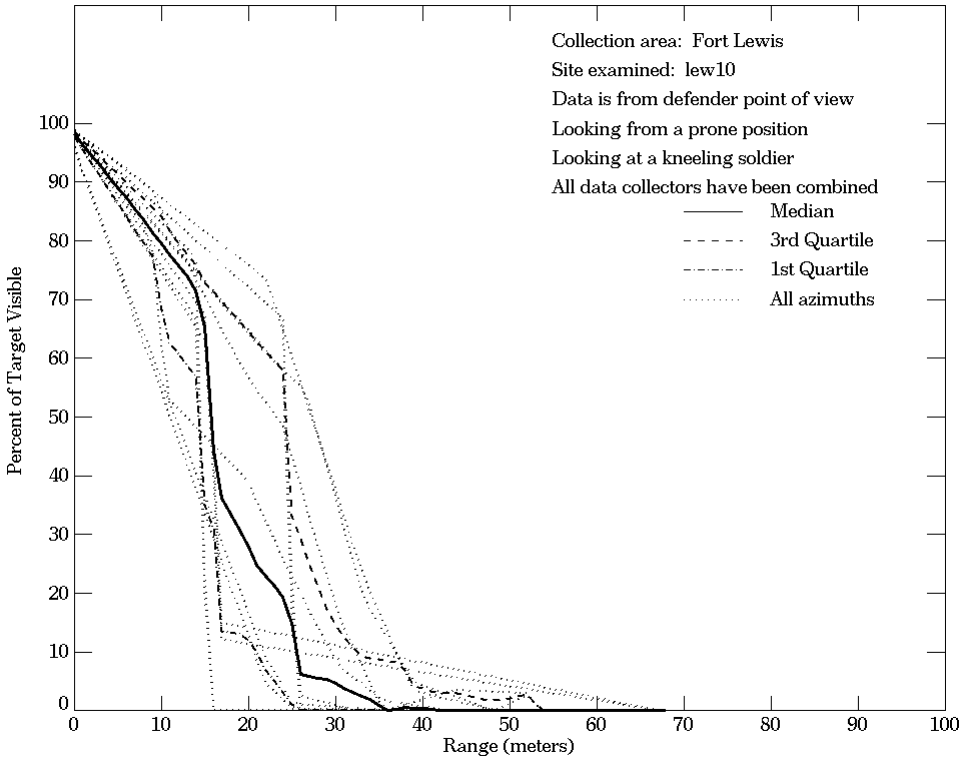

Figure E-61. Fort Lewis, From Defender Point of View, Site lew10

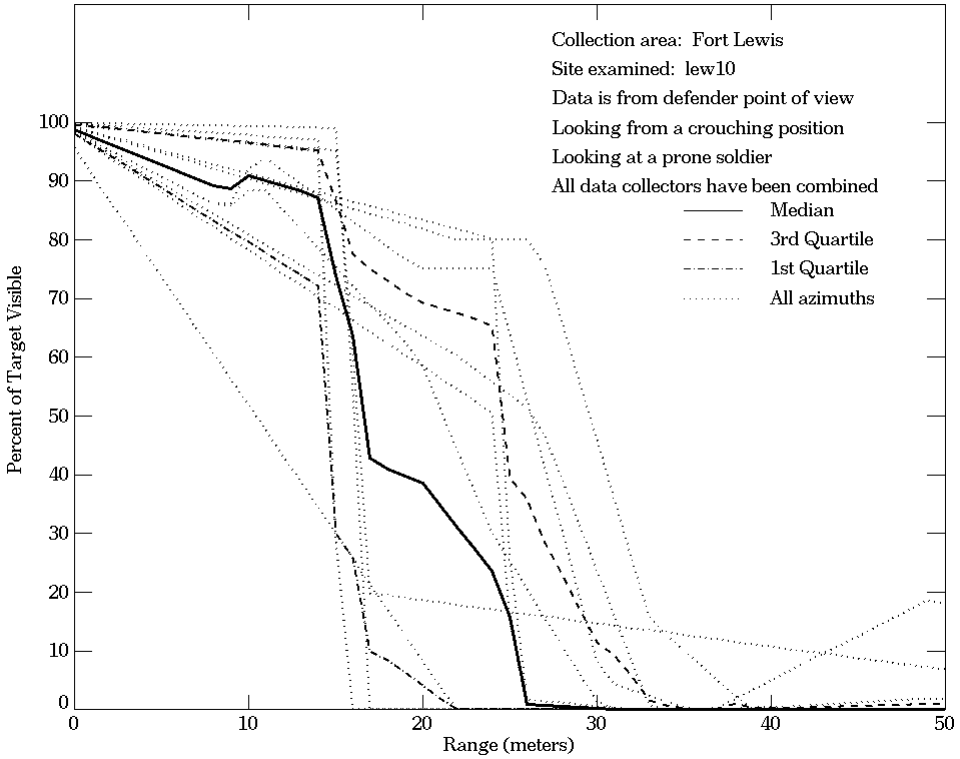

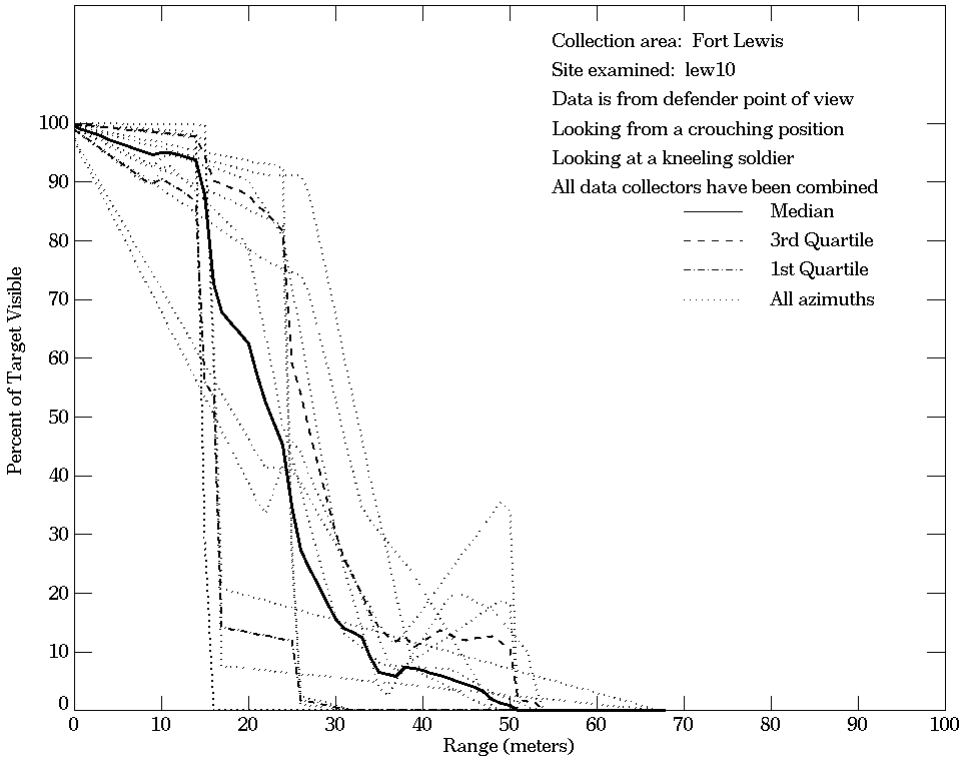

Figure E-61. Fort Lewis, From Defender Point of View, Site lew10 (Continued)

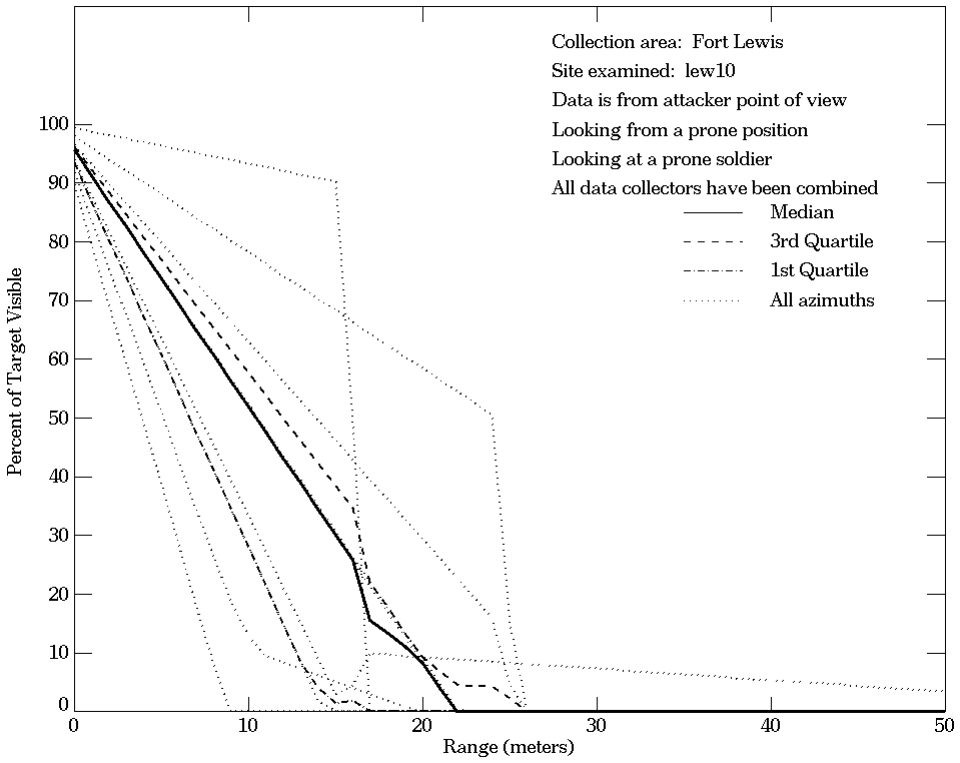

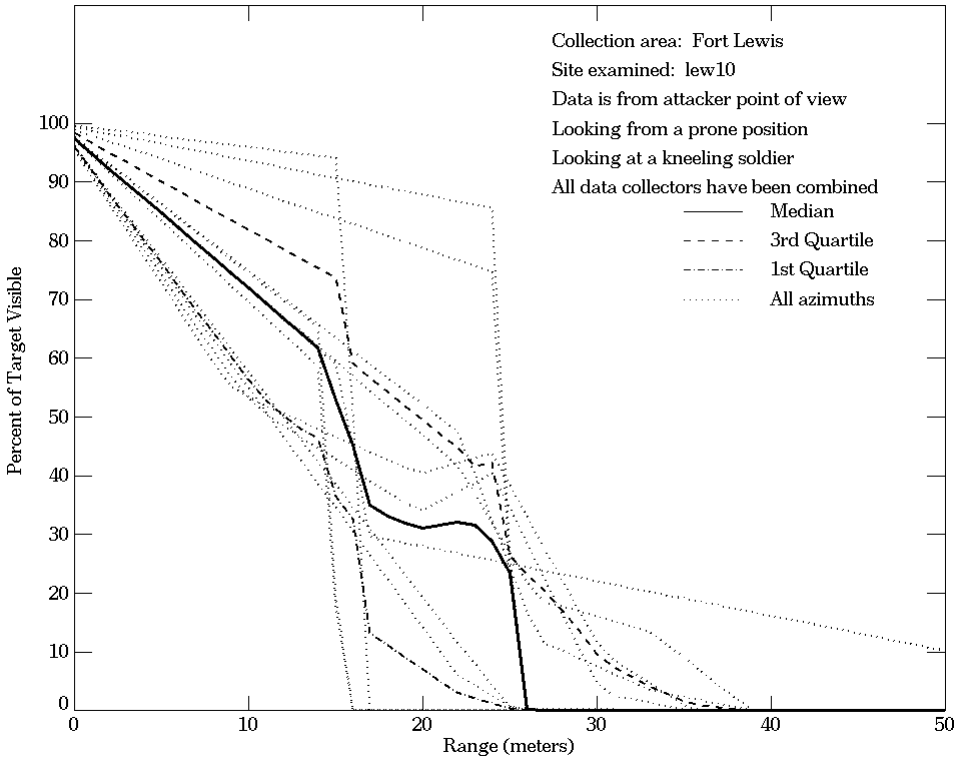

Figure E-62. Fort Lewis, From Attacker Point of View, Site lew10

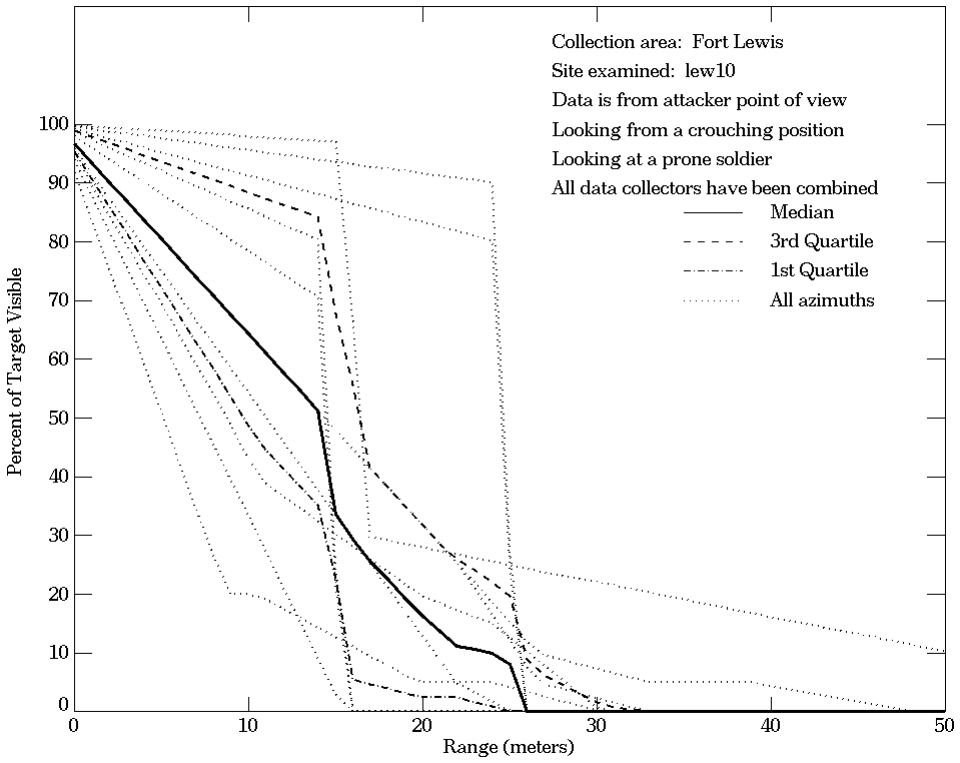

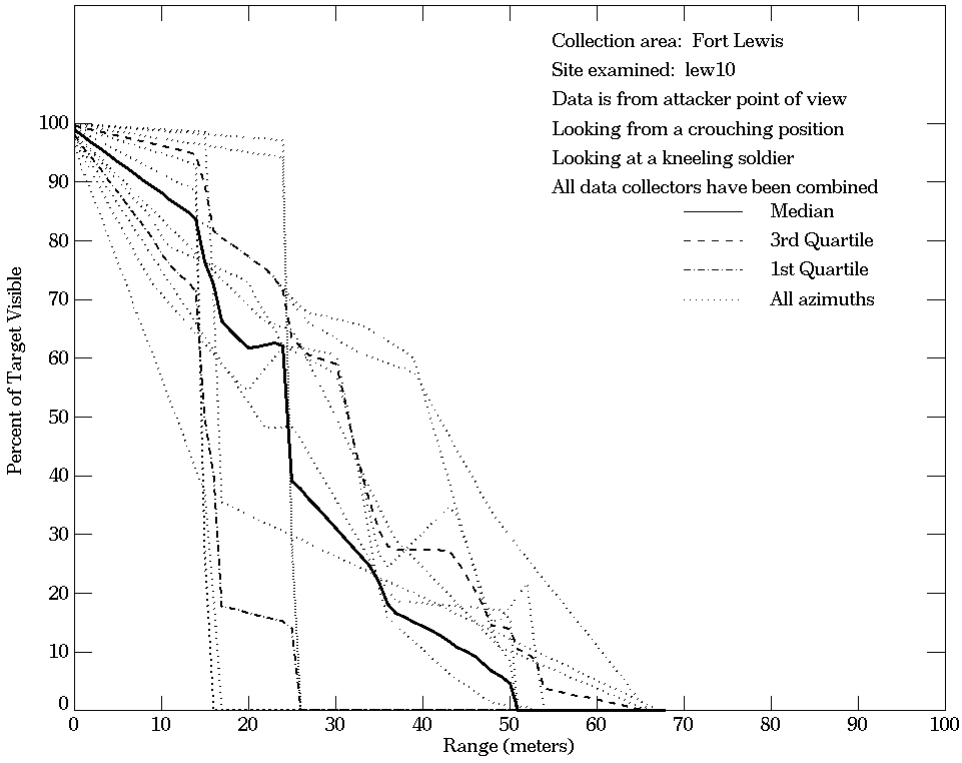

Figure E-62. Fort Lewis, From Attacker Point of View, Site lew10 (Continued)

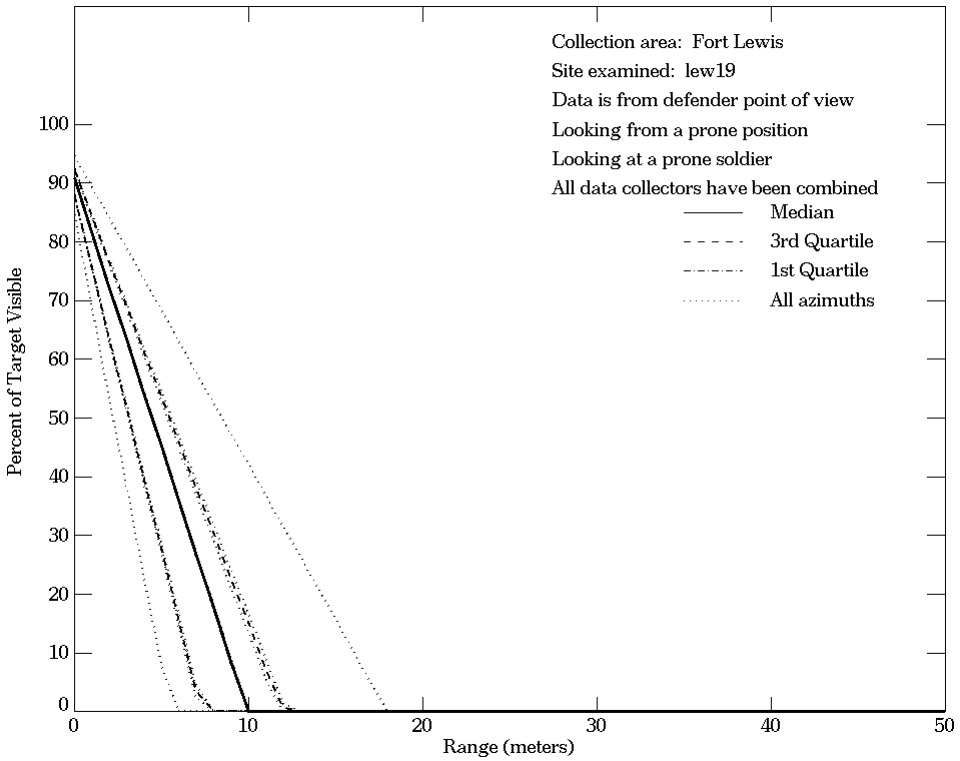

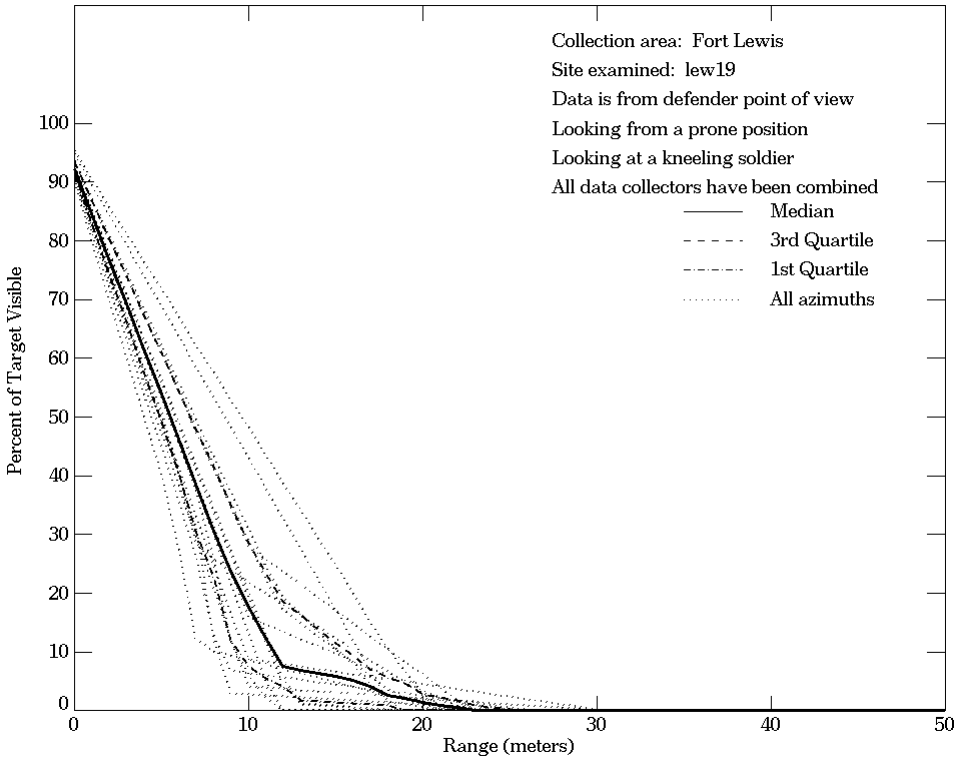

Figure E-63. Fort Lewis, From Defender Point of View, Site lew19

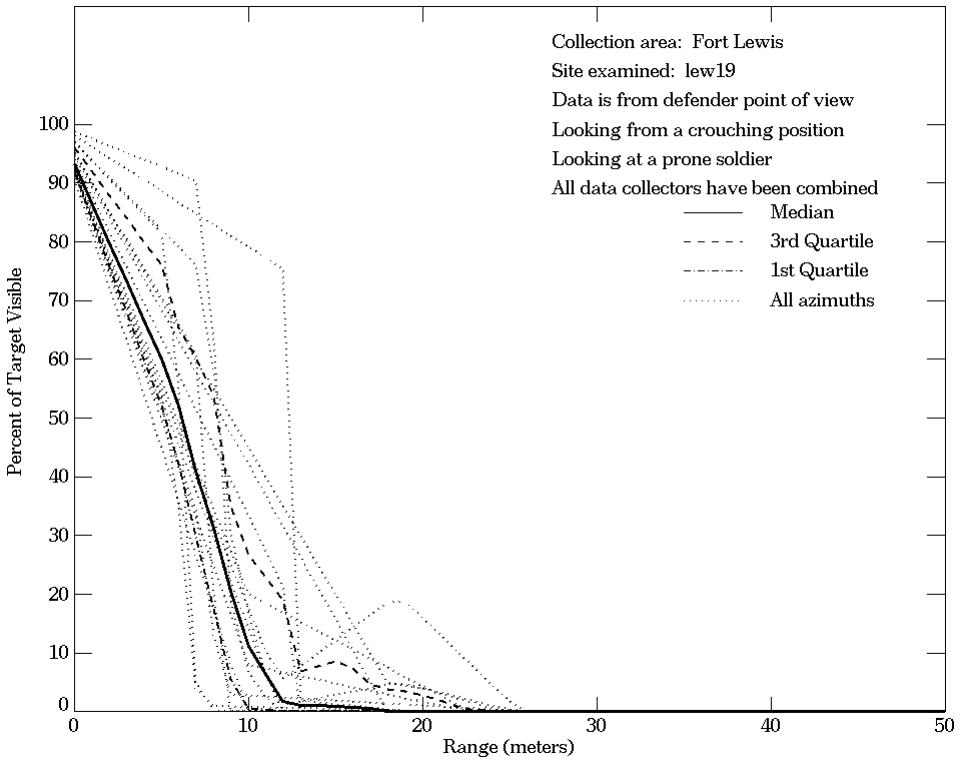

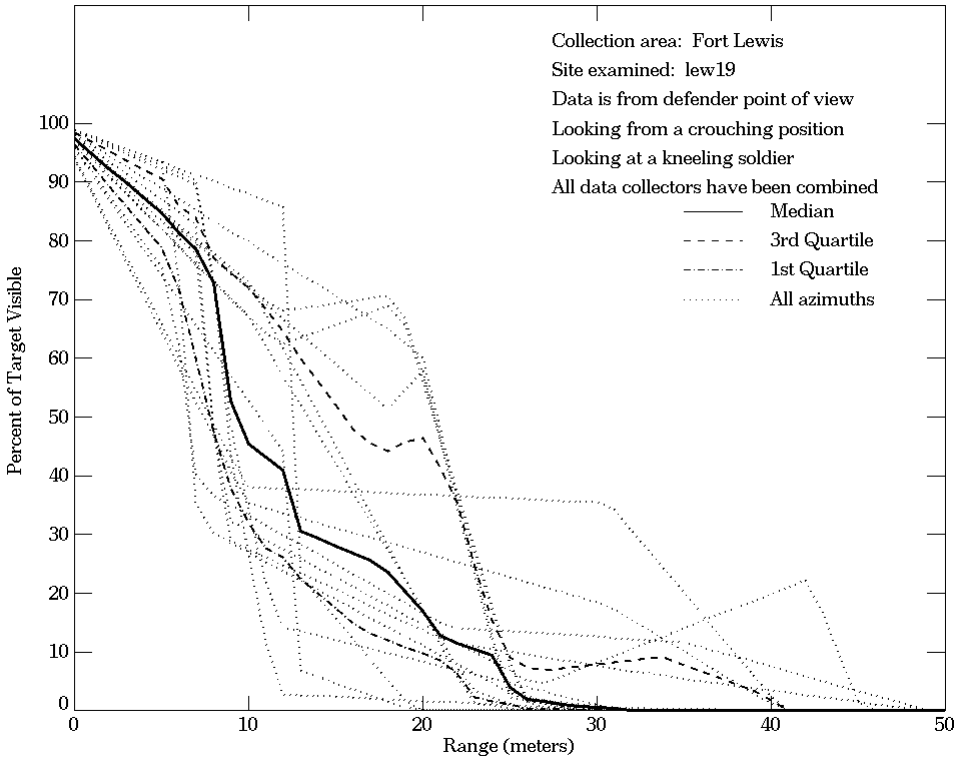

Figure E-63. Fort Lewis, From Defender Point of View, Site lew19 (Continued)

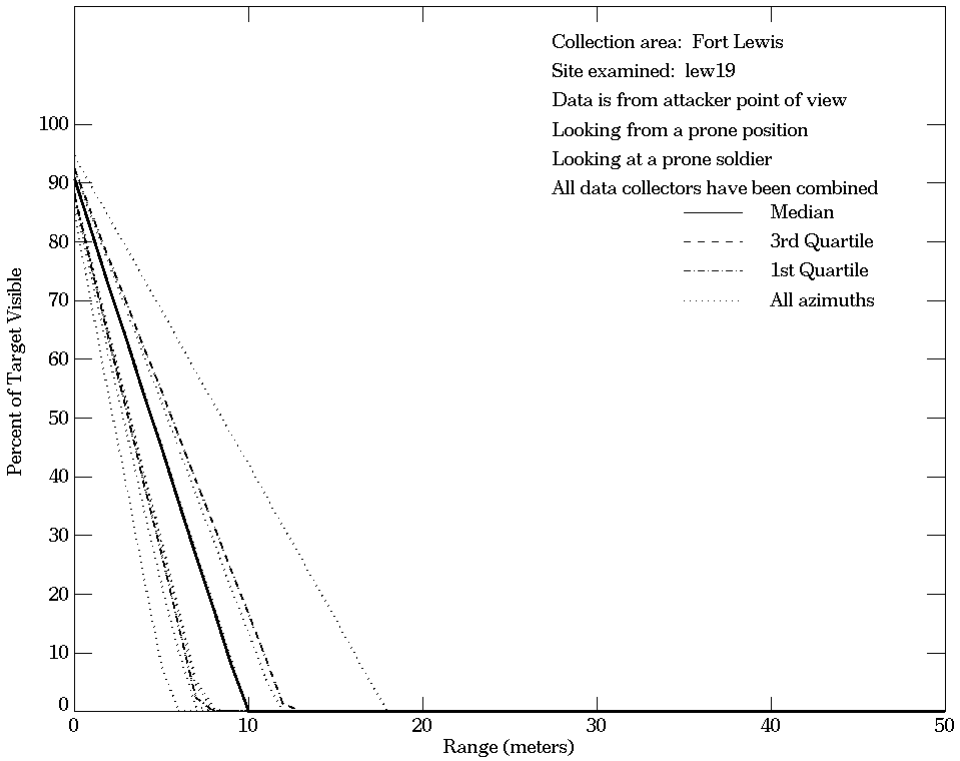

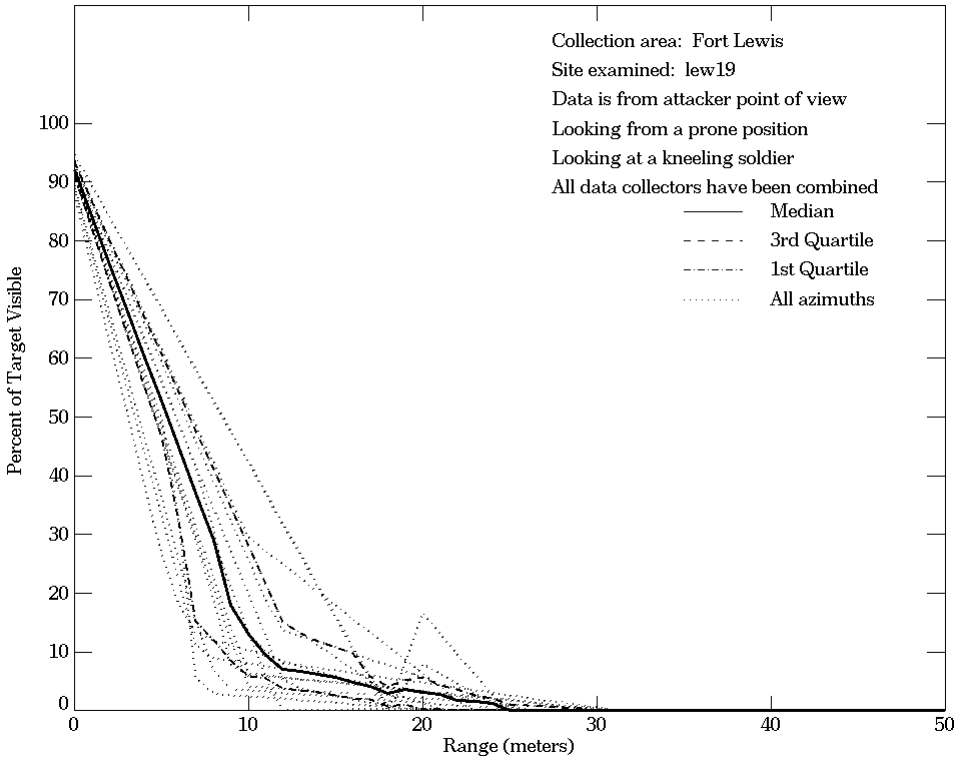

Figure E-64. Fort Lewis, From Attacker Point of View, Site lew19

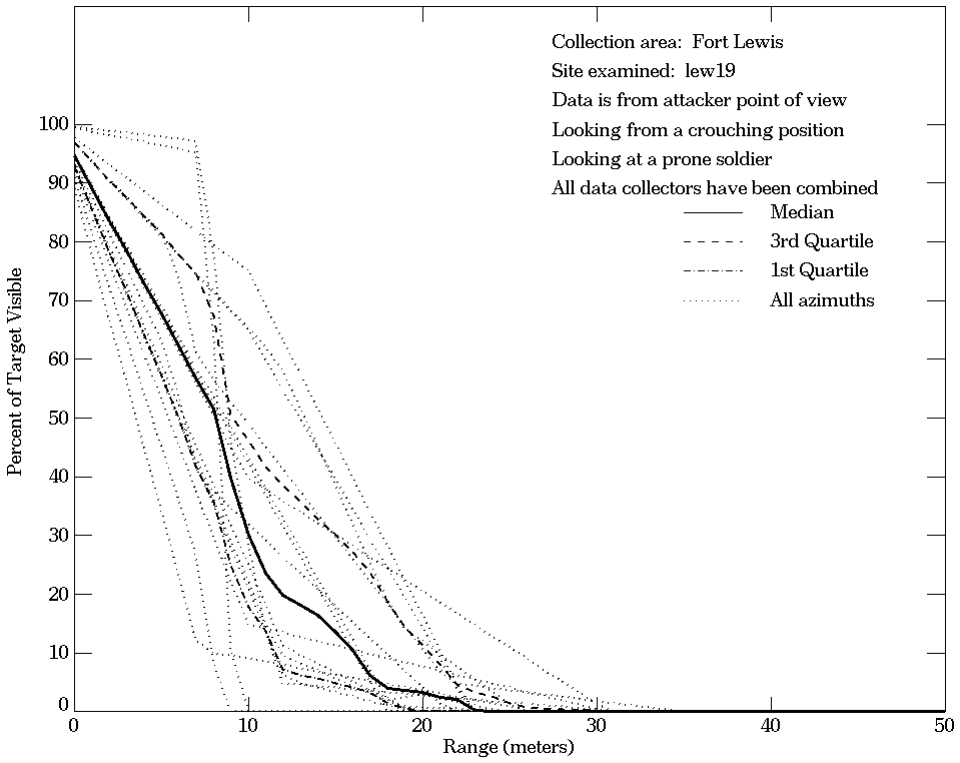

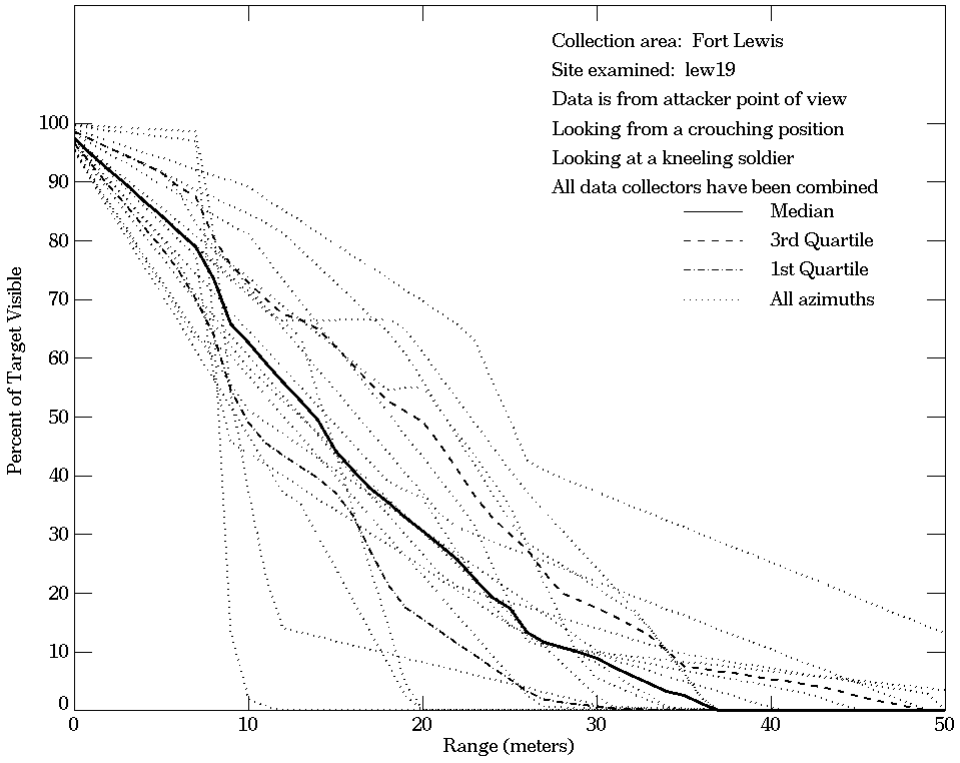

Figure E-64. Fort Lewis, From Attacker Point of View, Site lew19 (Continued)

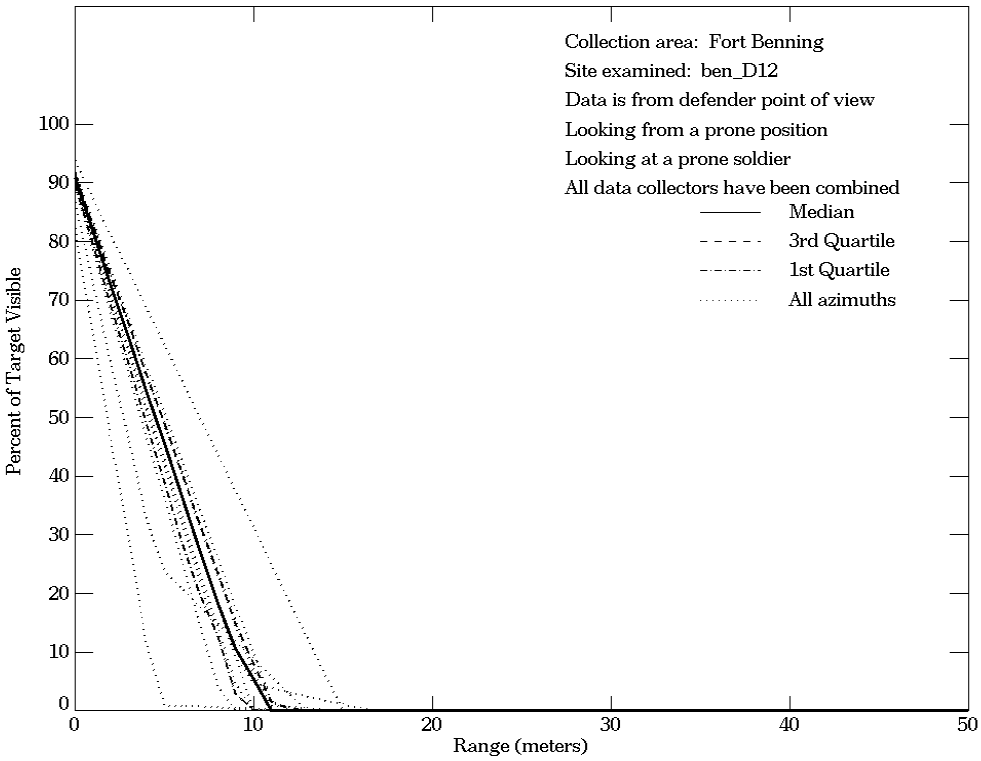

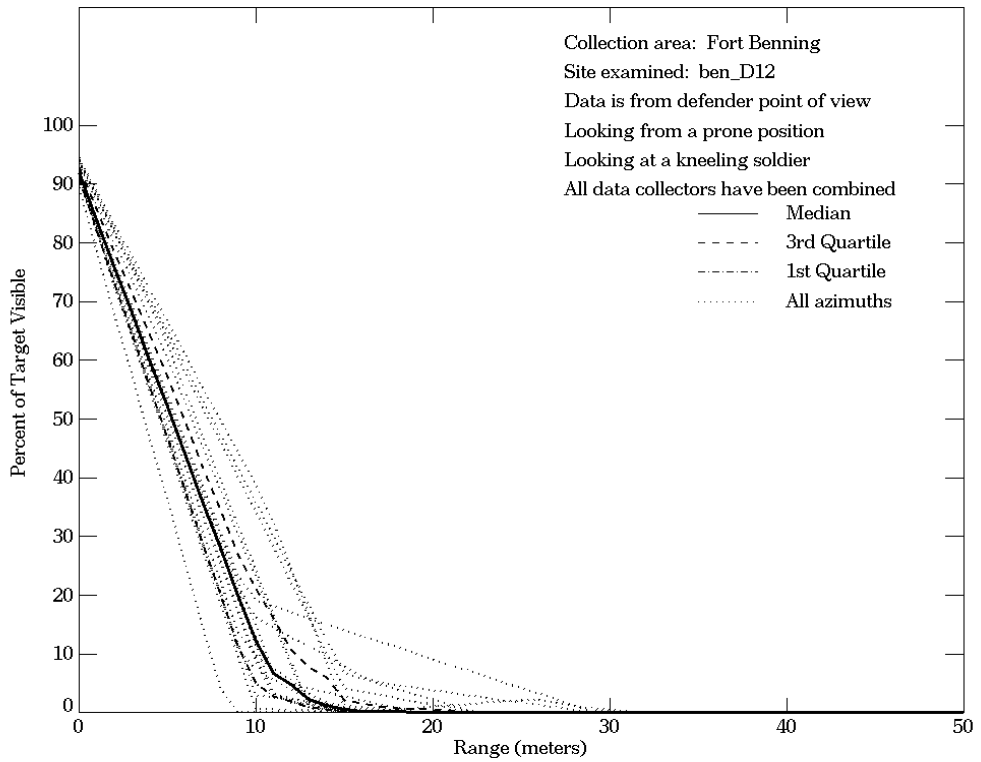

Figure E-65. Fort Benning, From Defender Point of View, Site ben_D12

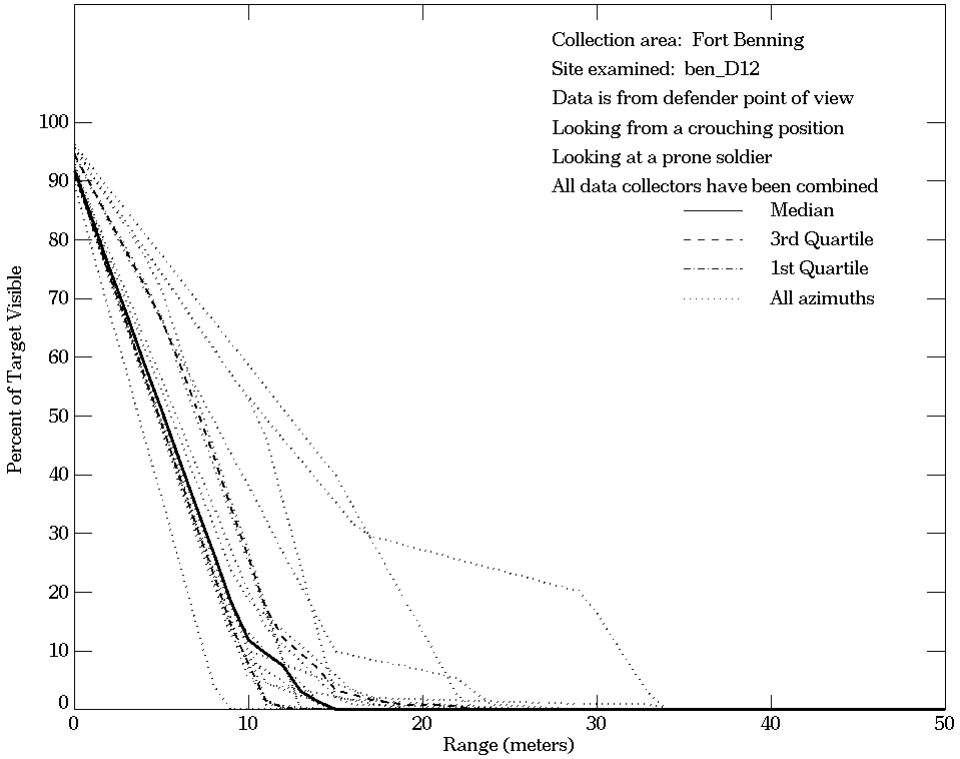

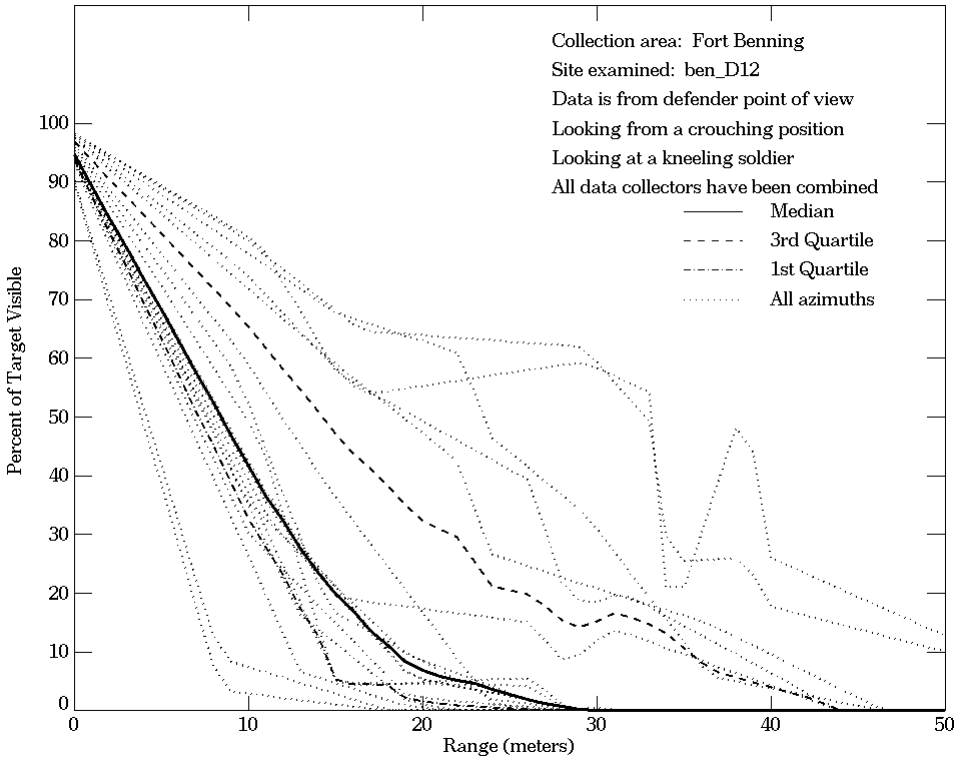

Figure E-65. Fort Benning, From Defender Point of View, Site ben_D12 (Continued)

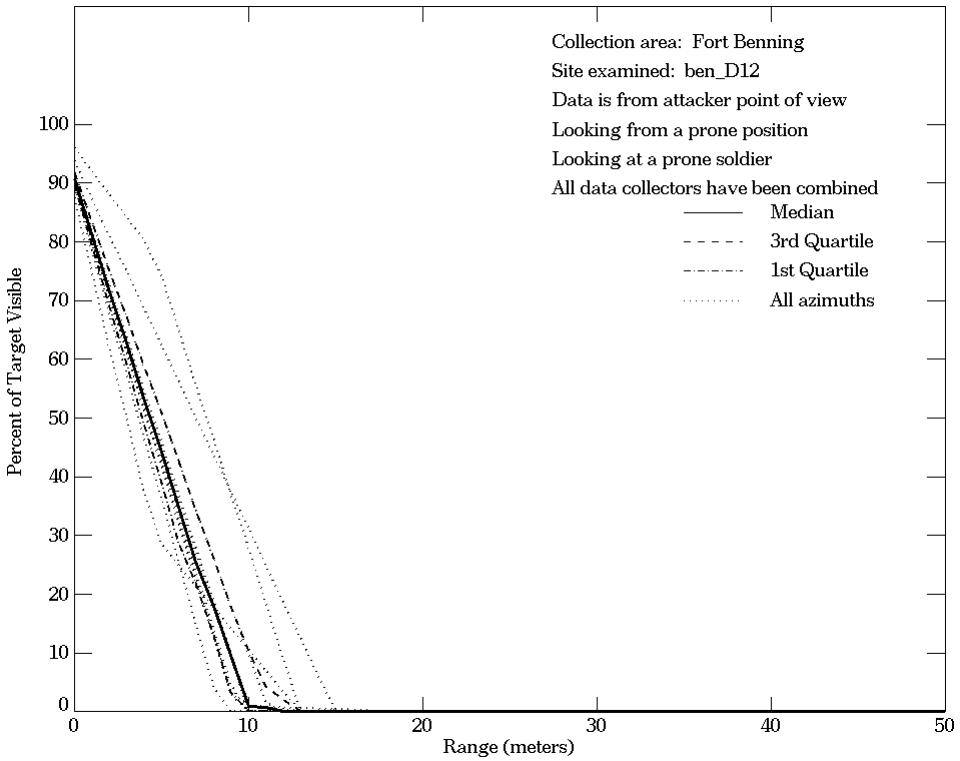

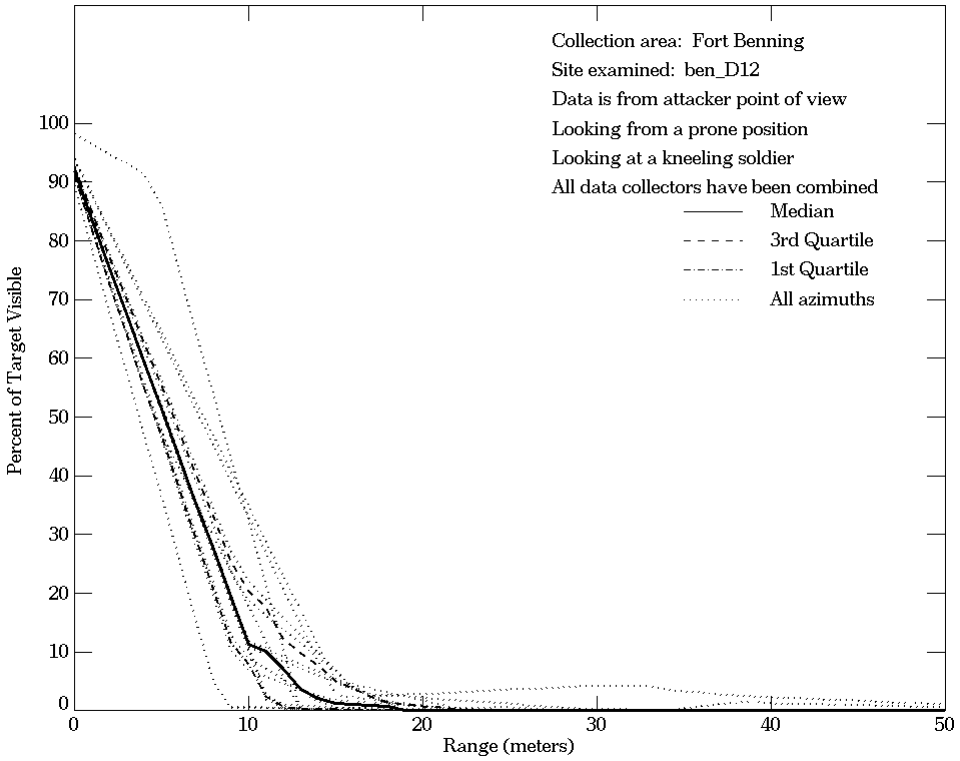

Figure E-66. Fort Benning, From Attacker Point of View, Site ben_D12

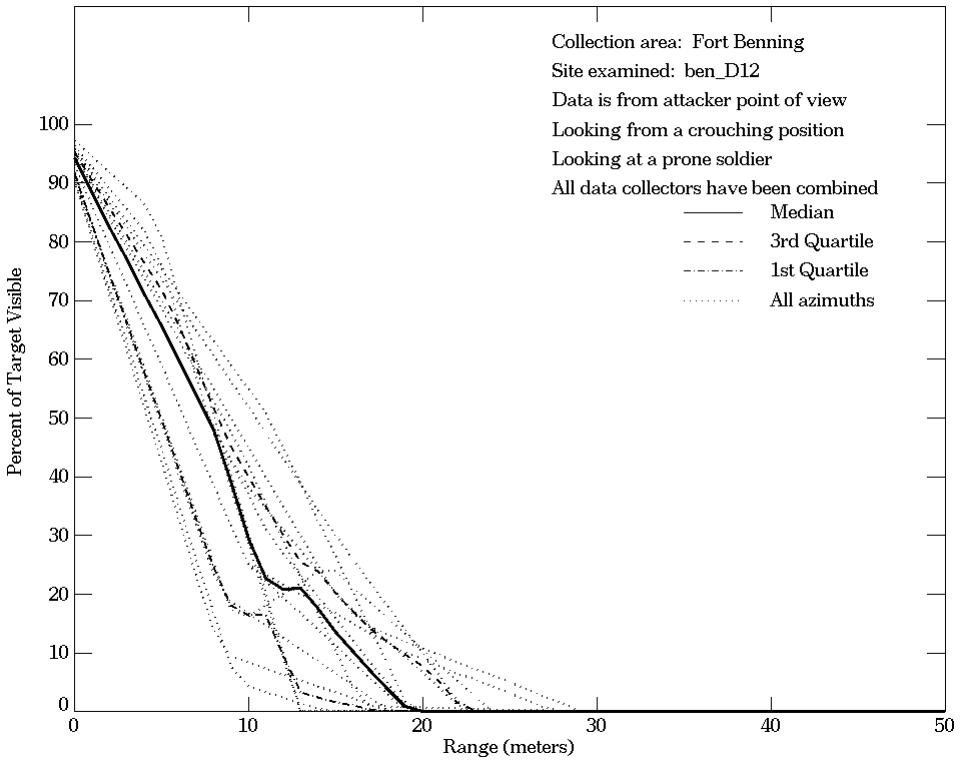

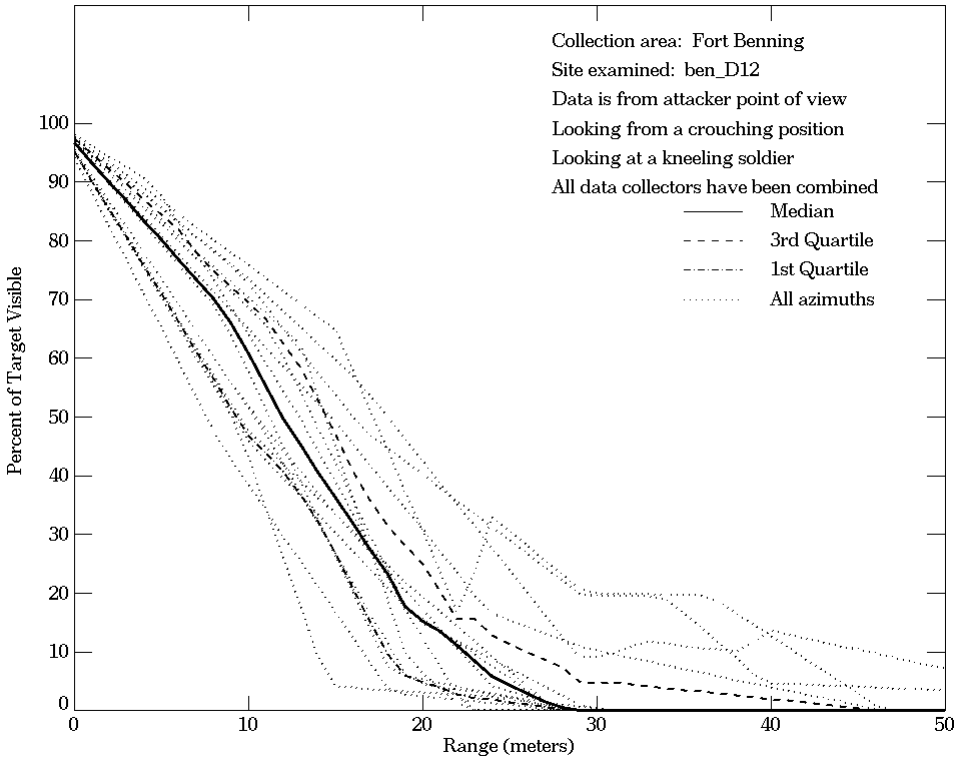

Figure E-66. Fort Benning, From Attacker Point of View, Site ben_D12 (Continued)

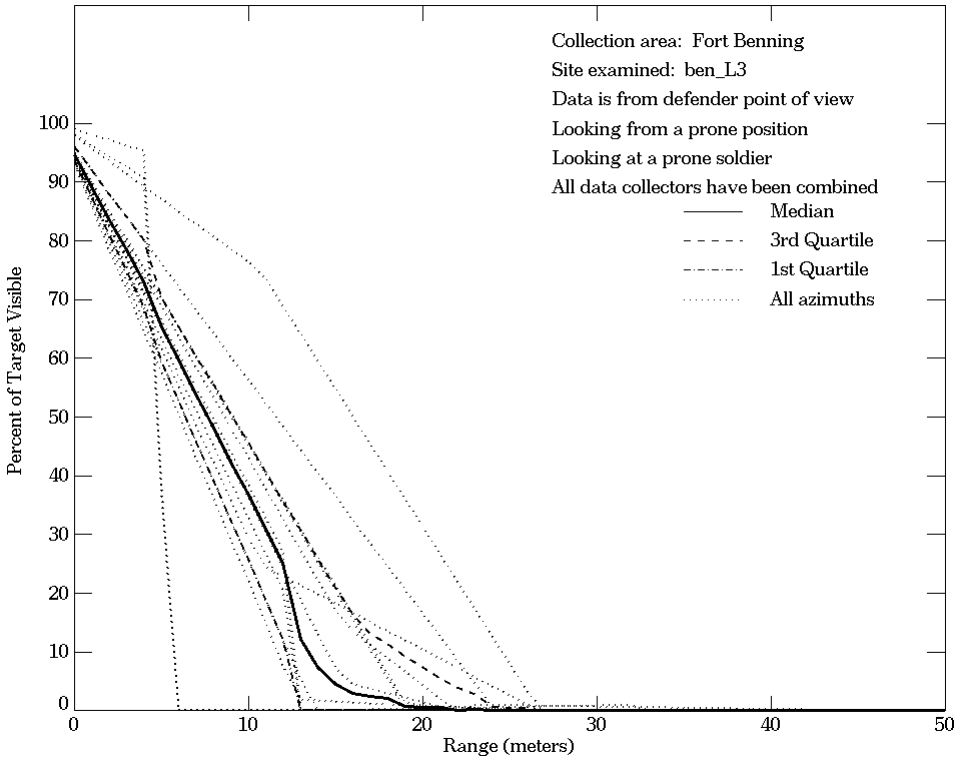

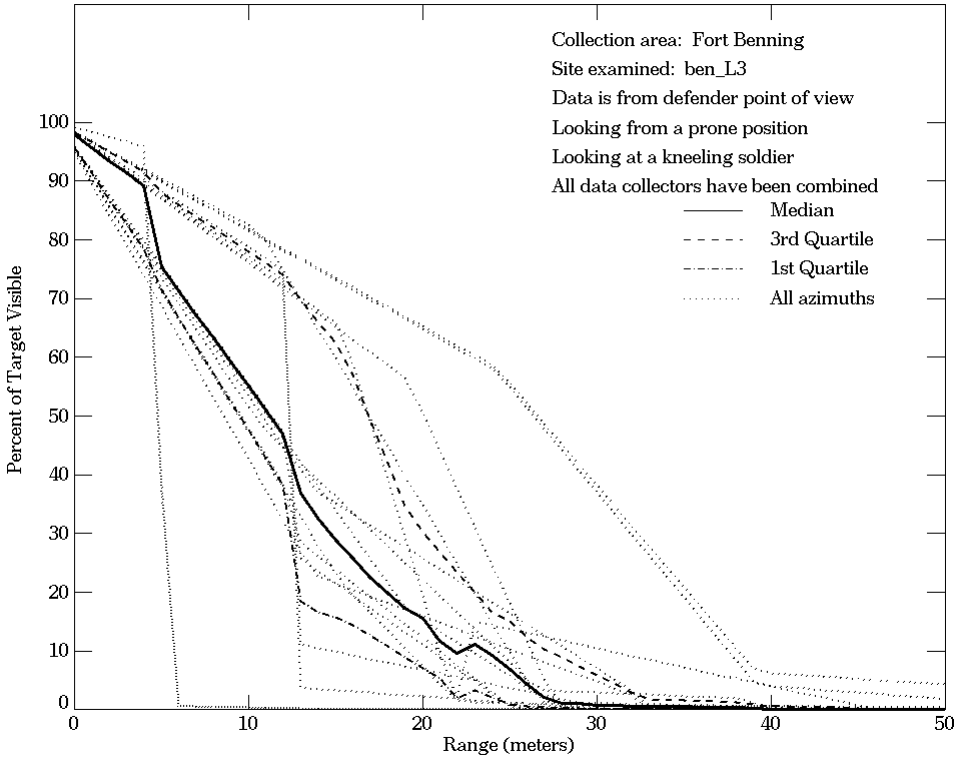

Figure E-67. Fort Benning, From Defender Point of View, Site ben_L3

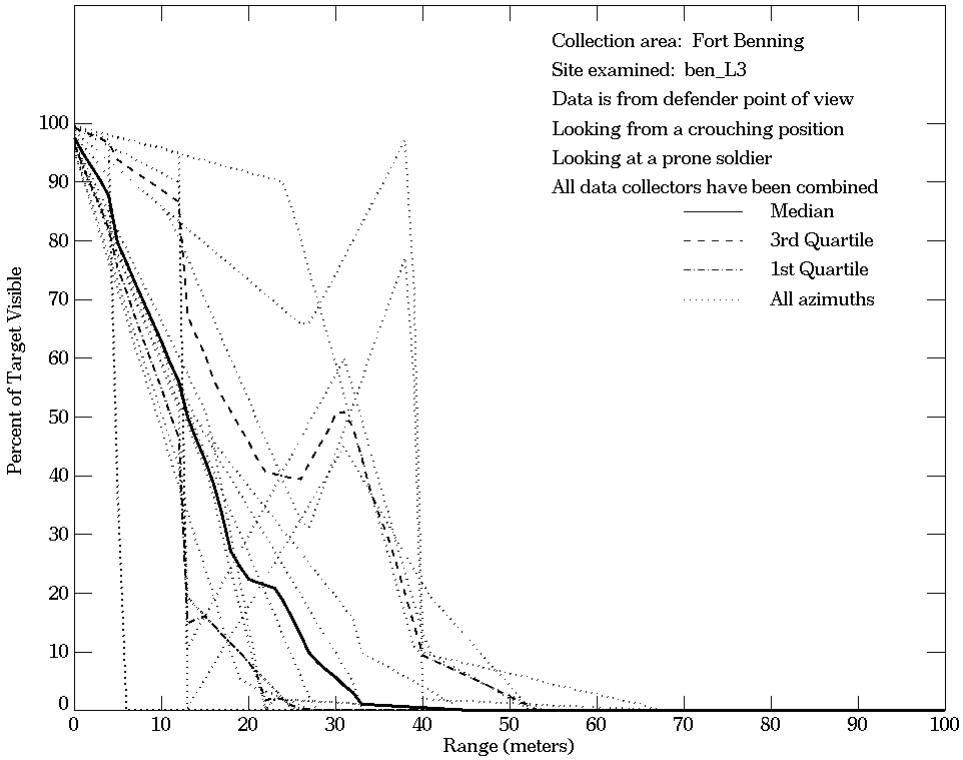

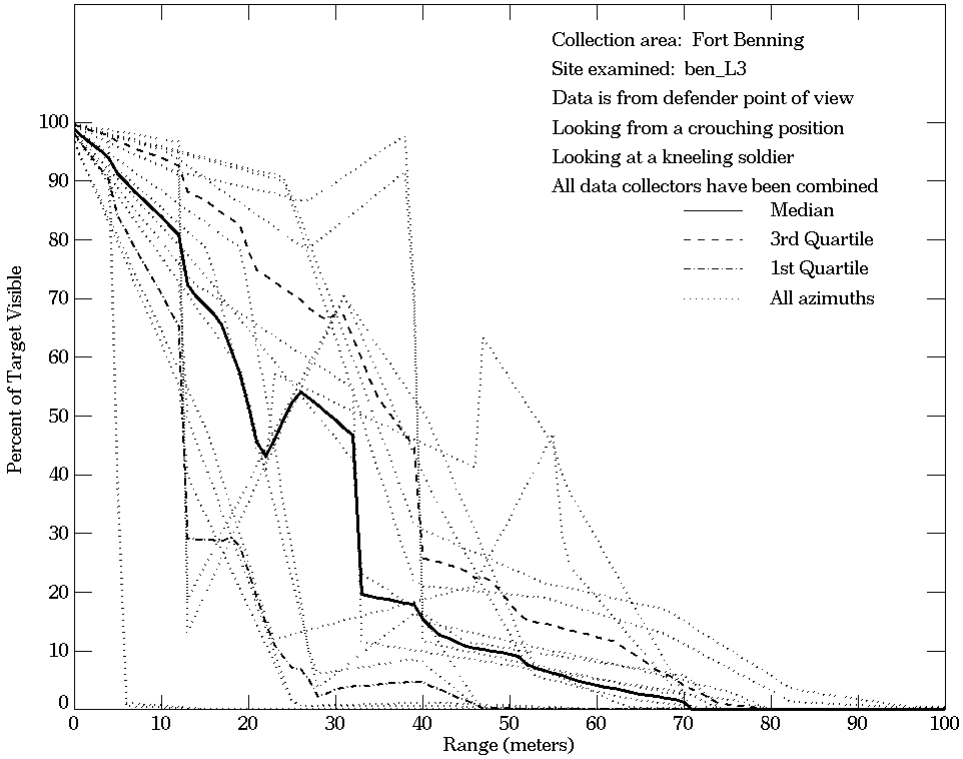

Figure E-67. Fort Benning, From Defender Point of View, Site ben_L3 (Continued)

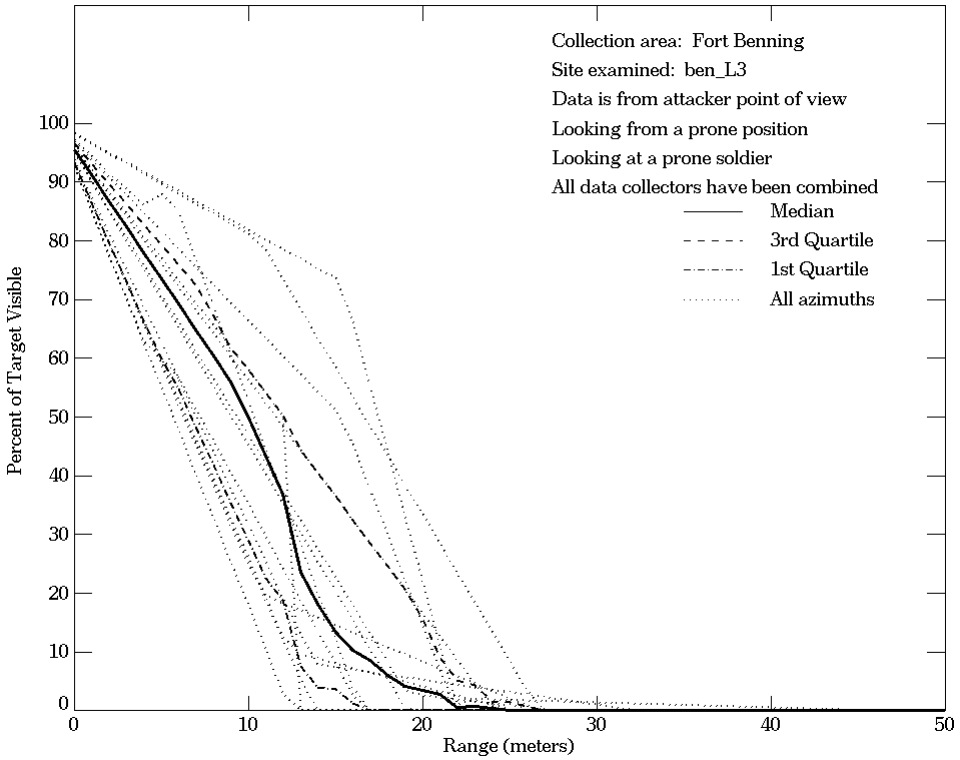

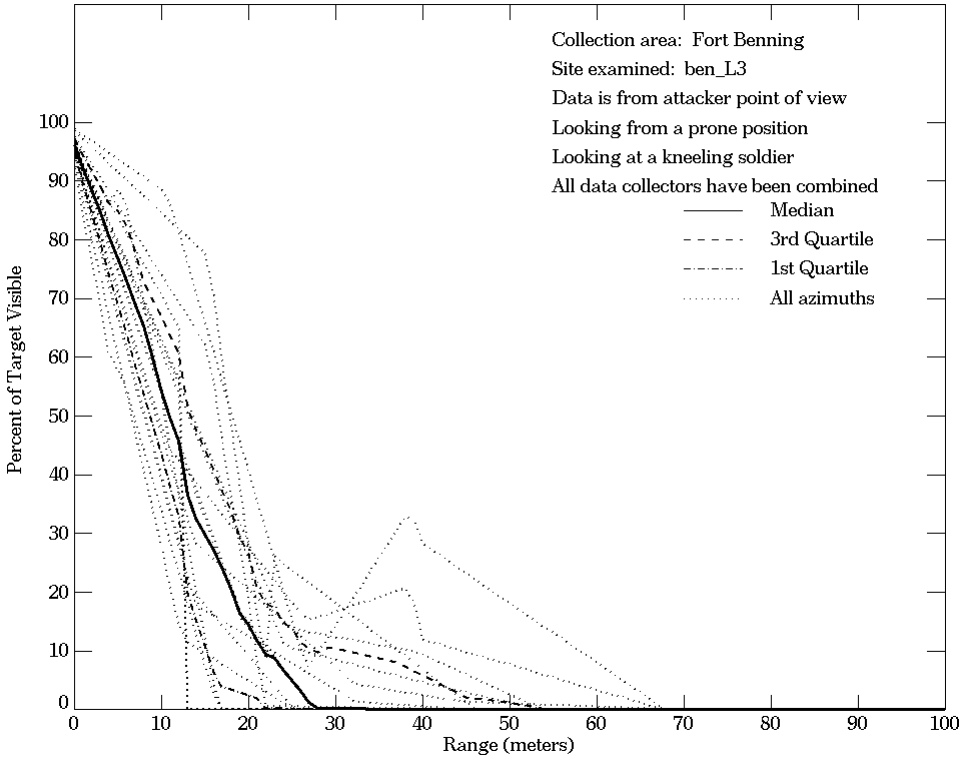

Figure E-68. Fort Benning, From Attacker Point of View, Site ben_L3

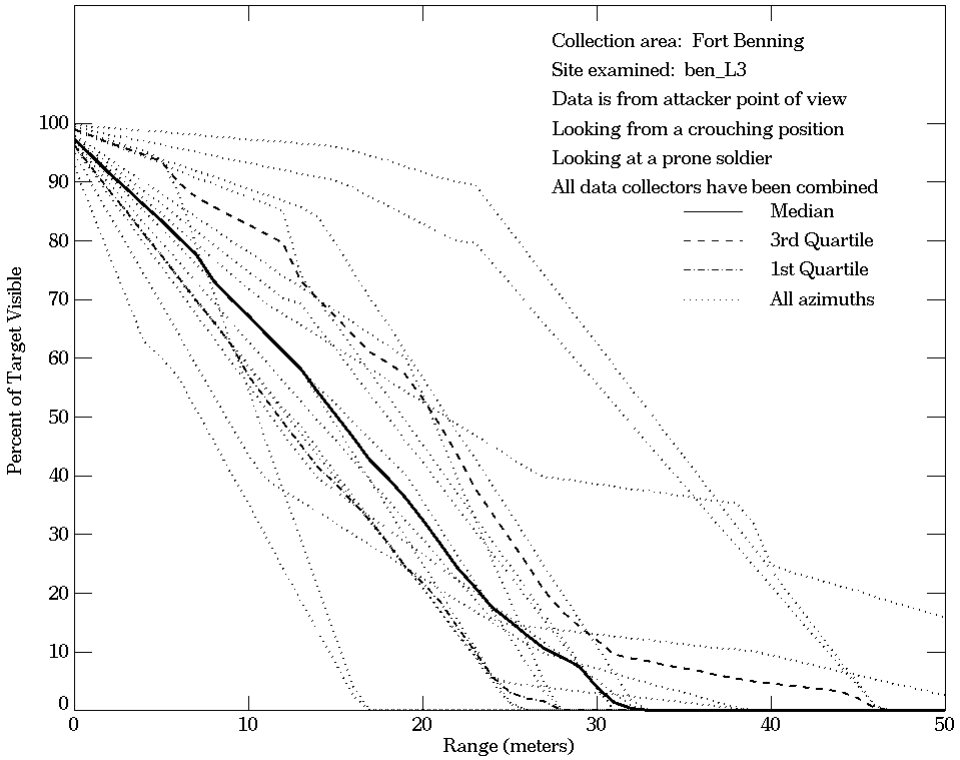

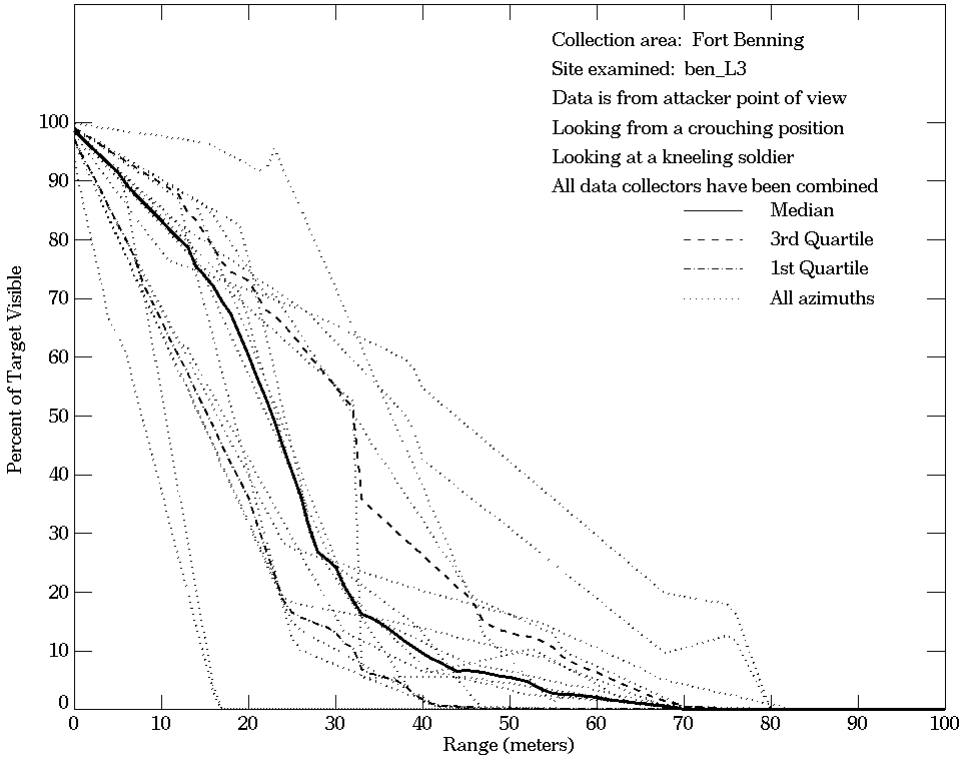

Figure E-68. Fort Benning, From Attacker Point of View, Site ben_L3 (Continued)

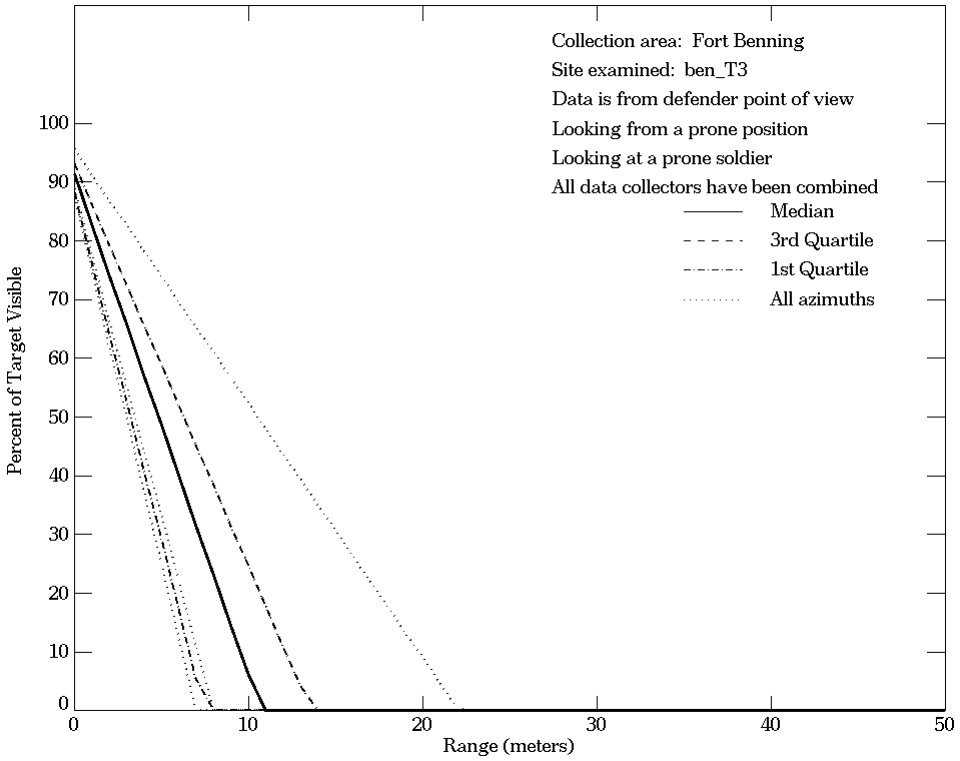

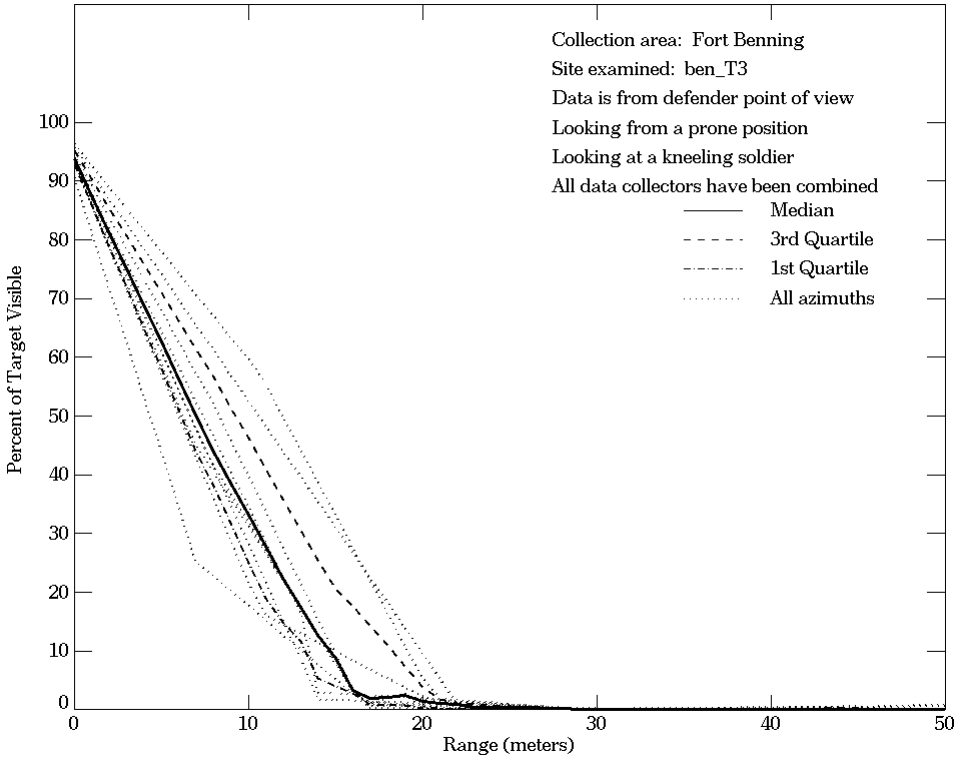

Figure E-69. Fort Benning, From Defender Point of View, Site ben_T3

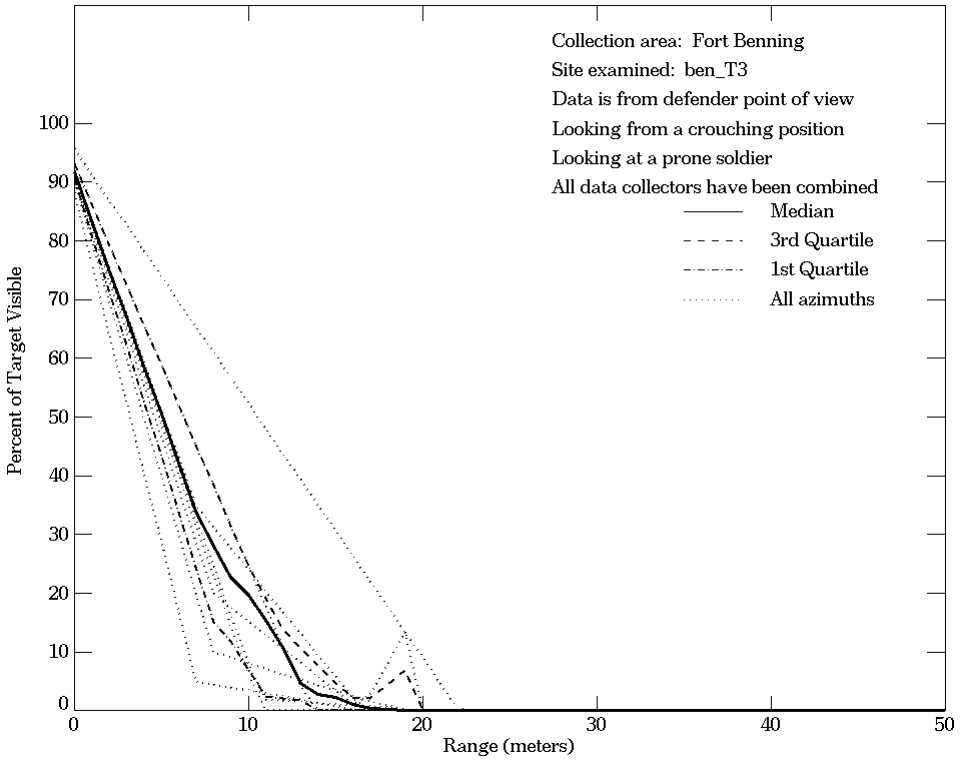

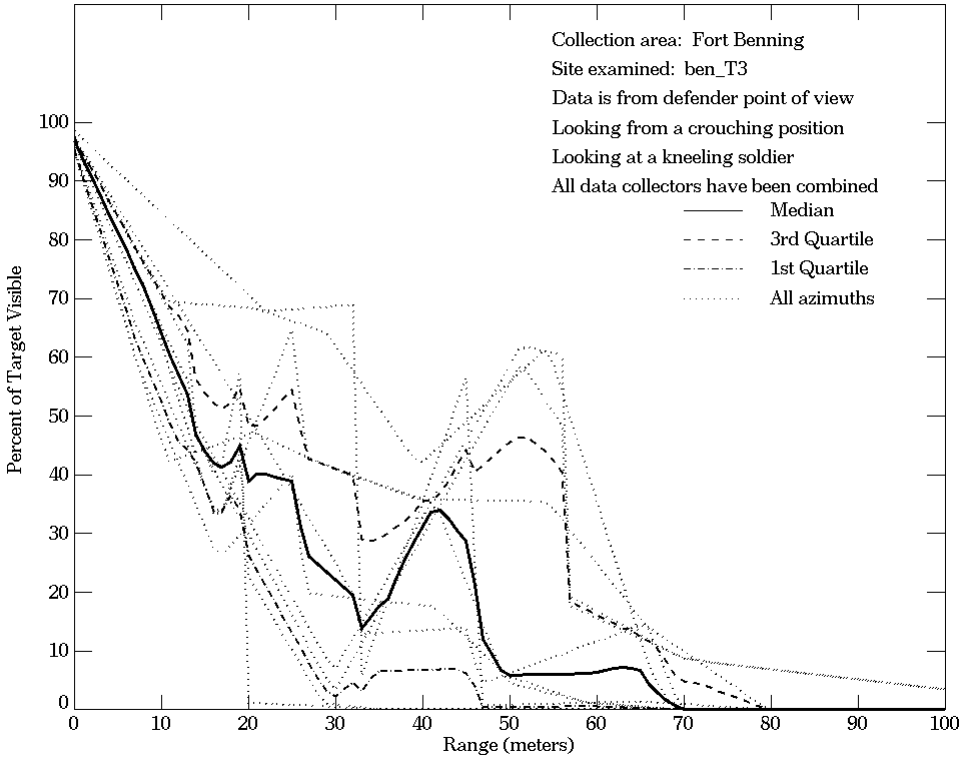

Figure E-69. Fort Benning, From Defender Point of View, Site ben_T3 (Continued)

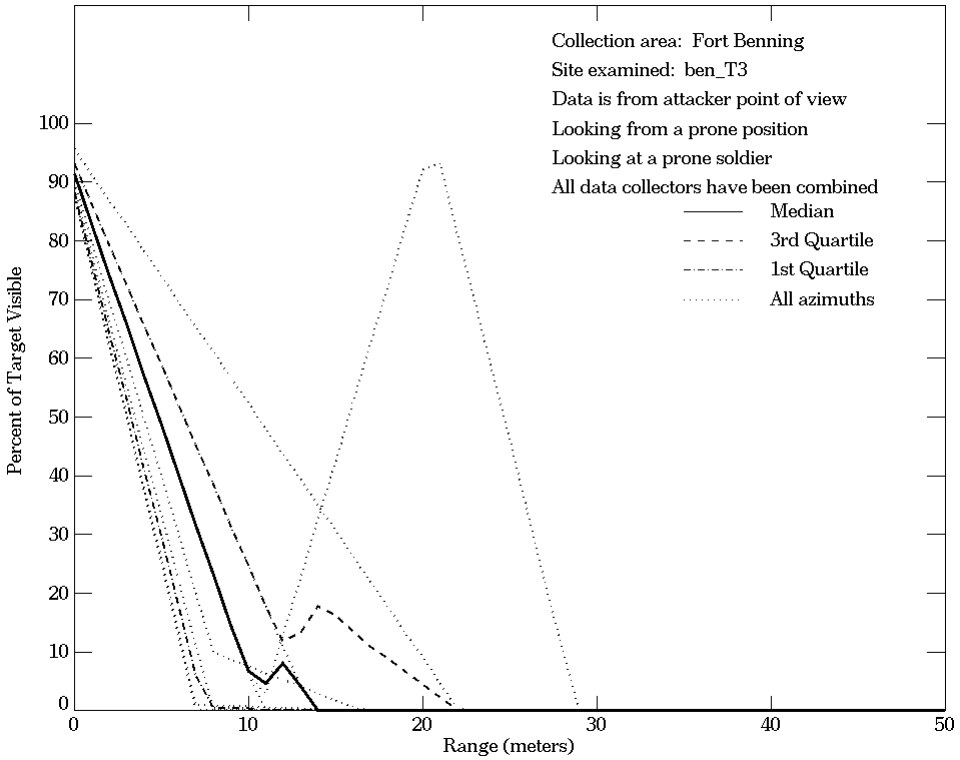

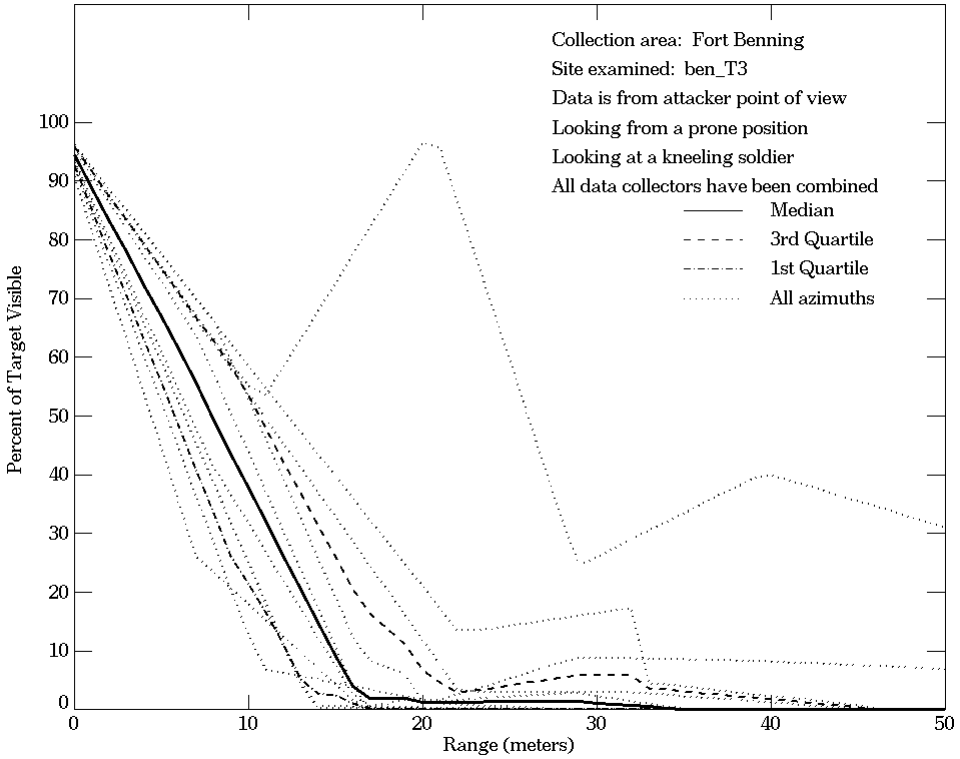

Figure E-70. Fort Benning, From Attacker Point of View, Site ben_T3

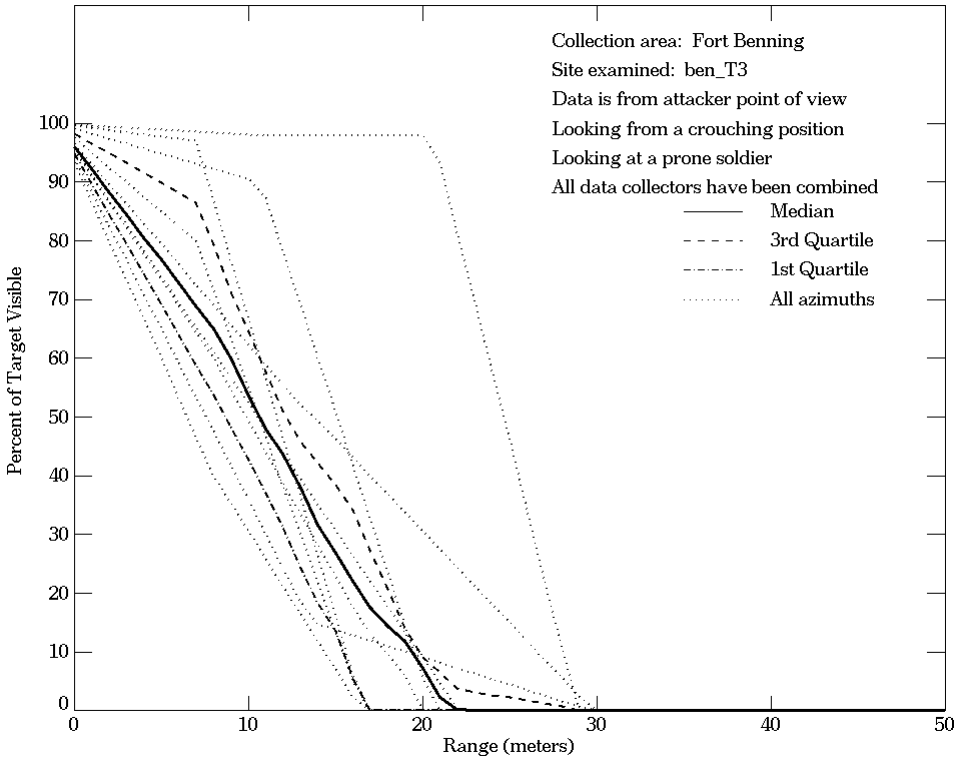

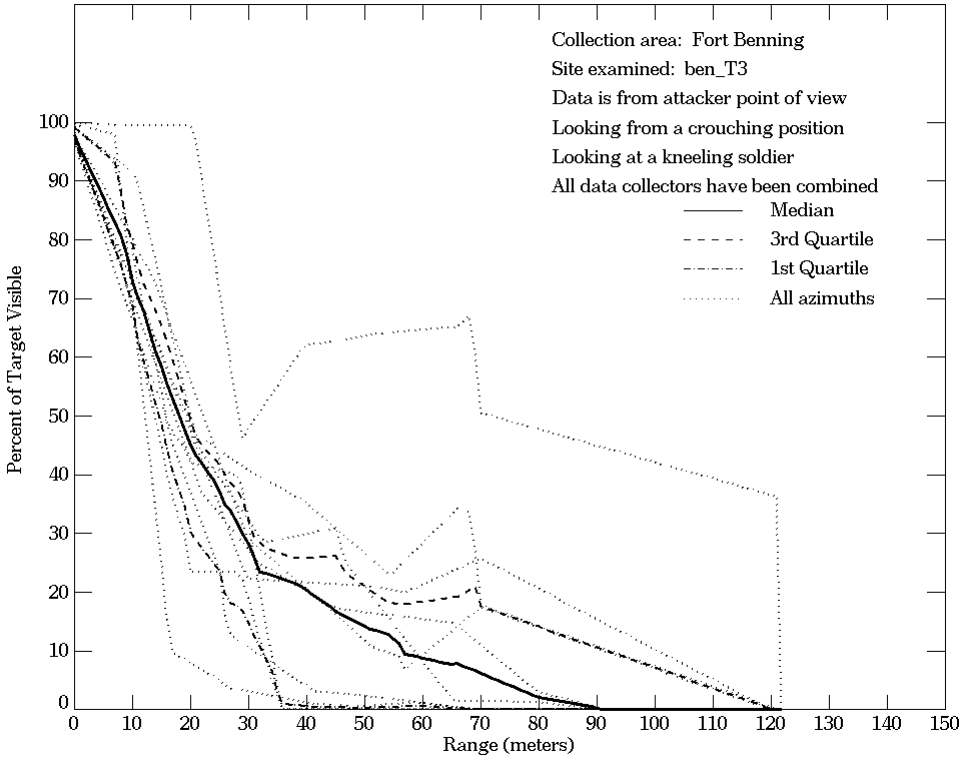

Figure E-70. Fort Benning, From Attacker Point of View, Site ben_T3 (Continued)

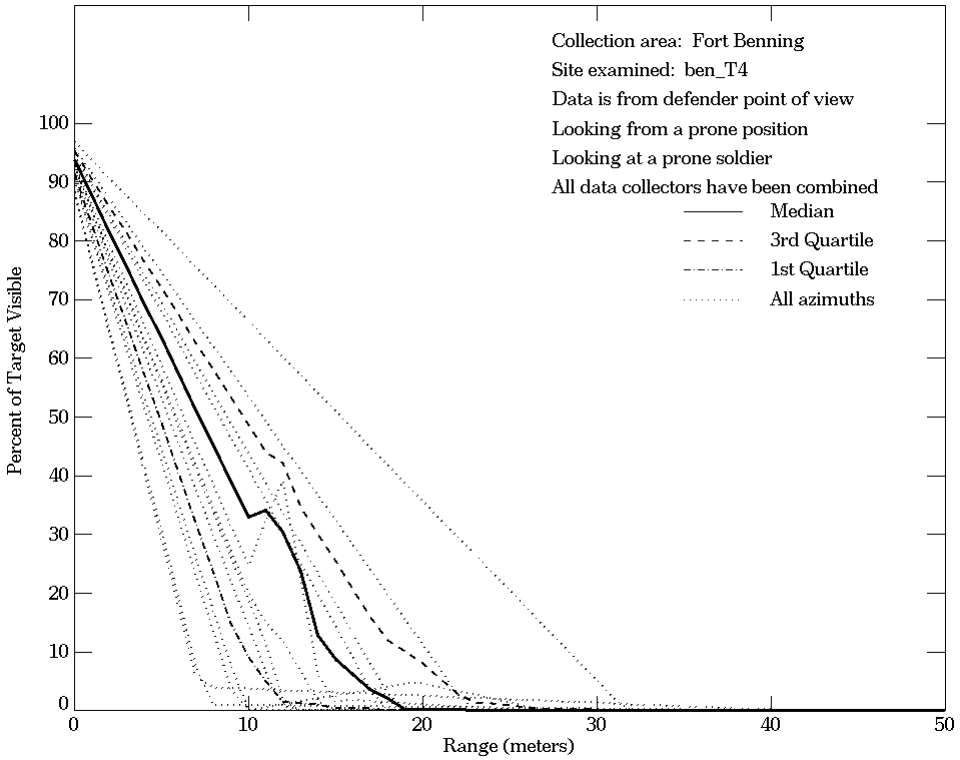

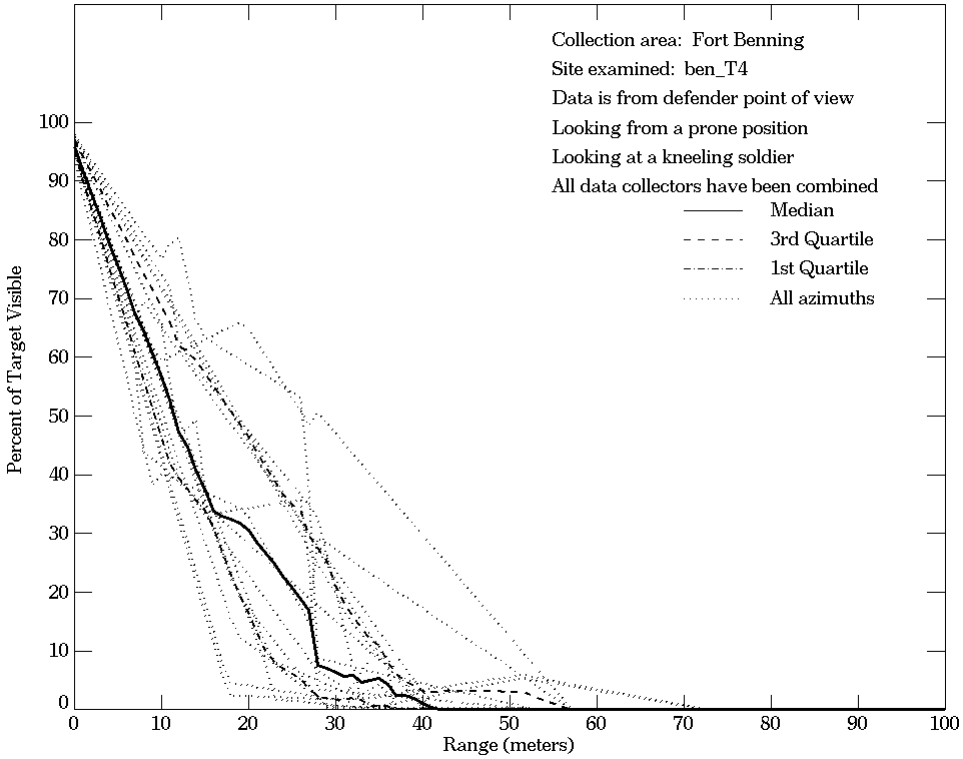

Figure E-71. Fort Benning, From Defender Point of View, Site ben_T4

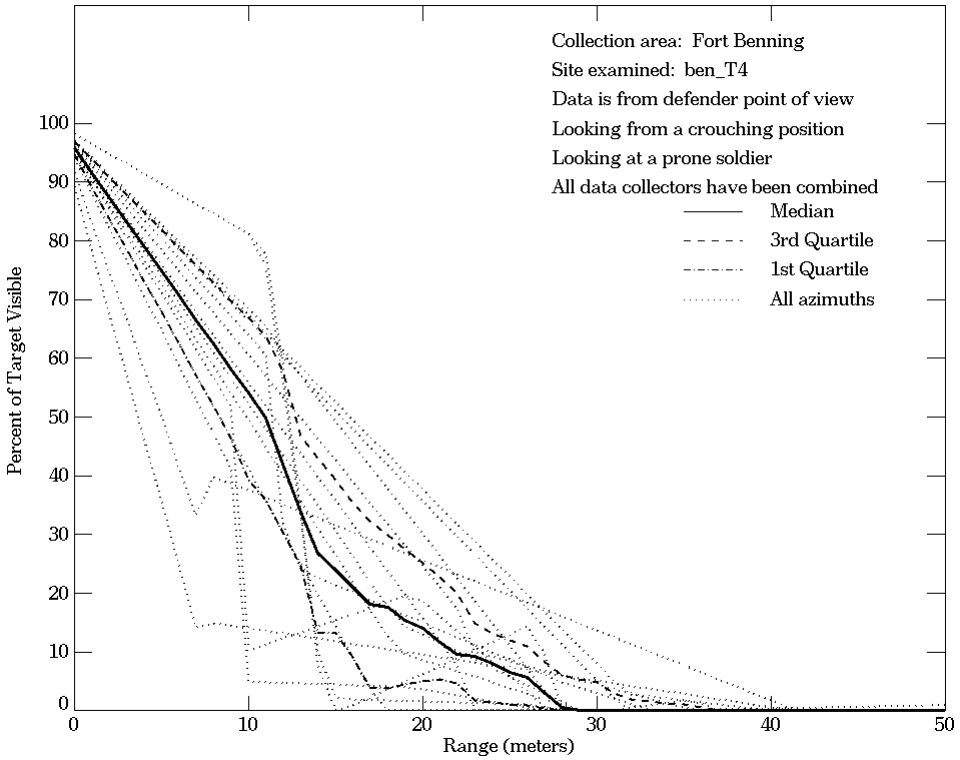

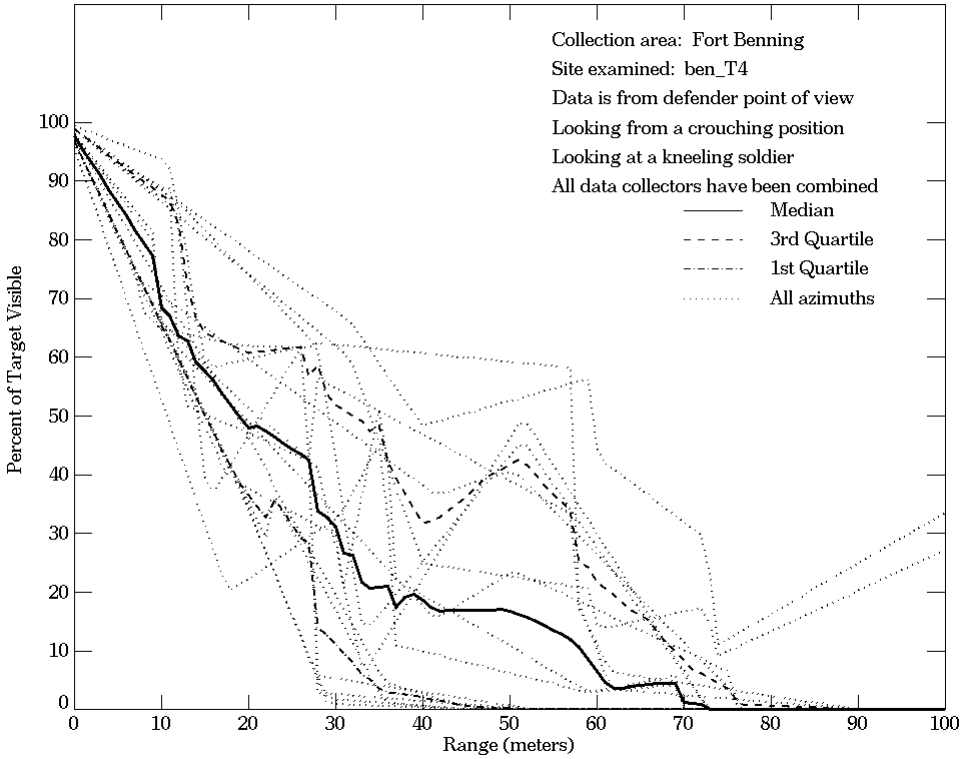

Figure E-71. Fort Benning, From Defender Point of View, Site ben_T4 (Continued)

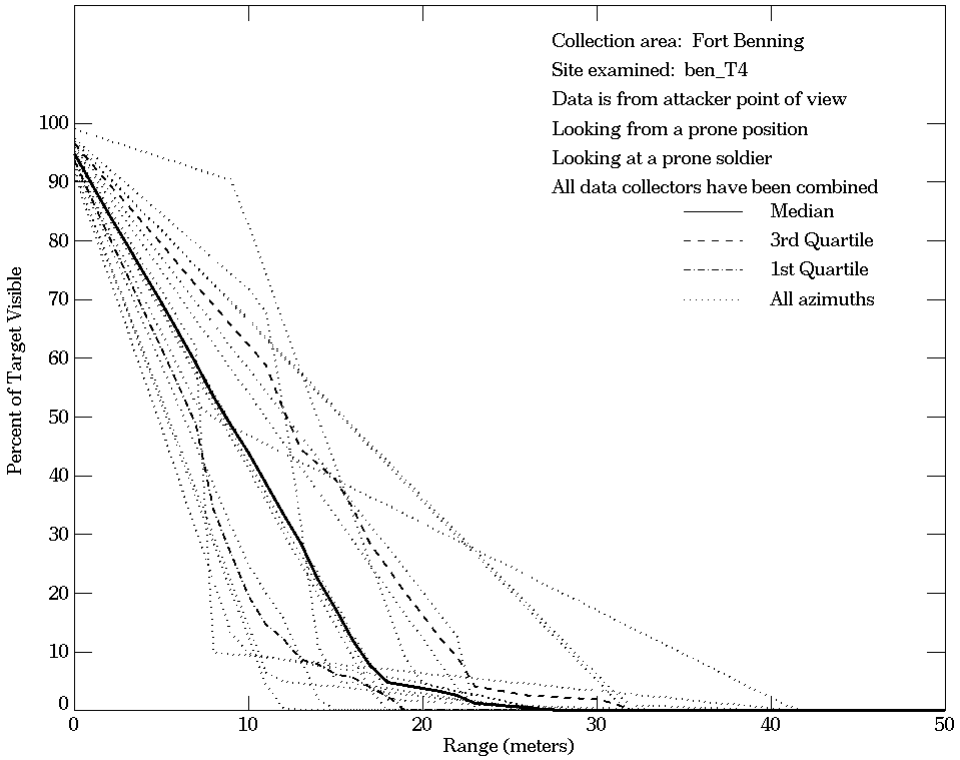

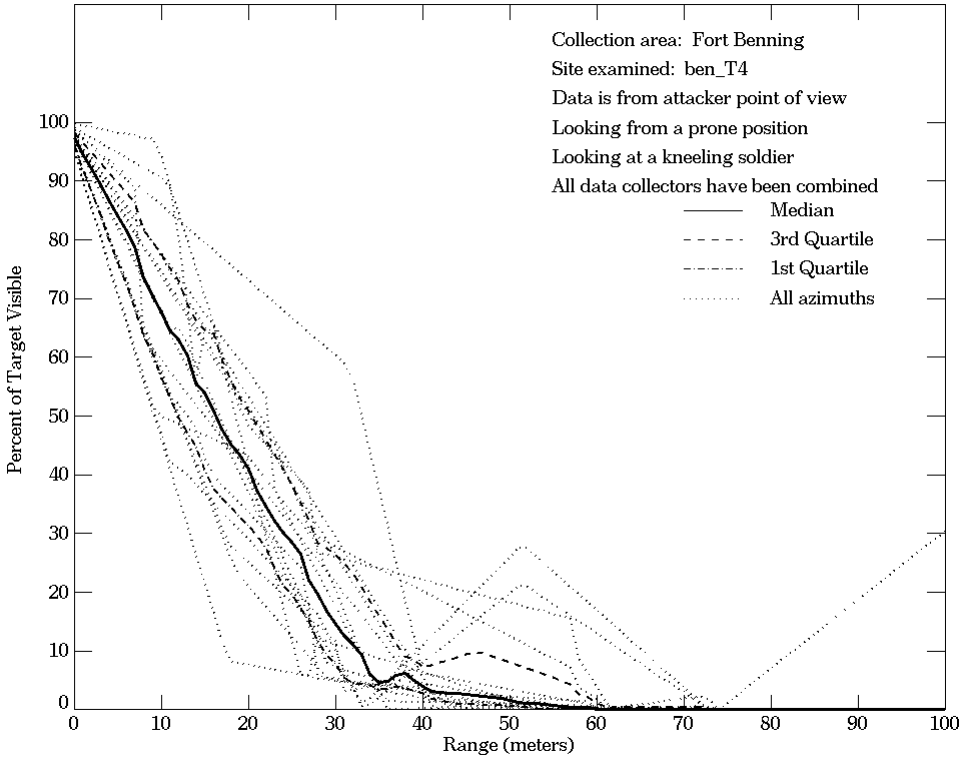

Figure E-72. Fort Benning, From Attacker Point of View, Site ben_T4

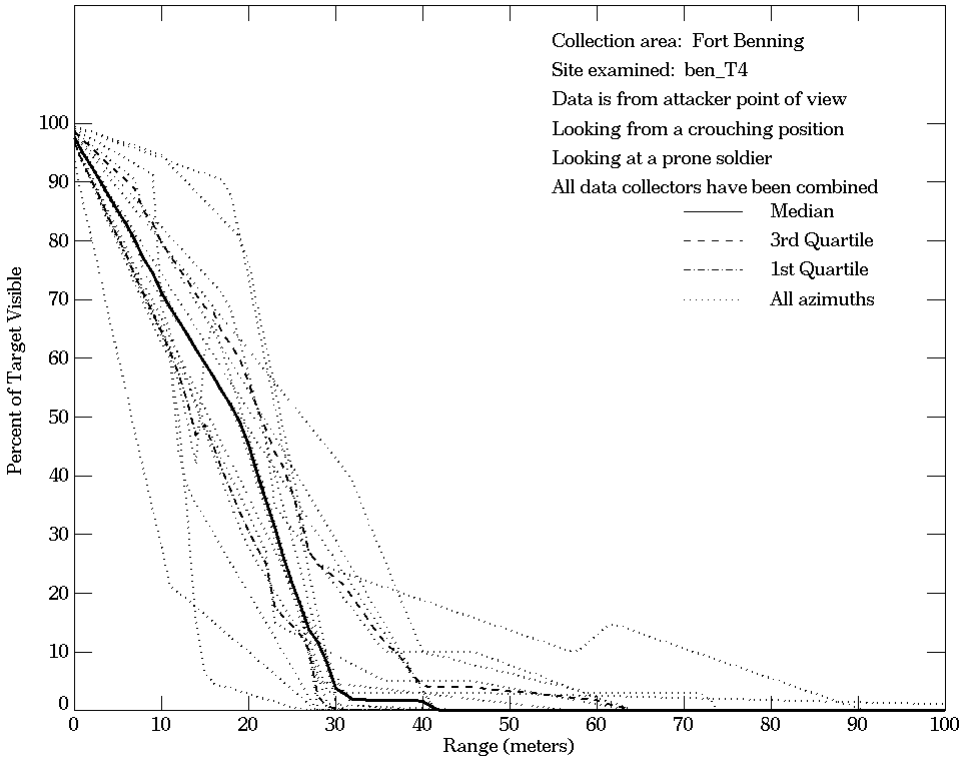

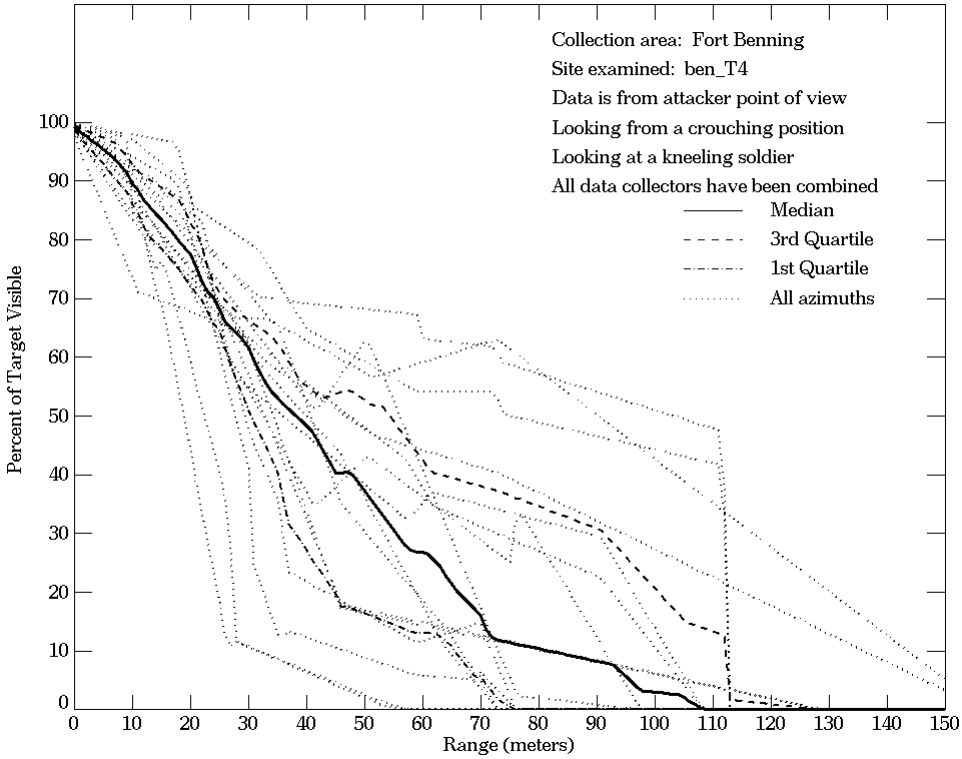

Figure E-72. Fort Benning, From Attacker Point of View, Site ben_T4 (Continued)

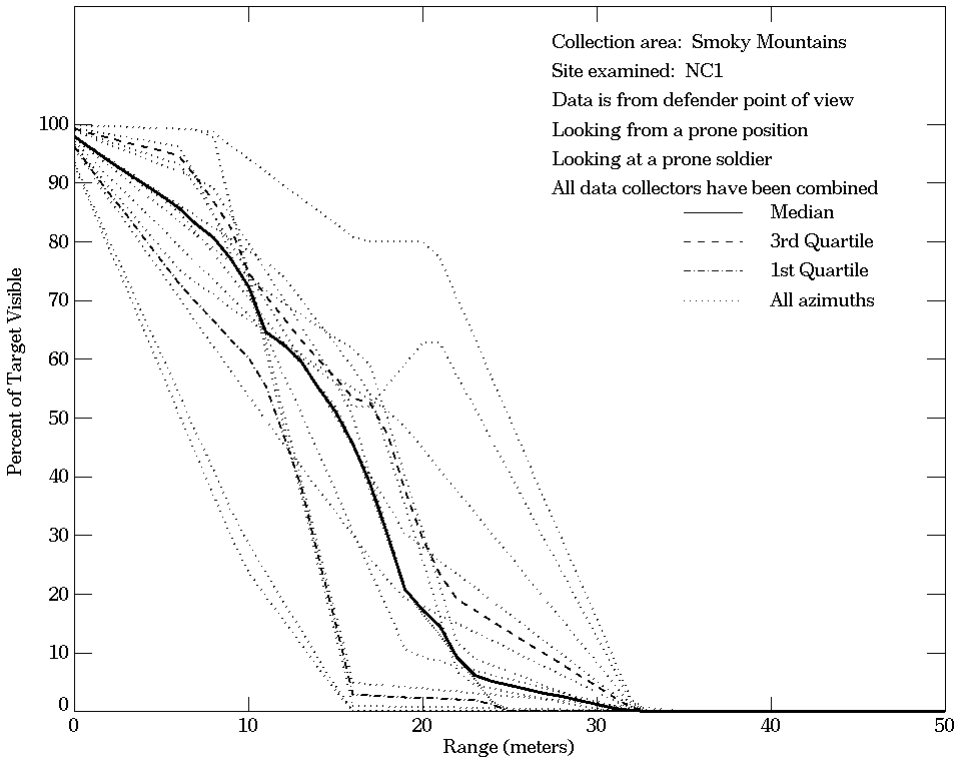

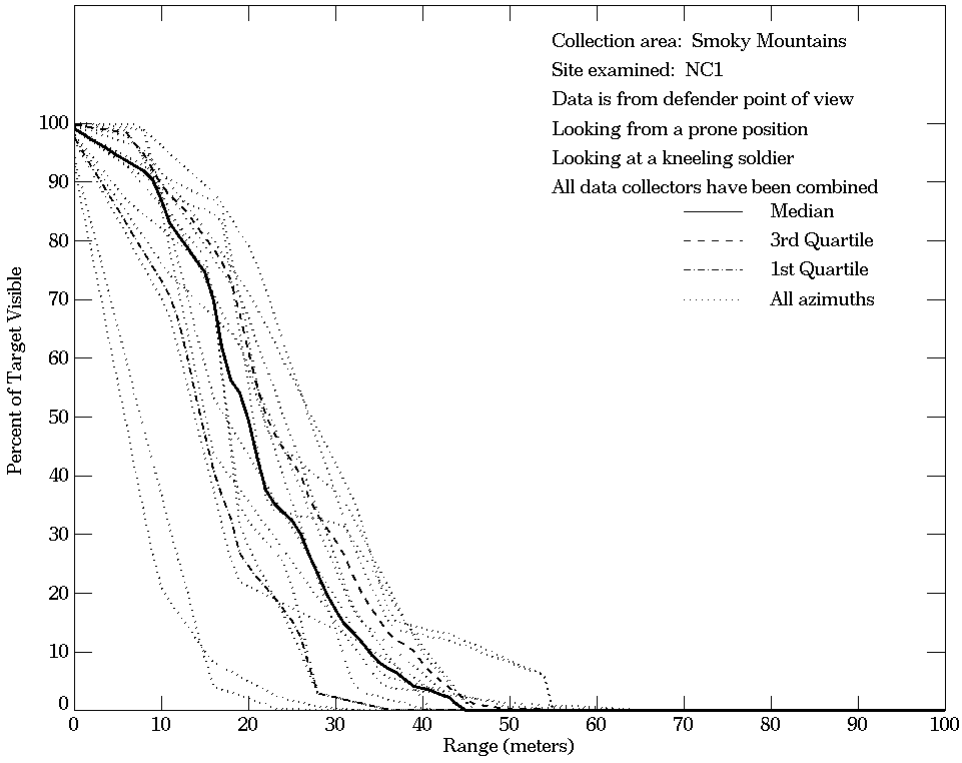

Figure E-73. Smoky Mountains, From Defender Point of View, Site NC1

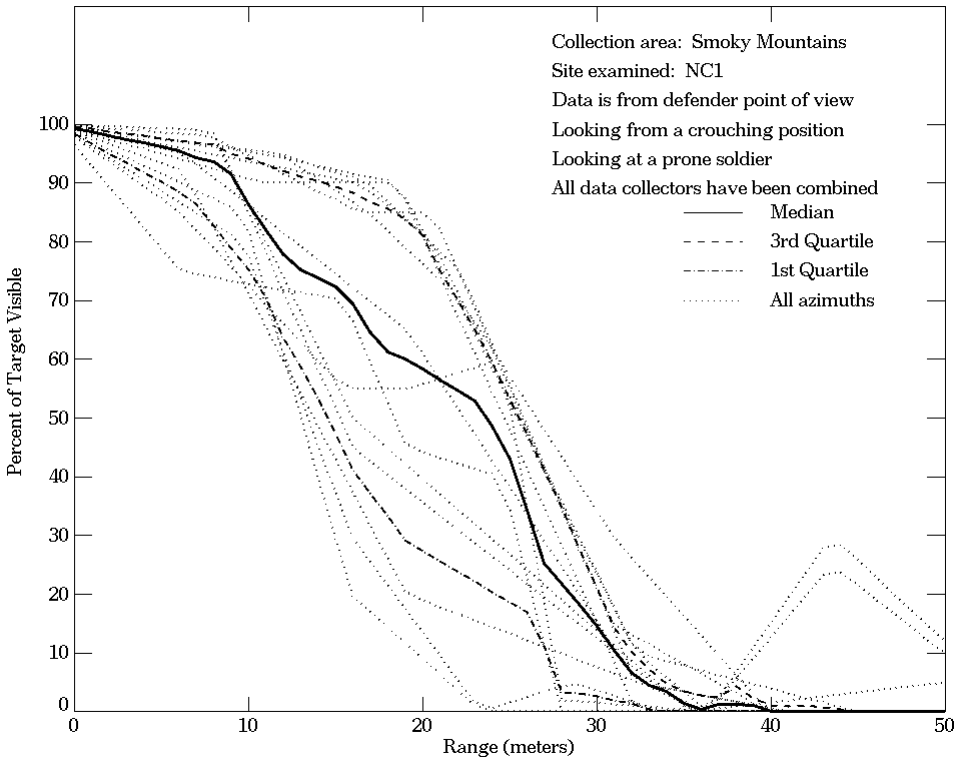

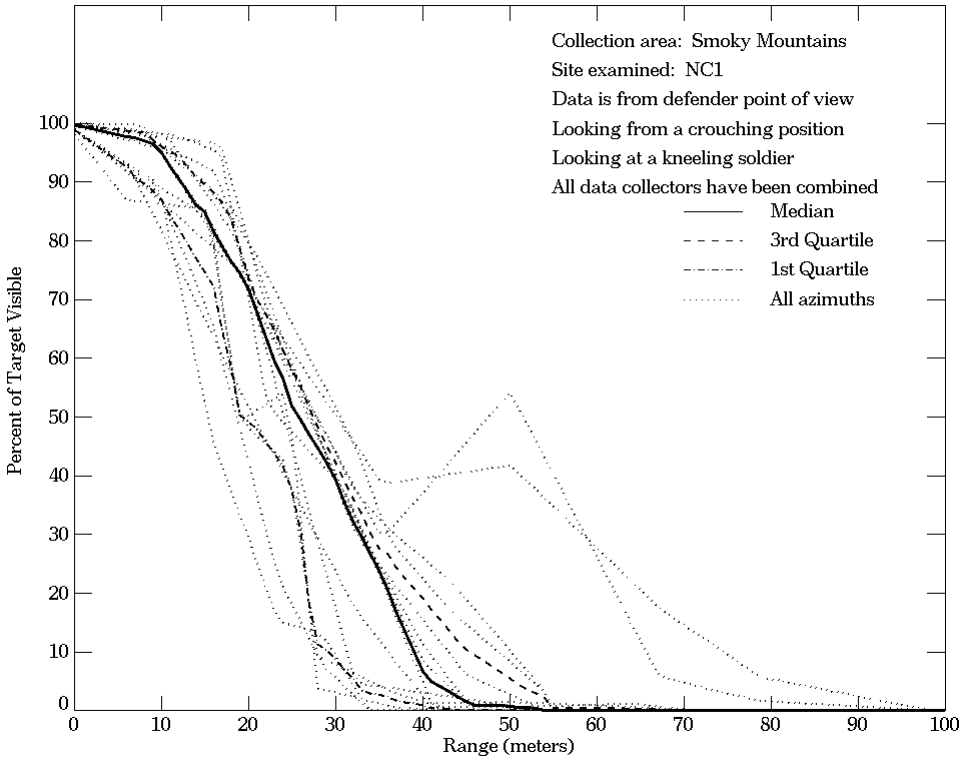

Figure E-73. Smoky Mountains, From Defender Point of View, Site NC1 (Continued)

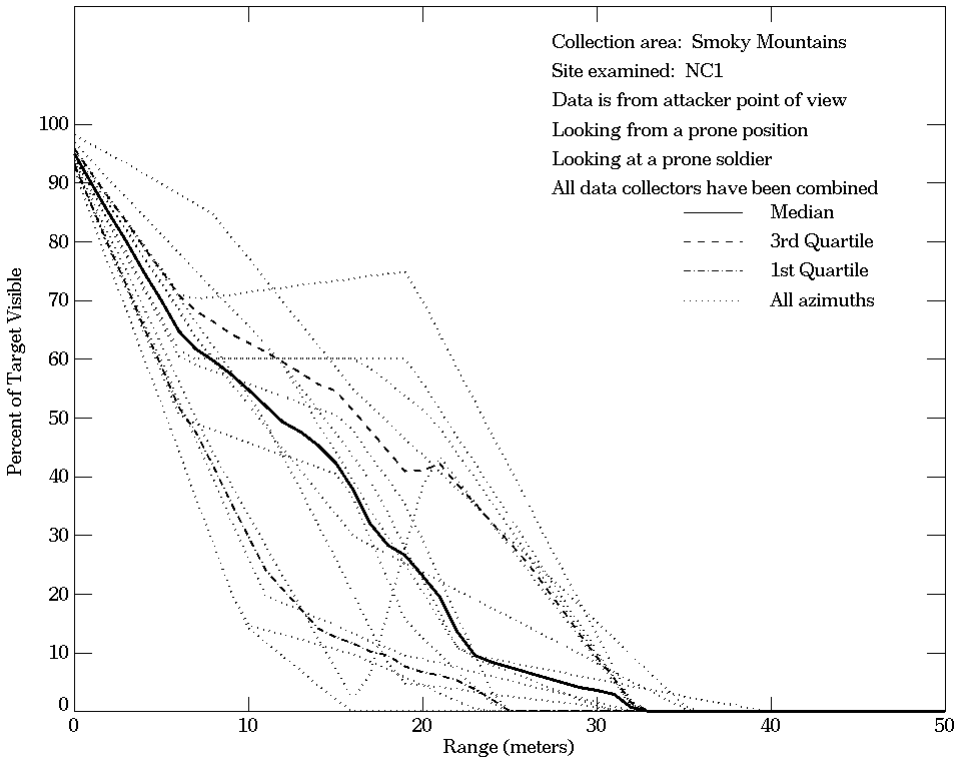

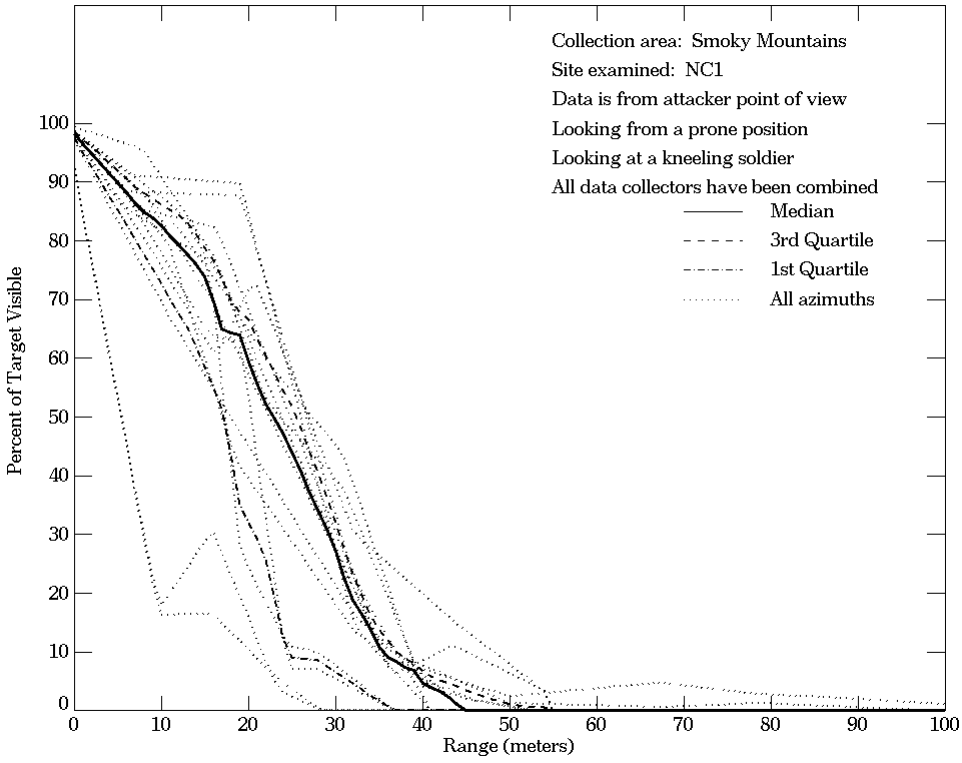

Figure E-74. Smoky Mountains, From Attacker Point of View, Site NC1

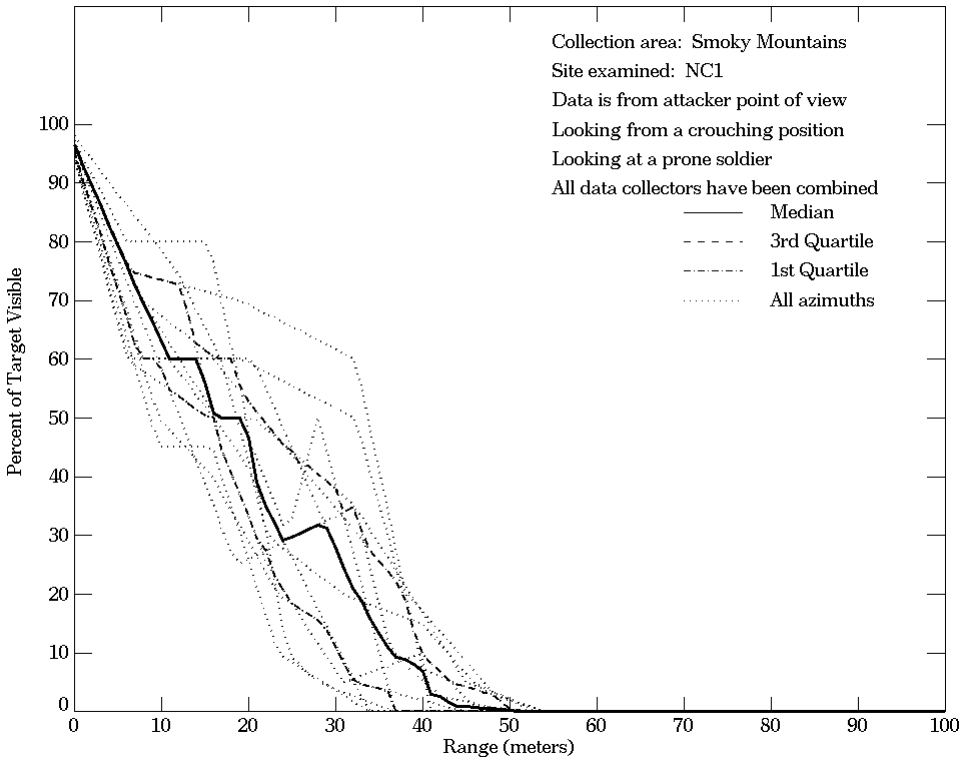

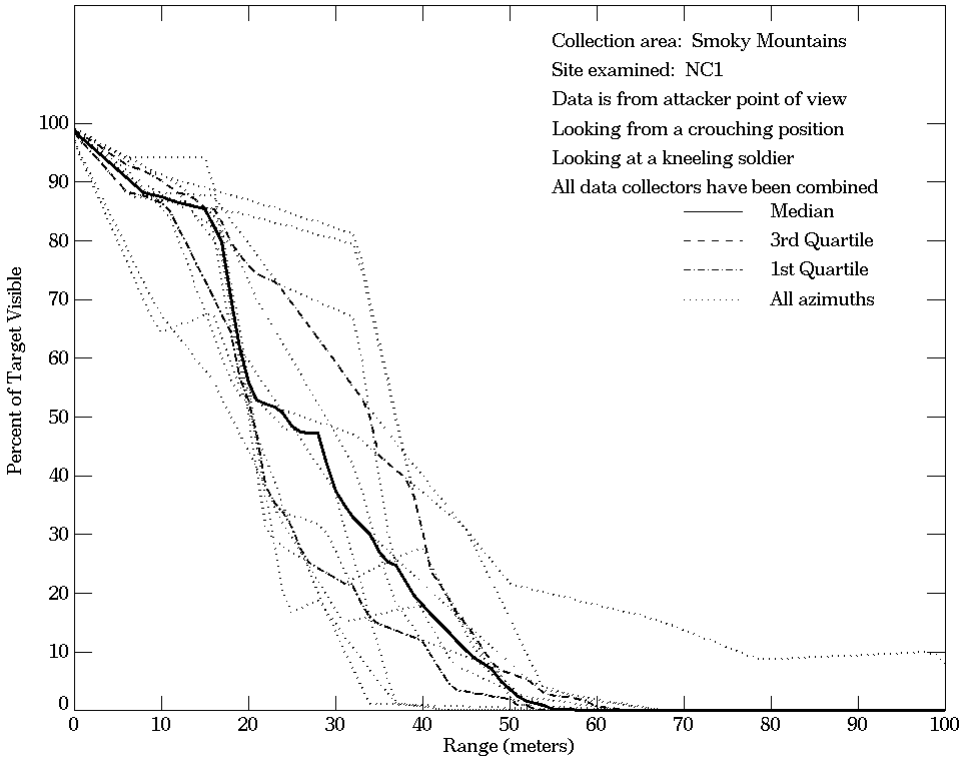

Figure E-74. Smoky Mountains, From Attacker Point of View, Site NC1 (Continued)

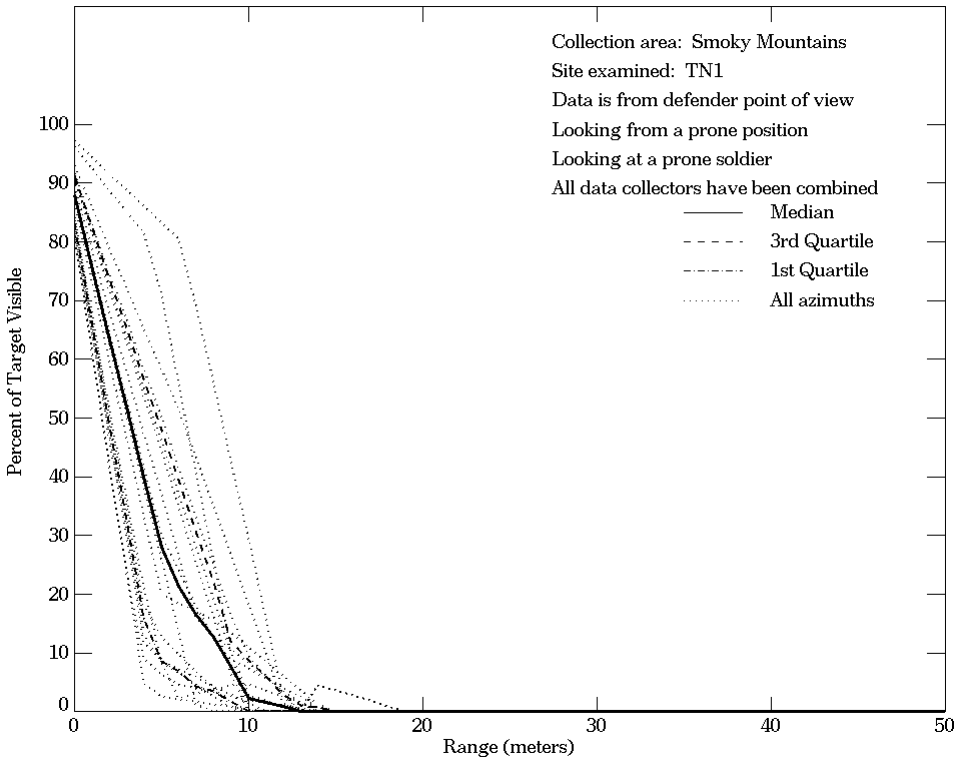

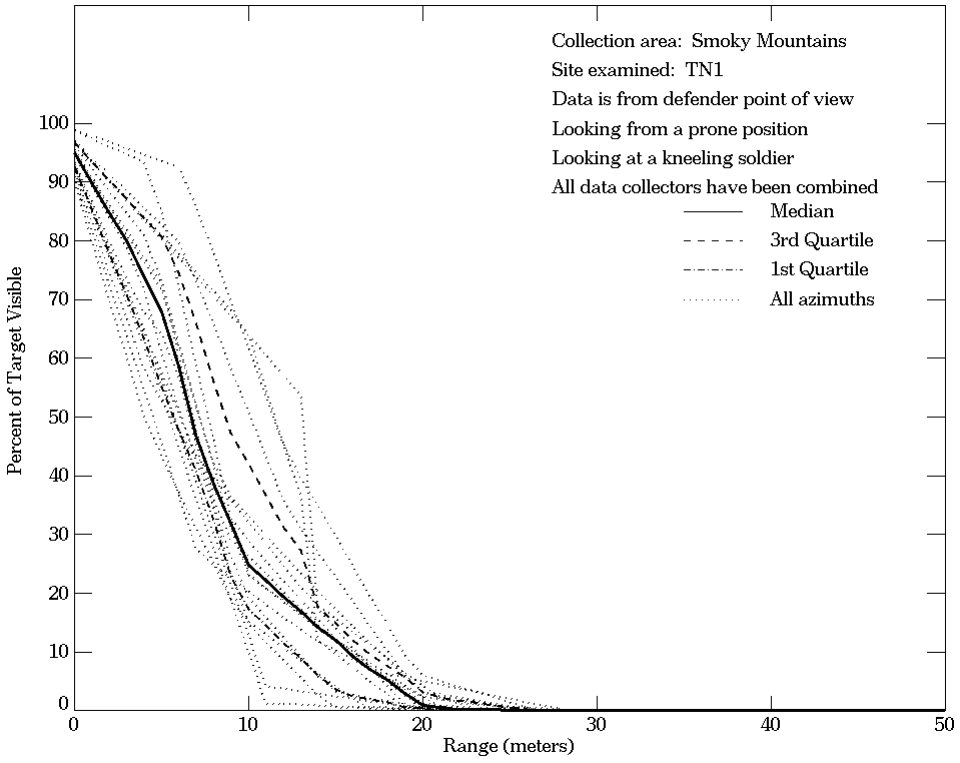

Figure E-75. Smoky Mountains, From Defender Point of View, Site TN1

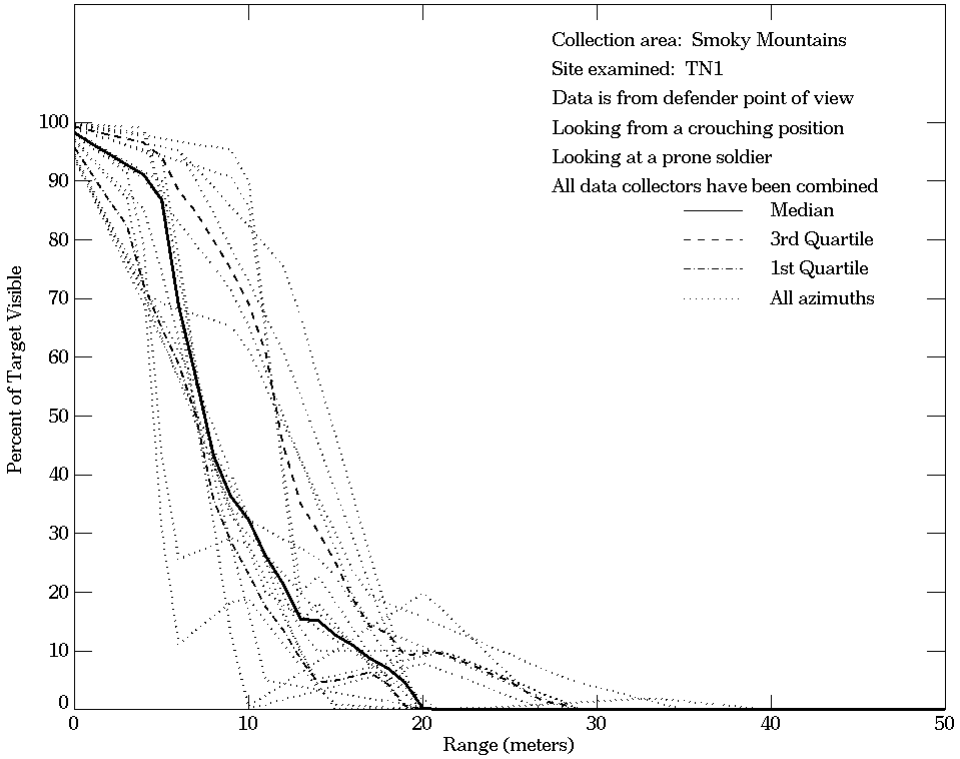

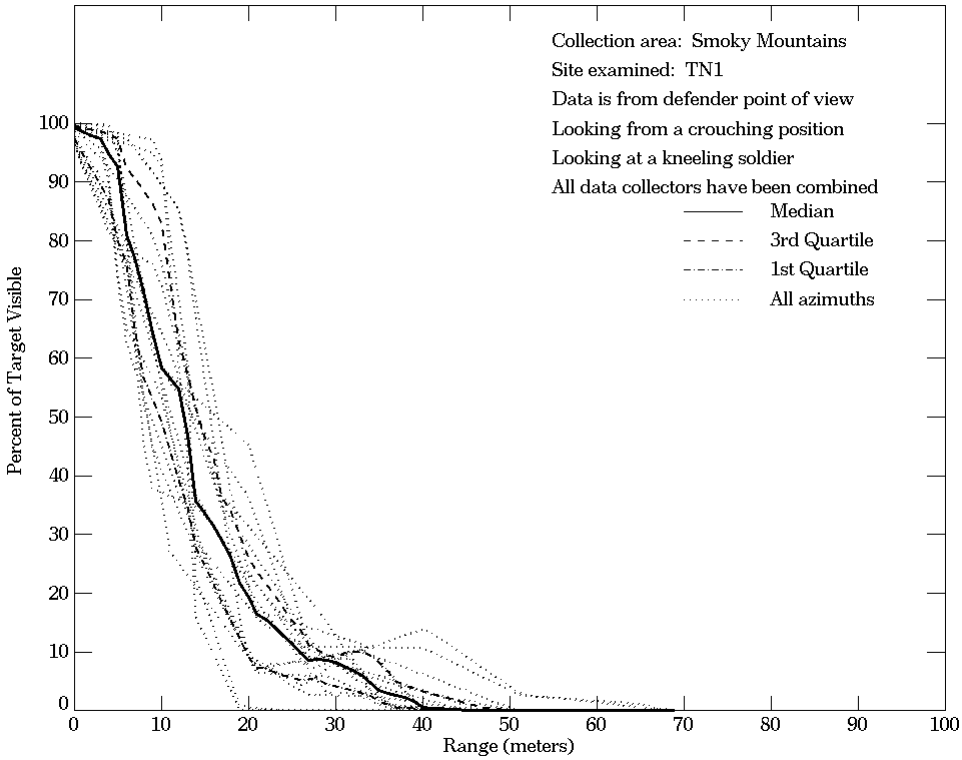

Figure E-75. Smoky Mountains, From Defender Point of View, Site TN1 (Continued)

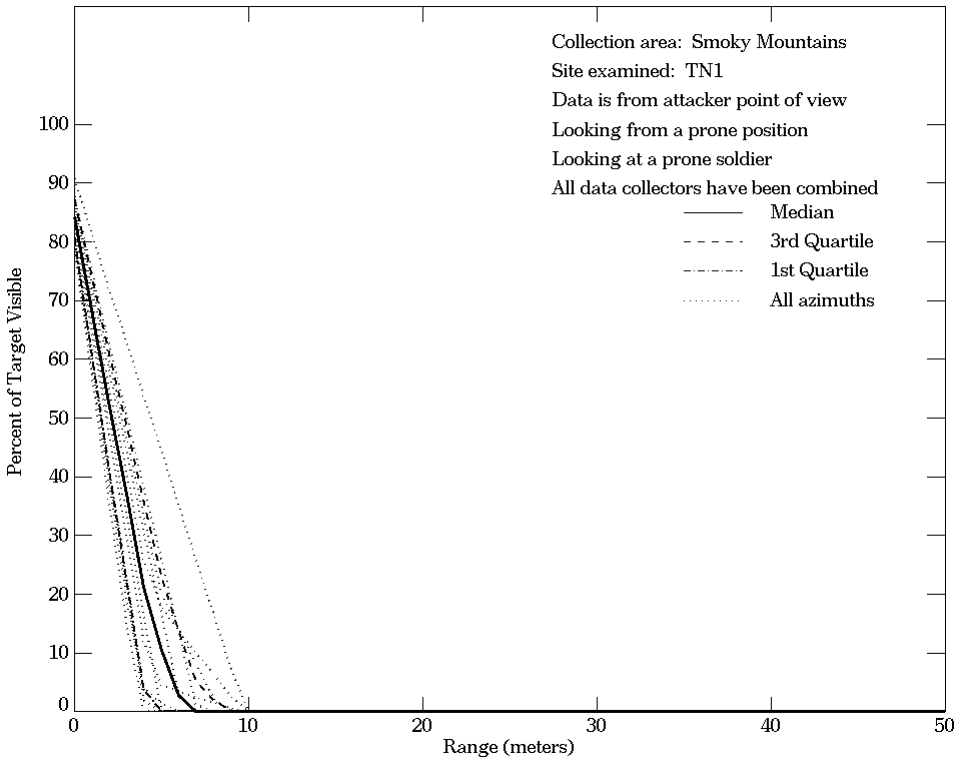

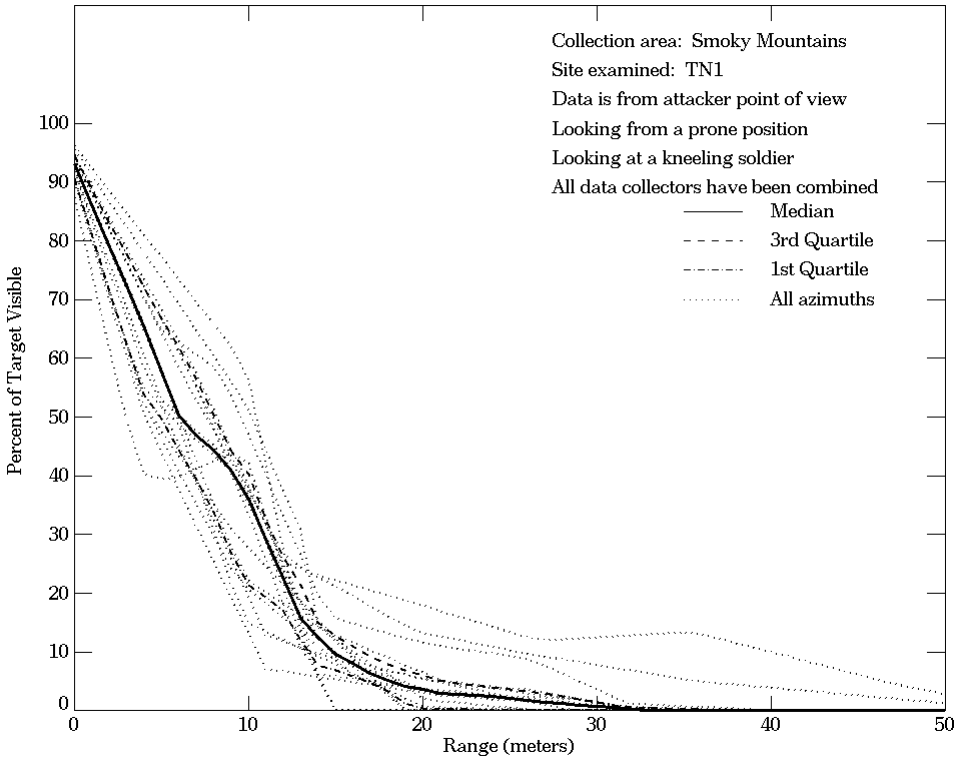

Figure E-76. Smoky Mountains, From Attacker Point of View, Site TN1

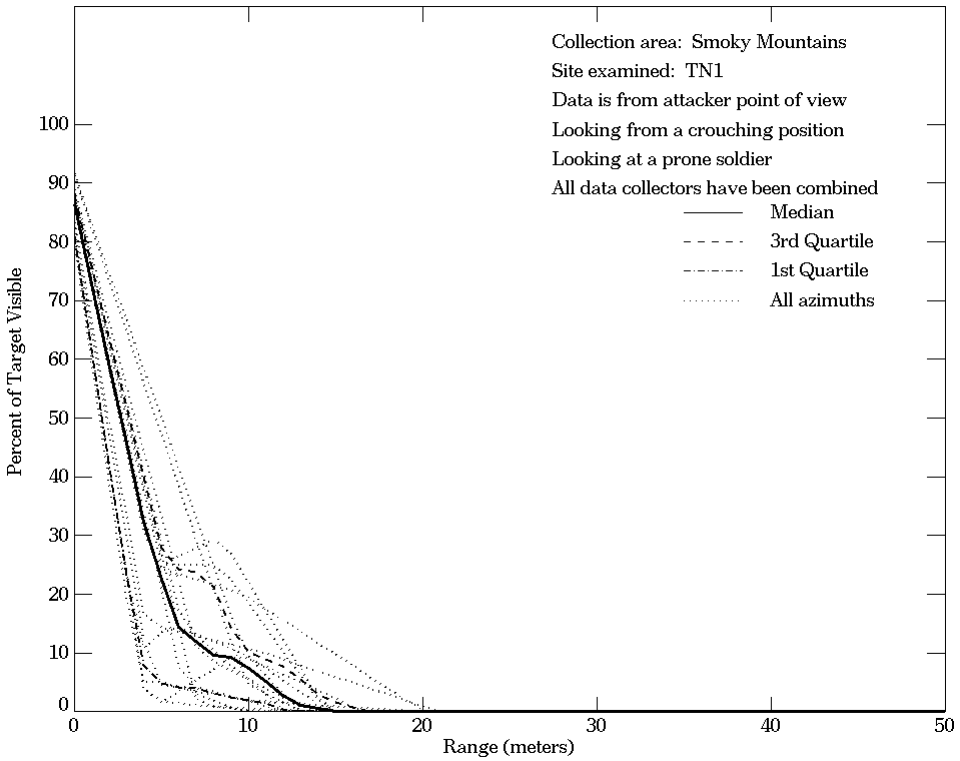

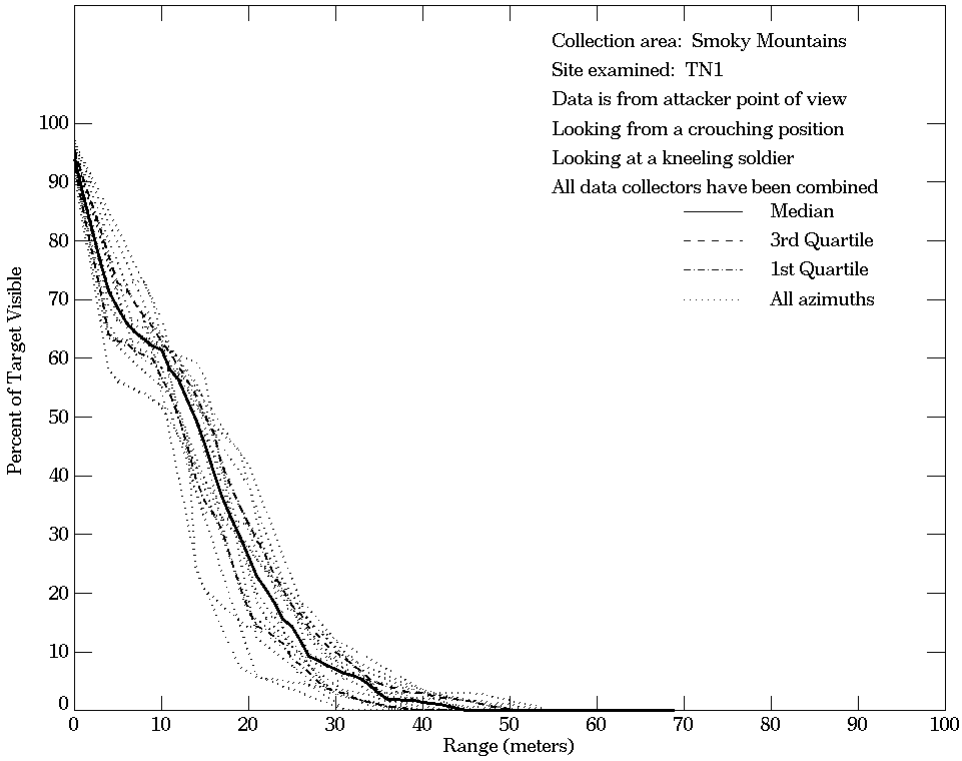

Figure E-76. Smoky Mountains, From Attacker Point of View, Site TN1 (Continued)

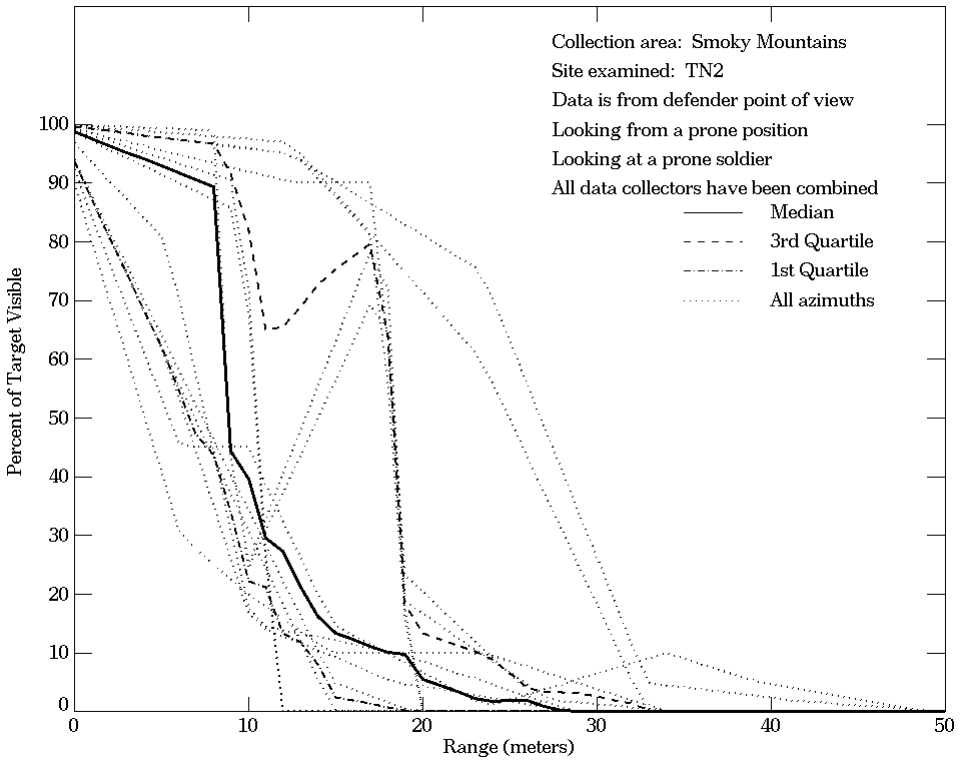

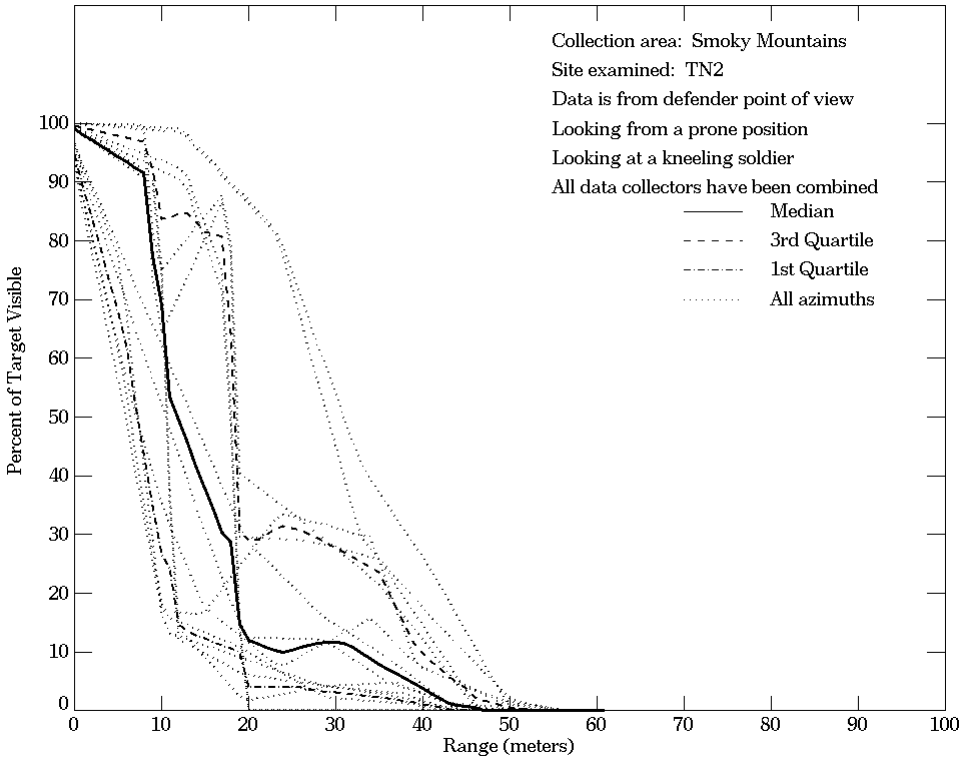

Figure E-77. Smoky Mountains, From Defender Point of View, Site TN2

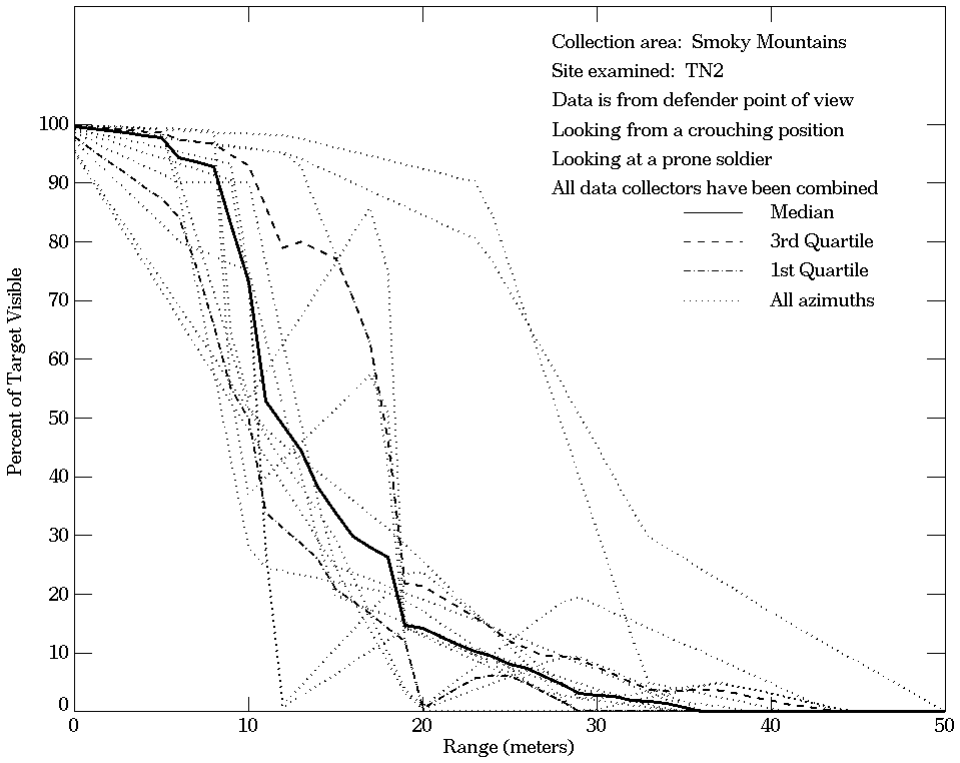

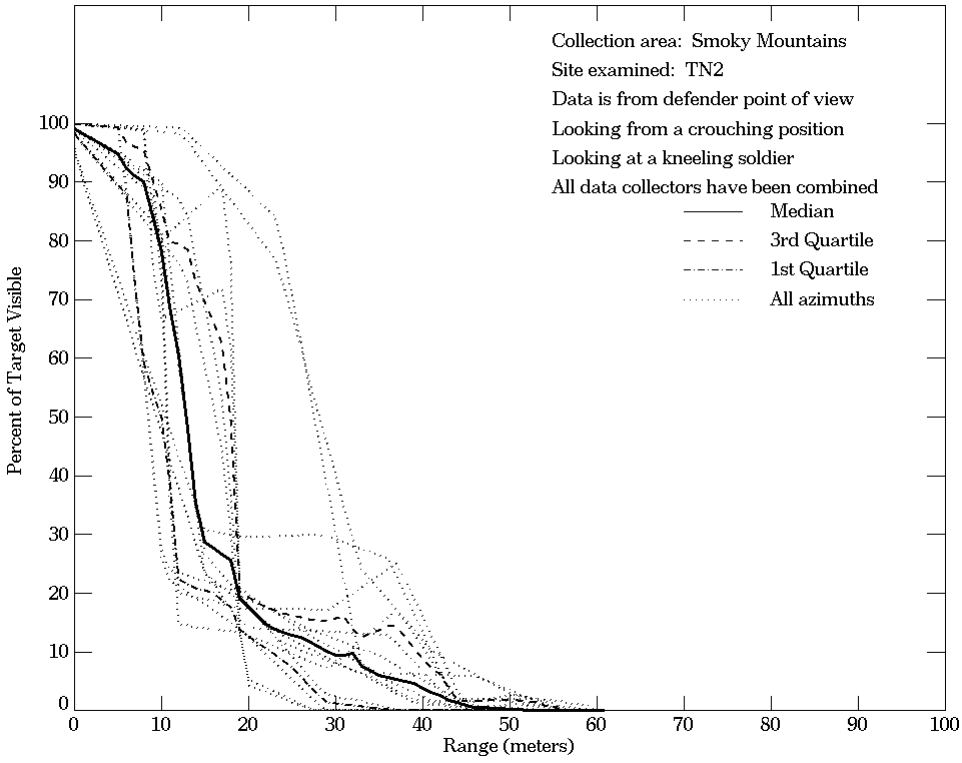

Figure E-77. Smoky Mountains, From Defender Point of View, Site TN2 (Continued)

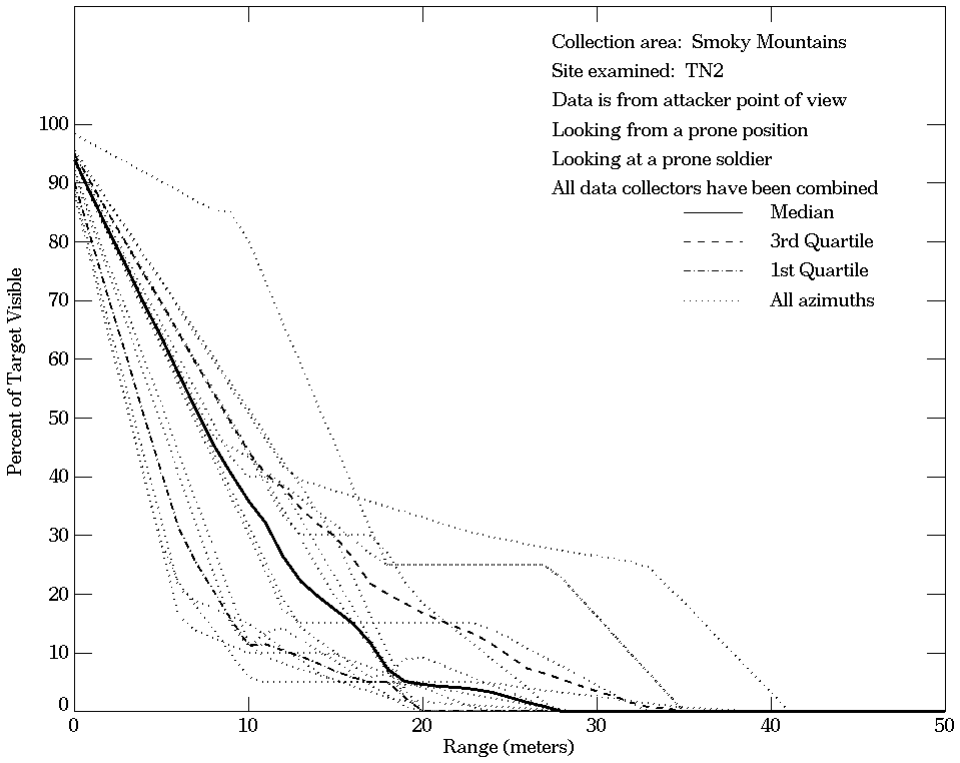

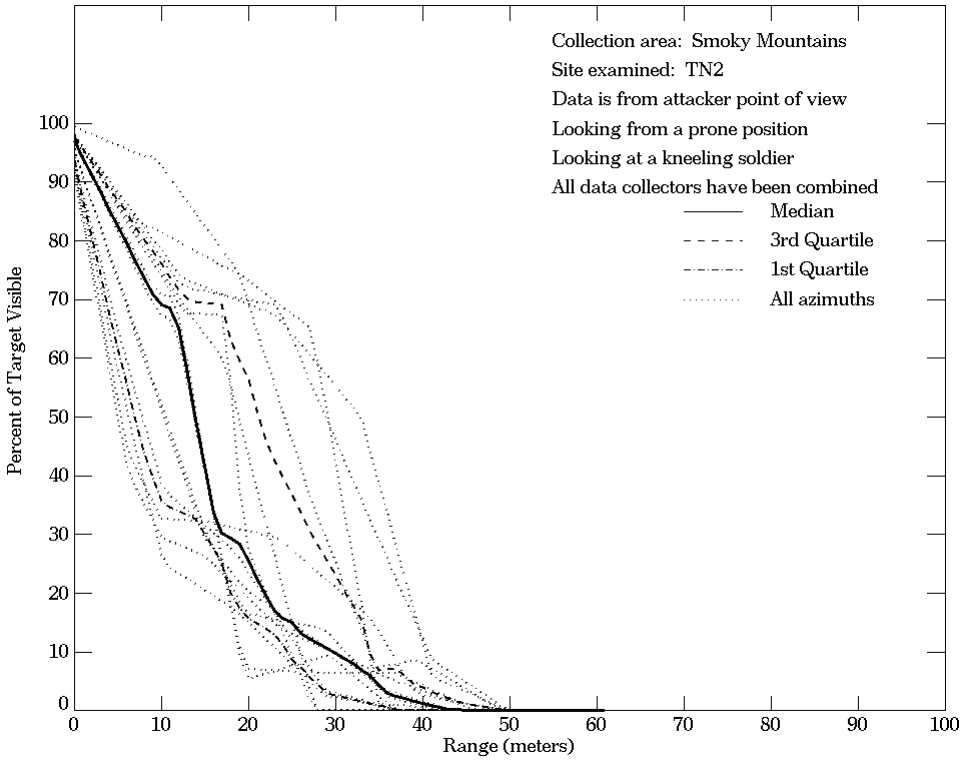

Figure E-78. Smoky Mountains, From Attacker Point of View, Site TN2

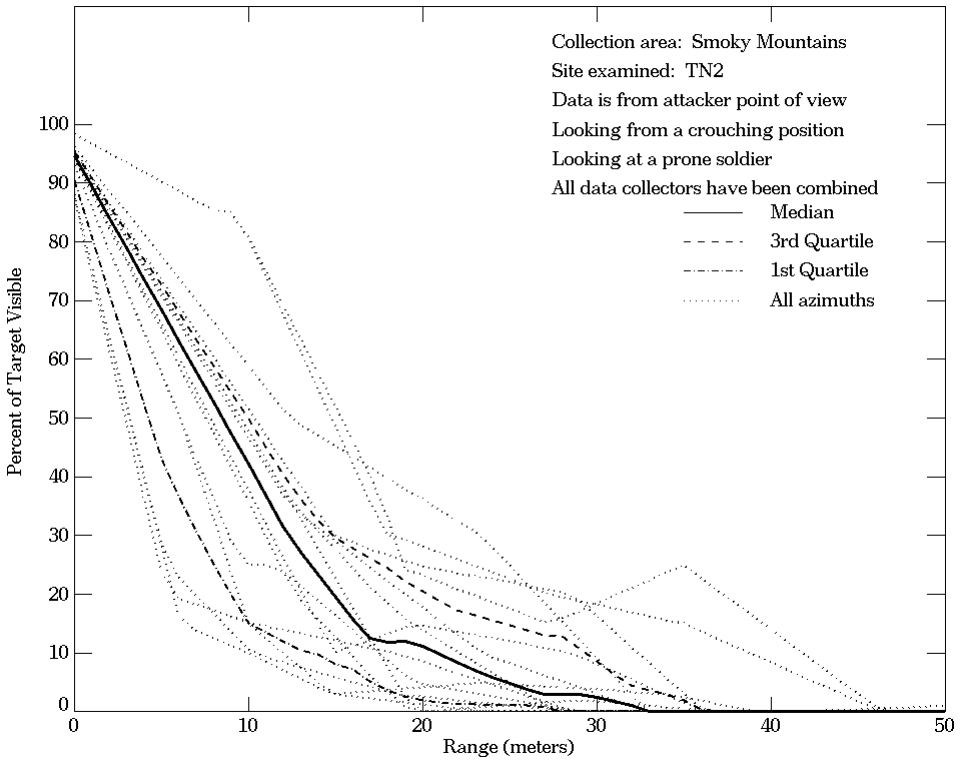

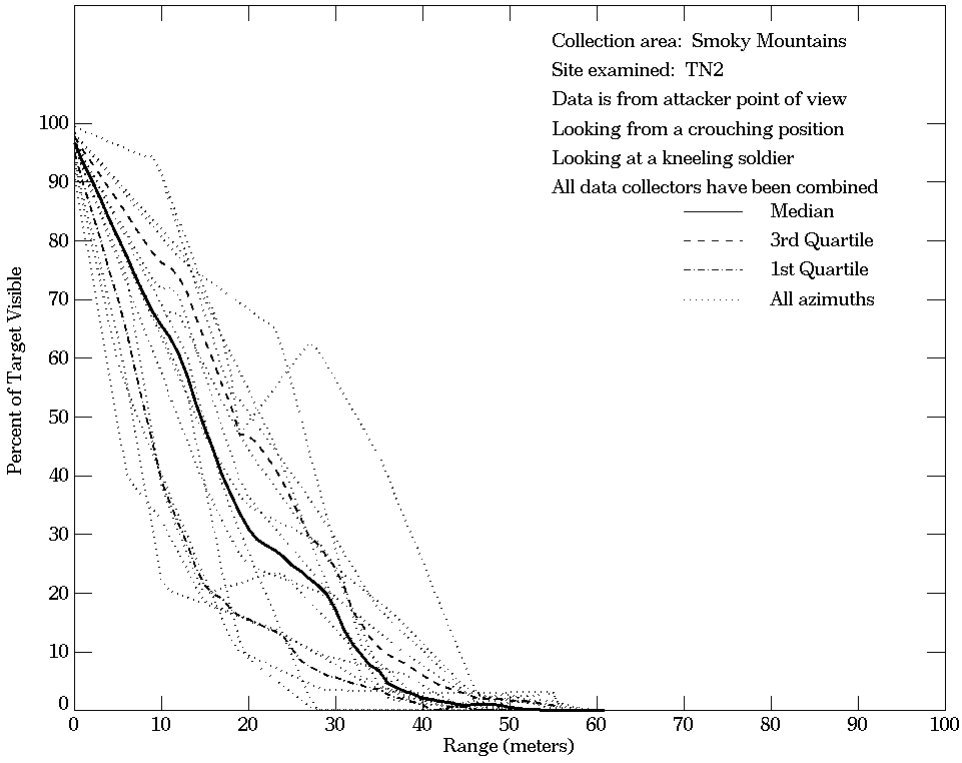

Figure E-78. Smoky Mountains, From Attacker Point of View, Site TN2 (Continued)

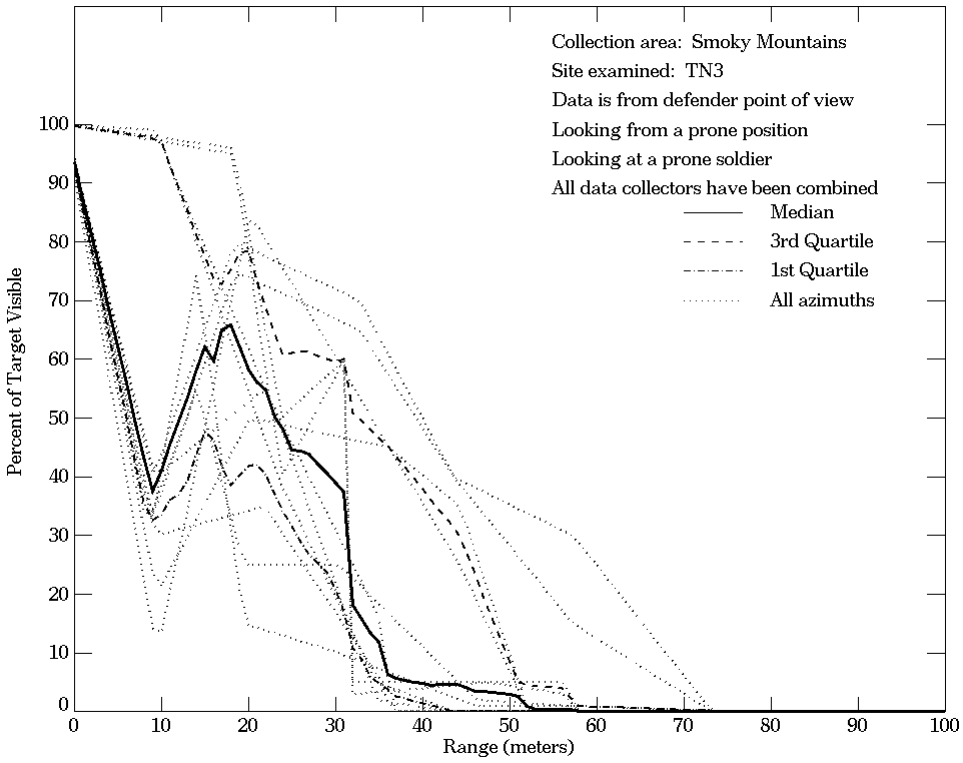

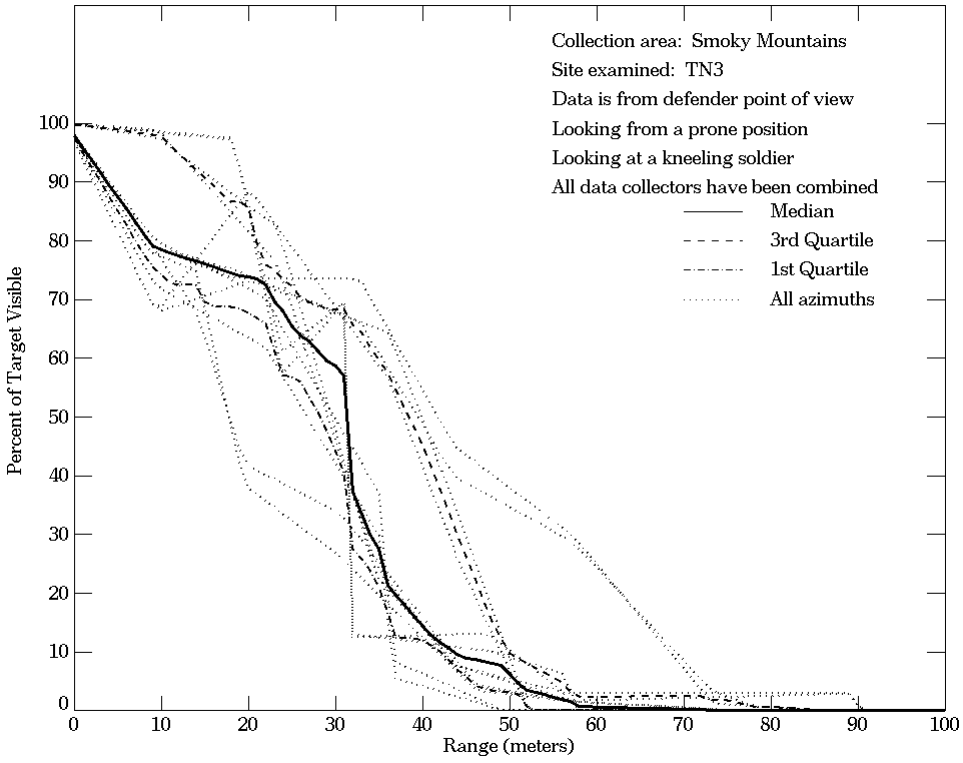

Figure E-79. Smoky Mountains, From Defender Point of View, Site TN3

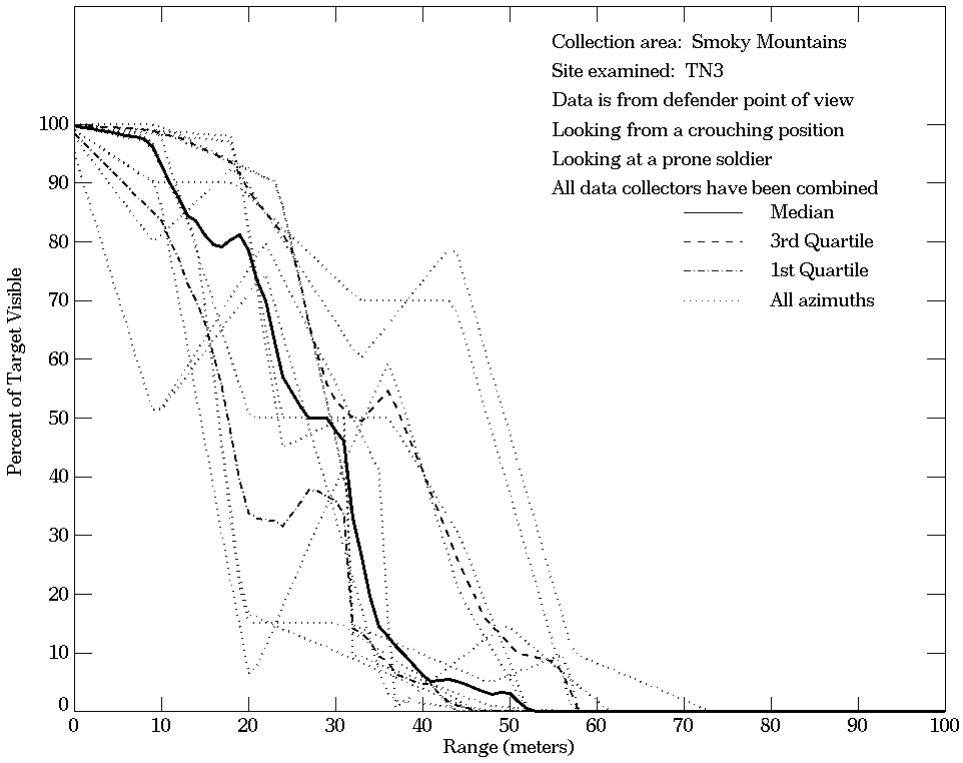

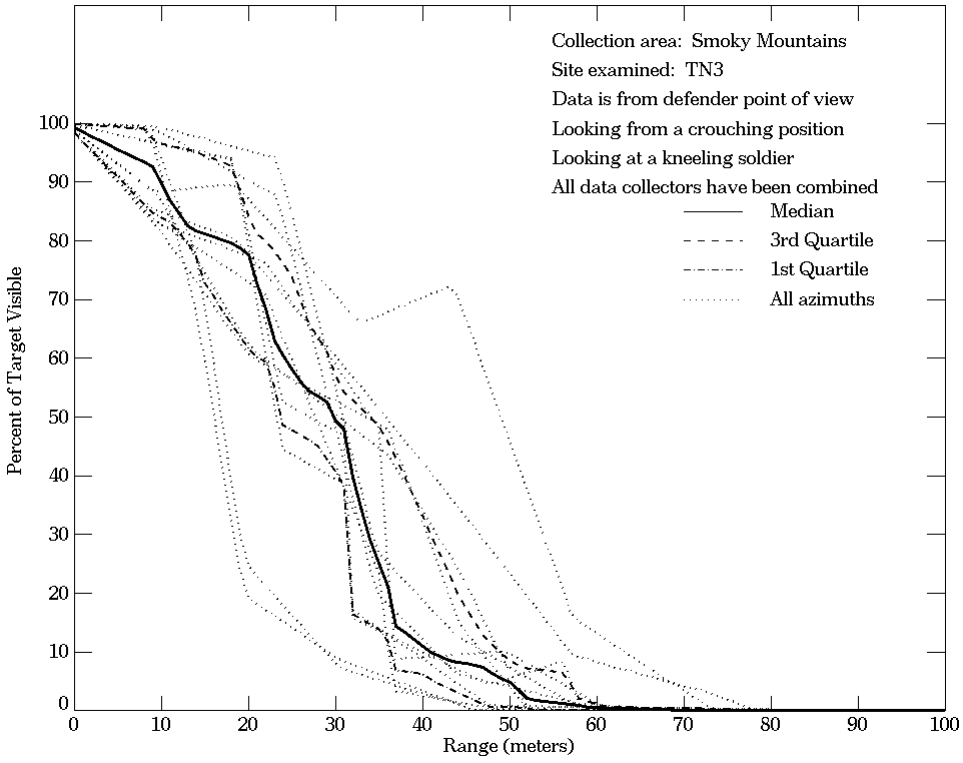

Figure E-79. Smoky Mountains, From Defender Point of View, Site TN3 (Continued)

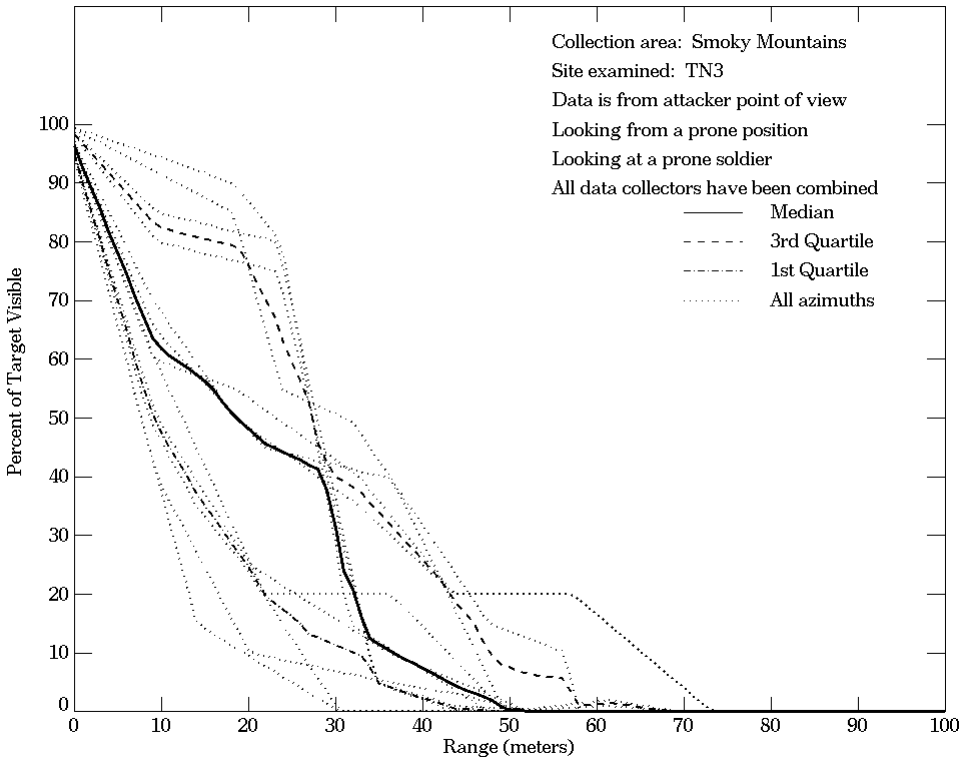

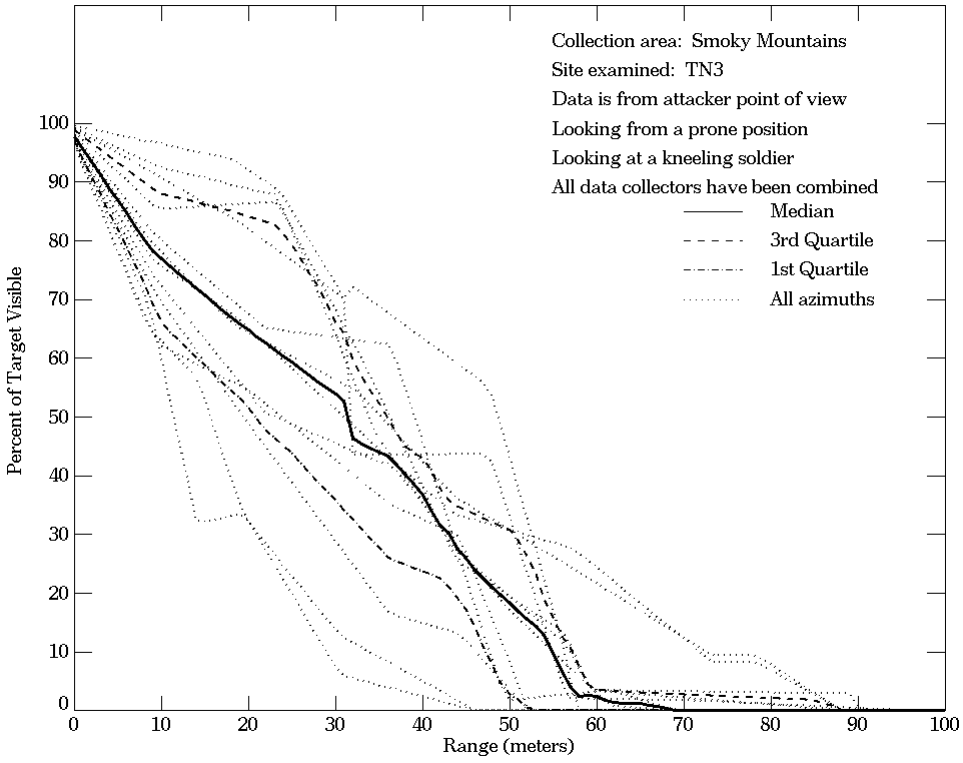

Figure E-80. Smoky Mountains, From Attacker Point of View, Site TN3

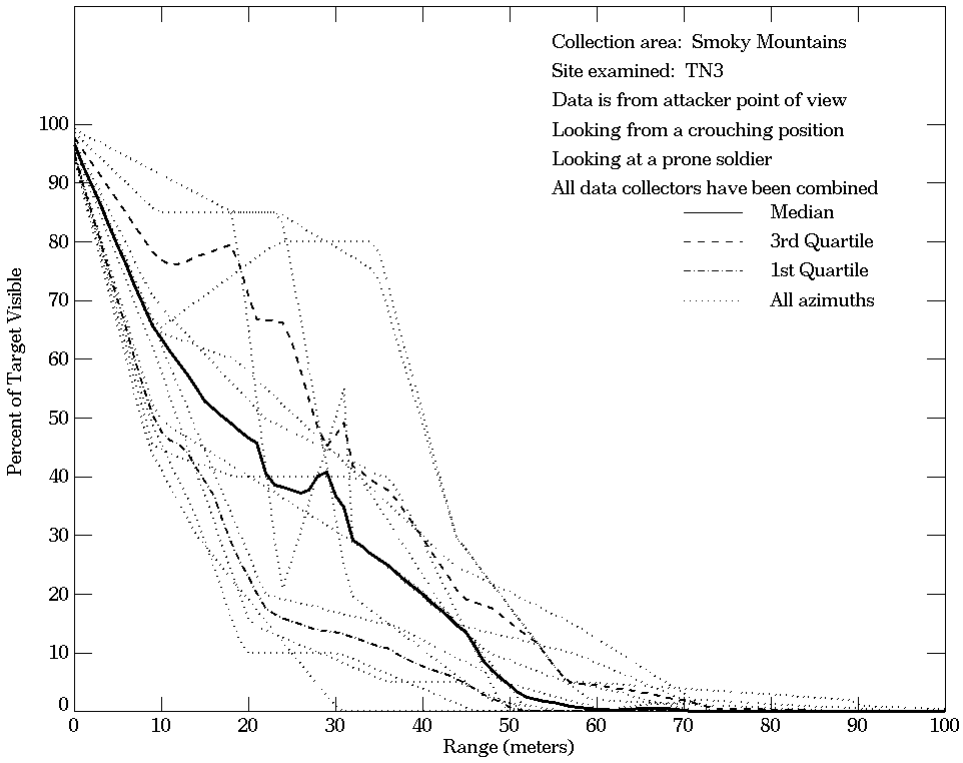

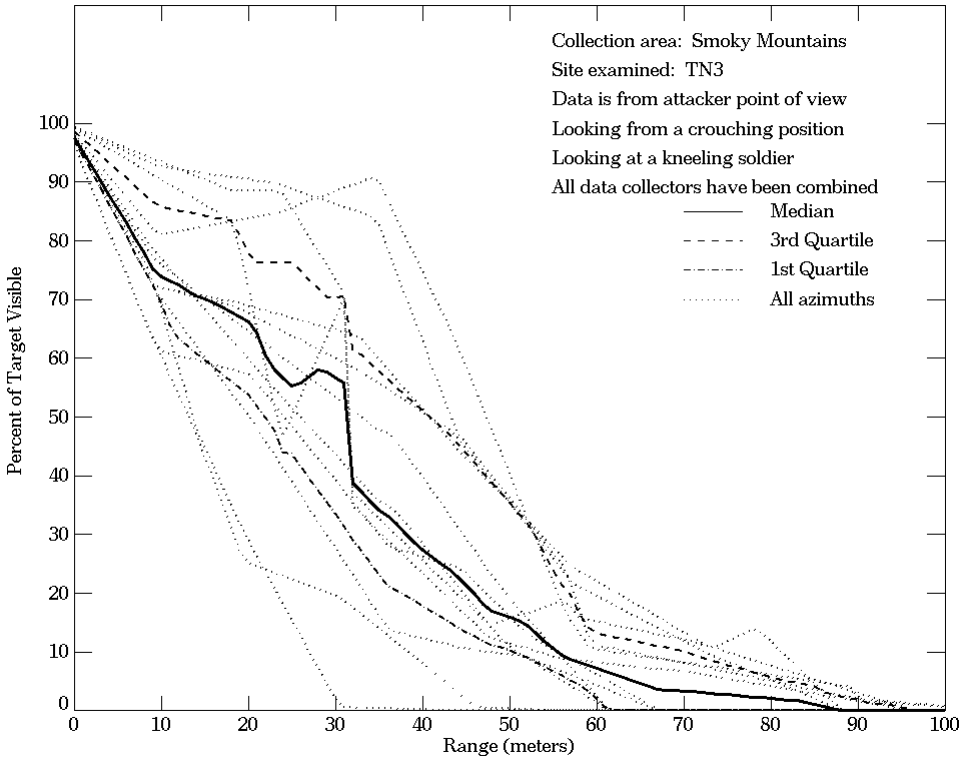

Figure E-80. Smoky Mountains, From Attacker Point of View, Site TN3 (Continued)

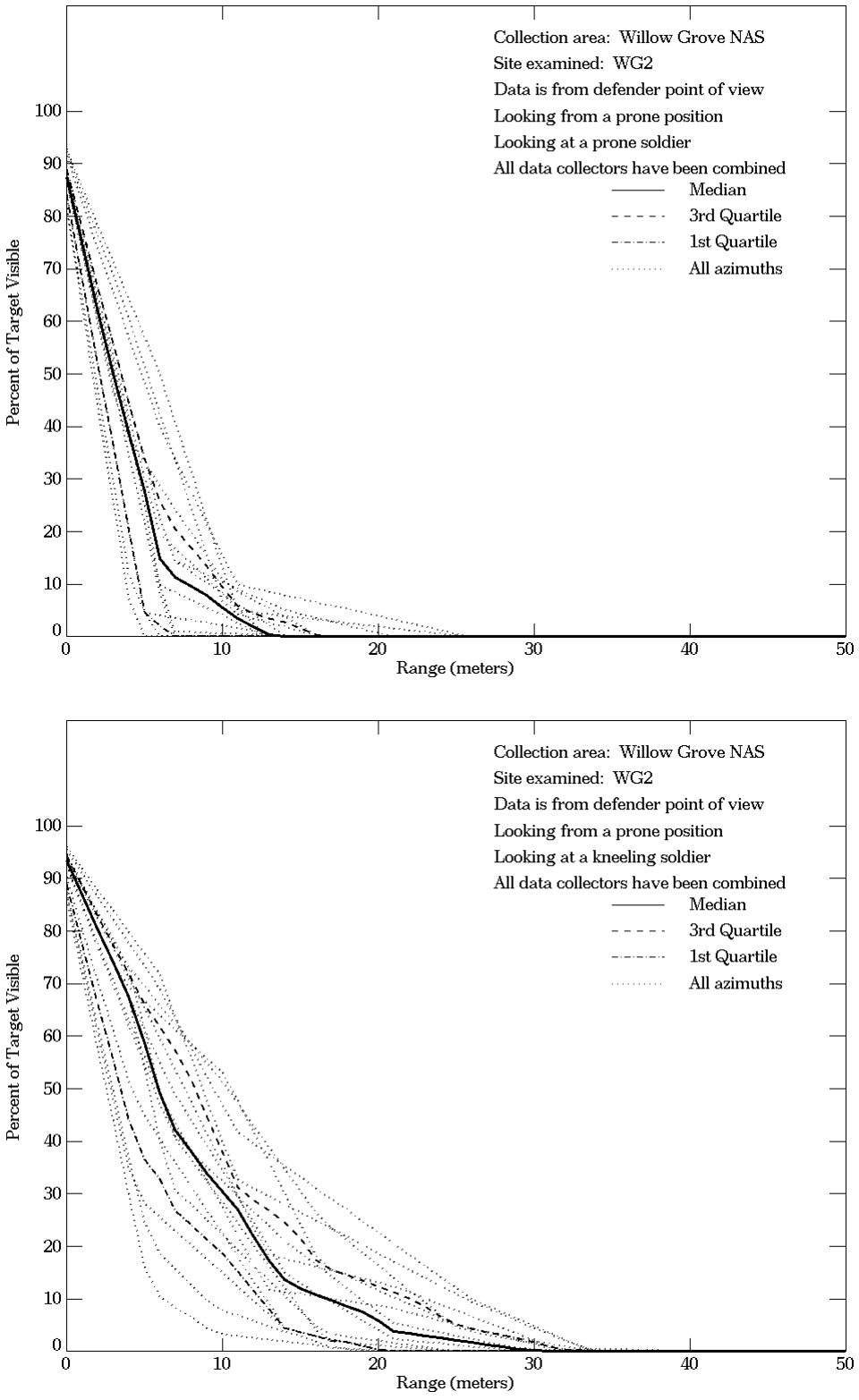

Figure E-81. Willow Grove NAS, From Defender Point of View, Site WG2

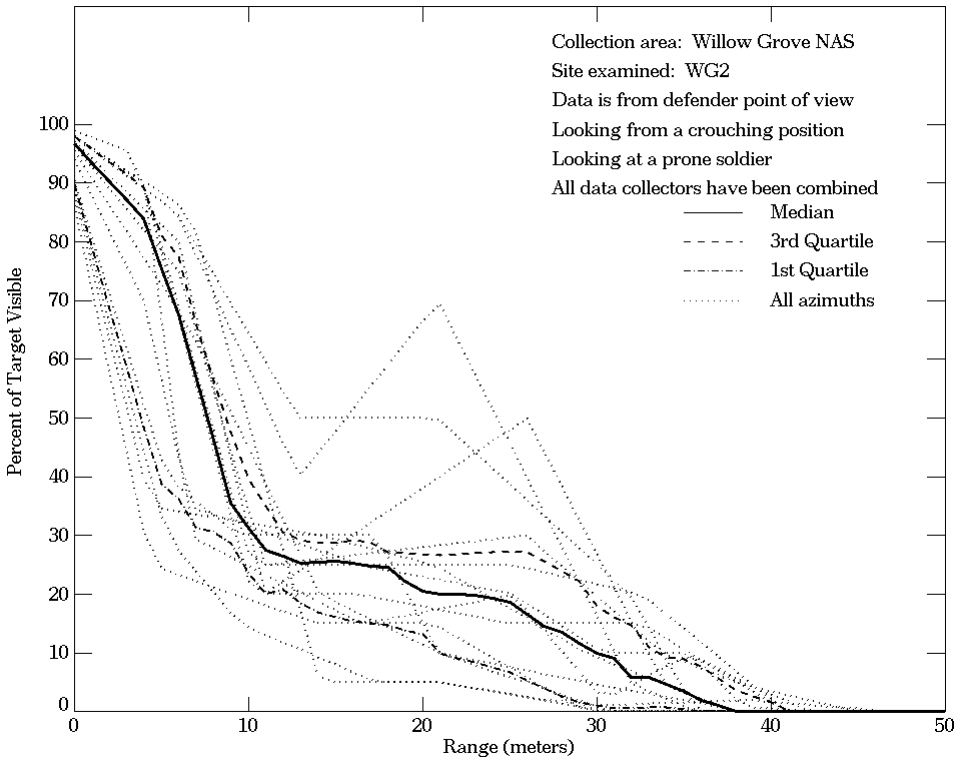

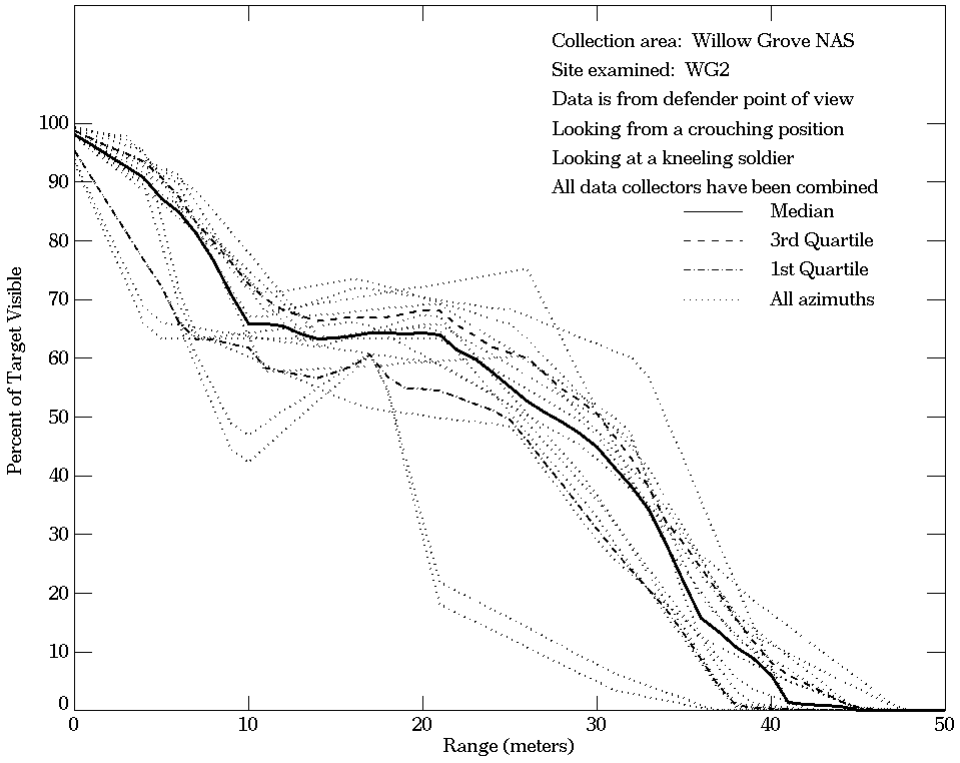

Figure E-81. Willow Grove NAS, From Defender Point of View, Site WG2 (Continued)

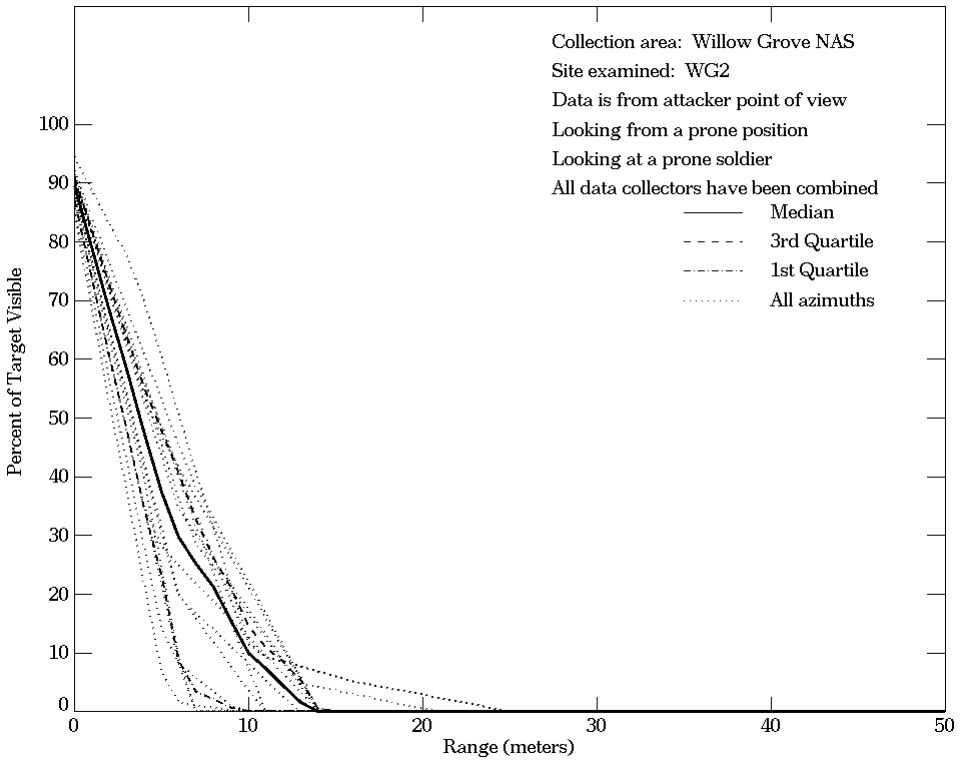

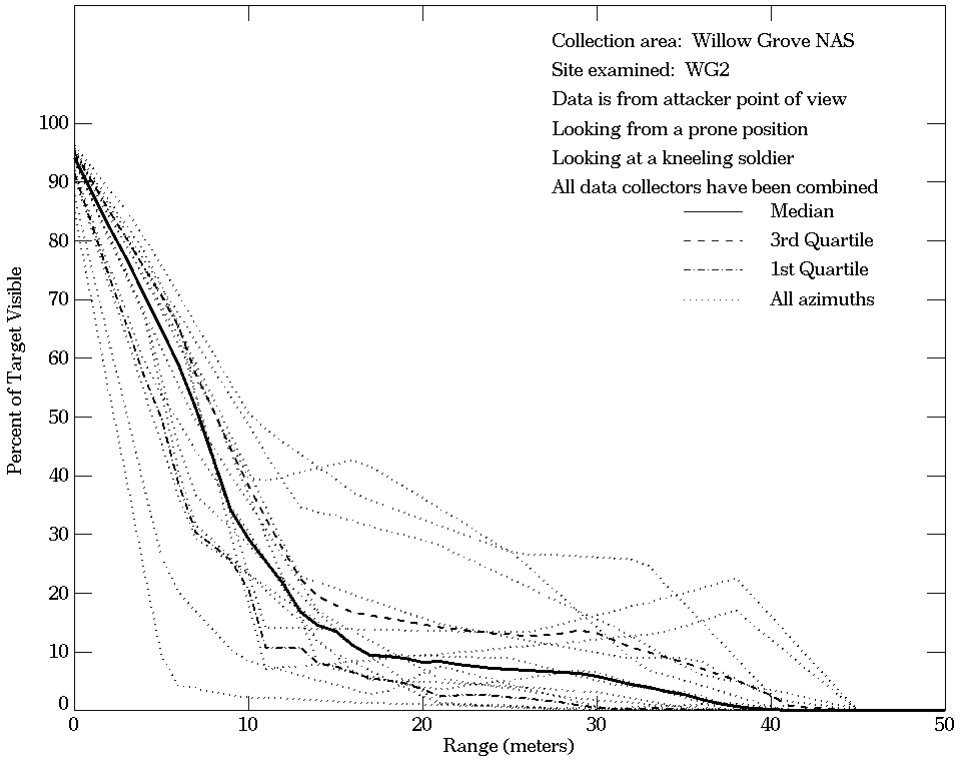

Figure E-82. Willow Grove NAS, From Attacker Point of View, Site WG2

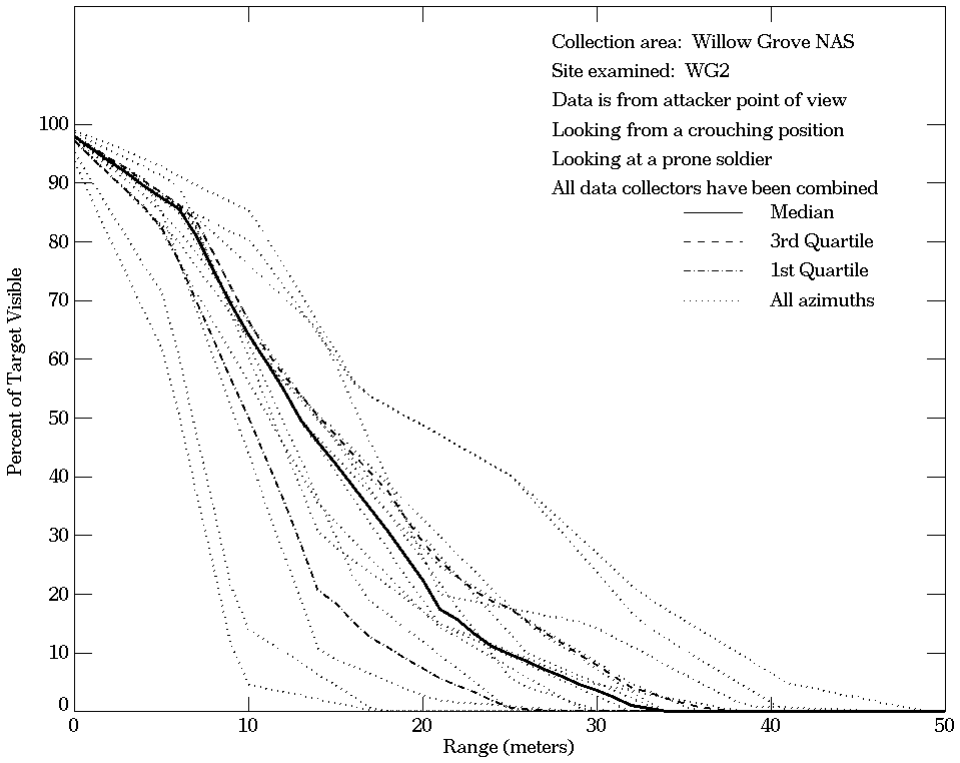

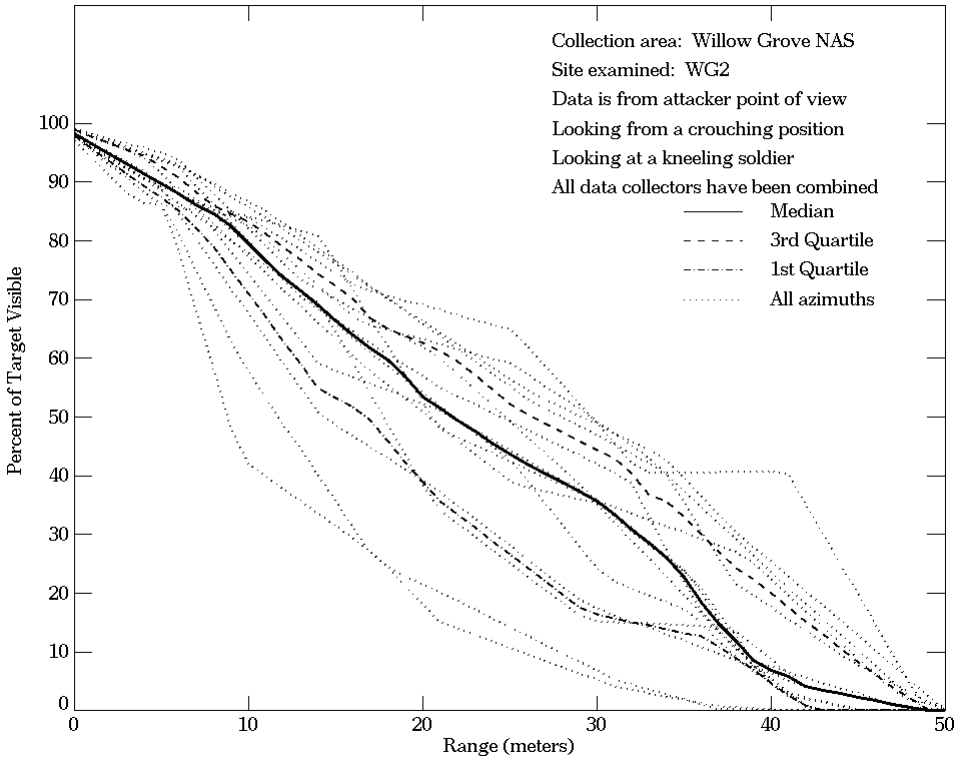

Figure E-82. Willow Grove NAS, From Attacker Point of View, Site WG2 (Continued)

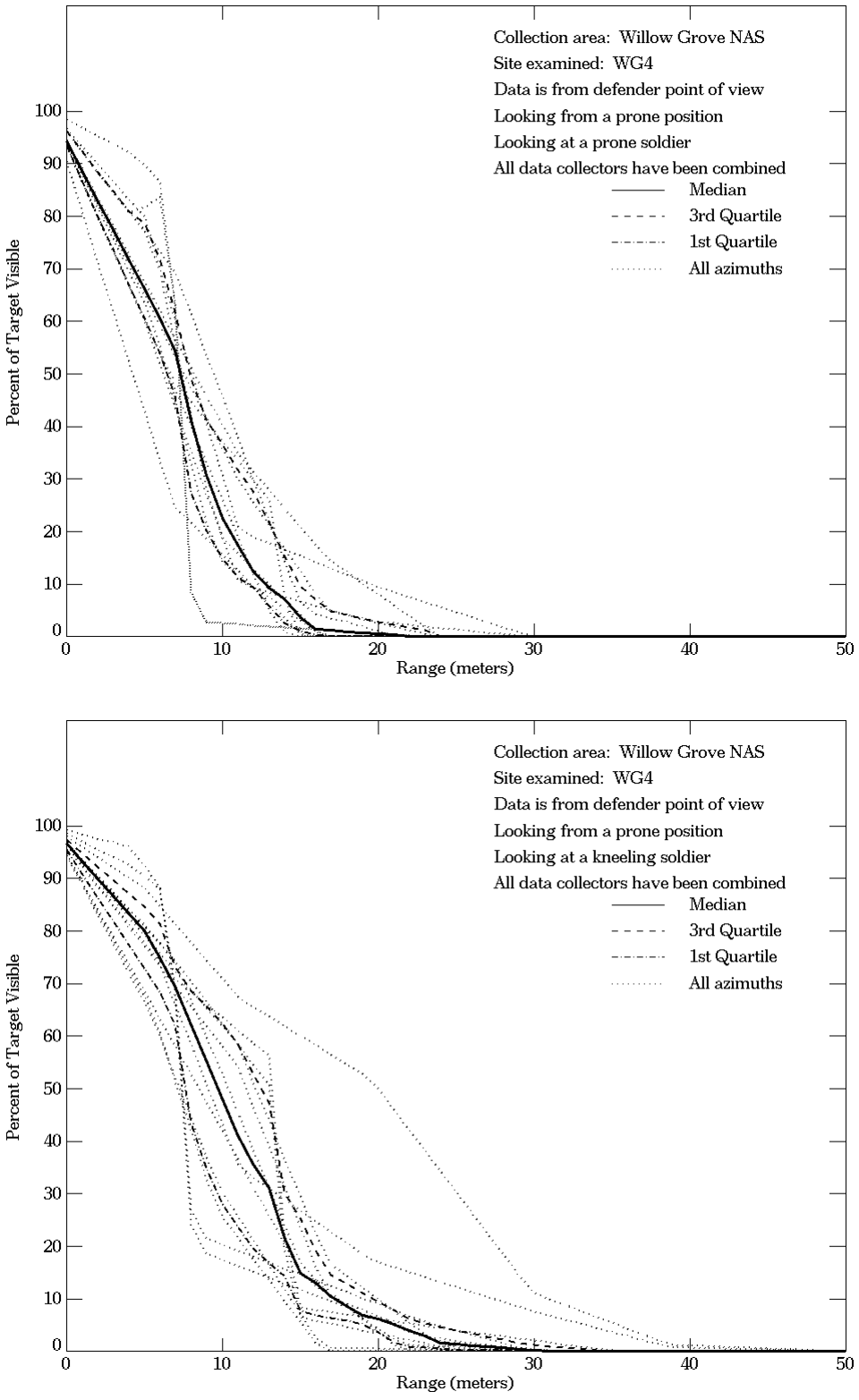

Figure E-83. Willow Grove NAS, From Defender Point of View, Site WG4

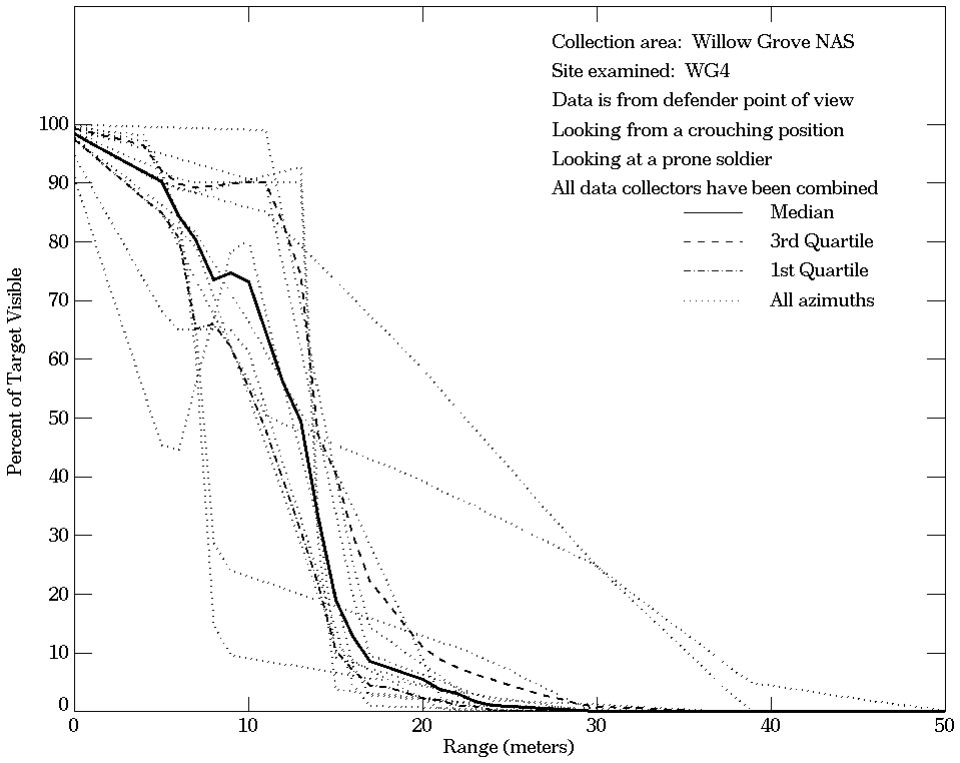

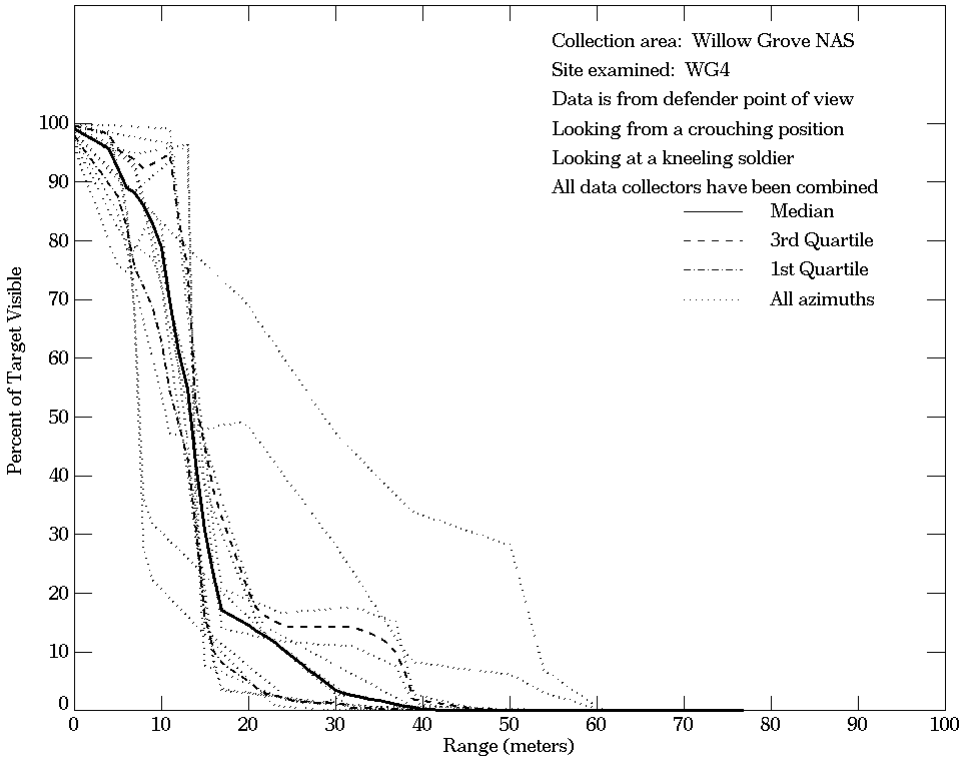

Figure E-83. Willow Grove NAS, From Defender Point of View, Site WG4 (Continued)

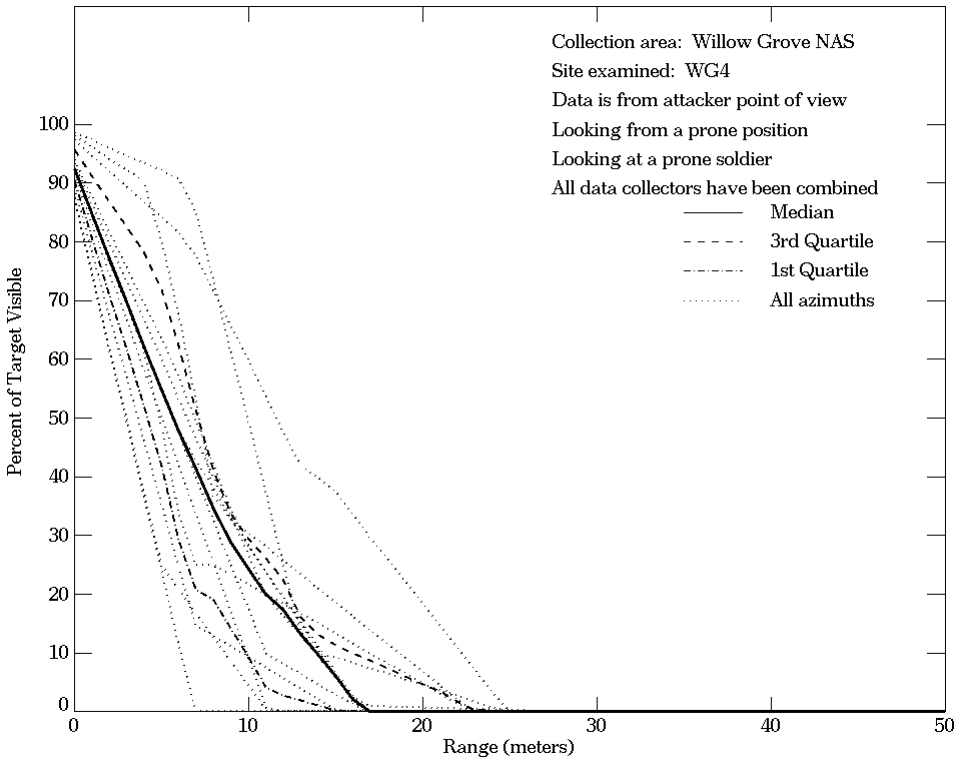

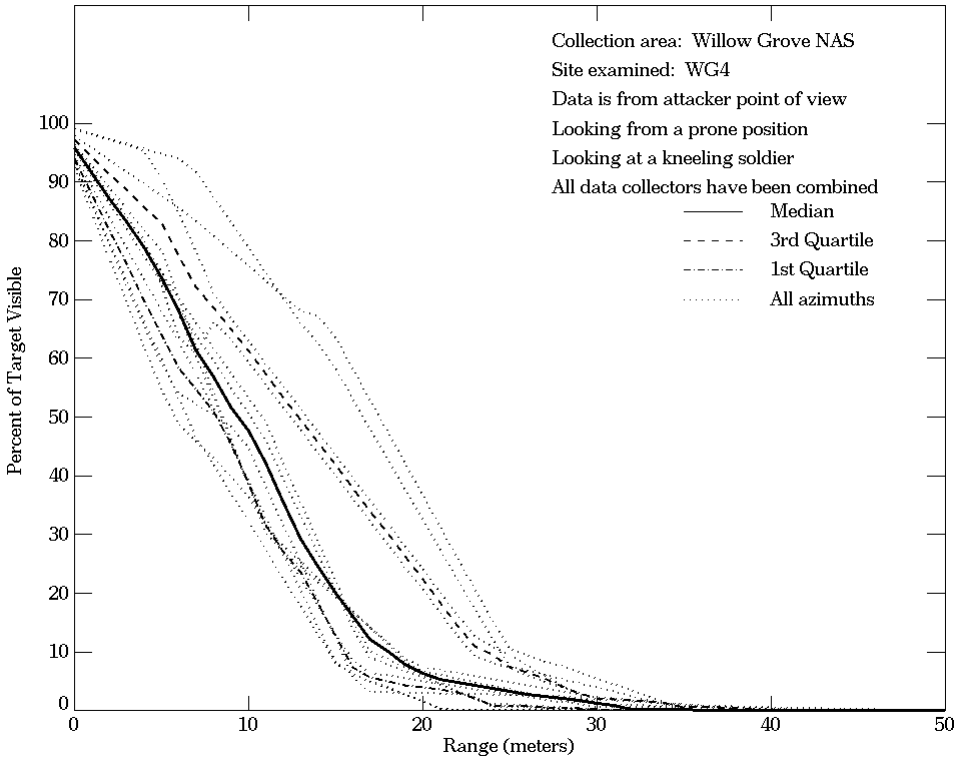

Figure E-84. Willow Grove NAS, From Attacker Point of View, Site WG4

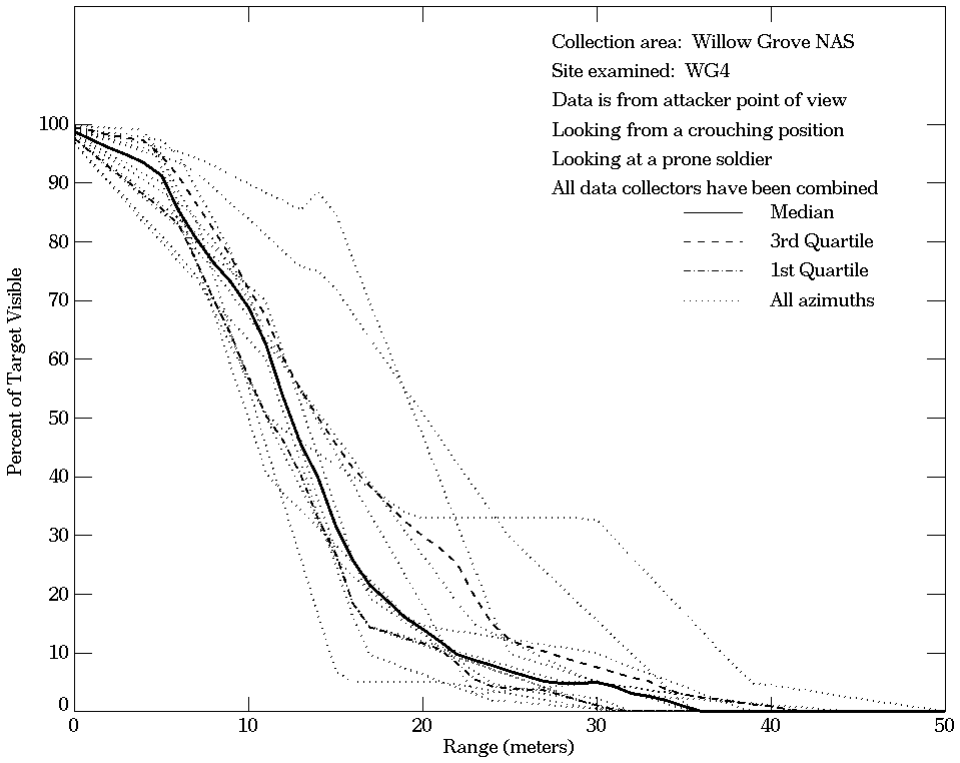

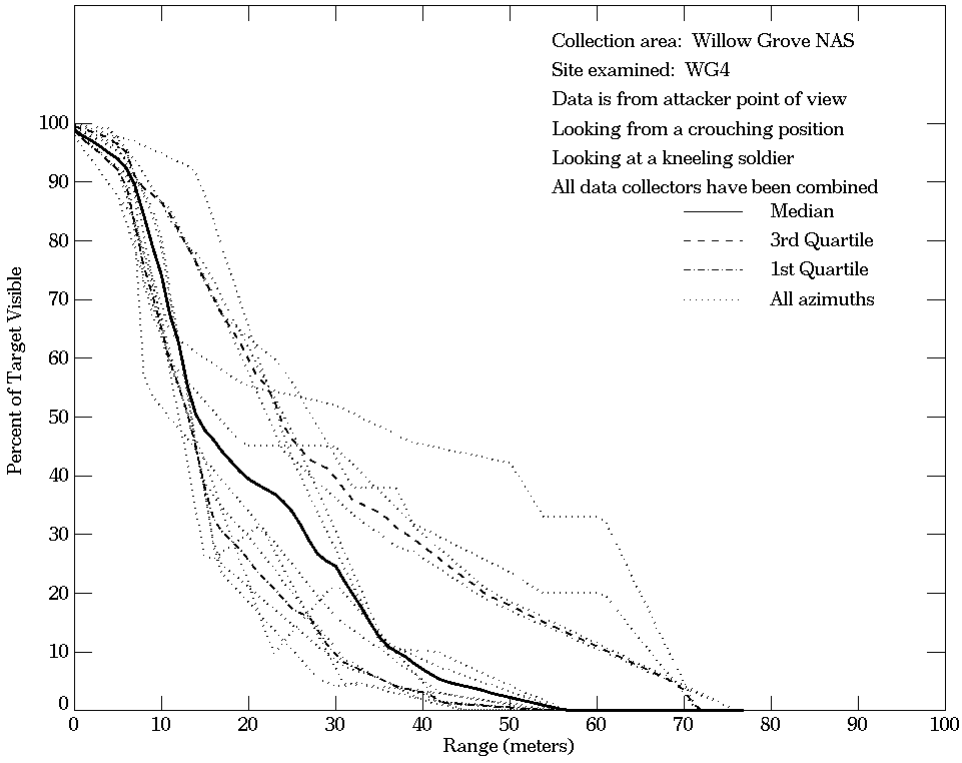

Figure E-84. Willow Grove NAS, From Attacker Point of View, Site WG4 (Continued)

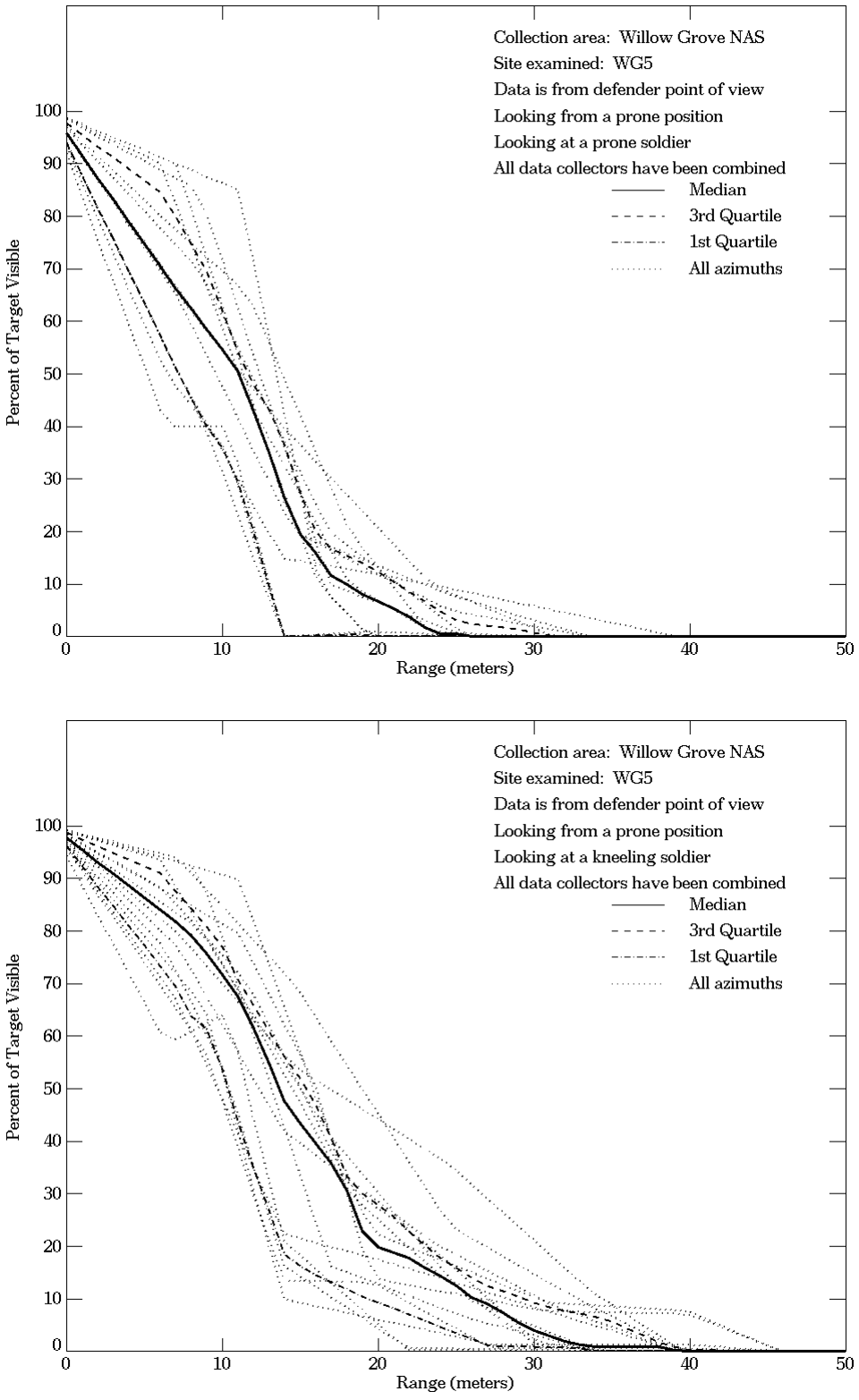

Figure E-85. Willow Grove NAS, From Defender Point of View, Site WG5

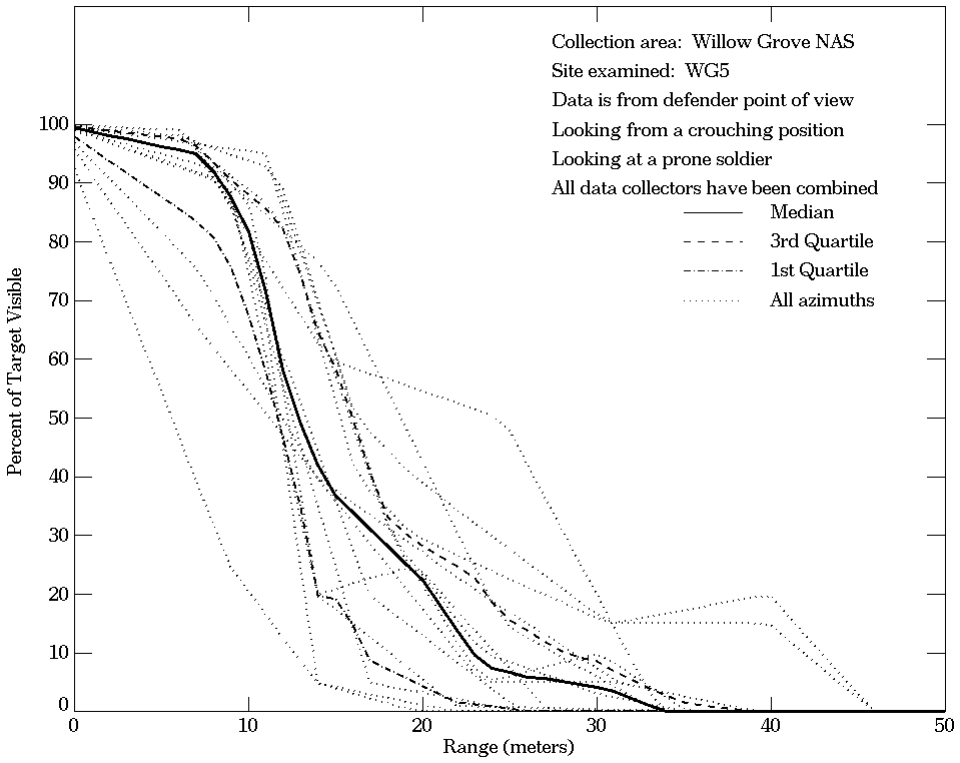

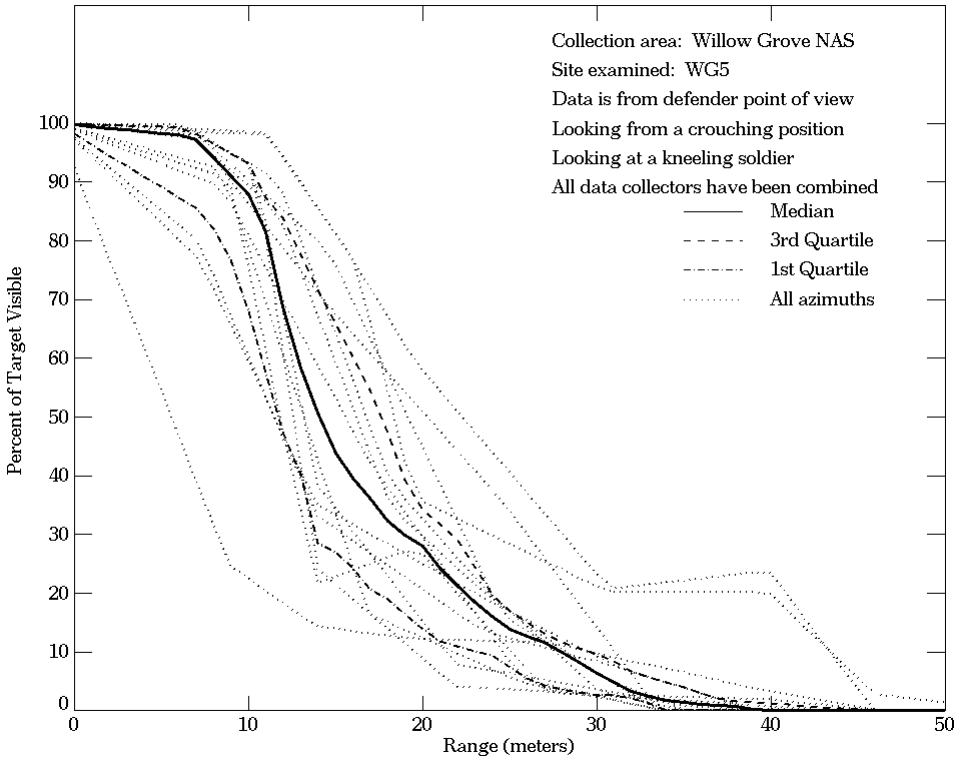

Figure E-85. Willow Grove NAS, From Defender Point of View, Site WG5 (Continued)

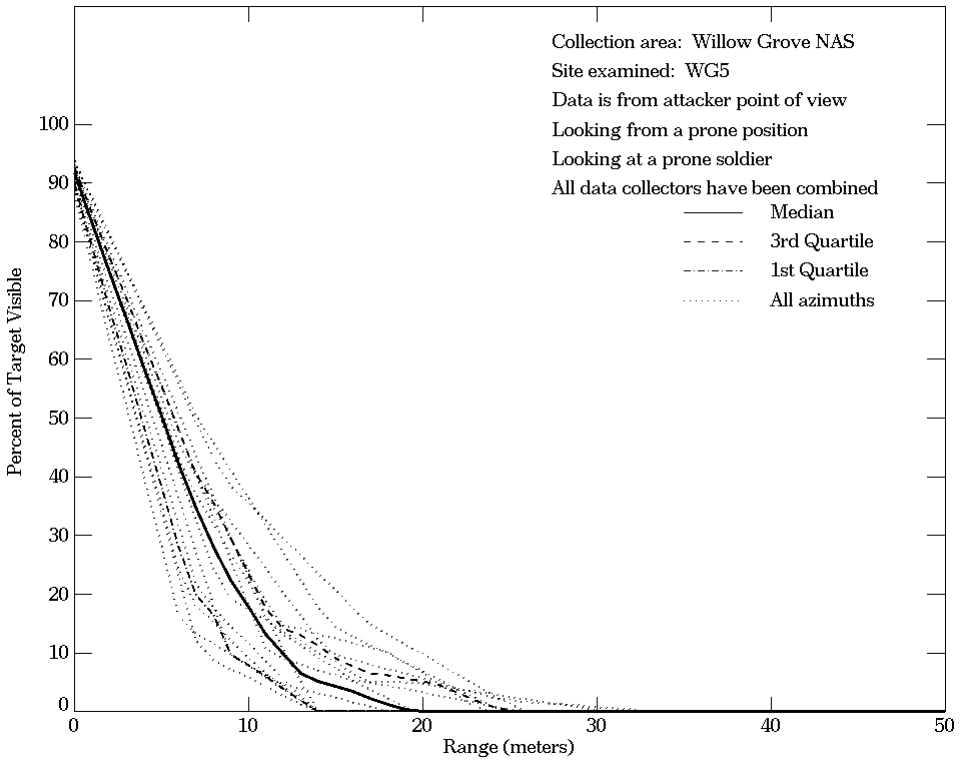

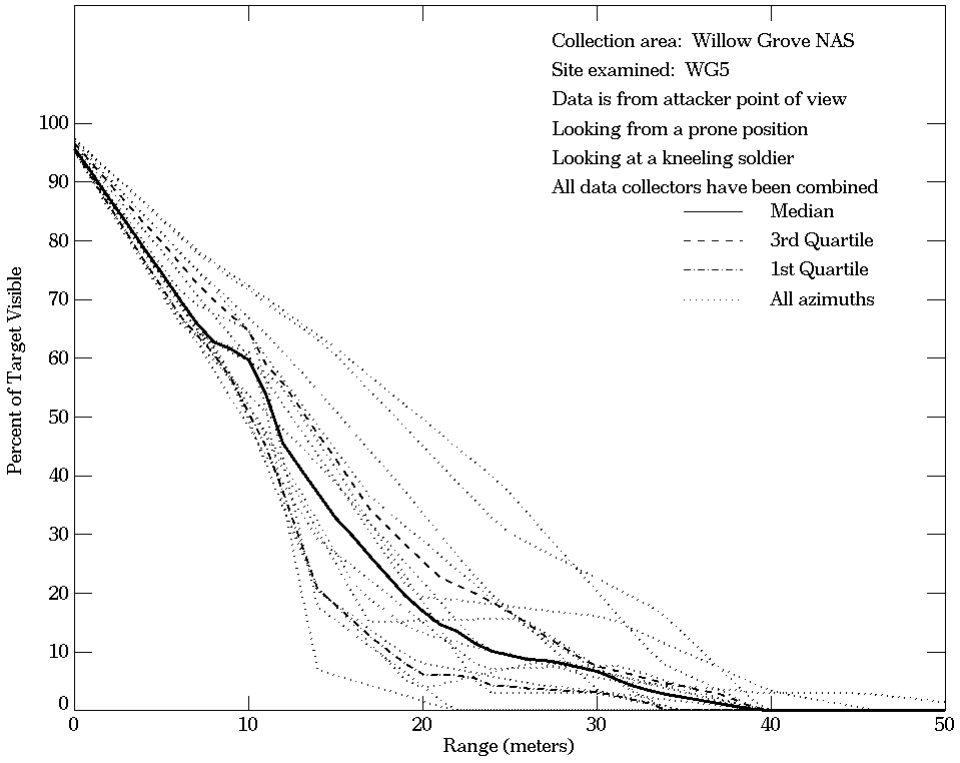

Figure E-86. Willow Grove NAS, From Attacker Point of View, Site WG5

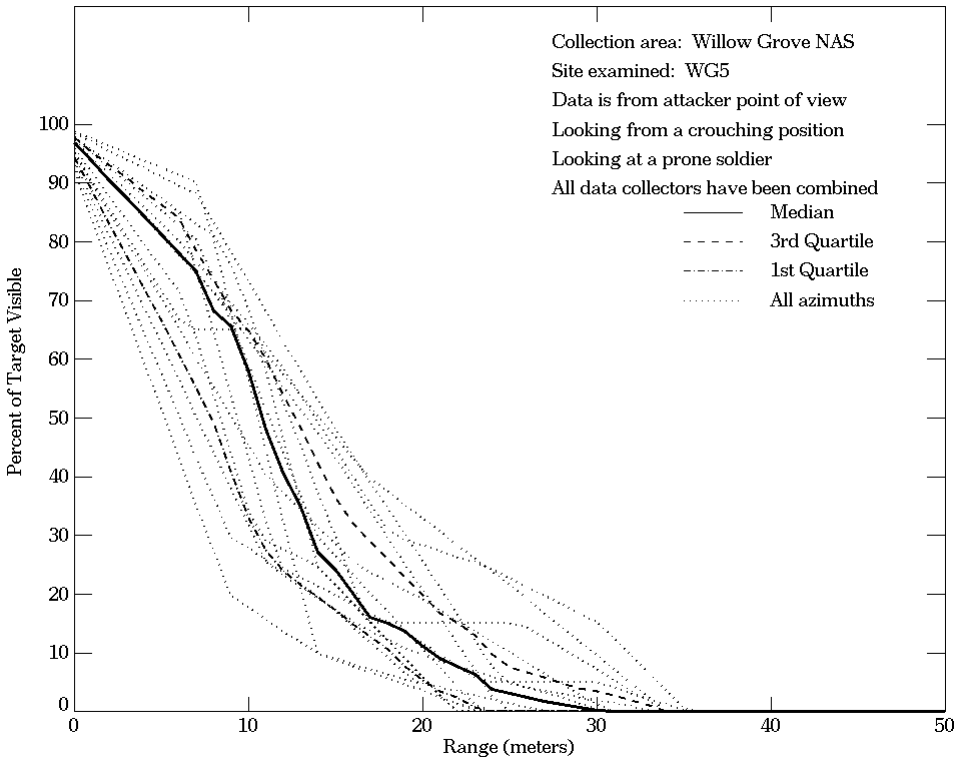

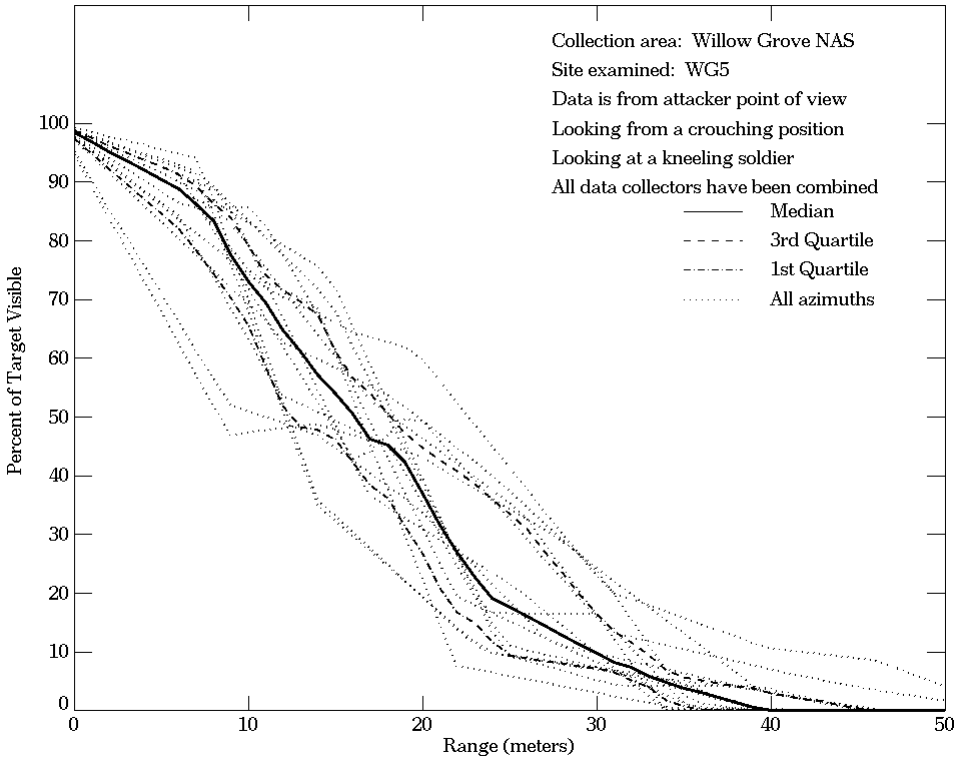

Figure E-86. Willow Grove NAS, From Attacker Point of View, Site WG5 (Continued)

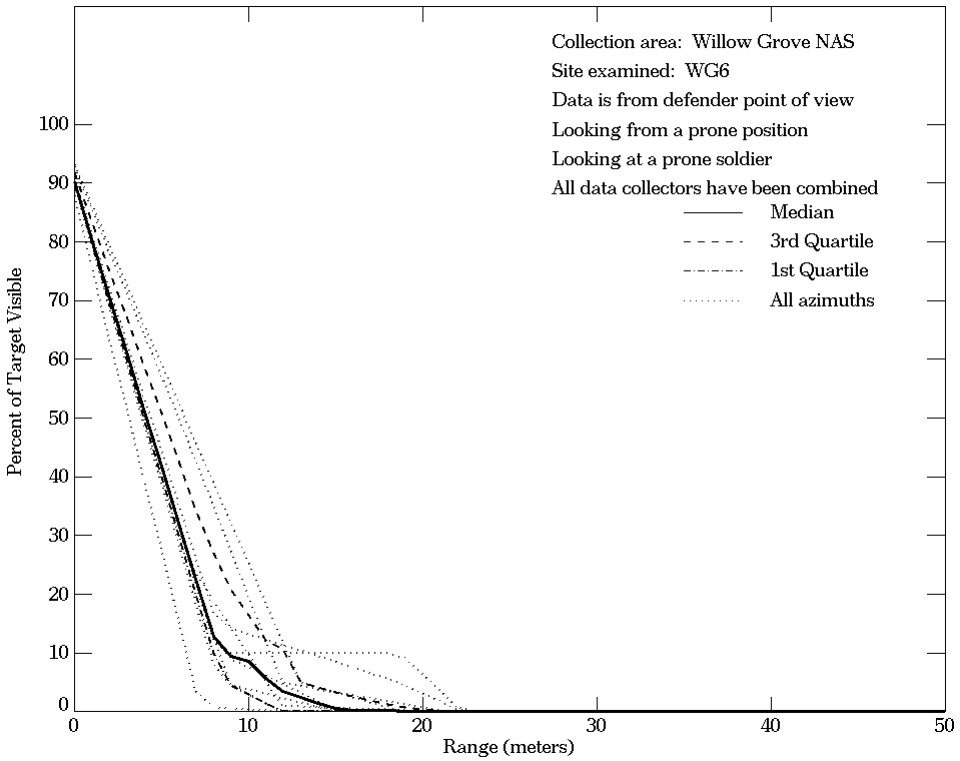

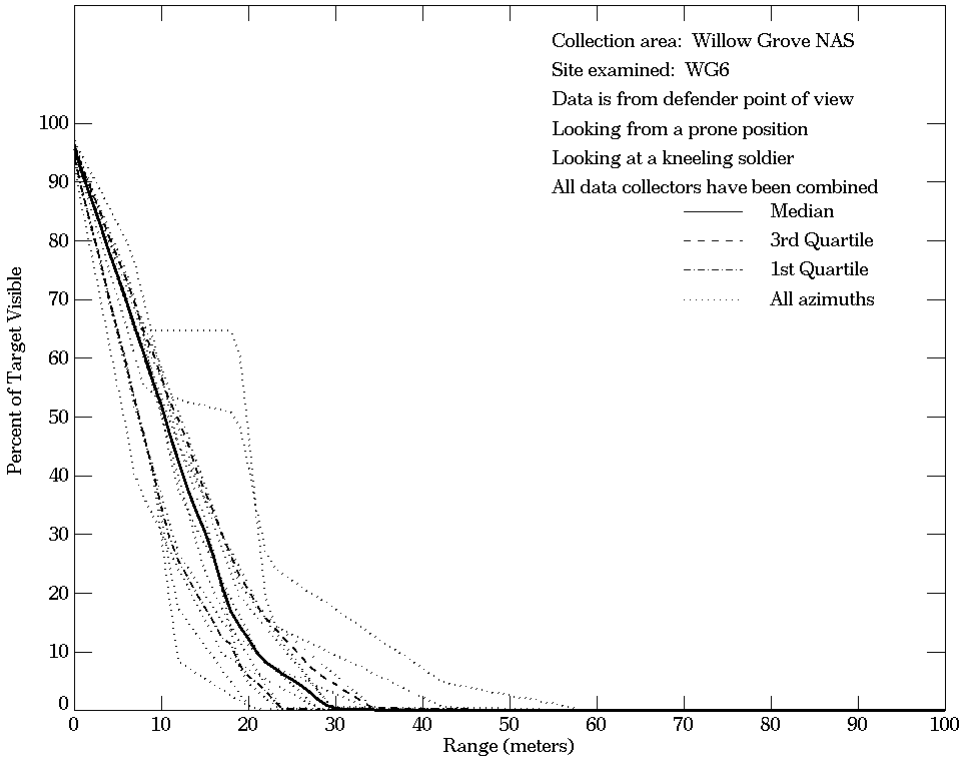

Figure E-87. Willow Grove NAS, From Defender Point of View, Site WG6

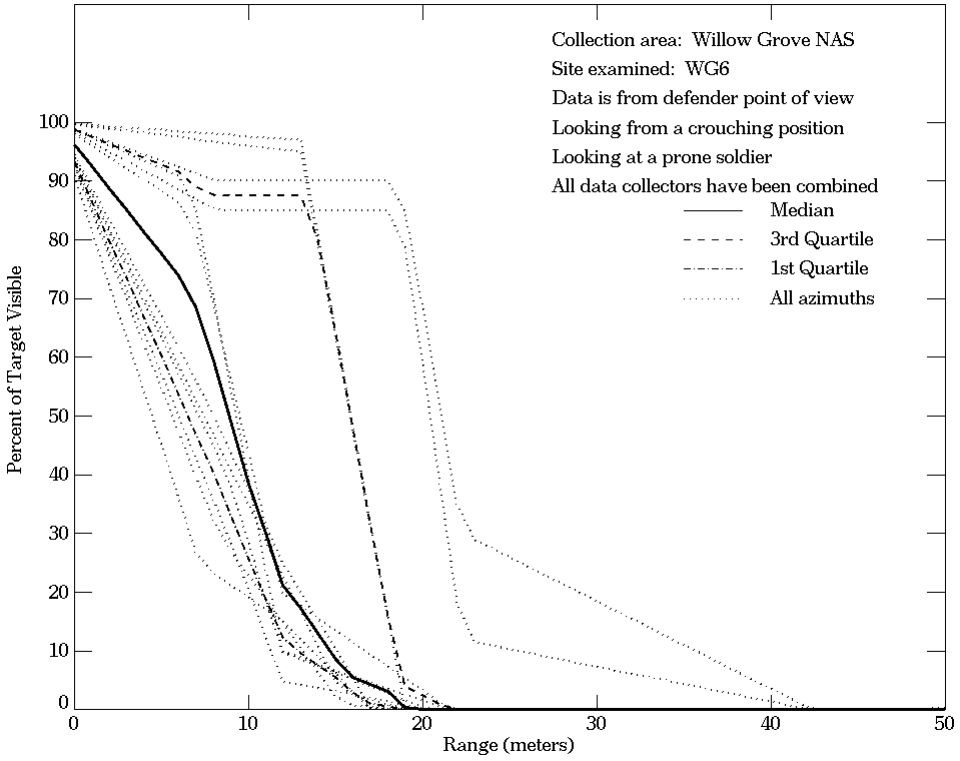

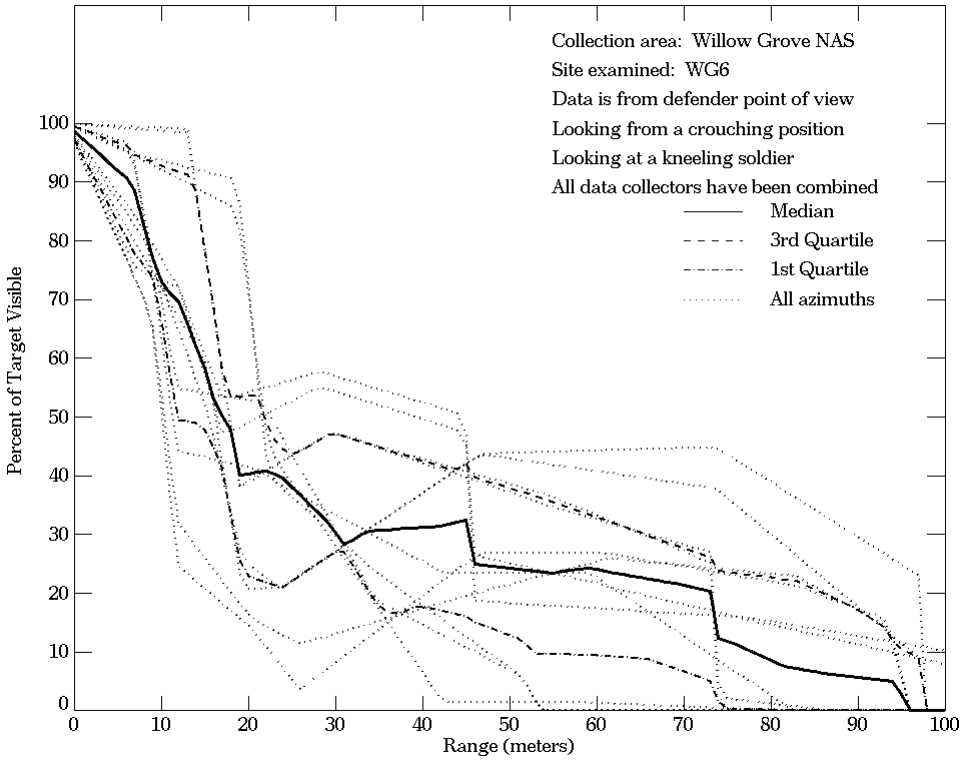

Figure E-87. Willow Grove NAS, From Defender Point of View, Site WG6 (Continued)

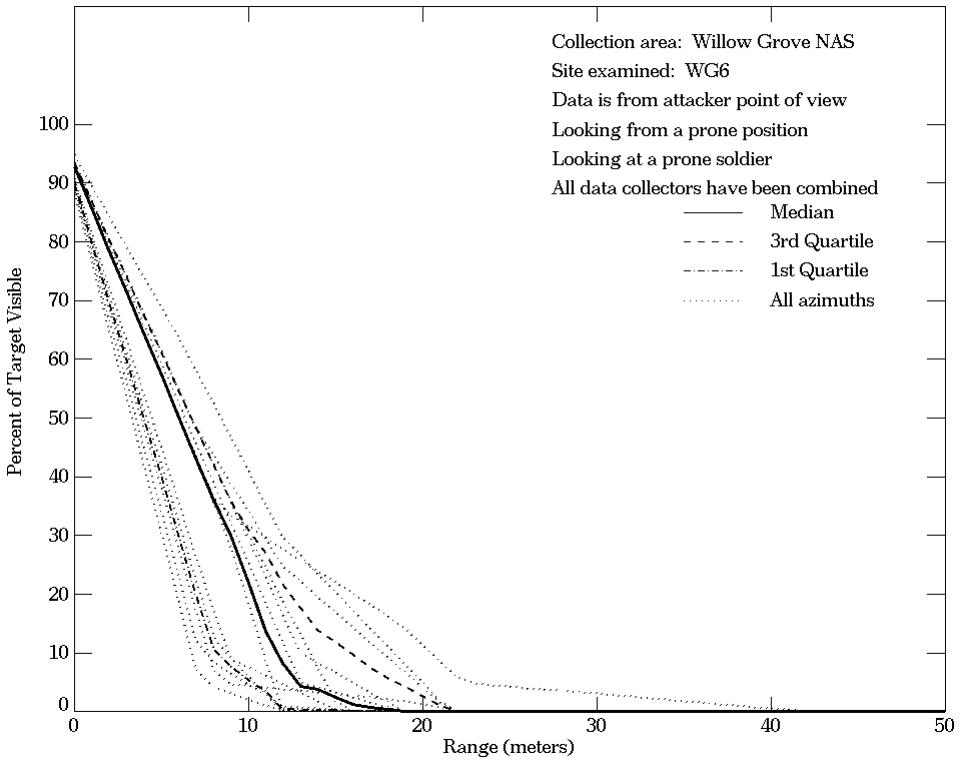

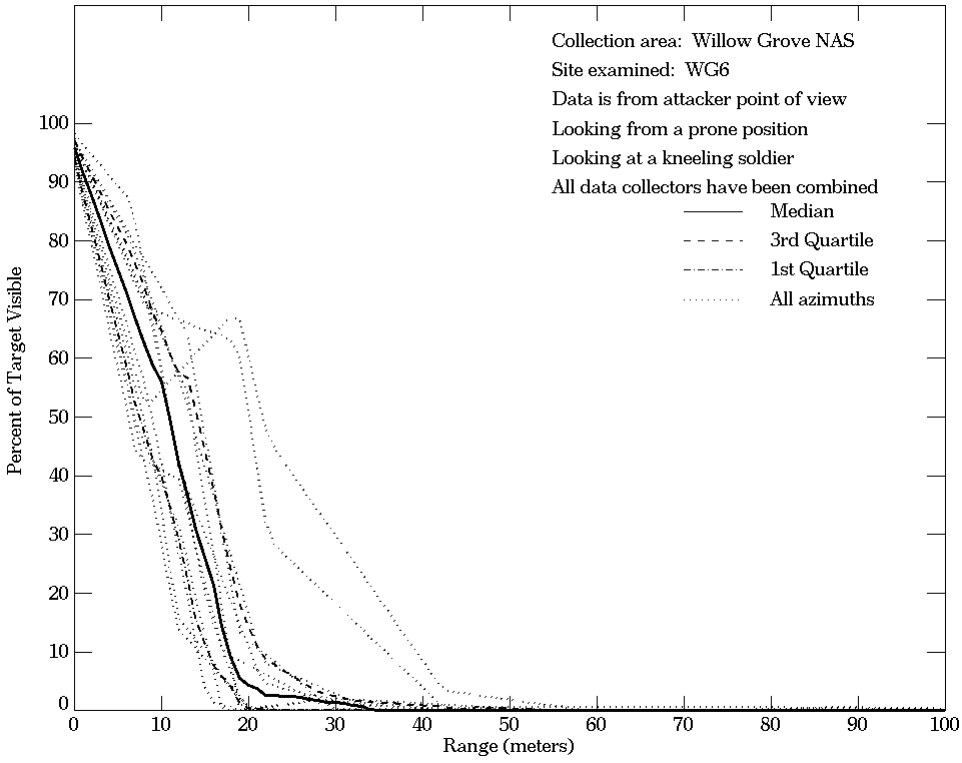

Figure E-88. Willow Grove NAS, From Attacker Point of View, Site WG6

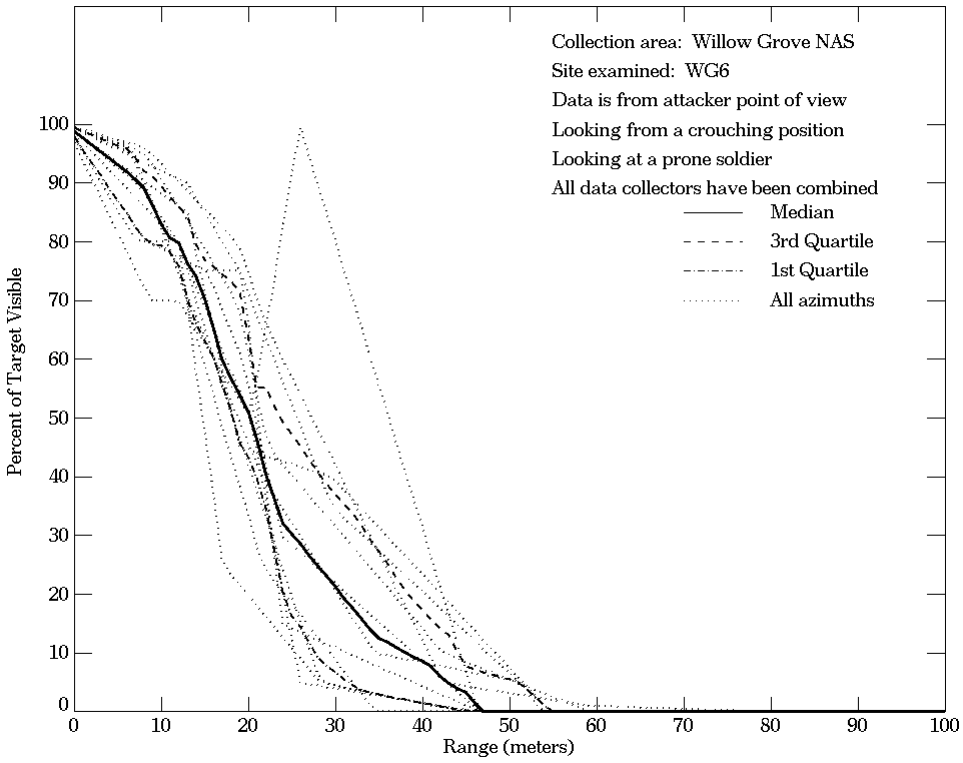

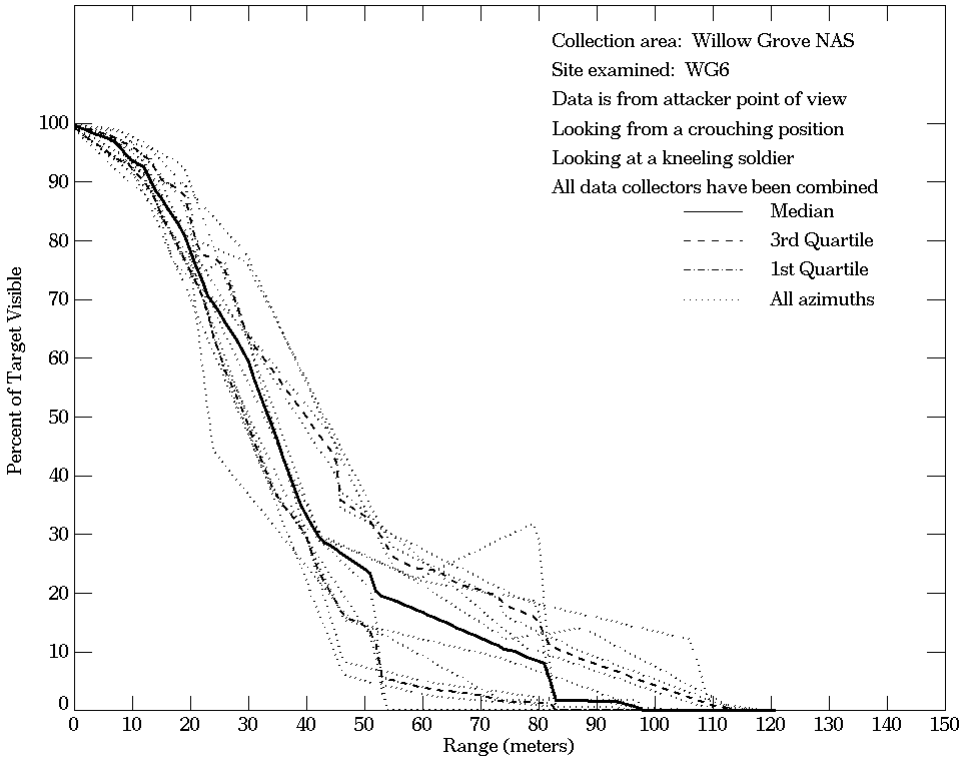

Figure E-88. Willow Grove NAS, From Attacker Point of View, Site WG6 (Continued)

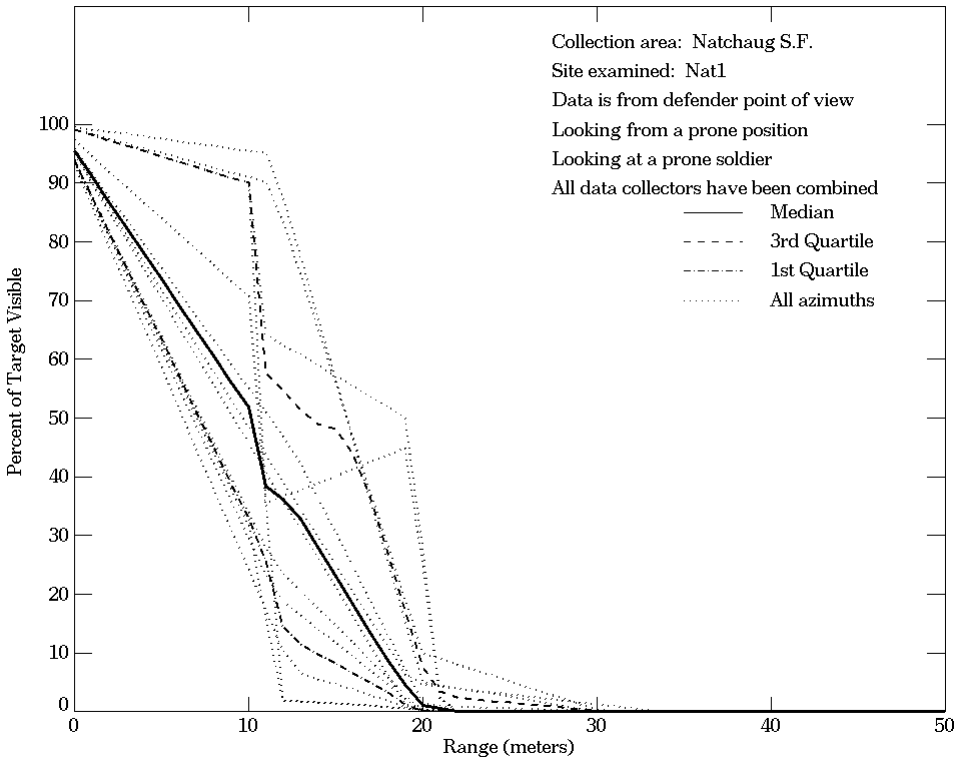

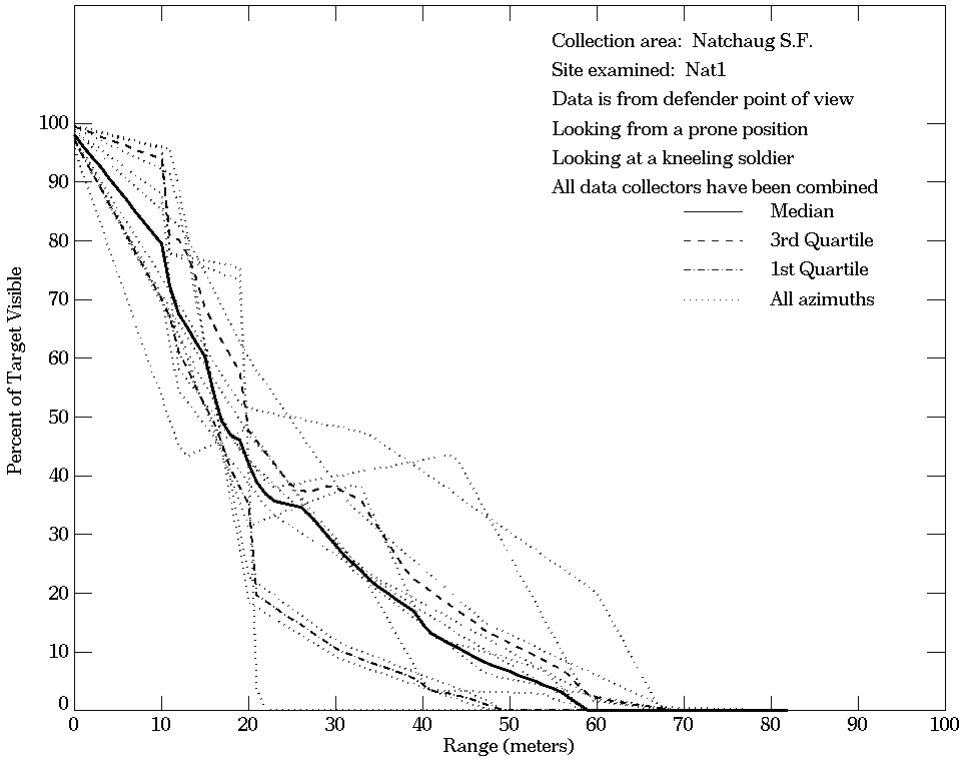

Figure E-89. Natchaug SF, From Defender Point of View, Site Nat1

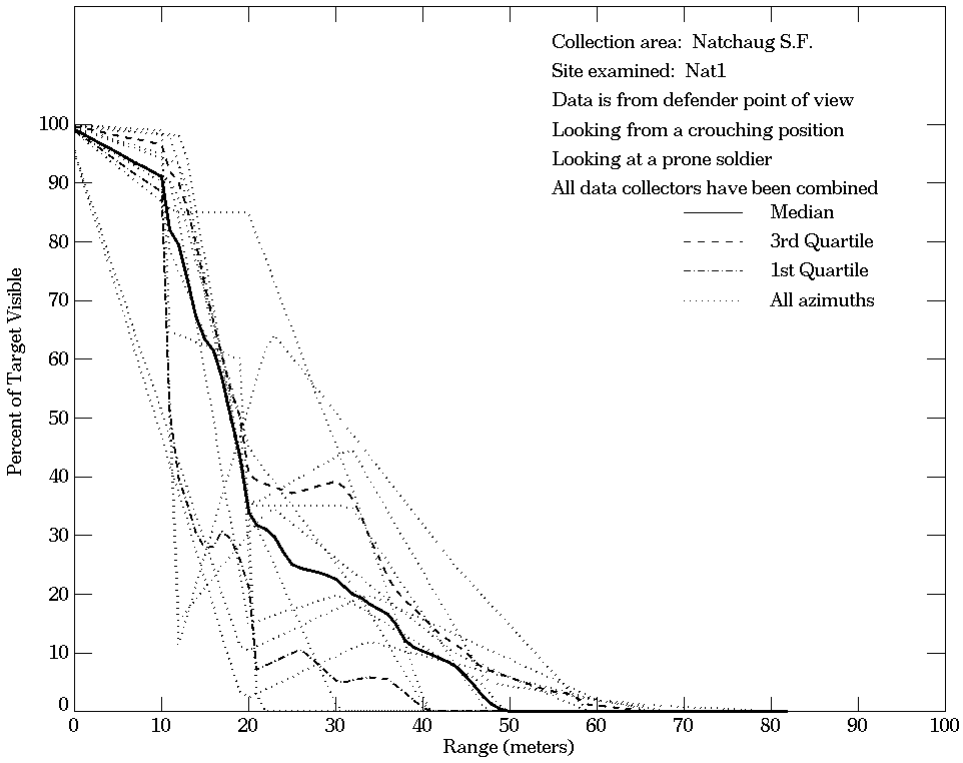

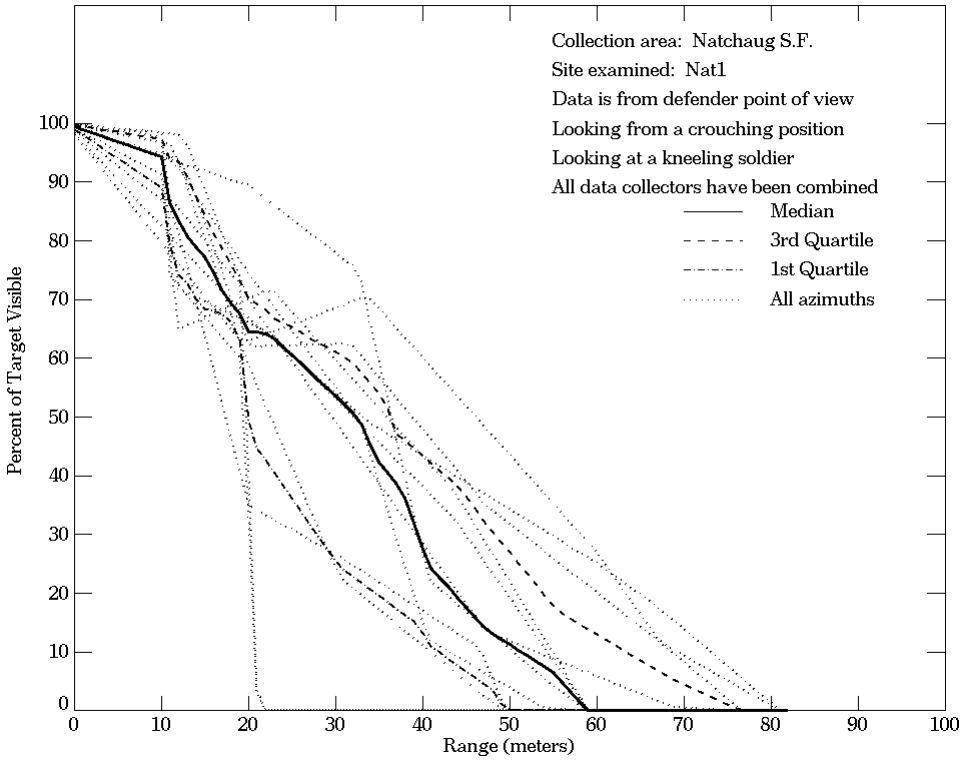

Figure E-89. Natchaug SF, From Defender Point of View, Site Nat1 (Continued)

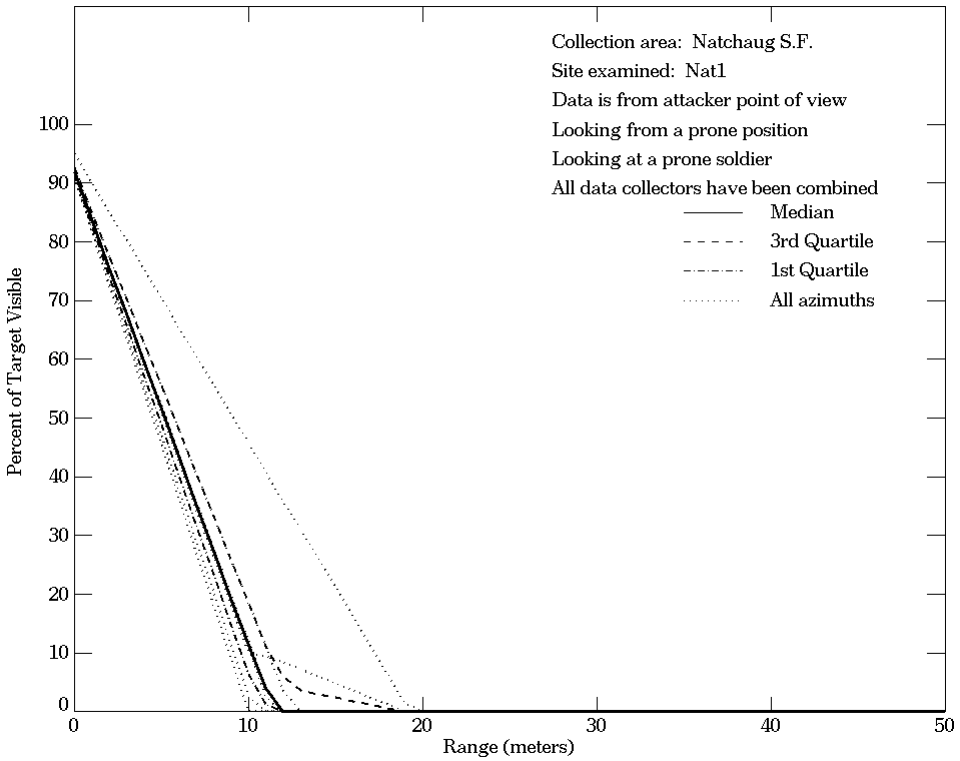

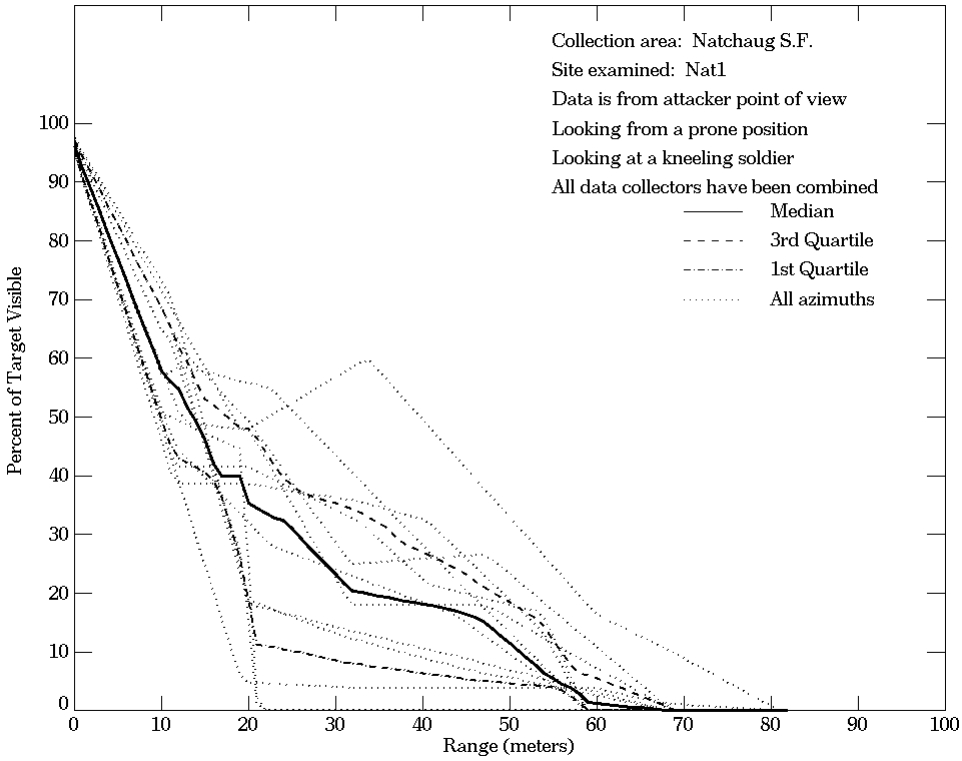

Figure E-90. Natchaug SF, From Attacker Point of View, Site Nat1

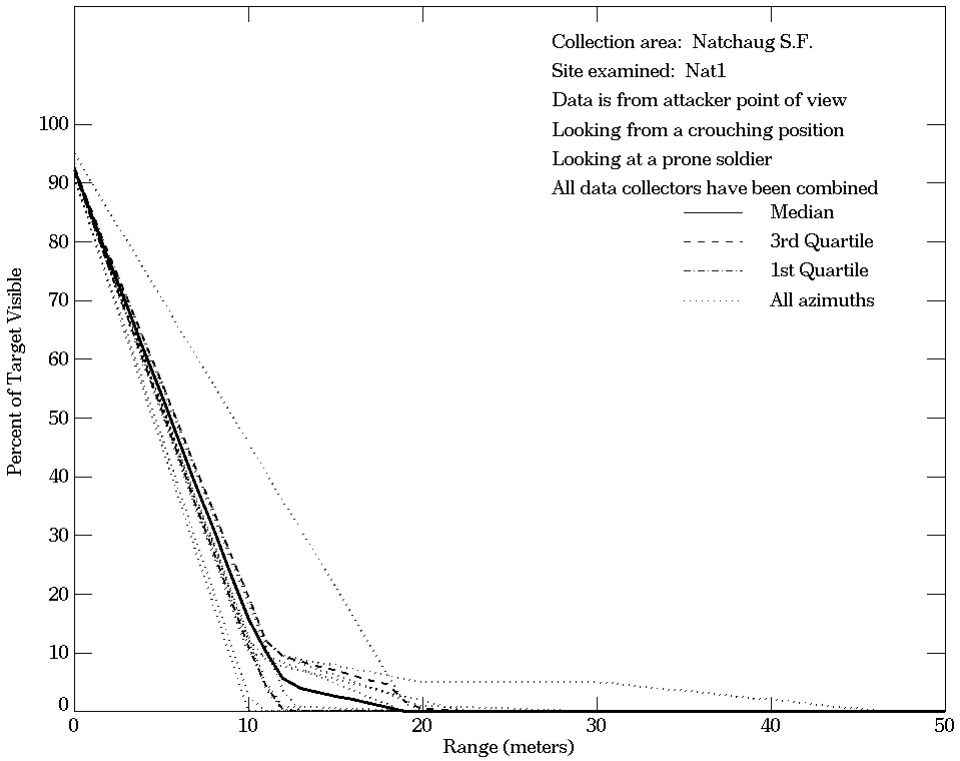

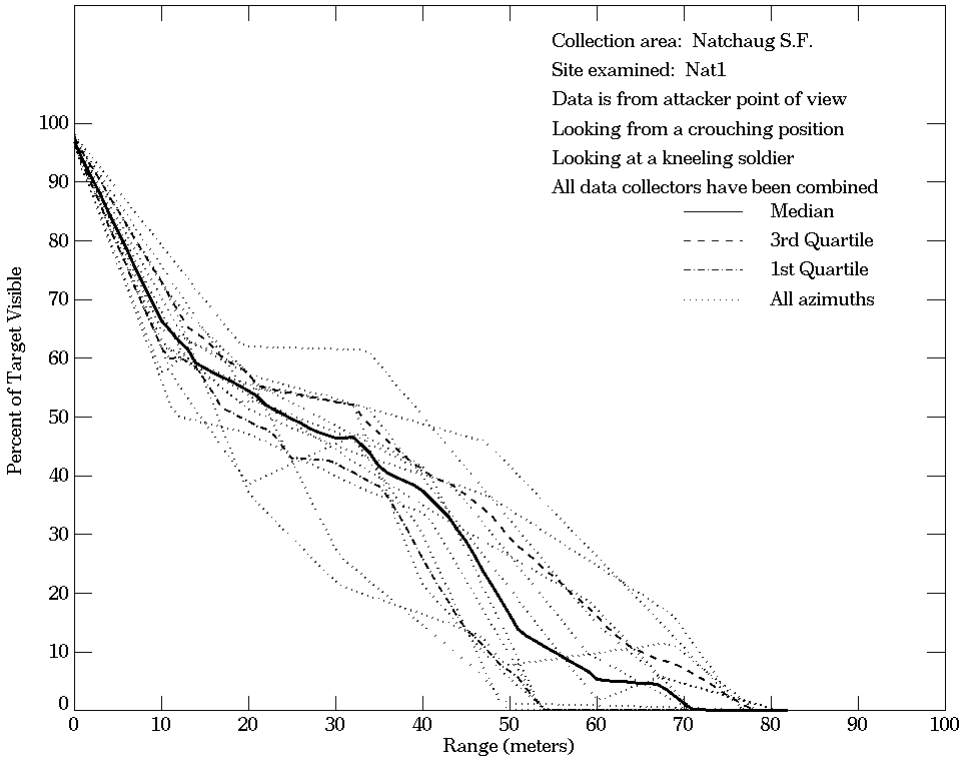

Figure E-90. Natchaug SF, From Attacker Point of View, Site Nat1 (Continued)

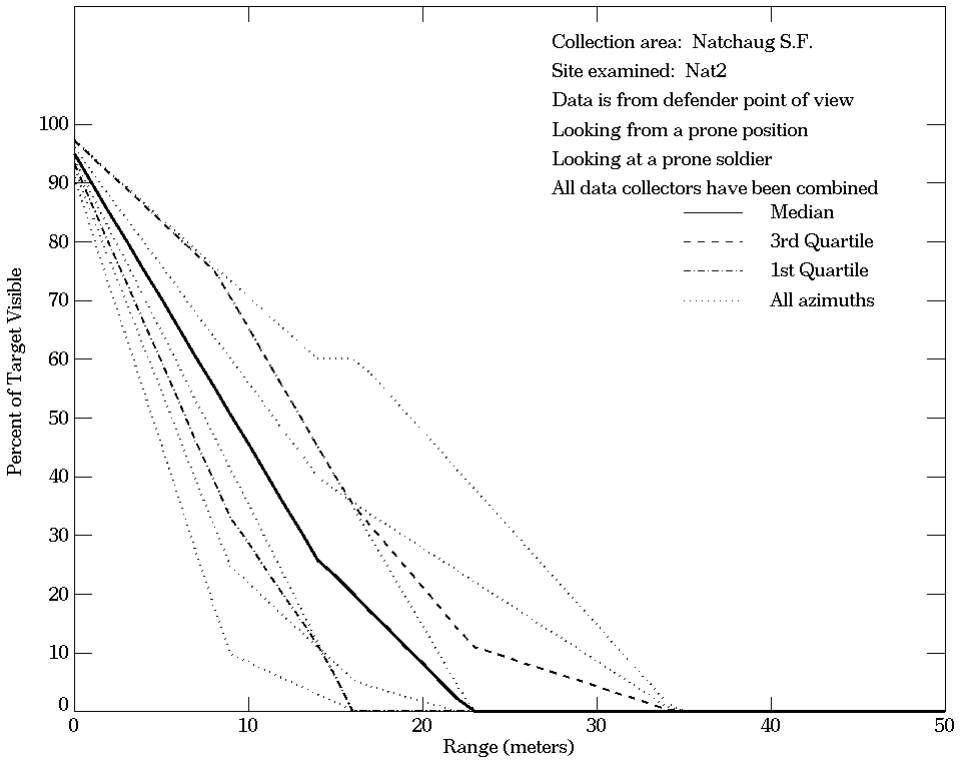

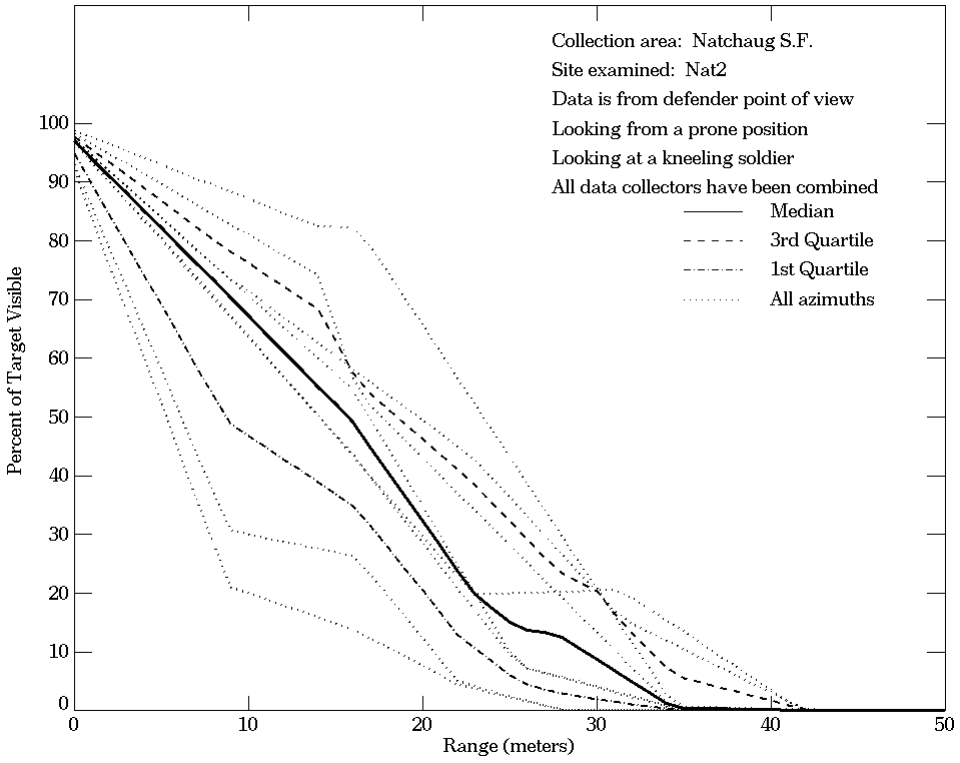

Figure E-91. Natchaug SF, From Defender Point of View, Site Nat2

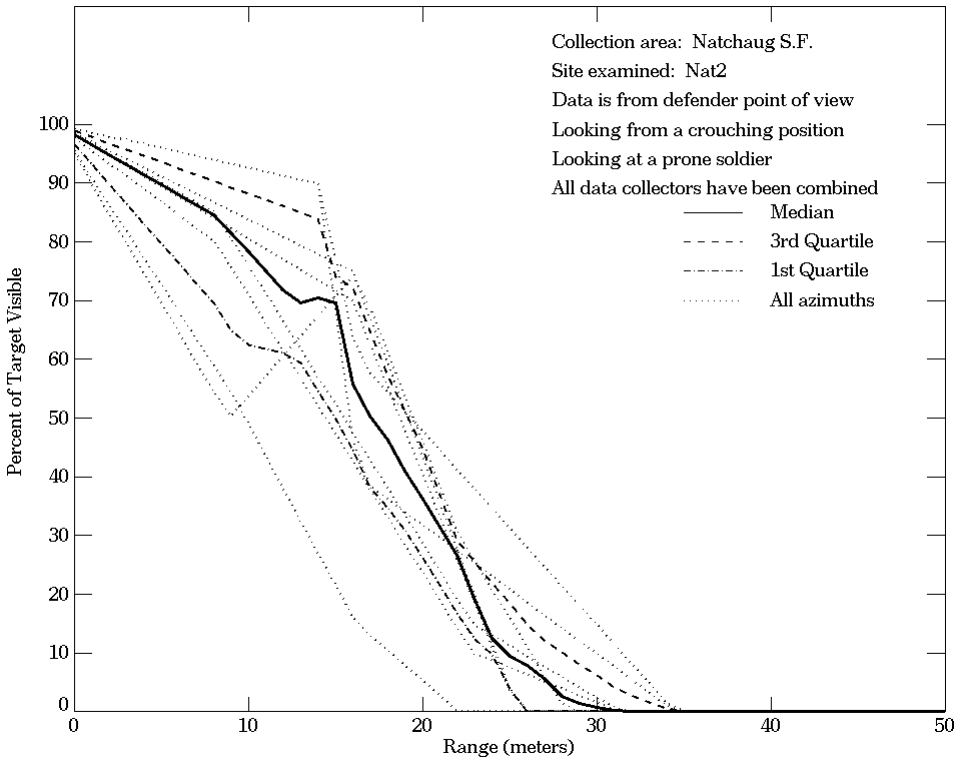

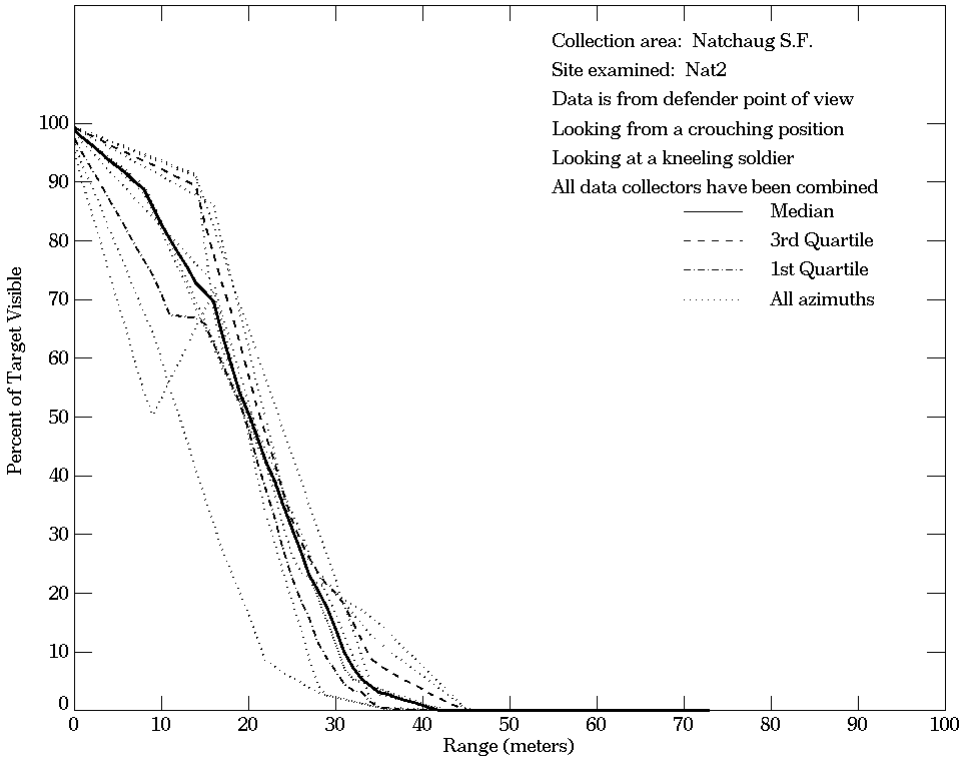

Figure E-91. Natchaug SF, From Defender Point of View, Site Nat2 (Continued)

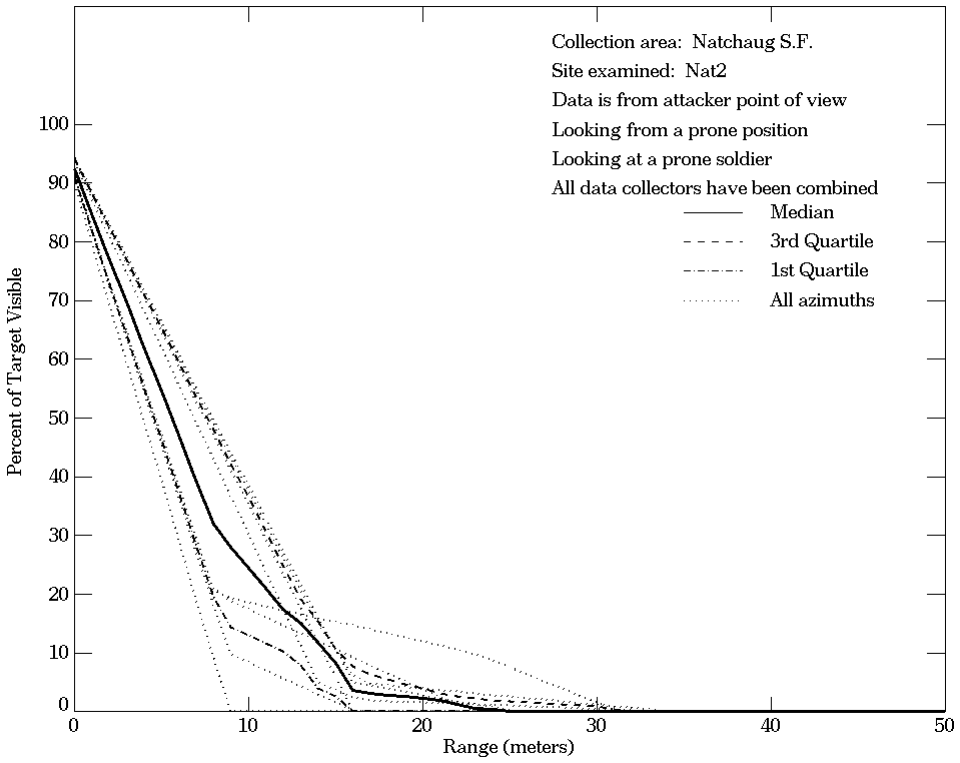

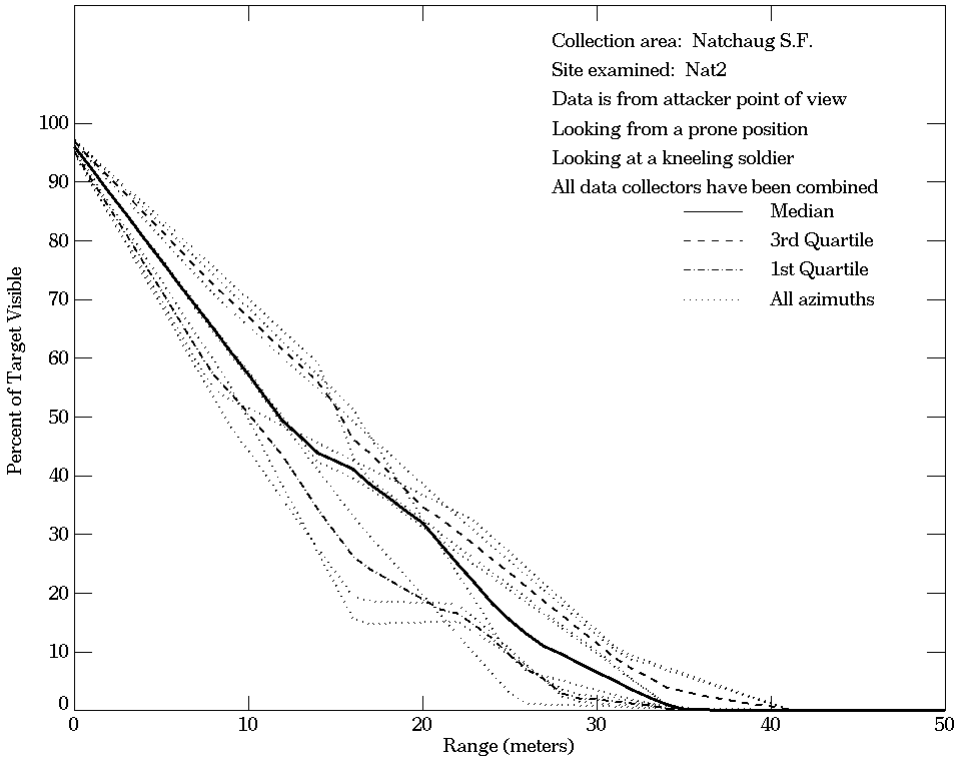

Figure E-92. Natchaug SF, From Attacker Point of View, Site Nat2

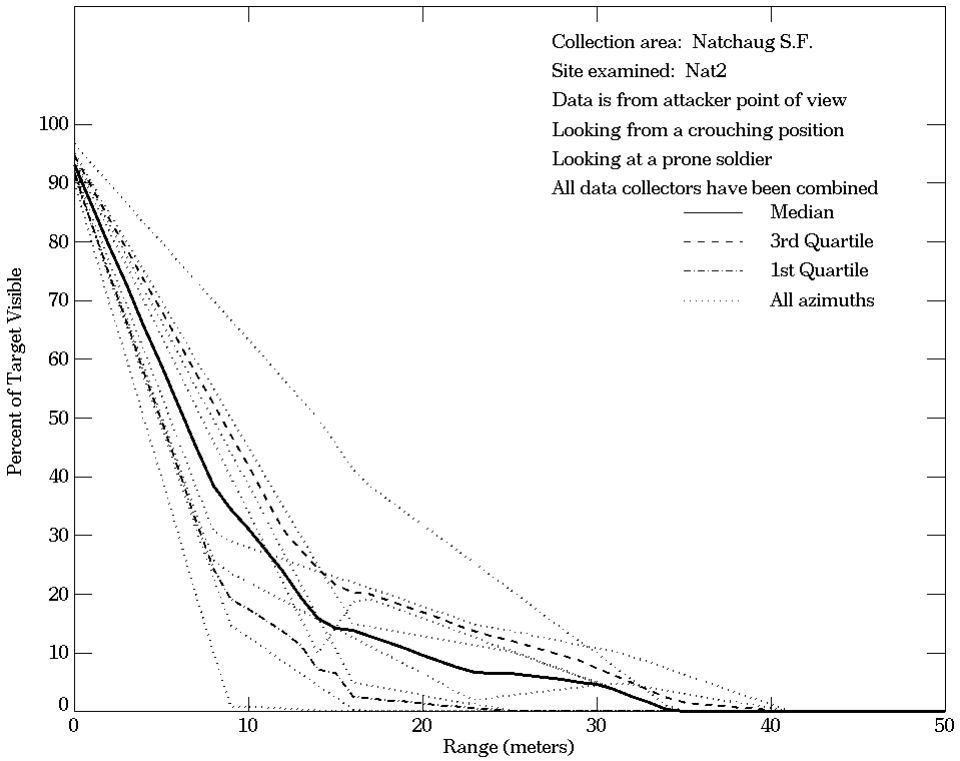

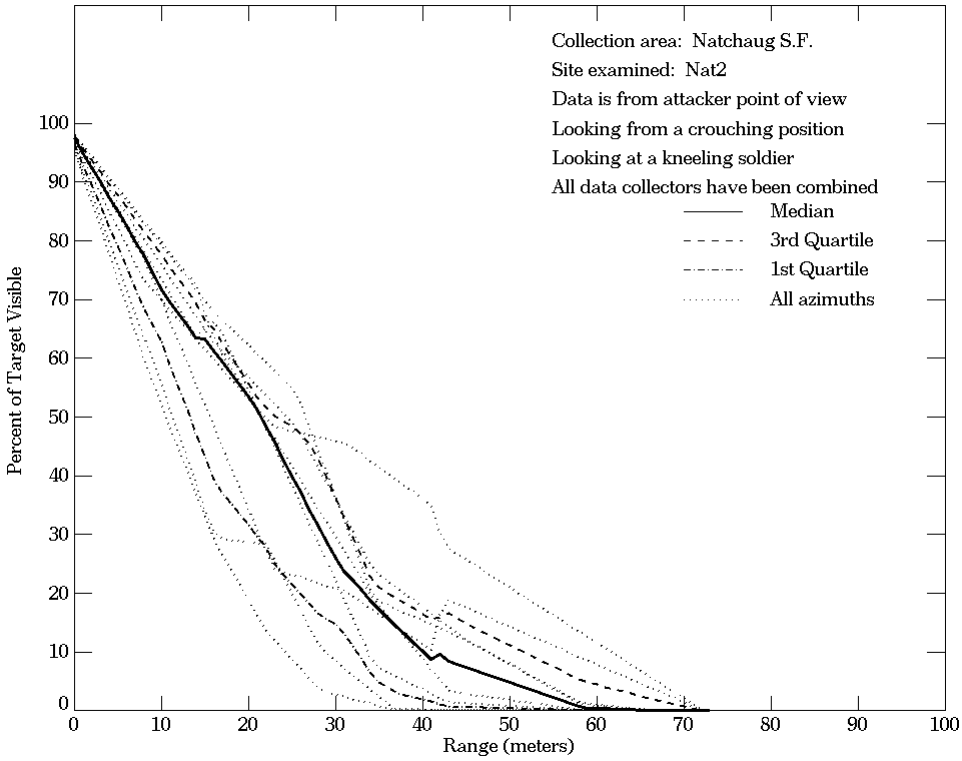

Figure E-92. Natchaug SF, From Attacker Point of View, Site Nat2 (Continued)

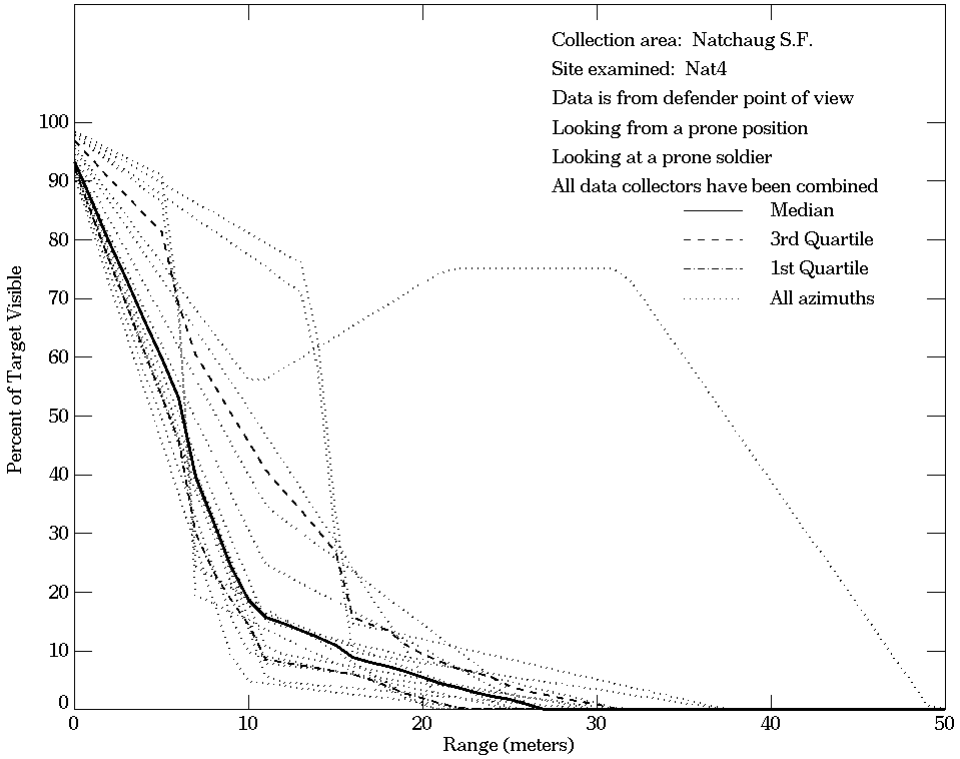

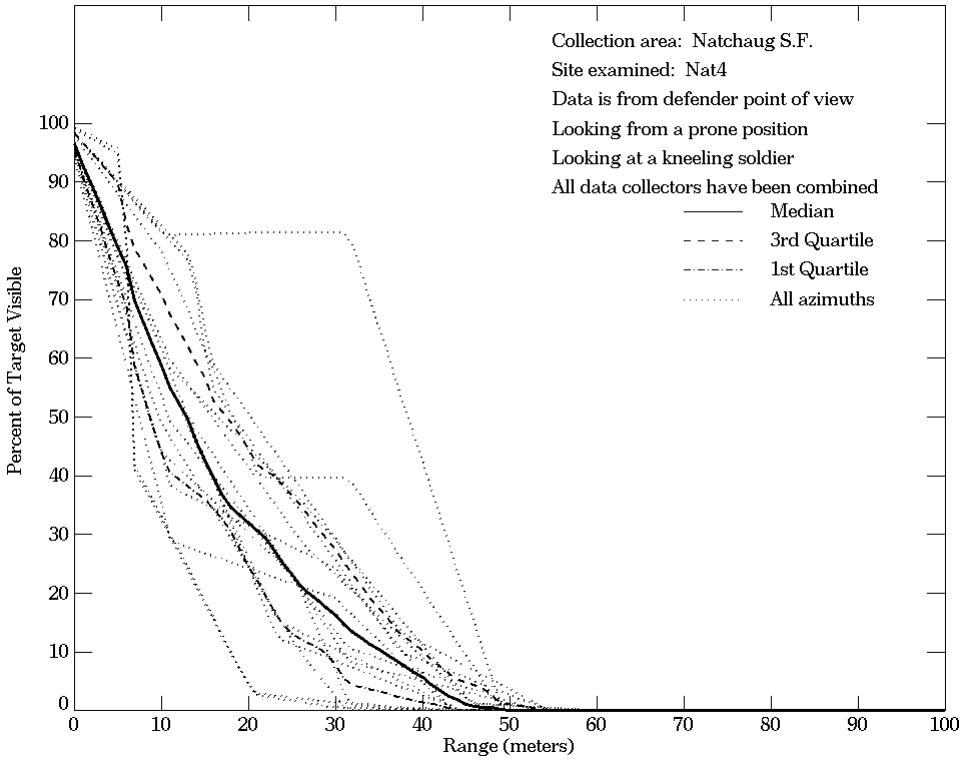

Figure E-93. Natchaug SF, From Defender Point of View, Site Nat4

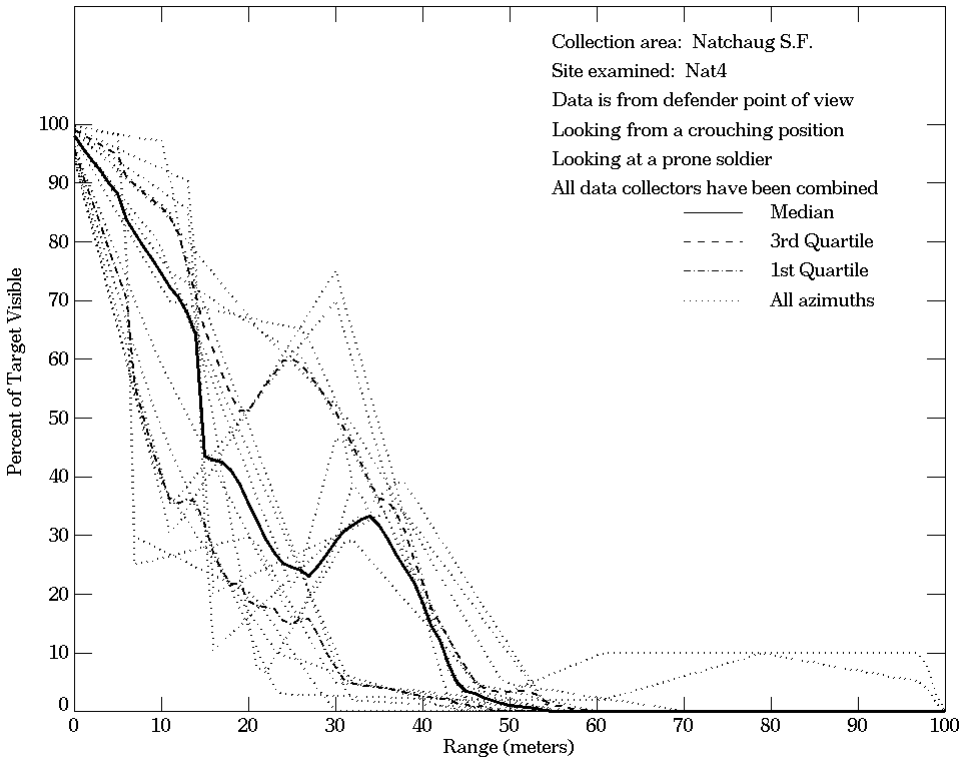

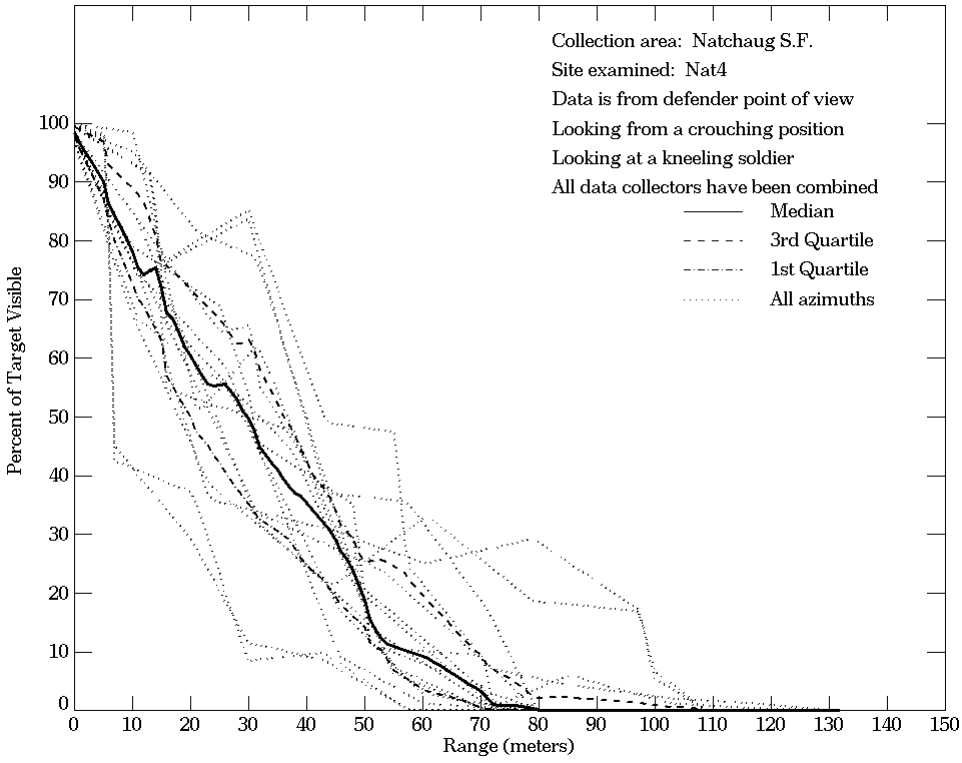

Figure E-93. Natchaug SF, From Defender Point of View, Site Nat4 (Continued)

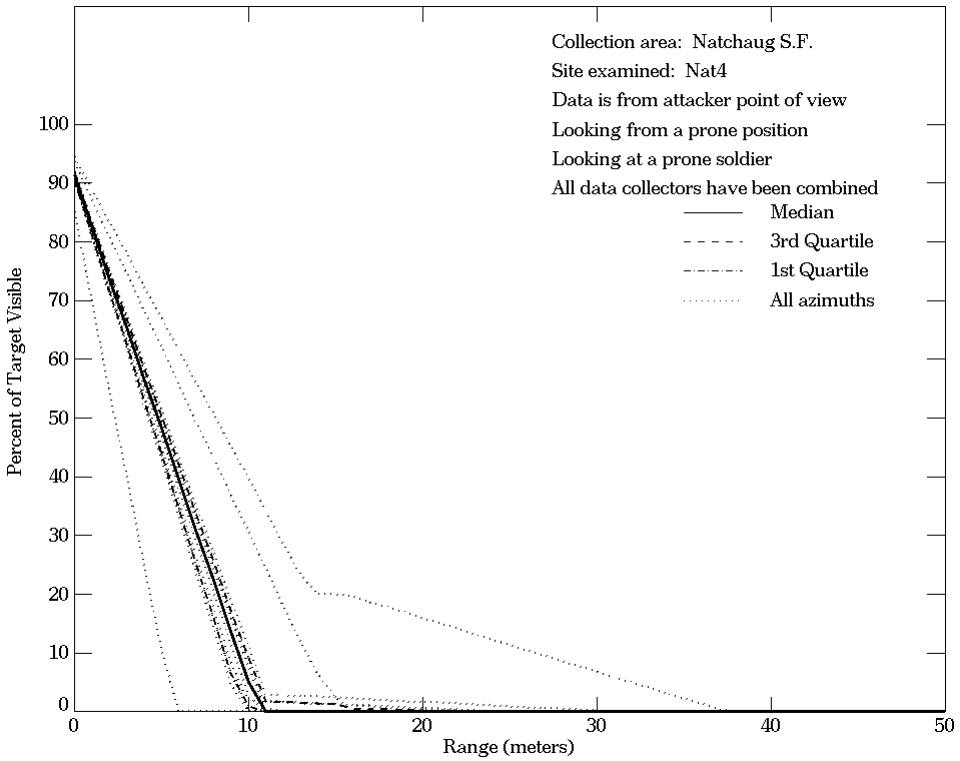

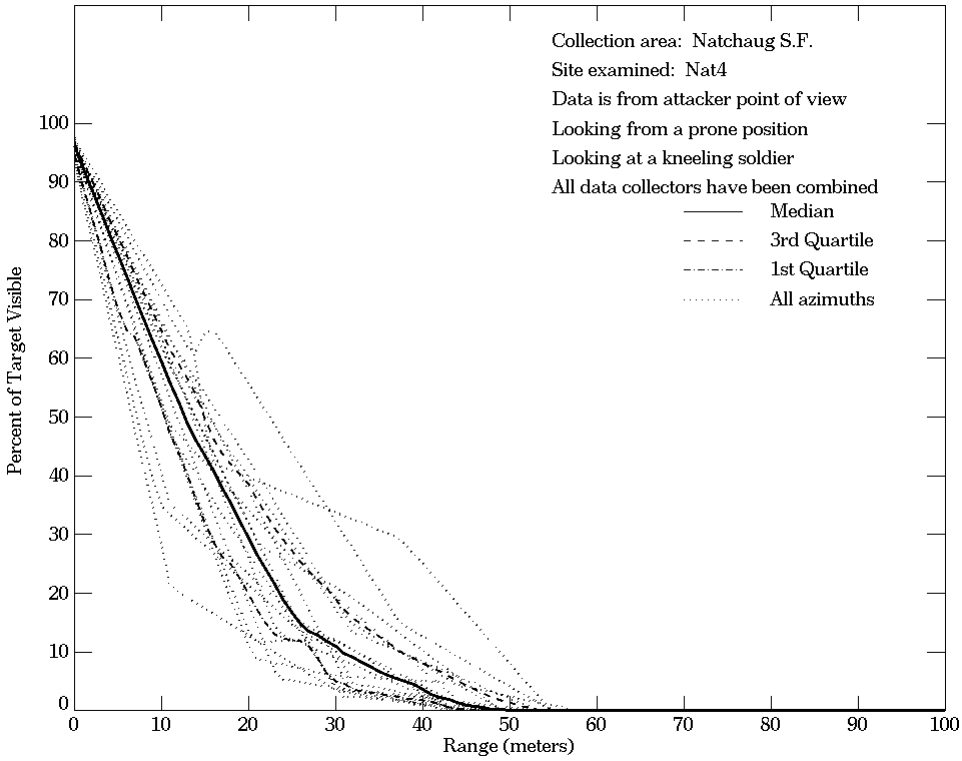

Figure E-94. Natchaug SF, From Attacker Point of View, Site Nat4

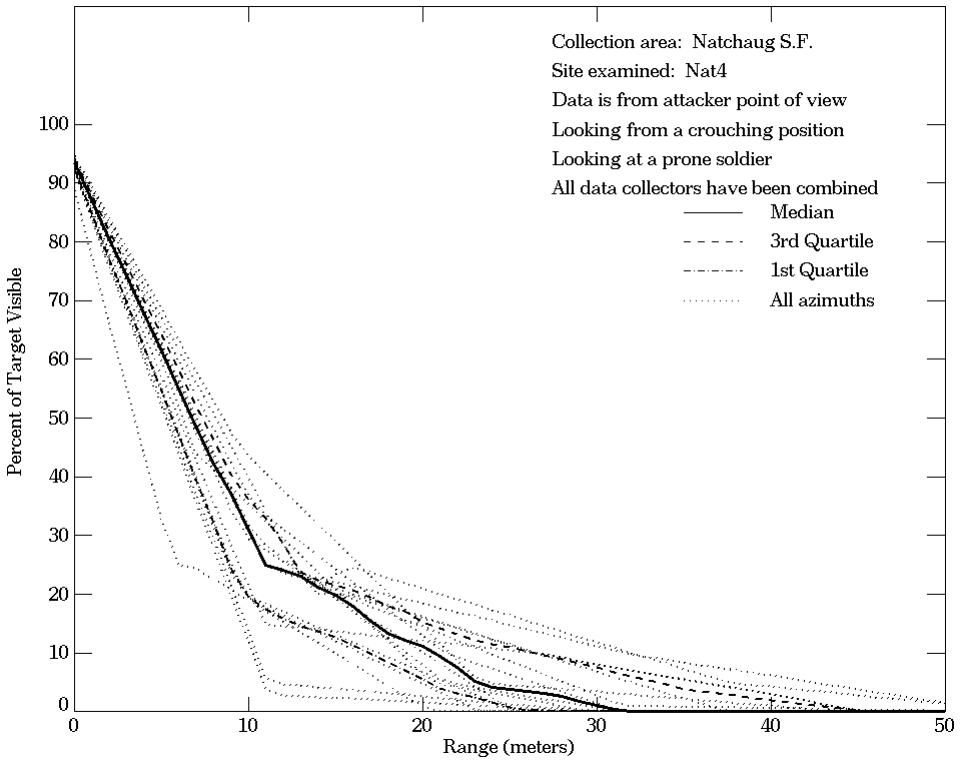

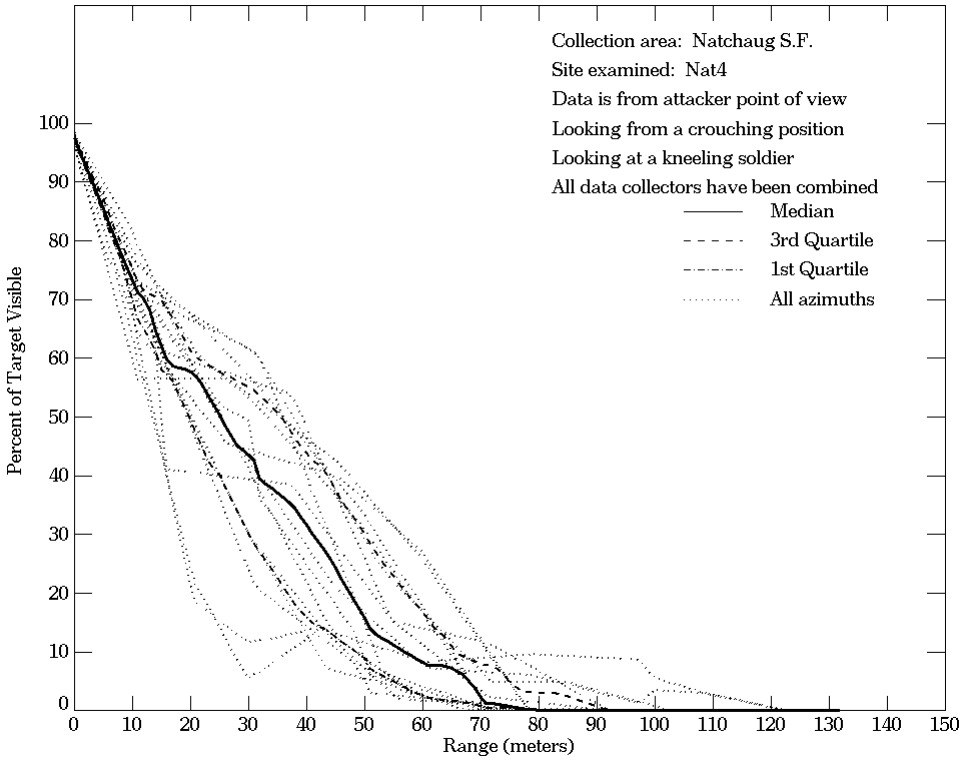

Figure E-94. Natchaug SF, From Attacker Point of View, Site Nat4 (Continued)

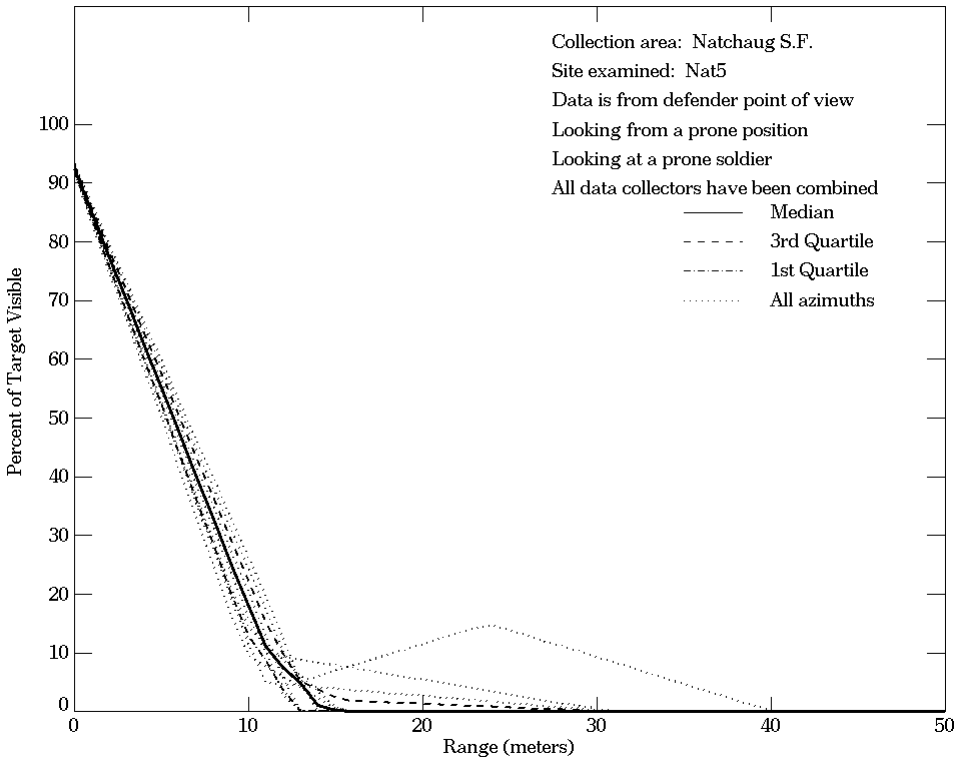

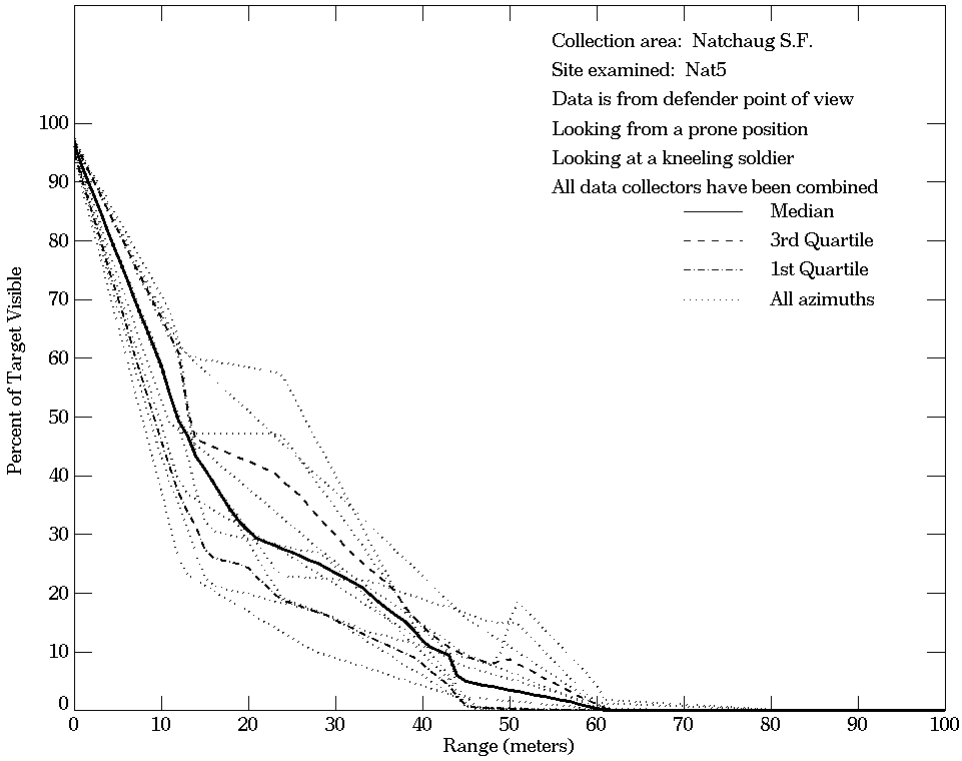

Figure E-95. Natchaug SF, From Defender Point of View, Site Nat5

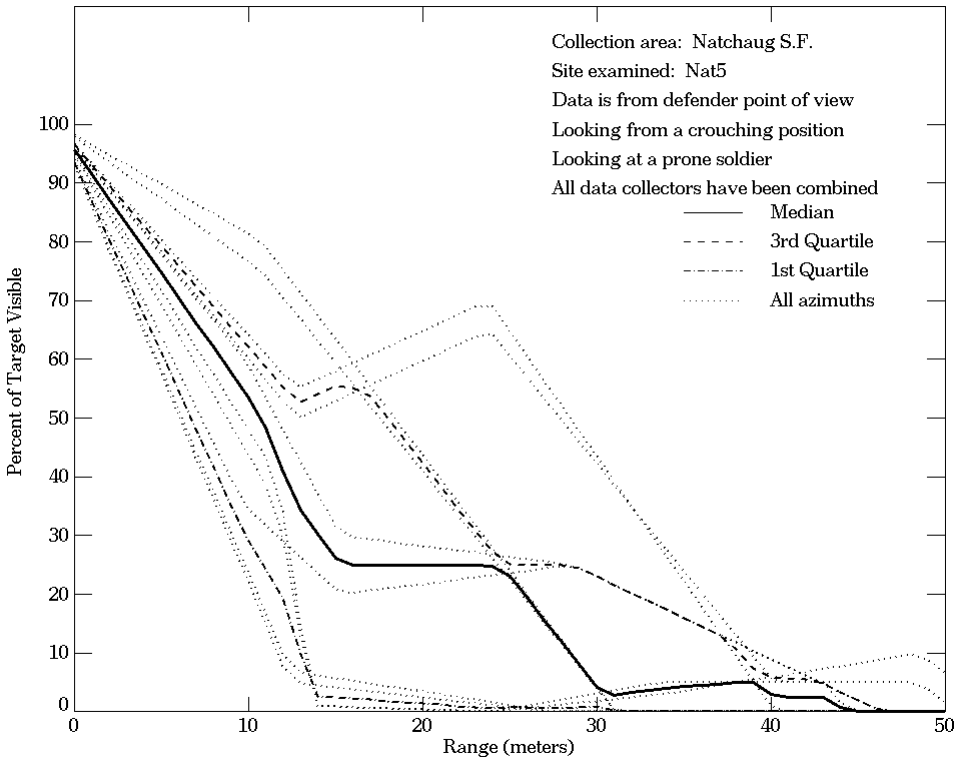

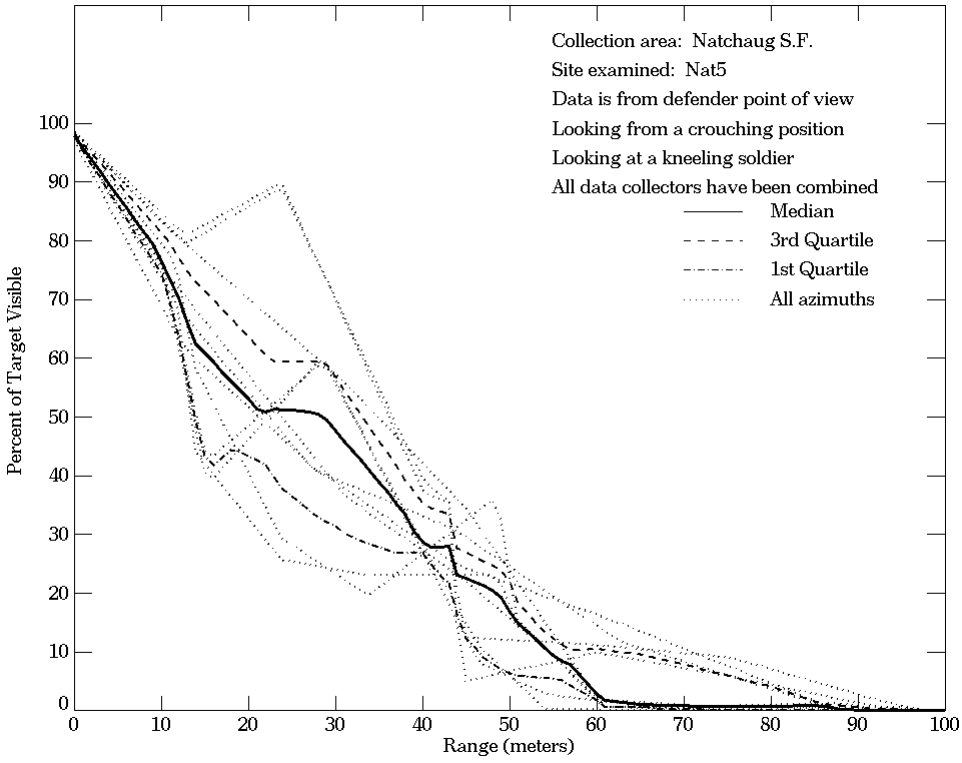

Figure E-95. Natchaug SF, From Defender Point of View, Site Nat5 (Continued)

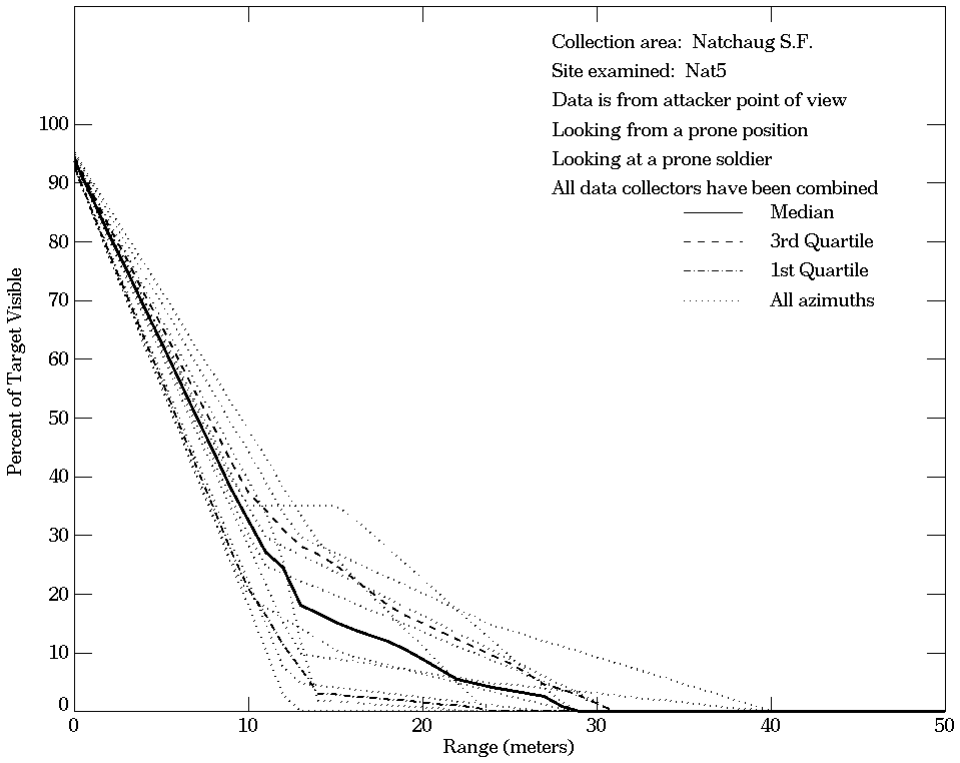

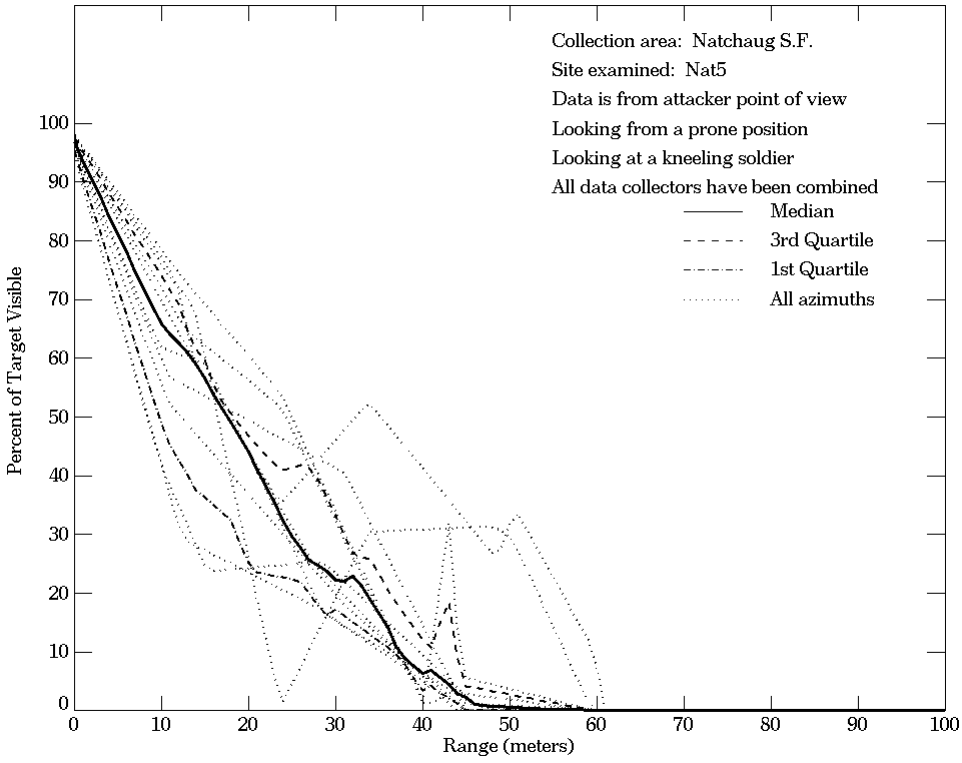

Figure E-96. Natchaug SF, From Attacker Point of View, Site Nat5

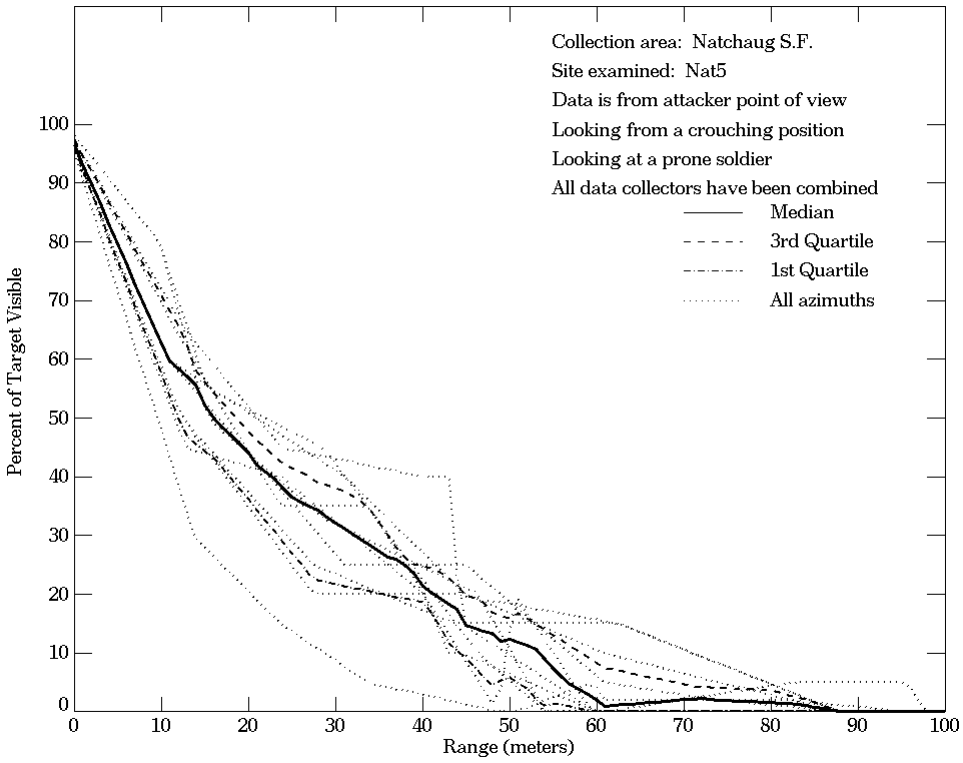

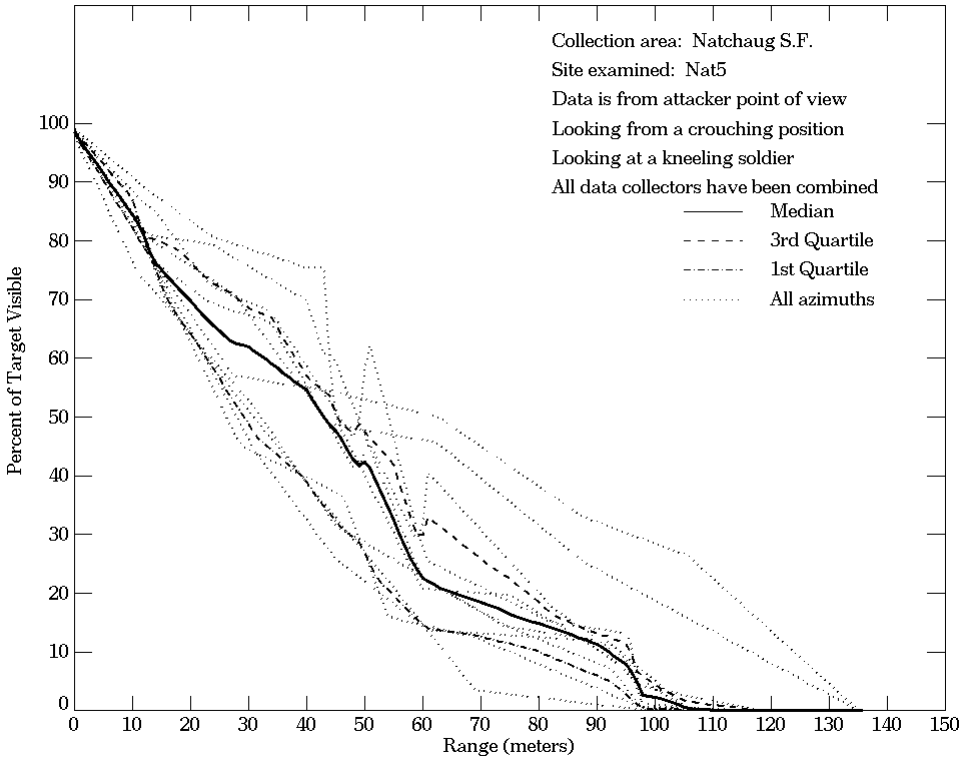

Figure E-96. Natchaug SF, From Attacker Point of View, Site Nat5 (Continued)

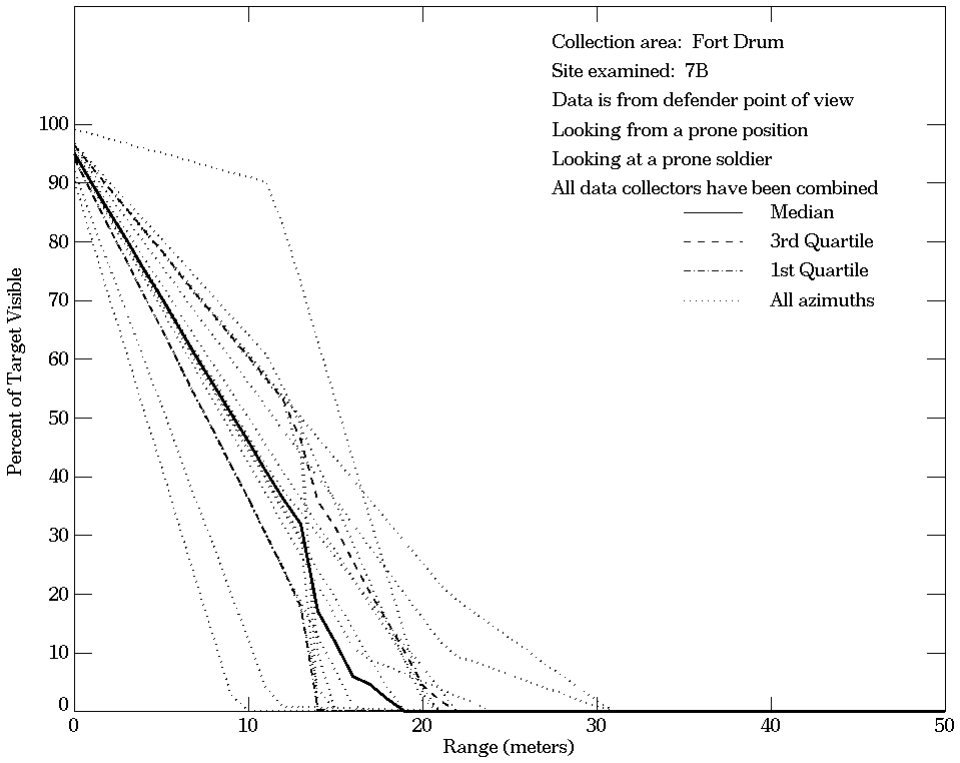

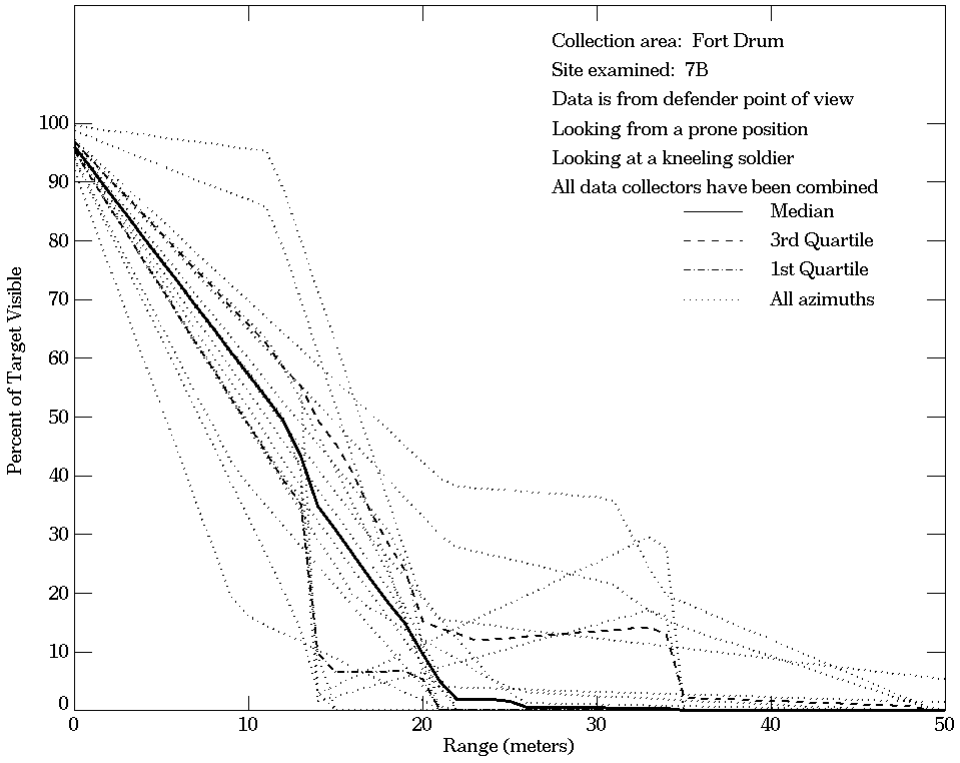

Figure E-97. Fort Drum, From Defender Point of View, Site 7B

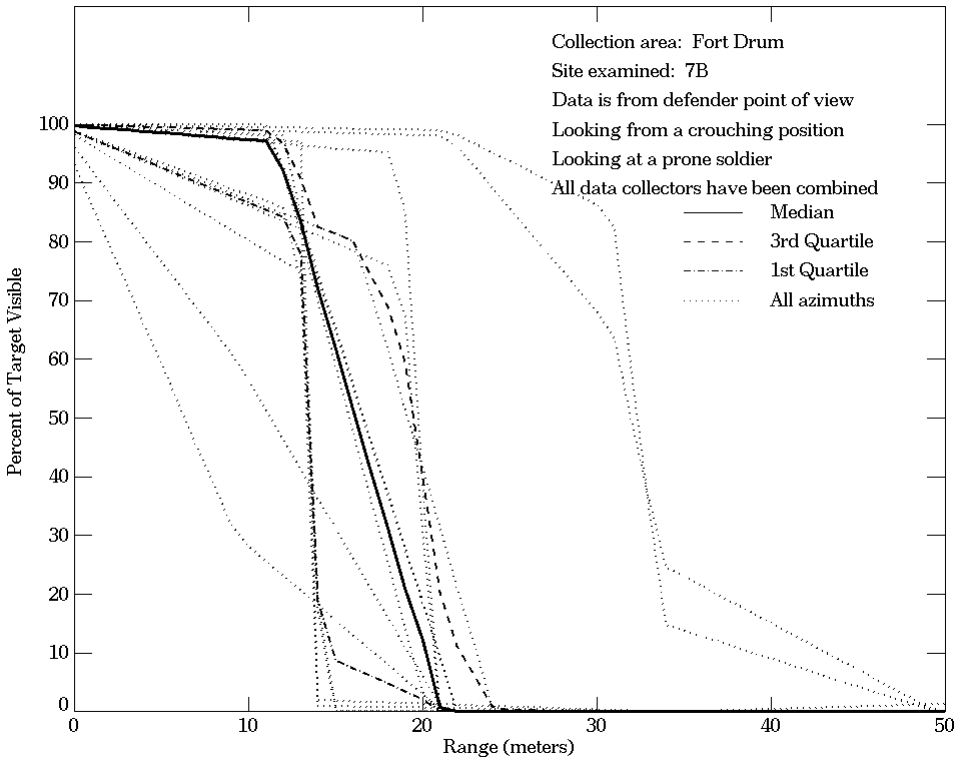

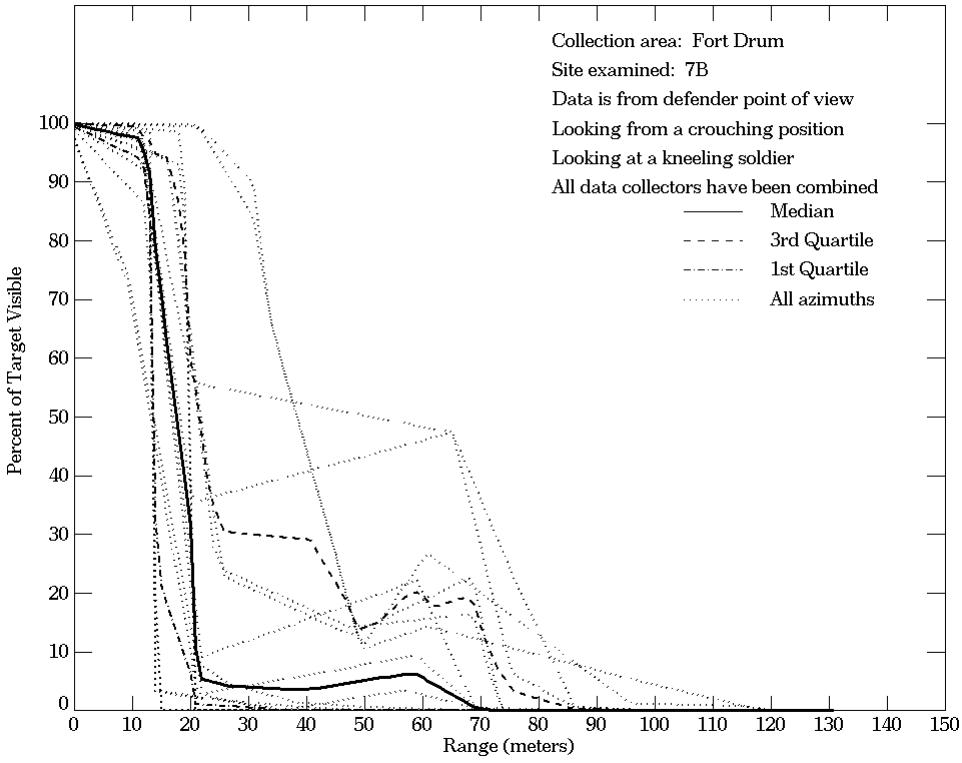

Figure E-97. Fort Drum, From Defender Point of View, Site 7B (Continued)

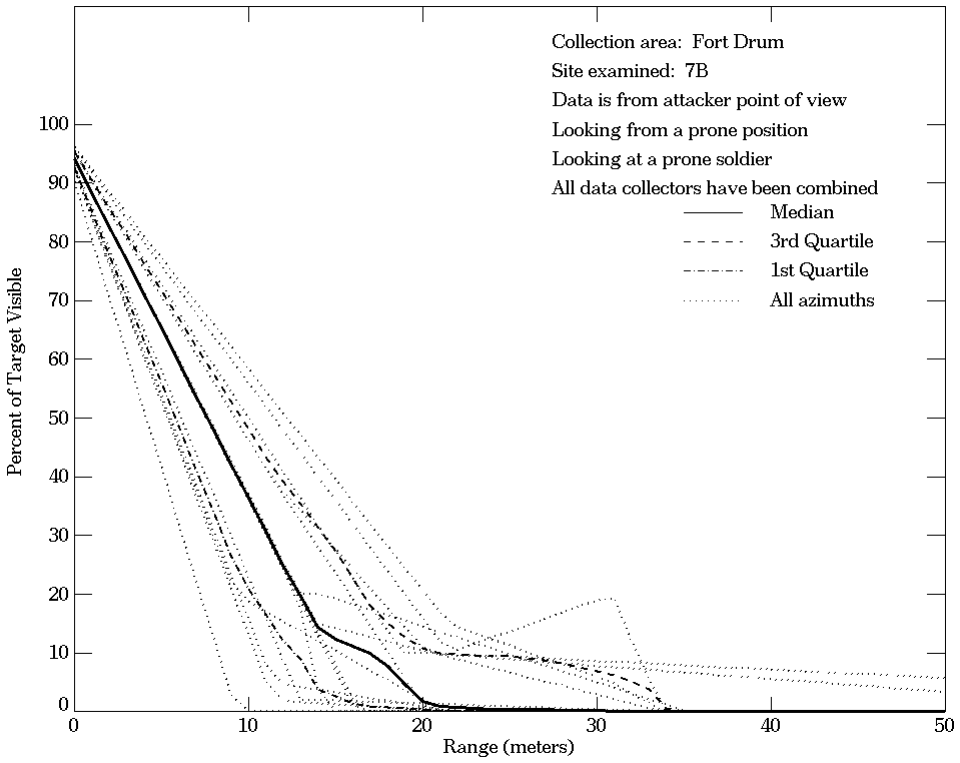

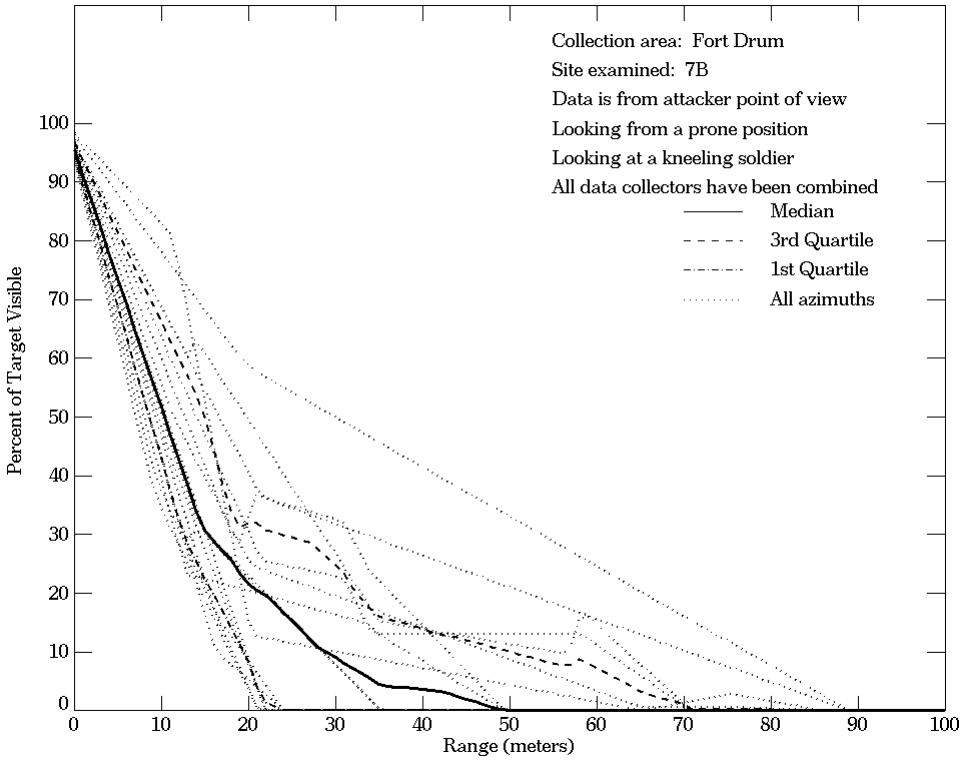

Figure E-98. Fort Drum, From Attacker Point of View, Site 7B

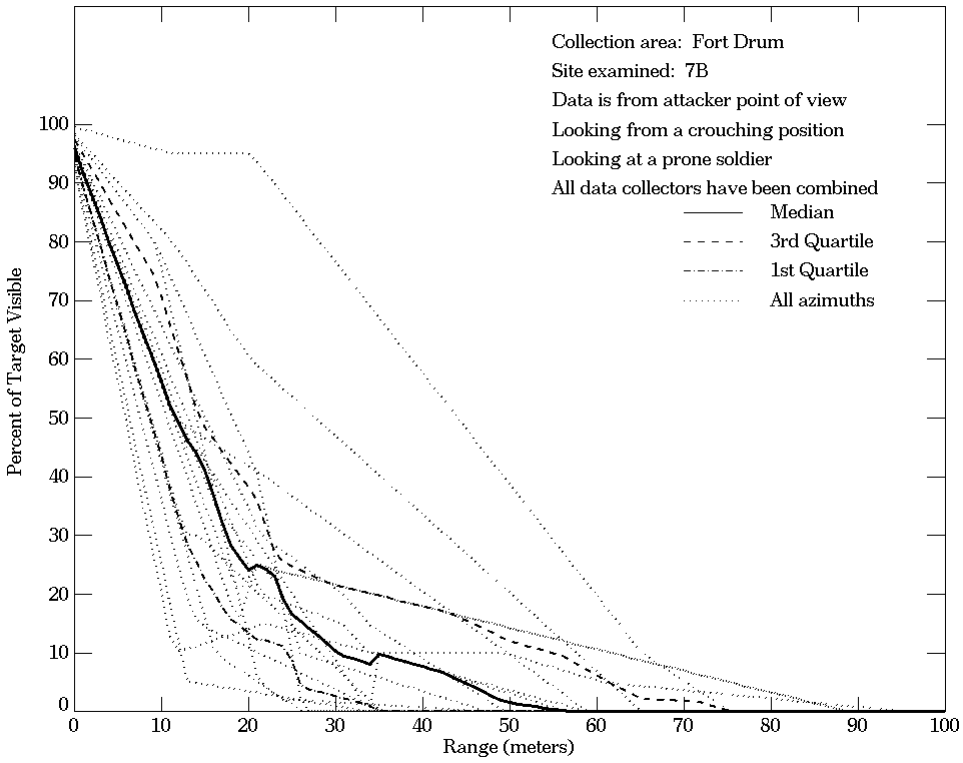

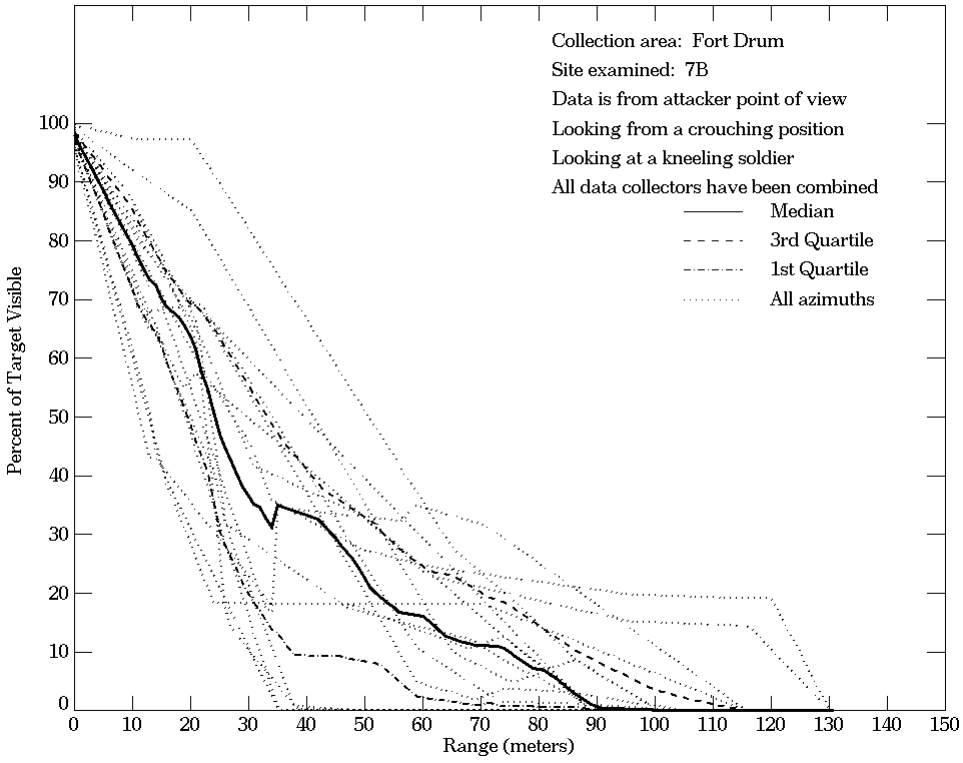

Figure E-98. Fort Drum, From Attacker Point of View, Site 7B (Continued)

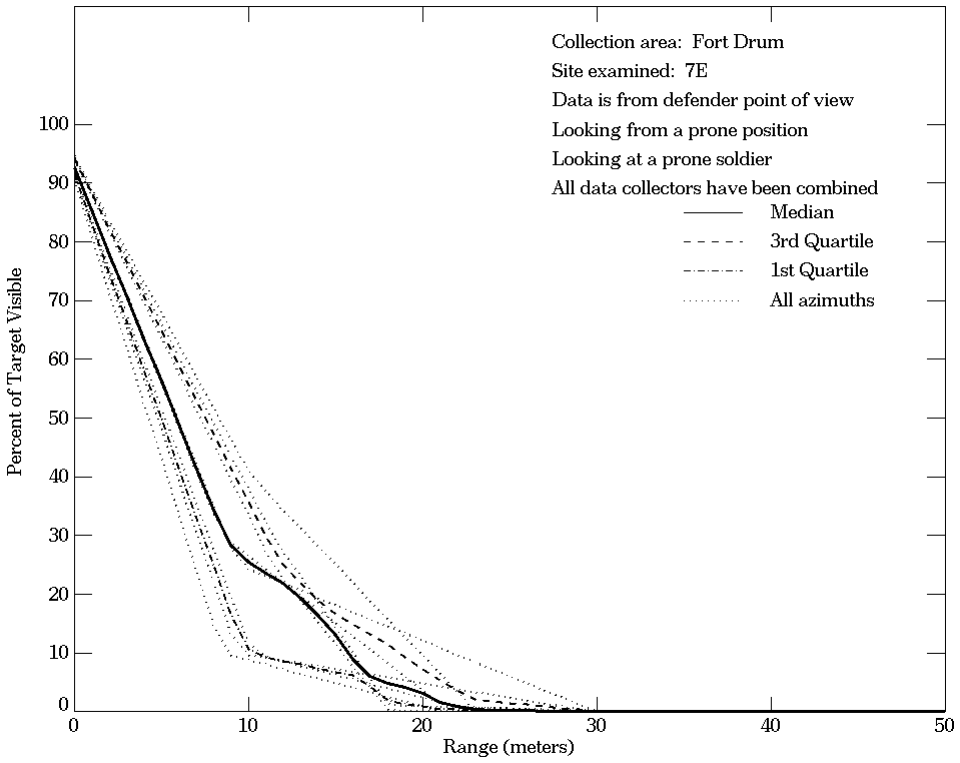

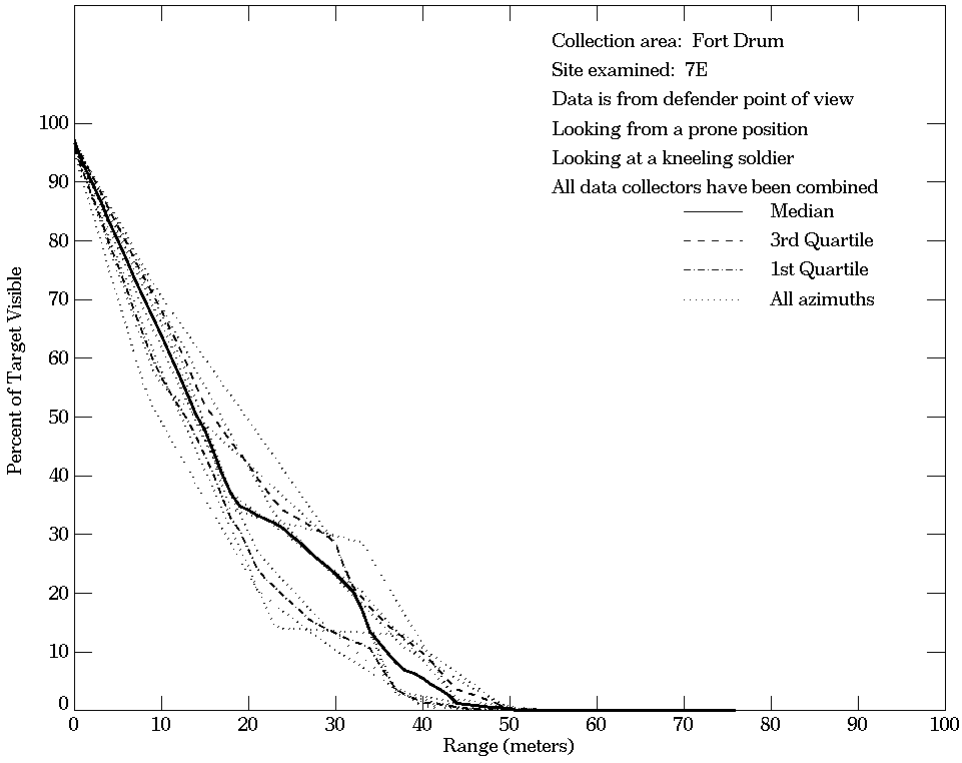

Figure E-99. Fort Drum, From Defender Point of View, Site 7E

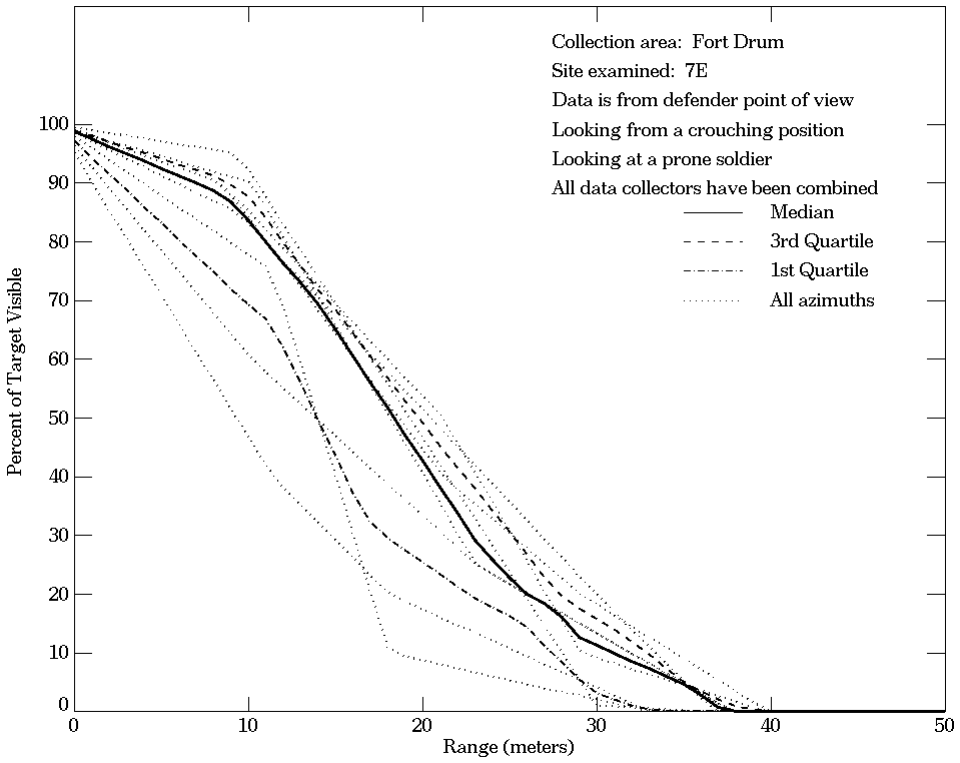

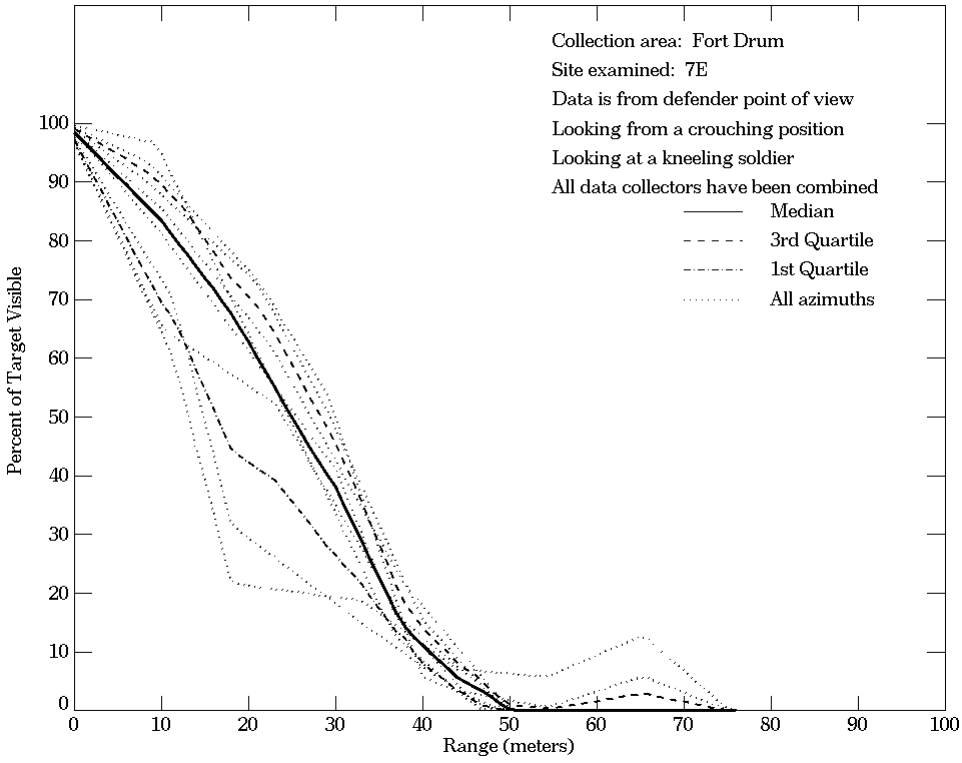

Figure E-99. Fort Drum, From Defender Point of View, Site 7E (Continued)

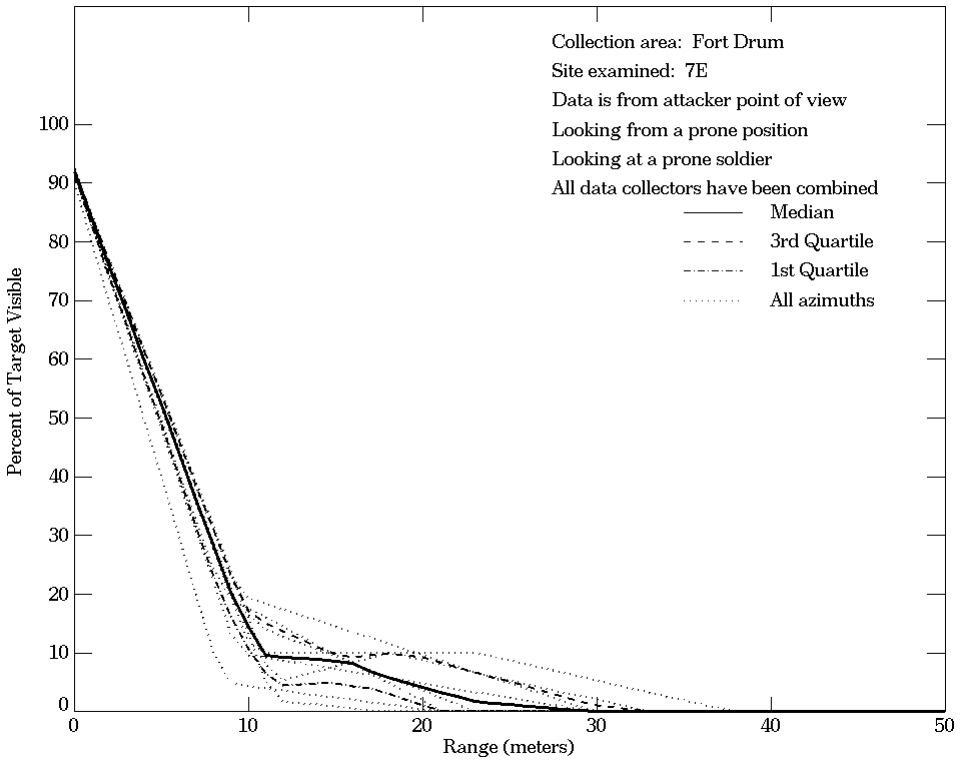

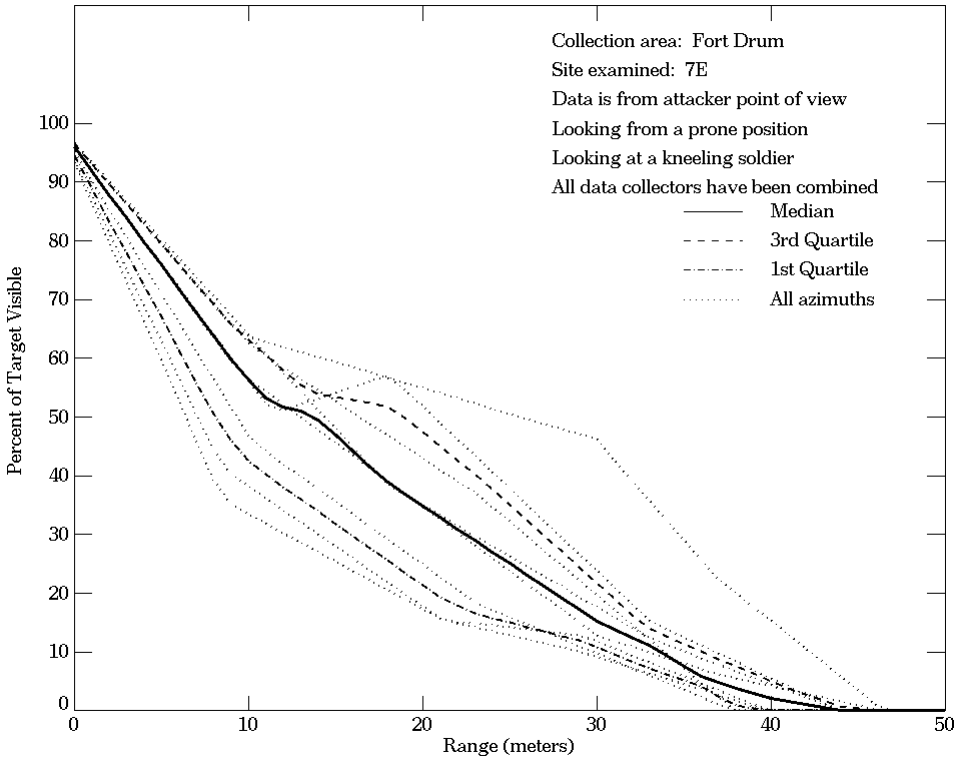

Figure E-100. Fort Drum, From Attacker Point of View, Site 7E

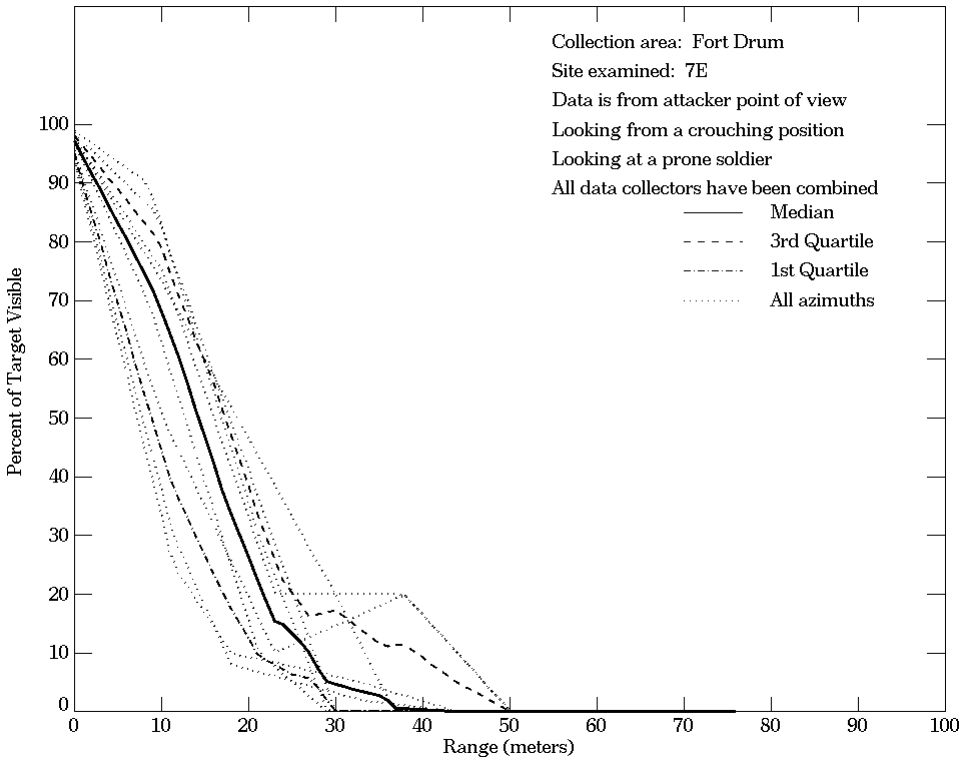

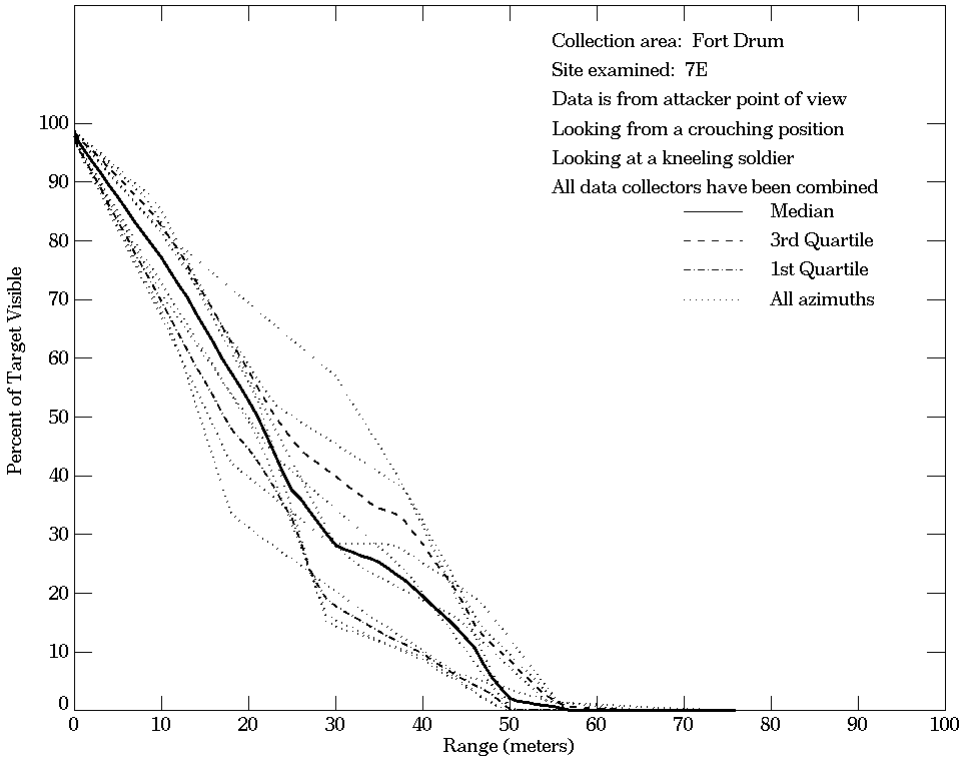

Figure E-100. Fort Drum, From Attacker Point of View, Site 7E (Continued)

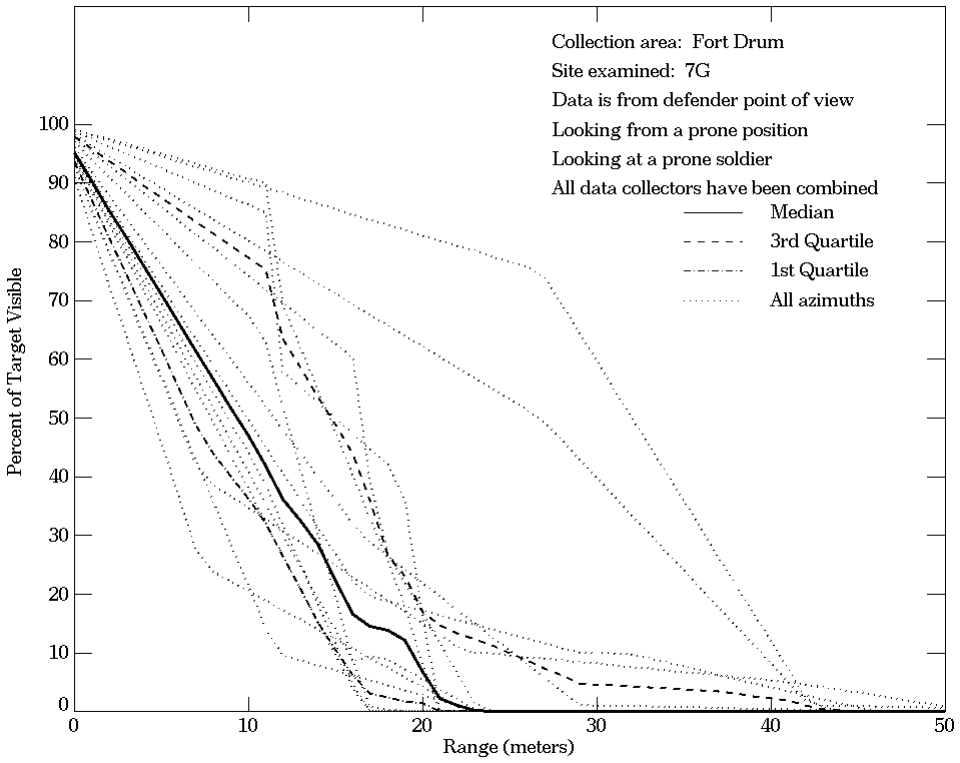

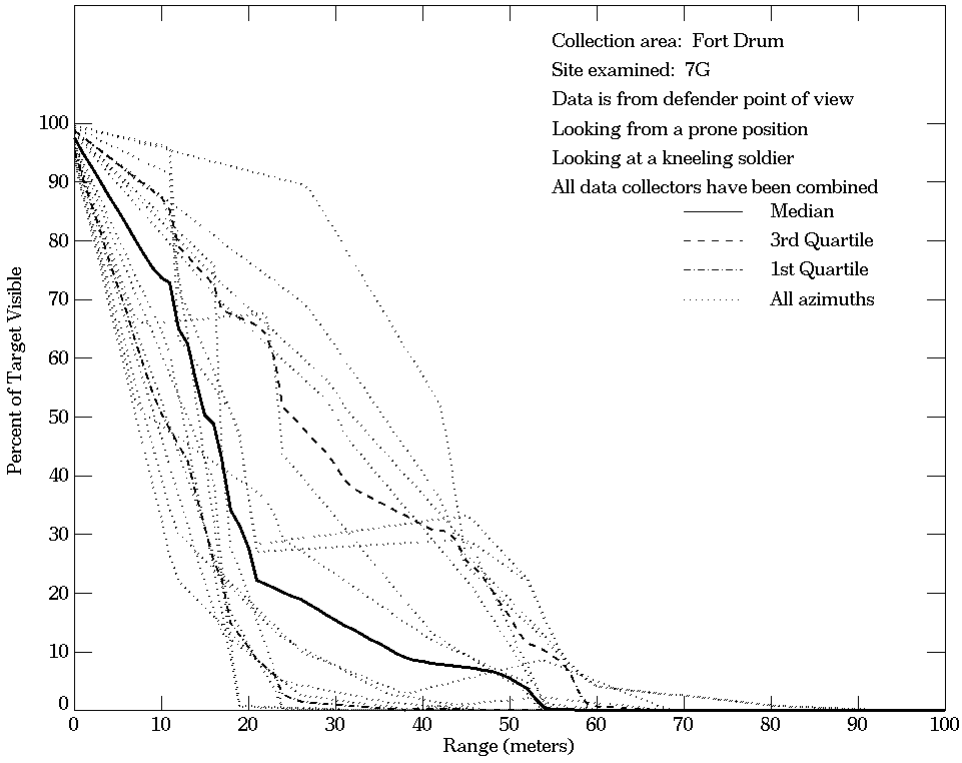

Figure E-101. Fort Drum, From Defender Point of View, Site 7G

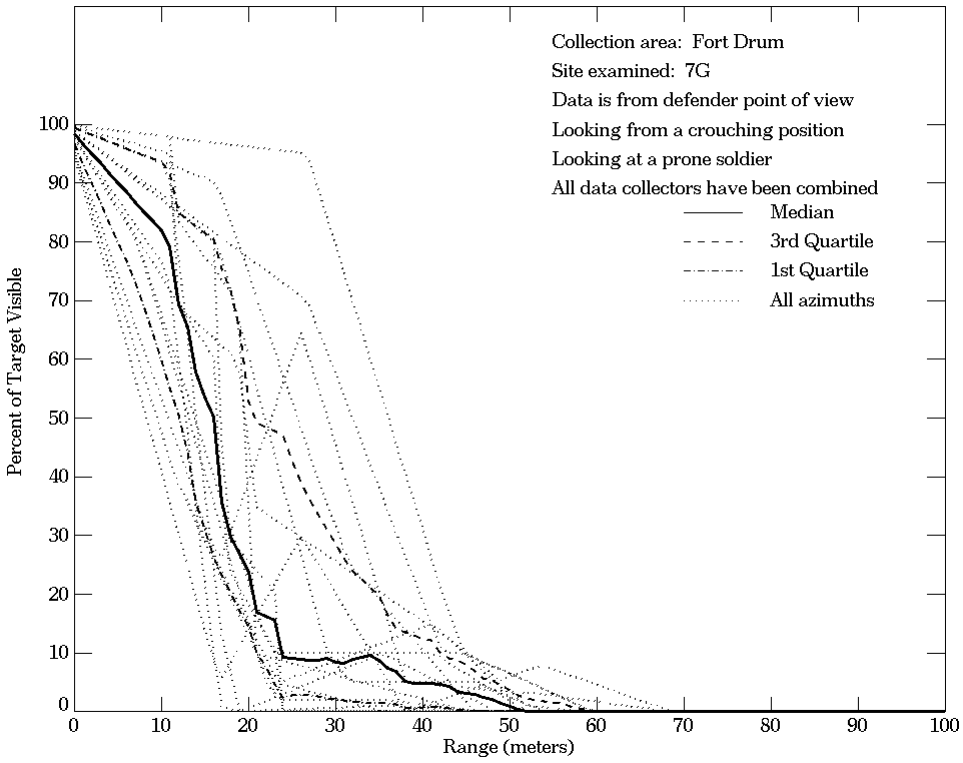

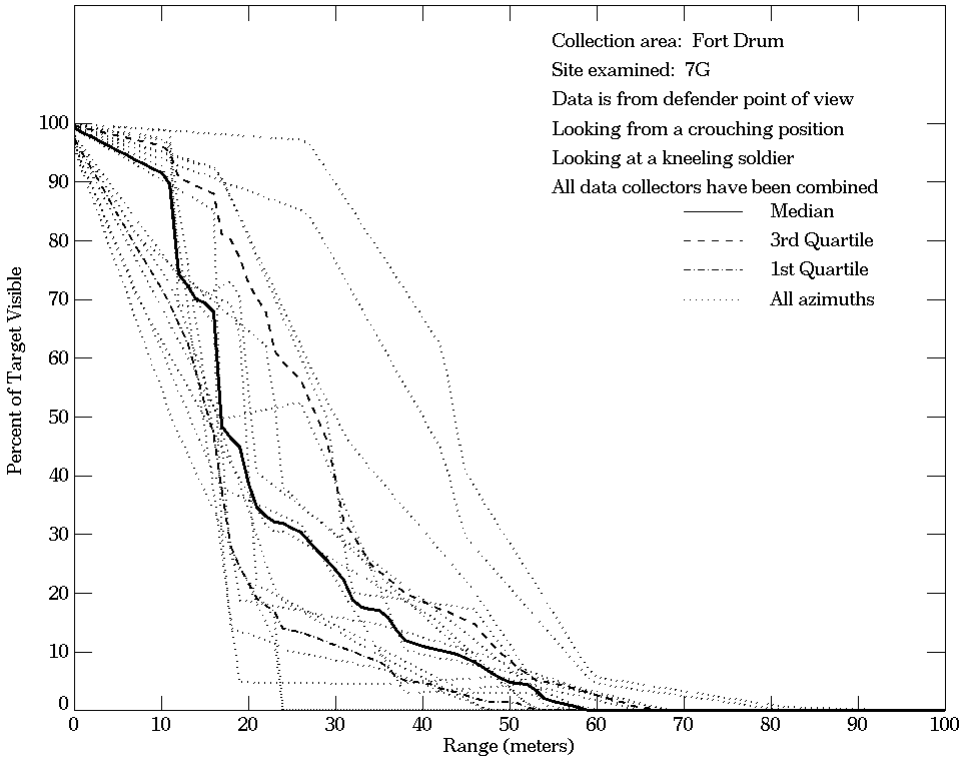

Figure E-101. Fort Drum, From Defender Point of View, Site 7G (Continued)

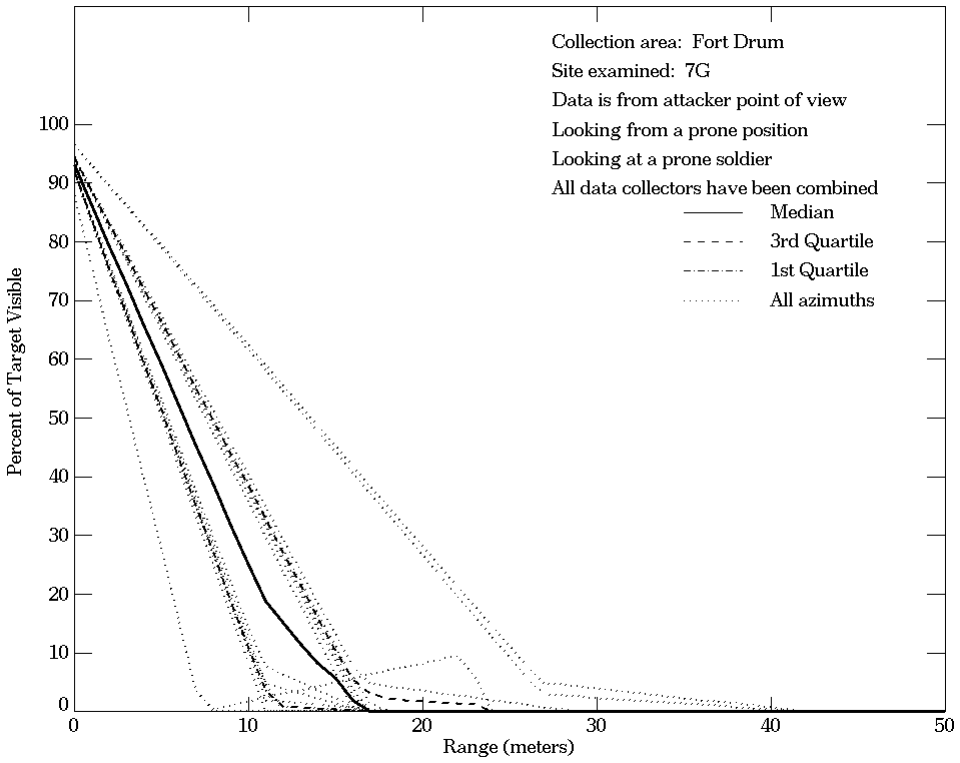

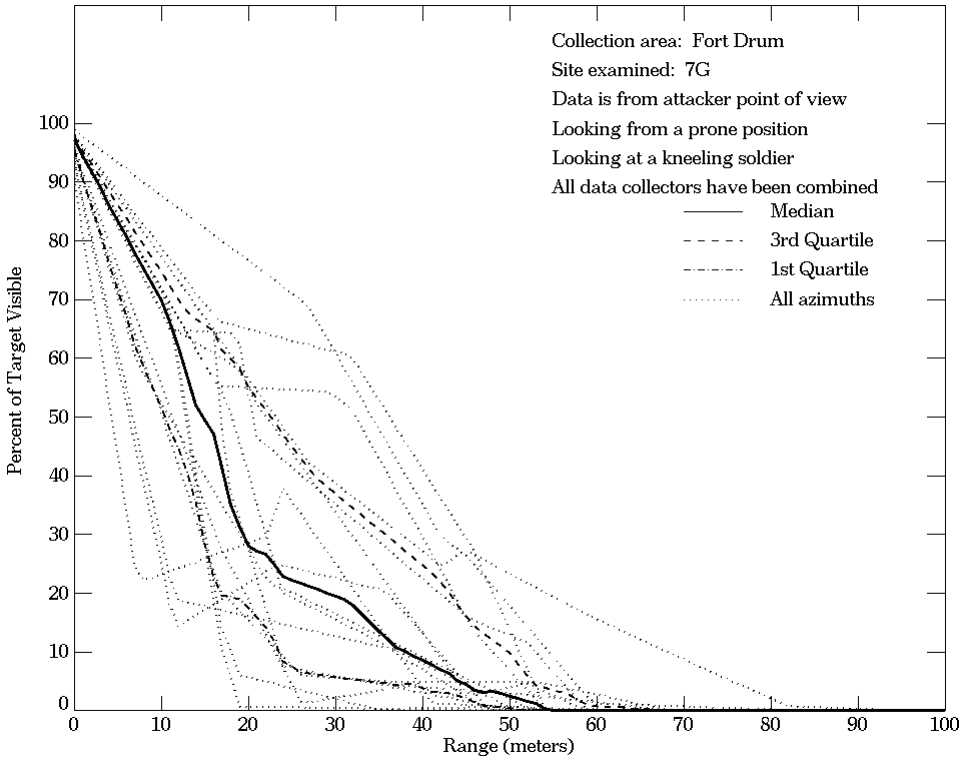

Figure E-102. Fort Drum, From Attacker Point of View, Site 7G

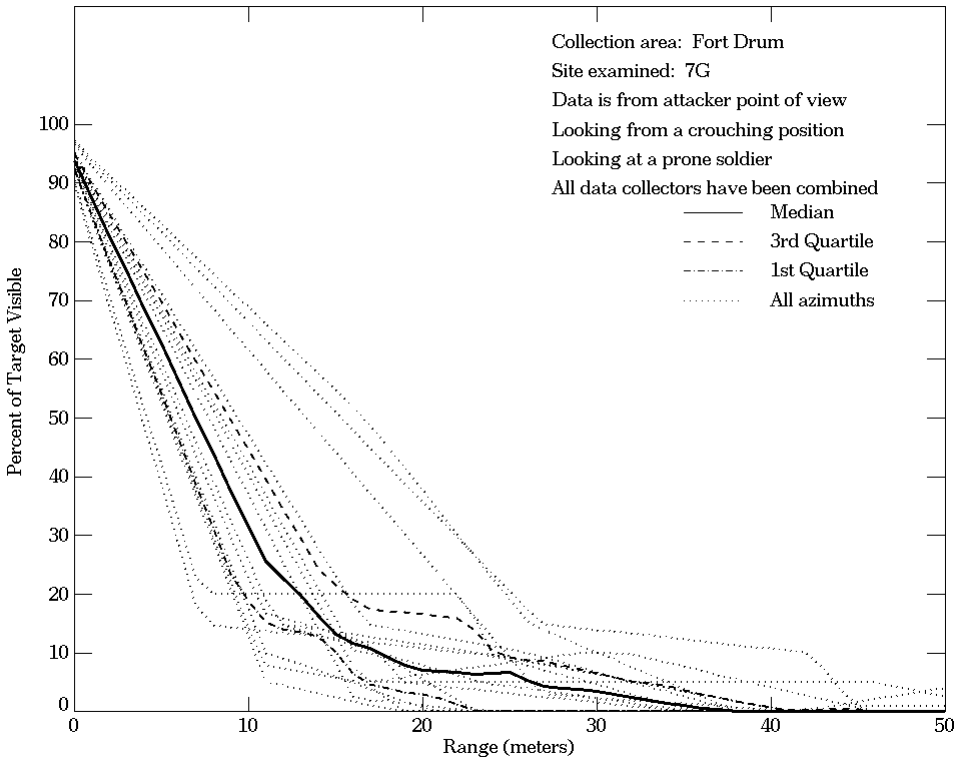

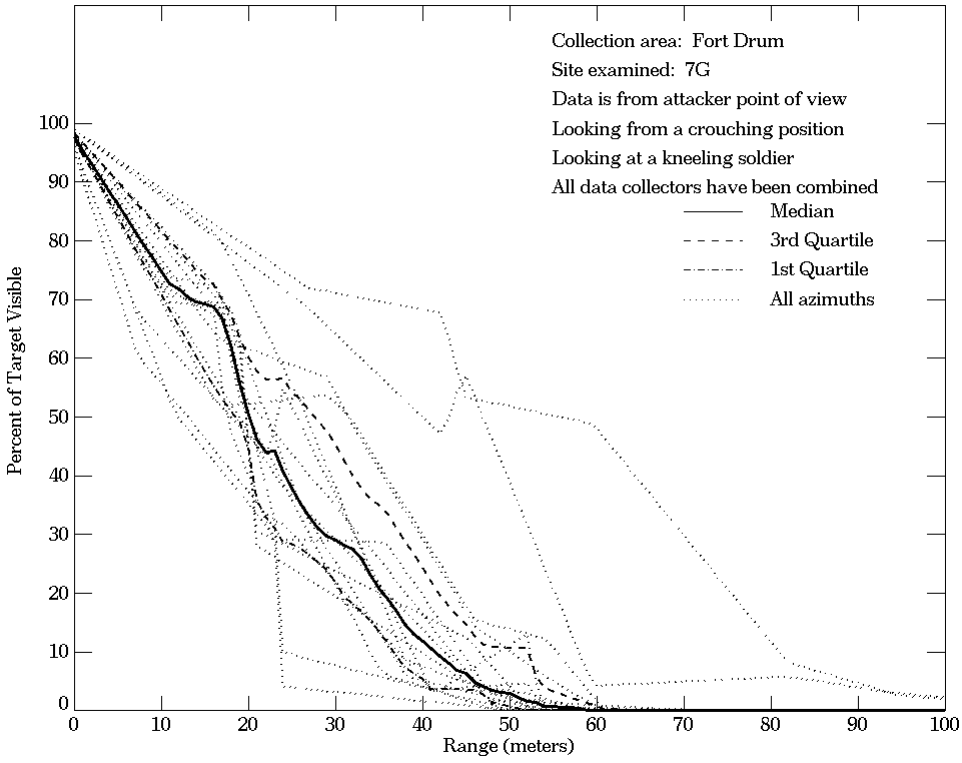

Figure E-102. Fort Drum, From Attacker Point of View, Site 7G (Continued)

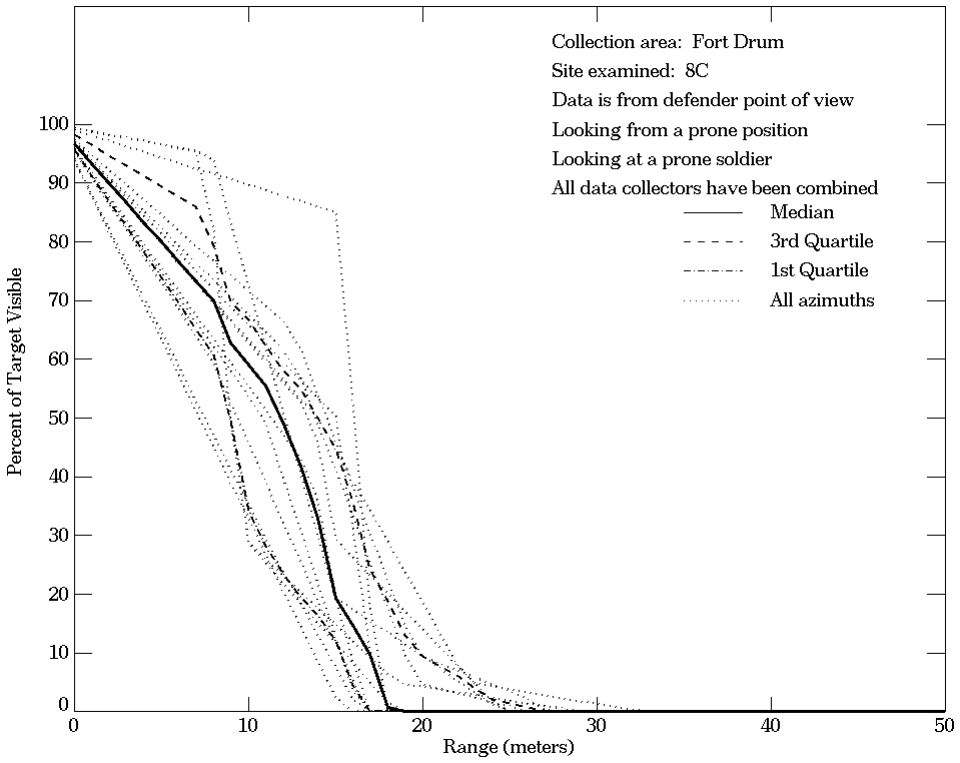

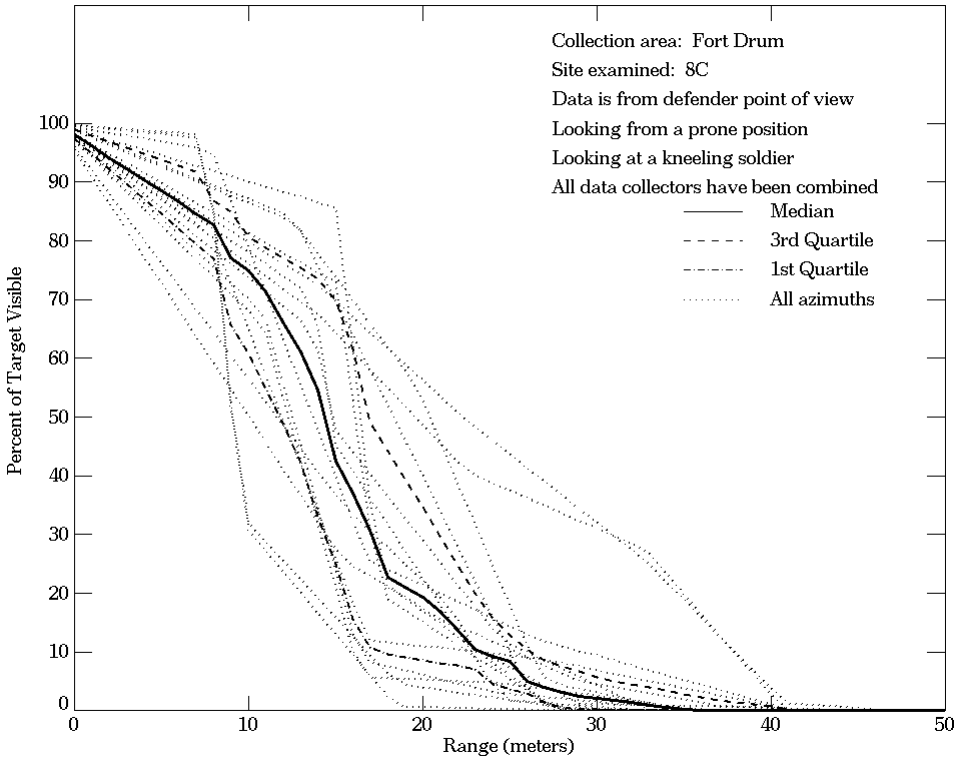

Figure E-103. Fort Drum, From Defender Point of View, Site 8C

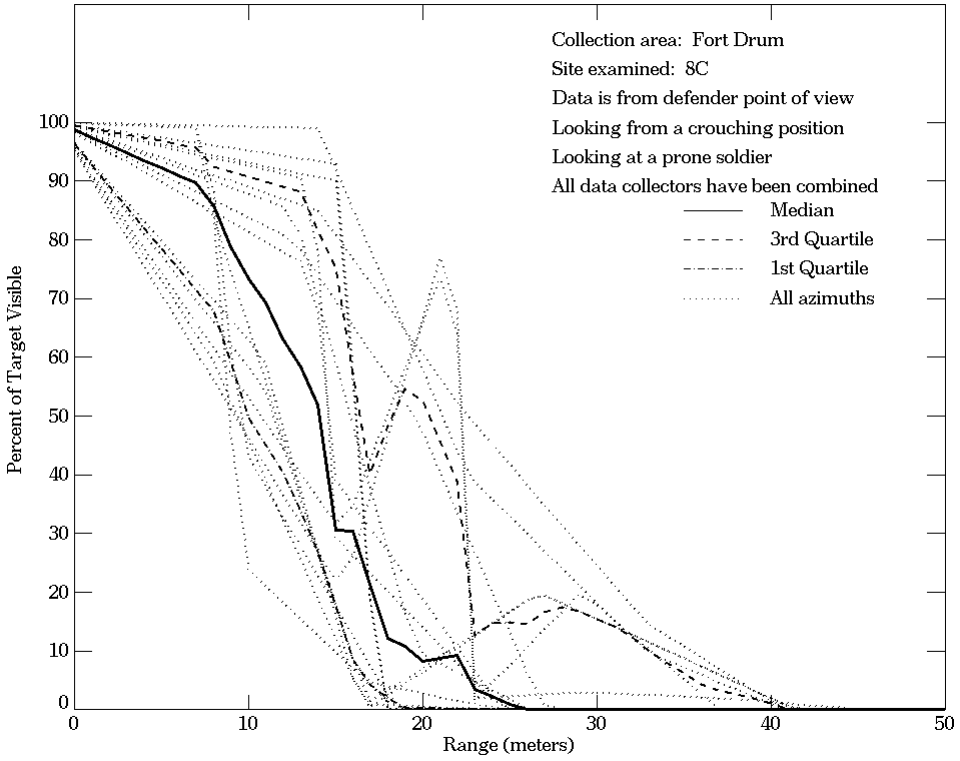

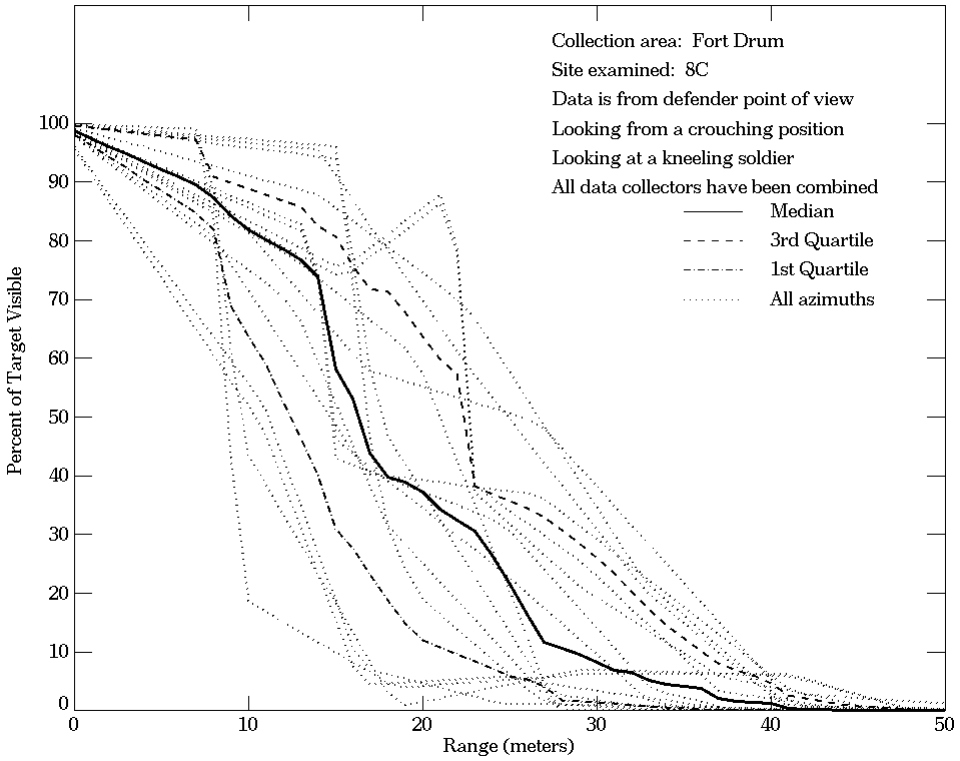

Figure E-103. Fort Drum, From Defender Point of View, Site 8C (Continued)

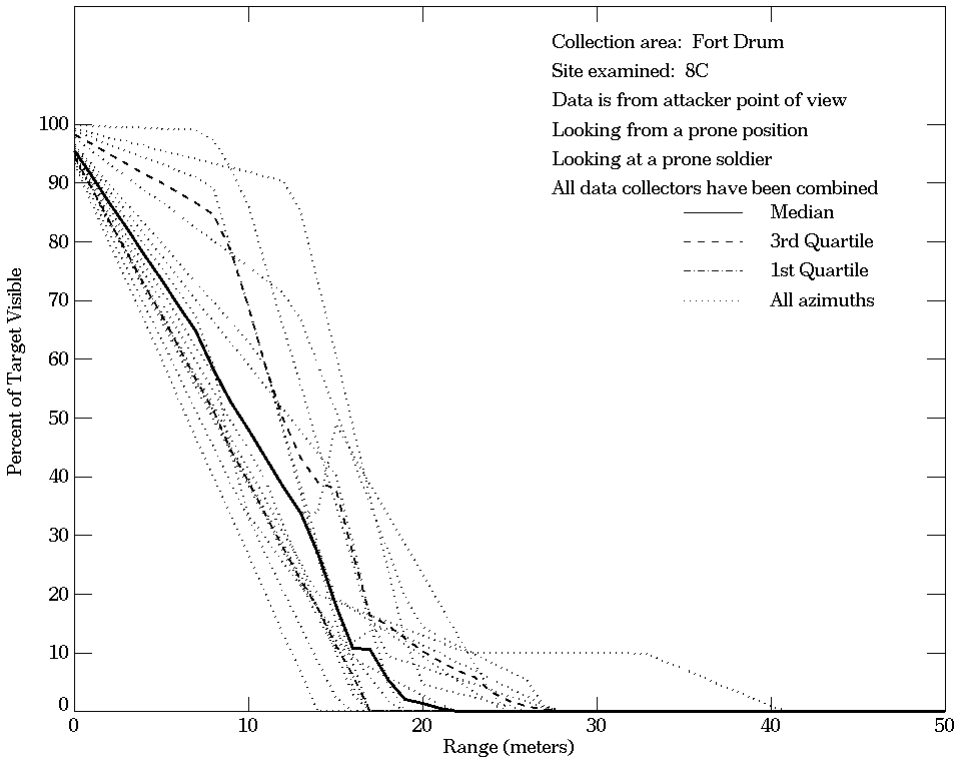

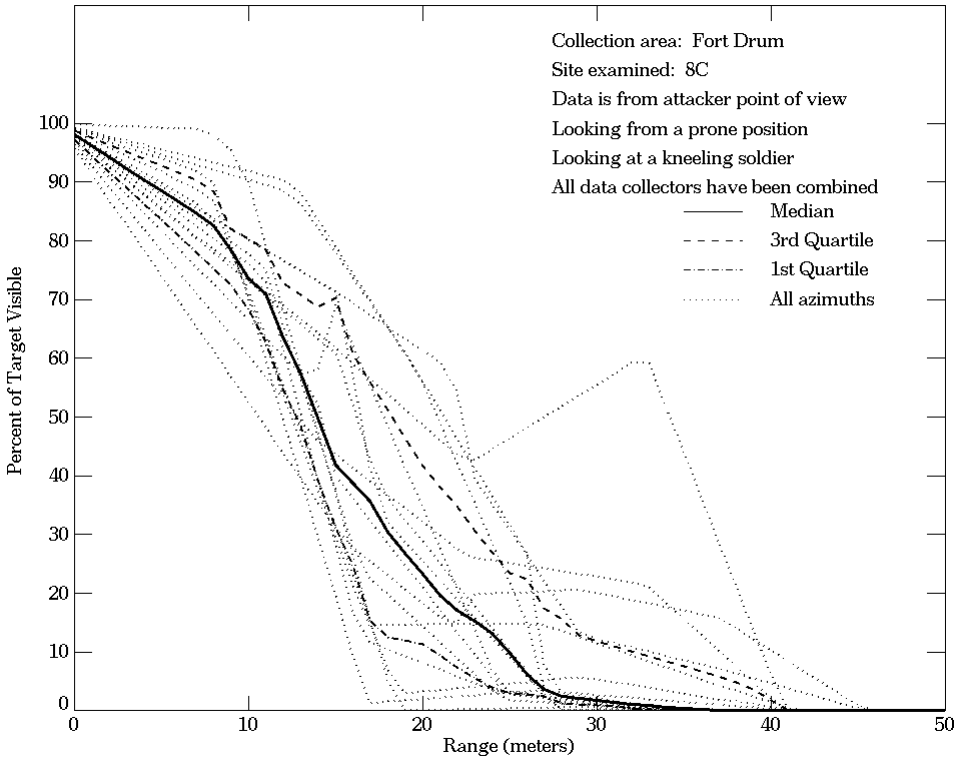

Figure E-104. Fort Drum, From Attacker Point of View, Site 8C

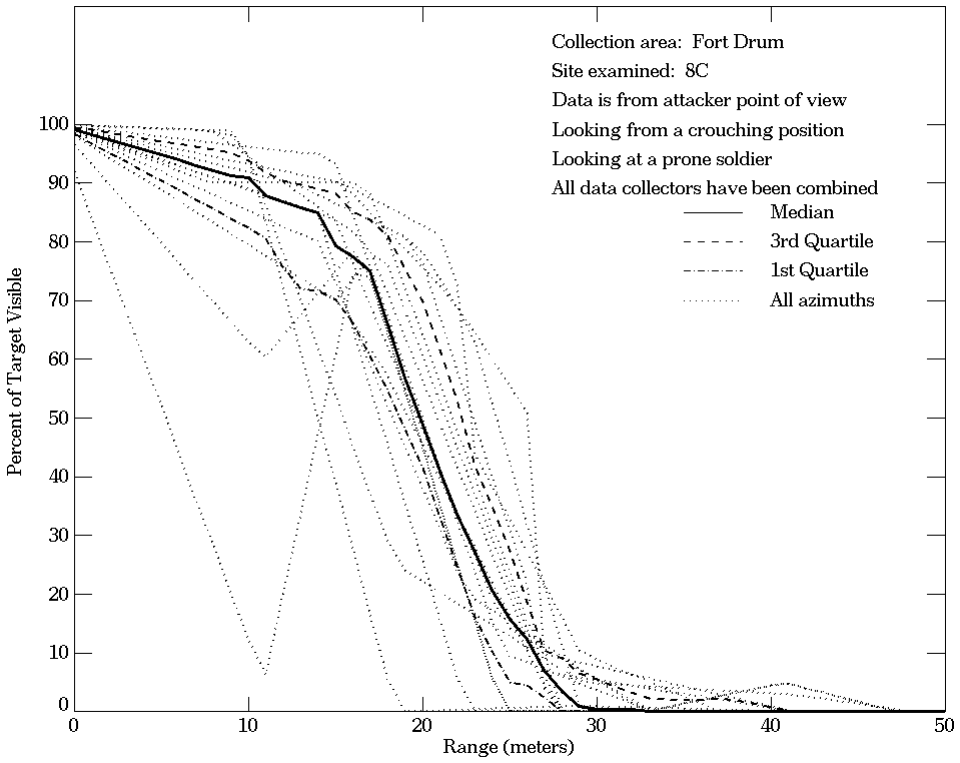

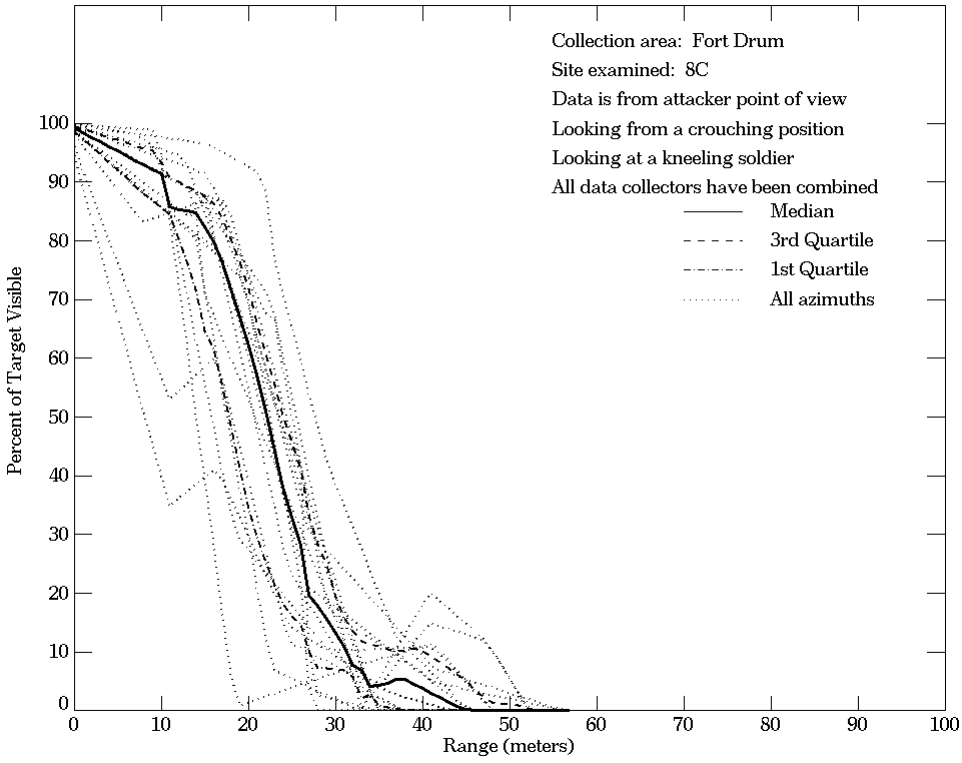

Figure E-104. Fort Drum, From Attacker Point of View, Site 8C (Continued)

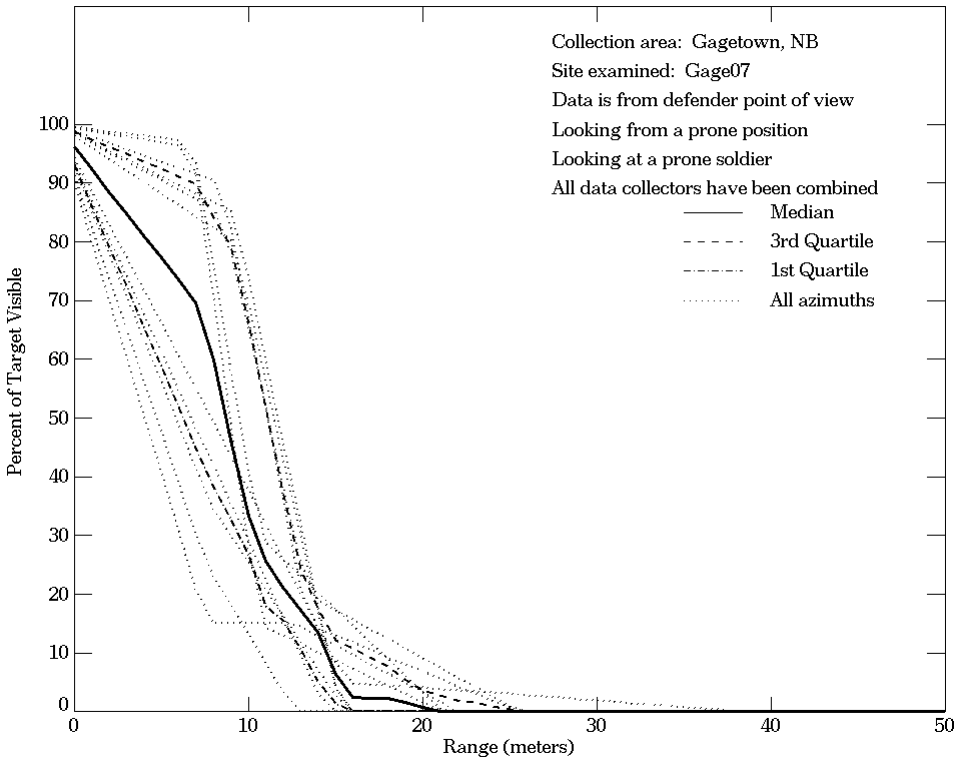

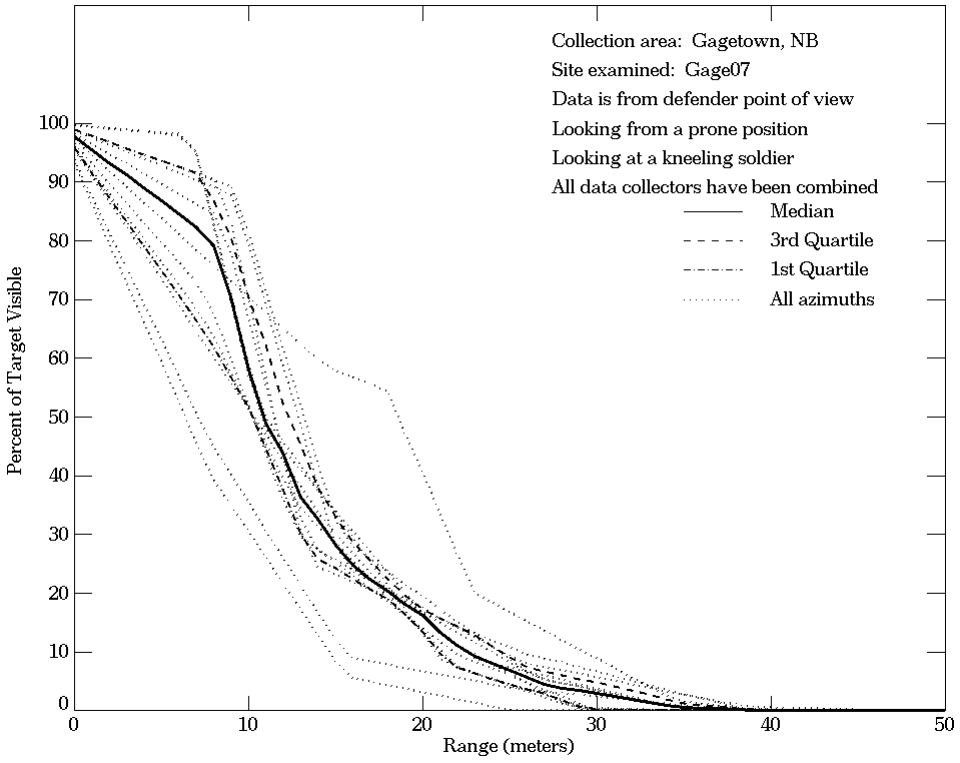

Figure E-105. Gagetown, NB, From Defender Point of View, Site Gage07

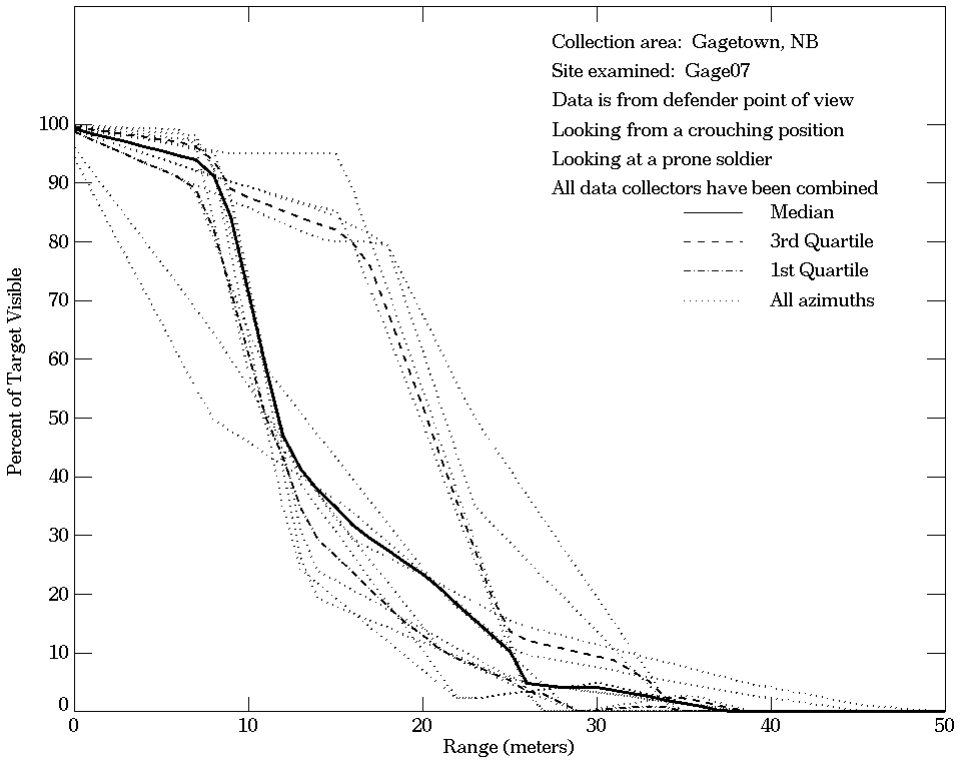

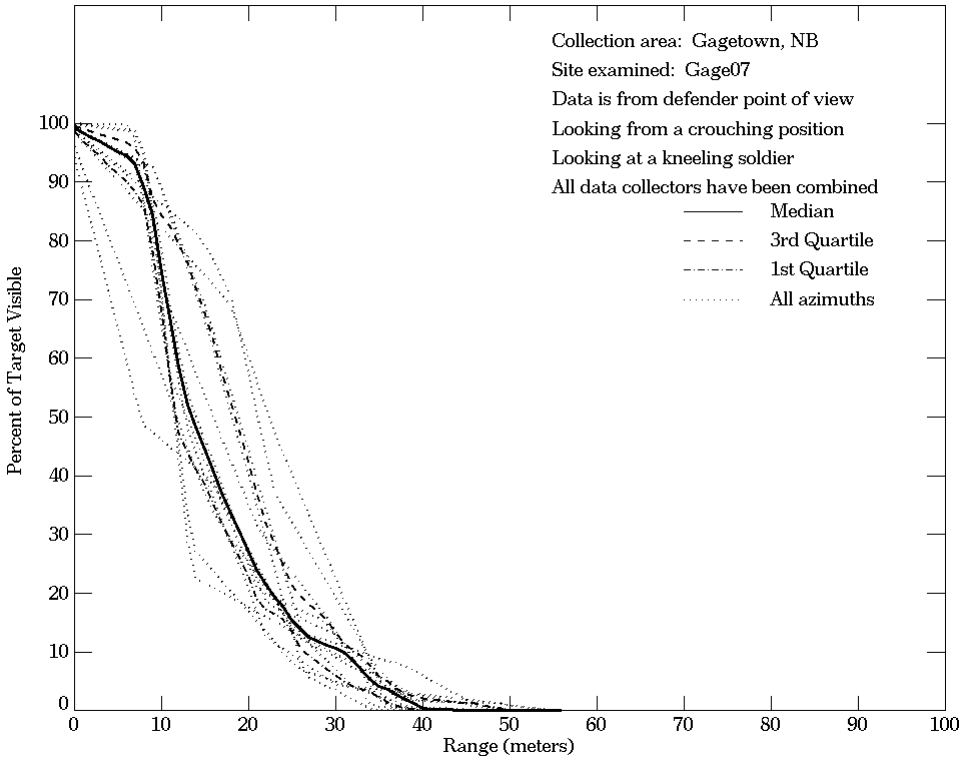

Figure E-105. Gagetown, NB, From Defender Point of View, Site Gage07 (Continued)

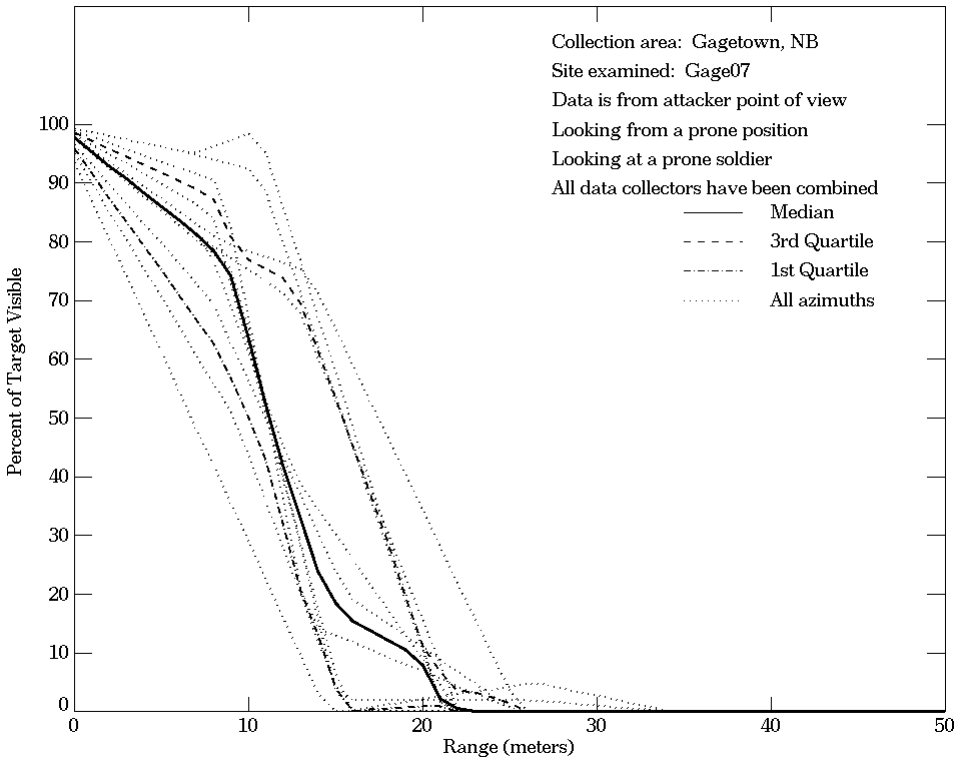

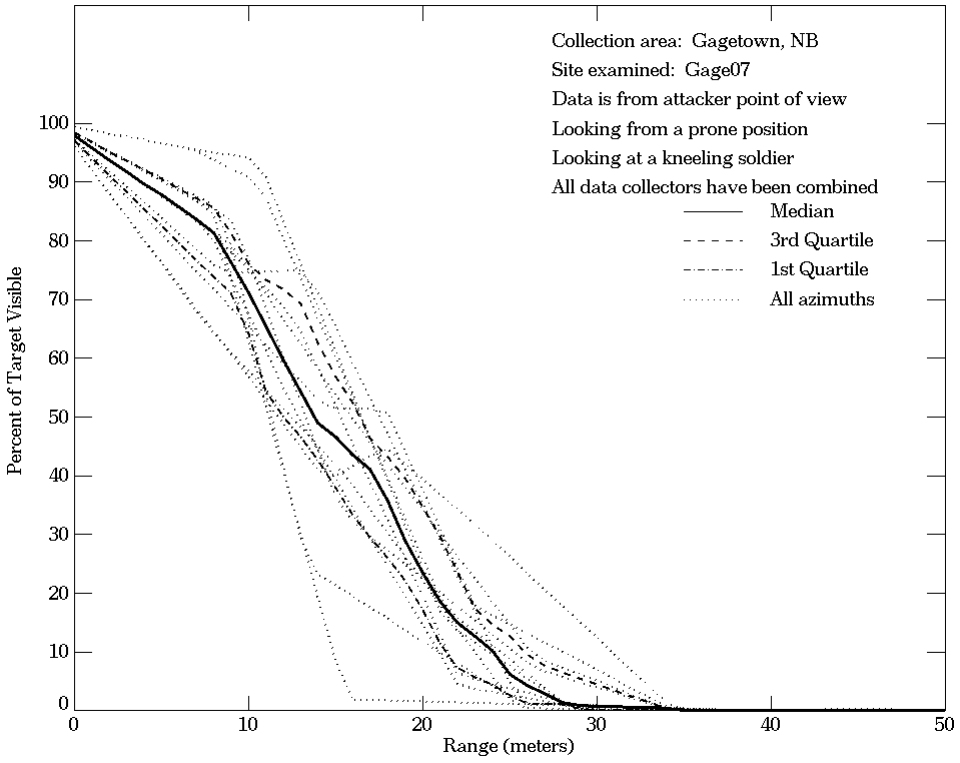

Figure E-106. Gagetown, NB, From Attacker Point of View, Site Gage07

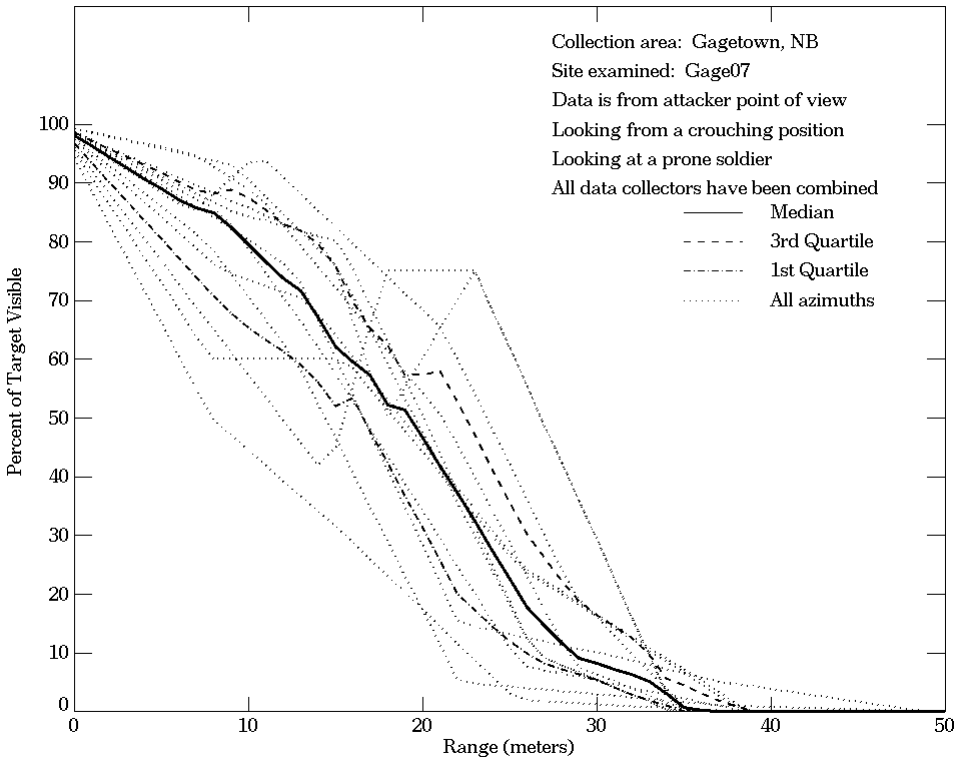

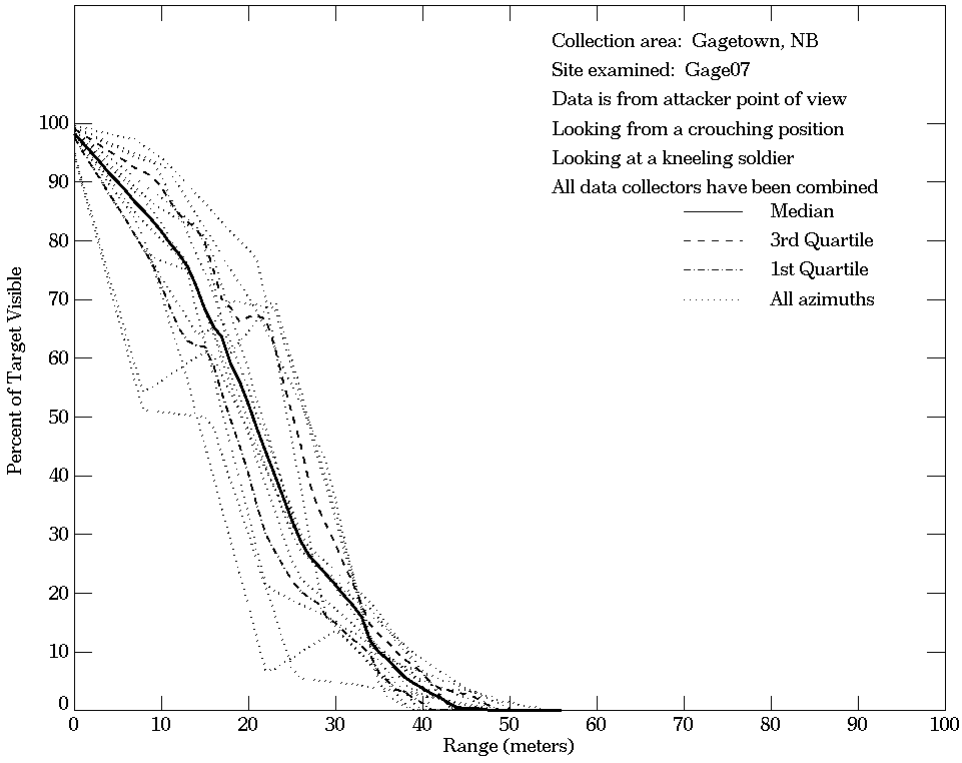

Figure E-106. Gagetown, NB, From Attacker Point of View, Site Gage07 (Continued)

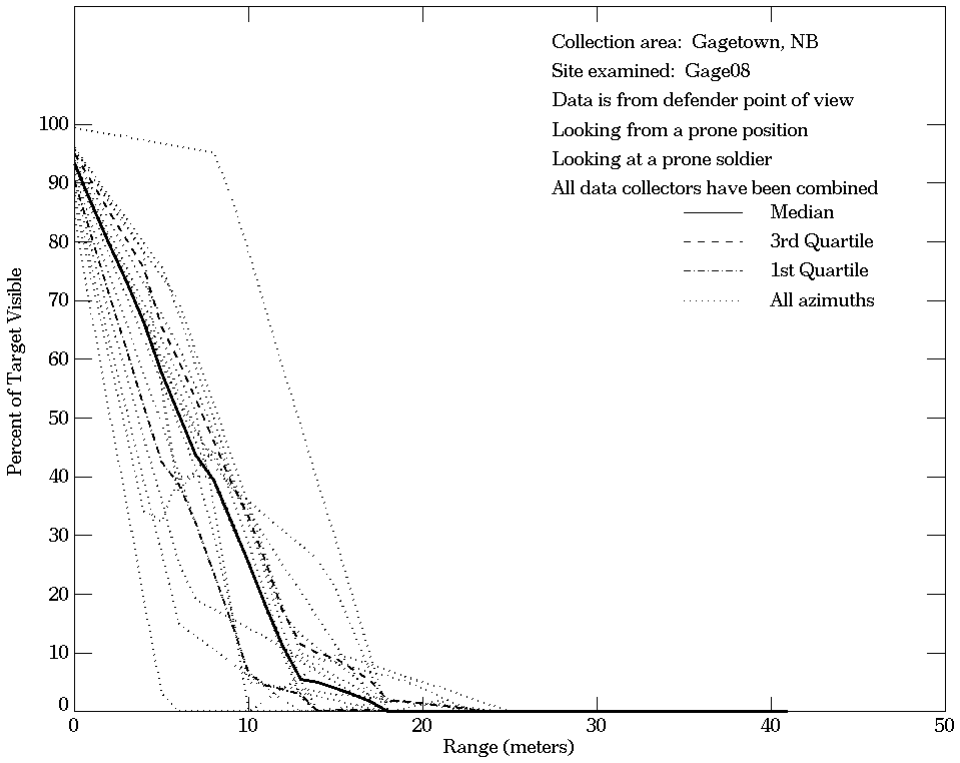

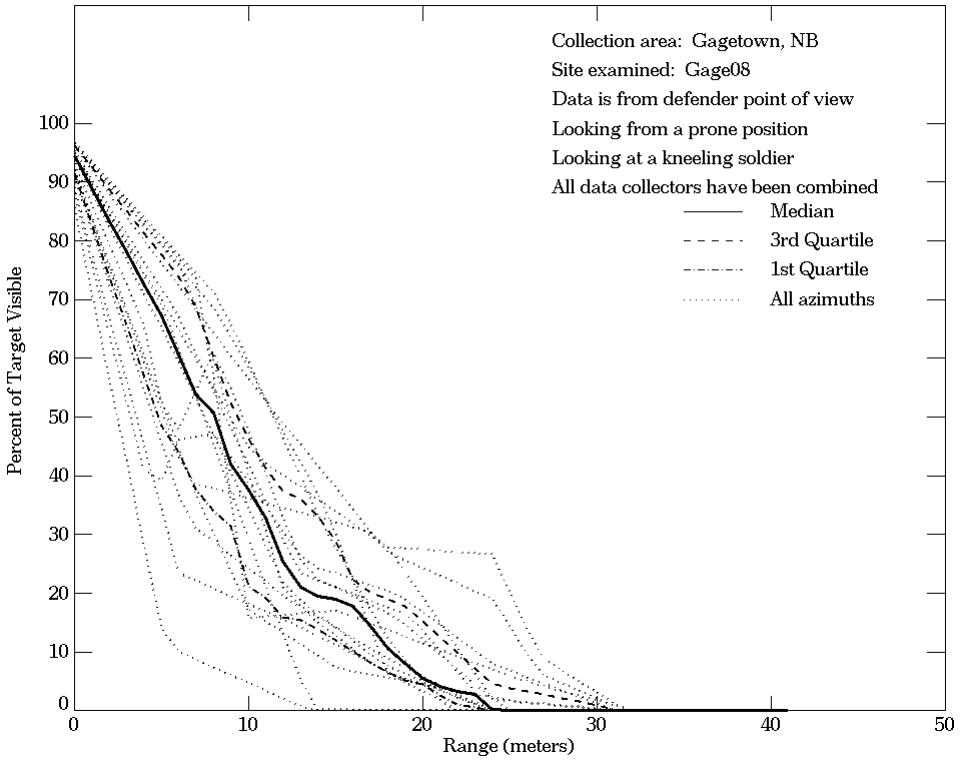

Figure E-107. Gagetown, NB, From Defender Point of View, Site Gage08

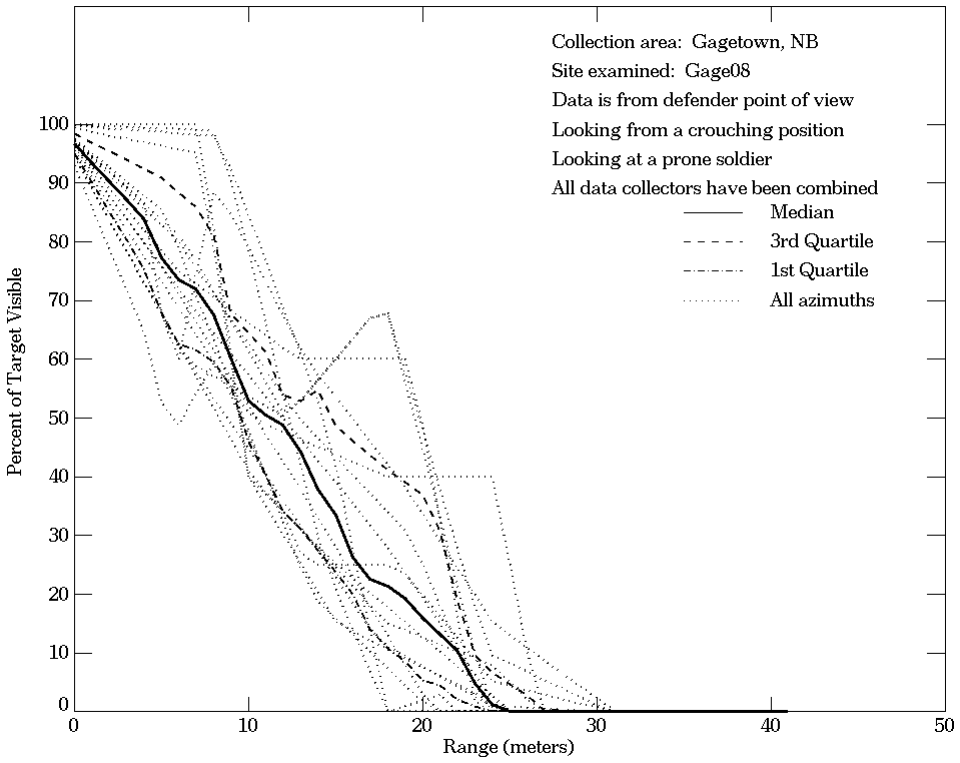

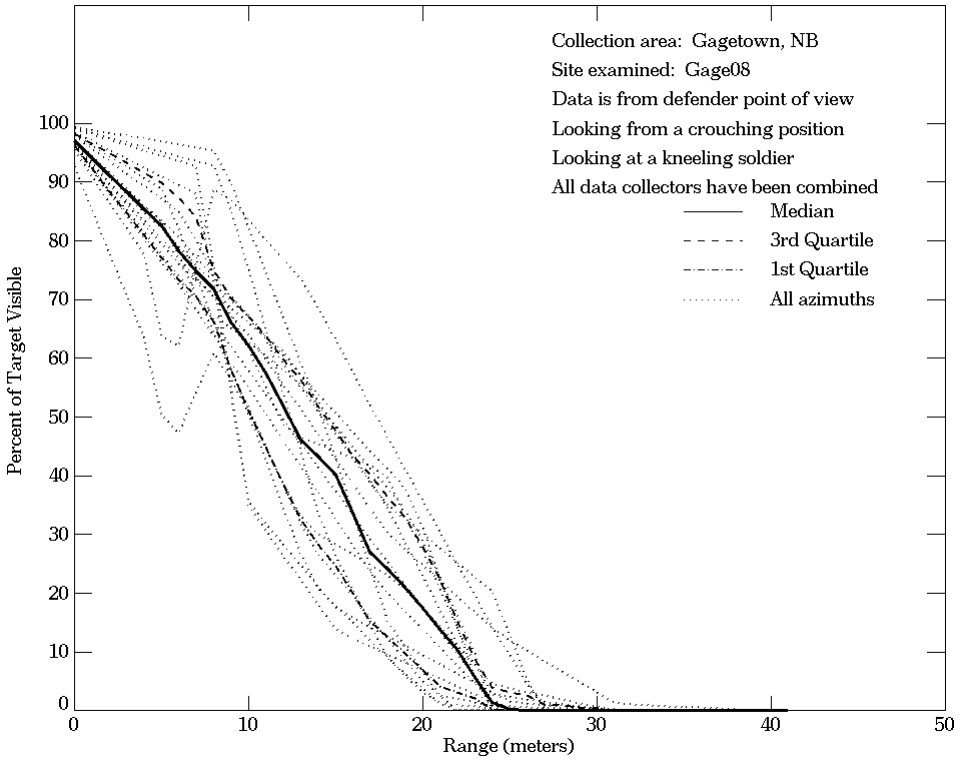

Figure E-107. Gagetown, NB, From Defender Point of View, Site Gage08 (Continued)

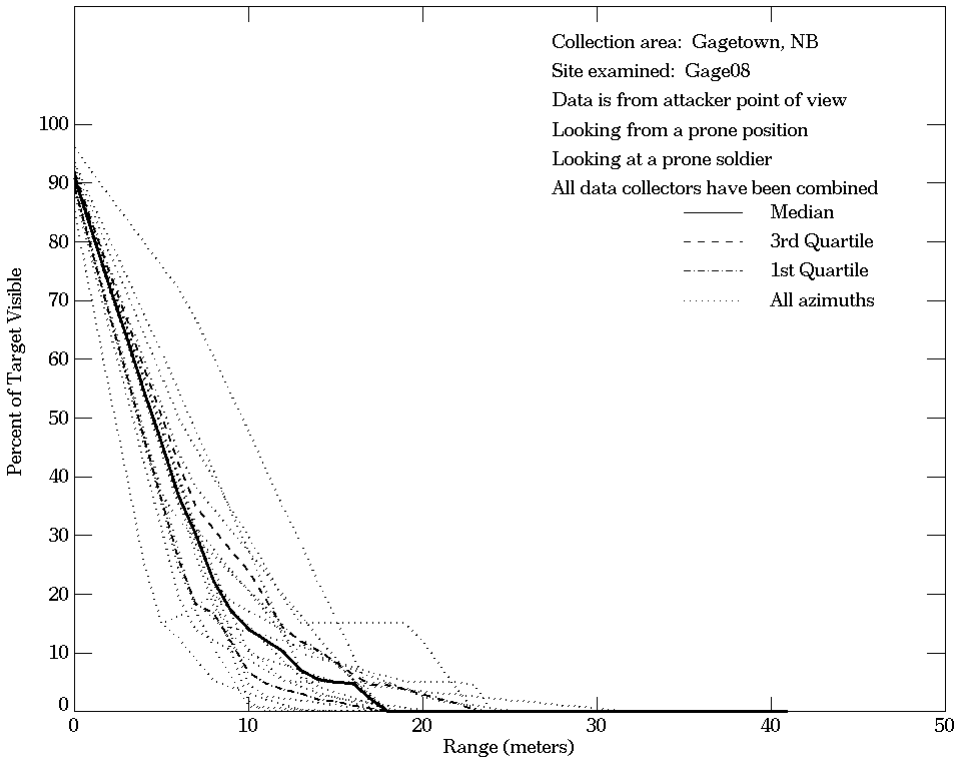

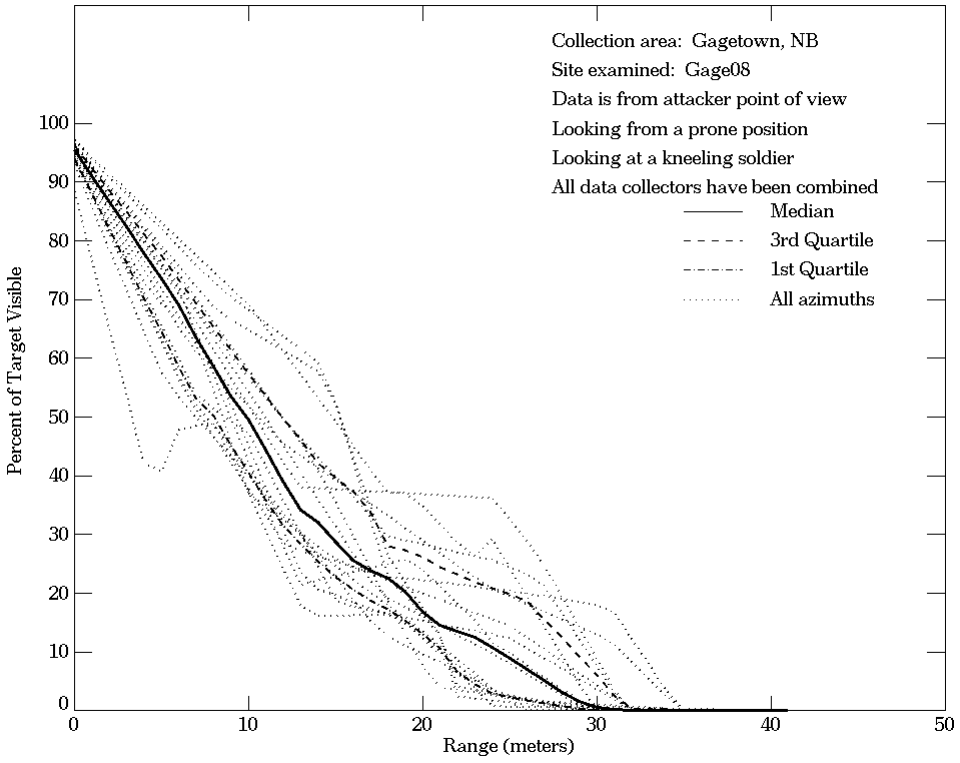

Figure E-108. Gagetown, NB, From Attacker Point of View, Site Gage08

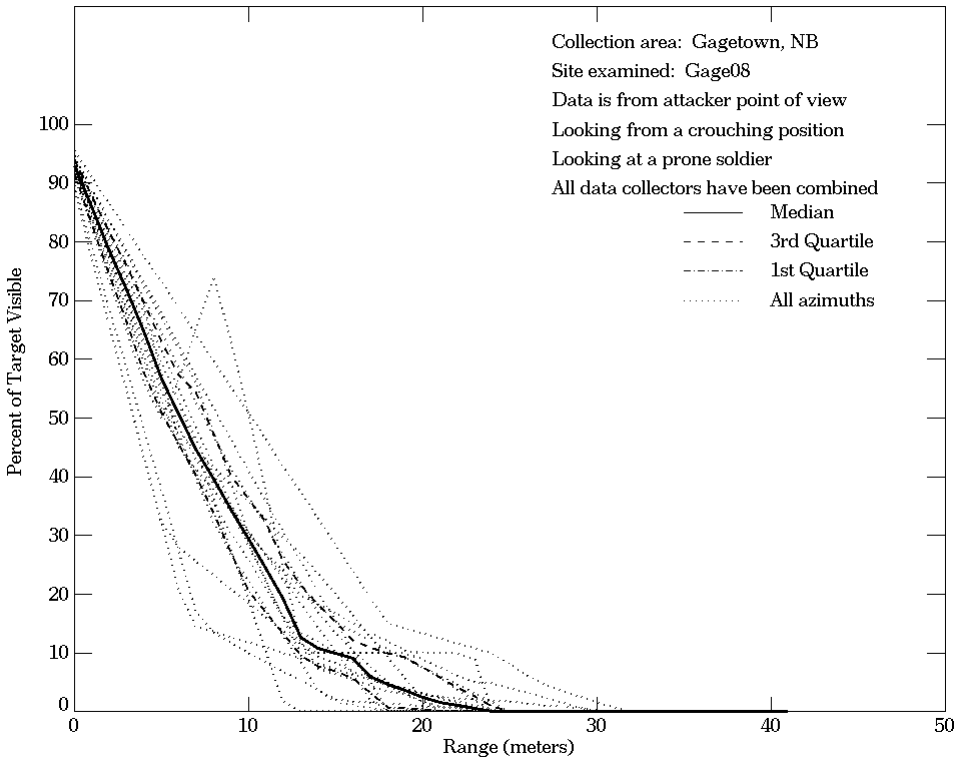

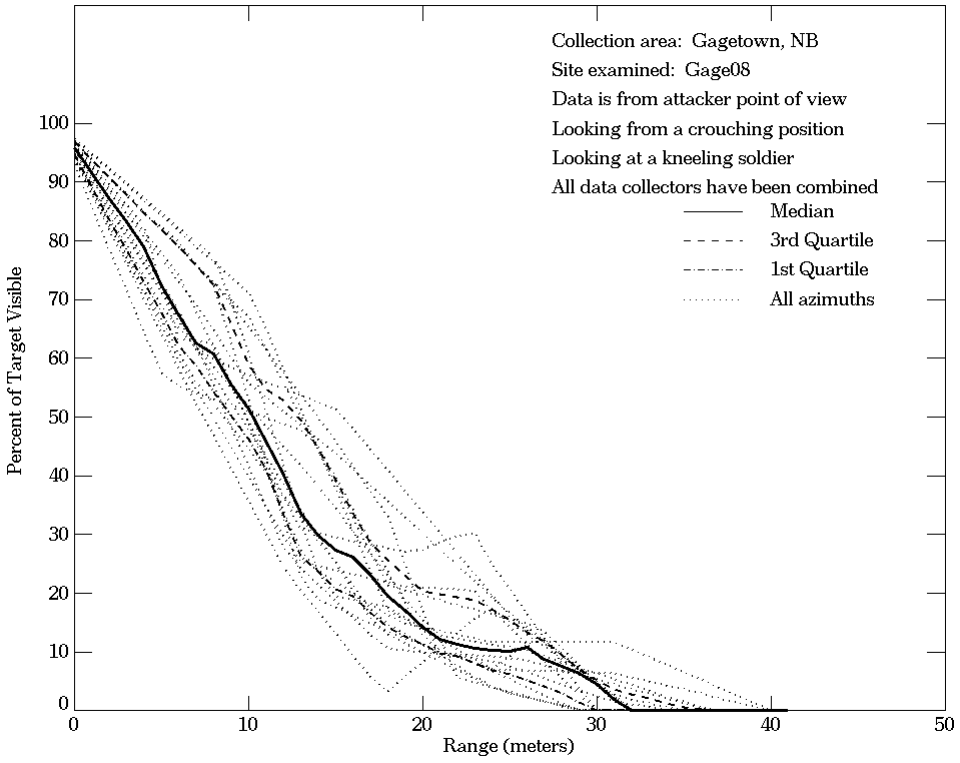

Figure E-108. Gagetown, NB, From Attacker Point of View, Site Gage08 (Continued)

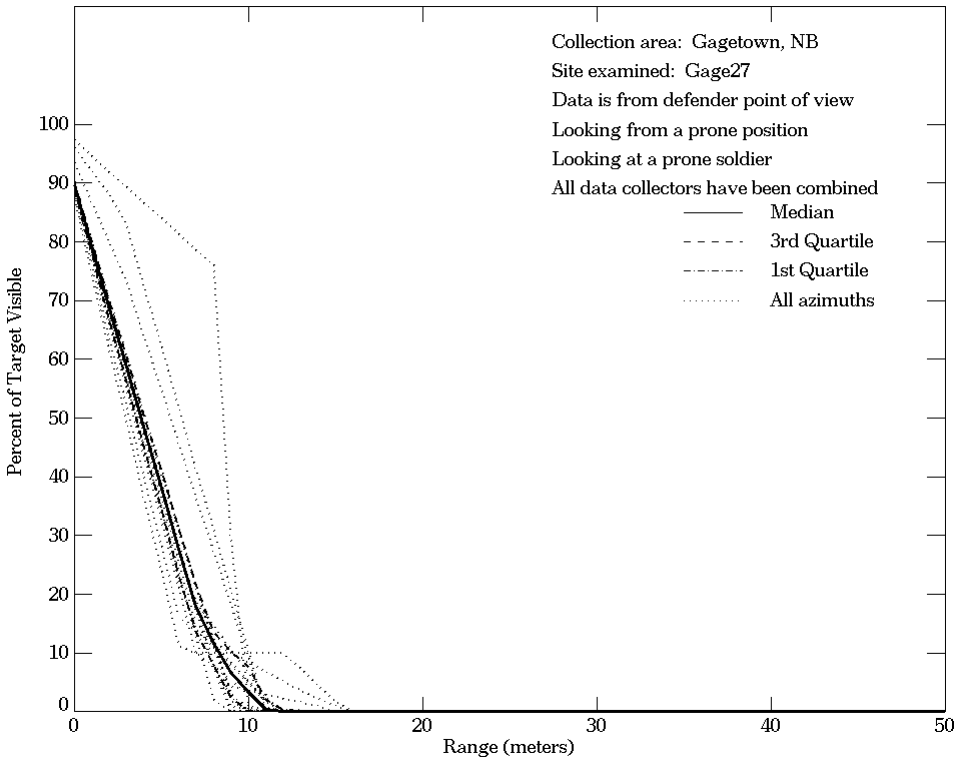

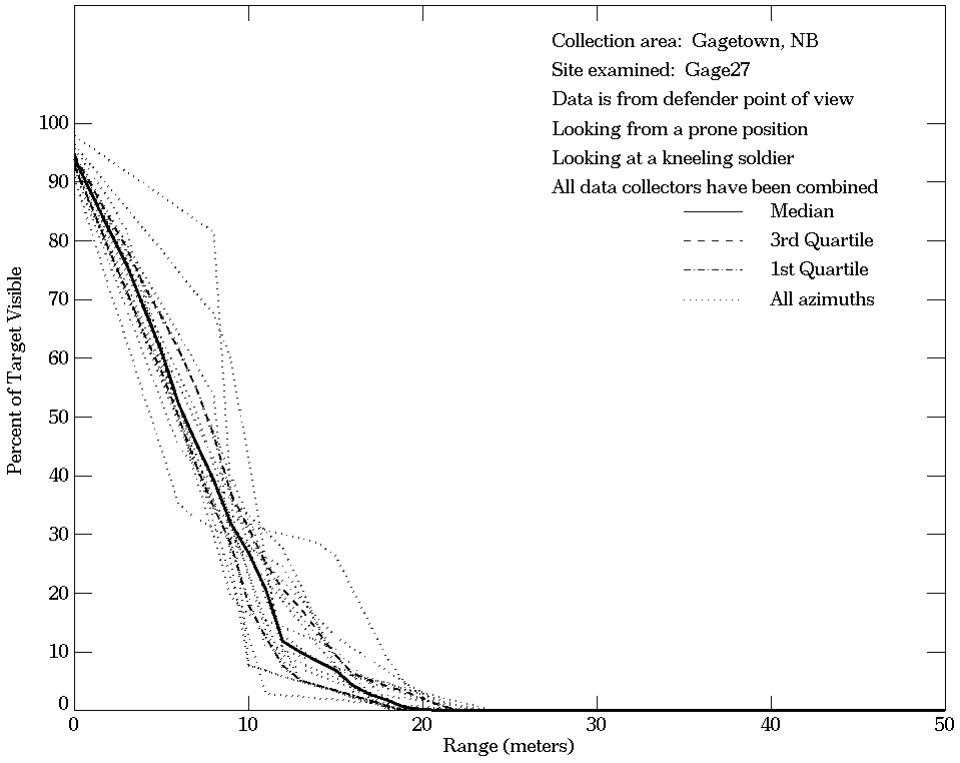

Figure E-109. Gagetown, NB, From Defender Point of View, Site Gage27

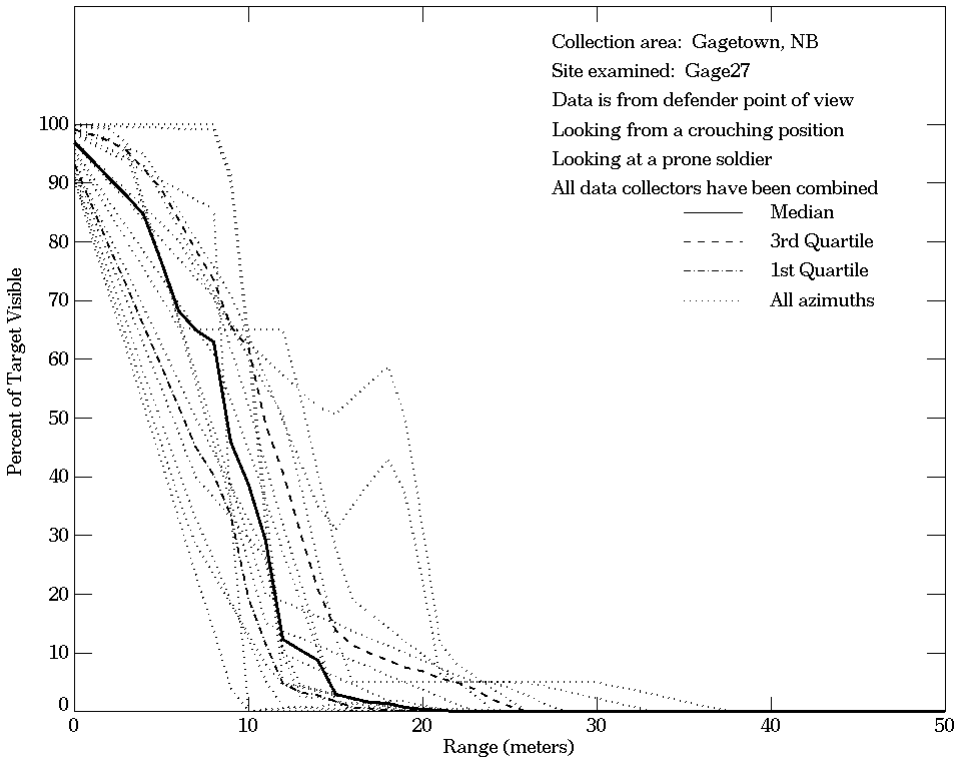

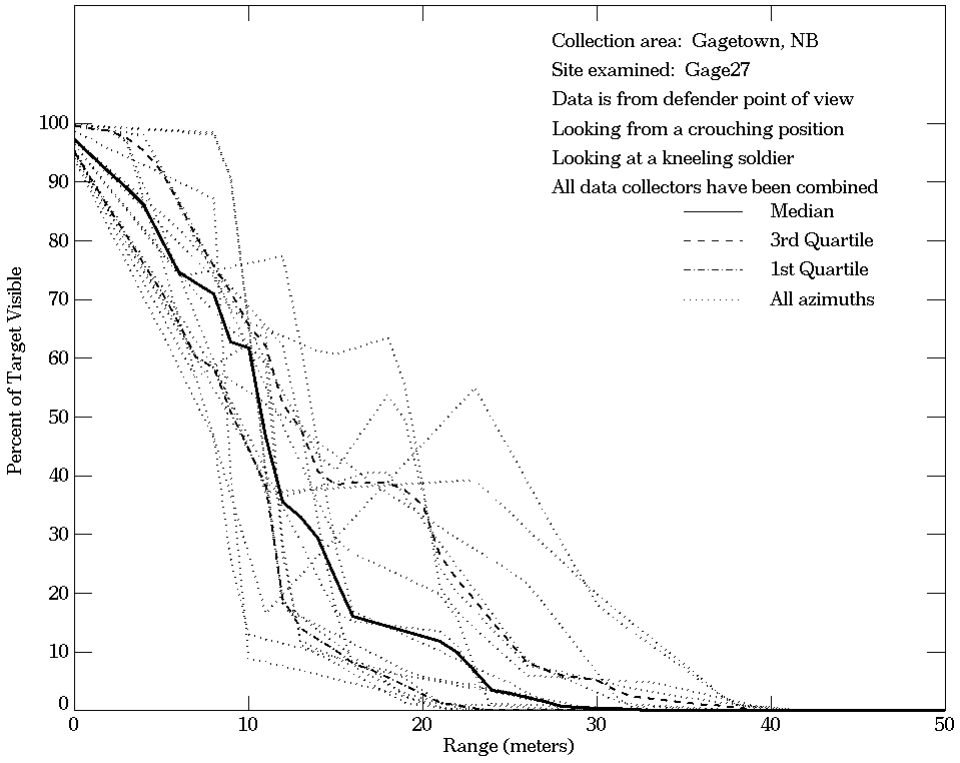

Figure E-109. Gagetown, NB, From Defender Point of View, Site Gage27 (Continued)

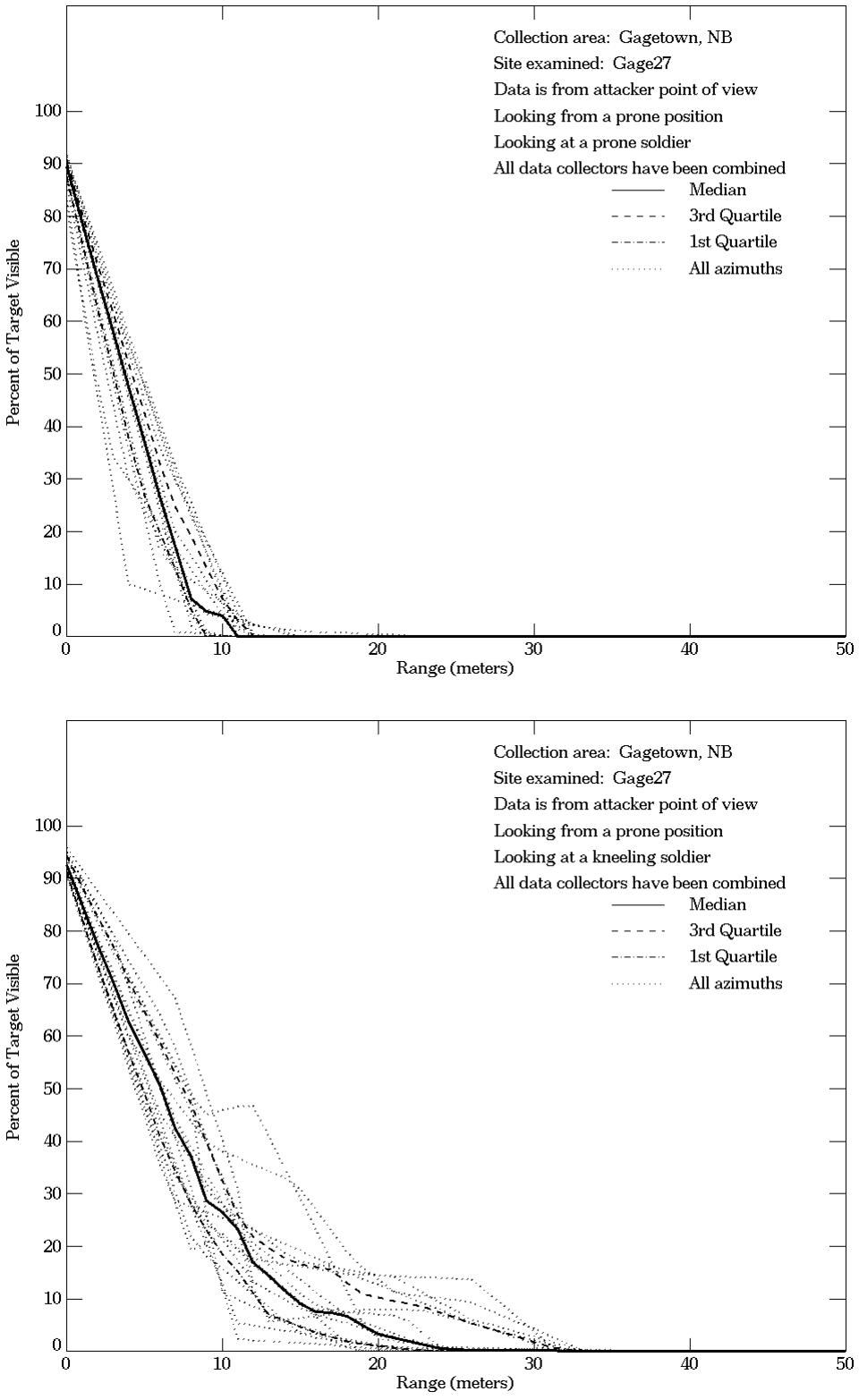

Figure E-110. Gagetown, NB, From Attacker Point of View, Site Gage27

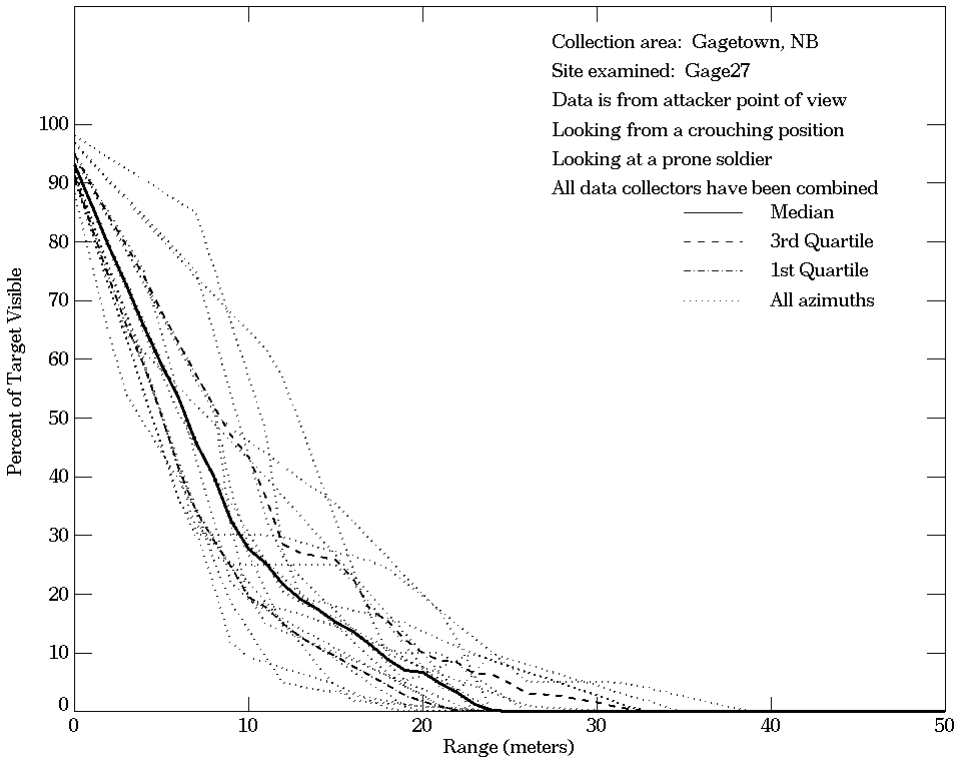

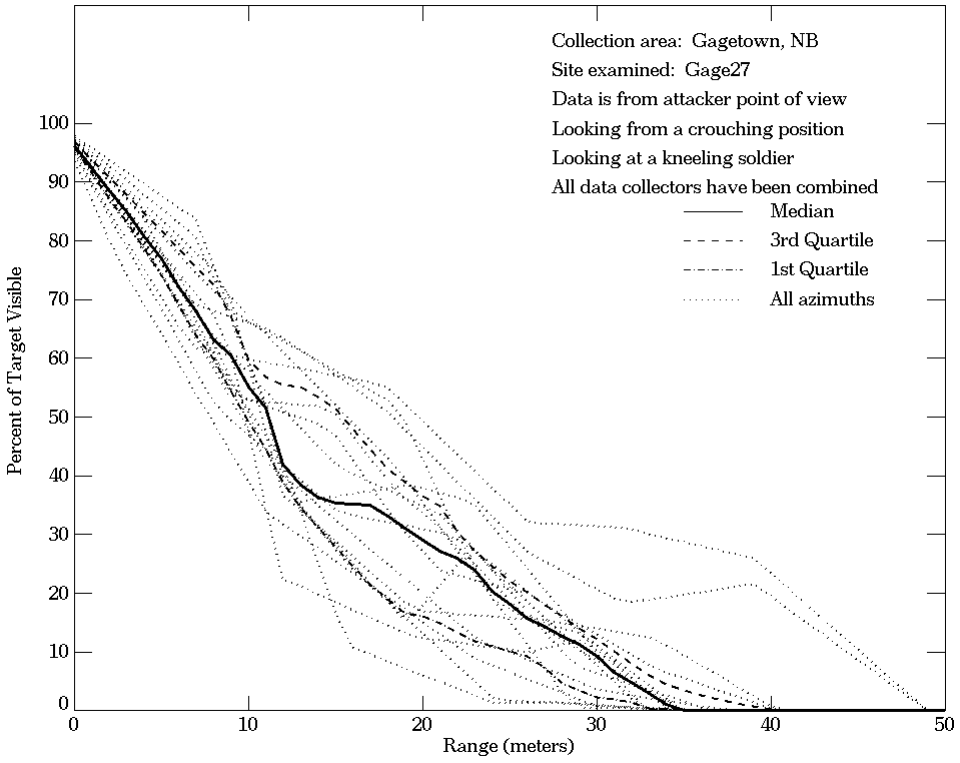

Figure E-110. Gagetown, NB, From Attacker Point of View, Site Gage27 (Continued)

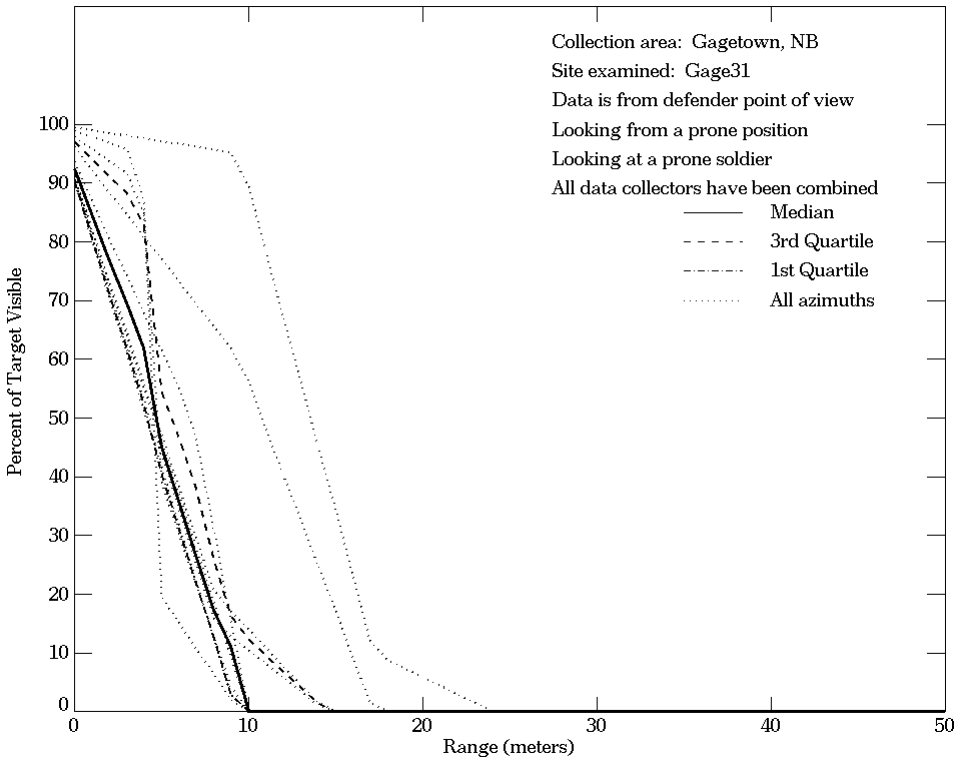

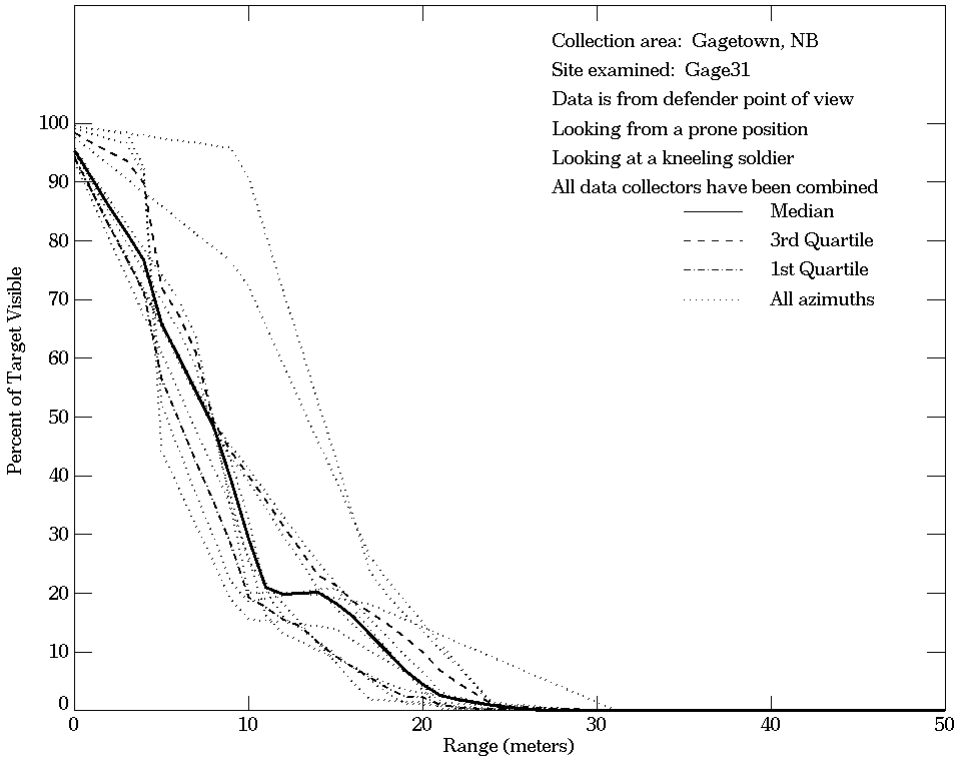

Figure E-111. Gagetown, NB, From Defender Point of View, Site Gage31

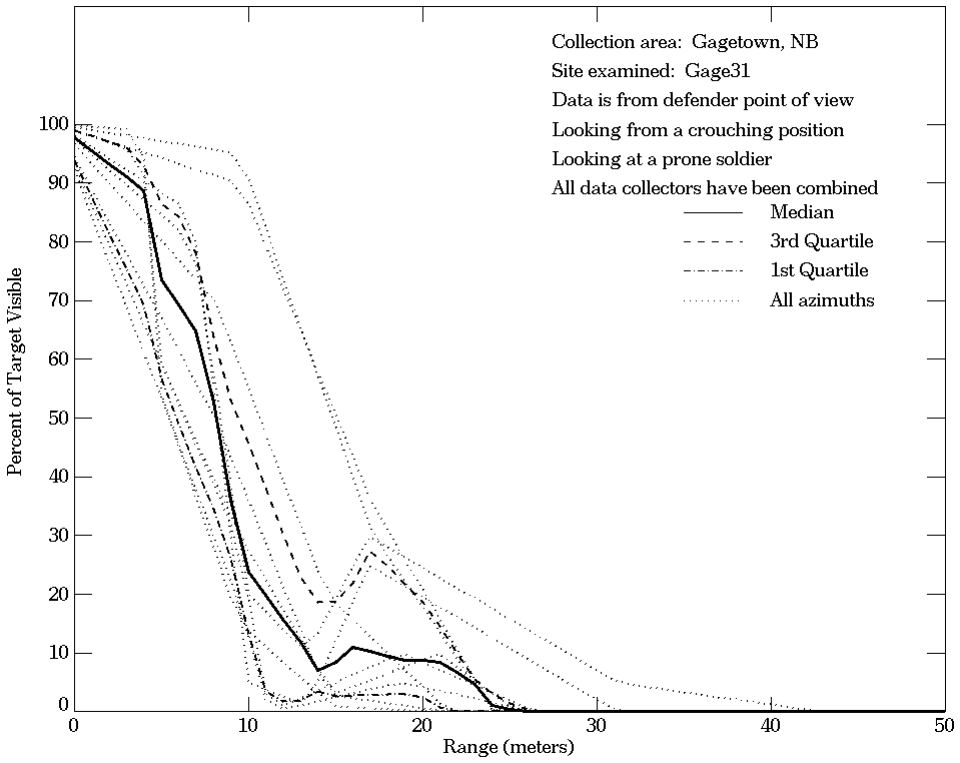

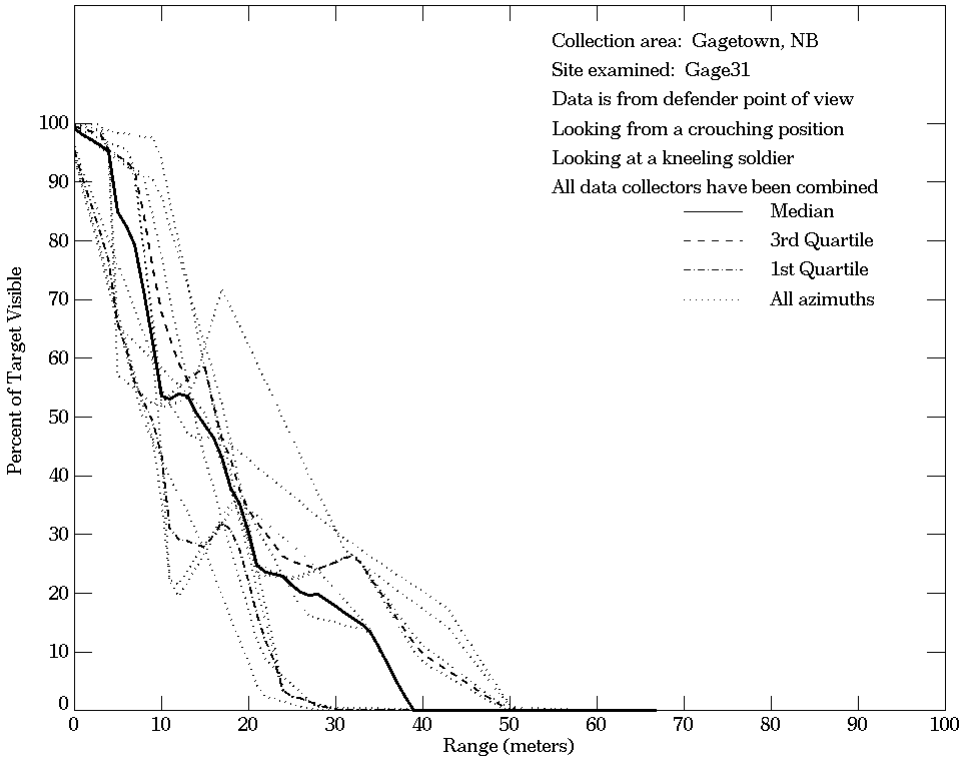

Figure E-111. Gagetown, NB, From Defender Point of View, Site Gage31 (Continued)

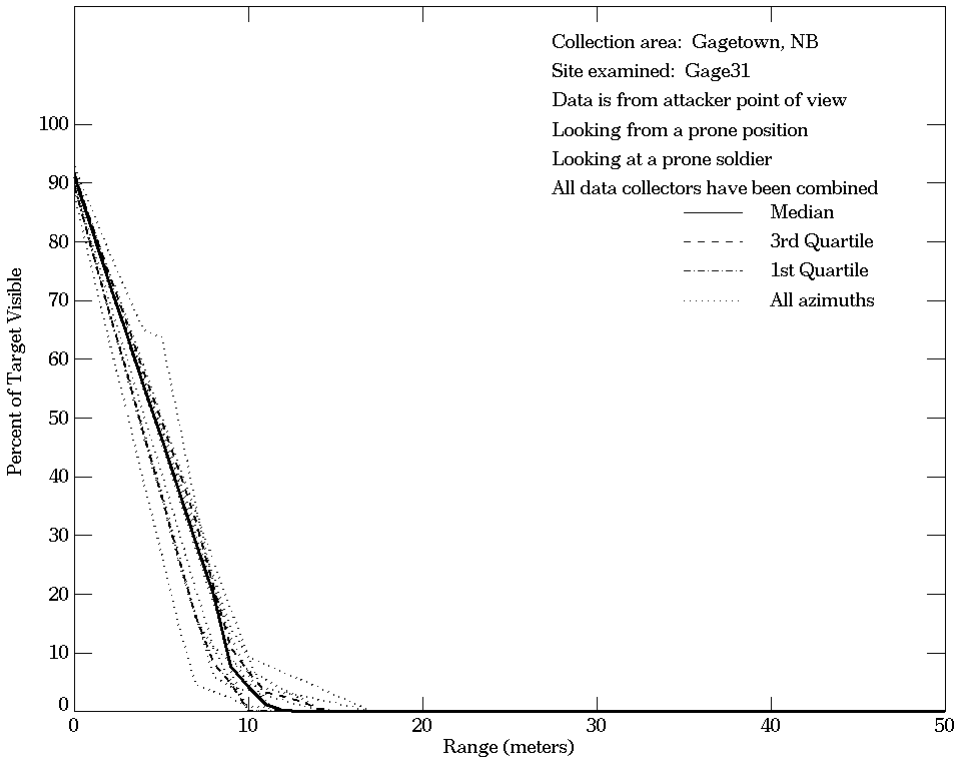

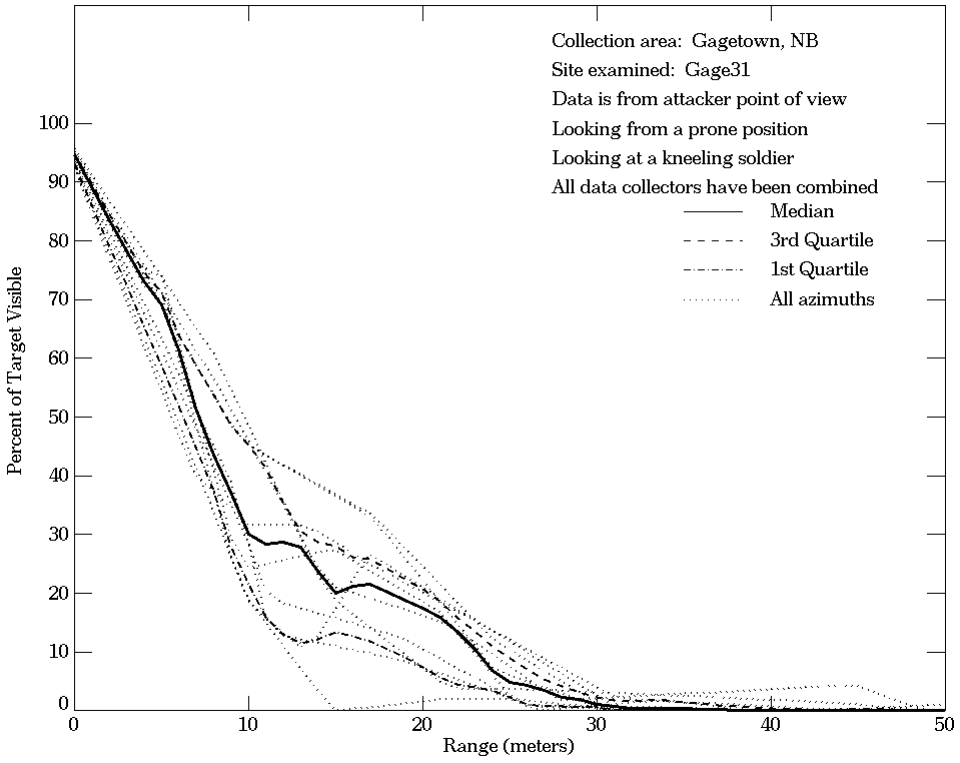

Figure E-112. Gagetown, NB, From Attacker Point of View, Site Gage31

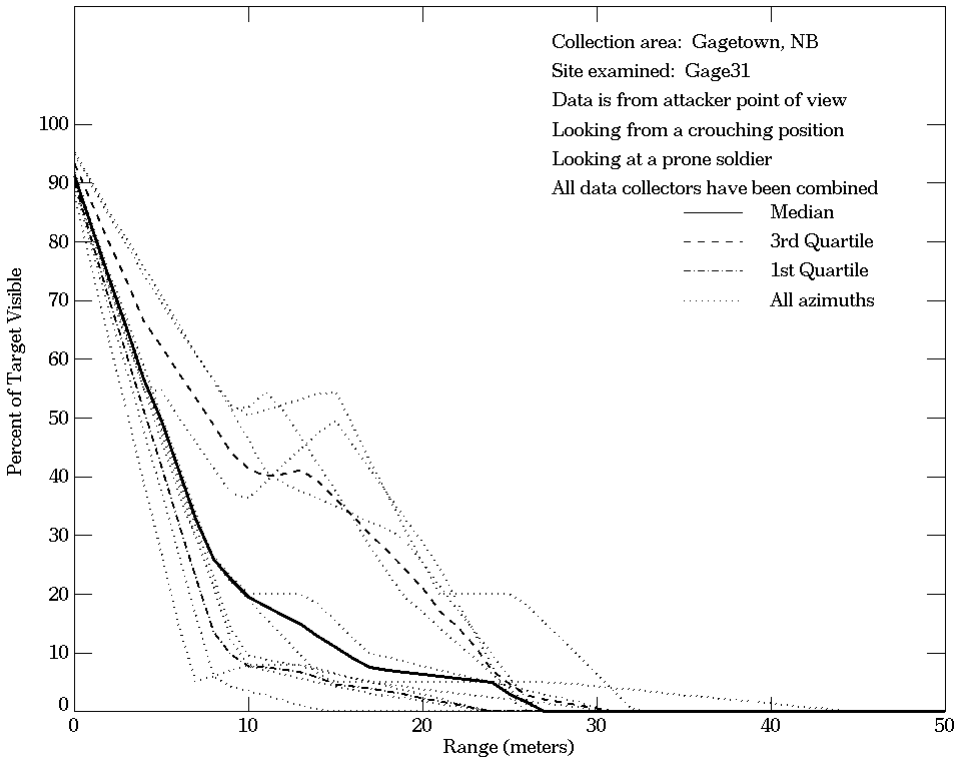

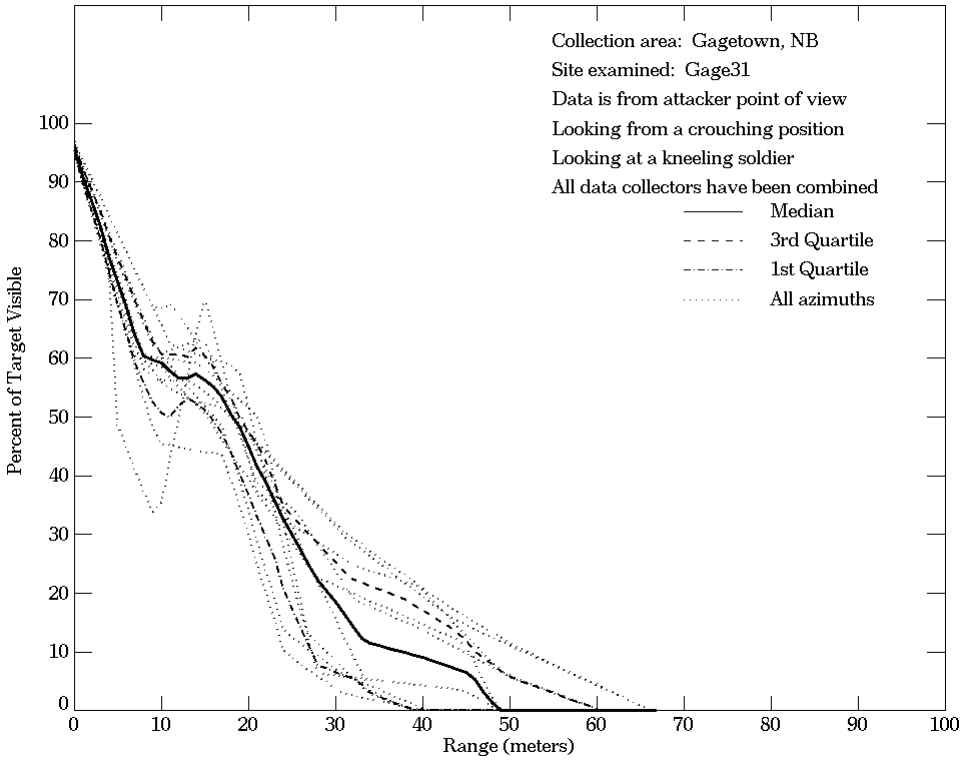

Figure E-112. Gagetown, NB, From Attacker Point of View, Site Gage31 (Continued)

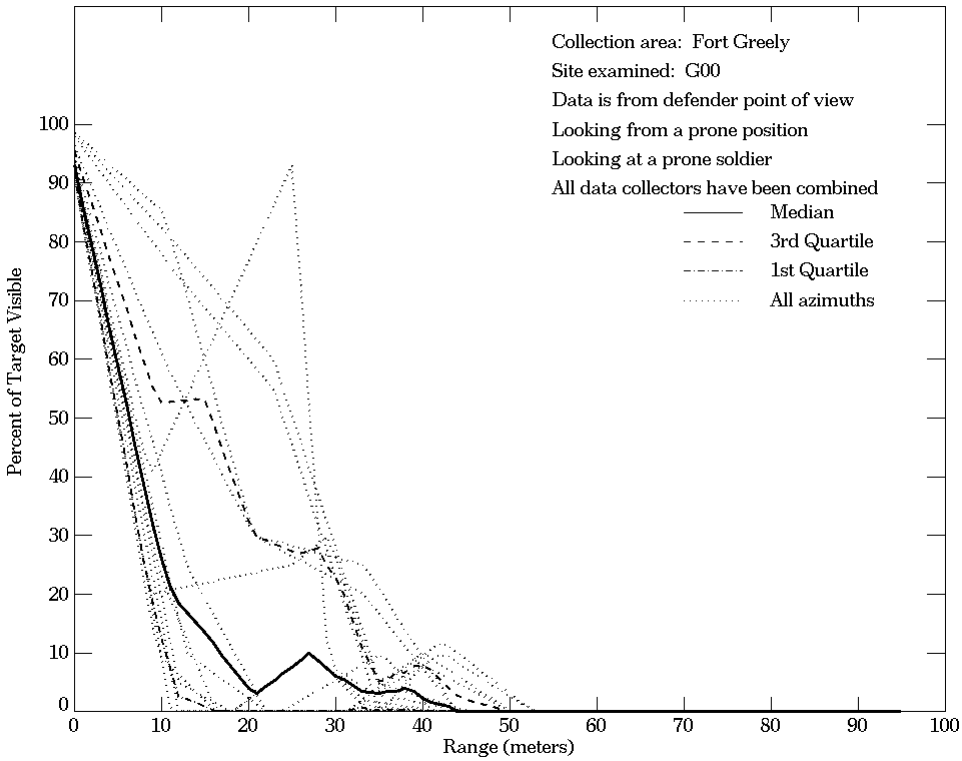

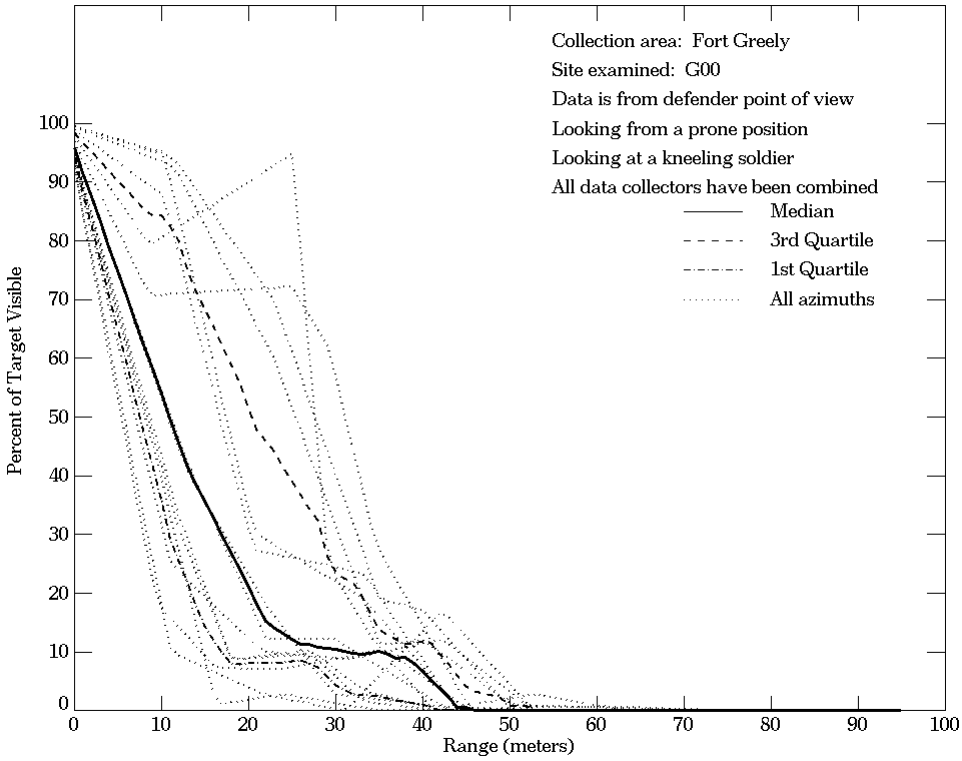

Figure E-113. Fort Greely, From Defender Point of View, Site G00

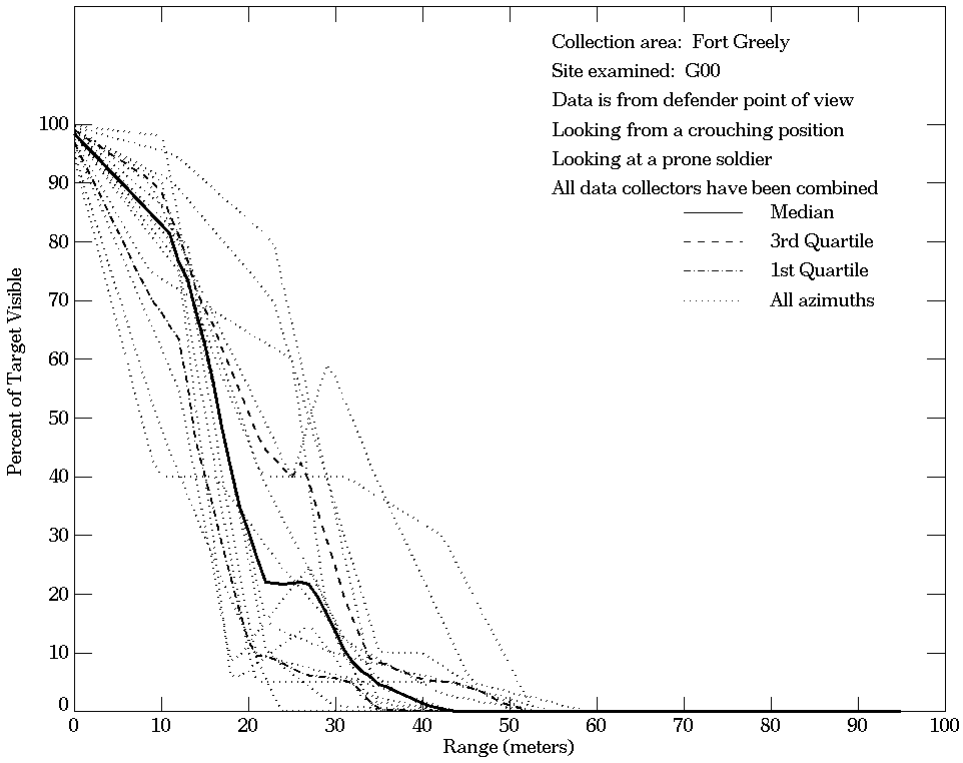

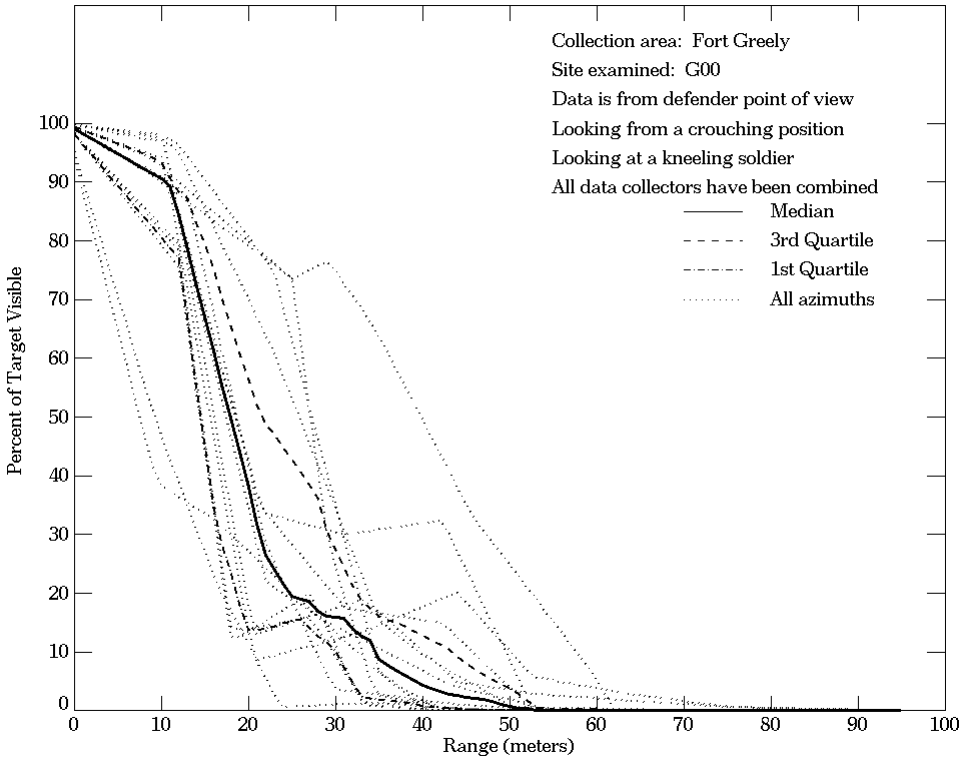

Figure E-113. Fort Greely, From Defender Point of View, Site G00 (Continued)

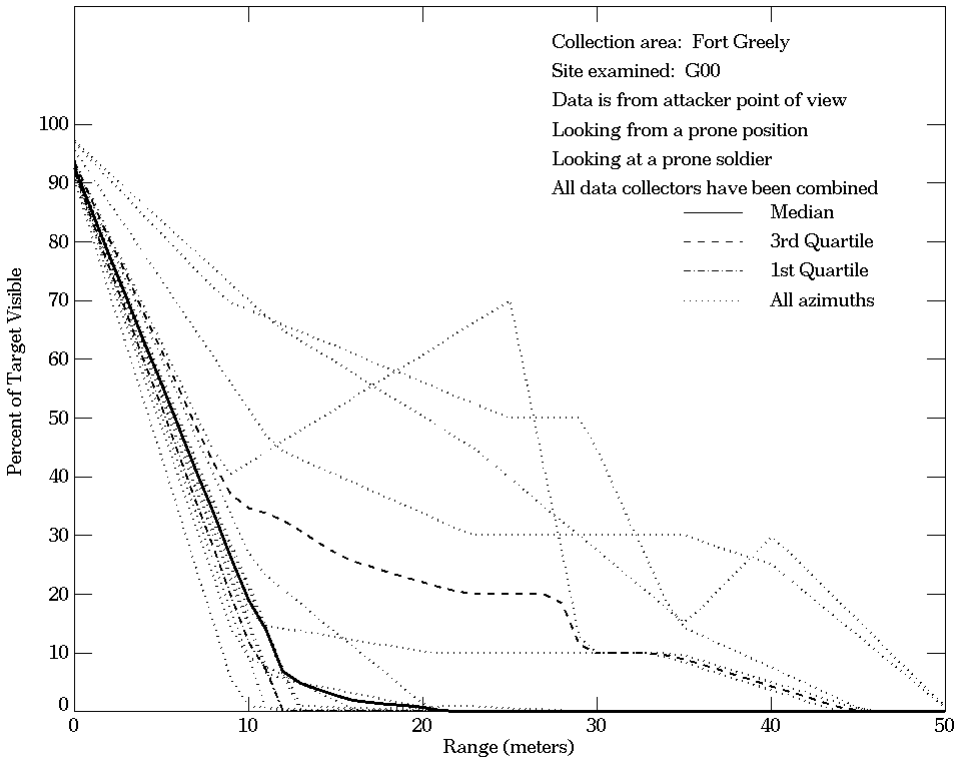

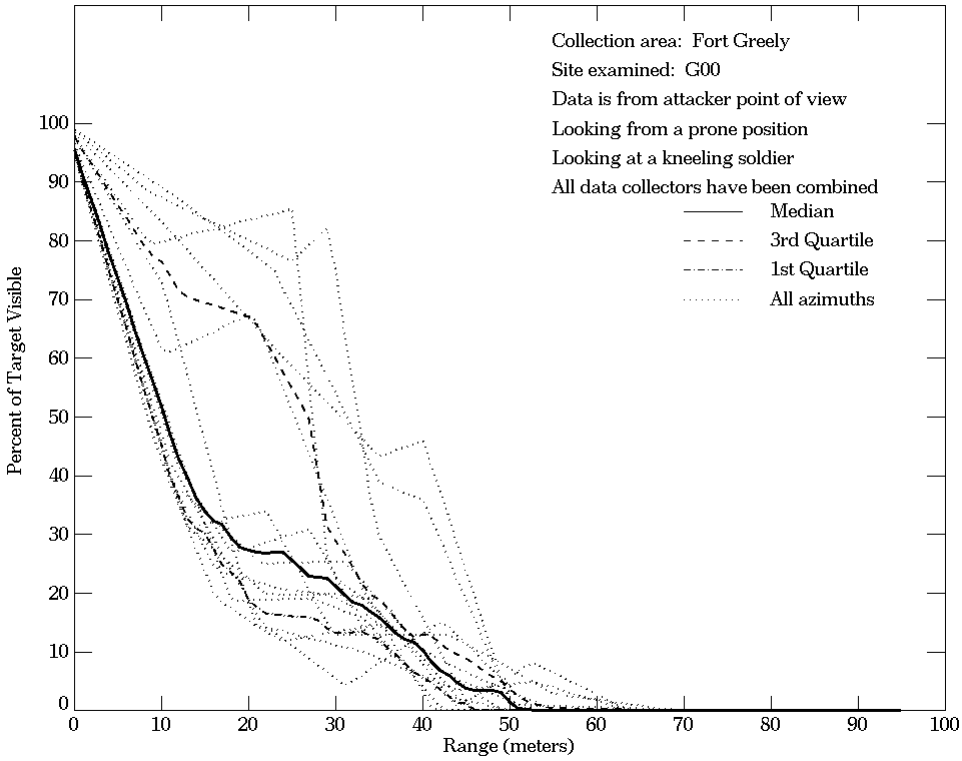

Figure E-114. Fort Greely, From Attacker Point of View, Site G00

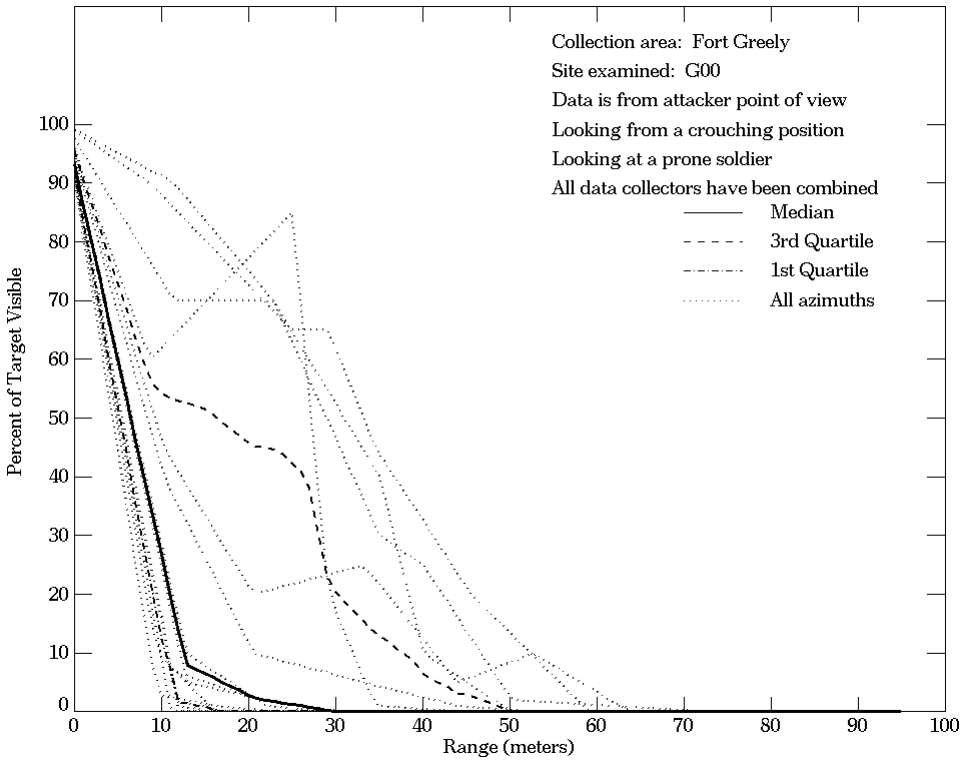

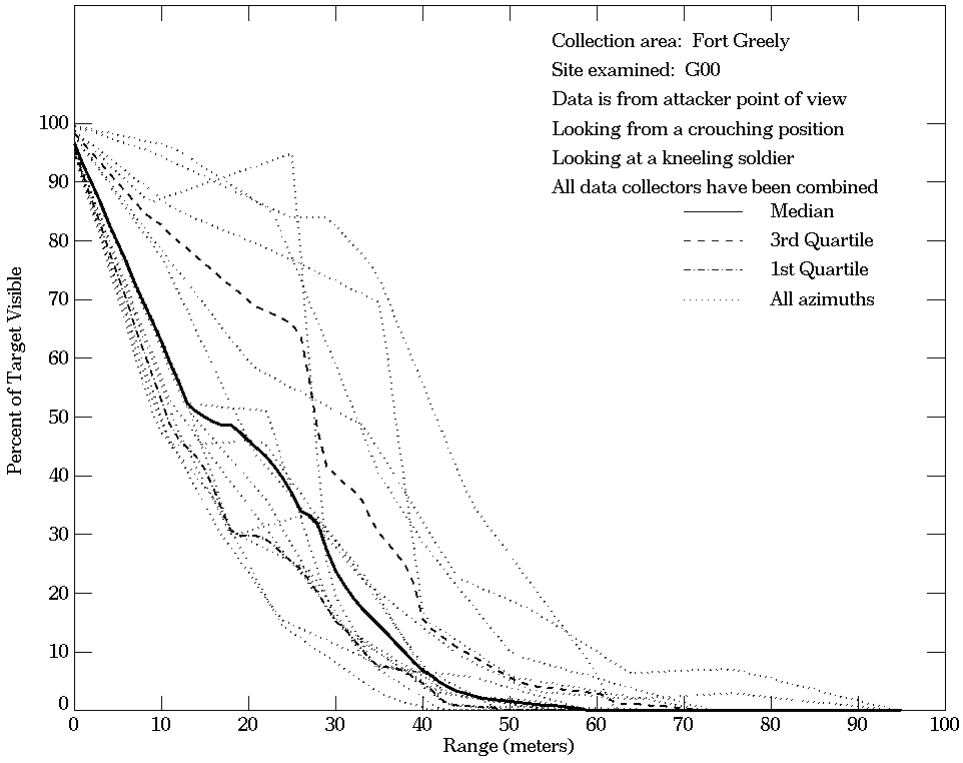

Figure E-114. Fort Greely, From Attacker Point of View, Site G00 (Continued)

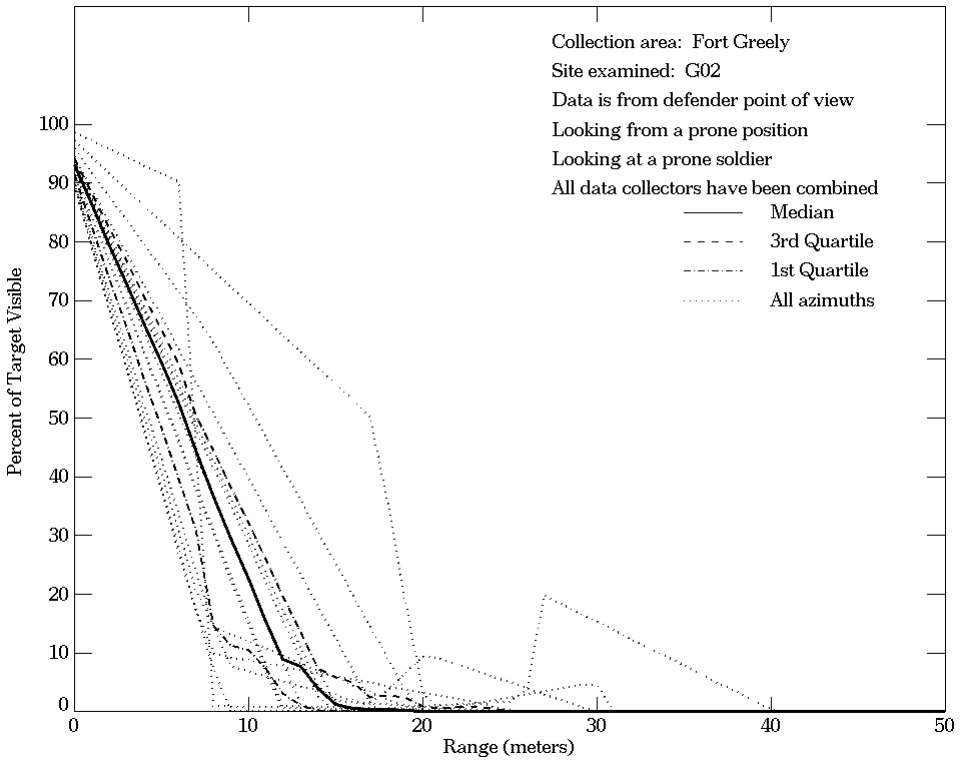

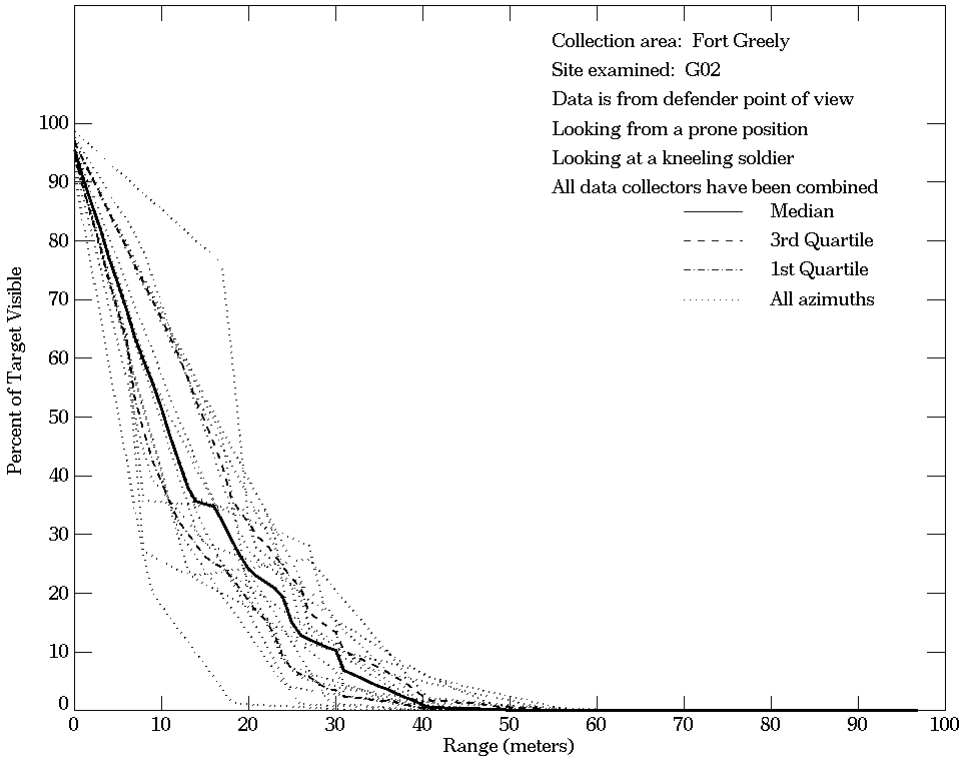

Figure E-115. Fort Greely, From Defender Point of View, Site G02

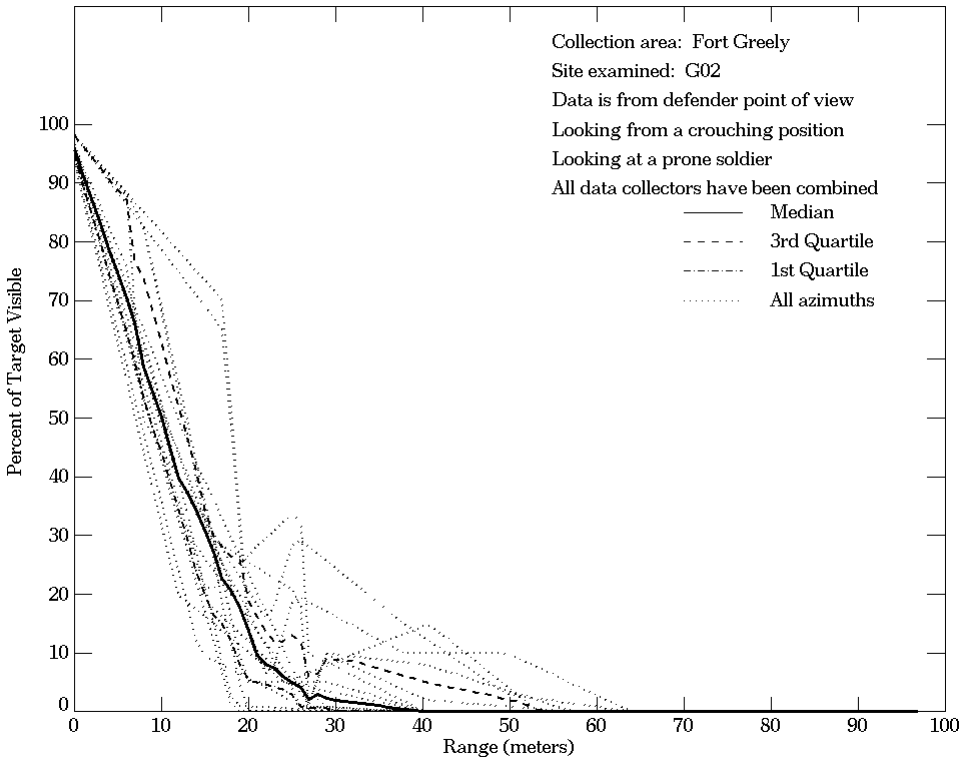

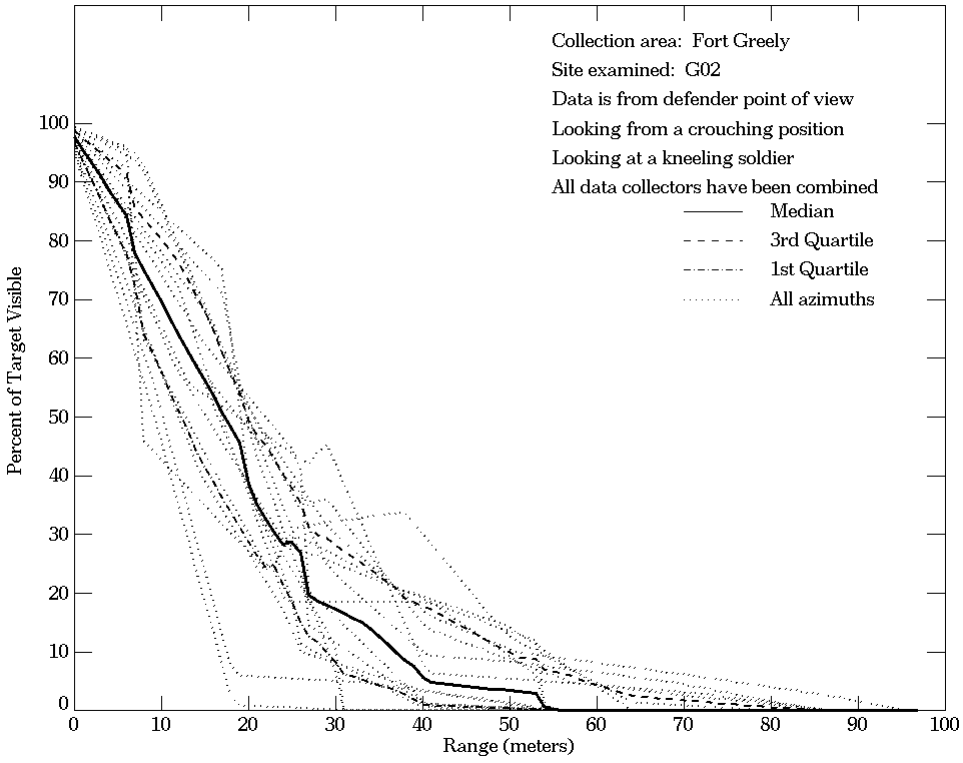

Figure E-115. Fort Greely, From Defender Point of View, Site G02 (Continued)

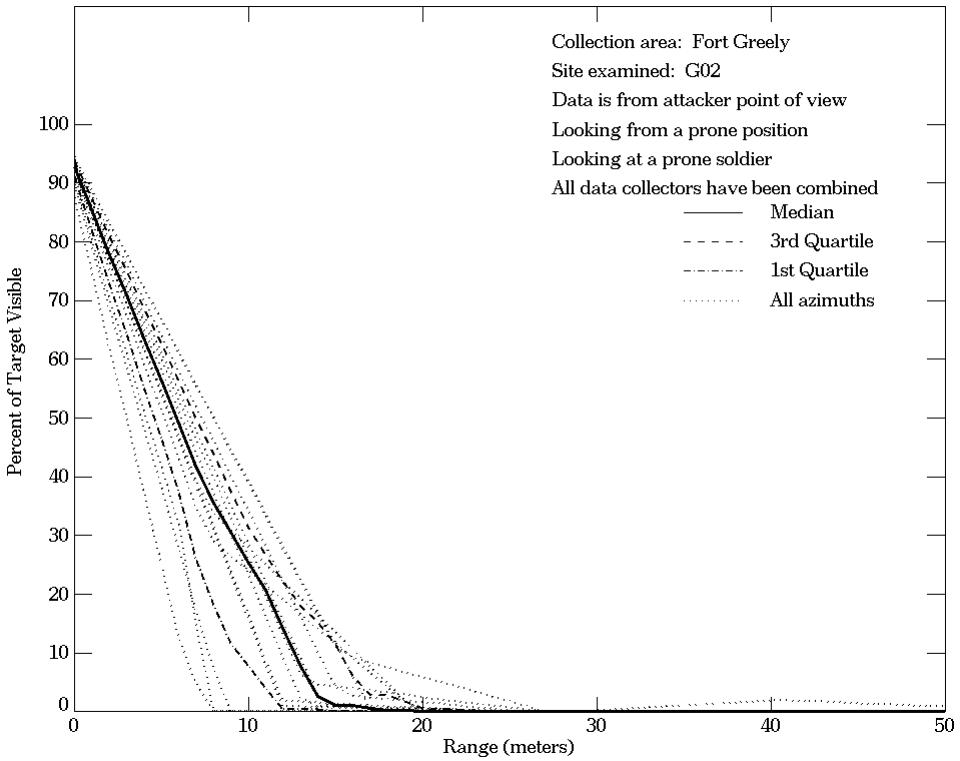

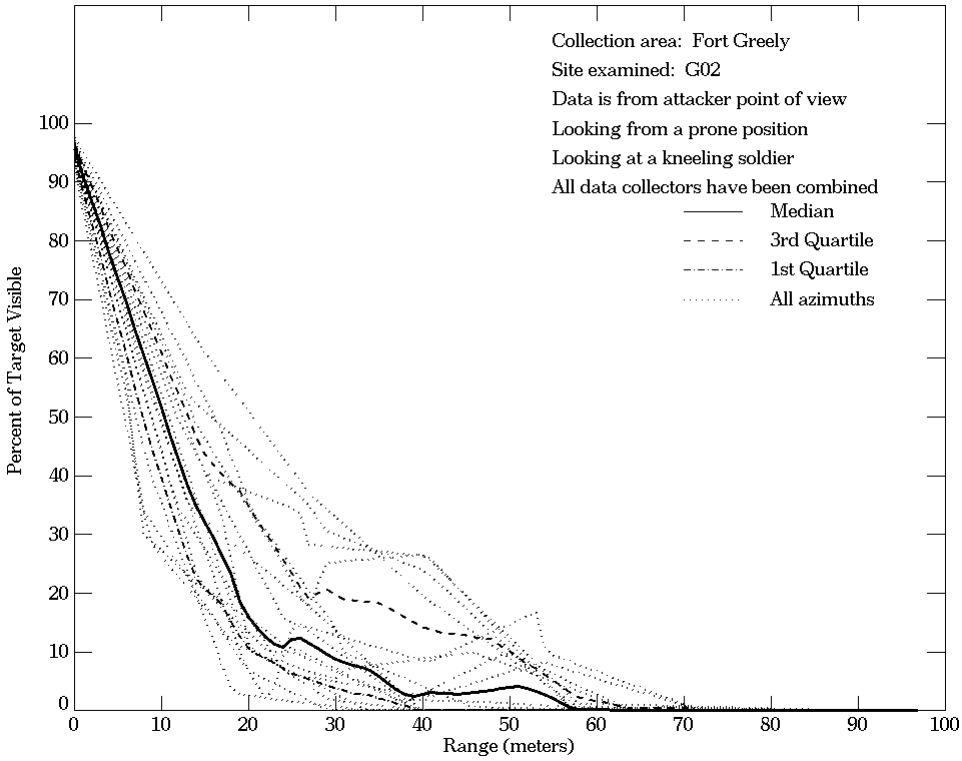

Figure E-116. Fort Greely, From Attacker Point of View, Site G02

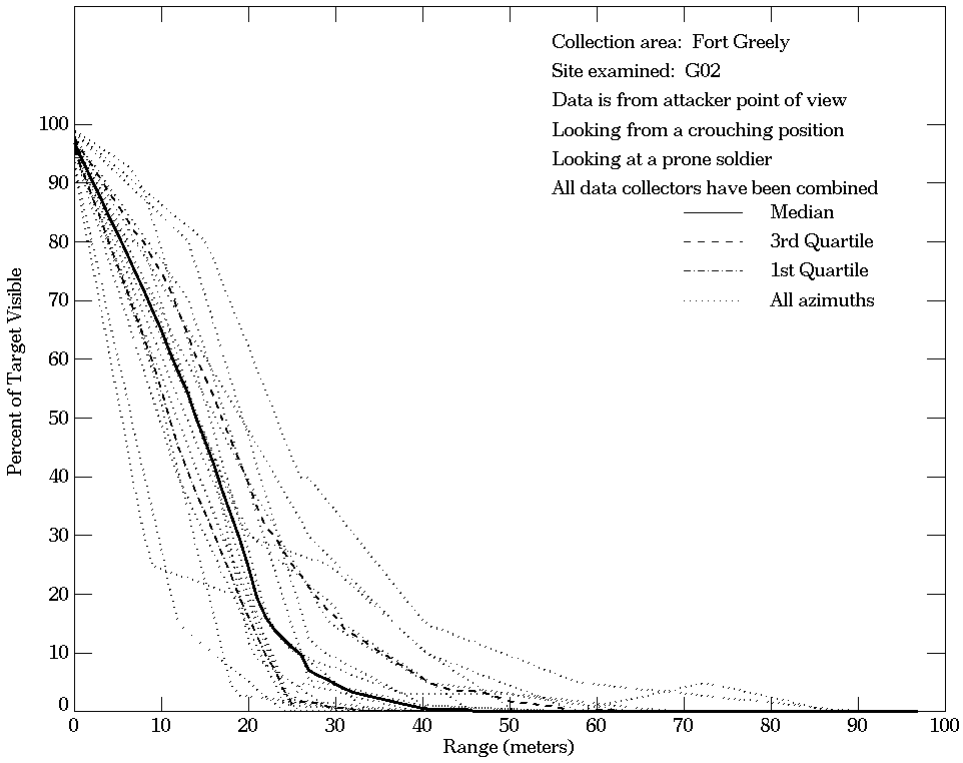

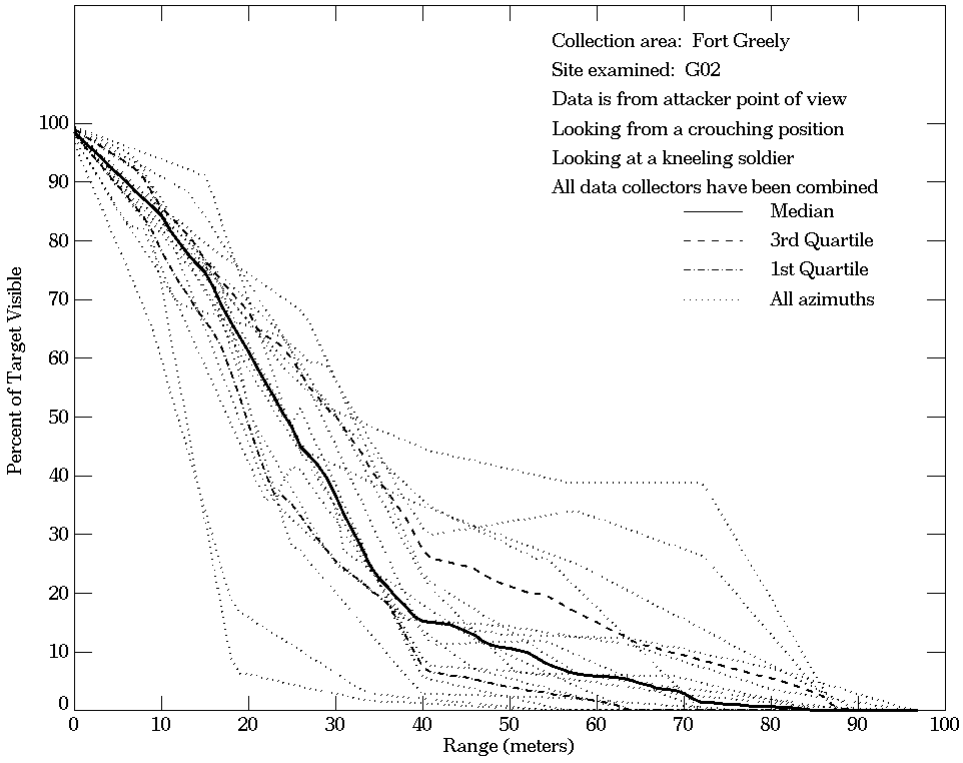

Figure E-116. Fort Greely, From Attacker Point of View, Site G02 (Continued)

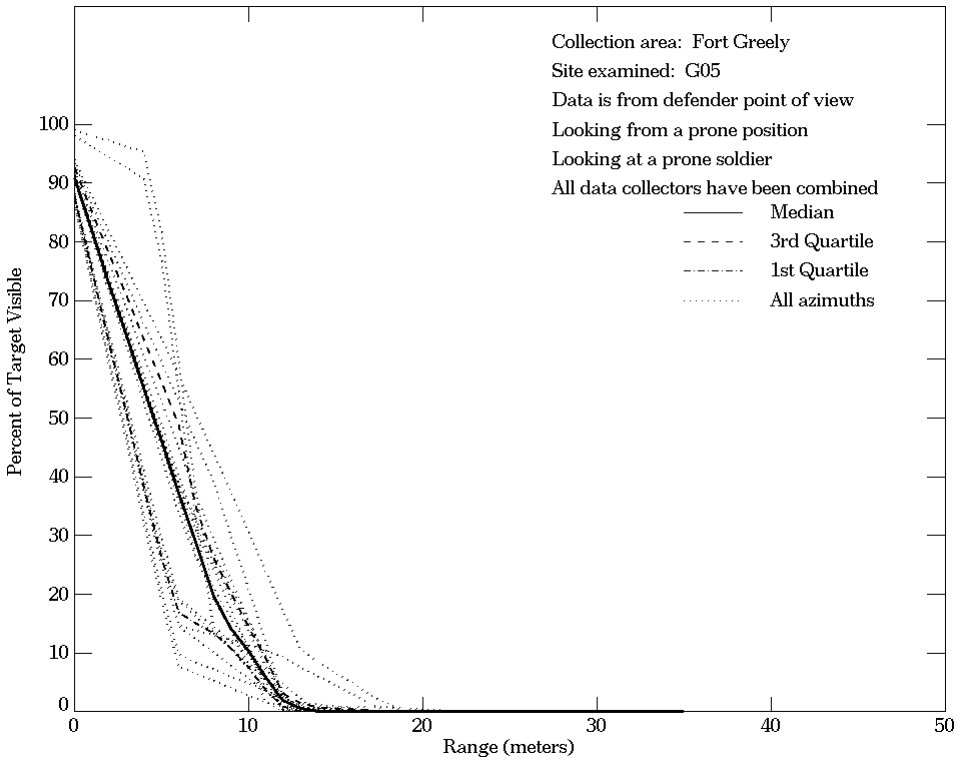

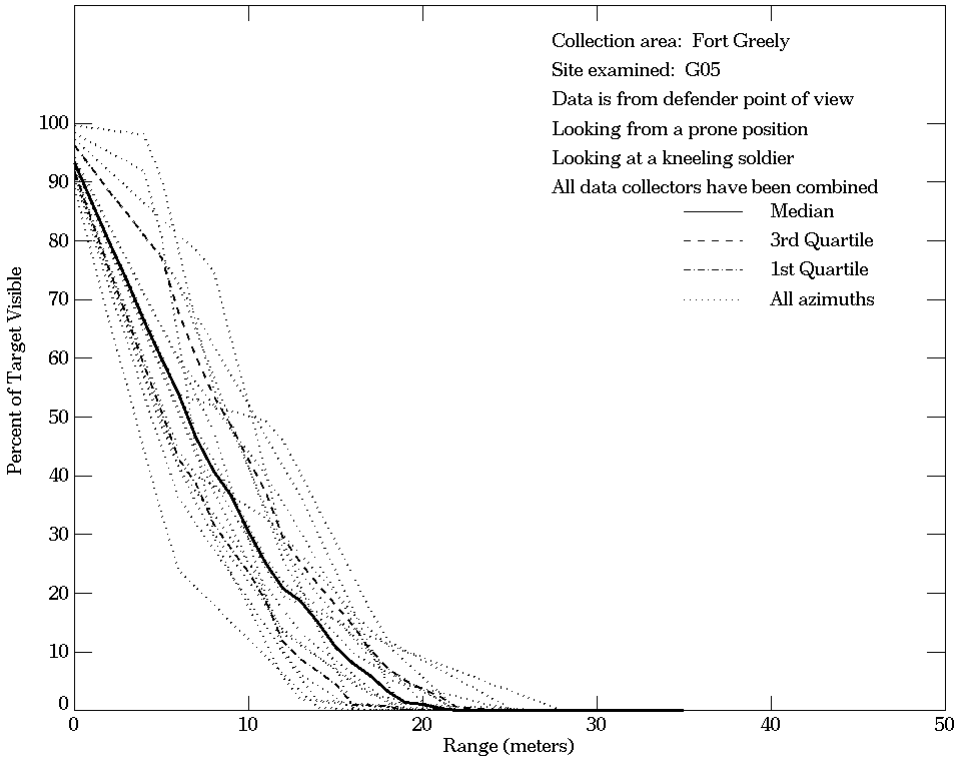

Figure E-117. Fort Greely, From Defender Point of View, Site G05

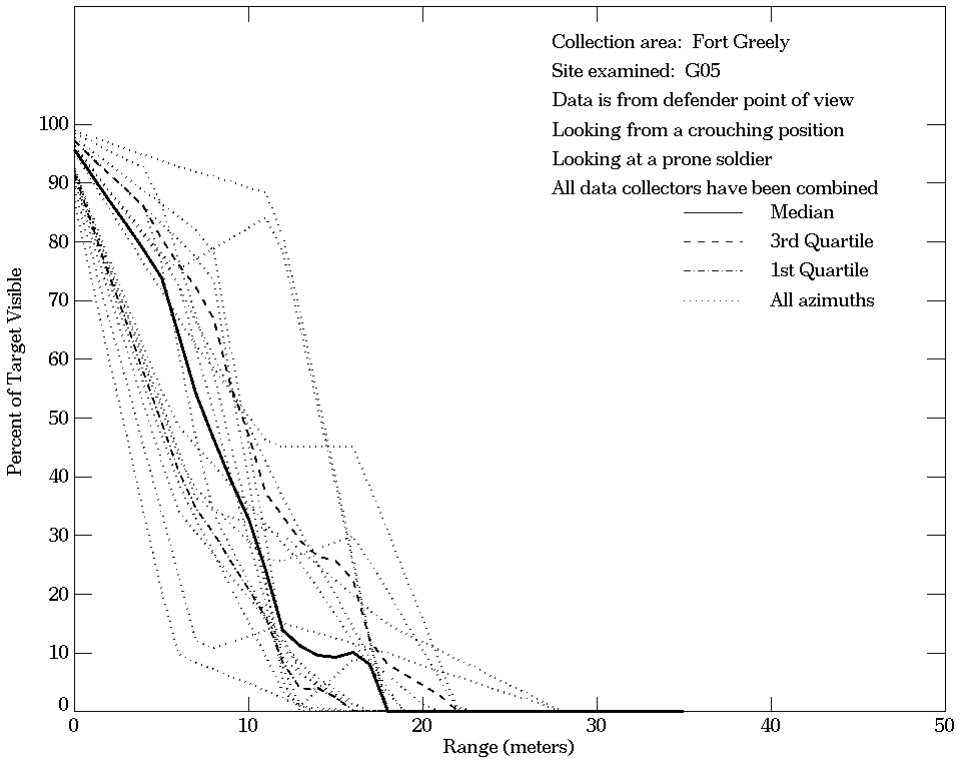

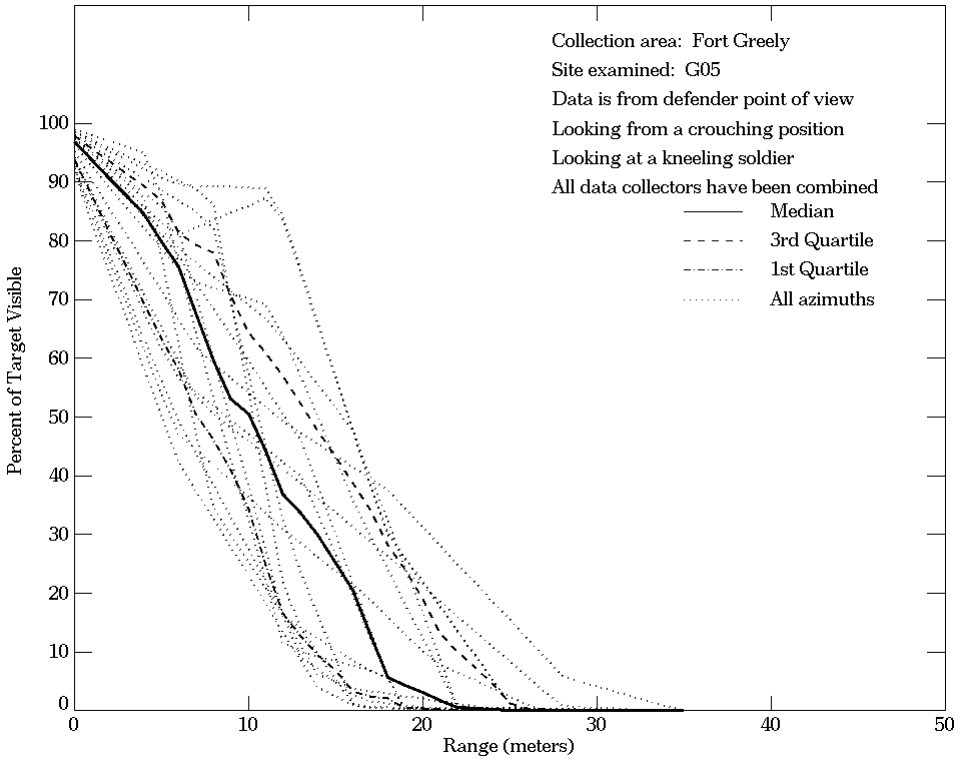

Figure E-117. Fort Greely, From Defender Point of View, Site G05 (Continued)

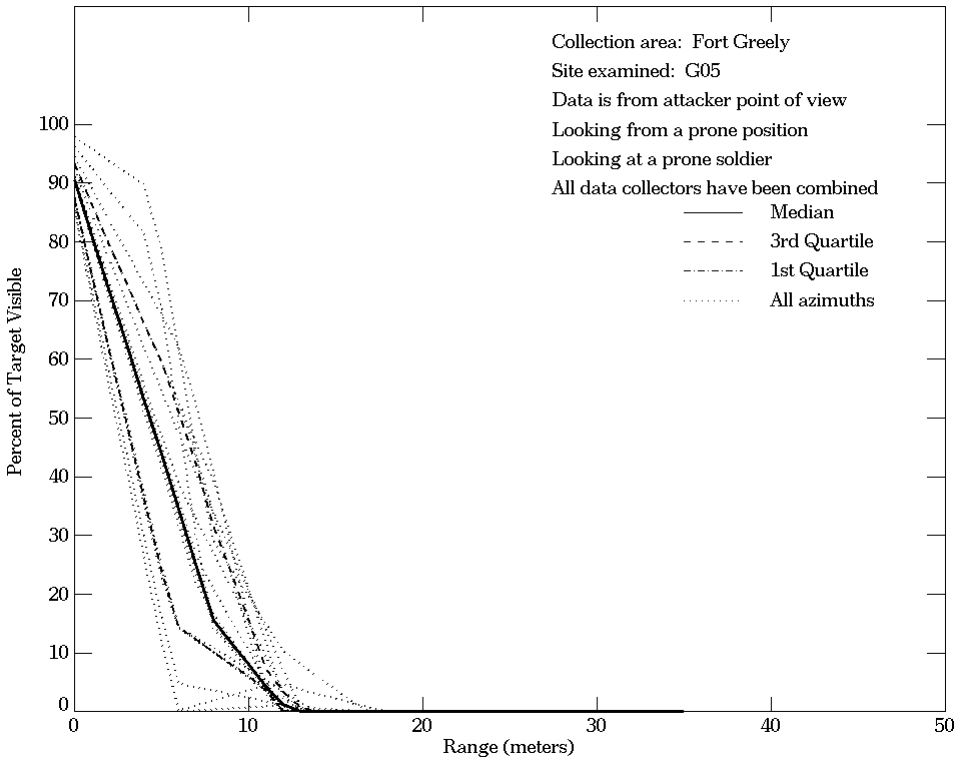

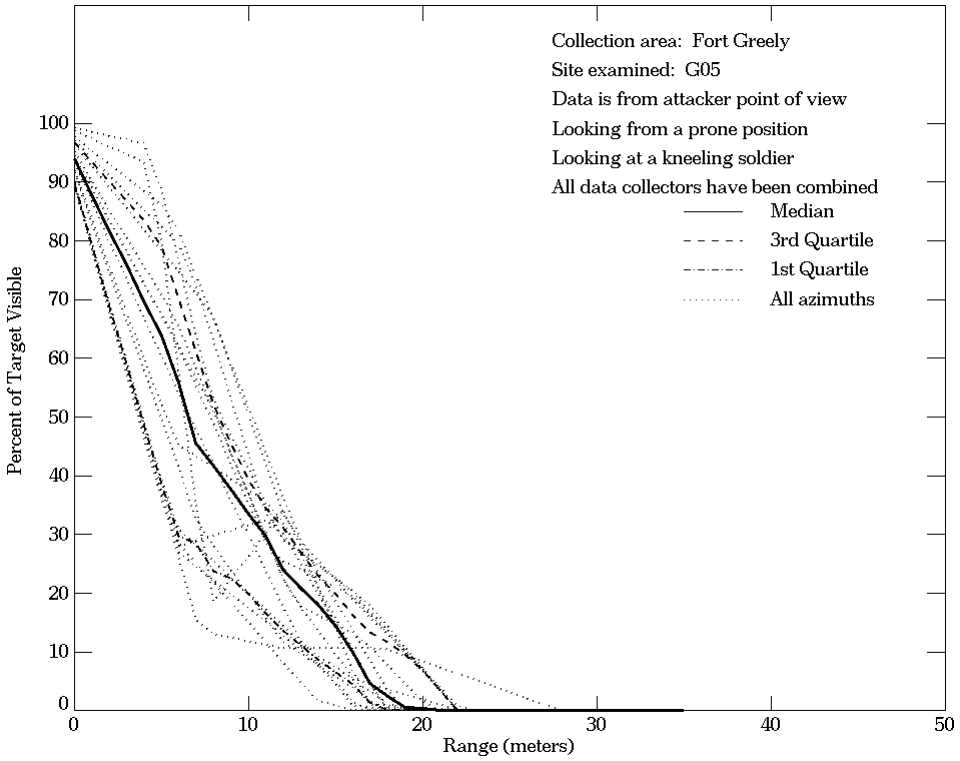

Figure E-118. Fort Greely, From Attacker Point of View, Site G05

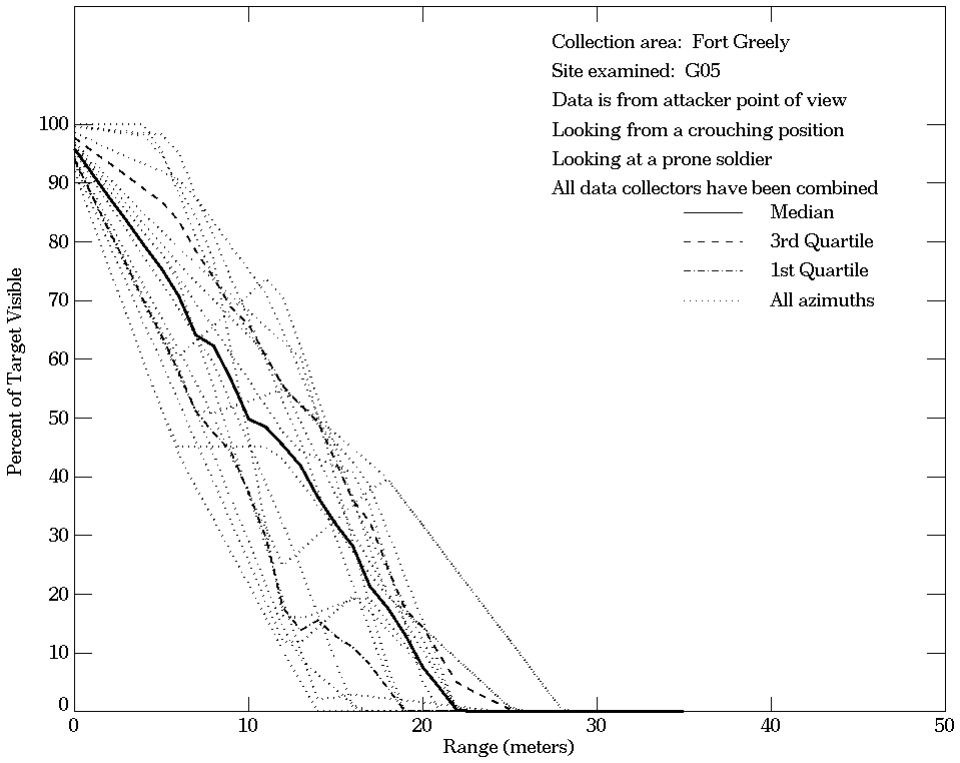

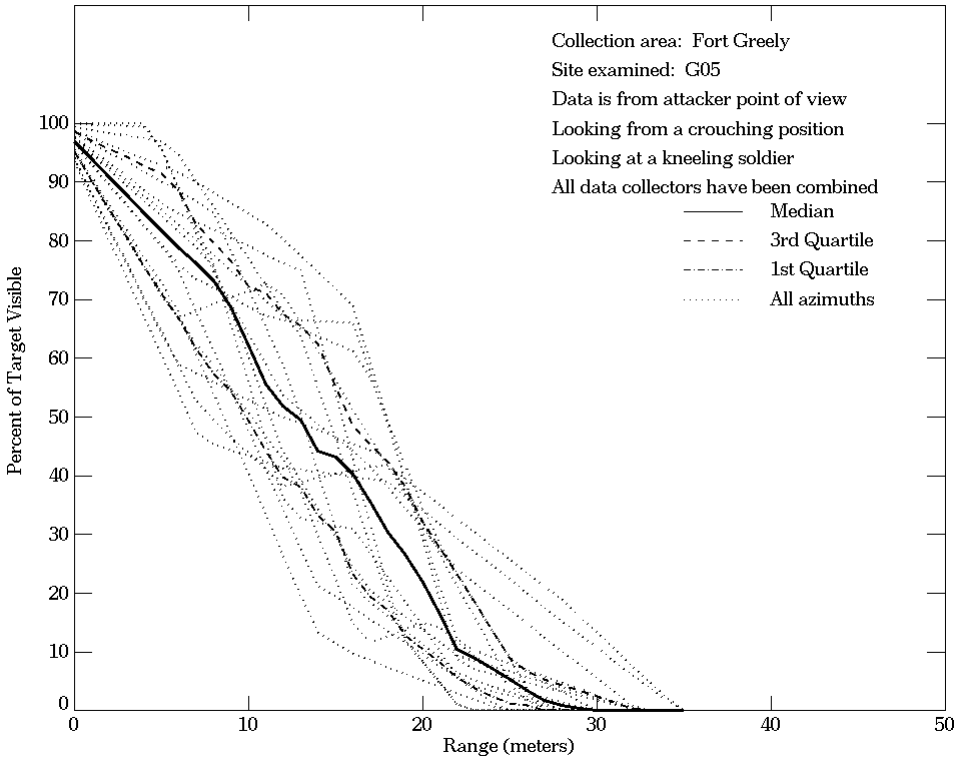

Figure E-118. Fort Greely, From Attacker Point of View, Site G05 (Continued)

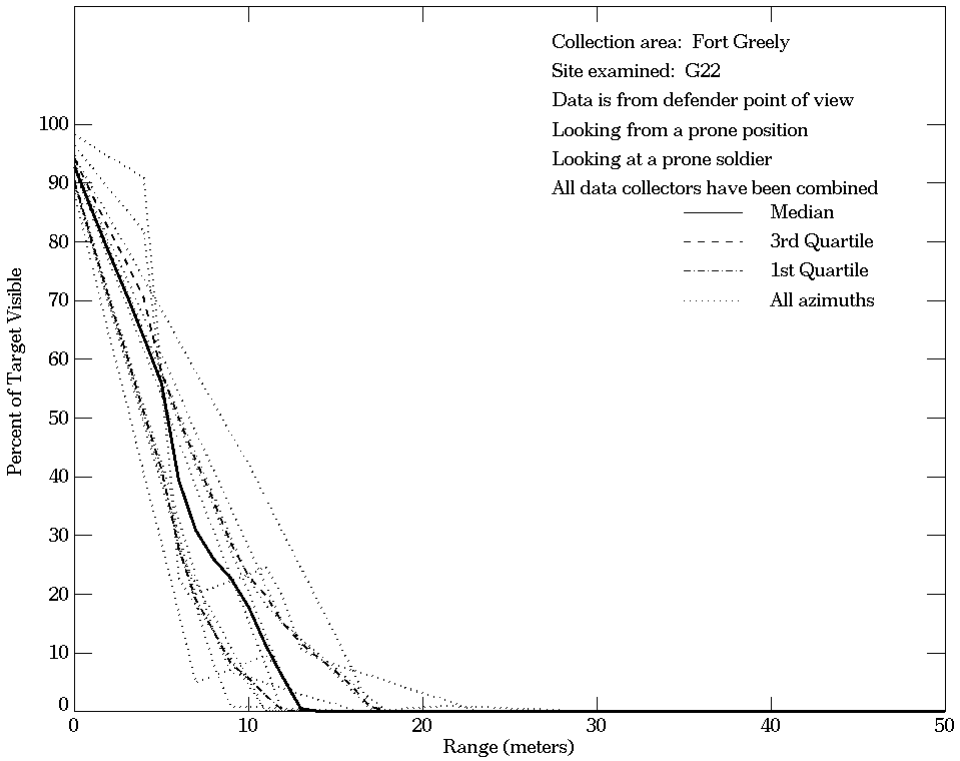

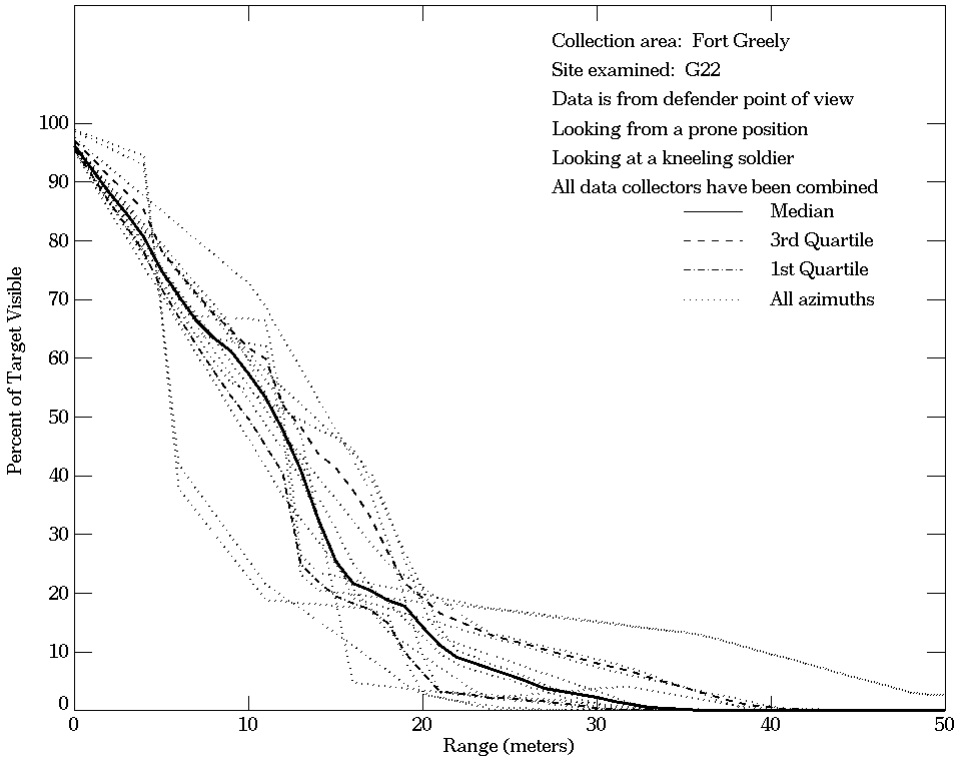

Figure E-119. Fort Greely, From Defender Point of View, Site G22

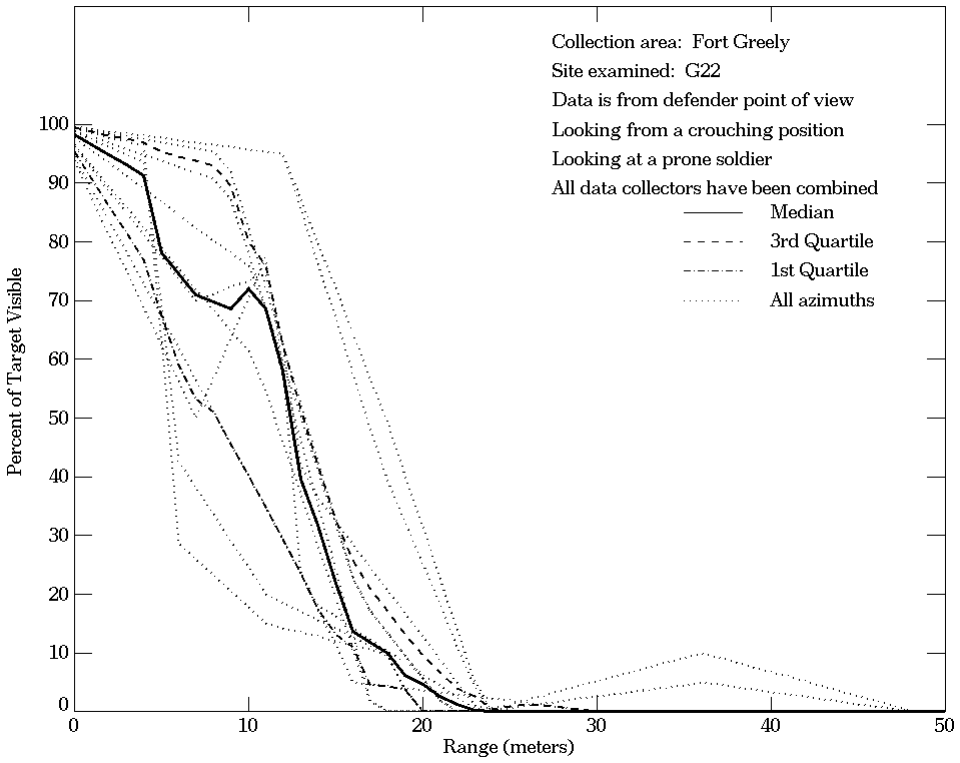

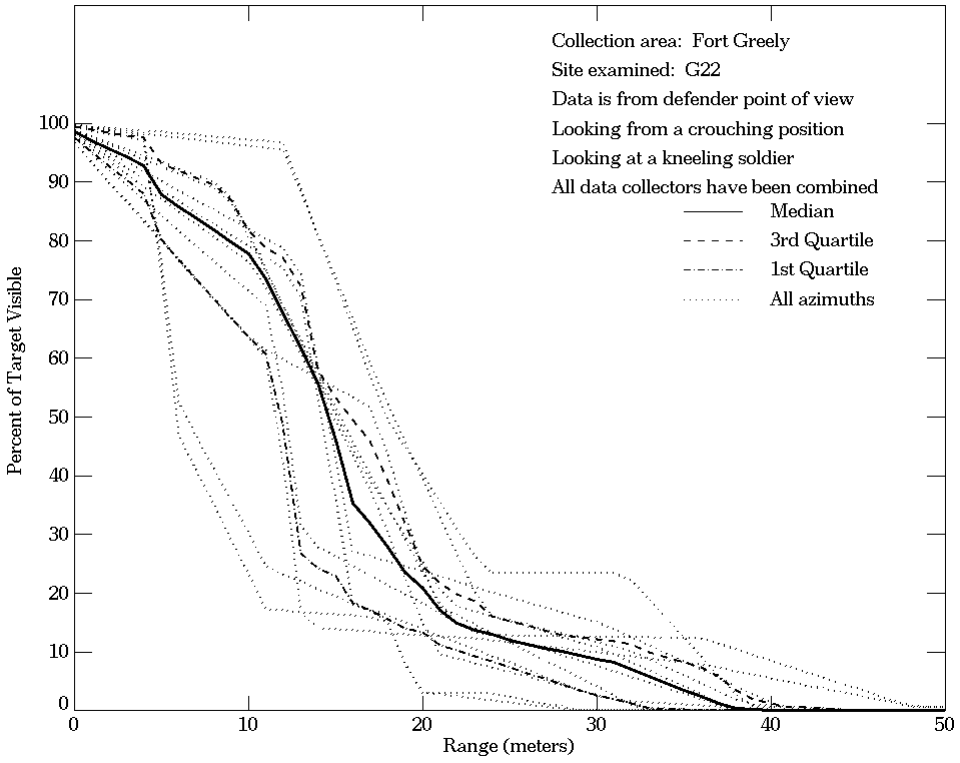

Figure E-119. Fort Greely, From Defender Point of View, Site G22 (Continued)

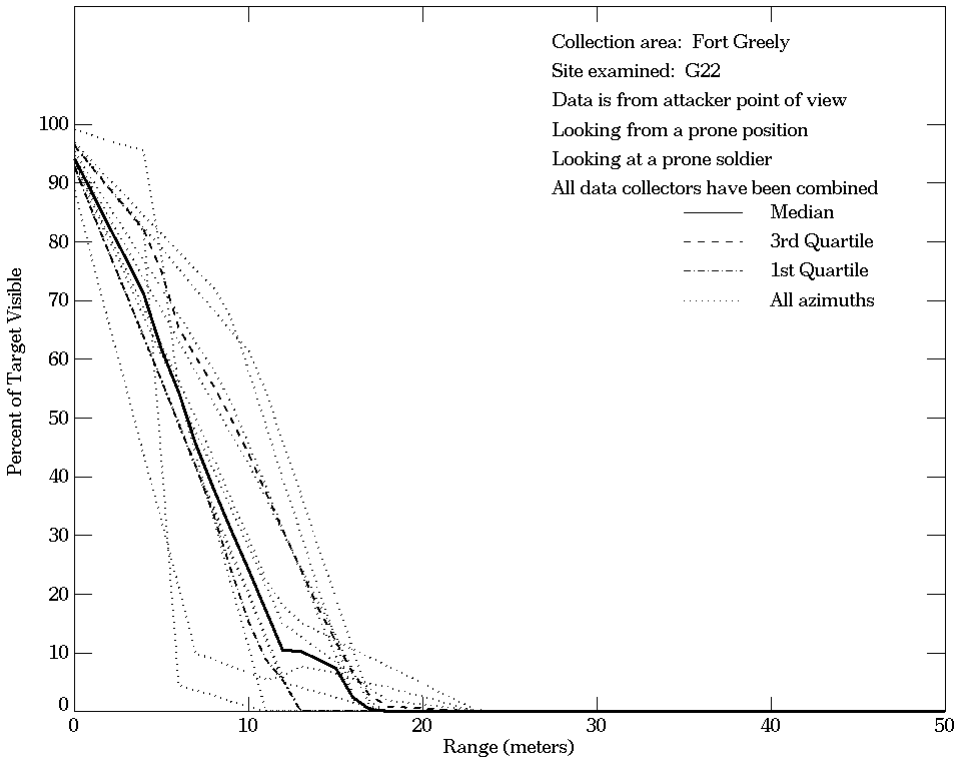

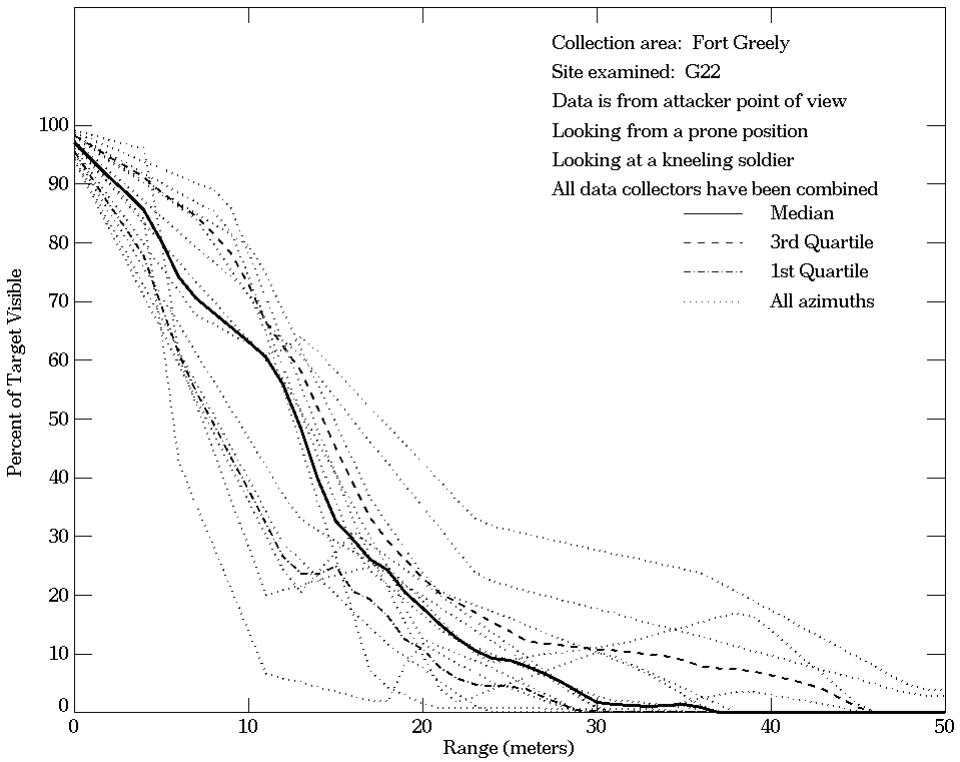

Figure E-120. Fort Greely, From Attacker Point of View, Site G22

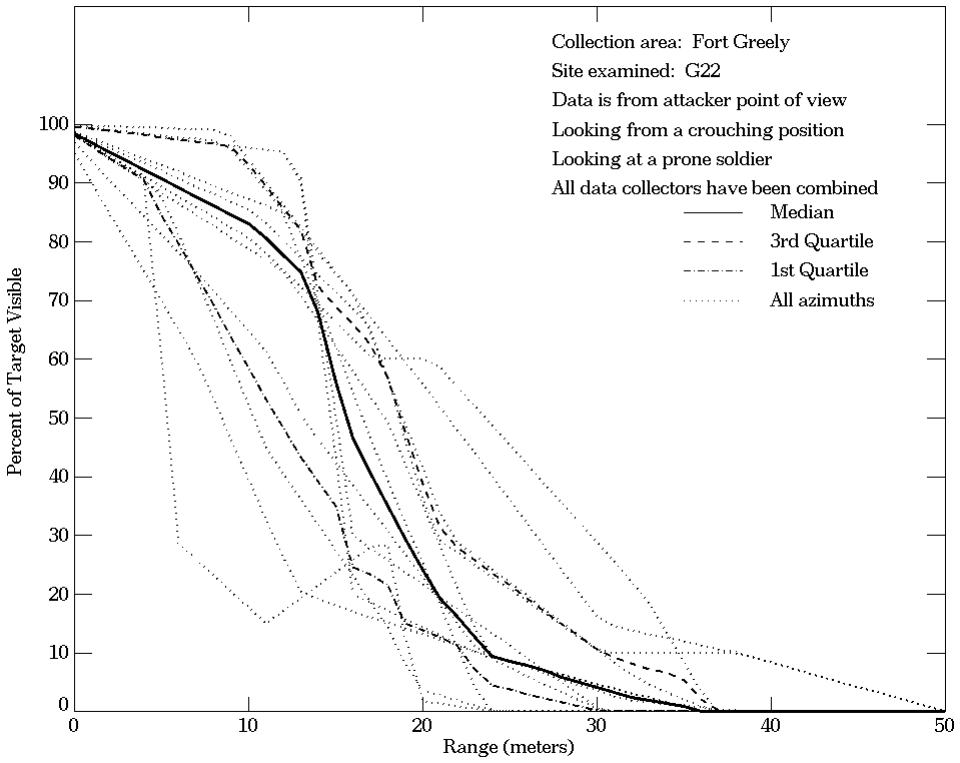

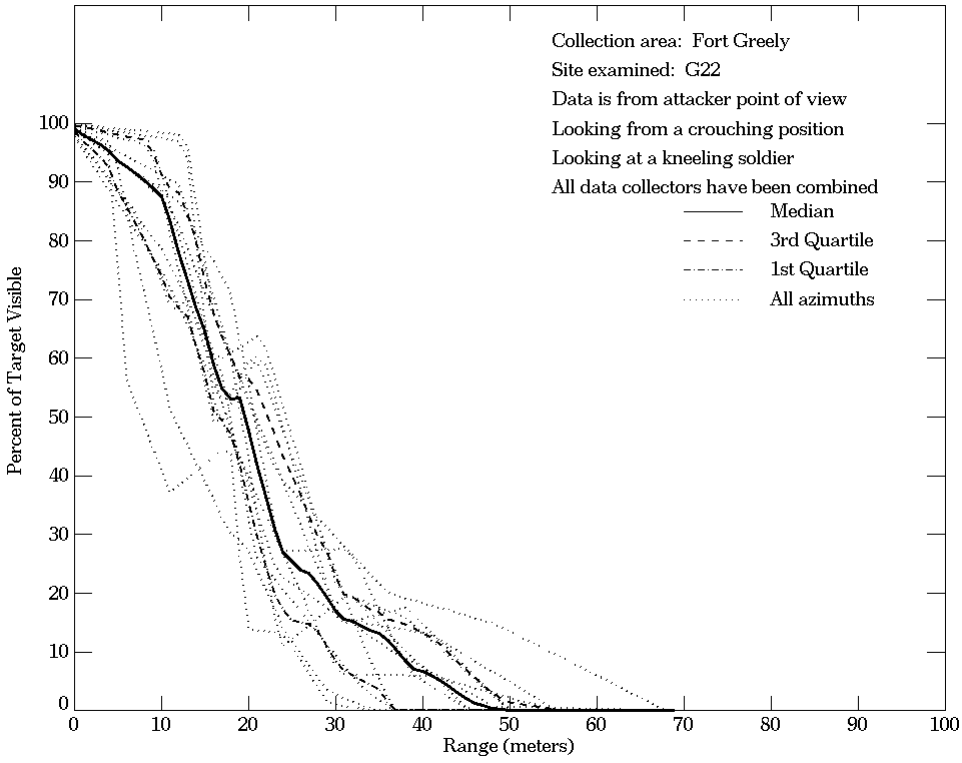

Figure E-120. Fort Greely, From Attacker Point of View, Site G22 (Continued)

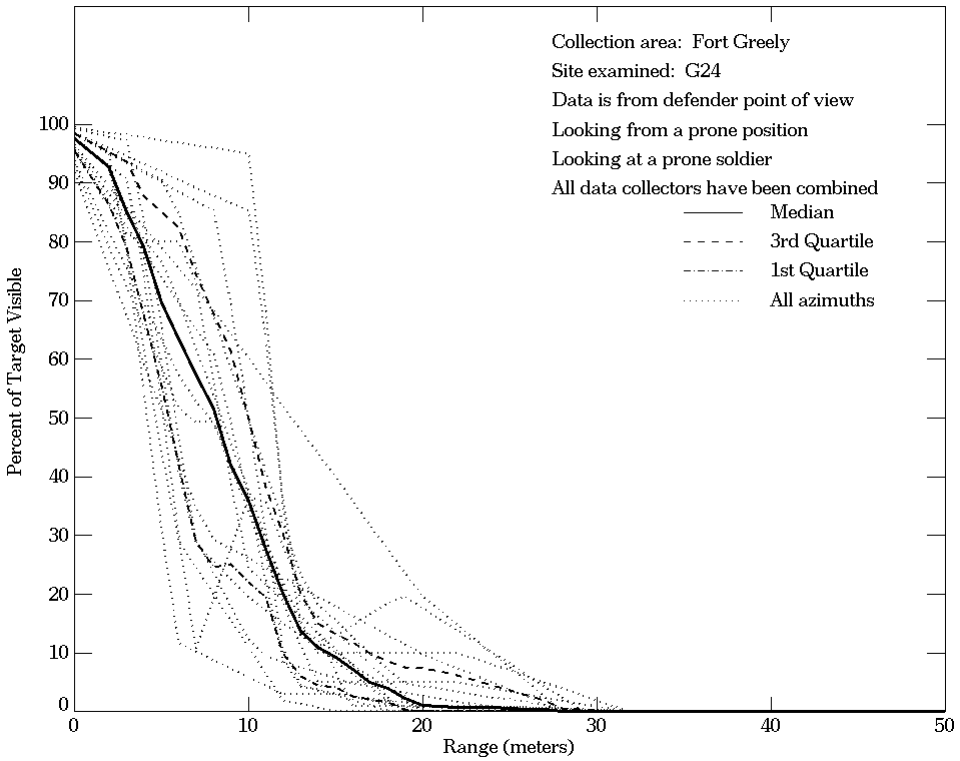

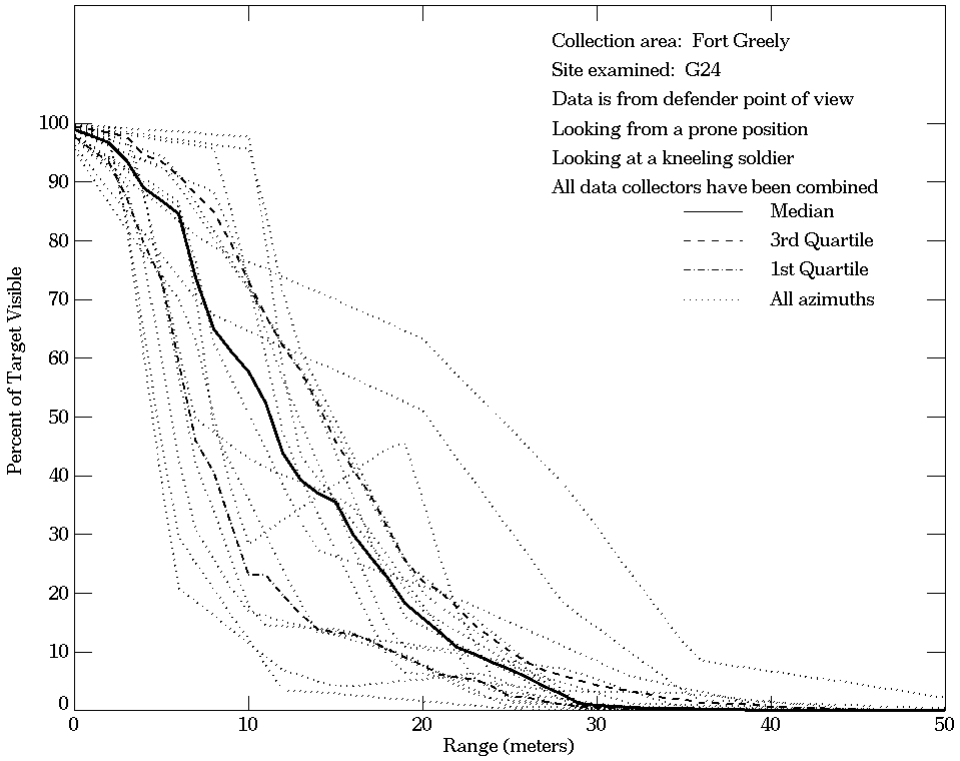

Figure E-121. Fort Greely, From Defender Point of View, Site G24

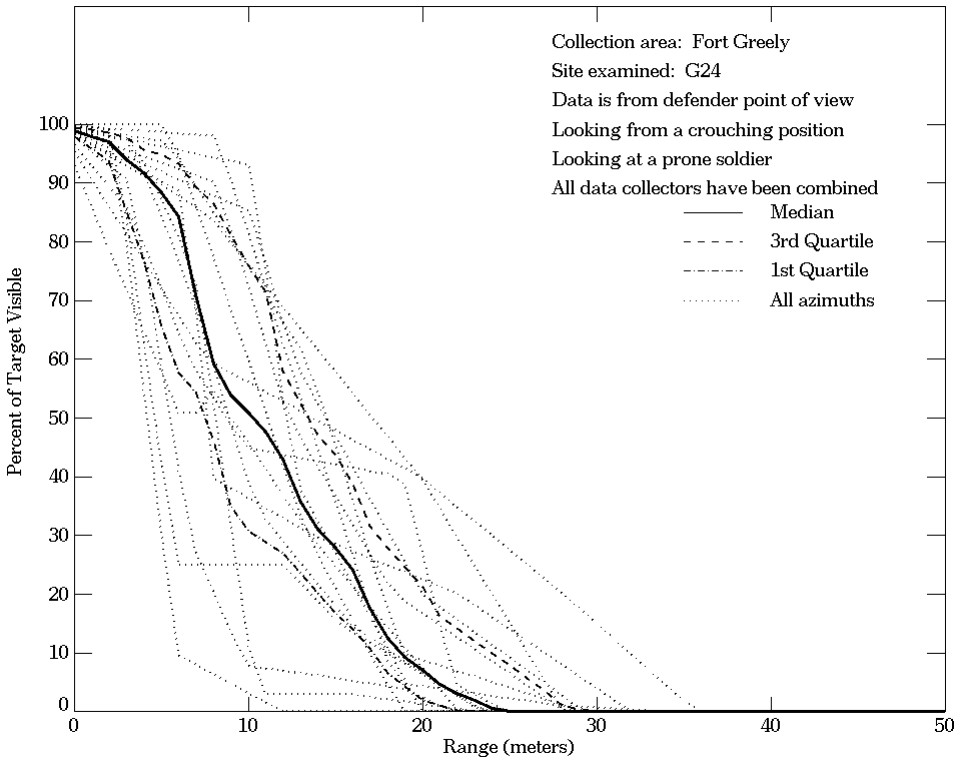

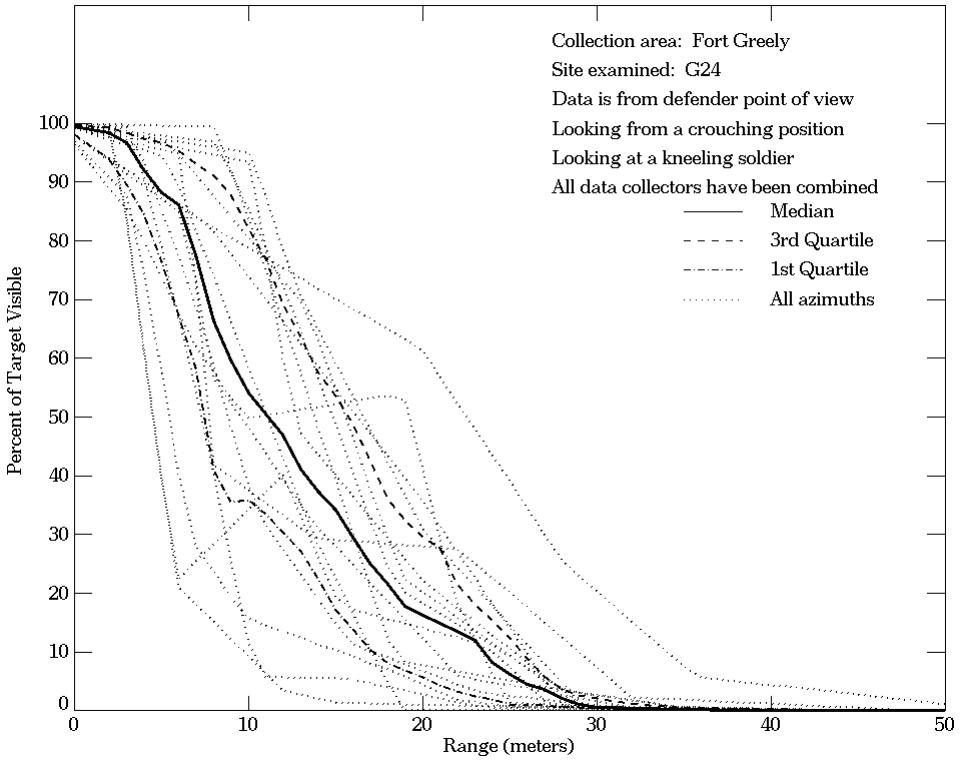

Figure E-121. Fort Greely, From Defender Point of View, Site G24 (Continued)

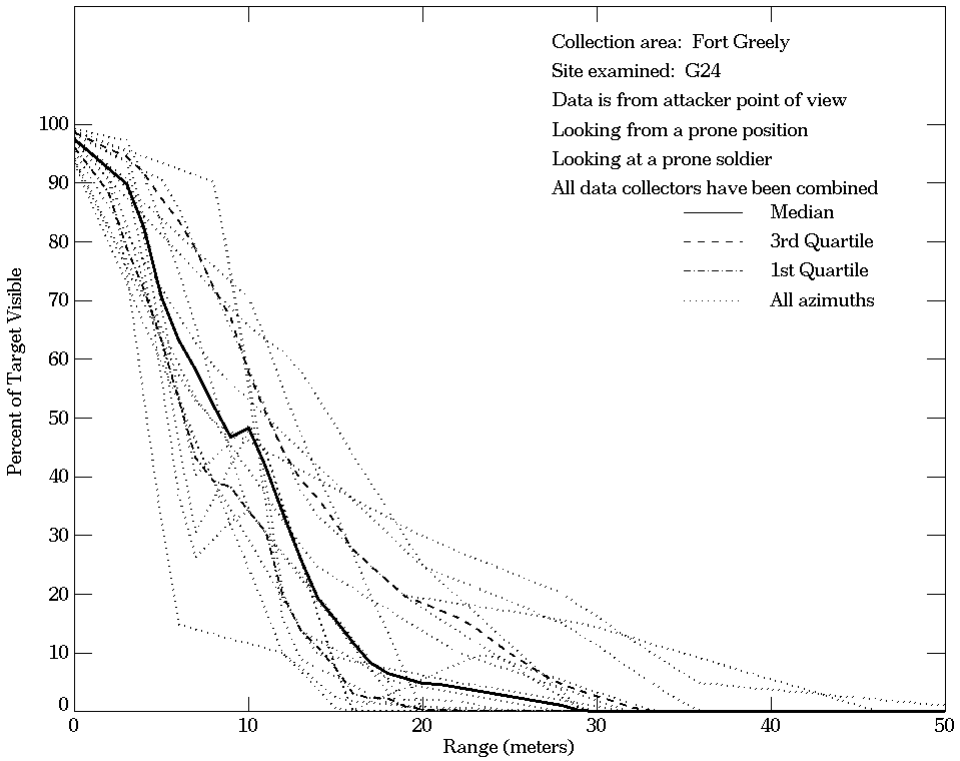

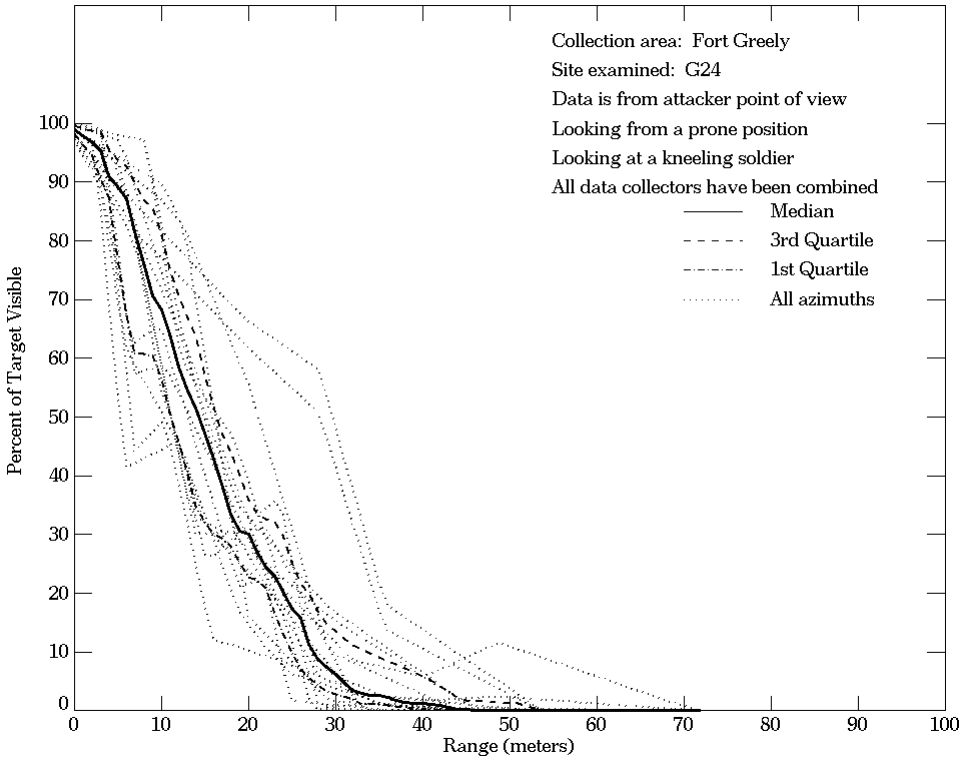

Figure E-122. Fort Greely, From Attacker Point of View, Site G24

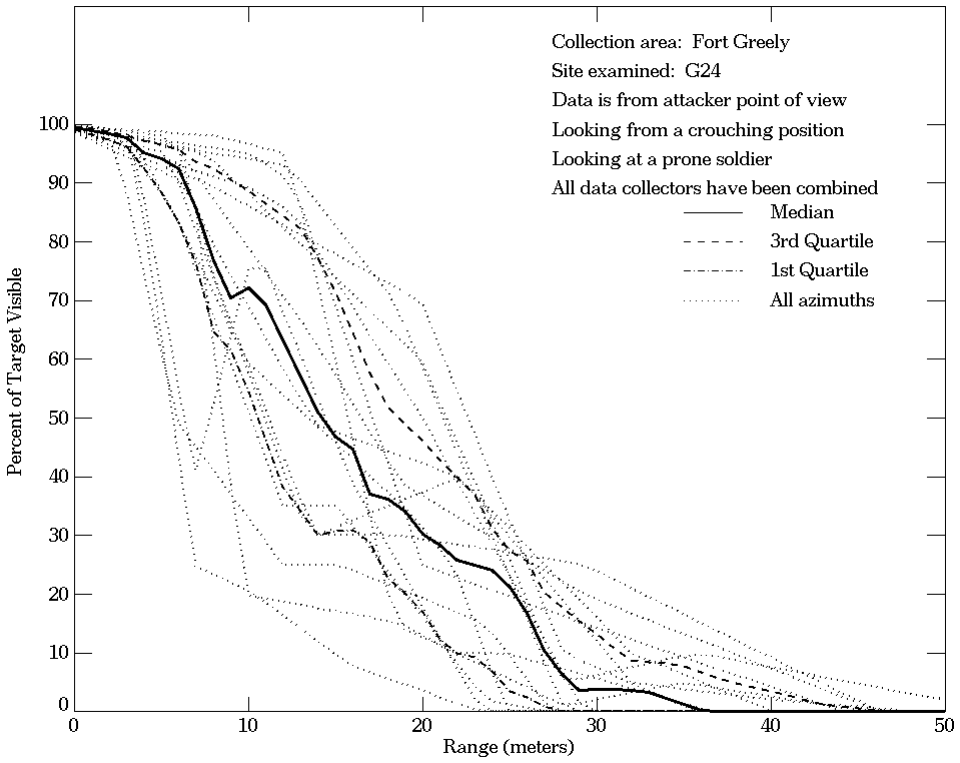

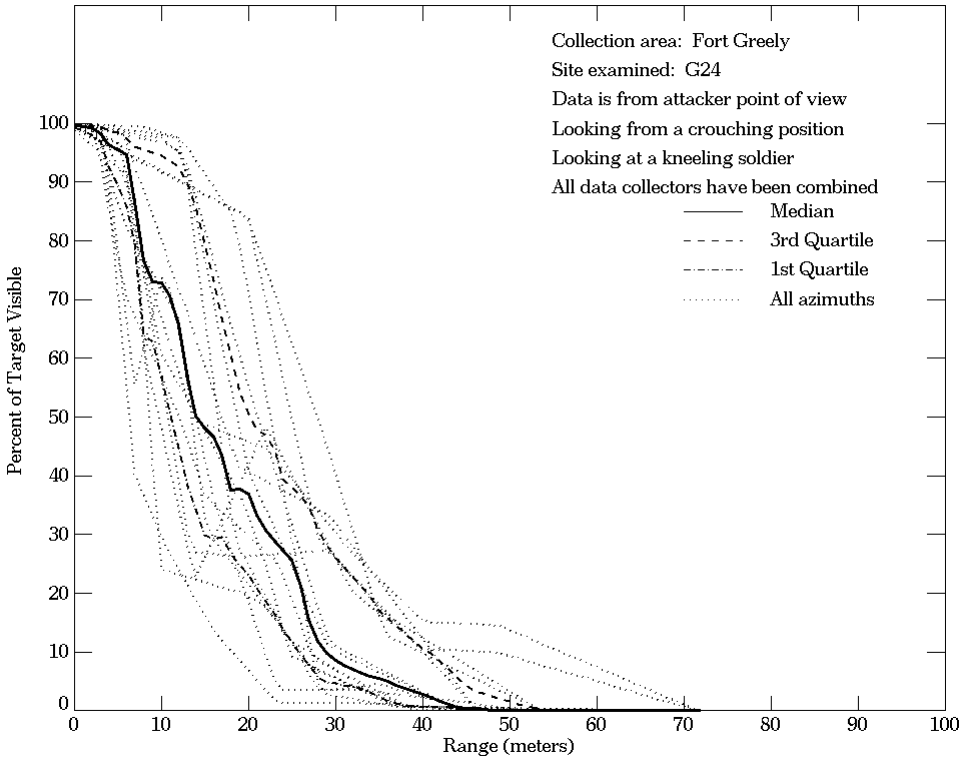

Figure E-122. Fort Greely, From Attacker Point of View, Site G24 (Continued)

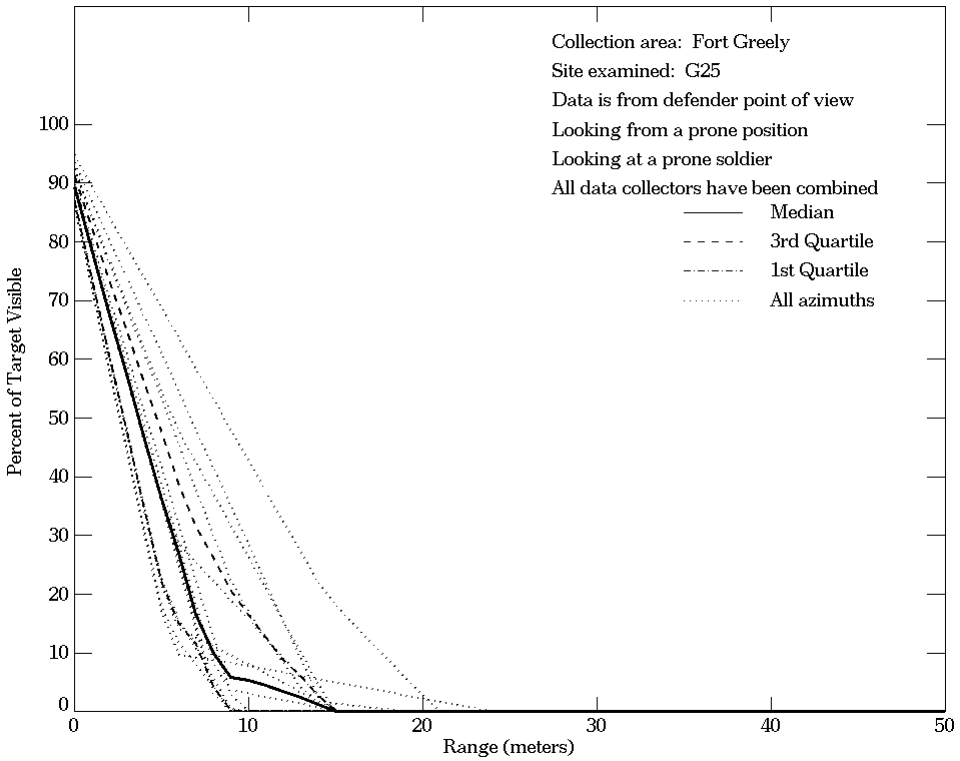

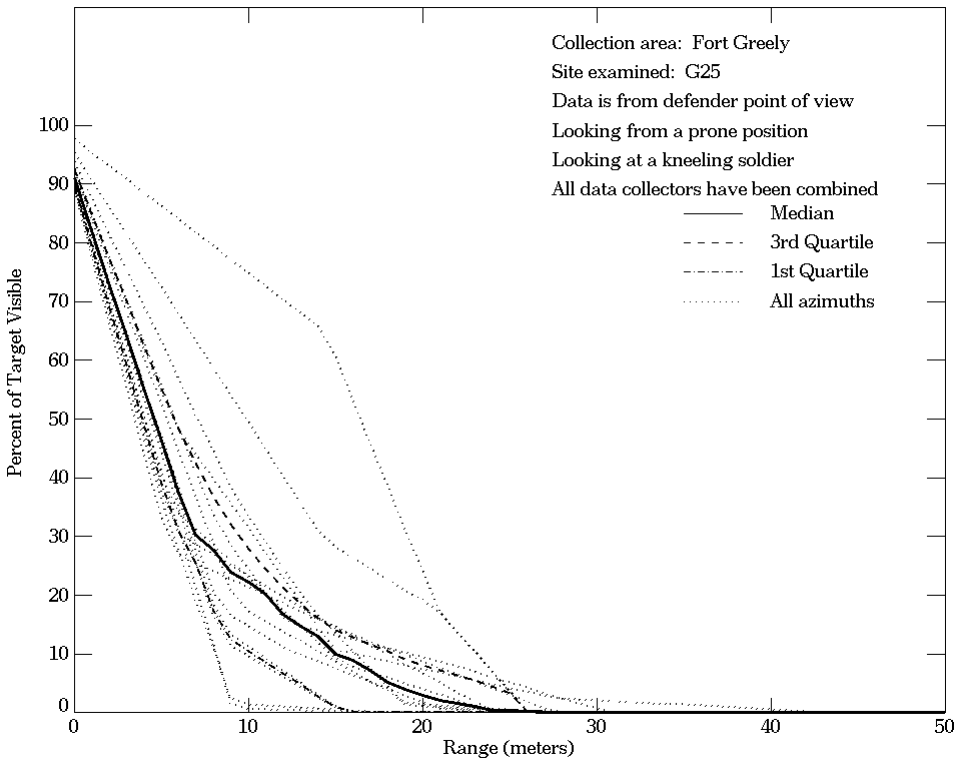

Figure E-123. Fort Greely, From Defender Point of View, Site G25

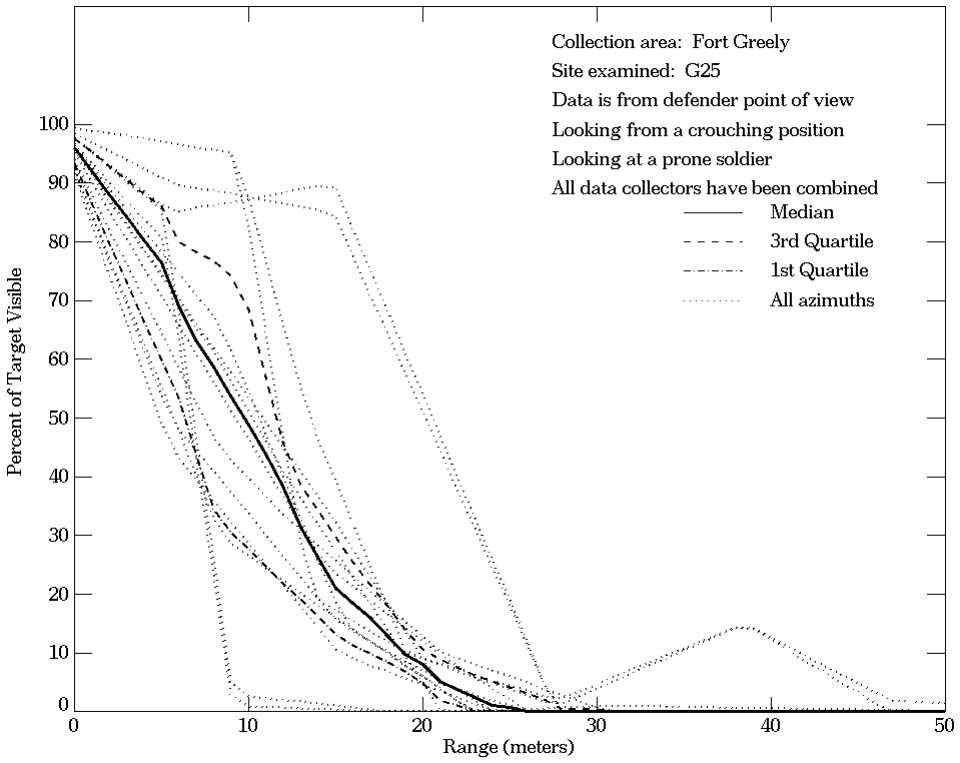

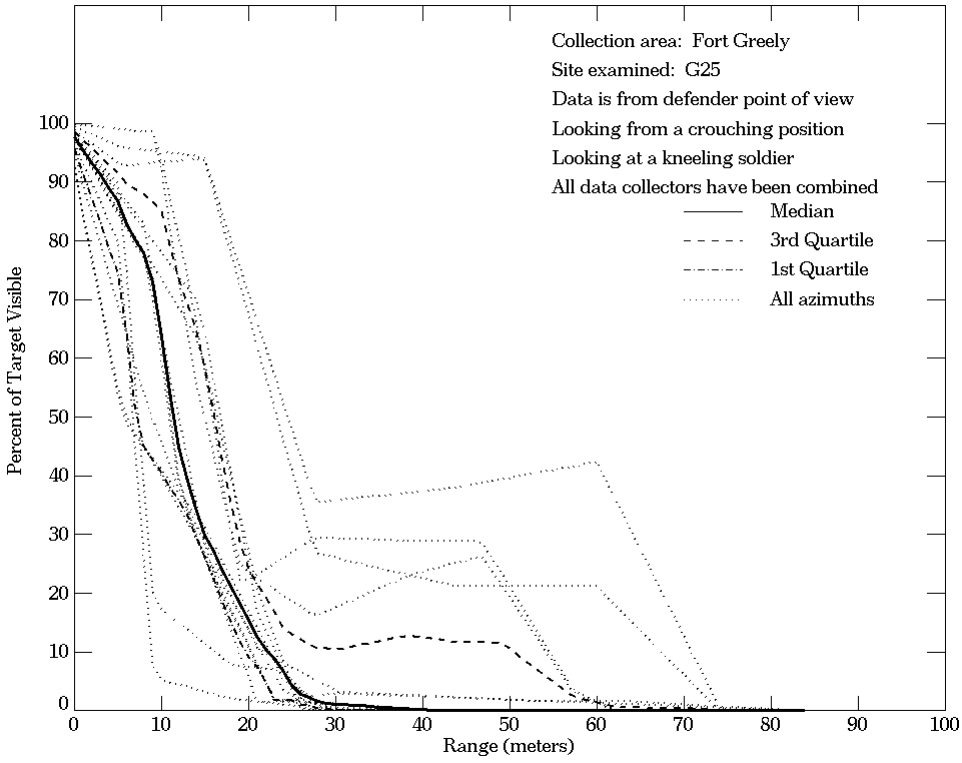

Figure E-123. Fort Greely, From Defender Point of View, Site G25 (Continued)

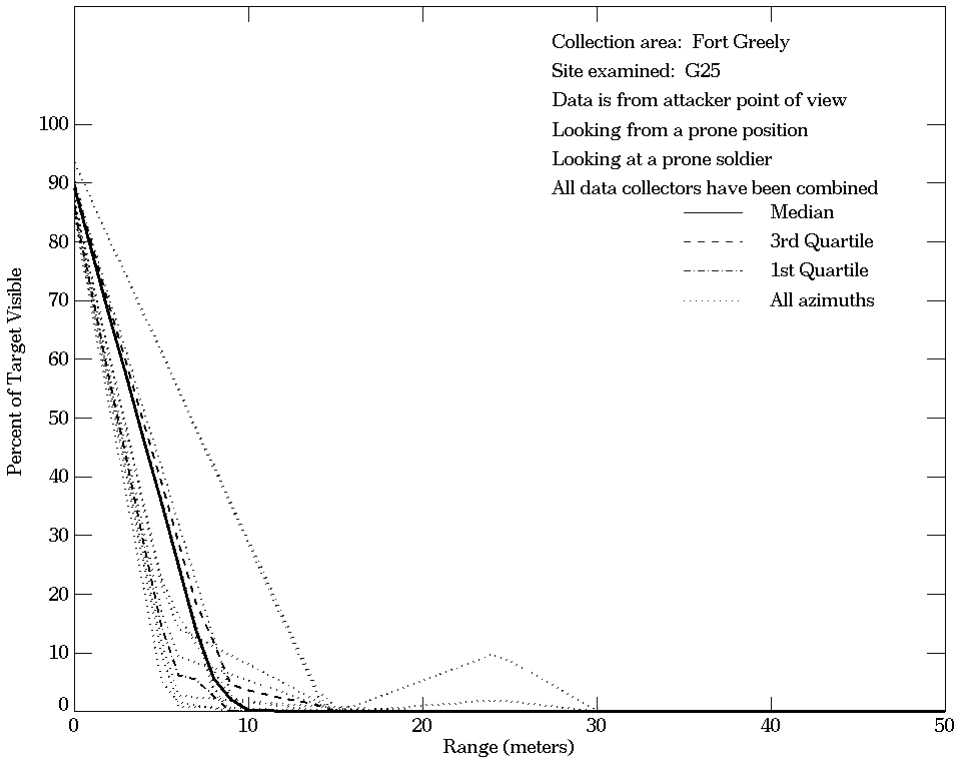

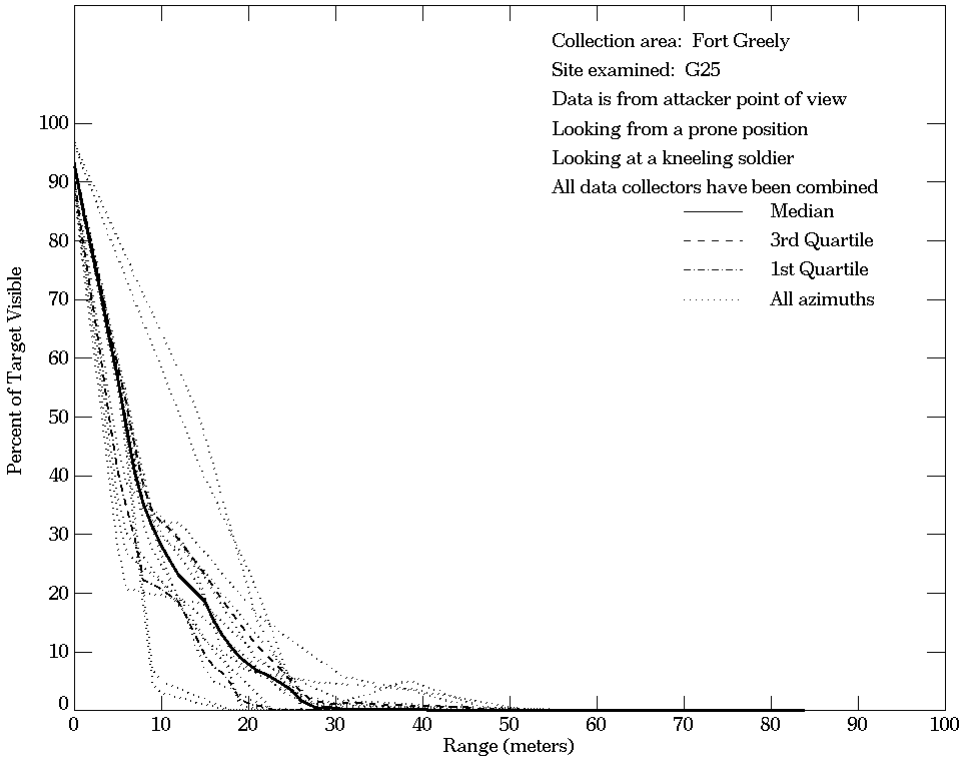

Figure E-124. Fort Greely, From Attacker Point of View, Site G25

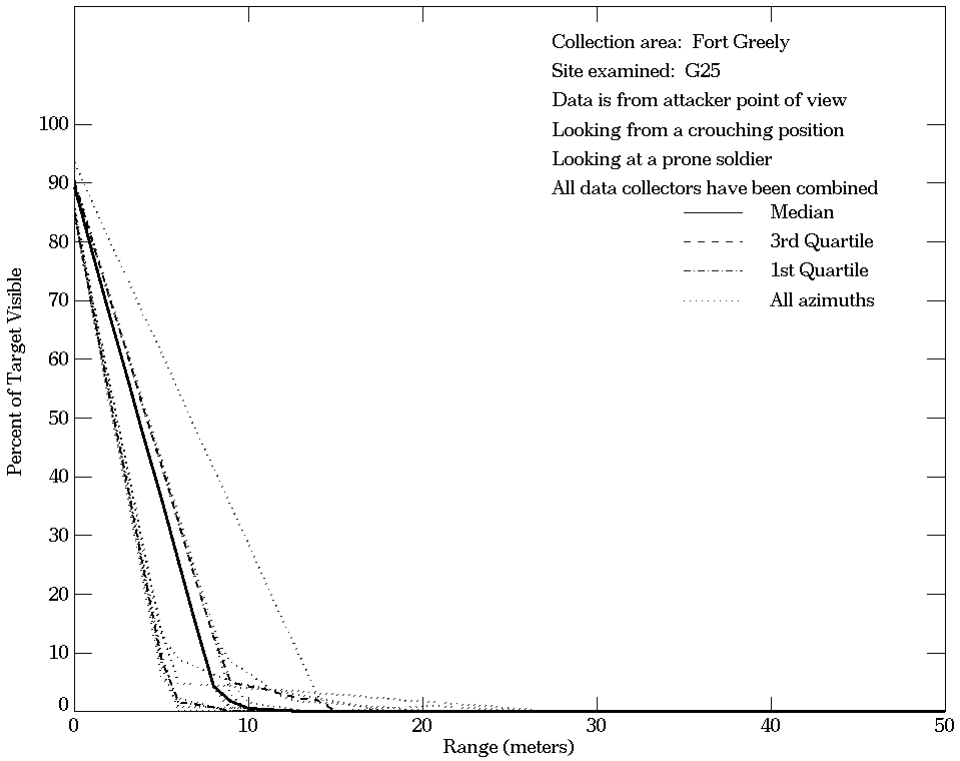

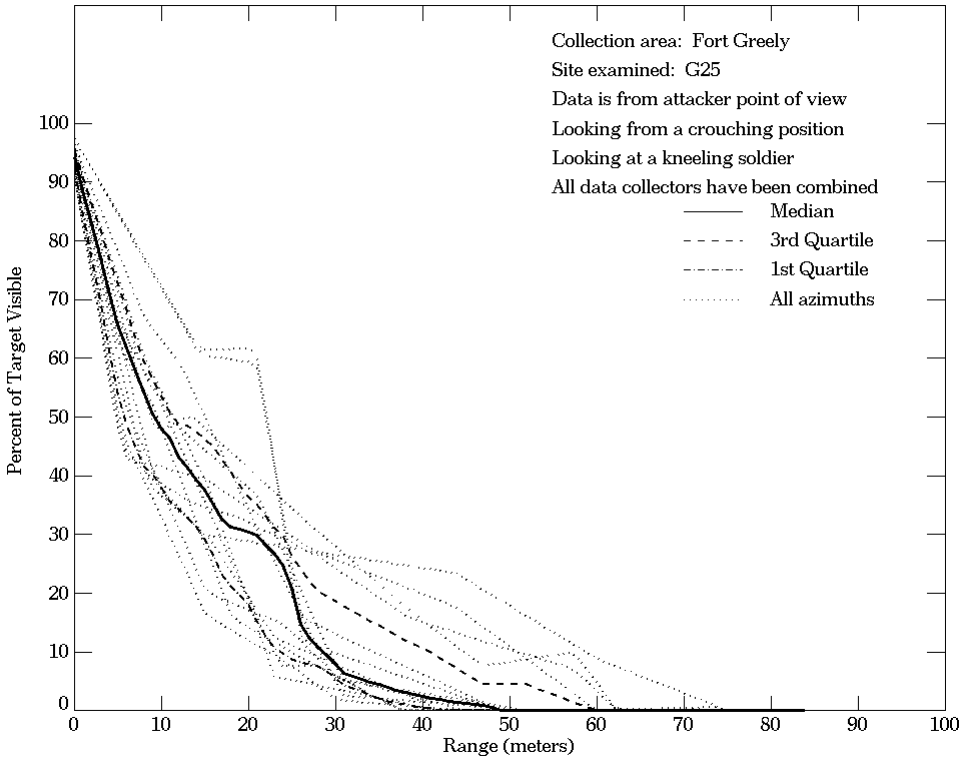

Figure E-124. Fort Greely, From Attacker Point of View, Site G25 (Continued)

Bibliography

Ahrens, C.D. (1991), Meteorology Today – An Introduction to Weather, Climate, and the Environment, New York, NY, West Publishing Company.

Champion, Danny C., Pankratz, Kent G., and Fatale, Louis A., "The Effects of Different Line-of-Sight Algorithms and Terrain Elevation Representations on Combat Simulations," White Sands Missile Range, NM, 88002, September 1995.

Coe, Gary Q. (1997), "Concept Exploration on the Virtual Battlefield," Military Operations Research, Volume 3, Number 4.

Mackey, Douglas C., Dixon, David S., Jensen, Karl G., Loncarich, Thomas C., Swaim, Jerry T., "CASTFOREM: Methodologies," White Sands Missile Range, NM 88002, March 1990.

Millikan, Justin A. (1998), "Lateral Vegetation Optical Density Modeling for Combat Simulation: The Red Banner II Field Trial," Salisbury, South Australia.

O'Connor, John D., O'Kane, Barbara L. PhD, Royal, Christopher K., Ayscue, Kathy L., Bonzo, David E., Nystrom, Beth M., "Recognition of Human Activities Using Handheld Thermal Systems," Fort Belvoir, VA 22060, April 1996.

Oliver, J.E. (1973), Climate and Man's Environment – An Introduction to Applied Climatology, New York, NY, John Wiley & Sons.

Olson, Warren K., "Warfighter Operational Evaluation Report - Modeling and Simulation Terrain Databases for McKenna MOUT Site, Fort Benning, Georgia," Institute for Defense Analysis, Washington D.C., 26 February 1997.

Petrides, George A. (1972), A Field Guide to Trees and Shrubs, Haughton Mifflin Company, Boston.

Petrides, George A. And Petrides, Olivia (1992), A Field Guide to Western Trees, Haughton Mifflin Company, Boston.

Seagraves, Mary Ann and Davis, John M. (1989). Target Acquisition Tactical Decision Aid Software Technical Documentation, Atmospheric Sciences Laboratory, WSMR, NM.

Scott, Macio (1985), NV&EOL Detection Model, TRASANA.

Strahler, A. N. (1967), Introduction to Physical Geography, New York, NY, John Wiley and Sons.

Strahler, A. N. and Strahler, A. H. (1987), Modern Physical Geography, Third Edition., New York, NY, John Wiley and Sons.

Trewartha, G.T., A.H. Robinson and E.H. Hammond (1968), Fundamentals of Physical Geography, New York, NY, McGraw-Hill Book Company.

Acronyms

A	
AC	apparent contrast
AFA	Air Force Academy
AFB	air force base
ARTEP	Army training and evaluation program
ATTN	atmospheric attenuation
B	
BB	background brightness
C	
C	contrast
C	Celsius
CASTFOREM	Combined Arms and Support Task Force Evaluation Model
CD-ROM	compact disk-read only memory
cm	centimeter
coeff	coefficient
CONUS	continental United States
D	
DVO	direct view optics
F	
F	Fahrenheit
FLIR	forward looking infrared
FOV	field of view
G	
GPS	Global Positioning System
I	
ID	identification
IR	infrared
ITCZ	intertropical convergence zone
K	
km	kilometer
L	
LOS	line-of-sight
M	
m	meter
M&S	modeling and simulation
MI	moisture index
mm	millimeter
MRC	major regional contingency
MRF	maximum resolvable frequency
MSR	main supply route

N	
N	resolvable cycles
N	north
NAS	naval air station
NIMA	National Imagery and Mapping Agency
O	
OCONUS	outside the continental United States
P	
PDET	probability of detection
PE	potential evapotranspiration
PLGR	precision lightweight GPS receiver
S	
S	south
SF	state forest
SOG	sky over ground
SSE	sum of squares error
T	
TB	target brightness
TEC	Topographic Engineering Center
TRAC-WSMR	TRADOC Analysis Center-White Sands Missile Range
TRADOC	Training and Doctrine Command
TSS	total survey station
TTPF	target transfer probability function
U	
US	United States
UTM	Universal Transverse Mercator

Distribution

	CD-ROM	Paper
DUSA-OR Mr. Hollis ATTN: SAUS-OR 102 Army Pentagon Washington, DC 20310-0102		1
DCSOPS ATTN: DAMO-ZDS (Mr. M. Moore) 400 Army Pentagon, 3A538 Washington, DC 20310-0400		1
DCSOPS ATTN: DAMO-ZS (LTC Timian) Army Modeling and Simulation Office 400 Army Pentagon Washington, DC 20310-0400		1
Commander, 7ATC ATTN: AEAGC-TD-TC Dr. Claude Miller Unit 28130 APO, AE 09114-5413	1	
Commander, US Army AMCOM ATTN: AMSAM-RD-AT-R (G. Tackett) Redstone Arsenal, AL 35898		1
Commander, JFKSWCS ATTN: CPT W. Rossa Chief, M&S Branch Concept Development Division Fort Bragg, NC 28307-5200		1
Commander, STRICOM ATTN: AMSTI-ET (Ms. P. Woodard) 12350 Research Parkway Orlando, FL 32826-3276	1	
Commander, STRICOM ATTN: AMSTI-ET (Mr. D. Stevens) 12350 Research Parkway Orlando, FL 32826-3276	1	
Commander, USAIC ATTN: ATZB-WC (Mr. J. Powell) Fort Benning, GA 31905-5400		1
Commander, USAIC ATTN: ATZB-WC (Mr. J. Derrico) Fort Benning, GA 31905-5400	1	
Commander, USAIC ATTN: ATZB-WC (Mr. G. Dutoit) Fort Benning, GA 31905-5400	1	

	CD-ROM	Paper
Commander, USAIC ATTN: ATZB-WC (Mr. J. Chervenak) Fort Benning, GA 31905-5400	1	
Commander, USAIC ATTN: ATZB-WC (Mr. B. McGlothlin) Fort Benning, GA 31905-5400	1	
Commander, USAIC ATTN: ATZB-CDI (Major B. Scott) Fort Benning, GA 31905-5400	1	
Commander and Director, WES ATTN: WES-GM (D. Bullock) 3909 Halls Ferry Road Vicksburg, MS 39180		1
Commander and Director, WES ATTN: CEWES (Mr. G. Mason) 3909 Halls Ferry Road Vicksburg, MS 39180	1	
Commander and Director, WES ATTN: CEWES-GE-YH (D. Lashlee) 3909 Halls Ferry Road Vicksburg, MS 39180	1	
Director, AMSAA ATTN: AMXSY-CA (Mr. Drake) 392 Hopkins Road Aberdeen Proving Ground, MD 21005-5071	1	
Director, AMSAA ATTN: AMXSY-CD (Mr. D. Hodge) 392 Hopkins Road Aberdeen Proving Ground, MD 21005-5071		1
Director, AMSAA ATTN: AMXSY-CD (D. Nuzman) 392 Hopkins Road Aberdeen Proving Ground, MD 21005-5071	1	
Director, AMSAA ATTN: AMXSY-CD (M. Burrough) 392 Hopkins Road Aberdeen Proving Ground, MD 21005-5071	1	
Director, AMSAA ATTN: AMXSY (R. Thompson) 392 Hopkins Road Aberdeen Proving Ground, MD 21005-5071	1	
Director, AMSAA ATTN: AMXSY-CA (B. Yaekel) 392 Hopkins Road Aberdeen Proving Ground, MD 21005-5071	1	

	CD-ROM	Paper
Director, AMSAA ATTN: AMXSY-CA (G. Comstock) 392 Hopkins Road Aberdeen Proving Ground, MD 21005-5071	1	
Director, AMSAA ATTN: AMXSY-CD (M. Schmidt) 392 Hopkins Road Aberdeen Proving Ground, MD 21005-5071	1	
Director, CAA ATTN: CSCS-OS (Mr. R. Johnson) Wilbur B. Payne Hall 6001 Goethals Road Fort Belvoir, VA 22060-5230		1
Director, CAA ATTN: OD-ARPO (Dr. K. Tatalias) Wilbur B. Payne Hall 6001 Goethals Road Fort Belvoir, VA 22060-5230	1	
Director, AMSAA ATTN: AMXSY-CD (T. Ruth) 392 Hopkins Road Aberdeen Proving Ground, MD 21005-5071		1
Director, USA TEC ATTN: CETEC-PD-PR (L. Fatale) 7701 Telegraph Road Alexandria, VA 22315-3864	20	10
Director, TRADOC Analysis Center ATTN: ATRC-FM (S. Solick) 255 Sedgwick Avenue Fort Leavenworth, KS 66027-2345		1
Director, TRADOC Analysis Center ATTN: ATRC-FSP-D (Mr. Orourke) 255 Sedgwick Avenue Fort Leavenworth, KS 66027-2345	1	
Director, TRADOC Analysis Center ATTN: ATRC-FPD (Mr. Pabone) 255 Sedgwick Avenue Fort Leavenworth, KS 66027-2345	1	
Director, TRADOC Analysis Center ATTN: ATRC-TD (Mr. Loental) 255 Sedgwick Avenue Fort Leavenworth, KS 66027-2345	1	
Director, TRADOC Analysis Center ATTN: ATRC-TD 255 Sedgwick Avenue Fort Leavenworth, KS 66027-2345	1	

	CD-ROM	Paper
Director TRADOC Analysis Center-Monterey Naval Postgraduate School PO Box 8692 Monterey, CA 93940-6672		1
Director, TRAC-WSMR ATTN: ATRC-WEA (D. Champion) White Sands Missile Range, NM 88002-5502		30
Director, TRAC-WSMR ATTN: ATRC-WSS-R White Sands Missile Range, NM 88002-5502		3
Technical Director Maneuver Support Battle Lab ATTN: ATSE-BL (Mr. V. Lowrey) 320 Engineer Loop, Suite 167 Fort Leonardwood, MO 65473-8929	1	
Technical Director Maneuver Support Battle Lab ATTN: ATSE-BL (Major G. Gage) 320 Engineer Loop, Suite 167 Fort Leonardwood, MO 65473-8929	1	
Senior Technical Advisor Maneuver Support Battle Lab ATTN: TPIO-TD (Mr. D. Lueck) 320 Engineer Loop, Suite 167 Fort Leonardwood, MO 65473-8929		1
USA Cadet Command ATTN: ATCC-H (Dr. A. Coumbe) Fort Monroe, VA 23651	1	
USA Soldier Biological Chemical Command (N) Natick Soldier Center ATTN: Dale Malabarba Kansas Street Natick, MA 01760		1
USA Soldier Biological Chemical Command (N) Natick Soldier Center ATTN: David Tucker Kansas Street Natick, MA 01760		1
US Army Yuma Proving Ground ATTN: STEYP-TD-ATO (Mr. A. Hooper) Yuma, AZ 85365-9110	4	1
US Army Yuma Proving Ground ATTN: STEYP-CD-P (Mr. J. Mitchell) Yuma, AZ 85365-9110	1	

	CD-ROM	Paper
US Army Yuma Proving Ground ATTN: STEYP-TD-ATO (Mr. R. Hernandez) Yuma, AZ 85365-9110		1
US Army Yuma Proving Ground ATTN: STEYP-TD-ATO (Mr. L. Vanderzyl) Yuma, AZ 85365-9110		1
US Army Yuma Proving Ground ATTN: STEYP-TD-ATO (Mr. T. McIntire) Yuma, AZ 85365-9110	1	
US Army Yuma Proving Ground Topic Test Center ATTN: STEYP-MT-TT (R. Ayala) Unit 7140 APO AA 34004-5000		1
US Army Yuma Proving Ground Topic Test Center ATTN: STEYP-MT-TT (L. Havrilo) Unit 7140 APO AA 34004-5000		1
US Army Yuma Proving Ground Topic Test Center ATTN: STEYP-MT-TT (L. Hay) Unit 7140 APO AA 34004-5000		1
NIMA LO TRADOC ATTN: Mr. R. Craven 415 Sherman Avenue Building 52, Room 326 Fort Leavenworth, KS 66027-2345		1
NIMA TRT ATTN: COTA (J. Miller) Mailstop P39 12310 Sunrise Valley Drive Reston, VA 20191-3449	1	
NIMA TRT ATTN: COTA (B. McMahon) Mailstop P39 12310 Sunrise Valley Drive Reston, VA 20191-3449	1	
NIMA TRT ATTN: COTA (LTC Hampel) Mailstop P39 12310 Sunrise Valley Drive Reston, VA 20191-3449	1	

	CD-ROM	Paper
NIMA TRT ATTN: COTA (J. Dale) Mailstop P39 12310 Sunrise Valley Drive Reston, VA 20191-3449		1
JWARS Office ATTN: Mr. C. Leake 1555 Wilson Road Arlington, VA 22209		1
DARPA/ISO ATTN: ARPA-ASTO (G. Lukes) 3701 North Fairfax Drive Arlington, VA 22203-1714		1
Institute for Defense Analysis ATTN: Dr. Dennis Deriggi 1801 N. Beauregard Street Alexandria, VA 22311-1772	1	
Institute for Defense Analysis ATTN: Warren Olson 1801 N. Beauregard Street Alexandria, VA 22311-1772		1
Institute for Defense Analysis ATTN: Tim Stone 1801 N. Beauregard Street Alexandria, VA 22311-1772	1	
Institute for Defense Analysis ATTN: Dr. Robert F. Richbourg 1801 N. Beauregard Street Alexandria, VA 22311-1772		1
Institute for Defense Analysis ATTN: D. Hue McCoy 1801 N. Beauregard Street Alexandria, VA 22311-1772		1
Mr. David Mason, DLOR 101 Colonel By Drive Ottawa, Ontario Canada K1A OK2		1
Mr. Pierre Ladouceur, DLOR 101 Colonel By Drive Ottawa, Ontario Canada K1A OK2		1
Mr. Justin A. Millikan, DSTO Operations Analysis and Evaluation Land Operation Division, DSTO PO Box 1500 Salisbury 5108 Australia		1

	CD-ROM	Paper
Mr. Dean Bowley Head RTA Studies Land Operation Division, DSTO PO Box 1500 Salisbury 5108 Australia		1
Dr. George Cran, DRA Building Q10 Fort Halstead Sevenoaks, Kent TN14 7BP United Kingdom		1
Mr. Terry Duell, EDE Army Tech and Eng Agency Private Bag 12 PO Ascot Vale Victoria 3032 Australia		1
Attache of Defence Science Embassy of Australia ATTN: Dr. G. C. L. Searle 1601 Massachusetts Avenue NW Washington, DC 20036		1
Applied Research Associates ATTN: Mr. J. Robinson 112 Monument Place Vicksburg, MS 39180		1
Computer Science Corporation ATTN: Mr. E. Landry 4815 Bradford Drive Huntsville, AL 35805	1	
Computer Science Corporation ATTN: Mr. B. Burgess 4815 Bradford Drive Huntsville, AL 35805	1	
Computer Science Corporation ATTN: Mrs. S. Siniard 4815 Bradford Drive Huntsville, AL 35805	1	
Computer Science Corporation ATTN: Mr. Monte Porter 4815 Bradford Drive Huntsville, AL 35805	1	
Joint Precision Strike Demonstration Project Office ATTN: Mr. J. Brown 10401 Totten Road, Suite 324 Fort Belvoir, VA 22060		1

	CD-ROM	Paper
Litton TASC Orlando ATTN: Mr. M. Butterworth 12443 Research Parkway, Suite 202 Orlando, FL 32826		1
Modeling and Simulation Operational Support Activity ATTN: Mr. John Gray 1901 N. Beauregard, Suite 400 Alexandria, VA 22311-1705		1
SAIC ATTN: Mr. S. McNully 6725 Odyssey Drive Huntsville, AL 35806-3301	1	
SAIC ATTN: Mr. J. Ferguson 1755 Jefferson Davis Highway Suite 202, Crystal Square 5 Arlington, VA 22202	1	
Technical Solutions Incorporated ATTN: Mr. G. Ober 7975 S. Main Mesilla Park, NM 88047	1	
Dave Davis Institute for Public Policy George Mason University 4400 University Drive MS3C6 Fairfax, VA 22030-4444	1	
DTIC 8725 John Kingman Road Suite 0944 Fort Belvoir, VA 22060-6218		1